The Dissertation Committee for Annette Summers Engel
Certifies that this is the approved version of the following dissertation:

Geomicrobiology of Sulfuric Acid Speleogenesis:
Microbial Diversity, Nutrient Cycling, and Controls on
Cave Formation

Committee:

Philip C. Bennett, Supervisor

Libby A. Stern

John M. Sharp

Barbara J. Mahler

Katrina Edwards

Geomicrobiology of Sulfuric Acid Speleogenesis: Microbial Diversity, Nutrient Cycling, and Controls on Cave Formation

by

Annette Summers Engel, B.A., M.Sc.

Dissertation

Presented to the Faculty of the Graduate School of

The University of Texas at Austin

in Partial Fulfillment

of the Requirements

for the Degree of

Doctor of Philosophy

The University of Texas at Austin

May, 2004

Acknowledgements

First and foremost, it is because of my family and friends who supported me throughout this long process, and it has been with their encouragement that I was able to complete this work. I honestly think that many of them thought this day would never come.... Now, a new stage of my life begins and I feel fortunate in knowing they champion me. I am greatly indebted to Scott for his love, patience, and strength. Without his devotion and never-ending sacrifices, finishing this work would have been much more difficult. *How many days of your vacations have you surrendered in search of one last stinky spring, or for collecting slime in some godforsaken place?* To Astrid and Jason, I am grateful for our friendship and will fondly remember all the margaritas we shared together. I extend very special thanks to Megan Porter, a truly wonderful person and valued friend. This research would have suffered if not for her collaboration, companionship, and intellectual banter.

I owe much to Phil Bennett and Libby Stern, both caring and supportive individuals, for all their creativity and guidance. They honed my crazed thoughts and refined many ideas. It is still unbelievable to me how these unsuspecting souls quickly embraced the research, donned gas masks with passion, and forcibly slithered into a smelly hole in the ground. Together, after logging some 1665 hours (!!!) in the caves with friends and colleagues, we unburied quite an unforgettable treasure in Lower Kane Cave.

University of Texas at Austin, and the National Speleological Society. Sample acquisition would not have been possible without the cooperation of the Bureau of Land Management, Cody Office, Wyoming.

Finally, I am especially grateful to my countless friends who took precious time from their lives to help with work in Lower Kane Cave. Their interest and enthusiasm for the research will not be forgotten, and I hope that someday I can repay their kindness. The purpose and heart of a caver, of my friends and companions, are described in the poem *In Praise of Limestone* by W.H. Auden. It is with these words that I end this dedication and begin the story:

If it form the one landscape that we, the inconstant ones,
Are consistently homesick for, this is chiefly
Because it dissolves in water. Mark these rounded slopes
With their surface fragrance of thyme and, beneath,
A secret system of caves and conduits; hear the springs
That spurt out everywhere with a chuckle,
Each filling a private pool…; when I try to imagine a faultless love
Or the life to come, what I hear is the murmur
Of underground streams, what I see is a limestone landscape.
W.H. Auden, excerpt from *In Praise of Limestone*

Geomicrobiology of Sulfuric Acid Speleogenesis: Microbial Diversity, Nutrient Cycling, and Controls on Cave Formation

Publication No. _____

Annette Summers Engel, Ph.D.

The University of Texas at Austin, 2004

Supervisor: Philip C. Bennett

Much of the terrestrial subsurface is inaccessible for study, but caves represent distinctive shallow subsurface habitats where biogeochemical processes can be easily examined. Previously defined speleogenesis models are almost entirely based on abiotic chemical and hydrologic controls, as biological controls on cave formation have not been considered significant. Hydrogen sulfide-rich groundwater discharges from springs into Lower Kane Cave, Wyoming, and the sulfuric acid speleogenesis model was introduced in the early 1970s as a cave enlargement process resulting primarily from hydrogen sulfide autoxidation to sulfuric acid and replacement of carbonate by gypsum on subaerially exposed surfaces. The reduced sulfur compounds serve as rich energy sources for microorganisms that colonize the cave in both subaqueous and subaerial

environments. Several evolutionary lineages of the class "*Epsilonproteobacteria*" dominate the microbial diversity of subaqueous mats, and these microbes support the cave ecosystem through sulfur cycling and chemolithoautotrophic carbon fixation. The "*Epsilonproteobacteria*" occupy microbial mats in additional sulfidic cave and spring habitats, expanding the evolutionary and ecological diversity of these previously unknown organisms. The interior of the Lower Kane Cave microbial mats is devoid of oxygen and this provides habitat for anaerobic metabolic guilds, dominated by sulfate-reducing and fermenting bacteria. These anaerobic groups are responsible for autochthonous hydrogen sulfide and volatile organosulfur gas production. Cycling of carbon and sulfur compounds by the subaqueous microbial communities affects sulfuric acid speleogenesis. Compared to the total flux of sulfide into the cave, little hydrogen sulfide volatilizes into the cave atmosphere or oxidizes abiotically. Instead, the primary loss mechanism is from subaqueous microbial sulfur oxidation. Consequently, despite the cave waters being slightly supersaturated with respect to calcite, the "*Epsilonproteobacteria*" generate sulfuric acid as a byproduct of their metabolism, locally depress pH, and focus carbonate dissolution. The hydrogen sulfide that volatilizes into the cave air is oxidized at the cave walls where interactions between cave-wall biological and physicochemical factors influence subaerial speleogenesis and low temperature authigenic quartz precipitation. The recognition of the geomicrobiological contributions to subaqueous and subaerial carbonate dissolution fundamentally changes the model for sulfuric acid speleogenesis and the mechanisms for subsurface porosity development.

Table of Contents

List of Tables

List of Figures

Chapter 1: Introduction

Microbial processes occurring in the absence of light have generally been considered insufficient to support ecosystem-level processes. Until recently, the dogma has been that life in the subsurface, if present and metabolically active, is dominated by heterotrophic consumption of surface-derived carbon. But the absence of light energy does not preclude life, as chemosynthesis also provides sustainable energy. Reactive rock surfaces and mineral-rich groundwater provide an assortment of potential energy sources for specialized microorganisms, defined as chemolithoautotrophs (literally a 'self-feeding rock-eater'), that gain cellular energy from the chemical oxidation of inorganic compounds and fix inorganic carbon. Consequently, chemolithoautotrophs play important roles in global chemical and ecosystem processes, as they serve as catalysts for reactions that would not otherwise occur or would proceed slowly over geological time.

While soil and shallow bedrock (<200 m depth) are major habitats for subsurface organisms, viable microbial communities are now known to be ubiquitous in the deep subsurface, including sedimentary basins, basaltic and granitic aquifers, geothermal systems, and caves. For the most part, this is attributable to chemolithoautotrophy. These environments are often limiting in organic carbon and couple relatively constant physicochemical conditions with protection from surface hazards, such as solar radiation or cosmological events. Some researchers have suggested that modern subsurface habitats are analogous to environments where life may have originated and existed on primitive Earth, or

even possibly in extraterrestrial systems (e.g., Schopf, 1983; Stevens, 1997; Pedersen, 2001). Consequently, it has been hypothesized that total subsurface primary productivity may even surpass the activity of surface photosynthetic organisms (Stevens, 1997; Gold, 1999). With this, the functional role of active microorganisms in subsurface systems remains poorly understood, although the potential for their impact on the surrounding geologic framework has recently been suggested (e.g., Ehrlich, 1996; Bachofen et al., 1998; Ben-Ari, 2002; Newman and Banfield, 2002). Because most subsurface habitats are relatively difficult to access, little is known about the biodiversity, community structure, ecosystem functioning, or nutrient cycling of terrestrial chemolithoautotrophically-based microbial ecosystems, or how these specialized microbes have impacted geochemical and geological processes through time.

In this study I investigate the interrelationships between microbial ecosystems and the surrounding geologic and hydrologic framework in aphotic, sulfidic habitats in the shallow subsurface. Groundwater bearing dissolved hydrogen sulfide, but negligible allochthonous carbon, discharges as springs into cave passages of several known systems, including the Lower Kane Cave, Wyoming. Hydrogen sulfide is an energy-yielding substrate for microorganisms, and consequently sulfidic caves are frequently colonized by thick subaqueous microbial mats dominated by sulfur-oxidizing bacteria. Although these caves are <50 m below the Earth's surface, they offer a valuable opportunity to examine biologic-geologic interactions and microbial processes occurring in the absence of sunlight. The microbial ecology, geochemistry, and nutrient cycling investigated in

2

Lower Kane Cave can be used as proxies for similar processes occurring in deeper subsurface settings, such as carbonate aquifers, that can otherwise only be accessed though wells.

MICROORGANISMS IN SULFIDIC CAVES

Caves represent distinctive habitats with complete darkness, relatively constant air and water temperatures, and a limited supply of easily degradable organic matter. Since darkness precludes photosynthetic activity, the minimal organic matter found in caves is usually derived from dead photosynthetic material that has been carried into the subsurface system via air currents, speleothem drip-waters, stream drainage, or as guano from cave-dwelling organisms (Poulson and Lavoie, 2000). Early biospeleologists assumed that microorganisms in caves were secondary degraders and were food sources for higher organisms because chemosynthetic activity was not evident or was limited in most cave systems (Caumartin, 1963; Northup and Lavoie, 2001). However, more recent research in caves, including those with sulfidic water, demonstrate that bacteria generate energy as primary producers and sustain complex cave ecosystems (Sarbu et al., 1996; Porter, 1999; Sarbu et al., 2000; Vlasceanu et al., 2000; Engel et al., 2001). For instance, chemolithoautotrophy, at the base of the Movile Cave, Romania, ecosystem, supports the most diverse cave ecosystem known, with 33 new cave-adapted taxa identified from 30 terrestrial invertebrate species (24 are endemic) and 18 species of aquatic animals (9 endemic) (Culver and Sket, 2000). Essentially, the chemolithoautotrophs utilize chemical energy that would otherwise be lost to the system.

3

Since the 1986 discovery of the chemolithoautotrophically-based ecosystem in Movile Cave (Sarbu et al., 1996), studies of sulfur-based, subaqueous cave microbial communities (i.e., living in microbial mats) have included geochemical and microscopy surveys (Hubbard et al., 1986; Olson and Thompson, 1988; Hubbard et al., 1990; Stoessell et al., 1993; Brigmon et al., 1994; Mattison et al., 1998; Garman, 2002), phylogenetic investigations based on 16S ribosomal RNA gene (rDNA)sequence analyses (Angert et al., 1998; Engel et al., 2001; Brigmon et al., 2003), stable isotope ratio analyses (Sarbu et al., 1996; Vlasceanu et al., 1997; Sarbu et al., 2000), and cultivation studies (Brigmon et al., 1994; Vlasceanu et al., 1997; Engel et al., 2001; Brigmon et al., 2003). Moreover, chemolithoautotrophic communities from subaerial cave-wall surfaces, associated with a variety of mineral deposits, have also been described (Maltsev et al., 1997; Hose et al., 2000; Vlasceanu et al., 2000; Northup and Lavoie, 2001; Northup et al., 2003; Barton et al., 2004). Sulfidic caves often have cave-wall biofilms that develop on gypsum and elemental sulfur surfaces, with exceedingly acidic condensation droplets, ranging from pH 0 to 4.

SULFURIC ACID SPELEOGENESIS

Karst landscapes form where soluble rocks dissolve, resulting in numerous geomorphic features including caves and conduit drainage systems (e.g., White, 1988; Ford and Williams, 1989; Palmer, 1991). The classic model for karst development (speleogenesis) involves carbonic acid dissolution, usually at shallow depths rarely far below the water table. More recently, sulfuric acid speleogenesis was proposed by S.J. Egemeier from work in Lower Kane Cave (Egemeier, 1981;

4

Hill, 1990; Jagnow et al., 2000). Based on observations of H_2S-bearing thermal springs, extensive gypsum deposits, and gypsum-replaced limestone cave walls, Egemeier (1981) proposed the original sulfuric acid speleogenesis model to include the volatilization of H_2S from the groundwater to the cave atmosphere and H_2S oxidation to sulfuric acid on moist subaerial surfaces, where the acid reacts with and replaces carbonate with gypsum:

$$H_2SO_4 + CaCO_3 + H_2O \rightarrow CaSO_4 \cdot 2H_2O + CO_2 \qquad (1\text{-}1).$$

Gypsum, which spalls from the cave walls, easily dissolves into groundwater, and the net result is mass removal and an increase in void volume. Cave formation due to sulfuric acid is now recognized in several active sulfidic caves in the United States, Romania, Italy, and Mexico (van Everdingen et al., 1985; Hubbard et al., 1990; Galdenzi and Menichetti, 1995; Sarbu et al., 1996; Hose et al., 2000; Sarbu et al., 2000), as well as in ancient hypogene caves, e.g. Carlsbad Cavern, New Mexico (Hill, 1990; Polyak et al., 1998). In addition to the subaerial processes, cave formation due to sulfuric acid in the Guadalupe Mountains has also been attributed to sulfuric acid dissolution at or just below the water table (Hill, 1990; Palmer, 1991; Jagnow et al., 2000).

Nearly all of the studies regarding sulfuric acid speleogenesis assumed that H_2S was oxidized, and consequently sulfuric acid produced, by abiotic processes (e.g., Egemeier, 1981). The role of sulfuric acid-generating bacteria in cave formation, while previously alluded to, has never been substantiated (Symk and Drzal, 1964; Hubbard et al., 1990; Palmer, 1991; Brigmon et al., 1994; Hill, 1995; Lowe and Gunn, 1995; Sarbu et al., 1996; Vlasceanu et al., 1997; Angert et al.,

1998; Hill, 2000; Hose et al., 2000; Palmer and Palmer, 2000; Sarbu et al., 2000; Vlasceanu et al., 2000; Engel et al., 2001). This study reexamines Lower Kane Cave, focusing not only on the microbial diversity of the cave, but also on the role microorganisms play in cave formation.

PRIMARY FIELD SITE: LOWER KANE CAVE, WYOMING

The Bighorn Basin

The Kane Caves are located in the Bighorn Basin near Lovell, Wyoming, on the western margin of the Bighorn and Pryor Mountain Belts (Figure 1-1). The mountains are Precambrian-cored anticlinal structures of Laramide age (late Cretaceous to Eocene). The Bighorn Basin is a large asymmetric structural basin that contains Cambrian to Quaternary sedimentary rocks. Along the flanks of the basin, near the cities of Thermopolis, Lovell, and Cody, there are structural anticlines associated with deep thrust faults and mountain uplift. The basin is well known for its extensive Paleozoic oil fields, including the Spence Dome field (Madison Limestone, Mississippian) south of the Kane Caves on the western side of the Bighorn River, the Crystal Creek field (Madison Limestone) to the east of the Bighorn River, and the Byron, Garland, Frannie, Alkali Flats, and Goose Egg fields (Pennsylvanian through Cretaceous strata) west and northwest of the Kane Caves (Stone, 1967). Many of the Tensleep (Pennsylvanian) and Phosphoria (Permian) fields contain high hydrogen sulfide gas (Biggs and Espach, 1960).

Thermal and non-thermal springs discharge along the flanks of the basin, commonly where faults are exposed at the surface (e.g., Five Springs at the Five Spring Fault) or where a river dissects an anticline (e.g., Spence Spring at the

Bighorn River level in the Sheep Mountain anticline) (Figure 1-1) (Egemeier, 1973, 1981; Heasler and Hinckley, 1985). Anomalous thermal gradients and groundwater temperatures have been recorded from sulfidic waters in the following areas: 1) southeast of the Little Sheep Mountain anticline south of Lovell, 2) within the Sheep Mountain anticline north of Greybull, 3) the region surrounding Thermopolis and the Thermopolis anticline, and 4) near Cody in the vicinity of the Shoshone River (Heasler and Hinckley, 1985). Groundwater circulation within the Paleozoic aquifers of the basin is controlled by flow along extensional fractures in fault-cored anticlinal or monoclinal folds (Jarvis, 1986; Spencer, 1986).

Karst topography is rarely exposed within the Bighorn Basin, or in the Bighorn or Pryor Mountains. The main cave-forming unit in the region is the Madison Limestone, although small caves and pits also form within the Bighorn Dolomite (Ordovician) at higher elevations within the Bighorn Mountains (Hill et al., 1976). There are numerous pits and small caves in the Bighorn Mountains where these units are exposed, and where Mississippian-Triassic strata are exposed in Little Sheep and Sheep Mountains due to dissection of the anticlines by the Bighorn River (Figure 1-1). Most caves north of these anticlines and within the Bighorn Mountains are epigenic systems (Hill et al., 1976), while several cave systems, especially larger ones, formed or were modified by hypogenic processes involving sulfuric acid (Hill et al., 1976; Egemeier, 1981). Lower Kane Cave and Upper Kane Cave both formed from sulfuric acid speleogenesis in the upper member of the Madison Limestone at the apex of the Little Sheep Mountain anticline along the Bighorn River (Figure 1-1). Lower Kane Cave has 325 m of

mapped horizontal length, of which 180 m is stream passage (Figure 1-2). There is only one known entrance into Lower Kane Cave. Upper Kane Cave is a dry cave 30 m above Lower Kane Cave, with 290 m of total horizontal length. Upper Kane Cave has extensive gypsum deposits.

Several other caves and springs are located along the Bighorn River in the vicinity of the Kane Caves (Figures 1-1 and 1-3). PBS spring, which is slightly thermal and sulfidic, discharges from the upper member limestone/dolostone of the Phosphoria Formation at the edge of Little Sheep Mountain along the Little Sheep Mountain fault (Figure 1-3). Hellspont Cave (Egemeier, 1981), or Coon Smell Cave (Hill et al., 1976), is 20 m long and has a thermal, sulfidic spring that discharges at the back of the cave. Salamander Cave is < 3 m long and has a large non-thermal, non-sulfidic spring (Figure 1-3). Spence Cave, in the Sheep Mountain anticline, also formed from sulfuric acid speleogenesis within the Madison Limestone along the Bighorn River (Figure 1-1) (Egemeier, 1973; 1981). Spence Cave is large, has several passage levels, and is similar to Upper Kane Cave in that it has dry passages and gypsum throughout (for a cave map and a complete description, refer to Egemeier, 1973 and 1981). Thermal, sulfidic springs discharge at river level within the Sheep Mountain anticline. The Bighorn-Horsethief Cave system is located 30 km north of the Kane Caves on the Wyoming-Montana border in the Bighorn Canyon (Hill et al., 1976) (Figure 1-1). This system is similar to Spence and Upper Kane Caves. Across the Bighorn Basin near Cody are the Spirit Mountain Caverns, with gypsum mineralization throughout the cave and reportedly high concentrations of H_2S at lower elevation passage levels (Hill et al., 1976).

Although not in the Bighorn Basin, Stinkpot Cave, near Jackson Hole along the Hoback River, also has sulfidic water and microbial mats (Hill et al., 1976).

Lower Kane Cave

General Cave Description

During this study (1999-2003) there were four springs discharging into the Lower Kane Cave passage (Figure 1-2). The Fissure, Upper, and Lower Springs issue from a fissure in the cave floor and Hidden Spring emerges from a hole in mud. The fissure in the cave floor, which corresponds to a fracture in the cave ceiling, is continuous throughout the entire length of the cave. There appears to be minimal offset of this fracture (<10 cm). The fissure is disrupted in places by secondary calcite that has precipitated over the open fracture; ~10 to 30 cm-wide holes through the calcite reveal the water-filled fissure underneath. In some places in the back of the cave the fracture is filled with sediment and/or gypsum. Faults with measurable offset are perpendicular to this continuous fracture (Figure 1-2), and these faults correspond to the springs outlets. Additionally, a resistant breccia composed of chert and limestone clasts with dolomitized cement protrudes into the passage at these fault zones.

Hydrology of the cave springs has a complex history, evident from recent exploration of the cave. During the study there were two open water-filled fissures near the back of the cave (Figure 1-4); no flow was observed, although Egemeier reports that the Terminal Spring flowed in 1969 (Egemeier, 1973). In 1999, the back of the cave near the Fissure Spring and Iron Pool was dry, and only the Iron Pool (Figure 1-4B) had water and red-pigmented biological material and

9

mineralization in the orifice. In 2000, sulfidic water discharged from the Fissure Spring (Figure 1-5A) and the back of the cave had 1-5 cm of water in the passage and thick orange- to red-colored microbial mats. As a consequence, a stream flowed from the Fissure Spring, along the north side of the cave wall and under gypsum mounds, into the Lower Spring orifice where it mixed with sulfidic water. During the late spring 2003 sampling trip, there was no discharge from the Fissure Spring, but flow reinitiated several days later. White microbial filament bundles are found below the Fissure Spring orifice (Figure 1-5B and 1-5C).

The Upper Spring discharges ~6 $L \cdot s^{-1}$ from a sediment-filled hole in a large pool, as estimated from salt-dilution traces (Figure 1-6A, 1-6B). The Upper Spring pool is ~2.5 m wide and up to 0.5 m deep, with white filament bundles on the pool edge and sediment bottom (Figure 1-6C). A stream channel, ranging from 5 to 10 cm in depth, flows from the orifice pool toward the cave entrance, and white filamentous mats fill the channel (Figures 1-7A, 1-7B). Because of underflow from the Fissure Spring, oxygenated water seeps into the Upper Spring pool and mixes with the incoming sulfidic water, allowing for the oxidation of iron sulfides. An area halfway between the Upper and Lower Spring orifices has a seep in which water emerges from under a gypsum pile (Figure 1-8A). A thick (~15 cm) red mat forms 5 cm from the gypsum pile (Figure 1-8B).

The Lower Spring has the deepest measurable orifice opening (2 m), and the orifice walls are coated with gray sediment/biological material and long white microbial filament bundles (Figure 1-9A). The water spills over the limestone lip, and a thick white mat develops downstream (Figure 1-9B). In early May 1999 the

Lower Spring microbial mat extended for > 2 m from the orifice, but following back-flooding of the Bighorn River June 1999, the mats were destroyed and consequently a mat <1 m length was present until 2003 when the mat again reached ~2 m. In 2001 through 2003, a slight trickle of sulfidic water issued from a small (~20 cm) hole in river mud at Hidden Spring (Figure 1-2), and sparse white filaments have been observed.

The Bighorn River infrequently floods Lower Kane Cave (Figure 1-10). The cave was flooded in May 1999, corresponding to a peak stage of 7.57 ft above the gaging station, approximately 1 km downstream from the cave (United States Geological Station (USGS) station #06279500 at Kane, Wyoming; 3660 ft above msl). The river stage and discharge records are maintained by the USGS (http://waterdata.usgs.gov/nwis/sw). Based on the available data, the minimum river stage required to flood the cave entrance is at least 7.57 ft. Consequently, there have been at least seven times since 1956 when the cave may have flooded (Figure 1-10). The consequences of flooding are believed to be moderately significant to the Lower Spring microbial mats. Because of a slight floor gradient, a river stage of 7.57 ft would backflood river water to approximately the end of the Upper Spring microbial mats, but the back of the cave and the Fissure Spring area would not be impacted.

There have not been any direct measurements to determine the age of Lower Kane Cave, but the timing of cave formation is loosely constrained by Bighorn River terraces. There is a small remnant terrace 24-m above the present river level near the entrance of Upper Kane Cave and a small terrace at the Lower Kane Cave

entrance (approximately 6 m above present river level). The 24-m terrace corresponds to a larger erosional terrace across the river, referred to as the Powell-Emblem or Sanatarium bench (Reheis, 1984). Egemeier (1981) suggests that this terrace may correspond to the Bull Lake glaciation, from 40 to 130 ka, but Reheis (1984) postulates that the 24-m terrace is much older, from 92 to 161 ka. Depending on the timing of emplacement of the upper terrace, the river level terrace may correlate to 38 ka, but also to the Pinedale glaciation at 10 ka. Additional research is needed to resolve this issue and to help constrain the age of the caves along the Bighorn River.

A Note Regarding Safety in Lower Kane Cave

Hydrogen sulfide (CAS:7783-06-4) is a colorless flammable gas (STEL = 15 ppm, IDLH = 100 ppm) that can cause headaches and nausea with prolonged low-level exposure (Beauchamp et al., 1984). Above 20 ppm, H_2S causes eye and mucous membrane irritation, and prolonged exposure can result in pulmonary edema. At all times while researchers were present, Lower Kane Cave air was monitored for H_2S, CO, and P_{O2} using an MSHA approved multigas monitor (PhD Ultra Atmospheric Monitor, Biosystems, Middleton, CT). While the concentration was typically less than STEL, all researchers worked under Level-C respiratory protection using a half-face air-purifying gas mask with organic/acid vapor cartridges (H_2S escape). These masks are effective for SO_2, organosulfur gases, and radon, but have only short term protection against high H_2S.

What initially attracted Egemeier (1973) to the Kane Caves was the prospect of economic deposits of ore minerals, and in particular uranium and

vanadium in the region (Wilson, 1960); Egemeier found the cave sediments were highly radioactive. Radioactivity (as total counts of combined $\alpha-$, $\beta-$, and $\gamma-$radiation) was measured using a Geiger counter in December 2001 (Figure 1-11). The highest concentrations were near the springs and along the anaerobic stream channels, as well as at the cave floor. The area around 215 m, associated with red microbial mats (Figure 1-8B), also had high radioactivity. Radioactivity on gypsum piles was low and considered to be at background levels.

A Note Regarding Sample Collection

Caves are valuable resources, both scientifically and recreationally, and karst regions are sensitive environments. Guidelines established by the National Speleological Society and the Conservation and Cave Management Organization were followed during the research; these guidelines suggest that researchers be 'professional, selective, and minimalistic'. During field work, all researchers attempted to alter the pre-existing features, water, and biota as little as possible. At all times, conservative sample quantities were collected and removal of material from the caves was limited in order to preserve the integrity of the mineralogic, hydrologic, and ecological systems. Permission to conduct research and to sample in Lower Kane Cave, Upper Kane Cave, and Hellspont Cave was granted by the Bureau of Land Management, Cody Office.

RESEARCH QUESTIONS

The primary research questions for this work are in five areas:

1. ***Relationships between microbial diversity and habitat geochemistry:*** **What** are the geochemical differences between the subaqueous (cave springs and stream) and subaerial (cave-wall) habitats? Is microbial community structure controlled by habitat geochemistry and geologic framework?

2. ***Microbial diversity and endemism:*** Are the microbes found in Lower Kane Cave unique to the cave, or are they widespread in other sulfidic systems, photic or aphotic? Can the presence of these microorganisms define any of the biogeochemical processes occurring in other systems?

3. ***Nutrient acquisition and cycling:*** What are the sources and availability of nutrients to the microbial cave ecosystem? What role do allochthonous and autochthonous substrates play in the ecosystem? Do microorganisms benefit or are they adversely affected by colonization of certain geologic materials?

4. ***Microbial role in speleogenesis:*** Can abiotic H_2S autoxidation be distinguished from biotic (microbial) oxidation? What are the consequences of microbial metabolism on the geologic/hydrologic surroundings? Is carbonate dissolution and speleogenesis affected depending on how or where sulfide is oxidized?

5. ***Process biosignatures:*** Are there diagnostic geologic, chemical, or isotopic characteristics of the habitats that can be used to fingerprint microbial activity in ancient systems?

HYPOTHESES AND RESEARCH APPROACH

I used an interdisciplinary approach to examine the cave microbial communities, nutrient sources and transfers, and the potential impact of the microorganisms to cave formation and modification during sulfuric acid speleogenesis.

Chapter 2: I hypothesized that the structure of microbial communities in the subaqueous microbial mats would reflect habitat geochemistry and substrate availability, and that shifts in community composition were controlled by dissolved oxygen and hydrogen sulfide. Additionally, I postulated that chemolithoautotrophy serves as the basis of energy production in the Lower Kane Cave ecosystem. As it is often difficult to ascertain the metabolism of certain organisms based only on 16S rDNA gene sequence phylogenies (e.g., Gray and Head, 2001), elemental composition (carbon to nitrogen ratios and sulfur content) and stable carbon and sulfur isotope ratio analyses of microbial mat morphotypes were combined with the 16S rDNA phylogenies to link hypotheses of ecosystem functionality with genetic identity (e.g., Boschker and Middelburg, 2002; Chesson et al., 2002).

Chapter 3: While many different types of sulfur-oxidizing bacteria have been found in sulfidic cave microbial mats, members of the "*Epsilonproteobacteria*" dominate the subaqueous mats from Lower Kane Cave. I hypothesized that these bacteria, which are successful colonizers of marine habitats (e.g., Alain et al., 2004), were also prevalent in terrestrial sulfidic caves and springs. I employed the full-cycle rRNA approach, including the construction of 16S rDNA clone libraries and application of 16S rRNA-targeted oligonucleotide

probes for fluorescence in situ hybridization (FISH), to characterize the microbial mats from Lower Kane Cave. I also applied the newly designed probes and polymerase chain reaction (PCR) primers to identify novel epsilonproteobacterial groups in microbial mats collected from other field locations.

Chapter 4: Molecular evidence indicated that the subaqueous microbial mats in Lower Kane Cave were much more complex than previously thought, and geochemical evidence revealed that the microbial mats were physically and chemically stratified. I hypothesized that molecular methods overlooked anaerobic microbial community diversity because populations were less abundant than the aerobes (i.e., "*Epsilonproteobacteria*"). I employed culture-based approaches, including the most probable number method and enrichment cultures using specific media, to characterize the diversity of anaerobic microbial communities.

Chapter 5: Inorganic and organic sulfur-containing compounds pass through multiple components of a microbial ecosystem and volatile components are released into the atmosphere. Although production and consumption of volatile sulfur gases (including hydrogen sulfide, methanethiol, dimethyl sulfide, and carbonyl sulfide) have been studied from photic marine and freshwater environments, virtually nothing is known about the flux of these gases from subsurface settings. I hypothesized that sulfur gases were produced and consumed by various metabolic guilds within the Lower Kane Cave microbial ecosystem, and potentially impact the local or global sulfur budgets. I employed culture-based approaches with time-series incubation experiments and gas chromatography (GC) to examine abiotic and biotic sulfur gas production and consumption. Hydrogen

sulfide flux and gas dynamics were characterized by direct-inject field GC inside Lower Kane Cave.

Chapter 6: The basic mechanism for sulfuric acid speleogenesis has been debated (Jagnow et al., 2000). While it was clear that specialized microbial communities take advantage of reduced sulfur compounds as energy sources, it was not clear that biotic pathways influence karstification. I hypothesized that microbial sulfur oxidation dominated over abiotic autoxidation, and microbially-derived sulfuric acid controlled speleogenesis. I combined the interdisciplinary results from 1) H_2S gas flux data (described in Chapter 5), 2) aqueous geochemistry and mineralogy, 3) the deployment of field microcosms, and 4) fluorescence in situ hybridization of colonized carbonate surfaces to examine the subaqueous sulfide loss mechanisms and the roles of sulfur-oxidizing bacteria on carbonate dissolution.

Chapter 7: The sulfuric acid speleogenesis model of Egemeier (1981) requires volatilization and oxidation of H_2S to sulfuric acid on cave-wall surfaces, which causes aggressive carbonate rock dissolution and replacement of limestone by gypsum. I hypothesized that the chemistry of condensation on subaerial cave-wall surfaces influenced dissolution and precipitation reactions occurring on the walls, and that gypsum replacement of the walls was an episodic process. I characterized the mineralogy of the cave walls, the microbiology of cave-wall biofilms, and the chemical and physical nature of condensation droplets in Lower Kane Cave. Moreover, microcrystals of authigenic quartz that form in the cave-walls biofilms and gypsum potentially represent a biogeochemical marker of cave-wall processes.

17
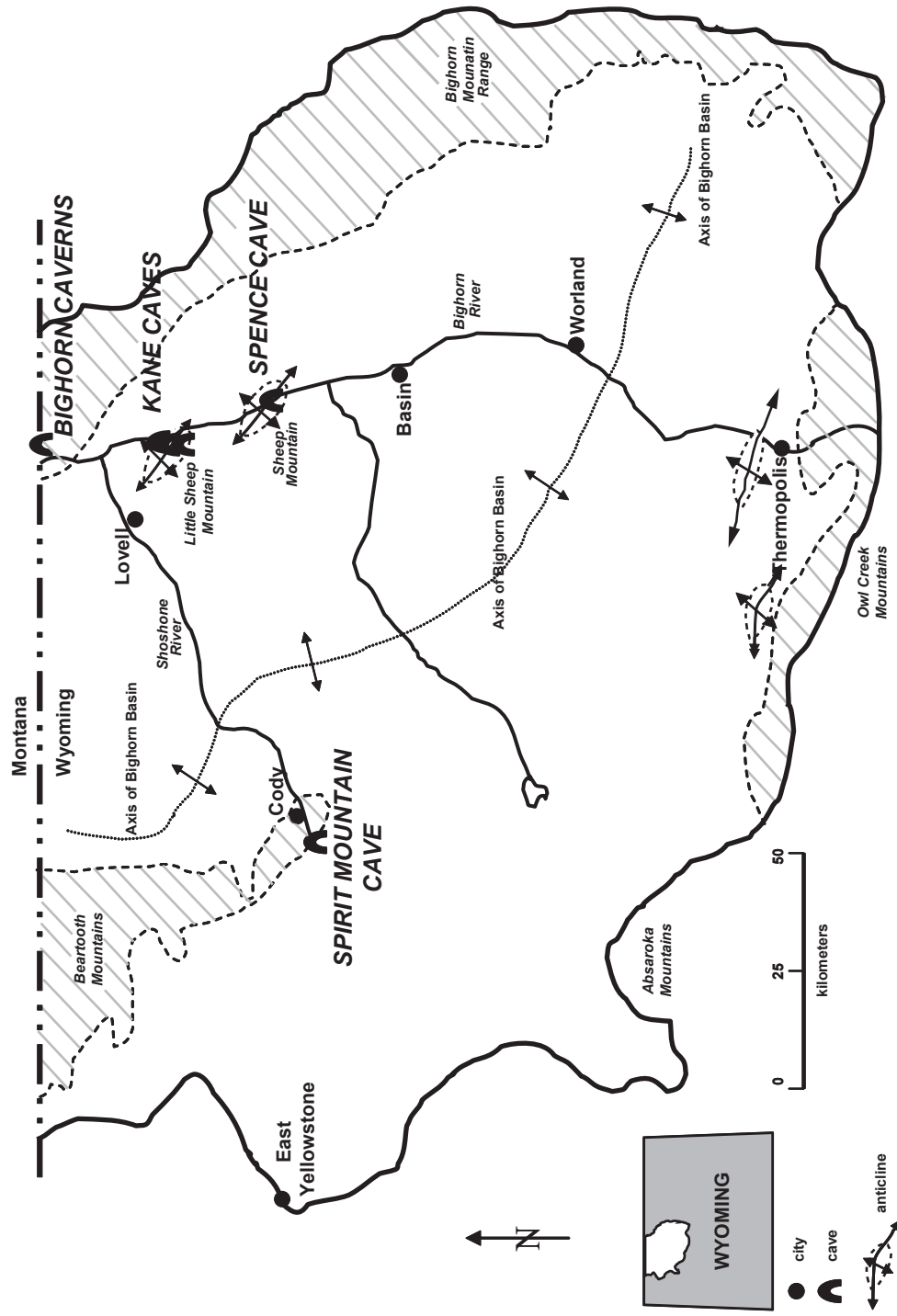
Figure 1-1: Bighorn Basin, Wyoming, showing major cities and physiographic features. Map modified from Egemeier (1981).
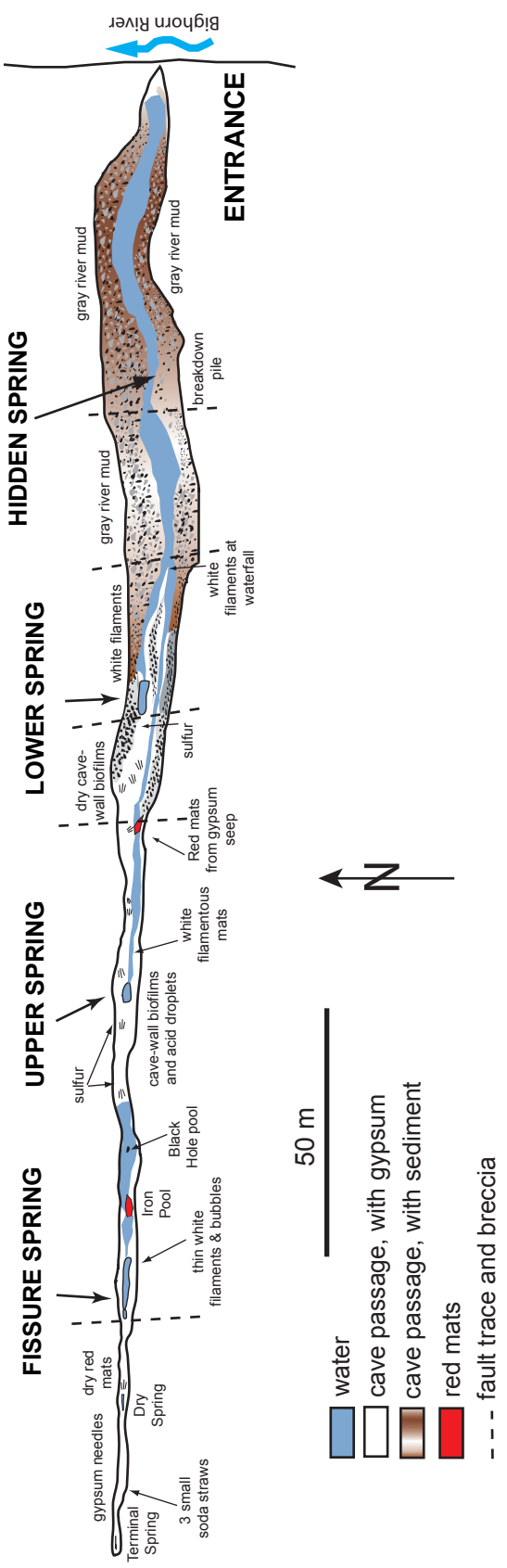
Figure 1-2: Plan-view map of Lower Kane Cave, Wyoming, showing major spring features. Map modified from Egemeier (1981) and annotated based on this current work.

19
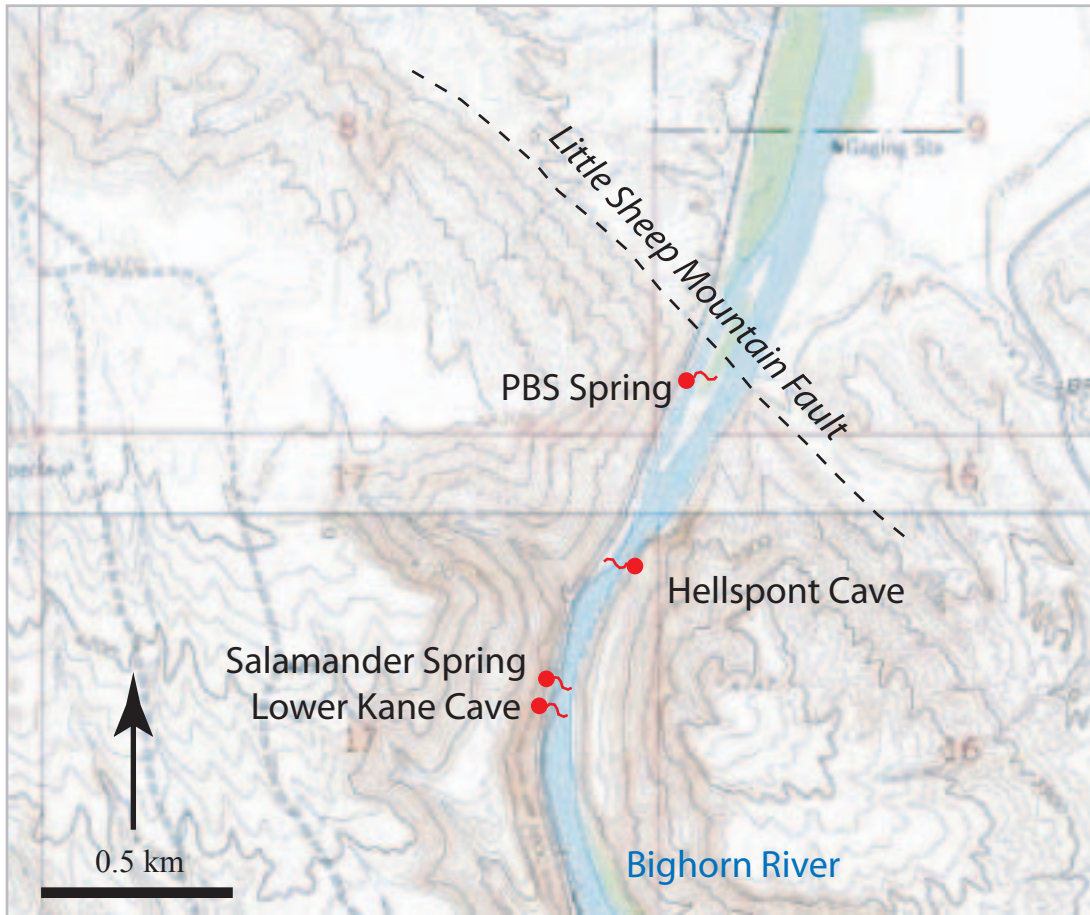
Figure 1-3: Topography associated with Little Sheep Mountain anticline and Bighorn River in the vicinity of the Kane Caves, Wyoming. Three springs discharge into the Bighorn River. The Upper Kane Cave passage (not shown) is 30 m directly above Lower Kane Cave.

Figure 1-4: (A) Looking toward the back of the cave, and into a small fissure in the floor filled with water. The cave walls are covered with gypsum and a brown crust. (B) Looking into the Iron Pool.

Figure 1-5: (A) Fissure Spring area, looking to the back of the cave. (B) Fissure Spring orifice. (C) White filaments and webs approximately 3 m from orifice.
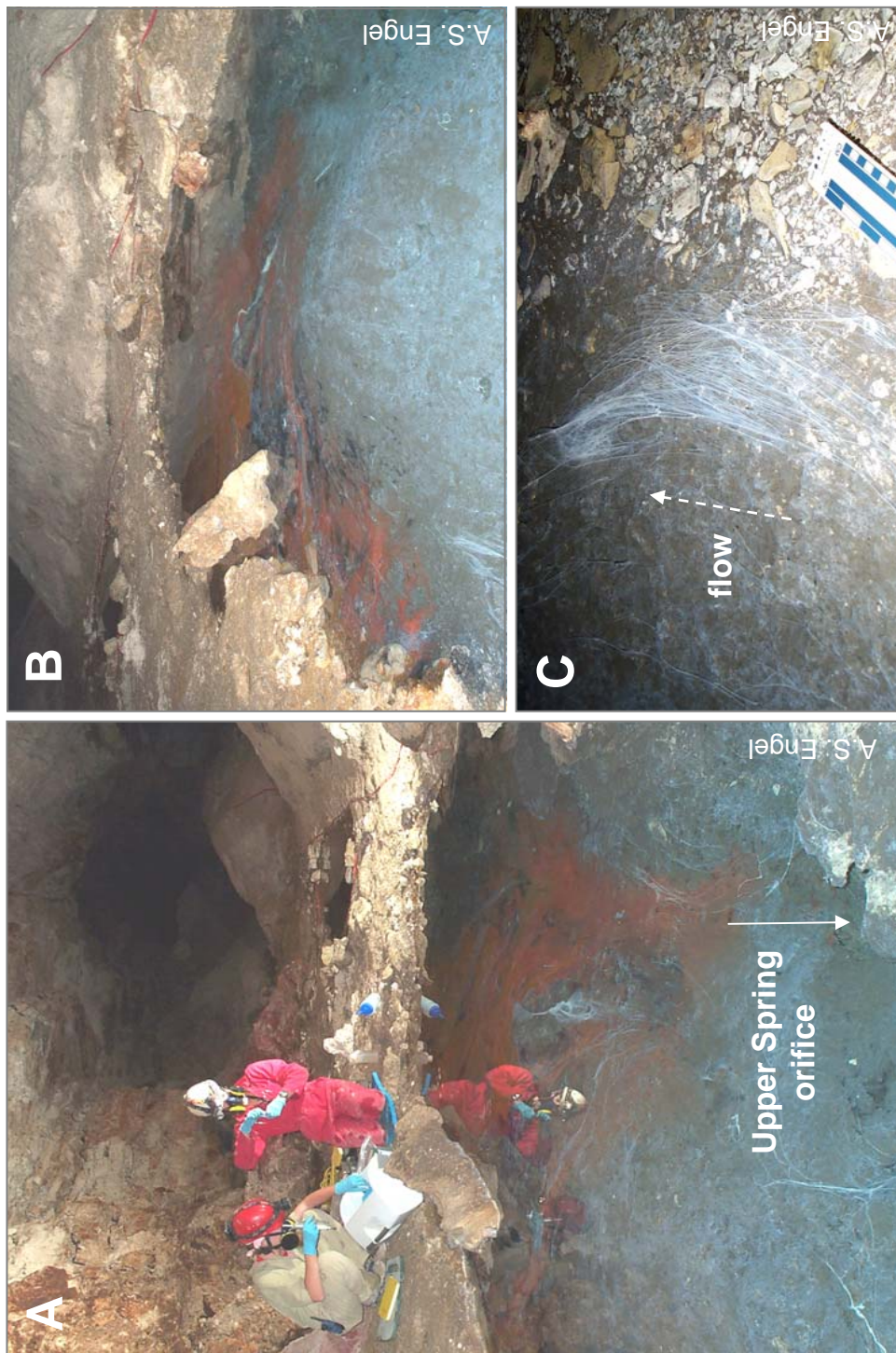
Figure 1-6: (A) Upper Spring area, looking to the back of the cave. (B) Upper Spring orifice pool. (C) White filaments on side of the orifice pool in ~5 cm deep water.

Figure 1-7: (A) Out-flow stream channel from Upper Spring orifice pool. (B) White filamentous microbial mats filling 0.5 to 1 m wide out-flow channel, looking downstream.
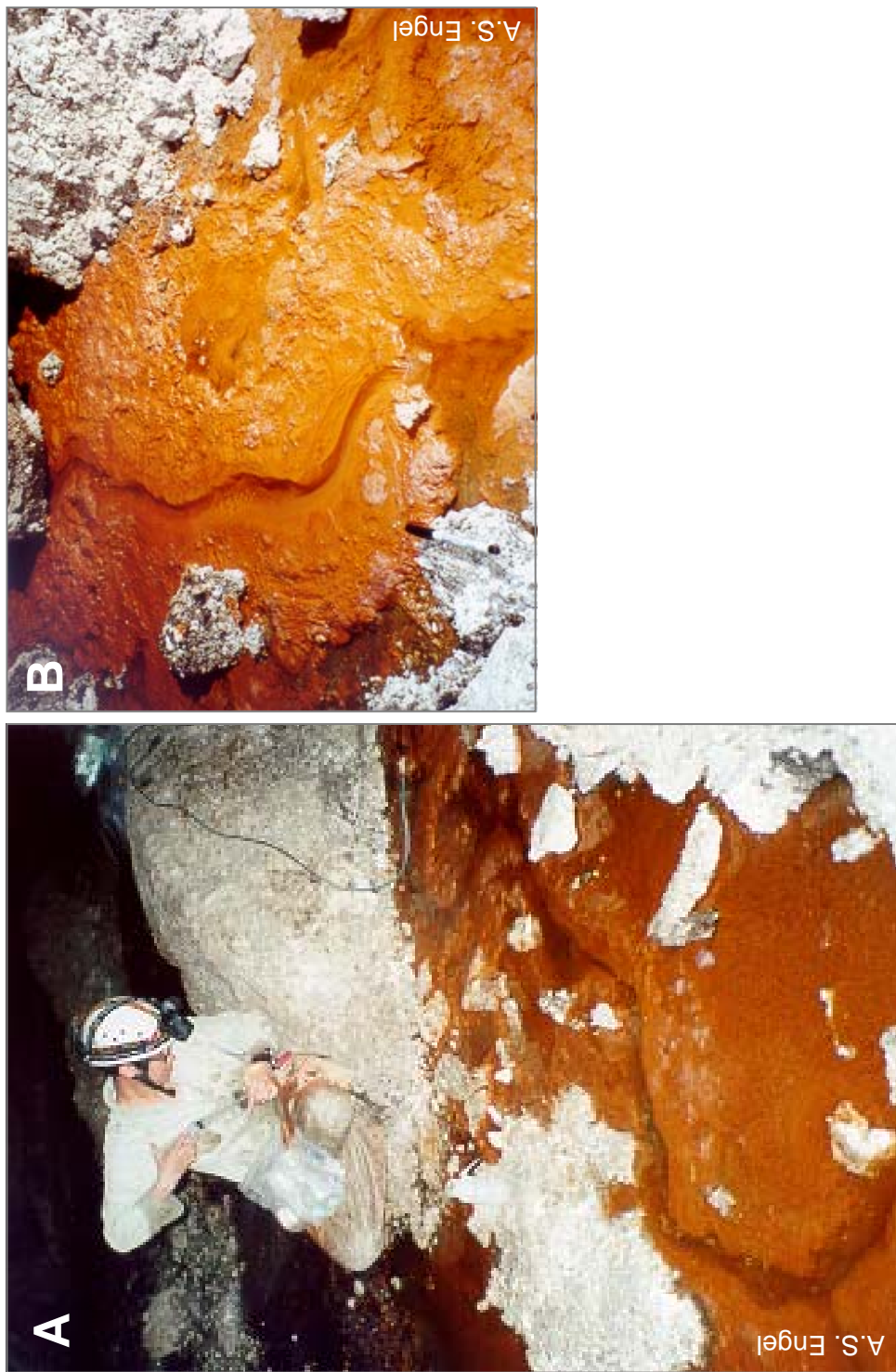
Figure 1-8: (A) Non-sulfidic water seep and downstream red mats under gypsum pile between Upper and Lower Spring. (B) Thick red mats; pen for scale in lower left corner.
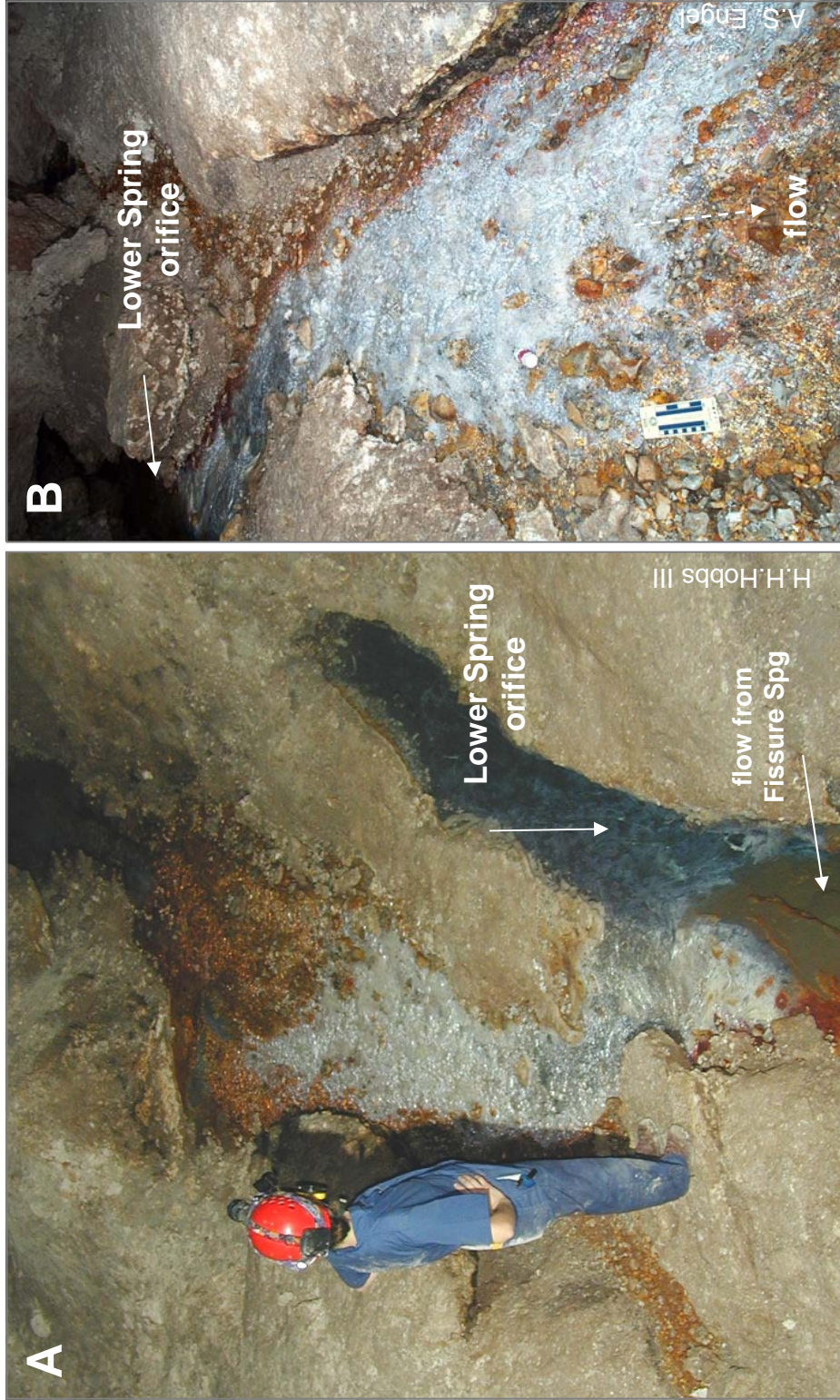
Figure 1-9: (A) Lower Spring orifice, with anaerobic water discharging from gray side and non-sulfidic water from upstream coming into the orifice in the foreground. (B) White filamentous microbial mats, ~1.5 m long, below spring orifice.
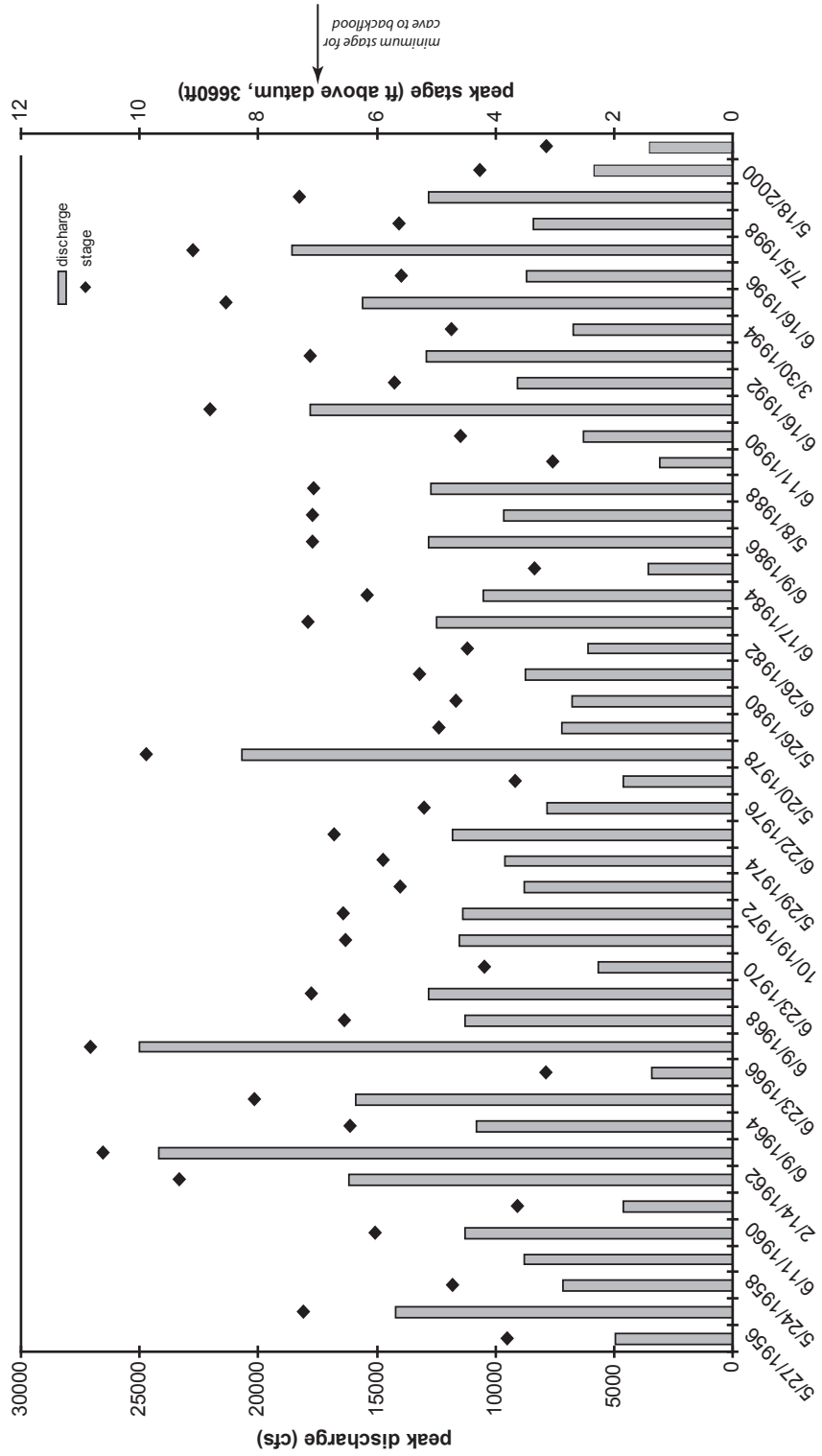
Figure 1-10: Peak discharge and peak stage data for the Bighorn River (USGS station # 06279500, Kane, Wyoming). Data from 1956 can be accessed at http://www.water.usgs.gov/nwis/.
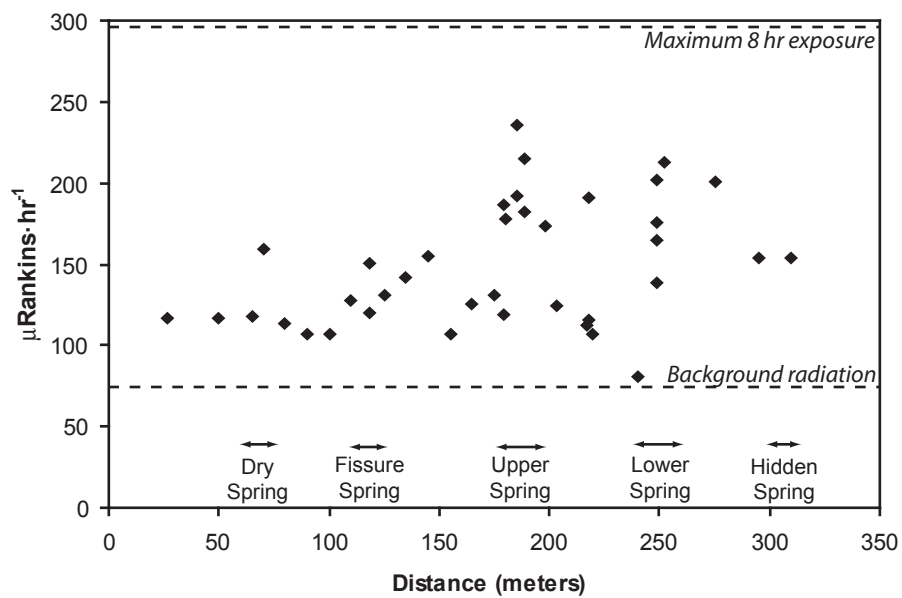
Figure 1-11: α-, β-, and γ-radiation measured as total counts in Lower Kane Cave, Wymoing, July 2002.

Chapter 2: Bacterial Diversity and Ecosystem Function of Filamentous Microbial Mats from Aphotic (cave) Sulfidic Springs Dominated by Chemolithoautotrophic "*Epsilonproteobacteria*"

ABSTRACT[1]

Filamentous microbial mats from three aphotic sulfidic springs in Lower Kane Cave, Wyoming, were assessed with regard to bacterial diversity, community structure influenced by geochemical changes, and ecosystem function using a 16S rDNA-based phylogenetic approach combined with elemental content and carbon and sulfur stable isotope ratio analyses. The bulk of the microbial mats had carbon isotope values (mean $\delta^{13}C$ = -34.7‰, 1σ = 3.6) consistent with chemolithoautotrophic carbon fixation from a dissolved inorganic carbon reservoir (cave water, mean $\delta^{13}C$ = -7.4‰; n = 8). The most widespread mat morphotype consisted of white filament bundles, with low C:N ratios (3.5–5.4) and high sulfur content (16.1-51.2%). Bacterial diversity was low overall, and the most prevalent taxonomic group was affiliated with the "*Epsilonproteobacteria*" (68%); six genetically distinct epsilonproteobacterial groups were identified. Other bacterial sequences were affiliated with *Gammaproteobacteria* (12.2%), *Betaproteobacteria* (11.7%), *Deltaproteobacteria* (0.8%), and the Acidobacterium (5.6%) and Bacteriodetes/Chlorobi (1.7%) divisions. Epsilonproteobacterial and bacterial group abundances and overall community structure within the microbial mats

---

[1] A portion of this chapter was used for the publication A.S. Engel, M.L. Porter, L.A. Stern, S. Quinlan, and P.C. Bennett, 2004, Bacterial diversity and ecosystem function of filamentous microbial mats from aphotic (cave) springs dominated by chemolithoautotrophic "*Epsilonproteobacteria*", <u>FEMS Microbiology Ecology</u>, accepted.

shifted from the spring orifices downstream, corresponding to changes in habitat dissolved sulfide and oxygen concentrations and metabolic requirements of certain bacterial groups. Most of the epsilonproteobacterial groups were identified from high sulfide and low oxygen concentrations were measured, whereas *Thiothrix* spp. and *Thiobacillus* spp. had higher abundances where conditions of low sulfide and high oxygen concentrations were observed. Genetic and metabolic diversity among the "*Epsilonproteobacteria*" maximizes overall cave ecosystem function, and these organisms play a significant role in providing chemolithoautotrophic energy to the otherwise nutrient-poor cave habitat. These results expand the evolutionary and ecological views of "*Epsilonproteobacteria*" in terrestrial habitats and demonstrate that sulfur cycling supports this subsurface ecosystem through chemolithoautotrophy.

INTRODUCTION

Microbial processes occurring in the absence of light have generally been considered insufficient to support ecosystem-level processes, and until recently, the dogma has been that life in the subsurface, if present and metabolically active, is dominated by heterotrophic consumption of surface-derived carbon (Caumartin, 1963; Pedersen, 2001; Naeem, 2002; Alfreider et al., 2003). But the absence of light does not preclude life, as reactive mineral surfaces and solute-rich groundwater provide energy sources sufficient for chemolithoautotrophic growth in the subsurface (e.g., Stevens, 1997; Kinkle and Kane, 2000). Chemolithoautotrophy is now recognized as an important ecosystem-level process in aphotic

environments, including deep terrestrial aquifers (Stevens and McKinley, 1995; Pedersen, 2001) and caves (Sarbu et al., 1996; Vlasceanu et al., 2000; Schabereiter-Gurtner et al., 2002). Because subsurface habitats are relatively difficult to access, however, little is known about the biodiversity, community structure, ecosystem functioning, or carbon cycling of terrestrial chemolithoautotrophically-based microbial ecosystems.

Caves represent distinctive habitats with complete darkness, relatively constant air and water temperatures, and a poor supply of easily degradable organic matter. Consequently, most cave ecosystems depend on allochthonous organic material for energy (Poulson and Lavoie, 2000; Simon et al., 2003). Previous investigations describing microorganisms in caves (e.g., Caumartin, 1963; Dickson and Kirk, 1976; Mikell et al., 1996), including from sediments and aquatic habitats, suggest that the microbes are similar to those found in surface environments and are only active under optimal growth conditions (Northup and Lavoie, 2001). However, groundwater bearing dissolved hydrogen sulfide and negligible allochthonous carbon discharges as springs into the passages of several caves (e.g., Egemeier, 1981; Sarbu et al., 1996; Angert et al., 1998; Hose et al., 2000); hydrogen sulfide is an energy-yielding substrate for some microorganisms, and areas of these sulfidic caves are colonized by thick subaqueous microbial mats (Brigmon et al., 1994; Angert et al., 1998), as well as extensive cave-wall biofilms (Hose et al., 2000).

Molecular phylogenetic studies based on 16S rRNA gene sequences (rDNA) have expanded our understanding of the microbial diversity in caves (e.g.,

Northup and Lavoie, 2001), including those with hydrogen sulfide-rich groundwater (Angert et al., 1998; Vlasceanu et al., 2000; Engel et al., 2001) and those without (Holmes et al., 2001; Schabereiter-Gurtner et al., 2002; Northup et al., 2003; Schabereiter-Gurtner et al., 2003; Barton et al., 2004). In sulfidic caves, the dominant bacterial groups from some subaqueous microbial mat communities belong to the *"Epsilonproteobacteria"* (Angert et al., 1998; Engel et al., 2001; Barton et al., 2002). Stable carbon isotope measurements and ^{14}C-radiolabeled substrate experiments suggest that chemolithoautotrophy is the base of these ecosystems (Sarbu et al., 1996; Porter, 1999; Sarbu et al., 2000). There has been relatively little study, however, of the biogeochemistry and ecological roles of the dominant groups involved with energy and nutrient transfers within these ecosystems, or on the physical or chemical controls that govern community structure and dynamics.

This purpose of this chapter was to characterize microbial ecosystems and nutrient cycling in sulfidic cave habitats, using Lower Kane Cave as a proxy for deeper subsurface environments. The objectives were to describe genetic and functional diversity, and to define how habitat geochemistry controls community structure. I hypothesized that community composition and structure reflect substrate availability, and specifically that community composition shifts with changes in the concentrations of dissolved oxygen and hydrogen sulfide. As it is often difficult to ascertain the metabolism of many organisms based on 16S rDNA-based phylogenies (e.g., Gray and Head, 2001), elemental composition and stable carbon and sulfur isotope ratio analyses were combined with 16S rDNA

phylogenies to link hypotheses of ecosystem functionality with genetic identity for the as yet uncultured microorganisms (Boschker and Middelburg, 2002; Chesson et al., 2002; Naeem, 2002). The results of the isotopic and phylogenetic characterization of the Lower Kane Cave ecosystem expand the evolutionary and ecological views of "*Epsilonproteobacteria*" in terrestrial habitats and demonstrate that sulfur cycling supports this subsurface cave ecosystem through chemolithoautotrophy.

MATERIALS AND METHODS

Sample Acquisitions

Samples of each microbial mat morphotype were aseptically collected from three of the sulfidic spring sites in Lower Kane Cave, Wyoming (Figure 1-2). Multiple mat samples were used for bulk biomass, elemental analysis, carbon isotope analysis, and DNA extraction and 16s rDNA clone library construction. To preserve the integrity of the sensitive ecological systems, conservative quantities of microbiological materials were collected. Sampling sites were numbered according to their location in meters from the back of the cave, with flow always toward the cave entrance (i.e. longer distances) (Figure 1-2): Fissure Spring (124-, and 127-m), Upper Spring (190-, 195-, 198-, and 203-m), and Lower Spring (one orifice and one mat sample from 248-m). Microbial mat morphotypes were collected separately and distinguished as white filaments (denoted as 'f'), white webs (denoted as 'w), yellowish-white mat (denoted as 'y'), and whitish-gray filaments (denoted as 'g'). White filament bundles in the water column or filaments from the surface of the mats were targeted for clone libraries; however, one library was

33

constructed with gray filaments ~2 cm below the top of the mat for comparison.

Geochemical Analysis

Geochemical data were acquired at the major microbiological sample locations, as well as throughout the cave, over a three year period. Unstable parameters (pH, E_H, and dissolved oxygen) were measured using electrode methods. Dissolved hydrogen sulfide (as total dissolve sulfide, $C_TS^=$), ferrous iron (Fe^{2+}), and low concentrations of dissolved oxygen were measured in the field using the Methylene Blue, Ferrozine and Rhodazine D colorimetric methods, respectively (CHEMetrics, Inc., Calverton, VA), using a MiniSpec 20 field spectrophotometer. Vertical profiles of dissolved oxygen through the mats were determined by fluorescence-quenching optical methods (Ocean Optics, Inc., Dunedin, FL). Unstable and reactive parameters (pH, oxygen, hydrogen sulfide, etc.) were also measured at several transects along and across the cave stream channels. Alkalinity (as total titratable bases, here dominated by bicarbonate) was determined in the field by titration to pH 4.5, and verified in the laboratory by end-point seeking autotitration. Anions and acid-preserved metals were determined by ion chromatography and inductively coupled plasma mass spectrometry, respectively. Dissolved organic and inorganic carbon (DOC and DIC, respectively) were determined by Dorhman DC-180 wet-oxidation carbon analyzer. Dissolved gas species (e.g., methane, aromatic hydrocarbons, hydrogen sulfide, organosulfur gases) from the spring and stream water were analyzed by headspace gas chromatography.

Scanning Electron Microscopy

Microbial mats were examined using scanning electron microscopy (SEM) by fixing biological material with a chemical critical-point drying method modified from Nation (1983). Briefly, samples were fixed with 25% gluteraldehyde, then freeze-fractured in liquid nitrogen, and freeze-dried. Samples were mounted on aluminum stubs, sputter-coated with gold, and examined using a JEOL JSM-T330A SEM in the Jackson School of Geosciences at the University of Texas at Austin.

Carbon, Nitrogen, and Sulfur Content

Aliquots of each morphotype (~2 ml) was individually homogenized, acidified with dilute HCl and rinsed with dH_2O (acidification and washing were repeated at least twice to ensure dissolution of carbonate mineral phases), followed by freeze-drying. Total organic carbon and nitrogen contents were determined by elemental analyzer interfaced with a FinniganMAT Delta Plus mass spectrometer at the University of Texas Marine Sciences Institute in Port Aransas, Texas, simultaneously with carbon isotope ratio analysis. Total sulfur content, as inorganic and organic sulfur compounds, was determined on a EuroEA3000 elemental analyzer (EuroVector, Milan, Italy).

Minimum bulk mat biomass was determined from dry weight analysis of the mats followed by comparison of the percent carbon in each aliquot, using methods described in and modified from Bratbak and Dundas (1984). Briefly, ~ 1 ml replicates were individually homogenized, acidified with dilute HCl, weighed, freeze-dried, and re-weighed to obtain the dry weight. The percentage of carbon in

each dried aliquot was determined by elemental analyzer. Cell carbon content was calculated from the standard conversion factor of 350 fg·C·cell^{-1} (assuming an average cell size of 1 μm^3; Bratbak and Dundas, 1984) to determine the number of cells per ml.

Carbon Isotope Methods

For carbon isotope ratio ($^{13}C/^{12}C$) analysis, organic carbon of 1 to 2 ml mat samples was prepared by acidifying the sample in dilute HCl to ensure removal of carbonate mineral phases. Most measurements were made by elemental analyzer interfaced with a continuous flow FinniganMAT Delta Plus mass spectrometer, but some measurements were also made by sealed tube combustion, vacuum purification, and using a dual-inlet VG Prism II mass spectrometer at the Jackson School of Geosciences. Microbial mat carbon isotope values were compared to the values obtained from cave water dissolved inorganic carbon (DIC), including a composite of $CO_{2(aq)}$, HCO_3^-, and CO_3^{2-} from the cave water. DIC was extracted for ^{13}C analysis by acidifying under vacuum with 100% phosphoric acid followed by cryogenic purification of the resulting CO_2 (method modified from Hassan, 1982). At the pH and temperature of the cave water (pH ~7.3 at 21.5^{o}C), the dominant DIC species was HCO_3^- (~90%) based on dissociation constants for $H_2CO_3^*$, HCO_3, and CO_3^{2-} species (Stumm and Morgan, 1996). Carbon isotope values for the Madison Limestone hostrock were also measured by reaction with 100% phosphoric acid (McCrea, 1950). All carbon isotope values are expressed in delta (δ) notation with respect to the international standard V-PDB, where

$$\delta^{13}C\ (\permil) = \left[\frac{{}^{13}C/{}^{12}C_{sample} - {}^{13}C/{}^{12}C_{standard}}{{}^{13}C/{}^{12}C_{standard}} \right] \times 1000 \qquad (4\text{-}1)$$

Sulfur Isotope Methods

Aqueous sulfide was collected by precipitating Ag_2S from filtered spring water with 10% $AgNO_3$ solution. Following sulfide removal, aqueous sulfate was collected by precipitating $BaSO_4$ with $BaCl_2$ (Carmody et al., 1998). Sulfur isotope ratios of sulfide, sulfate, and organic material were made with an elemental analyzer interfaced with a Micromass Optima mass spectrometer and ratios are expressed in delta notation with respect to the Cañon Diablo Troilite (CDT) standard.

DNA Extraction and PCR Amplification of 16S rRNA Gene Sequences

Approximately 0.2 to 0.5 ml mat morphotype material were aseptically collected and placed into tubes containing 0.5 to 1 ml sterilized DNA extraction buffer comprised of 10 mM Tris-HCl (pH 8), 100 mM EDTA, and 2% sodium dodecyl sulfate. Prior to DNA extraction and laboratory manipulation of the mat material, 9 μl Proteinase K (20 mg/ml) was added to each sample. Samples were physically disrupted by a series of freeze-thaw (3 times, $-80^{o}C$ to $65^{o}C$) cycles, followed by incubation at $55^{o}C$ overnight. RNase was added to the digests and incubated at $37^{o}C$ for up to 1 hr, following manufacturer instructions. Proteins and other cellular debris were precipitated in 7.5 M ammonium acetate by centrifugation. The supernatant was transferred to cold 100% isopropanol and then nucleic acids were precipitated overnight at $-20^{o}C$. DNA was pelleted by

centrifugation and pellets were washed in 70% ethanol, air-dried, and stored in either sterile water or TLE buffer. DNA quality and quantity from each extraction were determined on a GeneQuantII spectrophotometer (Amersdam Biosciences, Piscataway, NJ).

Nearly full-length community 16S rRNA gene sequences (>1300 bp) were PCR-amplified using the eubacterial primer pair 27f (forward, 5'-AGAGTTTGATCCTGGCTCAG-3') and 1492r (reverse, 5'-GGTTACCTTGTTACGACTT-3') (Lane, 1991). PCR is a method that amplifies a specific DNA sequence in vitro by repeated cycles of synthesis using specific primers and DNA polymerase. Amplification was performed with a Perkin Elmer 9700 thermal cycler and AmpliTaq Gold (Applied Biosystems, Branchnurg, NJ) under the following conditions: denaturation at $94^{o}C$ for 1 min, primer annealing at $42^{o}C$ for 1 min, chain extension at $72^{o}C$ for 1.5 min, repeated for 35 cycles. A control tube containing sterile water instead of DNA was used as a negative control; *Escherichia coli* DNA was used as a positive control.

16S rRNA Gene Clone Library Construction

Amplified PCR products were purified with the GeneClean II Kit (Bio101, Inc., Vista, CA), following manufacturer recommendations. Purified PCR products were cloned using the TOPO TA Cloning kit with *E. coli* TOP10F' cells, according to manufacturer instructions (Invitrogen, Carlsbad, CA). Molecular cloning involves the isolation and incorporation of a fragment of DNA (i.e., PCR product) into a cloning vector (a plasmid), where it is transformed into and perpetuated by a

population of host cells descended from a single cell. A collection of clones from one sample, each containing a replicated PCR product, comprises a clone library.

Bacterial 16S rDNA clone libraries were constructed from eleven microbial mat morphotype samples in the Department of Integrative Biology, Brigham Young University, Provo, Utah. Plasmids containing nearly-full length inserts were extracted using a standard alkaline lysis miniprep method (Ausubel et al., 1990). Clone plasmids were digested simultaneously using *Eco*RI and *Rsa*I (1U each) according to manufacturer's instructions (New England Biolabs) for restriction fragment length polymorphism (RFLP) analysis. RFLP patterns were visualized on 2% agarose gels stained with ethidium bromide and run in TBE (Tris-borate-EDTA)-buffer (refer to Appendix A for RFLP clone library results). Clones representing unique patterns from each library were selected for sequencing (Appendix A; Table A-1).

Sequencing of 16S rRNA Genes and Phylogenetic Analysis

Sequence inserts from plasmid minipreps for each clone to be analyzed were PCR-amplified using the plasmid-specific primer pair M13(-20) (5'-GTAAAACGACGGCCAGT-3') and M13(-24) (5'-AACAGCTATGACCATG-3'). PCR products were purified using Sephadex columns and sequenced using an ABI Big-Dye Ready Reaction kit (Perkin Elmer) with the primers 27f and 1492r in conjunction with the internal primers 704f (forward, 5'-GTAGCGGTGAAATGCGTAGA-3') and 907r (reverse, 5'-CCGTCAATTCCTTTRAGTTT-3'). Automated DNA sequencing was done on an ABI Prism 377X sequencer (Perkin Elmer) at Brigham Young University.

DNA sequences were submitted to the CHECK-CHIMERA program of the Ribosomal Data Base Project (RDP) II at Michigan State University (http://rdp.cme.msu.edu/html/) (Maidak et al., 2001) to screen for and to eliminate chimeric sequences. Clone sequences were subjected to BLAST searches within the GenBank database (http://www.ncbi.nlm.nih.gov/) to determine 16S rDNA sequence similarities to culturable and not yet cultured organisms (Appendix A; Table A-1).

Phylogenetic analyses were conducted by Megan L. Porter, Department of Microbiology and Molecular Biology, Brigham Young University, and detailed information can be found in Engel et al. (accepted). Briefly, nucleotide sequences were initially aligned using Clustal X (Thompson et al., 1997) and then manually adjusted based on conserved primary and secondary gene structure. Analyses were done after removal of segments that could not be unambiguously aligned corresponding to *E. coli* 16s rRNA secondary structure helices 9 and 10 (bp 181-226; all alignments), helix 17 (bp 452-481; all but the *Betaproteobacteria* alignment), helices 25 and 26 (bp 822-860; *Gammaproteobacteria* and Bacteroidetes/Chlorobi-Acidobacterium alignments), helix 30 (bp 1028-1032; *Betaproteobacteria* and *Deltaproteobacteria* alignments), and helix 33 (bp 995-1045; *"Epsilonproteobacteria"* and Bacteroidetes/Chlorobi-Acidobacterium alignments). All base pair positions correspond to *E. coli* numbering (Brimacombe et al., 1988). The minimum evolution criteria in the program PAUP* (Swofford, 2002), maximum likelihood criteria using a genetic algorithim (MLga) in MetaPIGA (Lemmon and Milimkovitch, 2002), and Bayesian inference coupled

with Markov chain Monte Carlo techniques (BMCMC) in MrBayes version 3.0b4 (Ronquist and Huelsenbeck, 2003) were used for phylogenetic analyses. As an indication of nodal support, bootstrap analyses were performed for minimum evolution (500 replicates) criteria using full heuristic searches. For BMCMC and MLga analyses, posterior probabilities were used for nodal support (Lemmon and Milimkovitch, 2002; Ronquist and Huelsenbeck, 2003).

Statistical Analysis and Sequence Population Diversity

To determine if the number of clones in each of the clone libraries was representative of microbial diversity, rarefaction curves were produced using the approximation algorithm aRarefactWin (Analytic Rarefaction, version 1.3, S. Holland, http://www.uga.edu/~strata/software/). The calculations for the program are based on Hurlbert (1971) and Heck et al. (1975). Rarefaction curves having 95% confidence levels were constructed by comparing the number of clones in each 16S rRNA gene library to the number of phylotypes from a particular library.

Estimates of clone library species richness and species dominance/evenness indices (combined to represent heterogeneity; e.g., Rousseau and Van Hecke, 1999; Ricotta, 2003) were calculated based on the number of phylotypes identified from RFLP and taxonomic affiliations from GenBank BLAST searches (Hughes et al., 2001; Martin, 2002; Hill et al., 2003). The nonparametric methods Abundance-based Coverage Estimator (ACE) and Chao1, and the Shannon-Wiener biodiversity function expressed as the Shannon Index (*H'*) were computed for each library using EstimateS (version 6.0b1, R.K. Colwell, http://viceroy.eeb.uconn.edu/estimates). Although there are problems with the interpretation of *H'* (refer to Hill et al., 2003,

for a complete discussion), it is the negative sum of each phylotype proportional abundance multiplied by the log of its proportional abundance, and is a measure of the difficulty in predicting the identity of the next individual sampled. The *H'* value is positively correlated to richness and evenness, but because it gives more weight to rare than to common phylotypes, it is more sensitive to absolute, but not relative, changes in abundance.

The Shannon Evenness (*E*) and the Simpson's Dominance index (*D*) were also calculated based on equations presented in Hill et al. (2003). *E* gives the ratio of *H'* to the maximum possible value of *H'* that could be obtained theoretically with the observed number of phylotypes; *E* is sensitive to changes in evenness of rare phylotypes such that an increase in abundance of a rare phylotype will increase *E* more than the equivalent reduction in abundance of a dominant phylotype (Hill et al., 2003). *D* strongly weights dominant phylotypes, which provides the probability that two clones chosen at random will be from the same phylotype. *D* is useful expression in this RFLP study because the dominant organisms are similar in all libraries (Hill et al., 2003).

A sequence similarity matrix was constructed for the closely related clone sequences from the "*Epsilonproteobacteria*" using corrected distances based on the model selected by Modeltest 3.06 (Posada and Crandall, 1998).

Nucleotide Sequence Accession Numbers

Nucleotide sequence data reported in this study are available in the GenBank database under the accession numbers AY208806 to AY208817 for LKC2-labeled clones, and AY510166 to AY510267 for LKC3-labeled clones.

RESULTS

Spring and Stream Geochemistry

The cave springs are all calcium-bicarbonate-sulfate water type and the geochemistry of the springs did not vary significantly from sample period to sample period (Table 2-1). Although the cave forms from sulfuric acid dissolution of limestone (Egemeier, 1981), the spring and stream pH was buffered to circum-neutral by ongoing carbonate dissolution. Incoming spring water had an average concentration of total dissolved sulfide ($C_TS^=$) of ~38 $\mu mol \cdot L^{-1}$ and non-detectable dissolved oxygen (Table 2-1). Incoming $C_TS^=$ was speciated as ~60% HS^-:40% H_2S (pK 7.04) based on the pH of the cave waters. The concentration of dissolved oxygen and $C_TS^=$ changed downstream in all transects, such that at the end of the microbial mats $C_TS^=$ decreased to non detectable and the concentrations of dissolved oxygen exceeded 40 $\mu mol \cdot L^{-1}$ (e.g., from the Upper Spring transect from 190 m to 203 m; Figure 2-1). The concentration of DOC in all the spring waters was extremely low, at <80 $\mu mol \cdot L^{-1}$ including methane.

Morphologic Description of the Microbial Mats

Four major mat morphotypes were distinguished by color and visual inspection in the cave when illuminated with white light. All three spring orifice pools contained long white filament bundles suspended in the water column. The Lower Spring (248 m) had the densest concentration of orifice bundles (Figure 2-2A), although the Upper Spring had the longest bundles at more than a meter in length. The entire microbial mat below the Lower Spring orifice pool was 2 to 5 cm

43

thick and less than 1 m in length; the mat was yellowish-white in appearance (Figure 2-2B). At the Upper Spring (190 m), long filament bundles in the orifice pool (Figure 2-2C, 2-2D) transitioned to shorter bundles that coalesced on the edges of the outflow channel (195 to 198 m), corresponding to a decrease in $C_TS^=$ and an increase in dissolved oxygen concentrations (Figure 2-1). Very thin, short (1 cm in length) whitish-gray filaments covered stream sediments in flowing water at the bottom of the outflow channel (195 m). Approximately 6 m downstream from the Upper Spring orifice, the gray filaments thickened and were stratigraphically below long white filaments and thin white webs that occasionally had a bumpy or knobby texture (Figure 2-2E). Oxygen microelectrode profiles at 203 m showed oxygen tension abruptly decreased ~3 mm below the mat-water interface and anaerobic conditions ($pO_2 < 10$ Pa) persisted within the 5 cm-thick mat interior, indicating that the mats are geochemically stratified. Gray filaments within the mat at 203 m (~2 cm below the white mat surface) were sampled to test for differences in the microbial community structure. For both the Upper and Lower Springs, dense white filamentous mats, with small (1-3 cm diameter) discontinuous yellow patches and feathery bundles (i.e., short, thick, and branching filaments), dominated the lower reach of the outflow channels (Figure 2-2F). Filament bundles near the orifice of the Fissure Spring (118 m) (Figure 2-2G) were also associated with web-like structures (125 m) (Figure 2-2H).

SEM examination of several mat samples revealed complex organic and inorganic structures as part of the overall mat structure. White filamentous material revealed a tight filament network (Figure 2-3A) with branching and non-branching

filaments averaging 1 μm wide (Figure 2-3B through 2-3D). Some thin filaments (~0.5 μm wide) were twisted and associated with long rods (Figure 2-3E and 2-3F). In comparison, gray sediment from the Upper Spring orifice (Figure 2-4) had few filaments and Fe-S framboids and crystallites were common (Figure 2-4A through 2-4D), indicating a reducing microenvironment within the sediments. Cell clusters were also observed (Figure 2-4E and 2-4F).

C:N Ratios, Sulfur Content, and Biomass Estimates

The N contents varied by mat morphotype (Table 2-2), and white filaments and white webs had the highest N content compared to gray filaments or gray sediment. Generally, the lower the C:N ratio, the higher the quality of the mat as a food source for the ecosystem (Fagerbakke et al., 1996). The mean C:N ratios for white filament morphotypes was 5.0 ($1\sigma = 0.8$), suggesting a high quality food source. The C:N ratios of gray filaments were significantly higher and more variable than white mat morphotypes, with a mean of 15.0 ($1\sigma = 10.5$). The C:N ratios were highest for gray filaments and sediment from spring orifice sites, suggesting that this biomass consisted of lower quality organic matter, while the C:N ratios for gray filaments at the end of the microbial mats approached those of the white mat morphotypes (Table 2-2).

The sulfur content of the white filaments was higher than the gray filaments (Table 2-2), presumably reflecting intracellular sulfur (as elemental S^0) rather than organosulfur compounds. Typically, in the absence of stored sulfur the highest bacterial cell sulfur content ranges up to 1% (w/w) (Fagerbakke et al., 1996).

However, the white filament sulfur content had a mean of 30.0% ($1\sigma = 11.2\%$), and the white webs had consistently the highest sulfur content. The gray filaments and sediment had significantly lower sulfur contents, with a mean of 1.9% ($1\sigma = 0.6\%$), consistent with predicted values for bacterial biomass (Fagerbakke et al., 1996). The sulfur content of white filaments was generally the same at the extreme upstream and downstream samples of the Upper Spring transect, but decreased by up to 10% in the middle stream reach (Table 2-2).

The biomass of the microbial mat samples was generally high ($\sim10^{10}$ cells·ml^{-1}), with less than an order of magnitude difference between white and gray filament morphotypes (Table 2-2). Biomass values may underestimate the actual biomass because cell conversion factors are for rod-shaped cells, and FISH suggests that the mats are dominated by filamentous morphotypes (Engel et al., 2003; refer to Chapter 3).

Carbon Isotope Systematics

The $\delta^{13}C$ value for the limestone bedrock was +0.95‰, and the DIC reservoir along the Upper Spring transect had an average $\delta^{13}C$ value of -7.5‰ (n = 7, $1\sigma = 0.1‰$), and DIC from the Fissure Spring orifice water had a slightly higher $\delta^{13}C$ value of -7.2‰. Microbial mat morphotypes had $\delta^{13}C$ values ranging from -23 to -41‰ (mean -34.1‰, $1\sigma = 4.1$) (Figure 2-5). The low $\delta^{13}C$ values reflect the large discrimination against ^{13}C exhibited by autotrophs (e.g., ~25 ‰ relative to total DIC for sulfur-oxidizing bacteria; Ruby et al., 1987).

Microbial mat morphotypes showed systematic variations in their carbon isotope compositions at most locations (Figure 2-5). At all three spring locations, gray filaments consistently had among the highest $\delta^{13}C$ values, whereas all coexisting white filaments had lower $\delta^{13}C$ values. More specifically, near the distal portions of the Upper Spring mats (203 m), white feathery bundles and yellow patches (Figure 2-2F) had some of the lowest $\delta^{13}C$ values, whereas the white webs and gray filaments had the highest $\delta^{13}C$ values (Figure 2-5). In contrast, however, the feathery bundles from the proximal region of the Upper Spring mats (196 m) had among the highest $\delta^{13}C$ values. Moving downstream, the $\delta^{13}C$ value of the white filaments in both Upper Spring and Fissure Spring decreased (Figure 2-5).

Sulfur Isotope Systematics

Allochthonous sulfide ($C_TS^=$) at the Upper Spring orifice had a $\delta^{34}S$ value of ~-22.5‰, and decreased downstream by approximately 1.6‰ (Figure 2-6). Dissolved sulfate had a $\delta^{34}S$ value of +13‰ and was invariable. The white filamentous morphotypes, containing high concentrations of sulfur (Table 2-2), had sulfur isotope values up to 2‰ lower than the allochthonous sulfide (Figure 2-6).

Clone Library Coverage, Species Richness, and Diversity

Eleven bacterial 16S rDNA clone libraries from four different microbial mat morphotypes were constructed and over 1000 clones were screened using RFLP (Appendix A). Although the RFLP method does not provide an absolute quantity of microbial groups within a community, it does provide an estimate of the proportional abundances of microbial groups in a given sample by assuming an

RFLP pattern of an abundant 'species' will be encountered more often in the clone library (Nübel et al., 1999; Morris et al., 2002). Nearly-full length 16S rRNA genes (>1300 bp) were sequences in both directions from selected clones. Sequences from the same RFLP pattern that had ≥98% sequence similarity were grouped as a phylotype, and this classification scheme was used to estimate community diversity (Table 2-3). This level of sequence similarity takes into account micro-variations in genetic sequences due to PCR and cloning biases and variations in 16S rRNA gene copies (Nübel et al., 1999; Speksnijder et al., 2001). Approximately 2% of the clone 16S rRNA gene sequences were chimera and removed from further analyses. Of the phylotypes identified, 44% had sequences that were ≥95% identical to GenBank sequences, corresponding to genus-level relationships (Stackebrandt and Goebel, 1994), and 30% of the sequences were ≥98% identical to GenBank sequences, corresponding to species-level relationships (Stackebrandt and Goebel, 1994). The remaining phylotype sequences had ≥90% sequence similarity to GenBank sequences (Table 2-3; Appendix A; Table A-1).

Rarefaction analysis was done to determine if the libraries had saturated coverage based on the number of clones obtained per library. The rarefaction curves indicated different patterns of diversity for different morphotype clone libraries (Figure 2-7). In the non-filament clone libraries (203g, 203w, 203y, and 248y), diversity was not fully covered compared to the saturation plateau reached for most of the white filament libraries (124f, 127f, 190f, 198f) (Figure 2-7). The non-filament libraries had higher phylotype richness overall and higher nonparametric estimates (ACE and Chao1; Table 2-4). As there was an overall

increase in the rate of phylotype accumulation in these unsaturated curves, major diversity within these libraries may not be well represented, although some of these libraries (e.g., 203y) do have high dominance (*D*) values (Table 2-4).

Species heterogeneity among the clone libraries was generally low and many of the white filament libraries showed overwhelming dominance by one of two phylotypes. Species richness was higher for the non-filament morphotypes, with the white webs from 203 m and the yellow patches from 203 m and 248 m showing the most diverse taxonomic representation among the eleven bacterial clone libraries (Table 2-3), even though observed species richness was lower than expected based on ACE and Chao1 values (Table 2-4). In comparison, although species richness of the white filament libraries varied, ranging from one to ten observed phylotypes, ACE and Chao1 estimates for the white filament libraries indicated that the observed phylotype numbers were close to the calculated values because of near-complete clone coverage for most of those libraries (Table 2-4). The diversity (*H'*)/dominance (*D*) indices changed for the white filament clone libraries downstream for both the Upper and Lower Spring transects, such that the *H'* values increased and *D* values correspondingly decreased (Table 2-4).

Phylogenetic Analysis of 16S rRNA Gene Clone Libraries

The 16S rDNA clones were affiliated with several bacterial phyla (Table 2-3; Figures 2-8 through 2-12). The majority of the sequences identified from the clone libraries belonged to the *Proteobacteria* taxonomic division, specifically the "*Epsilonproteobacteria*," (68%) *Gammaproteobacteria* (12.2%), *Betaproteobacteria* (11.7%), and *Deltaproteobacteria* (0.8%) classes, as well as other

49

bacterial divisions, including the Acidobacterium (5.6%) and Bacteroides/Chlorobi (1.7%).

The "Epsilonproteobacteria" class

The highest number of clones from all the libraries (68%) was assigned to the "*Epsilonproteobacteria*" (Table 2-3; Figure 2-8). Epsilonproteobacterial sequences from 17 phylotypes clustered into six groups based on phylogenetic position (Figure 2-8) and the sequence similarity matrix (Table 2-5), which suggests that genetic microdiversity was high (Fuhrman and Campbell, 1998). At least one epsilonproteobacterial phylotype was found in all clone libraries regardless of morphotype type or location (Table 2-3). The epsilonproteobacterial groups identified from Lower Kane Cave have few closely related sequences from the public sequence databases, suggesting that the diversity of these groups, and the "*Epsilonproteobacteria*" in general, is only now being realized.

The most abundant epsilonproteobacterial groups from all three springs formed two distinct clades, LKC group I and group II. No other epsilonproteobacterial phylotype was detected in a clone library if either LKC group I or II was absent. The closest relatives to LKC groups I and II were the two environmental clones, sipK119 and sipK94, respectively (98-99% similar in nucleotide sequence), from microbial mats with a string-of-pearls morphology in sulfidic marsh springs at the Sippenauer Moor, Regensburg, Germany (Rudolph et al., 2001; Moissl et al., 2002). Clone sequences from LKC group I were also closely related (97-99% similar in nucleotide sequence) to environmental clones obtained from a petroleum-contaminated, sulfidic groundwater storage cavity in

Japan (Watanabe et al., 2000; Watanabe et al., 2002) and two clones from microbial mats from the sulfidic Cesspool Cave, Virginia (Engel et al., 2001) (Figure 2-8). The closest cultured relative for LKC groups I clones is *Sulfuricurvum kujiense*; this organism is a slightly curved rod isolated as a chemolithoautotrophic sulfur-oxidizer, capable of growth on thiosulfate, elemental sulfur, and hydrogen sulfide, and able to use molecular oxygen, nitrate, or ferric iron as electron acceptors (Kodama and Watanabe, 2003). LKC group II clones were more distantly related (90-94% similar in nucleotide sequence) to miscellaneous marine, hydrothermal vent field and epibiont clones (e.g., Longnecker and Reysenbach, 2001; Lopez-Garcia et al., 2002) and clones from a sulfidic cave microbial mat in Parker Cave, Kentucky (Angert et al., 1998) (Figure 2-8). The phylogenetic affinities (Figure 2-8) and the sequence similarity matrix (Table 2-5) demonstrate that group I and group II are distinct from each other at more than the genus-level (85-87% similar in nucleotide sequence).

LKC group III did not form a distinct phylogenetic cluster and was defined by several phylotypes from five libraries, supported by the range of sequence similarities among the sequences and moderate boot-strap node values (Table 2-5; Figure 2-8). No LKC group III clones were found at the Lower Spring. The relatives to the epsilonproteobacterial LKC groups III and IV were similar to LKC group I clones (Table 2-5).

LKC group IV, comprised of clones only from the Upper Spring, clustered closely with *S. kujiense* (Kodama and Watanabe, 2003), and groundwater and cave environmental clones (Figure 2-8). Based on the similarity matrix, LKC groups III

and IV had low sequence similarity within the groups, although each library was distinct from all the other groups (Table 2-5).

LKC group V also had a wide range of sequence similarity (Table 2-5), indicating additional diversity within this group that could not be resolved by RFLP. LKC group V was most closely related to LKC group II clones (Table 2-5).

Seventeen clones from four morphologically diverse libraries, but mostly white filament morphotypes, belonged to the novel sequence cluster LKC group VI, which was genetically distinct from all the other epsilonproteobacterial groups (Table 2-5). The closest relatives to LKC group VI clones were environmental clones from subsurface acid mine drainage and groundwater (95-96% similar in nucleotide sequence).

The Gammaproteobacteria *class*

Twelve percent of all the clones belonged to the *Gammaproteobacteria* (Figure 2-9). Eighty-one clones formed one phylotype, closely related to the environmental clone sipK4 from sulfidic marsh springs (99-100% similar in nucleotide sequence) (Rudolph et al., 2001), which is also closely related to *Thiothrix unzii*. The relative abundance of this phylotype generally increased downstream from the orifice to the end of the mats for all three spring transects (Table 2-3). Cultured representatives from *Thiothrix* oxidize a variety of reduced sulfur compounds and several *Thiothrix* species have been identified from other sulfidic caves, including Parker Cave (Angert et al., 1998), underwater caves and karst springs in Florida (Brigmon et al., 2003), and Cesspool Cave (Engel et al., 2001). *T. unzii*, an aerobic sulfur-oxidizing bacterium that utilizes sulfide and

thiosulfate as sole sulfur sources and stores sulfur intracellularly (Howarth et al., 1999), and environmental clones closely related to *T. unzii* are also commonly associated with activated sludge and wastewater treatment plants (e.g., Wagner et al., 1994; Howarth et al., 1999), as well as sulfidic springs where it is the dominant group (Rudolph et al., 2001; Moissl et al., 2002).

Clone library 203g was dominated by clones belonging to the Enterobacteriaceae, specifically the *Pantoea* and *Serratia* genera (Figure 2-9). The libraries 203g and 248y had six clones closely related to *Serratia marcescens* (99% similar in nucleotide sequence).

Nine sequences from the 124f and 203w libraries were distantly related to *Beggiatoa* sequences (90% similar in nucleotide sequence), with one relative being the isolate *Beggiatoa* sp. MS-81-1c from a salt marsh, described as a narrow and non-vacuolate filament (Ahmad et al., unpublished GenBank submission) (Table 2-3; Figure 2-9). The weak sequence similarity to known *Beggiatoa* sequences and low bootstrap values between the clone group and *Beggiatoa* sequences (Figure 2-9), however, indicate that Lower Kane Cave clones may belong to a different, unclassified bacterial group within the *Gammaproteobacteria*. *Beggiatoa*-like filaments have been described from a marine cave in Italy using microscopy (Airoldi et al., 1997) and from microbial mats in Parker Cave, Kentucky (Thompson and Olson, 1988), although detailed phylogenetic investigations from Parker Cave did not support the presence of *Beggiatoa* (Angert et al., 1998).

The **Betaproteobacteria** *class*

Nearly twelve percent of the clones were affiliated with the *Betaprotoebacteria*, and were most closely related to *Thiobacillus* spp. (Figure 2-10). Three phylotypes were identified from two libraries. The closest relatives were the environmental clone 44a-B2-21 from acid mine drainage (Labrenz and Banfield, unpublished GenBank submission) and *Thiobacillus aquaesulis* (94-95% sequence similarity). Many *Thiobacillus* spp. oxidize reduced sulfur compounds (Kelly and Harrison, 1989), and *T. aquaesulis* is not an obligate sulfur-oxidizing chemolithoautotroph, but can grow as a facultative heterotroph on nutrient broth and yeast extract (McDonald et al., 1996). Thiobacilli have been described from caves (Vlasceanu et al., 1997; Angert et al., 1998; Hose et al., 2000; Vlasceanu et al., 2000; Engel et al., 2001), but environmental clones from those studies were not closely related to the Lower Kane Cave group.

The **Deltaproteobacteria** *class*

Less than 1% of the clones were closely related (96-97% similar in nucleotide sequence) to *Desulfocapsa thiozymogenes*, the environmental clone sipK94 from the string-of-pearls mats in Germany (Moissl et al., 2002), and the environmental clones SRB348 and SRB282 identified from the chemocline of the meromictic Lake Cadagno, Switzerland (Tonolla et al., 2000) (Table 2-3; Figure 2-11). *D. thiozymogenes* disproportionates thiosulfate, sulfite, or elemental sulfur to sulfate and sulfide (Janssen et al., 1996).

The Acidobacterium division

One phylotype representing 5.6% of all the clones obtained from this study was closely related (96-97% similar in nucleotide sequence) to uncultured environmental clones within the Acidobacterium division. Library 203w was dominated by this clone group, and rare clones from this phylotype were found in five additional libraries (Table 2-3). The closest relative was clone SJA-36 identified from an anaerobic bioreactor with trichlorobenzene contamination (von Wintzingerode et al., 1999) (Figure 2-12). The Lower Kane Cave phylotype also expands the *Acidobacteria*-group 7 described by Liles et al. (2003), which consists of only a few environmental clones from soil, as well as the *Acidobacteria*-subgroup-b described by Schabereiter-Gurtner et al. (2002) from La Garma Cave, Spain. Clone LKC3_156.13 had 92% sequence similarity to clone SJA-36, but also clustered as an unclassified taxonomic group within the Bacteroidetes phylum by phylogenetic analysis (Figure 2-12). Cultivated members of the *Acidobacteria* division are heterotrophs, although *Acidobacteria* have been found in many geochemically different environments, including neutral and acidic soils, marine and freshwater sediments, hot springs, deep-sea vents, and engineered systems (Barns et al., 1999; Schabereiter-Gurtner et al., 2002; López-García et al., 2003; Schabereiter-Gurtner et al., 2003).

The Bacteroidetes/Chlorobi division

Seven phylotypes, each represented by rare 'singleton' or 'doubleton' clones, belonged to the Bacteroidetes/Chlorobi (BC) taxonomic group (Table 2-3; Figure 2-12). Three phylotypes (BC groups I-III) were closely related to

environmental clones within the *Bacteroides* class, including clones from lakes and contaminated groundwater. Four phylotypes (BC groups IV-VII) were related to environmental clones within the *Sphingobacteria* class (including the genus *Cytophaga*) obtained from a wide habitat range, including deep-sea hydrothermal vent metazoans, gas hydrate sediment, soil, and contaminated groundwater.

DISCUSSION

Terrestrial subsurface environments are often inaccessible for study, limiting our understanding of ecosystem structure and dynamics, elemental cycling, and potential biogeochemical impacts to earth and atmospheric processes. The main research goals of this part of the study were to identify the bacterial groups characteristic of the cave microbial mats, to gain an understanding of how geochemistry may control microbial community diversity within the aphotic environment, and to elucidate potential ecosystem functioning and the impact of sulfur cycling and chemolithoautotrophy on the ecosystem. The results of this work suggest that similar microbial communities and concomitant microbially mediated biogeochemical cycles may be more widely dispersed in sulfidic groundwater habitats than previously recognized.

"Epsilonproteobacteria" Diversity and Ecophysiology

The majority of 16S rRNA gene sequences from the clone libraries were affiliated with the *"Epsilonproteobacteria,"* and specifically with two epsilonproteobacterial groups defined as LKC Group I and II (Figure 2-8). Additionally, there was a high level of genetic microdiversity within the

"*Epsilonproteobacteria*" identified in this study based on the range of sequence similarities for the obtained epsilonproteobacterial clones (Table 2-5).

Numerous 16S rDNA-based molecular surveys suggest that "*Epsilonproteobacteria*" successfully colonize a variety of geochemical settings, including caves (Angert et al., 1998; Engel et al., 2001; Barton et al., 2002), deep aquifers (Pedersen et al., 1997), terrestrial sulfidic springs and groundwater (Watanabe et al., 2000; Rudolph et al., 2001; Moissl et al., 2002; Watanabe et al., 2002; Elshahed et al., 2003; Kodama and Watanabe, 2003), oil fields (Voordouw et al., 1996), deep marine sediments and ocean water (Fenchel and Glud, 1998; Li et al., 1999a; Li et al., 1999b; Todorov et al., 2000; Madrid et al., 2001), hydrothermal vent sites (Moyer et al., 1995; Muyzer et al., 1995; Polz and Cavanaugh, 1995; Brinkhoff et al., 1999; Reysenbach et al., 2000; Corre et al., 2001; Longnecker and Reysenbach, 2001; Takai et al., 2003), in association with deep-sea animal life at vent sites (Haddad et al., 1995; Cary et al., 1997; Naganuma et al., 1997; Alain et al., 2002a; Lopez-Garcia et al., 2002; López-García et al., 2003), and in engineered systems including sewage sludge and contaminated waste (Engberg et al., 2000; On, 2001). Based on the geochemical diversity of these study sites and the lack of culture-based information from most phylogenetic groups within the "*Epsilonproteobacteria*", especially those groups identified from terrestrial settings, it is challenging to predict what the ecophysiological roles of "*Epsilonproteobacteria*" in Lower Kane Cave might be (Gray and Head, 2001).

In many environments "*Epsilonproteobacteria*" are implicated in sulfur cycling, and specifically in oxidizing reduced sulfur compounds; this is supported

by several culture-based studies (Finster et al., 1997; Stolz et al., 1999; Gevertz et al., 2000; Campbell et al., 2001; Nemati et al., 2001; Alain et al., 2002b; Miroshnichenko et al., 2002; Kodama and Watanabe, 2003; Takai et al., 2003). Additionally, in nearly all of these culture-based studies, the epsilonproteobacterial strains grew chemolithoautotrophically. Therefore, reasonable metabolic hypotheses can cautiously be made for the "*Epsilonproteobacteria*" from Lower Kane Cave based on cave biogeochemistry.

It is possible that the organisms represented by LKC groups I, III, and IV clones may have metabolic similarities to *S. kujiense*, which grows under microaerophilic to anaerobic conditions. However, alternative electron acceptors such as nitrate and ferric iron are exceptionally low in the cave waters (Table 2-1). Closely related phylogenetic groups, however, do not necessarily indicate similar ecophysiological characteristics (Fuhrman and Campbell, 1998), as Takai et al. (2003) showed that the observed phylogenetic distribution of epsilonproteobacterial cultures isolated from deep-sea vents did not correlate with substrate or electron acceptor preferences, oxygen requirements, or geographic location. These deep-sea vent cultures were non filamentous and affiliated with five distinct epsilonproteobacterial taxonomic groups, yet had high metabolic diversity which included sulfur and thiosulfate oxidation using nitrate or molecular oxygen (at 1% or 10%) or H_2-dependent sulfur-reduction (Takai et al., 2003).

Clearly, the high concentrations of dissolved sulfide discharging from the springs provide a rich energy source for sulfur-oxidizing bacteria. Although it is unlikely that abiotic autoxidation (i.e., chemical oxidation) and volatilization cause

sulfide loss exclusively, there was an observed decrease in dissolved sulfide concentrations downstream (Figure 2-1). Abiotic sulfide autoxidation is extremely slow in disaerobic water at pH ~7.4 (the autoxidation half-life was calculated at >800 hours; $H_2S:HS^-$ pK 7.04) and sulfide volatilization from the water to the atmosphere accounts for <8% of the sulfide loss in the stream based on gas flux experiments (see Chapters 5 and 6). With no other mechanism for $C_TS^=$ loss, there would be, for example, significantly higher sulfide concentrations at the end of the Upper Spring microbial mat, as well as at the cave entrance 150 m further downstream. However, a very rapid decrease in $C_TS^=$ is observed (Figure 2-1). Microbial catalysis under microaerophilic conditions causes rapid sulfide consumption; therefore, most of the epsilonproteobacterial groups identified must consume dissolved sulfide as sulfur-oxidizers (see Chapters 5 and 6).

Another line of evidence to suggest that "*Epsilonproteobacteria*" in the microbial mats oxidize sulfur compounds is from the measured $\delta^{34}S$ values (Figure 2-6). The decrease in $\delta^{34}S$ values for $C_TS^=$ from the cave spring to the end of the mats, by up to 2‰, indicates that allochthonous $\delta^{34}S$ values are being offset by biogenic sulfide generated by sulfate-reducing bacteria (e.g., *Desulfocapsa thiozymogenes*) within the mats (Canfield, 2001b). H_2S produced by sulfate-reducing bacteria would have more negative $\delta^{34}S$ values isotopes than the incoming sulfide, as the ^{34}S discrimination expressed by sulfate reduction is variable and can be as high as 45‰ (Canfield, 2001a; 2001b). In comparison, the processes of sulfide volatilization (Van Everdingen et al., 1985; Fry et al., 1986) and abiotic autoxidation (Fry et al., 1988) would result in a ^{34}S enrichment in the residual

59

dissolved sulfide. Because there is a high sulfur concentration in the microbial biomass, presumably as intracellular sulfur, the $\delta^{34}S$ values for microbial biomass are interpreted as a direct measure of the sulfide source utilized by the sulfur-oxidizers. Current thought is that sulfur-oxidizing bacteria exhibit negligible (+/-1‰) sulfur isotope fractionation during both the transformation of sulfide to elemental sulfur and elemental sulfur to sulfate (Toran and Harris, 1989). Specifically, if the bulk of the microbial biomass that oxidized reduced sulfur compounds utilized only allochthonous sulfide, then the $\delta^{34}S$ values for the mats would be nearly the same as the spring water sulfide (Kaplan and Rittenberg, 1964). The general ^{34}S depletion in the microbial biomass relative to the source (i.e., dissolved sulfide) suggests that sulfur-oxidizing bacteria utilize a mixture of both allochthonous and autochthonous sulfide (Toran and Harris, 1989; Canfield, 2001a).

Geochemical Controls on Community Structure and Ecosystem Function

Studies from aquatic environments suggest that shifts in community structure could result from changes in nutrient availability, salinity, light penetration, turbidity, oxygen content, sulfide, or pH (e.g., Skirnisdottir et al., 2000; Nübel et al., 2001). At present, however, there have not been any investigations that describe the controls on changing community structure from a freshwater aphotic habitat. Specifically, light penetration, turbidity, and salinity are not critical physicochemical conditions to influence cave microbial communities, and changes in the pH of the cave waters are not important because of the buffering of pH to circum-neutral conditions by dissolving carbonate rock. Instead, I propose

that 1) variations in dissolved hydrogen sulfide concentrations, 2) increasing dissolved oxygen concentrations downstream, 3) colonization of the springs and outflow channels by "*Epsilonproteobacteria*", and 4) changes in organic carbon production and storage as a result of chemolithoautotrophy by epsilonproteobacterial groups are the most critical parameters affecting microbial community structure within the microbial mats.

The relative abundances of epsilonproteobacterial and other taxonomic groups shifted moving downstream with changing dissolved sulfide and oxygen concentrations (Table 2-3). In general, the abundance of both epsilonproteobacterial LKC groups I and II decreased from the orifice pools downstream, and the highest abundance of epsilonproteobacterial LKC group I was from samples where the concentration of dissolved oxygen was very low at both the Fissure and Upper Springs. Clone libraries from the three spring orifices, which originated from areas continuously replenished by sulfidic spring water, were dominated by one epsilonproteobacterial group, whereas downstream libraries had higher bacterial diversity (Table 2-3). For example, at the Lower Spring, all clones screened by RFLP belonged to the epsilonproteobacterial LKC group II, whereas 1 m downstream in the microbial mat nine other bacterial groups were identified. At the three springs, there was also an increase in the abundance of *Thiothrix*- and/or *Thiobacillus*-like clones downstream, which is in accordance with the characterized metabolism and sulfide and oxygen preferences for these groups (e.g., Howarth et al., 1999). Specifically, *Thiothrix* spp. tolerate or require higher dissolved oxygen concentrations compared to what is known about the oxygen requirements for some

61

cultured "*Epsilonproteobacteria*". At the Upper Spring, LKC group III was most abundant in downstream libraries (203f) where the dissolved oxygen concentration was higher, suggesting that while this group may be involved with sulfur cycling, this group may prefer higher habitat oxygen content. The dominance of *Acidobacterium* in the 203w clone library, from the surface of the mat where dissolved oxygen is highest, suggests that this group prefers higher oxygen and lower sulfide concentrations.

Sulfur storage in the microbial mats from the three springs, as indicated by the sulfur content of the mats, also changed downstream (Table 2-2), which corresponds to the types of microbial groups present in the mats. The highest sulfur content was from white filament bundles collected from the orifices and from the mat termini; lower sulfur contents were measured from the filament libraries from the middle of the stream transects. There is no indication from cultures that "*Epsilonproteobacteria*" store sulfur intracellularly like *Thiothrix* spp. (Howarth et al., 1999), possibly as a mechanism to attenuate changes in substrate availability in the environment (Chesson et al., 2002). The marine epsilonproteobacterial strain "*Candidatus* Arcobacter sulfidicus" forms extracellular sulfur filaments (Taylor et al., 1999; Wirsen et al., 2002) and cultures of nitrate-reducing sulfur-oxidizing "*Epsilonproteobacteria*" form sulfur as the metabolic end-product when nitrate is limiting or absent (Gevertz et al., 2000; Nemati et al., 2001). Some neutrophilic *Thiobacillus* spp. are also known to precipitate sulfur outside the cell (Kelly and Harrison, 1989). Therefore, the high sulfur content in white filaments from the spring orifice samples, dominated by "*Epsilonproteobacteria*" could be due to

extracellular sulfur or sulfur accumulation due to nitrate-reduction. Higher sulfur content in downstream samples could also be due to incomplete sulfide oxidation to elemental sulfur by *Thiothrix* spp. The exceptionally low sulfur content in the 203y sample (8.6%) compared to other morphotypes may be because the thiobacilli oxidize sulfur within the mat morphotype due to the diminished dissolved sulfide concentration in the stream water. Therefore, the distribution of sulfur content in the microbial mats may explain how several bacterial groups with similar metabolic requirements (e.g., presence of reduced sulfur compounds) coexist, as there appears to be distinct differences in spatial and temporal resource use by the microbial populations in the mat morphotypes moving downstream (Chesson et al., 2002).

Based on experiments from deep-sea vent sites where "*Epsilonproteobacteria*" are the first to colonize virgin surfaces, López-García et al. (2003) suggest that epsilonproteobacterial groups initially and rapidly diversify metabolically within a habitat (natural or artificial), and thereby create microniches (such as anoxic regions) where other bacteria will subsequently colonize. High diversity among the specialized "*Epsilonproteobacteria*" would essentially maximize ecosystem functionality of other microbial groups and make the entire system more productive because of high growth rates, significantly higher biomass, and quick adaptations to specific geochemical conditions of the habitat. Additionally, Chesson et al. (2002) describe the tendency for the most productive species to also be the most dominant in a habitat, and thereby push others species to comparatively lower densities. These ecological caveats may explain why the

microbial mats in Lower Kane Cave have high diversity within the "*Epsilonproteobacteria*", but lower bacterial diversity overall.

The bacterial community composition of the 203g clone library is one of the most telling examples of the controls geochemistry has on community structure, and perhaps as an ecological consequence of "*Epsilonproteobacteria*" creating anoxic regions within the mat. The interior of the mat was dominated by clones with 99% nucleotide similarity to *Pantoea agglomerans* and environmental clones. *Pantoea* spp. are ubiquitous in natural and engineered environments, and are saprophytic, facultative anaerobes with diverse metabolic capabilities, including dissimilatory metal reduction. Recently, Northup et al. (2003) report a single *Pantoea* 16S rDNA clone from corrosion residues in Lechuguilla Cave, New Mexico, a cave that formed over several million years from sulfuric acid dissolution. This clone, however, is not closely related to those from Lower Kane Cave. There were also clones with 99% sequence similarity to *Serratia marcescens*, which is common to soil, water, and plants. *S. marcescens* is saprophylic and an opportunistic pathogen known to cause a variety of infections and diseases (Su et al., 2003). Although rare clones closely related to *D. thiozymogenes* were also identified from some samples (Table 2-3), preliminary culture investigation of gray filaments and other mat samples suggest that sulfate-reducing bacteria are present (see Chapter 4).

The presence of fermenting and sulfate-reducing bacteria in the deepest, most anaerobic portion of the mat is consistent with reducing conditions measured from oxygen microelectrodes, the presence of reduced mineral phases (Figure 2-4),

and the low C:N ratios for the gray sediment and filaments (Table 2-2). The ratios suggest enhanced processing of biological material due to heterotrophy, and possibly fermentation. While molecular methods allow for the characterization of organisms that are difficult, if not impossible to cultivate (e.g., Head and Gray, 1998), unfortunately molecular methods can create significant biases and underestimations of particular microbial groups, especially if abundances are $<10^7$ cells per volume (von Wintzingerode et al., 1997; Speksnijder et al., 2001). Therefore, because this part of the study focused on the white filament morphotypes, it is likely that the diversity of anaerobes is underrepresented with respect to total genetic diversity, and combined culture- and molecular-based approaches are necessary.

Chemolithoautotrophy in the Subsurface

Most caves are traditionally energy- and nutrient-limited, commonly fed by surface streams in which photosynthetically-derived organic matter and sediments, as well as microorganisms, are washed into the subsurface and deposited (Poulson and Lavoie, 2000; Simon et al., 2003). Previous studies have shown that most microorganisms in caves are not chemolithoautotrophs, but instead are translocated soil heterotrophs, chemoorganotrophs, or fecal coliform bacteria from contaminated surface water (Poulson and Lavoie, 2000). Mikell et al. (1996) estimate that $\geq 75\%$ of microbial communities in caves are heterotrophs. While it would be difficult to assess the metabolic pathways for all the microbial groups identified from the clone libraries using culture-based methods, or even to speculate about the metabolism for some groups with no cultured relatives, I used stable carbon isotope systematics

to interpret the source of carbon to the microbial mats, as well as to determine how carbon is cycled among different metabolic guilds. I propose that primary productivity was linked to the sulfur cycle through chemolithoautotrophy, as the geochemistry of the cave waters is consistent with reduced sulfur compounds being important components of the energy budget of the microbial ecosystem and because the most abundant microbial groups are associated with sulfur metabolism.

While the Bighorn River may have had a role in inoculating the cave with microorganisms during past flood stages (refer to Figure 1-10), I suggest that the microbial communities in Lower Kane Cave are endemic and virtually unaffected by surface hydrologic conditions, on the basis of these findings: 1) the discharging cave springs contribute little to no allochthonous DOC or particulate organic carbon to the microbial community (Table 2-1); 2) bacterial groups common to most soil environments, as evidence of translocated soil microbes, were not identified based on 16S rDNA phylogenies; and 3) the filamentous microbial biomass in Lower Kane Cave reaches at least 10^{10} cells·ml^{-1} (Table 2-2), significantly higher than 10^2 to 10^4 cells·ml^{-1} commonly found in aquatic cave systems (Brown et al., 1994). Furthermore, the overall carbon isotope compositions of the microbial biomass reflect significant isotopic discrimination against ^{13}C relative to the inorganic carbon source (Figure 2-5), with 77% of the microbial mat samples having δ^{13}C values ≤ 30‰, well below that of terrestrial biomass (Coplen et al., 2002), demonstrating that inorganic carbon is predominately fixed through chemolithoautotrophy. Porter (1999; unpublished data) verified chemolithoautotrophic productivity from the white filamentous microbial mats at

the Lower Spring by $H^{14}CO_3$-assimilation, which suggested that there was more than six times higher autotrophic productivity than heterotrophic productivity, as tested by ^{14}C-leucine-incorporation. The results of the 16S rRNA gene phylogenies also suggest that only a very minor component of the community is potentially heterotrophic.

Chemolithoautotrophy in a cave ecosystem is important because it serves as the base for the cave food web, increasing both food quality and quantity (Kinkle and Kane, 2000; Poulson and Lavoie, 2000). Movile Cave, Romania, was the first documented chemolithoautotrophically-based cave and groundwater ecosystem (Sarbu et al., 1996), and subsequently chemolithoautotrophy has been found in several different sulfidic caves systems around the world, including marine caves from Cape Palinuro, Italy (Airoldi et al., 1997), the Frasassi Caves, Italy (Vlasceanu et al., 1997; Sarbu et al., 2000), Cueva de Villa Luz, Mexico (Hose et al., 2000), Cesspool Cave (Engel et al., 2001), and the flooded Nullarbor caves, Australia (Holmes et al., 2001). The bulk of the white filament microbial biomass in Lower Kane Cave has low C:N ratios averaging 5.0, compared to a C:N ratio of 5.7 for microbial mats from Movile Cave (Kinkle and Kane, 2000). The C:N ratios for Lower Kane Cave mats match previously reported ratios for bacterial cells (C:N = 3 to 5; Paul and Clark, 1996), but also to periphyton in surface streams (C:N = 4 to 8; Gregory, 1983) and bacteria from a marine hydrothermal vent site (C:N = 3.8 to 9.4; Gugliandolo and Maugeri, 1998). These C:N ratios are consistent with an insignificant influx and processing of allochthonous carbon, and instead suggest that carbon is provided in situ through autotrophy. The especially low C:N ratios

for the white filaments from Lower Kane Cave suggest a high quality food that could be used by heterotrophic microorganisms and higher trophic levels (McMahon, 1975). Incidentally, there is a large population of snails (*Physa spelunca*) that graze on the microbial mats in Lower Kane Cave. In contrast, the high C:N ratios in the gray filaments indicate carbon storage and accumulation of processed biomass, but a reduction in nitrogen availability.

The mechanisms for inorganic carbon fixation were not evident based on carbon isotope analyses, as there are several different pathways for inorganic carbon fixation, and not all fixation pathways and their isotopic effects are known. Microorganisms that fix CO_2 by the Calvin reductive pentose phosphate pathway (Calvin-Benson-Bassham cycle), the predominant and most important CO_2-fixation pathway for photosynthetic and chemosynthetic bacteria, have isotopic values that fall into two categories based on the form of CO_2-fixing enzyme, ribulose- 1,5-bisphosphate carboxylase/oxygenase (RubisCO) (Robinson and Cavanaugh, 1995). The fixation pathway using the reductive citric acid (TCA) cycle imparts a smaller (~-10‰) carbon isotope fractionation (Preuß et al., 1989; Taylor et al., 1999; Wirsen et al., 2002). Nearly all of the mat samples from Lower Kane Cave had $\delta^{13}C$ values that fit into the RubisCO form I group, ranging between -27 to -35‰ (the '-30‰ group') (Robinson and Cavanaugh, 1995). Physicochemical conditions, such as velocity, water depth, temperature, pH, and CO_2 concentrations, can affect the effective isotope discrimination of autotrophs, which would result in tremendously different discrimination values (Preuß et al., 1989; Simenstad et al.,

1993; France, 1995; France and Cattaneo, 1998). However, the Upper Spring transect stream water maintains constant chemistry and turbulent flow.

Nutrient Spiraling

There were systematic differences in the carbon isotope composition among the mat morphotypes at any location, however, which suggests that there may be distinct carbon isotope effects imparted by specific populations due to autotrophic production versus heterotrophic consumption. Changing abundances of bacterial populations downstream could account for this observation if the downstream populations express larger ^{13}C discrimination. An alternative explanation for the downstream carbon (and sulfur) isotope trends may be that mat stratification, caused by redox conditions, creates an environment for nutrient spiraling, a process first described from surface stream ecosystems in which nutrients are cycled between multiple components of the ecosystem while being transported further downstream in each subsequent cycle (Newbold et al., 1981; Newbold et al., 1982; Newbold, 1982; Allan, 1995). Nutrient spiraling has neither been described from subsurface ecosystems, nor from chemosynthetic systems.

Variations in the $\delta^{13}C$ composition among the different microbial mat morphotypes (white filaments versus gray filaments) in downstream transects suggest carbon cycling between chemolithoautotrophs and heterotrophs. The physical model of the nutrient spiral is based on the energy transfer between redox (metabolic) environments, and without the metabolic complexity and juxtaposition of aerobic and anaerobic populations, nutrient spiraling would not occur. The autotrophically-fixed carbon, which may be respired as CO_2 with a low $\delta^{13}C$ value,

69

is transported downstream and preferentially reassimilated by autotrophs in the mat boundary layer; the proportion and intensity of recycling of the fixed carbon derived from respiration should increase downstream (Newbold, 1982). Downstream, filamentous sulfur-oxidizing bacteria form a thick mat that restricts the downward flux of oxygen into the mat interior, and the occupation of the exterior of the microbial mats by sulfur-oxidizers results in consumption of most of the available oxygen. This creates an anaerobic mat interior where compounds are transported by diffusion only, maintaining a habitat for obligate anaerobic populations. The anaerobic consortium, consisting of predominately sulfate-reducing and fermenting bacteria (refer to Chapter 4), generates biogenic sulfide that diffuses outward for consumption by the sulfur-oxidizers. Classically, the components of a nutrient spiral are transported by stream advection, and DIC, sulfate, and allochthonous sulfide move through the system in this manner. However, the effect of the anaerobic system bounded by the oxidizing system is a partial retention of both organic carbon and biogenic sulfide relative to stream advection, which promotes spiraling of sulfur between redox environments.

CONCLUSIONS

Molecular techniques and carbon and sulfur isotope ratio analyses were combined to examine the dynamics of microbial community structure and nutrient cycling in an aphotic sulfidic cave system. Microbial mat bacterial diversity was low overall, with most communities being dominated by several evolutionary lineages within the "*Epsilonproteobacteria*". Certain bacterial groups were found only in one microbial mat morphotype, and most bacterial groups were rarely found

or were completely absent in other morphotypes. The concentrations of dissolved oxygen and dissolved sulfide controlled the distribution of sulfur-oxidizers with differing requirements for oxygen, such that those preferring higher oxygen conditions were found at the end of the microbial mats where dissolved oxygen was highest. The "*Epsilonproteobacteria*" play a significant role in providing chemolithoautotrophic energy to the otherwise nutrient-poor cave habitat. Additionally, these filamentous sulfur-oxidizing bacteria initially colonize the cave springs, forming a dense mat that provides habitat for other bacterial groups with heterotrophic or chemoorganotrophic metabolism (Horner-Devine et al., 2003), and thereby increase mat species richness. The physical model of carbon and sulfur spiraling is based on the energy transfer between redox environments within the mats, and without aerobic and anaerobic metabolic complexity, nutrient spiraling would not occur. Spiraling carbon and sulfur between aerobe and anaerobe, autotroph and heterotroph, significantly extends the mat community.

Table 2-1: Geochemical parameters from representative Lower Kane Cave spring and stream water samples from August 2001, reported in $mmol \cdot L^{-1}$, unless otherwise noted.

Site	pH	T ($^\circ$C)	Cond (μS)	DO[a] ($\mu mol \cdot L^{-1}$)	S^{2-}[b] ($\mu mol \cdot L^{-1}$)	NPOC[c] ($mg\ C \cdot L^{-1}$)	Na^+	K^+	NH_4^+	Ca^{2+}	Mg^{2+}	HCO_3^-	Cl^-	NO_3^-	SO_4^{2-}	Si
Fissure																
Spring (118 m)	7.3	22	580	<0.2	39.7	0.66	0.25	0.009	0.012	1.69	0.94	3.43	0.12	0.001	1.19	0.17
Upper																
Spring (189 m)	7.39	21.3	577	<0.2	35.3	0	0.26	0.009	0.025	1.75	0.96	3.46	0.14	0.001	1.15	0.17
Stream																
Channel (205 m)	7.43	22	587	40	5.6	0.2	0.25	0.008	0.014	1.74	0.92	3.48	0.14	0.001	1.22	0.17
Lower																
Spring (248 m)	7.22	22.1	575	<0.2	39.4	0.13	0.25	0.009	0.025	1.66	0.91	3.42	0.13	0.002	1.18	0.17

[a] Dissolved oxygen, measured by the rhodazine D colorimetric method (CHEMetrics).
[b] Dissolved sulfide (as total dissolved sulfide, including H_2S and HS^-), measured by the methylene blue colorimetric method (CHEMetrics).
[c] Nonpurgable organic carbon, including methane.

Table 2-2: Biomass estimates and elemental analyses for microbial mat morphotypes. Site locations refer to distance (in meters) from the back of the cave.

Site (m)	Mat morphotype	Biomass (10^{10}cells·ml^{-1})	C:N	% N	% S
118	Gray sediment	2.9	28.8	0.3	0.3
120	Gray filaments & sediment		28.0	0.3	0.5
125	Gray sediment	2.6	17.1	0.4	1.5
128	Gray filaments & sediment		9.5	1.2	1.0
189	Gray sediment	1.8	23.6	0.2	1.7
192	Gray filaments	7.6	13.8	0.2	2.1
198	Gray filaments	0.73	7.9	0.6	1.3
203	Gray filaments	1.8	6.8	2.3	2.0
204	Gray filaments		6.0	3.9	2.0
248	Gray filaments	4.7	35.1	0.2	1.8
248	Gray filaments		6.7	5.5	1.5
120	White filaments		5.4	0.7	24.4
128	White filaments & webs		5.1	4.2	17.7
189	White filaments		3.6	4.1	38.1
192	White filaments		4.4	4.0	51.2
192.5	White filaments		3.6	6.1	41.6
196.5	White filaments		5.3	2.4	16.1
198	White filaments	1.8	5.2	2.4	26.7
201	White feathers		4.2	7.3	16.1
201	White filaments	1.8	3.5	4.6	26.6
203	White filaments		4.2	5.5	50.0
248	White filaments		4.9	5.8	32.7
201	White webs		4.4	2.3	38.5
203	White webs	2.9	4.7	4.1	35.4
248	White filaments & feathers		6.6	5.6	27.0
204	White feathers	2.0	4.2	6.1	37.3
203	Yellow patches	1.4	4.7	8.1	8.6

Table 2-3: Distribution of bacterial clones as they appeared in the microbial mat clones libraries.

Phylogenetic affiliation [a]	Representative clone sequences and phylotypes	Closest relative [a]	%[a]	19 124f[b][c]	22 127f	57 190f	270 195f	190 198f	127 203f	156 203w	102 203y	125 203g	199 248f	198 248y
				Fissure Spg				Upper Spring					Lower Spg	
Bacteroidetes/Chlorobi														
Group I	LKC3_198.43	Lake clone TLM10/dgge01	97	7										3
Group II	LKC3_156.56	Digestor clone vadinHA54	92							1				
Group III	LKC3_270.15	Groundwater clone ECP-C1	94				1							
Group IV	LKC3_102B.33	Groundwater clone WCHA101	91								1			
Group V	LKC2_127.25	Gas hydrate clone Hyd.B2.1	90						1					
Group VI	LKC3_19.50	Gas hydrate clone Hyd-B2-1	96	1										
Group VII	LKC3_102B.59													
Unclassified	LKC3_156.13	Groundwater clone SJA-36	92							1				
Acidobacterium	LKC3_156.1	Groundwater clone SJA-36	97	1			2		2	46	3			1
Proteobacteria														
"Epsilonproteobacteria"														
Group I	LKC3_22.5 (2)[d]	Sulfidic spring clone sipK119	98	80	66	77	47		2	1	1	1		10
Group II	LKC3_190.31	Sulfidic spring clone sipK94	98	3		28	54	81	29	7	1	1	76	17
Group III	LKC3_127.1 (7)	Sulfidic spring clone sipK119	96	5	4	7	6		30					
Group IV	LKC2_270.19 (3)	Groundwater clone 1028	96			8	1							
Group V	LKC3_127.28 (3)	Sulfidic spring clone sipK94	95			4	2		3					2
Group VI	LKC3_156.15	Acid mine clone 44a-B1-1	96	3						11	2			1
Gammaproteobacteria														
Thiothrix unzii	LKC3_22.33	Sulfidic spring clone sipK4	99	12	41	4	4		14					6
Beggiatoa spp.	LKC3_19B.17	*Beggiatoa* MS-81-1c strain	90	4						5				
Pantoea spp.	LKC3_125.3	*Pantoea agglomerans*	99									18		
Serratia spp.	LKC3_125.46	*Serratia marcescens*	99									6		6
Betaproteobacteria														
Group I	LKC3_102B.25	*Thiobacillus* clone 44a-B2-21	94							1				43
Group II	LKC3_198.35 (2)	*Thiobacillus aquaesulis*	95								70			1
Deltaproteobacteria	LKC3_190.37 (3)	*Desulfocapsa thiozymogenes*	96					6		1	1			
Total clones				116	111	127	117	87	81	74	79	26	76	91

[a] Affiliation based on taxonomic classifications from BLAST searches and percent sequence similarity to closest relative. Refer to Figures 2-8 through 2-12.
[b] Clone library reference number.
[c] Meter location along the cave stream; letter corresponds to morphotype: f, white filaments; w, white webs; y, yellowish-white mat; g, gray filaments.
[d] Number in parentheses represents number of phylotypes for each group if more than one, with phylotype defined as ≥98% sequence similarity.

74

Table 2-4: Bacterial clone library coverage and ecological indices.

Library (m)	Mat type[a]	No. clones	Number phylotypes observed	ACE[b,c]	Chao1[c]	Shannon-Wiener (H')[c]	Evenness (E)[d]	Simpson's Index (D)[d]
124	f	116	9	10.55	11.0	1.18	0.49	0.49
127	f	111	4	4.0	4.0	0.88	0.63	0.47
190	f	127	10	10.33	10.05	1.36	0.39	0.65
195	f	117	10	12.0	10.66	1.24	0.54	0.38
198	f	87	3	2.0	2.0	0.28	0.40	0.87
203	f	81	10	14.66	11.62	1.53	0.73	0.45
203	w	74	9	20.84	21.5	1.27	0.52	0.42
203	y	79	7	13.24	10.5	0.55	0.26	0.79
203	g	26	4	8.04	6	0.84	0.37	0.54
248	f	76	1	1.0	1.0	0	0	1.0
248	y	91	11	15.48	14.5	1.69	0.66	0.27

[a] Letter corresponds to morphotype: f, white filaments; w, white webs; y, yellowish-white mat; g, gray filaments.
[b] Abundance-based coverage estimator.
[c] Calculated by EstimateS, ver. 6.01b (http://viceroy.eeb.uconn.edu/estimates).
[d] H', E, and D calculated from equations provided in Hill et al. (2003).

Table 2-5: Percentage of 16S rDNA sequence similarity for Lower Kane Cave clones belonging to the "*Epsilonproteobacteria*."

"*Epsilonproteobacteria*"	Group I (n = 16)	Group II (n = 12)	Group III (n = 10)	Group IV (n = 3)	Group V (n = 3)	Group VI (n = 5)
Group I	99.1-100.0					
Group II	85.0-87.4	99.4-100.0				
Group III	94.6-98.6	85.0-91.5	91.0-99.8			
Group IV	92.9-98.2	85.0-90.6	88.7-97.9	95.0-97.9		
Group V	89.3-94.0	93.4-95.7	84.6-92.8	84.5-90.1	97.1-99.5	
Group VI	81.9-83.2	83.8-85.4	82.1-85.2	83.5-81.0	84.5-85.1	99.6-99.9
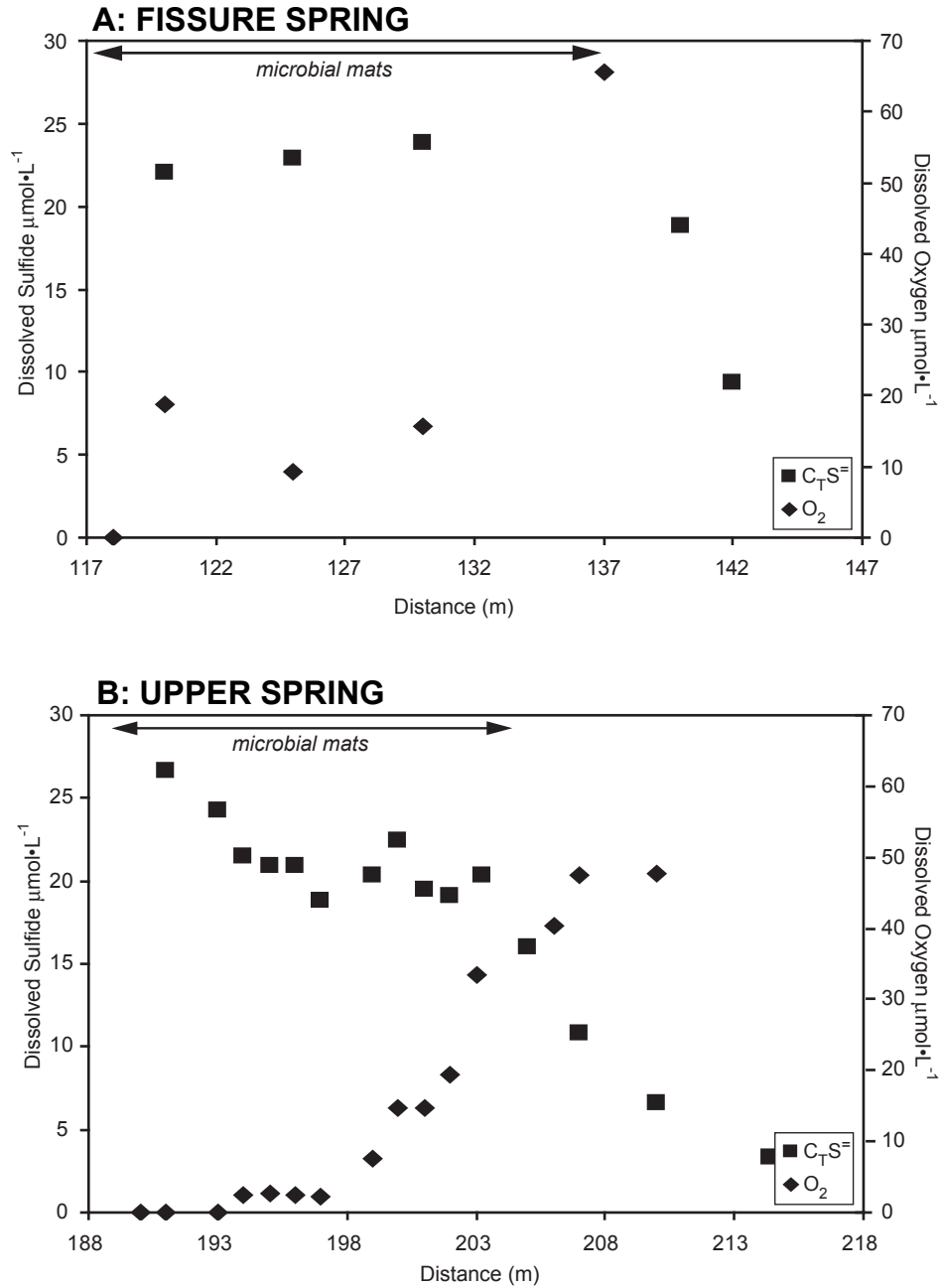
Figure 2-1: Total dissolved sulfide ($C_TS^=$) (■) and dissolved oxygen (◆) versus distance profiles from spring orifice through stream transects for the (A) Fissure Spring and (B) Upper Spring. Distance was measured from the back of the cave to the entrance.

Figure 2-2: Sampling sites, springs, and microbial mats in Lower Kane Cave, Wyoming. Black arrows in all photographs point in the direction of flow. (A) Lower Spring orifice (248 m) occupied by emergent sulfidic groundwater (flowing over the lip at the lower left) and white filament bundles. A thick white filamentous mat forms at the edge of the orifice. Orifice walls are made of limestone, while gypsum occurs around the edge of the orifice pool (upper right). (B) End of thick microbial mat below Lower Spring (248 m). The mat is composed of white filaments and dense gel-like yellow masses. Black spots on rocks at the edge of the mat (upper left) are snails (*Physa spelunca*, 2 mm long). Gas bubbles of carbon dioxide, methane, and hydrogen sulfide gases form in this portion of the mat. (C) Upper Spring Pool (190 m) area, looking upstream, with gray sediment on the orifice pool bottom and white filaments suspended in the water column. Water depth at the deepest part of the pool is ~ 2 m, although average water depth is 30 cm. (D) Upper Spring filament bundles suspended in the water column (190 m). (E) Knobby white webs on the surface of the mat within the Upper Spring channel (203 m). Thin white filaments are suspended in the water column above the webs. (F) Yellowish-white patches within white filament area at 203 m from the Upper Spring channel. Chert fragments are the stream bed substrate (lower center and lower left). Gas bubbles have also been observed at this locale. (G) Fissure Spring orifice (118 m). The orifice pool area consists of limestone cobbles and gray sediment, mostly clay. (H) Thin white filament bundles and white webs in the Fissure Spring outflow channel (125 m). Gas bubbles are also present.
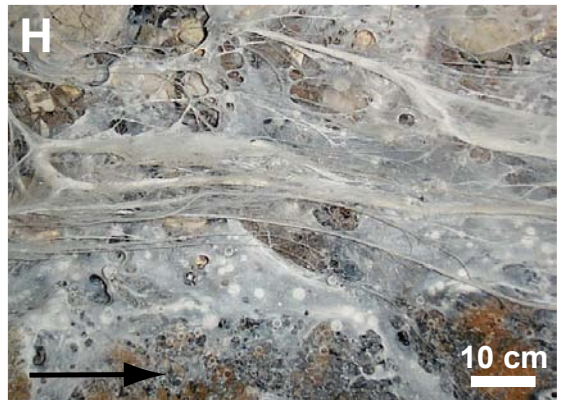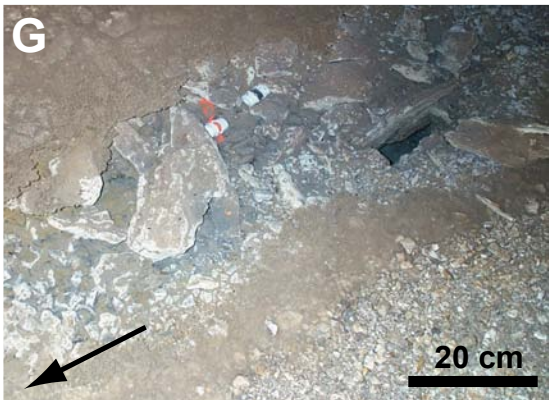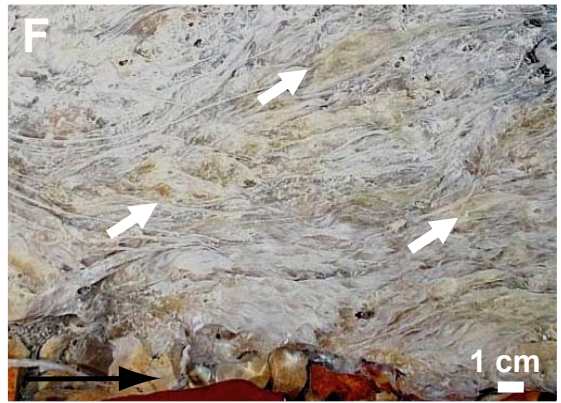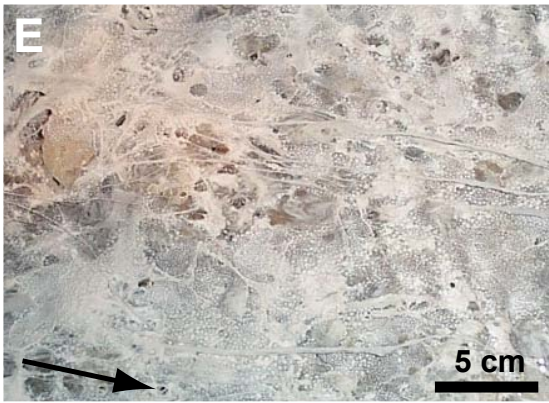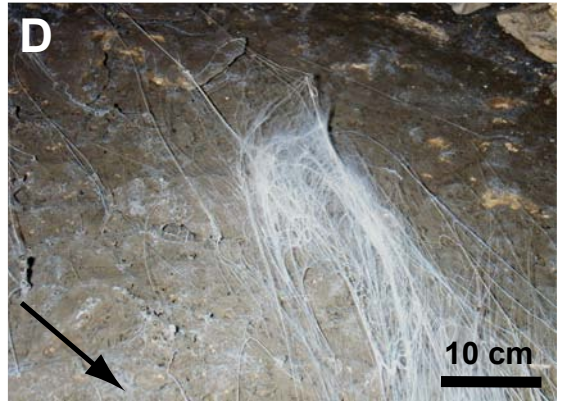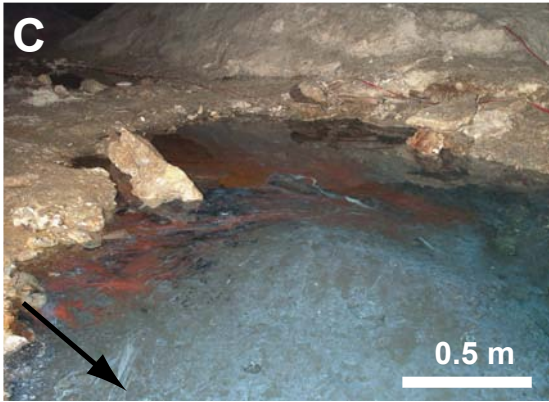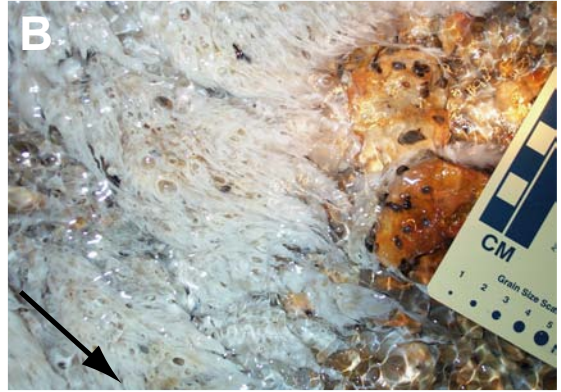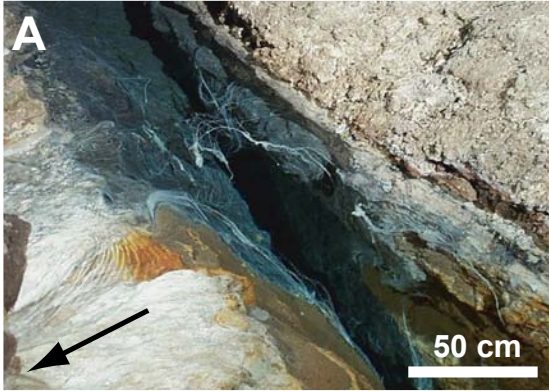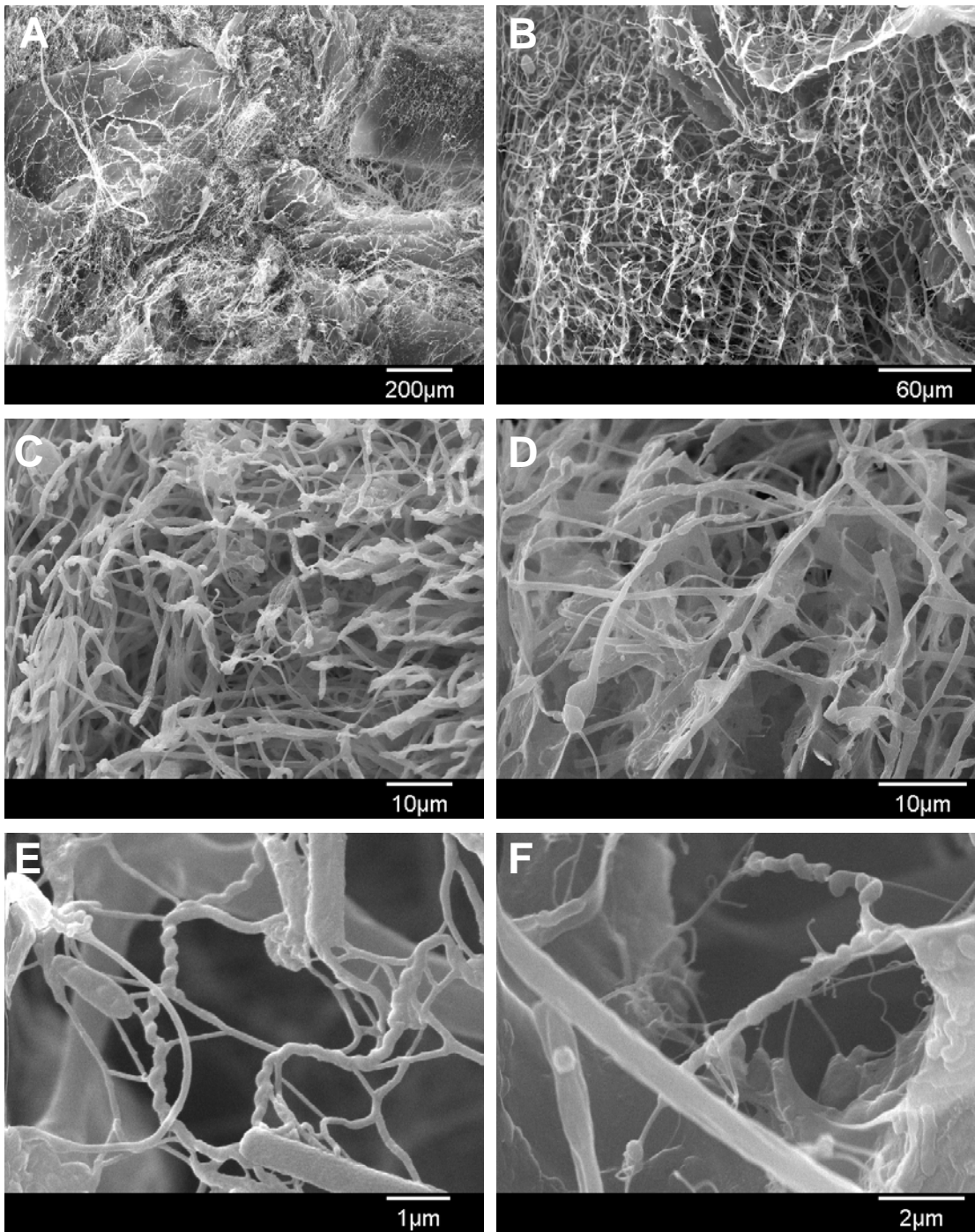
Figure 2-3: Scanning electron photomicrographs of white filamentous biomass from the 203 m sampling location in Lower Kane Cave, Wyoming. A 30 kV accelerating voltage was used. (A) and (B) Filament networks. (C) and (D) Branching and non branching filaments. (E) Twisted filaments and rods. (F) Filaments with intracellular sulfur.

79
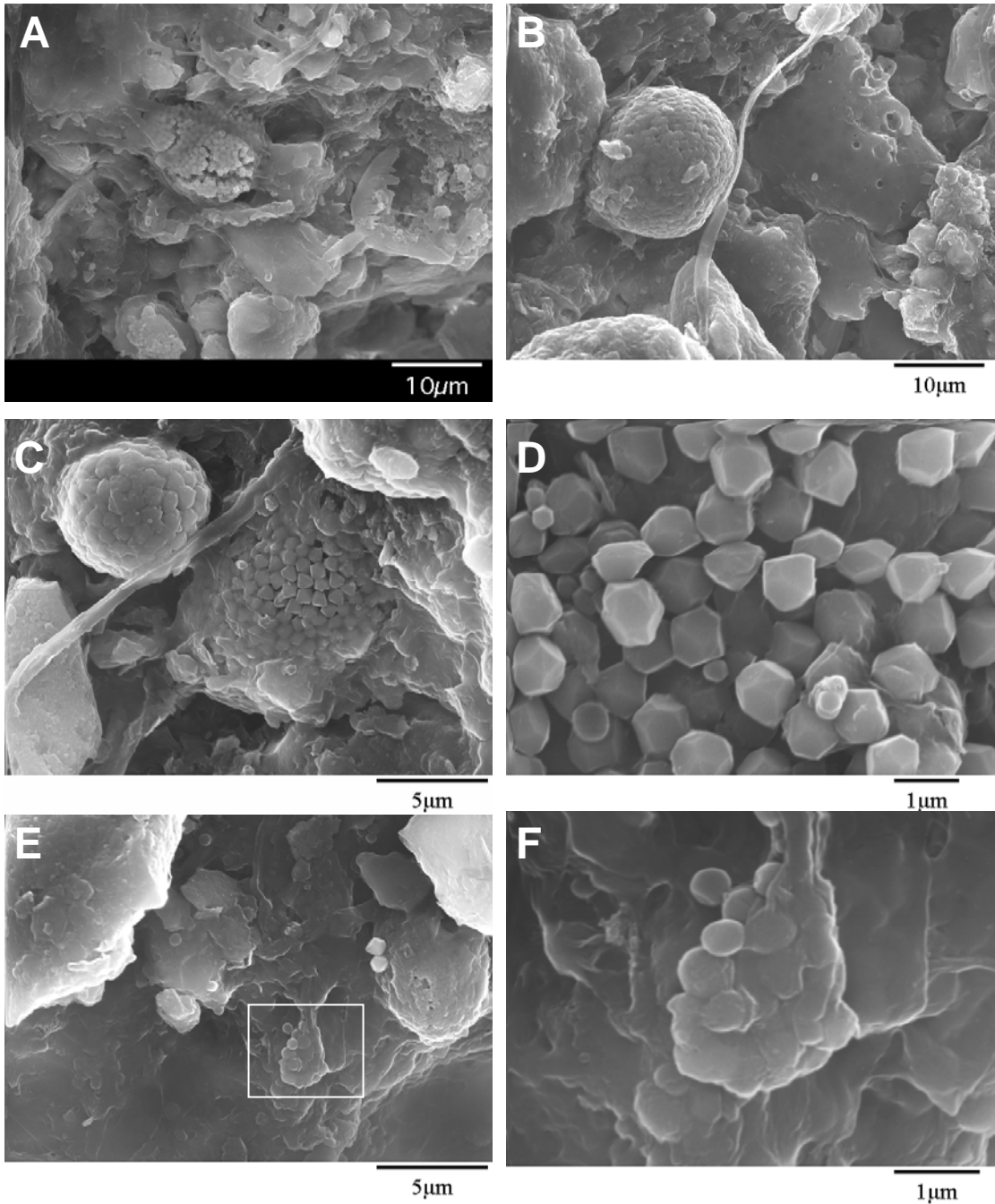
Figure 2-4: Scanning electron photomicrographs of gray sediment from the Upper Spring orifice (189-190 m). (A-C) Organic material and Fe-S framboids; (D) Close-up of individual Fe-S crystallites; (E) Biological material and cluster of cells (outlines in box) for photomicrograph (F) Cluster of cocci. Accelerating voltage for all images was 30 kV.
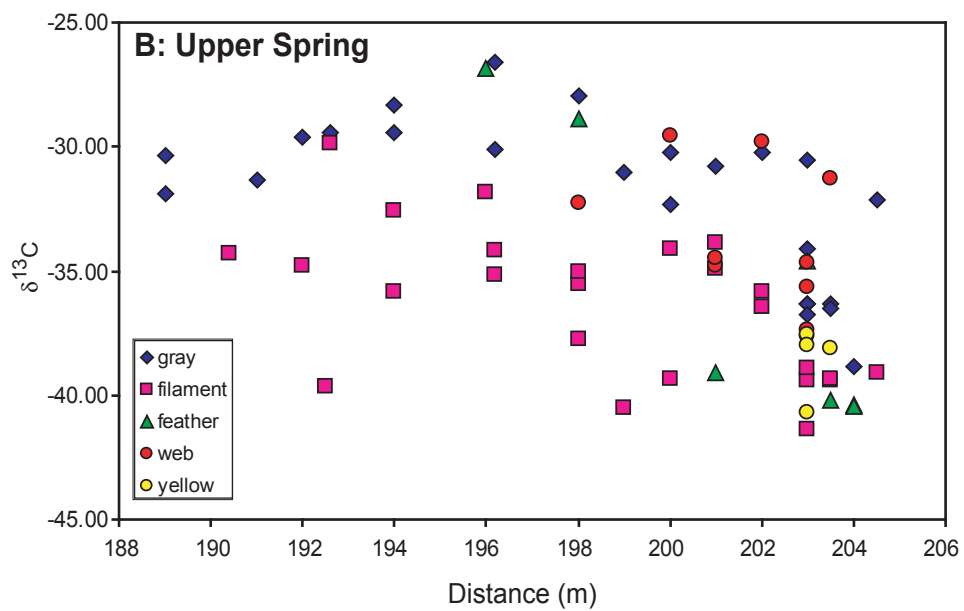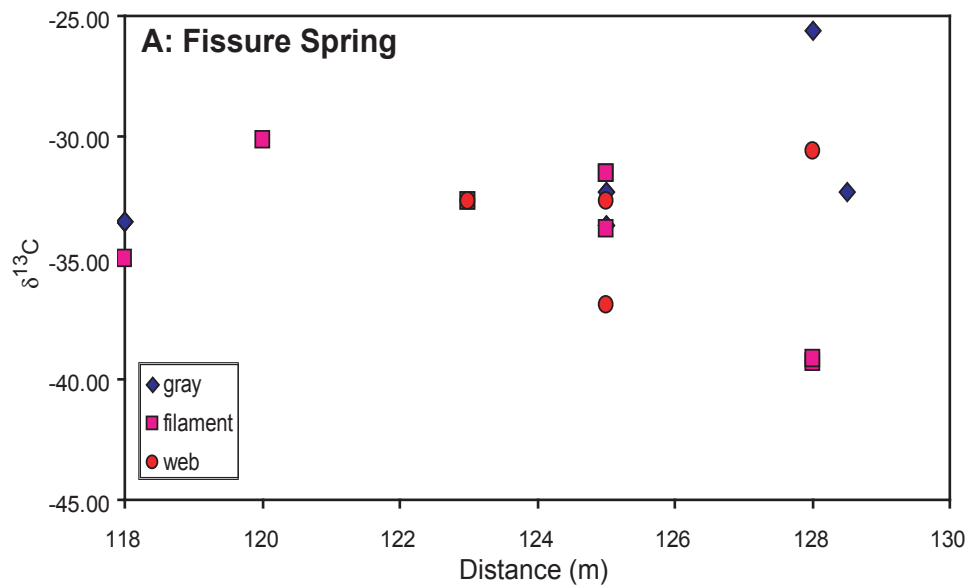
Figure 2-5: Carbon isotope composition of microbial mat morphotypes from (A) the Fissure Spring and (B) the Upper Spring.
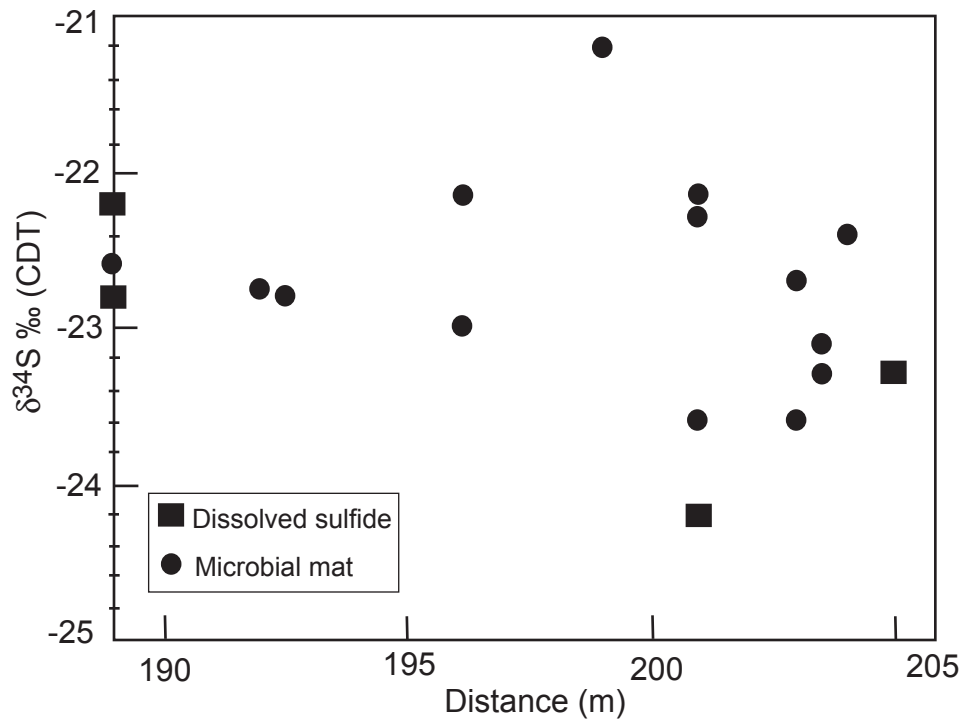
Figure 2-6: $\delta^{34}S$ values of dissolved sulfide (■) and bulk samples of white filamentous microbial mats (●) dominated by "*Epsilonproteobacteria*" versus distance along the Upper Spring flowpath.
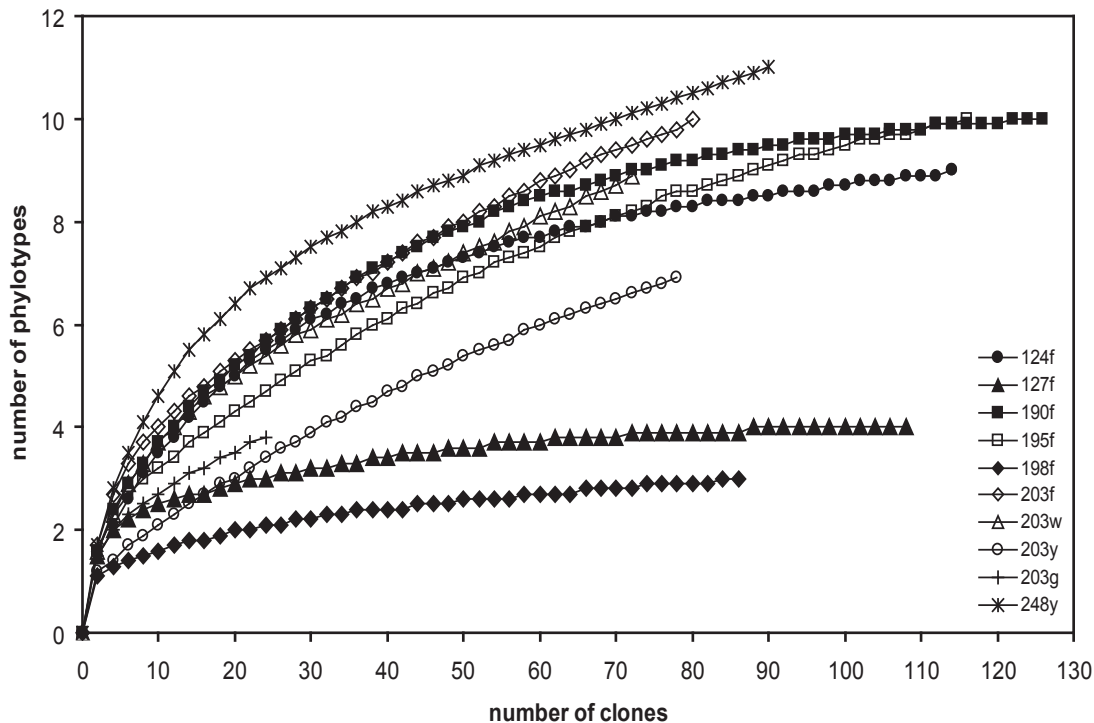
Figure 2-7: Rarefaction curves of the diversity in ten of the eleven 16S
rRNA gene sequence bacterial clone libraries based on phylo-
types identified from restriction fragment length polymorphism
(RFLP) patterns. Library 248f was excluded because only
one RFLP phylotype was identified.

Figure 2-8:   16S rRNA gene-based phylogenetic tree showing the phylogenetic position of clones from Lower Kane Cave within the *"Epsilonproteobacteria"*. Clones are labeled in bold with corresponding sample and clone numbers. Reference sequences (with GenBank accession numbers) were chosen to represent the diversity of the *"Epsilonproteobacteria"*. The tree was rooted with *Proteobacteria* representatives and other bacterial divisions. The tree is a representative topology from 188 trees of the same score inferred from minimum evolution analysis, with the differences among the minimum evolution trees due only to changes in the relative position of sequences within clades of Lower Kane Cave clones. The phylogenetic affiliations of the clones were confirmed by comparison with different reconstruction methods. Numbers along tree branches refer to support values for each node, corresponding to minimum evolution bootstrap proportions, MLga and BMCMC posterior probabilities (see text for details).

LKC3 22.17 [AY510189]
LKC3 57B.57 [AY510193]
Sulfidic spring clone sipK119 [AJ307940]
LKC3 22.54 [AY510180]
LKC3 57B.49 [AY510194]
LKC3 57B.17 [AY510188]
LKC3 22.53 [AY510181]
LKC3 57C.15 [AY510190]
LKC3 57C.33 [AY510195]
LKC2 270.64 [AY208817]
LKC2 57.8 [AY208807]
LKC3 57B.2 [AY510196]
LKC3 22.5 [AY510183]
LKC3 198.20 [AY510185]
LKC3 57.20 [AY510184]
LKC3 127B.2 [AY510182]
LKC3 19.39 [AY510191]
LKC3 22.81 [AY510192]
LKC3 198.15 [AY510186]
Petroleum-contaminated groundwater clone 1043 [AB030601]
Uncultured groundwater clone FTL212 [AF529098]
LKC3 22.72 [AY510167]
LKC3 57B.41 [AY510197]
Petroleum-contaminated groundwater clone 1049 [AB030606]
Petroleum-contaminated groundwater clone 1011 [AB030607]
Sulfuricurvum kujiense [AB080643]
LKC3 57B.22 [AY510200]
Cesspool Cave clone group CC-4 [AF207530]
LKC3 57C.10 [AY510199]
LKC2 270 19 [AY208816]
Cesspool Cave clone group CC-9 [AF207534]
Groundwater clone RA9C8 [AF407391]
LKC3 127.40 [AY510174]
LKC3 127.14 [AY510175]
LKC2 127.32 [AY208810]
LKC3 127.6 [AY510169]
LKC3 127.46 [AY510170]
LKC3 127.23 [AY510173]
LKC3 127B.27 [AY510171]
LKC3 127.39 [AY510172]
LKC3 57B.54 [AY510168]
LKC3 127B.26 [AY510177]
LKC3 270.5 [AY510187]
LKC3 127.43 [AY510176]
Petroleum-contaminated groundwater clone 1023 [AB030610]
Petroleum-contaminated groundwater clone KB2C [AB07495]
LKC2 270.16 AY208815]
LKC3 270.58 [AY510178]
LKC3 127.1 [AY510179]
LKC3 270.13 [AY510198]
LKC3 57B.56 [AY510201]
Thiomicrospira sp. [U46506]
Thiomicrospira denitrificans [L40808]
Pele's Vent clone PVB 55 [U15105]
Sulfurimonas autotrophica [AB088432]
Thiovulum sp. [M92323]
Meromictic lake sediment clone PENDANT-10 [AF142923]
Sulfidic spring clone sipK94 [AJ307941]
LKC3 190 31 [AY510209]
LKC3 127.4 [AY510206]
LKC3 102.21 [AY510214]
LKC3 57.4 [AY510210]
LKC3 270.57 [AY510215]
LKC3 159.12 [AY510213]
LKC3 156.14 [AY510208]
LKC3 127.29 [AY510216]
LKC3 125.31 [AY510207]
LKC3 57C.13 [AY510212]
LKC3 199.1 [AY510205]
LKC3 198.26 [AY510211]
LKC2 127 53 [AY208813]
Deep-sea hydrothermal field strain EM9I37-1 [AB091299]
Alvinella pompejana epibiont [L35521]
LKC3 127.36 [AY510203]
LKC3 127.28 [AY510204]
LKC3 198B.17 [AY510202]
Parker Cave clone SRang51 [AF047630]
Activated sludge clone rA10 [AF047626]
Hydrocarbon seep sediment clone GCA014 [AF154101]
Hydrothermal vent clone 49MY [AB091293]
Marine sediment clone NKB9 [AB013261]
Marine sediment clone JTB315 [AB015258]
Marine sediment clone a2b004 [AF420345]
Deep-sea hydrothermal field clone 42BKT [AB091292]
Deep-sea hydrothermal field strain E9S37-1 [AB091300]
Sulfidic spring clone ZB50 [AY327163]
Hydrothermal vent clone VC2_1 Bac1 [AF068783]
Riftia pachyptila's tube clone R103-B22 [AF449234]
Estuarine sediment clone 2BP-7 [AF121887]
Benzene-mineralizing consortium clone SB-17 [AF029044]
Rimicaris exoculata ectosymbiont [U29081]
Parker Cave clone SrangJ [AF047633]
Sulfidic spring clone ZB43 [AY327156]
Parker Cave clone SRang1.27 [AF047626]
Sulfidic groundwater clone 1065 [AB030598]
Candidatus 'Arcobacter' *sulfidicus* [AY035822]
Marine sediment clone NB1-k [AB013832]
Arcobacter butzlerii [L14626]
Oilfield groundwater strain FWKOB [AF144693]
Geospirillium sp. [Y18254]
Petroleum-contaminated groundwater clone 1014 [AB030587]
Sulfurospirillum deleyianum [Y13671]
Campylobacter jejuni [AF393203]
Helicobacter winghamensis [AF363063]
Flexispira rappini [AF034135]
Helicobacter pylori isolate MC123 [U01328]
Wolinella succinogenes [AF273252]
LKC3 156.15 [AY510218]
LKC3 102B.55 [AY510219]
LKC3 156.74 [AY510217]
LKC3 156.38 [AY510221]
LKC3 102B.15 [AY510220]
Acid mine drainage clone 44a-B1-40 [AY082468]
Acid mine drainage clone 44a-B1-1 [AY082456]
Petroleum-contaminated groundwater clone 1070 [AB030590]
Caminibacter hydrogeniphilus [AJ309655]
Nautilia lithotrophica [AJ404370]
Desulfocapsa thiozymogenes [X95181]
Desulfovibrio fairfieldensis [U42221]
Hydrogenophaga pseudoflava [AF078770]
Leptothrix.discophora [L33975]
Thiobacillus 44a.B2.21 [AY082471]
Thiothrix unzii [L79961]
Beggiatoa sp. [AF110276]
Escherichia coli K12 [NC_000913]
Cytophaga .sp [AB015525]
Bacteroides sp. [AB021162]
Thermotoga.subterranea [U22664]
Thermus aquaticus [L09663]

LKC Group I
LKC Group IV
LKC Group III
LKC Group II
LKC Group V
LKC Group VI

"*Epsilonproteobacteria*"

Miscellaneous strains & clones (marine & freshwater)

Arcobacter
Geospirillum
Sulfurospirillum
Campylobacter
Helicobacter/ Flexispira
Wolinella

Caminibacter
Nautilia

Outgroups

99/89/-
64/-/-
99/89/-
61/-/-
64/-/-
56/-/-
68/-/-
52/-/-
/-/100
97/100/100
99/100/100
72/100/100
100/100/100
90/100/100
53/-/-
50/-/-
98/94/80
86/-/-
85/88/100
85/88/100
100/100/99
85/100/100
60/100/-
-/62/-
77/-/99
-/81/100
-/64/-
94/100/100
77/100/71
73/-/56
67/75/100
78/-/65
68/100/100
91/100/100
96/100/100
67/100/100
56/-/-
90/-/69
100/100/100
-/69/-
71/-/-
87/100/100
99/100/100
65/-/-
100/100/100
100/100/100
100/100/100
83/100/100
100/100/100
96/88/100
99/100/100
94/100/100
-/-/81
-/88/100
100/100/100
95/100/-
81/-/79
91/-/-
100/100/100

─ 0.01 substitutions/site

85

Figure 2-9: 16S rRNA gene-based phylogenetic tree showing the phylogenetic position of *Gammaproteobacteria* bacterial clones from Lower Kane Cave. Clones are labeled in bold with corresponding sample and clone numbers. Reference sequences (including GenBank accession numbers) were chosen from the RDP to represent the diversity of each division. Each tree was rooted with different members of the *Proteobacteria* and other bacterial divisions. Tree topology was inferred from the results of minimum evolution (ME) analysis, and the phylogenetic affiliations of the clones were confirmed by comparison with different reconstruction methods. This tree is a representative topology from 14 trees. Numbers along tree branches refer to support values for each node corresponding to ME bootstrap proportions, MLga and BMCMC posterior probabilities.

86
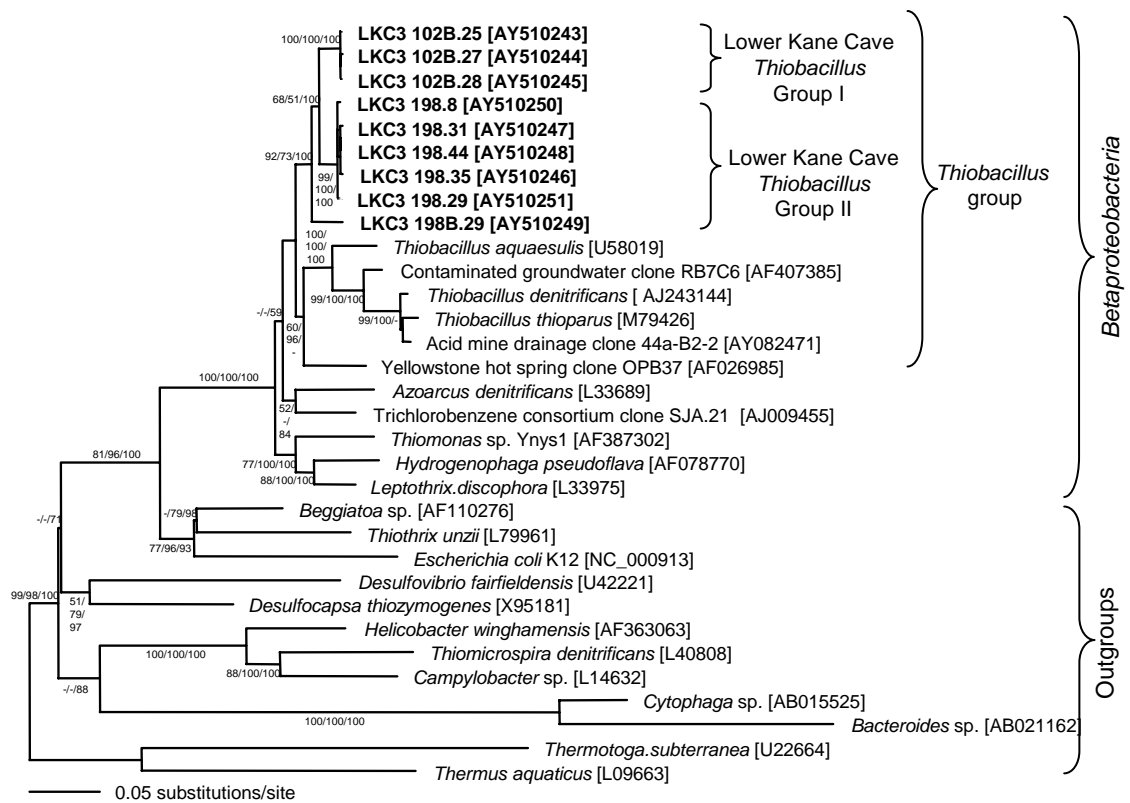
Figure 2-10: 16S rRNA gene-based phylogenetic trees showing the phylogenetic position of *Betaproteobacteria* bacterial clones from Lower Kane Cave. Clones are labeled in bold with corresponding sample and clone numbers. Reference sequences (including GenBank accession numbers) were chosen from the RDP to represent the diversity of each division. Each tree was rooted with different members of the *Proteobacteria* and other bacterial divisions. Tree topology was inferred from the results of minimum evolution (ME) analysis, and the phylogenetic affiliations of the clones were confirmed by comparison with different reconstruction methods. This tree is a representative topology of 2 trees of the same score inferred from ME analyses, with the differences among the ME trees from the same search due only to changes in the relative position of sequences within clades of the LKC clones. Numbers along tree branches refer to support values for each node corresponding to ME bootstrap proportions, MLga and BMCMC posterior probabilities.

87

-/84/79
Desulfocapsa thiozymogenes [X95181]
Lake clone SRB-348 [AJ389628]
84/100/- **LKC3 190.63 [AY510263]**
Sulfidic spring clone sipK108 [AJ307944]
83/100/100 Lake clone SRB-282 [AJ389626]
Desulfocapsa isolate Cad626 [AJ511275]
100/98/100 **LKC3 190.28 [AY510266]**
LKC3 190.37 [AY510265]
LKC3 190.75 [AY510267]
63/-/- -/94/ **LKC3 102.22 [AY510264]**
100 100/95/100 Contaminated groundwater clone WCHB1-67 [AF050536]
Vent sediment clone C1 B030 [AF420366]
82/53/100 73/-/62 *Desulfocapsa sulfoexigens* [Y13672]
Geobacter sulfurreducens [U13928]
-/64/85 96/100/87 Antarctica sediment *Desulfobacula* clone SB4-98 [AY177803]
56/-/- Antarctica sediment *Desulfuromonadales* clone LH5-30 [AY177804]
-/-/81 *Desulfovibrio fairfieldensis* [U42221]
90/76/88 *Beggiatoa* sp. [AF110276]
77/94/69 *Thiothrix unzii* [L79961]
62/77/- *Escherichia coli* K12 [NC_000913]
99/99/100 Acid mine drainage clone 44a-B2-2 [AY082471]
100/100/100 *Hydrogenophaga* pseudoflava [AF078770]
100/100/100 *Leptothrix.discophora* [L33975]
84/100/100 *Thiomicrospira denitrificans* [L40808]
Campylobacter sp. [L14632]
100/100/100 100/100/100 *Helicobacter winghamensis* [AF363063]
Bacteroides sp. [AB021162]
100/100/100 *Cytophaga* sp [AB015525]
Thermotoga subterranea [U22664]
Thermus aquaticus [L09663]

Desulfocapsa

Deltaproteobacteria

Outgroups

0.05 substitutions/site

Figure 2-11: 16S rRNA gene-based phylogenetic trees showing the phylo-
genetic position of *Deltaproteobacteria* bacterial clones from
Lower Kane Cave. Clones are labeled in bold with
corresponding sample and clone numbers. Reference sequences
(including GenBank accession numbers) were chosen from the
RDP to represent the diversity of each division. Each tree was
rooted with different members of the *Proteobacteria* and other
bacterial divisions. Tree topology was inferred from the results
of minimum evolution (ME) analysis, and the phylogenetic
affiliations of the clones were confirmed by comparison with
different reconstruction methods. The ME analysis of the
Deltaproteobacteria alignments resulted in a single tree.
Numbers along tree branches refer to support values for each
node corresponding to ME bootstrap proportions, MLga and
BMCMC posterior probabilities.
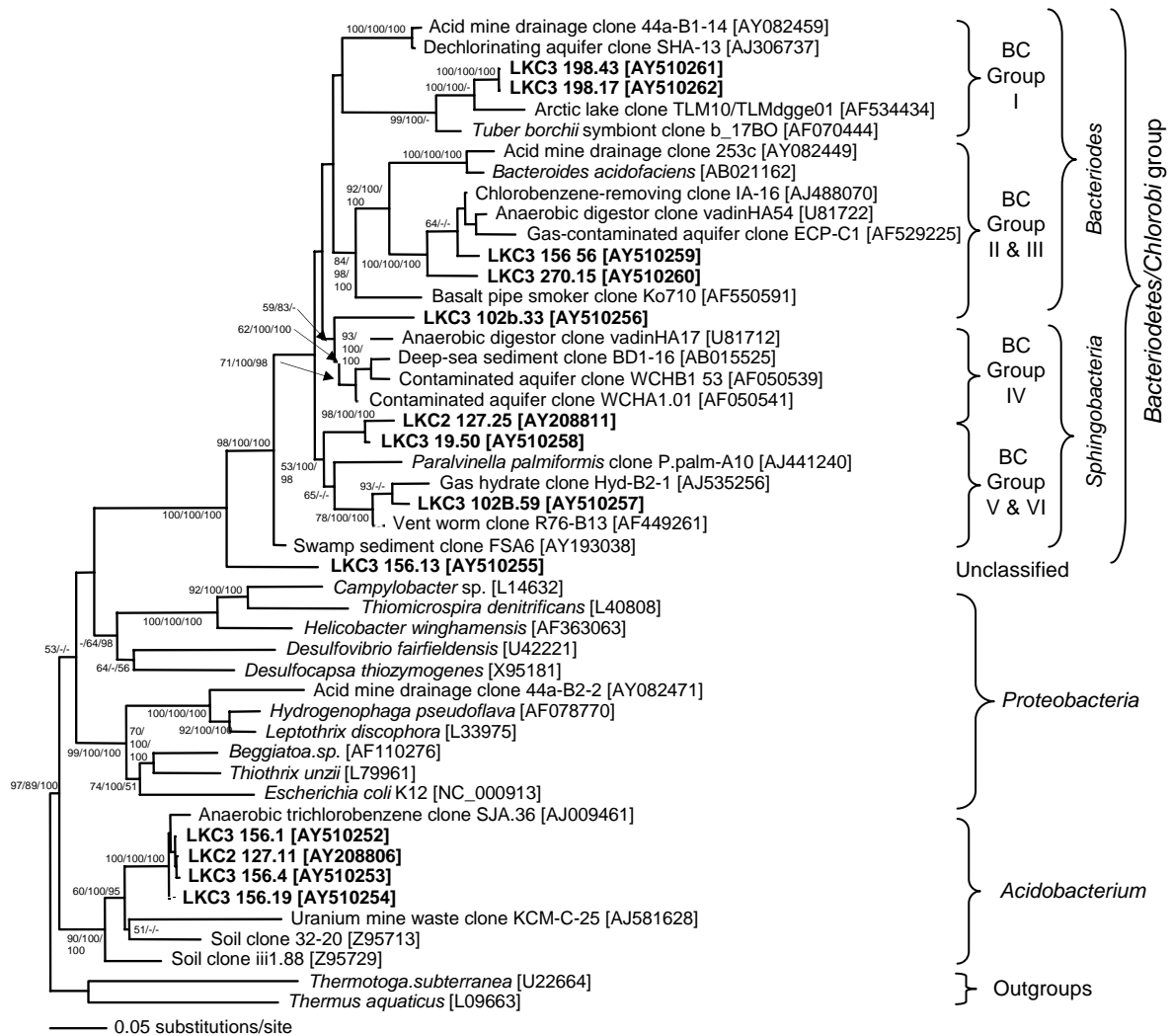
Figure 2-12: 16S rRNA gene-based phylogenetic trees showing the phylogenetic position of Bacteroidetes/Chlorobi and Acidobacterium bacterial clones from Lower Kane Cave. Clones are labeled in bold with corresponding sample and clone numbers. Reference sequences (including GenBank accession numbers) were chosen from the RDP to represent the diversity of each division. Each tree was rooted with different members of the *Proteobacteria* and other bacterial divisions. Tree topology was inferred from the results of minimum evolution (ME) analysis, and the ME analysis of the Bacteroidetes/Chlorobi-Acidobacterium alignments resulted in a single tree. Numbers along tree branches refer to support values for each node corresponding to ME bootstrap proportions, MLga and BMCMC posterior probabilities.

89

Chapter 3: Prevalence of Novel "*Epsilonproteobacteria*" from Filamentous Microbial Mats in Sulfidic Caves and Springs

ABSTRACT[1]

A molecular phylogenetic approach and fluorescence in situ hybridization (FISH) were used to survey white filamentous microbial mat populations in Lower Kane Cave, Wyoming. FISH probes were designed from thirty-two 16S ribosomal DNA (rDNA) gene sequences obtained from Lower Kane Cave clones belonging to two distinct clusters within the *"Epsilonproteobacteria,"* designated LKC group I and LKC group II. FISH proved to be an efficient tool for identifying and quantifying the previously uncharacterized, filamentous *"Epsilonproteobacteria"* from the cave microbial mats. Bacterial group quantification from six different Lower Kane Cave mat samples indicated that filamentous LKC group II populations dominated most of the bacterial communities (≤70% of the total bacteria). The microbial mats from Lower Kane Cave represent the first non-marine natural system demonstrably driven by the activity of *"Epsilonproteobacteria"*. Moreover, to demonstrate that these novel *"Epsilonproteobacteria"* are broadly distributed throughout sulfidic terrestrial habitats, occupying a range of physicochemical conditions, microbial mats from three additional sulfidic caves and nine surface-discharging mesothermal and thermal sulfidic springs were examined using lineage-specific

epsilonproteobacterial PCR primers based on the LKC sequences. Microbial mats from four geographically-distinct sulfidic caves in the USA and Italy, and nine surface-discharging springs were examined. Of the sites surveyed, positive amplification of 16S rDNA was obtained for both LKC groups I and II from two caves and five springs, ranging in water temperature from 8°C to 55°C. Several sites only had one group present. This work expands the evolutionary history and biogeographic diversity of the *"Epsilonproteobacteria"* and demonstrates the importance of this class to widespread biogeochemical cycling in terrestrial sulfidic habitats.

INTRODUCTION

The *"Epsilonproteobacteria"* class is, by and large, the most poorly characterized division within the *Proteobacteria* (Garrity and Holt, 2001; On, 2001). At present, the *"Epsilonproteobacteria"* consists of two genetically distinct orders, the *"Campylobacterales"*, and the *Nautiliales* (Miroshnichenko et al., 2004). The family *Campylobacteraceae* comprises the genera *Campylobacter*, *Arcobacter*, *Sulfurospirillum*, and *Thiovulum*, the family *"Helicobacteraceae"* is formed by the genera *Helicobacter* and *Wolinella*, and the family *Nautiliaceae* consists of the genera *Nautilia* and *Caminibacter* (Vandamme and De Ley, 1991; Miroshnichenko et al., 2004). While several genera within this group have been well characterized, such as *Helicobacter* and *Campylobacter* because of pathogenicity (On, 2001), most lineages have only been described from environmental 16S rRNA-based phylogenetic studies. Moreover, of all the genera described, *Thiovulum* and *Sulfurospirillum* are not associated with metazoans.

91

Many as yet uncultured phylogenetic groups have been characterized from environmental sequences retrieved from marine settings, including seawater and muds (Todorov et al., 2000; Madrid et al., 2001), deep-sea hydrothermal vent sites (Reysenbach et al., 2000; Corre et al., 2001; Longnecker et al., 2001; Takai et al., 2003), and associated with vent metazoans (Moyer et al., 1995; Reysenbach et al., 2000; Corre et al., 2001; Longnecker and Reysenbach, 2001; López-García et al., 2003; Takai et al., 2003; Alain et al., 2004). Recent culture-based investigations expanded the metabolic diversity of evolutionary groups from marine habitats (Takai et al., 2003; Alain et al., 2004), and several studies have resulted in new genera and species descriptions (Alain et al., 2002; Miroshnichenko et al., 2002; Alain et al., 2004; Miroshnichenko et al., 2004). In many investigations, "*Epsilonproteobacteria*" are characterized as mesophiles and occupy environments with low oxygen tensions, but many strains that have been isolated can also grow in the absence of oxygen (e.g., Luijten et al., 2003), and have been implicated in sulfur cycling, and especially oxidation (e.g., Finster et al., 1997; Gevertz et al., 2000; Nemati et al., 2001; On, 2001; Takai et al., 2003).

Comparatively, epsilonproteobacterial groups identified from terrestrial environments are only now being recognized (e.g., Engel et al., 2003), as little is known about the diversity, ecophysiology, and biogeochemical importance of terrestrial sulfur-based habitats. Environmental sequences of "*Epsilonproteo-bacteria*" have been retrieved from microbial mats at surface-discharging sulfidic springs (Rudolph et al., 2001; Barton et al., 2002; Moissl et al., 2002; Elshahed et al., 2003; Rzonca and Schulze-Makuch, 2003), groundwater associated with

92

hydrocarbons (Gevertz et al., 2000; Watanabe et al., 2000; Watanabe et al., 2002; Kodama and Watanabe, 2003), and caves with sulfidic springs and streams (Angert et al., 1998; Engel et al., 2001); Engel et al. 2003; Engel et al., in review). Kodama et al (2003) and Gevertz et al. (2000) isolated strains of rod-shaped cells from petroleum-contaminated groundwater and oil field production waters, respectively. Relatively little is known about "*Epsilonproteobacteria*" from non-marine settings because the terrestrial subsurface, including groundwater, is often inaccessible for study. However, the subsurface is reachable through caves and springs. Although springs vary geochemically and hydrogeologically, some of the most common types are associated with sulfidic water, and sulfidic caves and springs could be exceptional habitats for "*Epsilonproteobacteria*".

The main purpose of this chapter was to examine terrestrial sulfidic habitats for "*Epsilonproteobacteria*", based on initial 16S rRNA gene characterization of the filamentous microbial mats from Lower Kane Cave, Wyoming (Chapter 2) and previous work from other sulfidic caves (Angert et al., 1998; Engel et al., 2001; Barton et al., 2002). To identify and reliably quantify "*Epsilonproteobacteria*", I designed, evaluated, and applied two new 16S rRNA-targeted oligonucleotide probes specific for the detection of novel *"Epsilonproteobacteria"* using fluorescence in situ hybridization (FISH). With the complementary oligonucleotide sequences to target DNA, I also designed PCR primers to amplify lineage-specific epsilonproteobacterial DNA from microbial mats in other sulfidic caves and surface-discharging springs. The results of this work expand the geographic diversity of *"Epsilonproteobacteria"* to many different sulfidic springs and caves

that have been previously overlooked. The "*Epsilonproteobacteria*" play an important role in the widespread biogeochemical cycling of carbon and sulfur nutrients, and in subterranean geological processes.

MATERIALS AND METHODS

Sample Acquisition from Lower Kane Cave, Wyoming

Two major and two minor anaerobic, sulfidic springs discharge into Lower Kane Cave along a fracture zone (Figure 1-2; see Chapter 1). Samples for DNA extraction were obtained from microbial mats, and 16S rDNA clone libraries were constructed from a subset of six samples from the cave: Fissure Spring orifice white filament bundles (sample 21), Upper Spring orifice white filament bundles (samples 57 and 58), Upper Spring orifice white filament bundles (sample 114), Upper Spring thin white filaments (sample 190), Lower Spring orifice white filament bundles (sample 199), and Lower Spring yellowish-white mat (sample 198). Mat samples used for FISH were collected from the Fissure Spring orifice, Lower Spring orifice, the white filamentous mat from the Lower Spring, Upper Spring orifice, and three white filamentous mat samples from the Upper Spring stream channel (white mat 1, 2, and 3).

Sample Acquisition from Other Sulfidic Caves and Springs

White filamentous microbial mats from four sulfidic cave springs (12 to 22°C), four mesothermal (10 to 33°C) sulfidic surface-discharging springs, and eight thermal sulfidic surface-discharging springs (45 to 65°C) were sampled from the United States and Italy (Table 3-1). The broad geography and geochemical conditions were of interest in order to survey for "*Epsilonproteobacteria*" related to

those from Lower Kane Cave using epsilonproteobacterial-specific PCR primer sets. Refer to Appendix B for descriptions of the field sites. Spring pH and sulfide content were not significantly different (Table 3-1). There were several surface springs with phototrophic microbial biomass associated with the white filamentous mat morphotypes (Appendix B, Figures B-1 through B-10). All of the caves that were sampled formed in limestone or travertine, and almost all of the surface springs discharged from carbonates, either limestone or travertine (Table 3-1). The Lazio springs in Italy issued from volcanics (e.g., rhyolite), although the spring waters were also actively depositing travertine, and Palmetto Spring, Texas, discharged from sandstone, but the spring orifice was in an artificial concrete basin.

DNA Extraction

Approximately 0.2 to 0.5 ml of microbial mat from caves and springs were aseptically collected in the cave and transferred into 0.5 to 1 ml DNA extraction buffer containing 10 mM Tris-HCl (pH 8), 100 mM EDTA, and 2% sodium dodecyl sulfate (SDS). Total community DNA was extracted using an extraction protocol similar to the commercially available Purgene DNA extraction kits (Gentra Systems, Minneapolis, Minnesota), with the following modifications: 9 μl Proteinase K (20 mg/ml) was added to each DNA extraction buffer prior to digestion; a freeze-thaw (3 times at -80°C to 65°C) series was used; samples were incubated at 55°C overnight to digest cellular material; RNase was added to the digests and incubated at 37°C for up to 1 hr; and nucleic acids were precipitated in isopropanol overnight at -20°C.

PCR Amplification

For Lower Kane Cave samples, nearly full-length 16S rDNA gene sequences were PCR-amplified using the primer pairs 27f (forward, 5'-AGAGTTTGATCCTGGCTCAG-3') and 1492r (reverse, 5'-GGTTACCTT GTTACGACTT-3') for the domain *Bacteria*, according to the protocol described by Lane et al. (1991). Amplification was performed with a Perkin Elmer 9700 thermal cycler by Megan L. Porter at Brigham Young University, Department of Integrative Biology (Provo, Utah). The following conditions were used: denaturation at 95°C for 1 min, primer annealing at 42°C for 1 min, chain extension at 72°C for 1.5 min. Fifty PCR cycles were used. A control tube containing sterile water instead of DNA was used as a negative control.

For other cave and spring samples, 16S rDNA gene sequences were PCR-amplified using lineage-specific epsilonproteobacterial PCR primers designed during FISH probe design from the PROBE-DESIGN tools of the ARB software package (http://www.arb-home.de) (Ludwig and Strunk, 1996). For epsilonproteobacterial LKC group I, the primer pairs 'eps59f' (forward, 5'-AGTCGAACGATGAGAGGA-3') and 1492r for the domain *Bacteria* were used. For epsilonproteobacterial LKC group II, the primer pairs 'eps174f' (forward, 5'-CCCCATACTCCTTCTCAT-3') and 1492r. Amplification was performed in the Jackson School of Geosciences at the University of Texas at Austin with a MJ Research thermal cycler under the following conditions: denaturation at 95°C for 1 min, primer annealing at 45°C for eps59f and 47°C for eps174f for 1 min, chain extension at 72°C for 1.5 min. A control tube containing sterile water instead of

DNA was used as a negative control. Thirty cycles were done. PCR bands were visualized by electrophoresis on a 1% agarose gel.

Cloning, Sequencing, and Phylogenetic Analysis of 16S rRNA Genes

Amplified PCR products for Lower Kane Cave samples were purified with the GeneClean II Kit (Bio101, Inc., Vista, California), as recommended by the manufacturer. Purified PCR products were cloned using the TOPO TA Cloning Kit (Invitrogen, San Diego, California), following manufacturer's instructions.

The 16S rDNA clones obtained from Lower Kane Cave were lysed in 50 µl buffer (10mM Tris-HCl; 0.1 mM EDTA, pH 8.0) for 10 min at 96°C. Clones were randomly selected for sequencing, and sequence inserts were then PCR-amplified from lysed cells using plasmid-specific primer pairs M13(-20) (5'-GTAAAACGACGGCCAGT-3') and M13(-24) (5'-AACAGCTATGACCATG-3') and the following PCR conditions: denaturation at 94°C for 1 min, primer annealing at 55°C for 1 min, chain extension at 72°C for 3 min, for 35 cycles. PCR products were purified using Sephadex columns and sequenced using an ABI Big-Dye Ready Reaction kit (Perkin Elmer) using the primers 27f and 1492r in conjunction with internal primers 907r (reverse, 5'-CCGTCAATTC CTTTRAGTTT-3') and 704f (forward, 5'-GTAGCGGTGAAATGCGTAGA-3'). Automated DNA sequencing was done on an ABI Prism 377XL sequencer (Perkin Elmer) at Brigham Young University.

The DNA sequences were submitted to the CHECK-CHIMERA program of the Ribosomal Data Base Project (RDP) II at Michigan State University (http://rdp.cme.msu.edu/html/) (Maidak et al., 2001). Clone sequences were

97

subjected to BLAST searches within the GenBank database (http://www.ncbi.nlm.nih.gov/) to determine 16S rRNA gene sequence similarities to culturable and not yet cultured organisms.

The retrieved nucleotide sequences were first aligned using Clustal X (Thompson et al., 1997) and then manually adjusted based on conserved gene primary and secondary configuration. Phylogenetic analyses were done by Megan L. Porter at Brigham Young University, using maximum likelihood, minimum evolution, and maximum parsimony criteria in PAUP* (Swofford, 2000) and Bayesian inference in MrBayes (Huelsenbeck and Crandall, 1997). For minimum evolution, Bayesian inference, and maximum likelihood searches, a model of evolution was chosen based on likelihood ratio tests (Huelsenbeck and Crandall, 1997), as implemented in Modeltest 3.06 (Posada and Crandall, 1998). As an indication of nodal support, bootstrap analyses were performed for maximum likelihood (100 replicates), minimum evolution (500 replicates), and maximum parsimony (1000 replicates). For Bayesian inference analyses, posterior probabilities were used for nodal support. All trees were rooted using *Desulfocapsa thiozymogenes* (X95181) and *Hydrogenophaga pseudoflava* (AF078770) as outgroups.

16S rRNA Oligonucleotide Probes

Oligonucleotide probes specific for two epsilonproteobacterial clone groups from Lower Kane Cave (LKC group I and group II) were designed using the PROBE-DESIGN tools from ARB and probe designations according to Alm et al. (Alm et al., 1996). Probe LKC59 (S-*-eProt-0059-a-A-18) is specific for LKC

98

group I clones, and probe LKC1006 (S-*-eProt-1006-a-A-18) targets LKC group II clones. Probe specificity was verified using the RDP PROBE-MATCH function (Maidak et al., 2001) and the PROBE-MATCH tool of the ARB software package, and a 16S rRNA data set including all publicly available sequences from "*Epsilonproteobacteria*" (at the time of probe design, 238 epsilonproteobacterial GenBank sequences were available for comparison). Sequences and optimal hybridization conditions for probes LKC59, LKC1006, and other probes used, are listed in Table 3-2, including probe EPS710, designed to target environmental clones within the "*Epsilonproteobacteria*" (Watanabe et al., 2000) and *Sulfuricurvum kujiense* (Kodama and Watanabe, 2003). More information about the applied probes can be found at probeBase (http://www.microbial-ecology.net/probeBase) (Loy et al., 2003).

Fluorescence In Situ Hybridization (FISH), Microscopy, and Quantification

For FISH, microbial mat samples were collected and shipped on dry ice to Dr. Michael Wagner and Dr. Natuschka Lee in the Department of Microbial Ecology, Technische Universität in Munich, Germany. Samples were preserved in two ways (with respect to the general requirements for successful FISH of gram-negative and gram-positive bacteria) within 48 hr of collection: (i) with 4% (wt/vol) paraformaldehyde for 3 hr before final wash with saline phosphate buffer as described by Manz et al. (1992), and (ii) with ice-cold ethanol according to Roller et al. (1994).

I preformed all hybridizations and examined samples using a LSM510 confocal laser scanning microscopy (CLSM) (Zeiss, Oberkochen, Germany) in

Germany. Prepared cells were attached to Teflon-coated nonfluorescence slides and air-dried overnight before dehydrating by sequential washes in 50, 80, and 100% (vol/vol) ethanol for 3 min each. The probes were synthesized and directly labeled with the monofunctional, hydrophilic, sulfoindocyanine dyes indocarbocyanine (Cy3) and indodicarbocyanine (Cy5), or with FluosPrime (5,6-carboxyfluorescein-*N*-hydroxysuccinimide ester), purchased from Hybaid-Interactiva (Ulm, Germany). Hybridization and washes were performed as described by Manz et al. (1992). Briefly, the hybridization solution contained 5 M NaCl, 1 M Tris/HCl (pH 8), 10% [wt/vol] SDS, and formamide (as given in Table 3-2 for each probe). Cy3 and Cy5-labelled probes were applied at 30 ng·μl^{-1} each, while FluosPrime probes were applied at 50 ng·μl^{-1}. Washing buffer consisted of 5 M NaCl, 1 M Tris/HCl (pH 8), 10% SDS, and 0.5 M EDTA (pH 8) and was preheated to 48°C. The wash buffer salt concentration was adjusted to the hybridization buffer formamide concentration according to Manz et al. (1992).

Optimal hybridization stringency for probes EPS710, LKC59, and LKC1006 was determined by increasing the formamide concentration of the hybridization buffer in increments of 5 or 10% while maintaining a constant hybridization temperature of 46°C. Because of a lack of suitable reference cells, the optimal hybridization stringency for the probes was defined by the highest stringency allowing unambiguous visual detection of probe target cells in fixed samples of the white filamentous microbial mats from two different sampling locations ('Upper Spg white mat 1' and 'Upper Spg white mat 3').

To determine the percentage of all cells detected with the bacterial probe set, EUB338I-III mix-hybridized mat samples were additionally stained with 10 μl of a 10,000-fold dilute SYBR Green I (FMS Bioproducts, Rockland, Maine) working solution in the dark for 10 min at room temperature. Slides were then washed briefly with double-distilled H_2O and air-dried. Before examination, samples were covered with the antifading agent Citifluor AF1 (Chemical Laboratory, Caterbury, England). A CLSM equipped with a UV laser (351 and 364 nm), an Ar ion laser (450 to 514 nm), and two HeNe lasers (543 and 633 nm) was used to visualize FISH results. All images were recorded with a Plan-Apochromat 63x (1.4; oil immersion) objective. Image processing was performed with the LSM510 software (version 1.6). Quantification of probe-detected cells was achieved using Carl Zeiss Vision KS400 software in conjunction with the RAM (Relative Area Measurement) macro (Schmid et al., 2000).

Nucleotide Sequence Accession Numbers

The 16S rRNA gene sequences determined in this study, labeled with the prefix "LKC1", were submitted to GenBank, with accession numbers from AY191466 to AY191497.

RESULTS

Phylogenetic Analysis of 16S rRNA Clone Sequences from Lower Kane Cave

From six mat samples, 44 clones were randomly selected for sequencing in order to conduct a broad survey of the microorganisms present in Lower Kane Cave mat communities. Nearly full-length 16S rRNA gene fragments from the

clones were amplified and sequenced. None of the sequences were identified as chimera from RDP analysis. All clone sequences belonged to the *Proteobacteria* division; 85% of the clones were affiliated with the "*Epsilonproteobacteria*", 11% of the clones belonged to the *Betaproteobacteria*, and 4% of the clones clustered within the *Gammaproteobacteria*, and specifically *Thiothrix* spp.

The Lower Kane Cave epsilonproteobacterial clones clustered into two different clades, referred to as LKC group I and LKC group II, with high bootstrap values supporting their phylogenetic position (Figure 3-1), similar to results described in Chapter 2. The closest relatives to both LKC group I and group II were two environmental clones, sipK119 and sipK94, obtained from microbial aggregates with a string-of-pearls-like morphology in sulfidic springs at the Sippenauer Moor, Regensburg, Germany (Rudolph et al., 2001; Moissl et al., 2002). Group I clones, identified from the Fissure and Upper Spring orifice samples, clustered closely (98-99% similar in nucleotide sequence) with clone sipK119 and Cesspool Cave clone group CC-4 (Engel et al., 2001). The closest cultured representative of LKC group I sequences was *Sulfuricurvum kujiense* (Kodama and Watanabe, 2003). LKC group II clones, obtained from Upper and Lower Spring orifice and white mat samples, were closely related to the sipK94 clone (99% similar in nucleotide sequence), and more distantly to various marine and hydrothermal vent clones (91-94% similarity), as well as to Parker Cave clones (92-94% identical) (Angert et al., 1998).

Fluorescence In Situ Hybridization of Lower Kane Cave Microbial Mats

FISH probes were used to identify and to quantify specific microorganisms in the filamentous microbial mats from Lower Kane Cave (Appendix B). Thirty-two clone sequences, thirteen from LKC group I and nineteen from LKC group II (Figure 3-1), were used to design rRNA-specific oligonucleotide probes. Probes LKC59 and LKC1006 targeted clone sequences from group I and group II, respectively, based on the PROBE-MATCH function in the ARB software (Table 3-3). Although LKC group I is closely related to other environmental clones from groundwater and caves (Figure 3-1), probe LKC59 has at least one mismatch with these and all other rRNA gene sequences in the database. Probe LKC1006 also did not target any other sequences in the database, including clone sipK94 which has 99% 16S rRNA gene sequence similarity to LKC group II sequence (Figure 3-1). Another probe for LKC group II was LKC174, targeting base position 174; however, the LKC174 probe did not work for FISH (no hybridization signal was observed), possibly because the 16S rRNA target region was inaccessible; probe LKC174 was disregarded for further FISH analyses. The target sequence was used instead as a PCR primer for LKC group II. Three of the LKC group II clones possess a single mismatch within the target site of probe LKC1006 and might not be detectable by this probe (Table 3-3). These mismatches indicate either actual genetic microheterogeneity or originate from PCR and/or sequencing artifacts.

Optimal hybridization stringency was determined for the newly designed probes, as well as for the previously published probe EPS710 (Watanabe et al., 2000); (Kodama and Watanabe, 2003). Because no cultured strains possessing the

target sites for probes LKC59 and LKC1006 are available, optimal hybridization stringency was inferred by visual comparison of filament fluorescence from cave samples (Figure 3-2; Appendix B). For all three probes, mat filaments showed bright fluorescence if hybridization buffers with up to 30% formamide were used (Figure 3-2); under more stringent conditions (higher formamide concentrations), signal intensity decreased.

In the six samples analyzed, between 68% and 88% of the cells stainable with a general nucleic acid dye (SYBR green I) could be detected with a bacterial probe set (Table 3-2; Appendix B). Of the ten different group- and genus-specific probes applied, positive hybridization signals were observed with the probes BET42a, GAM42a, G123T, and ARCH915. Long filamentous cells hybridized strongly with probes GAM42a and G123T, indicating the presence of *Gammaproteobacteria*, and in particular *Thiothrix* spp., which also hybridized to EUB338I-IIImix (Figure 3-3A and 3-3B). Probe BET42a labeled small rods specifically, but weakly, in all samples (Figure 3-3C), indicating the presence of rare *Betaproteobacteria*. The FISH results for *Betaproteobacteria* and *Gammaproteobacteria* are similar to the results obtained from the 16S rRNA clone libraries (Chapter 2), in that these bacterial groups occur in the mats but are not dominant. In addition to the filamentous *Gammaproteobacteria*, the other filaments (Figure 3-3D) hybridized with EUB338I-IIImix, are likely "*Epsilonproteobacteria*". Interestingly, filaments that hybridized with GAM42a and G123T also hybridized with ARCH915. The PROBE-MATCH function in ARB suggested that the probe ARCH915 targeted some *Thiothrix* sequences,

104

particularly *T. unzii*, and therefore may not be a suitable probe when *Thiothrix* is present. No further analyses with the ARCH915 probe were done (Appendix B).

The three probes targeting subgroups within the *"Epsilonproteobacteria"* were used in different combinations to survey probe overlap. All probes exclusively hybridized to filamentous microbes, and conferred very bright signals to their target cells, indicating high rRNA contents (Amann et al., 1995). Filaments detected by probe LKC59 had an average diameter of 1 μm and appeared kinked or twisted, while straighter, longer, and slightly thicker filaments were detected by LKC1006 (Figure 3-4). Twisted filaments were observed with scanning electron microscopy (Figure 2-3E). Simultaneous hybridization with the epsilonproteobacterial probes LKC59 and EPS710 showed that they stained the same filamentous cells (Figure 3-4, row I), and as expected, neither probe EPS710 nor probe LKC59 overlapped with probe LKC1006 (Figure 3-4, rows II and III). In the study by Watanabe et al. (2000), probe EPS710 hybridized only to short rods during FISH. The different morphologies that hybridize to the EPS710 probe may indicate the potential for more group diversity than previously identified, and that the probe may confer genus-level or higher taxonomic specificity.

Epsilonproteobacterial filaments belonging to LKC group II dominated five of the six microbial mats examined and made up to 70% of the biovolume of those cells detectable by FISH with a bacterial probe set (Table 3-4). Only in Lower Spring white mats, which were dominated by *Thiothrix* spp., epsilonproteobacterial filaments occurred at relatively low numbers (4% of the bacterial biovolume). In contrast, epsilonproteobacterial filaments of LKC group I were below the detection

limit in three of the six samples investigated, and made up less than 10% of the biovolume in the other three samples (Table 3-4).

Distribution of "*Epsilonproteobacteria*" in Other Caves and Springs

The primer sequences for eprot59f (group I) and eprot174f (group II) were analyzed in GenBank for lineage-specificity (Table 3-5). Primer eprot59f showed a perfect match for the clone sipK119, the closest relative to LKC group I sequences. Other sequences, including members of the *Actinobacteria*, had one or more mismatches at the end of the primer. Primer eprot174f showed a perfect match for the epsilonproteobacterial clone T6-ph07-987 from deep-sea experimental chamber associated with *Alvinella* (Alain et al., 2004), but not for clone sipK119 (99% sequence similarity).

Previous 16S rRNA-based studies of several sulfidic springs have revealed the presence of "*Epsilonproteobacteria*" (Engel et al., 2001; Barton et al., 2002; Elshahed et al., 2003; Rzonca and Schulze-Makuch, 2003), and microbial mat samples from several of these sites (e.g., Table 3-1; Lower Kane Cave, Cesspool Cave, Glenwood Springs, and Soda Dam Spring) were used to test the utility of the new primers. Certainly, to verify that the phylogenetic groups of interest were amplified completely, the resulting PCR products should be cloned and sequenced. Additionally, a positive result does not always indicate that the organisms of interest are present if primers are not optimally applied (e.g., by using annealing temperatures that are not stringent). However, positive amplification using lineage-specific primers is a first step to circumvent the need to sequence many products randomly; if PCR is not successful following multiple approaches, no further

106

analyses are likely needed. Moreover, quantification is not possible by using this PCR-based method, so to determine if the groups are numerically important, additional studies using FISH are needed. FISH will also reveal the morphology of the microbial groups, which is important to demonstrate that the epsilonproteobacterial groups that hybridize with the LKC probes are filamentous in other habitats.

Positive PCR amplification with the lineage-specific primers was achieved for many white filamentous microbial mat samples; the general bacterial primer set was also used to verify results. Both epsilonproteobacterial primer sets had positive PCR amplification to Lower Kane Cave samples, as well as from Hellspont Cave and PBS Spring, sites downstream from Lower Kane Cave along the Bighorn River (Table 3-6; Figure 1-3). Based on phylogenetic relationships, the epsilonproteobacterial clone groups identified from Cesspool Cave were closely related to LKC group I (Engel et al., 2001), and PCR amplification with the eps59f/1492r primer set showed positive amplification, but not with the LKC group II primers (Table 3-6). "*Epsilonproteobacteria*" were also described from 16S rDNA investigations from the Drinking Spring at Glenwood Springs, Colorado (Barton et al., 2002), and Soda Dam spring, New Mexico (Rzonca and Schulze-Makuch, 2003); successful PCR amplification was obtained using both primer sets for Glenwood Springs, and only the eps59f/1492r set for Soda Dam spring (Table 3-6). PCR amplification with the eps59f/1492r primers was successful for mat samples from all the sulfidic caves and several springs (Table 3-6). The group II

primers successfully amplified all samples except those from Cesspool Cave and several springs (Table 3-6).

DISCUSSION

Defining the composition of microbial communities can aid in our understanding of biogeochemical cycling that occurs in remote and difficult-to-characterize habitats. Particularly for the terrestrial subsurface, little is known about microbial community structures because of the limited number of investigations done on such systems. The application here of the full-cycle rRNA approach to characterize microbial mats and "*Epsilonproteobacteria*" from cave and spring habitats, with Lower Kane Cave as the feature site, enabled assessment of the biogeochemical significance of these previously unknown "*Epsilonproteobacteria*" groups in a variety of environments.

The majority of 16S rRNA gene clones from Lower Kane Cave microbial mats from this investigation were assigned to two evolutionary lineages within the "*Epsilonproteobacteria*", designated LKC group I and II, neither of which have closely related cultured representatives. Several 16S rDNA sequences retrieved from groundwater at an underground petroleum storage cavity (Watanabe et al., 2000; Watanabe et al., 2002) and *S. kujiense* (Kodama and Watanabe, 2003), an anaerobic sulfur oxidizer recently isolated from this habitat, cluster with LKC group I (Figure 3-1). Two clone groups (CC-4 and CC-9) from Cesspool Cave (Engel et al., 2001) are also closely related to LKC group I (Figure 3-1). In contrast, LKC group II forms a monophyletic grouping with the 16S rRNA gene sequence of an uncultured filamentous epibiont associated with the vent annelid

108

Alvinella pompejana (Campbell et al., 2001), and clone groups from phylogenetic studies of Parker Cave, another sulfidic cave system (Angert et al., 1998), are found in sister clades (Figure 3-1).

Quantitative FISH with two newly developed 16S rRNA-targeted oligonucleotide probes specific for LKC group I and II revealed that both groups in Lower Kane Cave are filamentous bacteria. Filamentous "*Epsilonproteobacteria*" have not previously been identified, as most "*Epsilonproteobacteria*" are demonstrably rod-shaped, helical, curved, or ovoid in cell morphology (Miroshnichenko et al., 2004). Bright FISH signals observed for both groups also suggest that the microbes were physiologically active when the mats were collected (Amann et al., 1995). LKC group I filaments were detected in low abundances in three samples, and were not detected in other samples. In contrast, LKC group II filaments dominated five of six samples by biovolume, and represented 50% to 70% of the community bacterial biovolume (Table 3-4).

The FISH results do complement the 16S rDNA clone libraries, as described in Chapter 2, but disparate results also point to the importance of using more than one molecular method to characterize microbial communities. Specifically, the quantification results with FISH for LKC groups I and II (Table 3-4) are slightly different than the phylotype results from restriction fragment length polymorphism (RFLP) that suggest both LKC groups I and II have nearly the same population sizes in some of the microbial mat samples (Chapter 2; Table 2-3), although in any one filamentous mat sample either one of the groups could

dominate. For example, LKC group I clones were prevalent by RFLP in samples from the Fissure Spring, but not LKC group II as indicated by FISH (Table 3-4).

Results from FISH did not target high microdiversity within the "*Epsilonproteobacteria*" that was identified from RFLP (Chapter 2; Table 2-3 and Table 2-5; Figure 2-8). The FISH probes designed in this part of the study were intended for LKC groups I and II only, but probe LKC59 (LKC group I) could also target three of 17 clone sequences from LKC group III (Figure 2-8). Probe LKC1006 targeted only LKC group II clone sequences. Conversely, probe EPS710, designed by Watanabe et al. (2000) for a group of "*Epsilonproteobacteria*" from groundwater, targeted LKC group I, III, and IV clone sequences, indicating that the EPS710 probe could broadly hybridize to a large group of "*Epsilonproteobacteria*" in which most of the environmental clones are from groundwater and caves, much more broadly than the LKC probes or primers. Sequences for the LKC groups V and VI are not targeted by any 16S rRNA probe currently known, indicating additional diversity within the "*Epsilonproteobacteria*". Since these groups were not numerically important by RFLP, probes or primers were not constructed, although future work to describe complete epsilonproteobacterial diversity will require targeting these groups.

While high in situ abundance of free-living and eukaryote-associated "*Epsilonproteobacteria*" have been described from many marine environments, including hydrothermal vent and field communities and marine sediments, there has been no evidence that members of the "*Epsilonproteobacteria*" are also numerically important in terrestrial systems. The only exceptions currently known

are from two engineered systems and caves in which "*Epsilonproteobacteria*" exist in significant numbers. In the petroleum-contaminated groundwater associated with a storage cavity in Japan, between 12% and 24% of the total prokaryote cells could be identified via FISH as epsilonproteobacterial curved rods (Watanabe et al., 2000; Watanabe et al., 2002). Relatively low abundances of *Arcobacter* (4%) were identified with FISH from activated sludge in a wastewater treatment plant (Snaider et al., 1997). Epsilonproteobacterial abundance estimates from 16S rRNA clone libraries in Parker and Cesspool Caves, at 73% and 47% "*Epsilonproteobacteria*", respectively, are similar to the FISH biovolume estimates for LKC groups I and II (Angert et al., 1998; Engel et al., 2001). Although the mats from the sulfidic springs in Sippenauer Moor harbor "*Epsilonproteobacteria*" closely related to LKC group I and II, FISH analysis revealed that these mats are dominated not by "*Epsilonproteobacteria*", but by *Thiothrix* spp. and novel *Archaea* (Rudolph et al., 2001; Moissl et al., 2002). Consequently, the mats from Lower Kane Cave represent the first non-marine natural system demonstrably driven by the activity of "*Epsilonproteobacteria*".

"*Epsilonproteobacteria*" obviously are successful at colonizing a range of marine habitats, and one of the goals of this study was to determine if "*Epsilonproteobacteria*" potentially are as widespread in terrestrial sulfidic environments as they are in marine settings. Results suggest that terrestrial "*Epsilonproteobacteria*" can occupy a variety of physicochemical conditions, and specifically a range of thermal conditions (Table 3-1; Appendix B). Most of the sampling locations were associated with discharge from limestone or travertine

(Table 3-1), suggesting that the "*Epsilonproteobacteria*" may prefer to colonize habitats where acidity generated from their metabolism (e.g., sulfur oxidation) is potentially buffered by dissolving limestone.

The prevalence of "*Epsilonproteobacteria*" in terrestrial environments may be even more widespread than results of this study indicate, and the utility of the epsilonproteobacterial-specific probe and primer sets is significant. There are fewer terrestrial epsilonproteobacterial 16S rDNA gene sequences available in the public databases compared to marine-originating sequences, indicating a lack of information regarding the presence of "*Epsilonproteobacteria*" in terrestrial settings. The clone sequences previously retrieved from Cesspool Cave (Engel et al., 2001) and Sippenaeuer Moor (Rudolph et al., 2001) provided the first indications that at least LKC group I was more widely distributed in terrestrial sulfidic spring and cave habitats than previous research suggested. It is possible that other sites are occupied by members of the "*Epsilonproteobacteria*" that are not targeted by the eps59f or eps174f PCR primers. For instance, epsilonproteobacterial clone groups that are phylogenetically distinct from LKC clone groups have been reported from the sulfidic Parker Cave, Kentucky (Angert et al., 1998), and Zodletone Spring, Oklahoma (Elshahed et al., 2003) (Figure 2-8), indicating additional diversity not targeted by the lineage-specific primers applied in this study.

Because of the specificity of the epsilonproteobacterial primers designed in this study, however, it is highly probable that the epsilonproteobacterial groups in the systems I examined are closely related in nucleotide sequence to the Lower

112

Kane Cave groups, and may not be genetically distinct enough to suggest different microbial species. A low degree of genetic divergence within these groups would indicate that modern geographic isolation may not be a driving factor in the speciation of the LKC epsilonproteobacterial groups, in contrast to what has been demonstrated for some cyanobacteria from hot springs around the world (Papke et al., 2003). Obtaining the full-length 16S rRNA gene sequences, as well as other gene sequences, are required in the future to examine the significance of geographic isolation and genetic evolution for "*Epsilonproteobacteria*". At the onset, however, this study expands the geographic diversity of "*Epsilonproteobacteria*" to a variety of terrestrial photic and aphotic sulfidic habitats, suggesting that these groups may be more important ecologically and geologically than previously considered.

Table 3-1: Geographic and physicochemical information for sampling sites. Refer to Appendix B for complete site descriptions.

Cave, Spring, or Stream	Location	Temp °C	H₂Sᵃ ppm	pH	Rock type	Literature sources
Lower Kane Cave springs	Big Horn County, Wyoming	21	6-8	7.3	Limestone	Engel et al., 2003
Hellspont Cave spring	Big Horn County, Wyoming	22	12	7.1	Limestone	This study
Cesspool Cave spring	Allegheny County, Virginia	12	14-21	7.4	Travertine	Engel et al., 2001
Big Sulphur Cave stream water	Trigg County, Kentucky	15	NM	7.2	Limestone	This study
Frasassi Cave resurgent spring	Genga, Italy	13	6-24	7.4	Limestone	Sarbu et al., 2000; Vlasceanu et al., 2000
White Sulphur Springs	Schoharie County, New York	10	NM	6-7	Limestone	This study
PBS Spring	Big Horn County, Wyoming	13	5	7.2	Limestone	This study
Palmetto Spring	Gonzales County, Texas	17	NM	NM	Sandstone	This study
Thermopolis Hot springs	Hot Springs County, Wyoming	53-57	4.5	6.9	Limestone	Breckenridge and Hinckely, 1978
Glenwood Hot Springs	Garfield County, Colorado	48	1.6	6.4	Limestone	Glendon, 1989
Pah Tempe Mineral Hot Springs	Washington County, Utah	45-55	NM	NM	Limestone	This study
Fifth Water Hot Spring (aka Diamond Fork)	Utah County, Utah	50-54	NM	NM	Limestone	This study
Soda Dam Spring	Sandoval County, New Mexico	45	NM	6.5	Limestone	Goff and Grigsby, 1982; Rzonca and Schulze-Makuch., 2003
Le Zitelle Springs	Viterbo, Italy	46-65	NM	6.5-7.5	Volcanics, travertine	This study

ᵃNM: not measured

114

Table 3-2: Probe sequences used to screen cave microbial populations. Refer to Appendix B for screening results.

Probe	Target group	Probe sequence (5'→3')	Target Site[a]	FA[b]	References
EUB338	Eubacteria	GCT GCC TCC CGT AGG AGT	16S (338)	0-40	Daims et al., 1999
EUB338-II	Planctomycetes	GCA GCC ACC CGT AGG TGT	16S (338)	0-40	Daims et al., 1999
EUB338-III	Verrucomicrobia (and others)	GCT GCC ACC CGT AGG TGT	16S (338)	0-40	Daims et al., 1999
NonEUB	Negative control	ACT CCT ACG GGA GGC AGC	16S (338)	0	Wallner et al., 1993
ARCH344	Archaea	TCG CGC CTG CTG CIC CCC GT	16S (344)	0	Roller et al., 1994
ALF968	Alphaproteobacteria	GGT AAG GTT CTG CGC GTT	16S (968)	20	Neef et al., 1998
BET42a	Betaproteobacteria	GCC TTC CCA CTT CGT TT	23S (1027)	35	Manz et al., 1992
GAM42a	Gammaproteobacteria	GCC TTC CCA CAT CGT TT	23S (1027)	35	Manz et al., 1992
HGC69a	Actinobacteria	TAT AGT TAC CAC CGC CGT	23S (1901)	25	Roller et al., 1994
LGC345A	Firmicutes (with two other probes)	TGG AAG ATT CCC TAC TGC	16S (354)	20	Meier et al., 1999
LGC354B	Same as LGC344A	CGG AAG ATT CCC TAC TGC		20	Meier et al., 1999
LGC354C	Same as LGC344A	CGG CGT CGC TGC GTC AGG		20	Meier et al., 1999
CF319a	Some members of "Flavobacteria"	TGG TCC GTG TCT CAG TAC	16S (319)	35	Manz et al., 1996
G123T[c]	Thiothrix	CCT TCC GAT CTC TAT GCA	16S (697)	40	Kanagawa et al., 2000
EPS710	"Epsilonproteobacteria" Thiovulum groundwater subgroup	CAG TAT CAT CCC AGC AGA	16S (710)	30[d]	Watanabe et al., 2000
LKC59	Epsilonproteobacterial Group 1 from Lower Kane Cave	TCC TCT CAT CGT TCG ACT	16S (59)	30	This study
LKC1006	Epsilonproteobacterial Group 2 from Lower Kane Cave	CTC CAA TGT TTC CAT CGG	16S (1006)	30	This study

[a] E. coli rRNA position (Brosius et al., 1981).
[b] Formamide percentage (vol/vol) in the FISH hybridization buffer.
[c] Used in conjunction with a competitor probe G123T-C (5'-CCTTCCGATCTCTACGCA-3') (Kanagawa et al., 2000).
[d] This formamide concentration differs from the one suggested in the original publication (Watanabe et al., 2000) because a different hybridization temperature was used.

115

Table 3-3: Difference alignment of the target regions of the 16S rRNA for LKC-specific probes.

Probe and target	Target sequence [a]
LKC59 probe sequence (5'-3')	TCCTCTCATCGTTCGACT
Target sequence	AGUCGAACGAUGAGAGGA
LKC Group I clones[b]	------------------
Uncultured Cesspool Cave clone CC-4 [AF207530]	-------------U----
Uncultured groundwater clone 1023 [AB030610]	-------------U----
LKC1006 probe sequence (5'-3')	CTCCAATGTTTCCATCGG
Target sequence	CCGAUGGAAACAUUGGAG
Most LKC Group II clones[c]	------------------
LKC1.114_5 [AY191480]	---G--------------
LKC1.199_5 [AY191494]	-U----------------
LKC1.199_6 [AY191495]	---------U--------

[a] -, identical to the probe sequence.
[b] Based on nine LKC group I clones with 16S rRNA gene sequences at this position.
[c] Based on fifteen LKC group II clones.

Table 3-4: Quantification of epsilonproteobacterial filaments of LKC Group I and II with specific FISH probes.[a]

| | Relative Biovolume, % (SE) | | | | | |
| | Fissure Spring | | Upper Spring[b] | | Lower Spring | |
Group	Orifice	White mat 1	White mat 2	White mat 3	Orifice	White mat
EUB338I-III mix / SYBR Green I ratio	88 (2)	87 (3)	77 (3)	80 (3)	74 (1)	68 (4)
LKC Group I / EUB338I-III mix	<8[c] (2)	<10[c] (1)	<1	<1	2 (1)	<1
LKC Group II / EUB338I-III mix	64 (5)	67 (4)	70 (2)	57 (2)	50 (1)	4 (1)

[a] Relative biovolumes are given as percentages, and the number in parentheses is the standard error (SE).
[b] White mat 1 and white mat 2 were separated by 4 m, and white mat 2 and white mat 3 were separated by 5 m.
[c] This value is most likely overestimated because of relatively weak filament signal intensity and high background.

117

Table 3-5: Difference alignment of the LKC-specific PCR primers.

Primer and Sequences	Sequence Match[a]
eprot59 primer sequence (5'-3')	AGTCGAACGATGAGAGGA
LKC Group I clones	------------------
Uncultured spring clone sipK119 [AJ307940]	------------------
Uncultured *Actinobacteria* clone ARK10173 [AF468440] and 2 others	----------------G
Uncultured clone T2772c [AF019024]	----------------G
eprot174 primer sequence (5'-3')	CCCCATACTCCTTCTCAT
LKC Group II clones	------------------
Uncultured "*Epsilonproteobacteria*" clone T6-ph07-987 [UEP576005]	------------------
Uncultured "*Epsilonproteobacteria*" clone BD7-9 [AB015584] and 2 other deep-sea clones [AB015582 and AF468745]	---------------CC ---------------TC

[a] -, identical to primer sequence.

Table 3-6: Geographic and physicochemical information for additional sampling sites. Refer to Appendix B for PCR and electrophoresis gel details.

Location	Bacterial primers		
	eprot59f	eprot174f	8f/1492r
Lower Kane Cave	✓[a]	✓	✓
Hellspont Cave	✓	✓[b]	✓[b]
Cesspool Cave	✓	✗	✓
Big Sulphur Cave	✓	✓	✓
PBS Spring	✓	✓	✓
Frasassi Caves Spring	✗	✓	✓
White Sulphur Springs	✓	✓	✓
Palmetto Spring	✗	✗	✓
Thermopolis Hot Springs	✗	✗	✓
Glenwood Hot springs	✓	✓	✓
Pah Tempe Hot Springs	✓[b]	✓[b]	--
Diamond Fork Spring	✗	✓[b]	--
Soda Dam Spring	✓	✗	✓
Le Zitelle Spring	✗	✗	✓

[a] ✓, positive PCR amplification; ✗, negative PCR amplification; --, not attempted.
[b] Determined by M.L. Porter, Brigham Young University (refer to Appendix B).

Figure 3-1: 16S rRNA gene-based phylogenetic tree showing the positions of 32 clones from Lower Kane Cave (designated 'LKC1' and labeled in bold with corresponding sample and clone numbers) within the "*Epsilonproteobacteria*". Reference sequences (with GenBank accession numbers) were chosen from the RDP to represent the diversity of "*Epsilonproteobacteria*" members. The topology of the tree was inferred from results of the maximum likelihood analysis and the phylogenetic affiliations of the LKC clones were confirmed by comparison with different reconstruction methods. Specificity of the "*Epsilonproteobacteria*" FISH probes applied in this study is shown. The tree was rooted with the sequences of *Desulfocapsa thiozymogenes* and *Hydrogenophaga pseudoflava*, shown as an arrow 'to outgroups.' Numbers at branch intersections refer to bootstrap values for each node from maximum likelihood / maximum parsimony / minimum evolution / and Bayesian inference posterior probabilities (values below 50% or where only one method supports a node are not shown).

100 / 94 / 51 / 100 — Parker Cave clone SrangJ [AF047633]

Parker Cave clone SRang1.27 [AF047626]

62 / 61 / 64 / 100 — Activated sludge clone rA10 [AB021361]

60 / 85 / - / 90 — Marine sediment clone NKB9 [AB013261]

Marine sediment clone SB-17 [AF029044]

Hydrothermal vent clone VC2.1Bac1 [AF068783]

Estuarine sediment clone 2BP-7 [AF121887]

Rifta pachyptila's tube clone R103-B22 [AF449234]

Marine sediment clone a2b004 [AF420345]

68 / 61 / 59 / 91

LKC1.57_5 [AY191473]
LKC1.198_2 [AY191489]
LKC1.57_1 [AY191469]
LKC1.199_3 [AY191492]
LKC1.199_1 [AY191490]
LKC1.57_9 [AY191474]
LKC1.199_2 [AY191491]
LKC1.190_2 [AY191487]
LKC1.199_6 [AY191495]
LKC1.199_5 [AY191494]
LKC1.57_25 [AY191476]
LKC1.57_13 [AY191475]
LKC1.190_1 [AY191486]
LKC1.199_9 [AY191497]
LKC1.190_3 [AY191488]
LKC1.199_4 [AY191493]
LKC1.199_8 [AY191496]
LKC1.114_5 [AY191480]
LKC1.57_3 [AY191471]

Lower Kane Cave Group II

FISH Probe LKC1006

51 / - / - / 69

100 / 97 / 97 / 100

91 / 98 / 99 / 100

Sulfide spring clone sipK94 [AJ307941]

Alvinella pompejana epibiont [L35521]

Rimicaris exoculata ectosymbiont [U29081]

85 / 72 / 72 / 100 — *Sulfurospirillum barnesii* [U41564]

Campylobacter jejuni [AF393203]

LKC1.114_6 [AY191481]
LKC1.57_4 [AY191472]
LKC1.21_5 [AY191468]
LKC1.114_7 [AY191482]
LKC1.114_8 [AY191483]
LKC1.114_12 [AY191485]
LKC1.58_1 [AY191477]
LKC1.21_2 [AY191467]
LKC1.58_3 [AY191478]
LKC1.57_2 [AY191470]
LKC1.114_2 [AY191479]
LKC1.21_1 [AY191466]
LKC1.114_11 [AY191484]

Lower Kane Cave Group I

FISH Probe LKC59

81 / 91 / - / 74

81 / 65 / 89 / 100

FISH Probe EPS710

Sulfide spring clone sipK119 [AJ307940]

86 / 71 / 72 / 99 — Cesspool Cave clone CC-4 [AF207530]

Groundwater clone 1023 [AB030610]

90 / 77 / - / 100 — Deep Groundwater clone JN5bf [Z69270]

Sulfuricurvum kujiense strain YK-1 [AB053951]

Groundwater clone KB2 [AB074955]

100 / 100 / 100 / 100 — Shallow Groundwater clone FTL212 [AF529098]

Shallow Groundwater clone RA9C8

Cesspool Cave clone CC-9 [AF207534]

63 / 93 / 99 / 95

53 / - / - / 82 — *Thiovulum* sp. [M92323]

100 / 99 / 100 / 100 — *Thiomicrospira denitrificans* [L40808]

Pele's Vent clone PVB 12 [U15104]

100 / 100 / 100 / 100 — *Flexispira rappini* [AF034135]

Helicobacter pullorum [L36144]

Acid mine drainage clone 44a-B1-1 [AY082456]

To outgroups

— 0.01 substitutions/site

120

Figure 3-2: A series of fluorescence images for probe LKC1006 with varying formamide concentrations to optimize hybridization stringency (optimal formamide is 30% for this probe). Columns: A, LKC1006 (labeled with Cy3, colored in red); B, EUB338I-III mix (labeled in Cy5, colored in light blue). When the two probes overlap, the fluorescence color is pink. Scale bar is 20 μm.
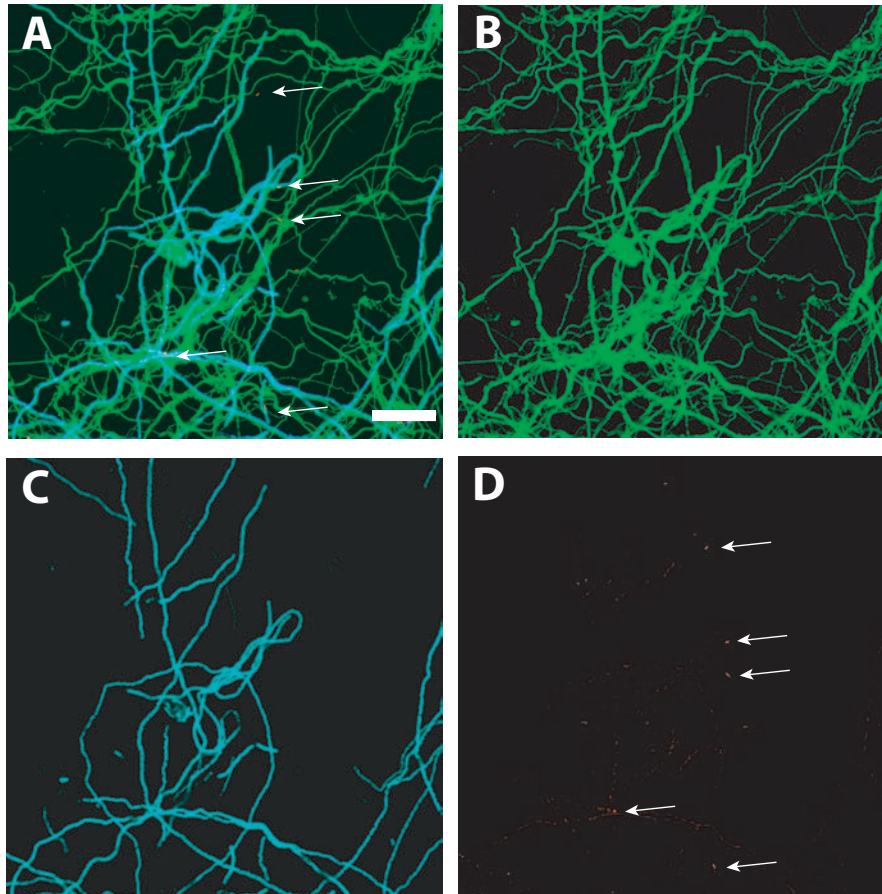
Figure 3-3: (A) Overlapping fluorescence in situ hybridization probes; green, EUB338I-III mix; light blue, GAM42a for *Gammaproteobacteria* (e.g., *Thiothrix* spp.); red and arrows, BET42a for *Betaproteobacteria* (e.g., *Thiobacillus* spp.). (B) EUB338I-III probes mix; (C) GAM42a probe only; (D) BET42a probe only. Scale bar is 20 μm.
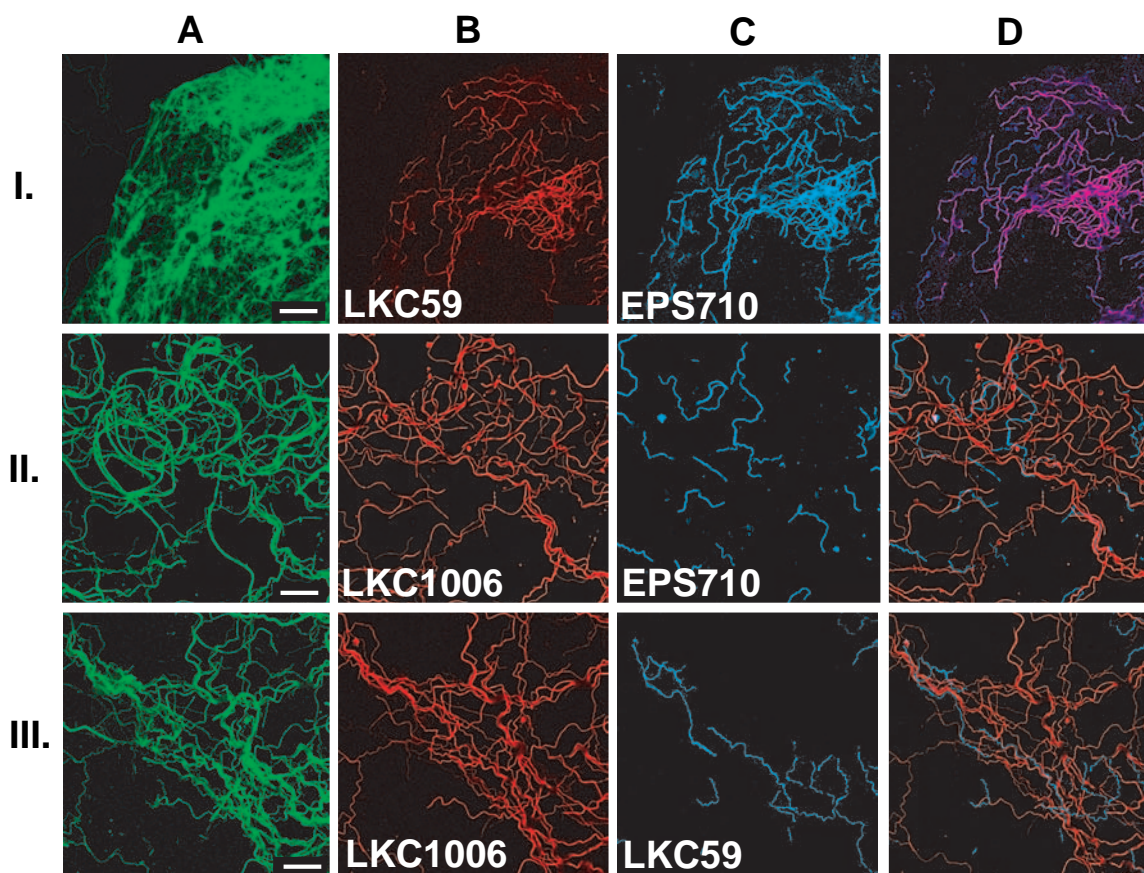
Figure 3-4: Fluorescence in situ hybridization of Lower Kane Cave microbial mat samples with probes EUB338I-III mix, newly designed probes LKC59 and LKC1006. Rows: I, Fissure Spring orifice filaments; II, Upper Spring white mat 1; III, Upper Spring white mat 2. Columns: A, EUB338I-III mix (labeled with FluosPrime, colored in green); B and C, epsilonproteobacterial LKC group probe or EPS710 probe (labeled with Cy3 and colored in red, or labeled in CY5 and colored in light blue); D, overlap of columns B and C. If Cy3- and Cy5-labeled probes overlap, the filmaents appear pink. Scale bar is 20 μm.

Chapter 4: Diversity of Anaerobic Microorganisms in Cave Microbial Mats: Using a Culture-based Approach to Understand Carbon and Sulfur Cycling

ABSTRACT

Hydrogen sulfide-rich groundwater discharges from springs into Lower Kane Cave and Hellspont Cave, Wyoming, where filamentous sulfur-oxidizing bacteria form thick microbial mats, and through chemolithoautotrophy, these bacteria serve as the energetic base of the cave ecosystems. Spring waters entering the caves, as well as the interior of the microbial mats, are devoid of oxygen, and a culture-based approach was used to characterize and to enumerate anaerobic metabolic guilds, including sulfate- and sulfur-reducing bacteria, fermenting bacteria, iron-reducing bacteria, sulfur-oxidizing nitrate- reducing bacteria, and methanogens. Anaerobic microbes were more abundant in mat samples, with up to 10^6 cells·ml^{-1}, compared to water or sediment samples. Sulfate-reducers and fermenters represented the dominant culturable groups from the mats, while sulfur-reducers, iron-reducers, and methanogens were in low abundance ($<10^3$ cells·ml^{-1}). Eight fermentation pathways were identified from Lower Kane Cave enrichments, suggesting that fermenters play a significant role in degrading the chemolithoautotrophically produced organic carbon. This work expands the diversity of some anaerobic metabolic guilds to microbial mats in sulfidic caves, and demonstrates that anaerobic processes are as vital to the cave ecosystem as chemolithoautotrophy.

INTRODUCTION

Ecosystems are arranged structurally and functionally such that there is a producer component and a consumer component, and the primary goal in ecology is to understand the spatial arrangements of these organisms (Eiler et al., 2003; Horner-Devine et al., 2003). While autotrophs generate organic carbon, predominately carbohydrates (e.g., Hayes, 2001), consumers decompose the carbon, releasing and recycling new compounds back into the ecosystem (Wardle, 2002). While characterizing ecosystem primary productivity is essential, understanding the diversity of microbial consumers and the variety of carbon breakdown pathways are also crucial aspects for differentiating total ecosystem functioning.

A significant finding from previous molecular-based investigations of the microbial mats in Lower Kane Cave, as presented in Chapter 2, is that sulfur-oxidizing bacterial communities do not occur in isolation, but have the potential to form a complex mat structure with diverse metabolic guilds (Engel et al., 2003; Engel et al., accepted). While sulfate-reducing bacteria (SRB) have long been implicated in the degradation of organic contaminants in many different habitats (e.g., Widdel and Bak, 1992; Stoessell et al., 1993; Voordouw et al., 1996; Ulrich et al., 1998; Minz et al., 1999a; Minz et al., 1999b; Rios-Hernandez et al., 2003), colonization of sulfidic caves by SRB, or even sulfur-reducing bacteria (S^0RB), has not been previously recognized. Other microorganisms responsible for fermentation or methanogenesis have been characterized from total community 16S rRNA gene

sequences retrieved from subaqueous cave mats (Angert et al., 1998; Engel et al., 2001), but most groups have not been intensely studied in detail.

Molecular methods allow characterization of a microbial community that may be difficult, if not impossible, to cultivate (Head et al., 1998). Unfortunately, molecular techniques can create significant biases and underestimations of particular microbial groups, especially if certain organisms have extremely high dominance, or conversely abundances $\leq 10^7$ cells per volume (von Wintzingerode et al., 1997; Speksnijder et al., 2001). Although Leff et al. (1995) suggest that only 1% of environmental bacteria can be cultured, and that standard culturing methods do often introduce a selective bias toward microorganisms able to grow quickly and to utilize substrates provided in the medium ("r-strategists") more efficiently than other organisms in the community (McDougald et al., 1998), culturing does allow quantification of metabolically active organisms (Palleroni, 1997).

Based on previous geochemical and molecular investigations (Chapter 2), I anticipated that redox stratification of the mats would result in a range of metabolically active anaerobic microorganisms in the microbial mats, and that most would be concentrated in their anaerobic interior. Molecular methods may have overlooked less abundant populations of anaerobic microorganisms in the microbial mats, and this chapter describes a culture-based approach to characterize anaerobic microbes in both Lower Kane Cave and Hellspont Cave, Wyoming (Figure 1-1). I used the most probable number (MPN) method for enumeration and enrichment to examine a variety of anaerobes from mat samples, including many different groups

126

of fermenting bacteria, sulfur-oxidizing nitrate-reducing bacteria, iron-reducing bacteria, three different types of sulfate-reducing bacteria, sulfur-reducing bacteria, and three methanogenic groups. This work demonstrates that anaerobic microbial processes that cycle carbon and sulfur are as vital to the cave ecosystem as chemolithoautotrophy.

MATERIALS AND METHODS

Sampling Strategy and Protocol

Several iterations of the enrichment culturing and biomass estimate techniques were done from 2000 to 2003. Microbial mat samples from Lower Kane Cave and Hellspont Cave were collected aseptically, placed into 15-ml sterile Falcon tubes, and shaken vigorously to disrupt the mat structure prior to inoculation into enrichment media. Shaking proceeded for 1 to 5 min, depending on the type of mat being sampled (i.e., longer times for white filaments, shorter durations for gray sediment). No dispersion amendments were added to the mat samples (e.g., Tween20) because some microbes can utilize these substrates (Holdman and Moore, 1972).

Aliquots of disrupted mat material, ranging from 0.1 ml to 0.5 ml depending on the dilution series, were inoculated by syringe into pre-reduced and sterile (PRAS prepared; Holdman and Moore, 1972) medium in the first bottle in a dilution series, per media type. Serial dilutions were performed in triplicate per sampling site, per enrichment medium; for a 10-fold dilution series, there would be a 30 total bottles in three separate dilution series. For Lower Kane Cave samples,

all of the first bottle inoculations were done in the cave. At Hellspont Cave, because of sampling restrictions and hazardous sulfide levels, samples were brought out of the cave and manipulated. Samples were removed from the cave within 1-3 hr of inoculation, and bottles were sonicated for 2 min to promote disaggregation and homogenization prior to material transfer. All serial dilutions were initiated within 3-7 hr of collection. Several bottles of sterile media (no inoculations) were used as controls. All bottles were incubated in the dark at room temperature ($\sim$21-23 ^{o}C).

Anaerobic Biomass Estimates from Enrichment Cultures

Microbes were enumerated for each metabolic group using the MPN method (Hurely and Roscoe, 1983). A 10-fold serial dilution series was used for cultivable fementers, and SRB, and a 5-fold serial dilution series was used for S^0RB, methanogens, and iron-reducers. Upon returning to the laboratory, inoculated bottles were transferred to a Coy anaerobic chamber with N_2:H_2 mixed gas to maintain anaerobic conditions. The computer program MPN Calculator (Build 2.0; M. Curiale, http://members.ync.net/mcuriale/mpn/index.html) was used to calculate MPN biomass estimates from bottles having positive growth, using 95% confidence intervals (Appendix C).

Fermenting Bacteria

Fermentative bacteria were initially enumerated using 25% Schaedler's Broth (Difco Laboratories, Detroit, MI) dispensed into 25 ml serum bottles. The medium was prepared per manufacturer instructions. Growth, as visible turbidity,

128

was scored positive after two days. Strain isolates were obtained non-selectively on solid 25% Schaedler's Broth and screened for a variety of fermenting abilities and possible H_2S production using triple-sugar iron (TSI) broth (Difco). TSI agar is traditionally used to screen for the physiological activities of some Enterobacteriacea groups (Hajna, 1945). Cells were grown on TSI agar slants in an anaerobic chamber, and growth was screened within 18-24 hr. A combination of cell growth, acid production, gas generation, and medium blackening caused by H_2S production in the butt of the tube and/or in the slant describes a specific pathway (although it should be noted that a particular combination of attributes may not be specific to just one group of organisms; (Hajna, 1945). Following TSI screening, strains were maintained on a modified low-nutrient (MLN) broth of (w/v) 1% sucrose, 0.5% peptone, 0.3 % yeast extract, 0.2% glucose, and 0.2% NaCl.

Sulfate-reducing Bacteria

Sulfate-reducing bacteria (SRB) are divided into two broad physiological subgroups: Group I SRB use lactate, pyruvate, ethanol, or other fatty acids as carbon sources, and Group II SRB oxidize acetate (Widdel and Bak, 1992). Certain species from both SRB groups are capable of growing chemolithoautotrophically with hydrogen as the electron donor, sulfate as the electron acceptor, and CO_2 as the sole carbon source (Widdel and Bak, 1992). Carbon-utilizing SRB were cultured from media designed for this work from modified Baar's and Postgate's C media (MacFarlane and Gibson, 1991). Three components were mixed: 400 ml of

Component I with 2 g $MgSO_4·7H_2O$, 2 g $NaSO_4$, 0.5 g NH_4Cl, 0.06 g $CaCl_2·2H_2O$; 200 ml of Component II with 0.5 g K_2HPO_4; and 400 ml Component III having the carbon source(s) and 0.1% yeast extract (Fisher Scientific). Components I and II were pre-autoclaved (121 ^{o}C, 20 min), before mixing with boiled Component III. Non-acetate oxidizers (Group I SRB) were provided with a mixture of 20 mM 60% Na-lactate and 20 mM Na-formate. Group II SRB were provided with 20 mM acetate. SRB Groups I and II capable of autotrophic growth were cultured using only Components I and II. Per liter, 10 ml Wolfe's trace element solution was added to each media mixture. Media were PRAS-prepared, with the exception that to reduce the potential for blackening of the media from abiotic iron reduction by cysteine or evolved microbial H_2S during growth, 0.01% L-cysteine (Fisher) was added as a PRAS reducing agent. Media were dispensed anaerobically into 10 ml serum bottles, crimp-sealed with butyl rubber caps and aluminum seals, and autoclaved to 121°C (20 min). Following inoculation, Groups I and II SRB bottles were pressurized with N_2 and CO_2, whereas the autotrophic bottles were pressurized with a 70:30 mixture of H_2:CO_2 to 140 kPa.

Instead of scoring positive growth from visual medium blackening due to the formation of iron-sulfides, from cell and iron-sulfide turbidity, or by using lead-acetate paper (e.g., Bekins et al., 1999), bottles were scored for positive growth by measuring evolved headspace H_2S with gas chromatography (GC) (refer to Chapter 5 for GC details). This is a much more sensitive and accurate method for

determining sulfate-reducing activity. SRB growth was found to be very rapid and growth was scored by GC after 7 days.

Sulfur-reducing Bacteria

A sulfur-reducing bacteria (S^0RB) medium was designed for this study, and consisted of the following components: Component I, 0.5g NH_4Cl in 400 ml, and Component II, 0.5 g K_2HPO_4 in 200 ml; Component III, 20 mM Na-formate, 2 mM Na-acetate, and 1 g Difco yeast extract in 400 ml. Components I and II were autoclaved separately (121^oC, 10 min) and mixed with pre-boiled Component III and PRAS preparation. No cysteine was added to the medium. Elemental sulfur flowers were washed with distilled H_2O, and crushed with a sterile mortar and pestle under water to hydrate surfaces. Approximately 5 ml sulfur slurry were dispensed anaerobically into 25 ml serum bottles prior to the addition of 10 ml media. Bottles were individually purged with a 90:10 mixture of N_2:H_2, crimp-sealed with butyl rubber caps and aluminum seals, and autoclaved at 112 ^oC (S^0 melts at 121^oC) for 20 min. Evolved gases were measured using GC after 2 weeks. Uninoculated bottles were also incubated to ensure no contamination occurred due to the lower autoclaving temperature.

Iron-reducing Bacteria

Iron-reducing medium was previously described by Lovely and Phillips (1986) and Bekins et al. (1999). The medium was dispensed in 25 ml serum bottles and autoclaved for 15 min. After inoculation, bottles were pressurized with a 70:30

mixture of $H_2:CO_2$ to 140 kPa. Positive growth was scored after 6 weeks by the bipyridine method (Bekins et al., 1999).

Methanogens

A variety of methanogens were enriched for using PRAS-prepared dilute mineral salts media previously described in Bekins et al. (1999). Briefly, mineral salts media were amended with 20 mM Na-acetate for methanogens that utilized acetate, and in separate medium 20 mM 60% Na-formate was amended for formate-utilizing methanogens. Hydrogen-oxidizing methanogens were enumerated on only mineral salts medium pressurized with a 70:30 mixture of $H_2:CO_2$ to 140 kPa. The use of acetate, formate, or hydrogen distinguishes among different groups of methanogens based on nutrition (Garcia et al., 2000); methanogens that produce methane from methyl-compounds (methylotrophs) were not enumerated. After inoculation, bottles were incubated a minimum of 6 weeks, and scored positive from GC analysis of evolved headspace methane.

Denitrifying Bacteria

Nemati et al. (2001) suggest that if sulfur-oxidizers use nitrate as an alterative electron acceptor at low O_2 tensions, and if sufficient nitrate is not available, then elemental sulfur will accumulate in culture as an indication of positive growth,

$$5HS^- + 2NO_3 + 7H^+ \rightarrow 5S^0 + N_2 + 6H_2O \qquad (4\text{-}1)$$
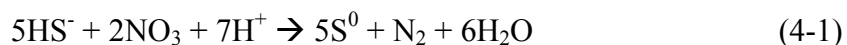
Using this scheme to test for the presence of nitrate-reducing sulfur-oxidizing bacteria from the microbial mats, the following solutions were combined: Solution

A, 2.0 g KH_2PO_4, 2.0 g KNO_3, 1.0 g NH_4Cl, 0.8 g $MgSO_4 \cdot 7H_2O$ in 940 ml dH_2O; Solution B, $Na_2S_2O_3 \cdot 5H_2O$ in 40 ml dH_2O; Solution C, 1.0 g $NaHCO_3$ in 20 ml dH_2O; Solution D, 2.0 g $FeSO_4 \cdot 7H_2O$ in 1.0 ml 0.1N H_2SO_4. Solutions A, B, and D were autoclaved separately at 121 $^{\circ}$C (15 min). Solution C was 0.22 μm-filter-sterilized. The four solutions were combined anaerobically, 2.0 ml sterile Wolfe's trace element solution was added, and medium was dispensed into 250 ml Erlenmeyer flasks in an anaerobic chamber. Flasks were sealed with rubber stoppers to limit oxygen diffusion following inoculation, and flasks were shaken for 2 weeks at ~200 rpm. Medium color was noted (yellow representing sulfur, S^0, accumulation) and cell growth was visualized using phase-contrast microscopy.

RESULTS

Diversity and Biomass of Anaerobic Enrichment Cultures

Several attempts were made to estimate biomass from the Lower Kane Cave and Hellspont Cave microbial mats (Table 4-1; Appendix C). In most of the mat samples analyzed, sulfate-reducers and/or fermenters represented the highest MPN estimates, with up to 10^6 cells·ml^{-1}. However, compared to the overall biomass estimates from the microbial mats of approximately ~10^{10} cells·ml^{-1} (Table 2-2), the MPN estimates of anaerobic microorganisms were up to four orders of magnitude less. There was little correlation in cell count or metabolic guild to the type of mat morphotype cultured (e.g., between white versus gray morphotypes). For instance, iron-reducers grew from gray sediment in the Upper Spring, but were also present in the white webs and stream water (Figure 4-1; Appendix C).

Moreover, there were nearly equal abundances of S^0RB in white and gray filament types, although less S^0RB in the stream and orifice water. Excluding the higher abundances for methanogenic and iron-reducing groups in the Hellspont Cave sample (Figure 4-2), there were no statistical differences in the abundances of fermenters or SRB between Hellspont and Kane cave samples.

Sampling was focused at the Lower Kane Cave Upper Spring microbial mats (Figure 4-1). SRB abundance increased from the orifice downstream through the microbial mats, but SRB were less abundant in the cave stream at 215 m. Both SRB Groups I and II were present in nearly all the samples, including mat and water, with less than 1- to 1000 fold differences in cell abundance overall (Figure 4-1; Appendix C). In some samples, fermenting bacterial biomass was almost equivalent to or surpassed SRB (Figure 4-1). Chemolithoautotrophic SRB were not detected in all samples, and generally had up to four orders of magnitude less cells than SRB Groups I or II. S^0RB were detected in most samples, with relatively low biomass overall with up to 10^2 cells·ml^{-1}. There were a few iron-reducers enumerated (up to 10^3 cells·ml^{-1}) in microbial mat samples, but none were detected in spring or stream water. Methanogens were rarely enumerated, with <14 cells per 100 ml^{-1} from the Upper Spring gray sediment and stream channel white filament samples, consistent with low detectable CH_4 in the water. (Figure 4-1); hydrogenotrophic methanogens most abundant in Hellspont Cave (Figure 4-2). Four of eight enrichment cultures for nitrate-reducing sulfur-oxidizing bacteria,

although not enumerated, had positive growth, and cells from the enrichments were single-celled rods (~ 1-2 μm long) (Table 4-1).

Fermentation Diversity

Of the 28 fermenting bacterial strains isolated from 13 mat samples, most of the strains were classified as 'A/A, G', representing acid production in the tube butt and slant (A/A) and gas production (G) (Table 4-2). There were three variations in gas production; gas was produced throughout the agar, only in the butt, or only in the slant (Table 4-2). Eight strains produced H_2S, as well as other gases and acidity. Overall, there were eight distinct types of growth identified. Three strains did not change medium pH or generate gas, although they did grow.

DISCUSSION

Diversity and Ecology of Anaerobic Microorganisms

Anaerobic microorganisms are common in marine and freshwater habitats, from anoxic sediments and bottom waters to rice paddies (e.g., Bak and Pfenning, 1991; Widdel and Bak, 1992; Wind et al., 1999; Scholten et al., 2002), and even in oxic regions of microbial mats (Minz et al., 1999a; Minz et al., 1999b). Of the anaerobic microbial guilds, especially SRB and S^0RB, many have not been studied in detail from groundwater and springs from karst terrains. Although one group of SRB and several types of fermenters were identified from 16S rDNA sequences retrieved from the microbial mats (Chapter 2), culture-based methods indicate that anaerobic microbial diversity is greater than previously determined, as is subsequent ecosystem functional diversity.

135

There are several reasons why the results of this culture-based study must be considered 'estimates' of microbial diversity. First, culturing techniques can distort the original population abundances and community structure, as there is no one medium that can suit all the organisms (e.g., McDougald et al., 1998). Secondly, enrichment techniques can narrow community structure by providing selective media that eliminate large groups of physiologically distinct bacteria. A rich nutrient source may allow a rare, lesser abundant metabolic group to compete ecologically, and thereby artificially offset community structure. Moreover, assessments of ecosystem function can be distorted if organisms utilize multiple electron acceptors in enrichments that are not available in the natural habitat.

The apparent dominance of SRB among the anaerobic metabolic groups enumerated here from Lower Kane and Hellspont Cave microbial mats was not surprising, as dissolved sulfate concentrations in the cave waters are high. Interestingly, the abundance of SRB in white and gray mat morphotypes was not significantly different, although there were more SRB in both groups in the more distal mat samples compared to mats proximal to the orifice. These results suggest that either microhabitats with low oxygen tension exist in more aerobic portions of the mat (white morphotypes), or that the SRB tolerate more oxygenated conditions (e.g., Minz et al., 1999a).

The estimated abundances of Group I and II SRB were similar; in most samples these groups had equal biomass values (Figure 4-1; Appendix C). Although SRB can use a variety of electron donors, the most common low-

molecular weight organic compounds are lactate and formate (Group I SRB) and acetate (Group I SRB) (Widdel and Bak, 1992). There is some evidence that Group I SRB associate closely with Group II SRB, as some formatotrophs do not completely oxidize lactate to CO_2, but instead oxidize it to acetate that is then completely oxidized to CO_2 by a Group II SRB (Ehrlich, 1996). This may explain why the abundance of these groups overlaps in some samples, suggesting that carbon is actively cycled between the groups.

Fermenting bacteria generate low molecular weight compounds, including amino acids, carbohydrates, and organic acids and alcohols, as intermediaries from the breakdown of complex organic matter (Ehrlich, 1995). TSI agar was used to test for mixed-acid fermentation from sugar breakdown, which yields either lactic, acetic, and succinic acids, formic acid (or CO_2 and H_2), ethanol, or 2,3-butanediol (Stainer et al. 1986). Other fermentation pathways common to anaerobic microorganisms, such as propionate, butyrate, or succinate fermentation, or fumarate reduction, could not be examined using TSI agar. Therefore, although it is apparent that a range of fermentation processes are evident based on culturing, actually assigning a specific pathway to an organism or genera is only a speculative process. A combination of culture- and molecular-based approaches will be essential to characterize the fermenting bacteria in the future.

Eight fermentation pathways were detected from culture, indicating there is a range in metabolic preferences and capabilities for the microbes from the cave microbial mats (Table 4-2). The most common fermentation pathway identified

involved acid production from mixed-sugar metabolism to organic acids, indicated by a reduction in medium pH below 4.5. CO_2 production was also common, and bacteria associated with sugar metabolism and gas production include *Escherichia, Proteus*, and most species of *Salmonella, Aeromonas* (Stainer et al., 1986). CO_2 production is an indication of formate cleavage by the enzyme formic hydrogenase, and formic acid (the end fermentation product) is replaced by CO_2 and H_2. Four of the 28 strains generated acidity but not CO_2 gas, a pathway characteristic of organisms that do not have formic hydrogenase, such as some species of *Shigella*. Of the 28 strains, eight produced H_2S, which is characteristic of species from *Citrobacter, Salmonella,* and *Proteus*. Sulfide production results from breakdown of the sulfur-containing amino acid cysteine, or thiosulfate disproportionation. However, Kolmos and Schmidt (1987) caution that some H_2S-producing Enterobacteriaceae were not detected using TSI agar.

For three strains, medium pH was not lowered and no gas was produced, which could indicate one of four possibilities: 1) no fermentation; 2) fermentation occurred but did not reduce pH because large amounts of 2,3-butanediol or ethanol were produced, which would also not generate CO_2; 3) only lactose fermentation was occurring, but strains lacking certain enzymes for efficient breakdown may not grow fast enough to illicit a medium pH reaction; or 4) since colony growth was obvious for these strains, it is also possible that peptone catabolism was occurring, in which there neither would be acid nor gas production. Butanediol and ethanol production are common to *Serratia,* and species from several other genera

including *Erwinia*, produce butanediol (Stainer et al. 1986); *Serratia* spp. was identified in a 16S rDNA clone library from a gray filament sample (Chapter 2; Table 2-3), suggesting that *Serratia* may have been at least one of the strains isolated. Lactose fermentation is characteristic of *Escherichia* and *Enterobacter*, but absent in *Shingella*, *Salmonella*, and *Proteus* (Stainer et al. 1986).

While not abundant, iron-reducers were enumerated from several mat samples. The concentration of Fe^{3+} is low in the cave (Table 2-1), and could be one reason why iron-reducers are not abundant. The presence of Fe-S framboids in the gray mat interior (Figure 2-4), however, may indicate microbial Fe^{3+} reduction. Iron-reducers can also use humic substances (Lovley and Phillips, 1986), and acetate is likely the major electron donor. Some iron-reducers ferment glucose, or can use monoaromatic compounds and fatty acids (Lovely, 2001). Competition with SRB, which represents a much larger biomass, for carbon substrates may be another reason why iron-reducers are not prevalent.

Enrichment cultures for nitrate-reducing sulfide-oxidizing bacteria were successful for half of the mat samples examined. However, although some sulfur-oxidizing organisms could reduce nitrate in the laboratory, this does not mean that sulfur oxidation through nitrate reduction also occurs in the cave microbial mats. Using the enrichment scheme from Nemati et al. (2001) for *Thiobacillus denitrificans* and *Thiomicrospira* spp., incomplete oxidation of sulfide to sulfate occurs if nitrate is not sufficient; the result is an accumulation of elemental sulfur. Brunet and Garcia-Gil (1996) suggest that if sulfide concentrations are <50 μmol·

L^{-1}, as they are in Lower Kane Cave, nitrate is reduced to N_2. Conversely, at higher sulfide concentrations incomplete nitrate reduction to nitrite, NO, and N_2O occurs, which can inhibit sulfate reduction and methanogenesis (Scholten et al., 2002). As the concentration of sulfide is below the reported threshold, nitrate is likely reduced completely to N_2, if reduction is occurring at any significant rate. More often than not, however, nitrate is a limiting nutrient in freshwater habitats, as it is in Lower Kane Cave (Table 2-1), making sulfide-dependent nitrate reduction either non-existent or indicating that nitrate is kept at an exceedingly low concentration because is so tightly cycled between production and consumption.

Methanogens are ubiquitous in most anaerobic environments with decomposing organic material (Garcia et al., 2000). Conversely, methanotrophy, a metabolic pathway not investigated in this study, is an important metabolic pathway in Movile Cave, Romania (Hutchinson et al., 2003), where the concentration of methane in the cave water is greater than that measured at Lower Kane Cave (Sarbu et al., 1996). It is well known that competition between methanogens and SRB is significant, and if the concentration of dissolved sulfate is high, this has been shown to inhibit methanogenesis (e.g., Garcia et al., 2000). Therefore, the low concentration of methane in Lower Kane Cave, lack of methanogens, and high sulfate concentration supporting high SRB biomass, suggest that methanogenesis is not a prominent physiology in the microbial mats.

Implications for Carbon and Sulfur Cycling

There have been many ecological studies (albeit from surface environments such as forests and soils) that indicate habitat diversity is an important determination for organism diversity, and therefore the organisms that affect niche diversity also affect the biological diversity of other organisms in that habitat (Naeem, 2002; Wardle, 2002). The microbial mats are grossly structured with white filamentous mat morphotypes of sulfur-oxidizing "*Epsilonproteobacteria*"- and *Thiothrix*-dominated communities in contact with flowing stream water, covering a microbial consortium within a gray mat interior. Niche development by the sulfur-oxidizers provides habitat for anaerobic microorganisms within the mat interior, while conversely the benthic orifice and stream sediments are depleted in anaerobic microbes by the absence of a mat structure.

Clearly, organic carbon quality and quantity are important factors in influencing the types of physiological processes that will occur in an ecosystem (Eiler et al., 2003; Horner-Devine et al., 2003). Horner-Devine et al. (2003), based on work in shallow phototrophic ponds, also suggest that primary productivity influences the composition and richness of bacterial communities. Although chemolithoautotrophically-based cave ecosystems have been previously described with respect to metazoans (Sarbu et al., 1996; Airoldi et al., 1997; Hose et al., 2000; Sarbu et al., 2000; Vlasceanu et al., 2000; Engel et al., 2001; Garman, 2002), the diversity and dependence of anaerobic microbial guilds from chemosynthetic primary productivity have not been considered. Based on 16S rDNA sequences

141

retrieved from the microbial mats (refer to Chapter 2), bacterial diversity increased downstream, including both the "*Epsilonproteobacteria*" and the other bacterial groups. In caves, one of the consequences of chemolithoautotrophy is that the quality and quantity of organic carbon is greater than most aphotic ecosystems typically have (Sarbu et al., 1996; Kinkle and Kane, 2000; Poulson and Lavoie, 2000; Simon et al., 2003). The bulk of the white filamentous microbial biomass in Lower Kane Cave has low C:N ratios (refer to Chapter 2; Table 2-2), indicative of an extremely high quality food source (McMahon, 1975), but also consistent with an insignificant influx and processing of allochthonous carbon.

In Lower Kane Cave, the trend of microbial biomass stable carbon isotope values demonstrates nutrient spiraling (Chapter 2), which suggests that carbon is cycled through an active microbial detrital loop and possibly that a significant portion of autotrophic biomass is cycled heterotrophically (Allan, 1995; Porter, 1999). A percentage of heterotrophic carbon recycling can be based on the raw ratio of heterotrophic productivity to autotrophic productivity, and this ratio is doubled to assume 50% growth efficiency (Kirchman et al., 1993; Engel et al., 2001). Porter (1999) determined the rate of chemolithoautotrophic primary productivity in Lower Kane Cave, by $H^{14}CO_3$ assimilation, to be 96.5 ± 6.0 mg C·grams dry weight (gdw^{-1})·hr^{-1} for the white channel mats. By comparison, the heterotrophic productivity by ^{14}C-leucine incorporation was only 14.8 ± 5.7 mg C·gdw^{-1}·hr^{-1} (Porter, 1999). Therefore, ~ 30% of the autotrophic productivity in Lower Kane Cave is processed through heterotrophy. Comparatively,

bacterioplankton utilization of phytoplankton production in a variety of open ocean systems ranges from 10-40% (Kirchman et al., 1993, and references therein).

While allochthonous sulfide most likely originates from dissimilatory sulfate reduction deeper in the Bighorn Basin, as determined on the basis of sulfur isotope values (see Chapter 2; Carmody et al., 1998), SRB within the cave also generate autochthonous sulfide (refer to Chapter 5). Sulfur isotope values support that there is a component of autochthonous sulfide with lower $\delta^{34}S$ values, compared to allochthonous sulfide, that is incorporated by sulfur-oxidizing bacterial biomass (Figure 2-6; Chapter 2 for discussion). While fermenting bacteria in mixed anaerobic communities are key to carbon cycling, the contribution of fermenting bacteria to sulfur cycling has not been well established. Results from this study indicate that some of the fermenting bacteria have the ability to generate H_2S from reduced inorganic and organic sulfur compounds, thereby also affecting sulfur cycling inside the cave. This led to the hypothesis that fermenting bacteria, in addition to SRB and S^0RB, can contribute to autochthonous H_2S gas production, as well as other reduced sulfur gases, in the microbial mats (Chapter 5).

In conclusion, although resolving the detailed structural and functional aspects of the anaerobic microbial community are not possible based only on the culture-based assessments used in this study, results do indicate 1) higher abundances of culturable anaerobes in the mats than sediment or water; 2) little difference in the abundance of SRB groups in white or gray mat morphotypes, suggesting that the conditions for SRB anaerobic growth are favorable throughout

the subaqueous cave environment; 3) many different fermentation pathways, indicating a variety of ways the chemolithoautotrophically produced organic carbon can be processed in the microbial mats; 4) methanogenesis is not a significant carbon cycling pathway in the anaerobic microbial mats; and 5) a large component of autotrophically produced carbon is cycled through a detrital microbial loop. This study expands the diversity and importance of anaerobic microorganisms in cave microbial mats and demonstrates the importance of these organisms to the cave ecosystem, despite low biomass.

Table 4-1: Culture groups, sampling sites, and microbial mat morphotypes in Lower Kane and Hellspont Caves, Wyoming.

Group[a]	HC	118 g	189 w	189 g	193 g	195 g	195 f	198 g	198 f	201 g	201 f	203 g	203 f	203 k	203 y	203 fe	215 r	216 w	248 w	248 g	248 f
2001 Sampling Sites (meters and morphotype)[b]																					
FB	✓		✓[c]	✓								✓	✓				✓	✓	✓	✓	✓
ASRB	✓		×	✓								✓	✓				✓	✓	✓	✓	
LFSRB	✓		✓	✓								×	×				✓	✓	✓	✓	
HSRB	✓		×	✓								✓	×				✓	✓	✓	✓	
IRB	✓		✓	✓								×	×				×	✓	✓	✓	
AM	✓		×	×								×	×				×	×	×	×	
LFM	✓		×	×								✓	×				×	×	×	✓	
HM	✓		×	×									✓				×	✓	×	×	
2002 Sampling Sites																					
FB	✓	✓	✓	✓	✓	✓	✓	✓	✓	✓	✓	✓	✓	✓	✓	✓			✓	✓	
ASRB	✓	×	✓	✓	✓	✓	✓	✓	✓	✓	✓	✓	✓	✓	✓	✓			×	✓	
LFSRB	✓	×	✓	✓	✓	✓	✓	✓	✓	✓	✓	✓	✓	✓	✓	✓			×	✓	
HSRB		×	✓	✓	✓	✓	✓	✓	✓	✓	✓	✓	✓	✓	✓	✓			×	✓	
IRB			✓	✓	✓	✓		✓		✓		✓	✓								
MM		×	×	×	×			×		×		×	×						✓	×	
HM		✓	×	✓	×			×		×		×	✓						×	×	
2003 Sampling Sites																					
S⁰RB			×	✓	✓	✓	✓	✓	✓	✓	✓	✓	✓	✓				×		×	
SONR			×	×	✓			✓				✓	✓							×	✓

[a] Type of physiologic group: FB, fermenting bacteria; ASRB, acetate-utilizing sulfate-reducing bacteria (SRB); LFSRB, lactate-/formate-utilizing SRB; HSRB, autotrophic SRB; IRB, iron-reducing bacteria; AM, acetate-utilizing methanogens; LFM, lactate-/formate-utilizing methanogens; HM, autotrophic methanogens; MM, mixed acetate- and formate-utilizing methanogens; S^0RB, sulfur-reducing bacteria; SONR, sulfur-oxidizing nitrate-reducing bacteria

[b] Number represents meter location along cave stream from back of the cave. HC: Hellspont Cave spring sediment. Letter represents mat morphotype: w, water; g, gray filaments or sediment; f, white filaments; fe, white feathers; k, knobby-web; y, yellow patches; r, red mats

[c] Box symbols: ✓, positive growth; ×, negative growth; no symbol means the enrichment was not attempted.

Table 4-2: Results from isolation and screening of fermenting bacterial strains using TSI agar.

| Strain | Colony Description | General Shape[a] | Triple Sugar Iron (TSI) Agar Growth | | | | | | Symbol[b] (slant/butt, gas, black) |
			Growth	Acid Slant	Acid Butt	Gas Slant	Gas Butt	H$_2$S	
1-1-2	Yellow, shiny colony	0.7 μm rods	+	+	+	+	+	-	A/A, G
1-3-2	White, smooth colony edges, smooth	Dumb-bell rods	+	+	+	-	-	-	A/A
2-2-2	White, spreading colony edges	Rod	+	+	+	+	+	+	A/A, G, B
2-3-2	White, shiny colonies	Rods	+	+	+	+	+	+	A/A, G, B
3-1-2	White, slimy and shiny colonies, smooth edges	Rods	+	+	+	+	-	-	A/A, G
3-2-2	White, slimy and puffy colonies, swarming	~1 μm rods	+	+	+	+	+	+	A/A, G, B
4-2-2	White, shiny colony, smooth, swarming	Rods	+	+	+	+	+	-	A/A, G
4-3-2	White, tiny, smooth	Rods	+	+	+	-	-	-	A/A
5-3-2	Yellow, small colonies, swarming	Rods	+	+	+	-	-	-	A/A
6-3-2	White, slimy, small	Rods	+	+	+	+	+	+	A/A, G, B
7-2-2AA	Brown, flat and spreading colonies	Rods	+	-	+	-	+	-	K/A, G
7-22AB1	White, irregular spreading colony edges	~1 μm fat rods	+	-	-	-	-	-	NC/NC
7-22AB2	White, smooth edges, grows into medium	Rods	+	-	-	-	-	-	NC/NC
8-2-2	Pink, tiny colonies, smooth edges	Rods	+	+	-	-	-	-	A, K
10-3-2	White, bumpy colonies, shiny	Rods	+	+	+	+	+	-	A/A, G
2ferm4-1-5A	White, shiny colonies	ND	+	+	+	-	+	-	A/A, G
2ferm4-1-5B	White, shiny colonies	ND	+	+	+	-	+	-	A/A, G
2ferm7-1-3A	White, smooth colony edges	ND	+	+	+	-	+	-	A/A, G
2ferm1-1-1A	White, slimy colonies	ND	+	-	+	-	+	-	K/A, G
Ferm-2-1-5	White, flat and small colonies	ND	+	-	-	-	-	-	NC/NC
Ferm-4-1-5A	White, small and shiny	ND	+	+	+	+	+	+	A/A, G, B
Ferm7-1-5A	White, shiny colonies	ND	+	+	+	+	+	+	A/A, G, B
Ferm8-1-5A	Pink, shiny colonies	ND	+	-	+	-	+	-	K/A, G
Ferm10-1-5A	White	ND	+	+	+	-	-	-	A/A
Ferm11-1-5-A	White, swarming	ND	+	-	+	-	+	+	K/A, G, B
Ferm13-1-5A	White, smooth edges	ND	+	+	+	+	+	-	A/A, G
Ferm15-1-5A	Yellow, shiny and slimy colonies	ND	+	+	+	+	+	+	A/A, G, B
Ferm19-1-5-A	White	ND	+	+	+	-	+	-	A/A, G

[a] ND, not determined.
[b] Symbols and interpretation: K, alkalinity, medium turns red; A, acid production, medium turns yellow; NC, no medium color change; G, gas production in medium; B, black precipitate in medium due to H$_2$S gas.

Figure 4-1: Most-probable number estimates for various anaerobic bacteria from Lower Kane Cave water, sediment, and microbial mat samples. Number at left represents site location, in meters, from the back of the cave forward (the spring orifice is the lowest number). SRB, sulfate-reducing bacteria (groups I and II, and autotrophic); S^0RB, sulfur-reducing bacteria; IRB, iron-reducing bacteria. Error bars are 95% confidence intervals calculated by MPN program (Hurley and Roscoe, 1983).

cells·ml^{-1}

Legend:
- Fermenting bacteria
- Group II SRB
- Group I SRB
- Autotrophic SRB
- S^{0}RB
- IRB
- Methanogens detected

Sample labels (top to bottom):
- 189 orifice water
- 189 gray sediment
- 193 gray filaments
- 195 white filaments
- 195 gray filaments
- 198 white filaments
- 198 gray filaments
- 201 white filaments
- 201 gray filaments
- 203 white webs
- 203 filaments
- 203 gray filaments
- 215 stream water

X-axis labels: 0.1, 1, 10, 100, 1000, 10^4, 10^5, 10^6, 10^7, 10^8

148

Figure 4-2: Most-probable number estimates for various anaerobic bacteria from Hellspont Cave orifice sediment. Error bars are 95% confidence intervals.

Chapter 5: Production and Consumption of Hydrogen Sulfide and Volatile Organosulfur Compounds in a Sulfidic Cave System

ABSTRACT[1]

Hydrogen sulfide gas ($H_2S_{(g)}$) and volatile organosulfur compounds (VOSC) were examined in filamentous microbial mats formed in anaerobic, sulfidic water in Lower Kane Cave, Wyoming. Total dissolved sulfide ($C_TS^=$) decreases from upstream to downstream through the microbial mats, while $H_2S_{(g)}$ at the air-water interface directly over the microbial mats averages 30 ppmv, corresponding to an average $H_2S_{(g)}$ flux of 44 $\mu mol \cdot m^{-2} \cdot min^{-1}$. The measured $H_2S_{(g)}$ volatilization accounts for less than 8% of the $C_TS^=$ flux into the cave, and abiotic sulfide autoxidation accounts for <0.014% $C_TS^=$ loss, suggesting that the primary $C_TS^=$ loss mechanism is caused by oxidation of $C_TS^=$ by subaqueous sulfur-oxidizing bacteria. Incubations of cave water and microbial mat samples demonstrate that $H_2S_{(g)}$ and VOSC are of biogenic origin, and are cycled by aerobic and anaerobic mat communities. Anaerobic laboratory enrichment cultures of fermenting, sulfate-, and sulfur-reducing bacteria from the cave microbial mats were screened for sulfur gas production. Enrichments of sulfur-reducing bacteria generated only $H_2S_{(g)}$, but sulfate-reducing and fermenting bacteria produced VOSC, in order of abundance: $H_2S_{(g)}$, methanethiol, dimethyl sulfide, and carbonyl sulfide. Twenty-nine percent of fermenting bacteria strains generated $H_2S_{(g)}$ with

---

[1] A portion of this chapter originated from the paper A.S. Engel, L.A. Stern, and P.C. Bennett, 2004, Microbial contributions to cave formation: new insights into sulfuric acid speleogenesis, <u>Geology</u>, v. 32 (5) p. 369-372.

growth medium, and two of the isolated strains produced $H_2S_{(g)}$ when thiosulfate and cysteine were present in the growth medium, but not with sulfate; methanethiol was produced when methionine was present. In anaerobic enrichment cultures and natural mat incubations, generation of methanethiol and dimethyl sulfide was always preceded by the generation of $H_2S_{(g)}$. Inhibition of microbial sulfate reduction by addition of molybdate in the incubations resulted in diminished to no VOSC production. There was no correlation between VOSC concentration and methane gas production, indicating that methanogenesis is not an important sulfur gas consumption mechanism in this system. Natural mat samples, dominated by active sulfur-oxidizing bacteria, degraded methanethiol and dimethyl sulfide aerobically when supplemented with VOSC. Active cycling of VOSC by anaerobes and aerobes from a freshwater, subterranean environment has not been previously demonstrated. As photochemical degradation of these gases is not possible, sulfur-based microbial mat communities in the subsurface represent a new terrestrial source for sulfur gases and the impact of subterranean microorganisms to the global sulfur cycle should be considered.

INTRODUCTION

Bacterial processes are largely responsible for recycling inorganic and organic sulfur-containing compounds within the sulfur cycle, and volatile components are released into the atmosphere (Taylor, 1991; Kelly et al., 1994). Hydrogen sulfide gas ($H_2S_{(g)}$) and volatile organosulfur compounds (VOSC), including carbonyl sulfide (COS), methanethiol (MT), dimethyl sulfide (DMS), and

dimethyl disulfide (DMDS), contribute to the global sulfur cycle, and consequently these sulfur gases have been intensively studied with respect to their contribution to acid precipitation and global warming (Legrand et al., 1991; Bates et al., 1992; Bodenbender et al., 1999; Watts, 2000). Understanding natural abiotic and biogenic emission is vital to evaluate the magnitude of anthropogenic perturbations to the global sulfur cycle. Marine and volcanic gas emissions make up a significant fraction of the global sulfur flux; while terrestrial biogenic emissions may be insignificant at the global scale, they are likely more important to local cycles (e.g., Andreae and Andreae, 1988; Bates et al., 1992; Watts, 2000). Attempts to estimate natural terrestrial emissions from surface environments have had variable results, showing disparate emission patterns spatially and temporally.

Most studies of natural $H_2S_{(g)}$ and VOSC production and consumption rates have investigated marine environments (Zinder et al., 1977; Visscher et al., 1991; Bodenbender et al., 1999; Fritz and Bachofen, 2000; Kristensen et al., 2000; Visscher et al., 2003), freshwater limnic systems (Stoner et al., 1994; Fritz and Bachofen, 2000), hot springs (Stoner et al., 1994), soil (Conrad, 1996; Yang et al., 1998), and flooded sediments and wetlands (Lomans et al., 1997; Lomans et al., 1999a; Lomans et al., 1999b; DeLaune et al., 2002). However, virtually nothing is known about the production of reduced sulfur gases from terrestrial, aphotic environments (caves) or sulfidic groundwater systems, although $H_2S_{(g)}$ has been detected in several caves (Galdenzi and Menichetti, 1995; Sarbu et al., 1996; Angert et al., 1998; Hose et al., 2000). $H_2S_{(g)}$ and VOSC have been identified rarely in caves, including from Lower Kane Cave, Wyoming (Egemeier, 1981), and

Cueva de Villa Luz, Mexico (Boston et al., 2001). VOSC in the subsurface do not photodegrade, and consequently cycling of reduced sulfur gases in the aphotic unsaturated zone may be a significant source of sulfur to the global budget. This is particularly important geologic environments from which gases can diffuse into the atmosphere, such as fractured bedrock or karst. Sulfur-based microbial communities can utilize the ubiquitous reduced sulfur compounds in anaerobic, sulfidic groundwater, and sulfur cycling may be more widely dispersed in the terrestrial subsurface than currently recognized.

This study describes the production and consumption of $H_2S_{(g)}$ and VOSC in Lower Kane Cave by sulfur-based microbial communities. While there have been investigations of VOSC utilization by some microbial groups, including *Thiobacillus* spp. (Kanagawa and Kelly, 1986) and *Hyphomicrobium* (DeBont et al., 1981), these organisms have mostly been studied in engineered systems (e.g., sewage sludge) or in photic microbial mats (e.g., Visscher et al., 1991). "*Epsilonproteobacteria*", the dominant sulfur-oxidizing bacteria in the Lower Kane Cave microbial mats (refer to Chapter 2 and 3; Engel et al., 2003), have not been previously linked to VOSC consumption or utilization. Based on gas chromatography (GC) methods designed specifically for the cave environment, I report $H_2S_{(g)}$ and MT gas flux rates from the subterranean sulfidic springs and microbial mats, as well as detailed regarding microbially mediate sulfur gas transformations from native microbial mat samples and laboratory enrichment cultures.

Cave Gas Sampling and Flux Measurements

A description of Lower Kane Cave, Wyoming, and its geological and hydrological setting are presented in Chapter 1 (Figure 1-1 and 1-2). Cave atmosphere components (CO_2, CH_4) and sulfur gases (H_2S, COS, SO_2, CS_2, MT, DMS) were determined in the cave by direct-inject GC on a SRI 310 (SRI Instruments, Torrance, CA) using either a Restek XL sulfur column and TCD/FID detectors, or a 60m 0.53mm MXT-1 column with FID/FPD detectors, respectively. In the cave, the MXT-1 column resulted in better gas separation with an isothermal run.

The GC was placed in an area of the cave previously determined to have extremely low to negligible sulfur gases, away from the cave stream (Figure 5-1A). A gas-powered Honda generator was placed at the cave entrance and 150 m of heavy-duty-outdoor extension cord was extended through the cave to the GC. $H_2S_{(g)}$ flux at the water-mat boundary layer was measured using a 16-cm^2 flux chamber suspended over the water and partially submerged to approximately 2 to 10 mm into the cave water (Figure 5-1B). Cave air was pumped through a reactive copper intake tube connected to the chamber to remove ambient VOSC (Figure 5-1C), and the chamber gas was withdrawn and pumped through Teflon tubing to a 1 ml Teflon sample loop for injection into the GC (Figure 5-1D). The entire gas flow path from the flux chamber to the GC was Teflon due to the reactivity of sulfur gases. The chamber gas outflow was monitored continuously for CO_2 (Comfort

Chek 100/200 CO_2 analyzer, Bacharach, Inc., Pittsburgh, PA) and flow rate using a mass flow meter. Replicate flux measurements were determined with variable pumping rates to achieve a representative flux rate. Individual gas samples were also collected throughout the cave in cleaned and non-reactive plastic syringes, and samples were analyzed immediately by GC. Dissolved gases in the stream were measured from sample bottles by headspace GC and by the bubble-strip method (Chapelle et al., 1997).

Enumeration of Anaerobic Enrichment Cultures

Microbes from the cave water and microbial mats were enriched using the most probable number (MPN) method in pre-reduced anaerobic media specific to certain physiologic groups, including fermenting bacteria, chemolithoautotrophic, acetate-, and lactate-/formate-utilizing sulfate-reducing bacteria (SRB), sulfur-reducing bacteria (S^0RB), methanogens, and iron-reducers. Gas evolution (H_2S, COS, MT, DMS, CH_4, CO_2) was measured by GC in the enrichment headspace (Chapter 4).

Isolation of Fermenting Bacteria and Metabolism of Sulfur Compounds

Some strains of fermenting bacteria (isolates obtained as described in Chapter 4) were tested for utilization of different sulfur substrates, including thiosulfate, sulfate, cysteine, and methionine. 100 µl of cell suspension was harvested from strain isolates, washed with filter-sterilized tap water, and inoculated into fresh serum bottles containing 10 ml MLN media (Chapter 4) supplemented with one of the following: 2.5 mM NaS_2O_3; 4 mM $MgSO_4 \cdot 7H_2O$ + 9 mM $NaSO_4$; 0.01% L-cysteine (Fisher); or 0.01% L-methionine (FisherBiotech).

155

MLN broth with no addition of sulfur compounds was a live-control. In each sulfur substrate series, a killed cell suspension was used as a sterile control (121°C, 20 min). All bottles were pressurized with N_2 to ensure anaerobic conditions. One bottle was used to measure microbial growth as optical density (OD) using a Perkin Elmer Lambda 6 UV/VIS spectrophotometer at a wavelength of 588 nm (traditionally, 600 nm is used to measure cell absorbance, but there was interference at 600 nm by the medium). pH was measured by electrode and headspace gas was quantified by GC. Growth rate for each strain was calculated using the modified Monod expression

$$OD_{(t)} = OD_o\ e^{\mu t} \qquad\qquad (5\text{-}1),$$

where $OD_{(t)}$ is the optical density at time t, OD_o is the optical density at the start, and μ is the specific growth rate. Doubling times (t_d) were calculated using

$$\mu = \ln 2\ /\ t_d \qquad\qquad (5\text{-}2)$$

Gas Cycling by Native Microbial Mat Communities

H$_2$S and VOSC production from homogenized mat samples

In separate cave-incubated and laboratory-incubated gas production experiments, approximately 100 ml of aseptically collected and homogenized microbial mat from the end of the Upper Spring and Lower Spring, and 150 ml of 0.22-µm-filtered (cold-sterilized) spring water, were dispensed into sterile 500 mL black Teflon chambers equipped with gas-sampling and electrode ports. Microcosms were amended with 10 ml of a gypsum-saturated, cold-sterilized solution to provide dissolved sulfate. For the cave incubations, a control chamber

156

containing 250 ml filter-sterilized spring water and 10 ml gypsum-saturated solution was used. The laboratory incubations had two controls: one sterile control with 250 ml filtered spring water and 10 ml gypsum-saturated solution, and another killed control of autoclaved (121 $^{\circ}$C, 30 min) microbial mat. Microcosms were incubated in the cave or at room temperature, and pH in the live chambers was monitored continuously using an Accumet portable pH/mV meter with a double-junction pH electrode (Fisher Scientific). For the laboratory incubations, sterilized pieces of Iceland Spar calcite (Wards Scientific), totaling 1 g for closed-chamber microcosms and 0.1 g for serum bottles, were added prior to mat inoculation to maintain circum-neutral pH and to provide an inorganic carbon source to autotrophic populations. Emitted sulfur gases and headspace CO_2 from cave-incubated chambers were measured in the cave by GC and using the portable Comfort Chek CO_2 monitor, respectively, and O_2 was measured by GC using a CTR-1 column. For the laboratory chambers, sulfur gases, methane and hydrocarbons, and CO_2 were separated by GC with FPD, FID, and TCD, respectively.

Inhibition of H$_2$S and VOSC production from homogenized mat samples

Aerobic and anaerobic gas production and consumption were measured in sterile 60-ml glass serum bottles inoculated with 10 ml homogenized microbial mat material, 20 ml cold-sterilized spring water, and 2 ml gypsum-saturated, filtered solution. Some bottles were supplemented with 4mM Na-molybdate to inhibit microbial sulfate reduction, while others were supplemented with 25 mM 2-bromoethanesulfonic acid (BES) to inhibit methanogenesis (Oremland and Capone,

1988; Lomans et al., 1997; Scholten et al., 2000), or with ~30 μl HgCl-saturated solution for a killed control. Abiotic controls were prepared from bottles of 30 ml cold-sterilized spring water and 2 ml gypsum-saturated solution, and of sterilized mat (121 $^{\circ}$C; 20 min). Bottles were sealed with butyl rubber stoppers and aluminum seals, and were incubated in the dark at room temperature (~21-23 $^{\circ}$C).

VOSC consumption by homogenized mat samples

Cold-sterilized spring water was purged with a mixed-sulfur gas standard (71.0 ppmv COS, 75 ppmv MT, 68.5 ppmv DMS) for 2 hr to examine VOSC degradation. Purged water was cold-sterilized into glass serum bottles and 10 ml homogenized aliquots of microbial mat were added. Some bottles were amended with 25 mM BES or $HgCl_2$ for a killed control. One bottle with mat was sterilized by autoclaving (121 $^{\circ}$C; 20 min). Immediately following sealing and gentle shaking, headspace samples were taken to determine starting gas concentrations. Samples were incubated in the dark at room temperature.

RESULTS

Hydrogen Sulfide Dynamics in the Cave

Field description

Cave spring waters had pH values ranging from 7.1 to 7.3 and a nearly constant temperature of 21.5 $^{\circ}$C (Table 2-1). Total dissolved sulfide ($C_TS^=$) at all orifice discharge pools averaged 30 $\mu mol \cdot L^{-1}$, but decreased rapidly from the discharge point downstream through the microbial mats (refer to Chapter 2; Figure 2-1). The total flux of $C_TS^=$ at the Upper Spring was calculated from the incoming concentration and the stream discharge determined by salt dilution tracing.

Discharge $C_TS^=$ flux, determined from the 191-m concentration of dissolved sulfide, was ~8700 μmol·min^{-1} (Table 5-1). $C_TS^=$ was not detected downstream from the mat terminus at the Lower and Upper Spring (2 and 20 m flow path distance from the orifice, respectively), although $C_TS^=$ (~20 μmol·L^{-1}) was measured 25 m from the Fissure Spring where the mats ended (Figure 2-1A).

At the Upper Spring orifice, water had no detectable dissolved O_2 (Table 5-1) and $H_2S_{(g)}$ was not detectable directly over this anaerobic spring water (Figure 5-2; Appendix D). Along the outflow channel, $C_TS^=$ was approximately constant as dissolved O_2 increased. From the orifice and along the stream channel, the water transitioned from anaerobic to disaerobic (O_2 = 0.1 to 5.0 μmol·L^{-1}), with 21 μmol·L^{-1} $C_TS^=$. The mats abruptly terminated at 205 m, and here dissolved O_2 exceeded 45 μmol·L^{-1} while $C_TS^=$ decreased to <6 μmol·L^{-1} (Figure 2-1B).

The approximately constant, and subsequently steep and concave-down $C_TS^=$ vs. distance profile (Figure 5-3A) is not the expected shallow, concave-up first-order loss profile characteristic of abiotic first-order loss mechanisms (Millero et al., 1987; Brezonik, 1994). A first-order loss curve was estimated from the initial $C_TS^=$ at the spring and the distance at half-$C_TS^=$ [$t_{1/2}$ = ln2/k; Brezonik, 1994] and an estimated stream velocity of 0.5 m·s^{-1} along the proximal 6 m channel from the orifice. The observed $t_{1/2}$ was ~0.5 min (k = 1.5) (Figure 5-3A). Stream velocity decreased to 0.2 m·s^{-1} at the mat terminus as the stream channel widened, and another first-order loss curve was estimated from the $C_TS^=$ at 203 m, near the end of the mat, with an observed $t_{1/2}$ ~ 0.2 min (k = 3.0) (Figure 5-3A).

Field flux experiments and theoretical volatilization

Although $H_2S_{(g)}$ flux varied along the outflow channel at different sampling times, the highest $H_2S_{(g)}$ flux was consistently quantified from directly over the microbial mats from the 193 to 194-m locations where dissolved $C_TS^=$ was relatively lower than $C_TS^=$ at the spring orifice (Table 5-1; Figure 5-2). MT was measured above the detection limit (<1 ppmv) from a flux chamber at 191 m, but upon repeating the experiment, MT was not detected again. The average concentration of $H_2S_{(g)}$ at the air-water interface for the entire stream length was 22 ppmv; this steady state concentration resulted in an average $H_2S_{(g)}$ flux of 44 μmol m^{-2} min^{-1} (Table 5-1).

The measured $H_2S_{(g)}$ flux was compared to a theoretical volatilization rate calculated from the 2-film model of Liss and Slater (1974) (Table 5-1), using the average water depth of 10 cm and an average channel width of 1 m. It was assumed that the shallow stream channel results in a completely mixed aqueous system and a purely fluid film-controlled volatilization rate. Volatilization half-life was determined from the first-order liquid phase mass transfer coefficient,

$$K_L = \frac{\left(H'/RT\right)k_g k_l}{\left(H'/RT\right)k_g + k_l} \qquad (5-3)$$

where k_g is the gas phase exchange coefficient, k_l is the liquid phase exchange coefficient, H' is the dimensionless Henry's constant, T is temperature in Kelvin, and R is the gas constant; k_g and k_l are estimated from the ratio of the mass of water vapor and CO_2, respectively, to the mass of H_2S (Liss and Slater, 1974). Dissolved H_2S was speciated from $C_TS^=$ for pH (H_2S:HS^- pK = 7.04; Stumm and Morgan,

1996). The theoretical volatilization rate yielded an estimated flux of 23 μmol m^{-2} min^{-1}, with a first-order volatilization half-life ($t_{1/2}$) of 13 min (Table 5-1). This compares very closely to the actual volatilization $t_{1/2}$ of ~6 min based on the mean measured $H_2S_{(g)}$ flux. Over the entire length of the Upper Spring stream channel, however, the total $H_2S_{(g)}$ volatilization accounted for less than 8% of the total influx $C_TS^=$ (Figure 5-3B), suggesting that the bulk of subaqueous $C_TS^=$ is lost by other mechanisms, not by volatilization.

Abiotic autoxidation rates

The rates of abiotic autoxidation were estimated to evaluate their contribution to $C_TS^=$ loss. The rate of sulfide autoxidation in water is a complex function of temperature, salinity, reactant concentration, dissolved metal concentration, pH, and the presence of ferric hydroxides (Millero, 2001; Millero et al., 1987). At low sulfide concentrations and low temperatures, the sulfide loss rate is first-order with respect to sulfide concentration and first-order with respect to oxygen, and second-order overall for the disappearance of sulfide (Millero et al., 1987):

$$d[H_2S]_T\Big/dt = k_2[C_TS^=]\,[O_2] \qquad\qquad (5\text{-}4)$$

where $[O_2]$ is the concentration of dissolved oxygen, $[C_TS^=]$ is the total concentration of all sulfide species, and k_2 is the second-order rate constant. At pH values near the pK of H_2S, k_2 consists of two components, k_0 and k_1, corresponding to the oxidation of H_2S and HS$^-$, respectively. Therefore, the second-order rate of sulfide oxidation, in water at 25°C at pH <6, is dominated by k$_0$ of ~11 L·mol^{-1}·hr^{-1},

with an activation energy of 43.5 kJ·mol^{-1}. For pH >8 the rate is dominated by HS^{-} oxidation, with a second-order rate constant of ~48 L·mol^{-1}·hr^{-1} at 25°C, with an activation energy of 53.5 kJ·mol^{-1} in freshwater (Millero et al., 1987). Using a pH of 7.3 at 22°C, a second-order rate constant of 40 L·mol^{-1}·hr^{-1} was estimated.

Using these rate constants, the calculated C_TS$^{=}$ autoxidation under the conditions in the disaerobic cave waters (20 μmol·L^{-1} C_TS$^{=}$ and a constant O$_2$ of 20 μmol·L^{-1}; conditions at 201 m) is extremely slow. The autoxidation rate of dissolved sulfide was estimated from the kinetic data determined at 25.0 ^{o}C for low ionic strength aqueous systems using a constant [O$_2$] to yield a pseudo-first order rate constant and half-life (Zhang and Millero, 1983; Millero et al., 1987). For the analysis, the point along the stream where [O$_2$] = C_TS$^{=}$ was chosen, because for kinetic evaluation, choosing the point where starting concentration [A]$_0$ = [B]$_0$ for a second-order overall reaction, greatly simplifies the evaluation. For a closed system under these conditions, the half-life is (Brezonik, 1994):

$$t_{1/2} = \frac{1}{k_2 [C_T S^{=}]_0} \qquad (5\text{-}5)$$

and was estimated to be 1250 hr at the 201 meter-location along the stream channel. Alternatively, the concentration of dissolved oxygen can be fixed so that the second-order reaction can be evaluated as a pseudo first-order reaction, where the rate is independent of the variable component (H$_2$S) and dependent only on the fixed concentration of dissolved oxygen:

$$t_{1/2} = \frac{\ln 2}{k_2 [O_2]_0} \qquad (5\text{-}6)$$

and was estimated at 866 hr at 201 m. Upstream, where the concentration of oxygen was lower, the rate was much slower, while the rate increased slightly downstream with increasing oxygen, and the half-life decreased by a factor of ~3 at 215 m (Table 5-1). Therefore, $C_TS^=$ autoxidation rate represented ~0.014% of the potential abiotic loss in this oxygen-limited system with low concentrations of dissolved metals (Figure 5-3B).

Microbial Mat Sulfur Gas Production and Consumption Experiments

Enrichment cultures of anaerobic microorganisms

Microbial mat sampling was focused at the Upper Spring mats. Sulfur gas, and specifically $H_2S_{(g)}$, production was used to detect SRB and S^0RB growth in MPN enrichment cultures, and sulfur gases were also measured from the headspaces of fermenting bacteria enrichment bottles (Table 5-2). SRB cell abundance based on MPN increased downstream, from the orifice water and orifice sediment samples moving through the microbial mats. Both lactate/formate (Group I)- and acetate (Group II)-utilizing SRB were present in nearly all the microbial mat samples, with 1- to 1000-fold differences in cell abundance overall (refer to Chapter 4; Figure 4-1). In some samples, fermenting bacterial biomass was almost equivalent to or surpassed SRB abundances (Figure 4-1). S^0RB were detected in most samples, with relatively low biomass overall (10^2 cells·ml^{-1}). Methanogens were rarely detected by MPN, with <14 cells·100 ml^{-1} (Figure 4-1). While $H_2S_{(g)}$ was generated in SRB, S^0RB, and some fermenting enrichment bottles, MT was detected in cultures of SRB Groups I and II and some fermenter enrichments (Table 5-2). COS was only generated from Group I SRB and fermenter enrichments from

the Upper Spring orifice samples (Table 5-2). DMS was produced in the headspace

of rare fermenter and SRB Group II enrichment cultures (Table 5-2),

Sulfur gas production from fermenting bacteria

Twenty-nine percent of the fermenting bacterial strains produced $H_2S_{(g)}$

when provided with thiosulfate or sulfur-containing amino acids. Two of these

strains (LKC-232 and LKC-322) were used to measure rates of $H_2S_{(g)}$ production

given various inorganic and organic sulfur sources, and to test for possible VOSC

formation from natural precursors (Figure 5-4). Both strains produced $H_2S_{(g)}$ from

thiosulfate (Figure 5-4A and 5-4B); MT was only detected in bottles supplemented

with methionine (Figure 5-4C). Strain LKC-232 reached exponential growth earlier

when supplemented with thiosulfate than LKC-322, and had a faster doubling time

at $0.19 \cdot hr^{-1}$ compared to $0.43 \cdot hr^{-1}$ for LKC-322 (Figure 5-4D and 5-4E). The

addition of thiosulfate strongly stimulated $H_2S_{(g)}$ formation, compared to the small

$H_2S_{(g)}$ concentrations measured in bottles supplemented with SO_4^{2-}, cysteine, and

methionine at levels approximately that of the control, suggesting those $H_2S_{(g)}$

concentration profiles represent background sulfur assimilation rates.

Native mat incubations

$H_2S_{(g)}$ was present in the headspace initially, but decreased to non-

detectable after 57 hr (Figure 5-5A; M-series). After a lag phase (~15 hr), the

concentration of $H_2S_{(g)}$ in live mat samples increased rapidly, while MT was not

generated in the live samples until after 200 hr (Figure 5-5B). COS and DMS were

not detected in any bottles (Figure 5-5C). Decreases in oxygen concentration in the

live mat incubations corresponded to increases in $H_2S_{(g)}$, but not in the sterile water

or killed controls (Figure 5-5D). The observed increase in headspace oxygen in the live sample incubations, with a corresponding rapid decrease in $H_2S_{(g)}$, may be related to oxygen leaking into the chambers during the course of the experiment and subsequent sulfide oxidation.

Homogenized mat incubations and inhibition experiments

Two different types of microbial mats were collected for three separate incubation experiments (Figure 5-6 through 5-8). In the A- and B-series, the concentration of headspace $H_2S_{(g)}$, MT, COS, and DMS were measured (Figures 5-6 and 5-7). $H_2S_{(g)}$ concentrations in the A- and B-series increased rapidly within the first day (6-15 hr) (Figures 5-6A and 5-7A), but in the C-series, $H_2S_{(g)}$ production occurred from 16-79 hr (Figure 5-8A). Headspace MT in the live mat incubations increased after 50 hr (e.g., Figure 5-6B), faster than observed from the M-series. MT was not detected from the C-series. While $H_2S_{(g)}$ concentration varied over time, the concentration of MT steadily increased in the live incubations (Figures 5-6B and 5-7B). COS was not measured from filtered spring water, suggesting that COS was produced biogenically in the mat environment (Figures 5-6C and 5-7C).

Inhibition of sulfate reduction and methanogenesis allowed for an examination of the possible roles of these anaerobic groups to sulfur gas cycling. Limited $H_2S_{(g)}$ evolved in molybdate-amended samples in any incubation series, resulting from either 1) unsuccessful inhibition of sulfate reduction, or 2) sulfur assimilation and $H_2S_{(g)}$ production by fermenting bacteria at low O_2 levels (e.g., Figure 5-6A). For the B-series, significant $H_2S_{(g)}$ was only produced in the BES-amended bottle, but not in the molybdate-amended bottle (Figure 5-7A). MT

headspace evolution was the same for BES-amended samples, but not the molybdate-amended samples, suggesting that MT production may be from SRB activity. In the A- and B-series, however, MT was detected in the molybdate-amended bottles, although at lower concentrations than the unamended incubations or BES-amended incubations. This indicates that other metabolic groups, such as the fermenting bacteria (e.g., Figure 5-4D and 5-4E), may also be responsible for MT production under low O_2 conditions. In the B-series (Figure 5-7C), COS increased in the unamended live mat incubations under low oxygen conditions, above the concentration in the filtered water (Figure 5-9C, 5-9F), but not in the BES-amended sample, indicating that COS production may be linked to methanogenic activity. Conversely in the A-series, COS increased in the BES-amended sample, suggesting association with sulfate reduction (Figure 5-6C). DMS was detected earlier in the BES-amended incubation than in an unamended sample in the A-series, but at the same rate in the B-series (Figures 5-6D and 5-7D).

Rapid increases in $H_2S_{(g)}$ concentrations corresponded to an increase in headspace CO_2 in the A- and B-series (Figures 5-6E and 5-7E), but to a more subdued increase in the C-series (Figure 5-8E). CO_2 did not increase in the headspaces of the sterile water and killed controls in any of the incubation series, indicating the CO_2 production was a results of microbial activity. The rapid increase in headspace CO_2 in the A- and B-series, coinciding with decreases in O_2, may be related to aerobic CO_2 utilization by aerobic chemolithoautotrophs (e.g., sulfur-oxidizers), and that CO_2 consumption slows when O_2 becomes low. This is

supported by the rates of $H_2S_{(g)}$ increase corresponding to decreases in headspace O_2 to <15% (Figure 5-6F, 5-7F, 5-8F).

VOSC consumption by homogenized mats

No $H_2S_{(g)}$ was detected from the spring water following sparging with VOSC (Figure 5-9); however, $H_2S_{(g)}$ was measured in the autoclaved microbial mat control, possibly because of VOSC degradation. The concentrations of both MT and DMS in the filtered water were nearly equal to the concentrations of the standard gases used for sparging. COS was extremely low following sparging, suggesting that the gas concentration in the water had not equilibrated and should have been sparged longer. Initially, headspace concentrations of MT and DMS were lower in the live microbial mat incubations compared to those from the headspace of the sterile water sample, suggesting aerobic microbial consumption of both gases, as the samples still had oxygen present (Figure 5-9F). MT increased above the concentration in the sterile sample after 16 hr (Figure 5-9B), corresponding to a rapid increase in headspace CO_2 (Figure 5-9E) and decreases in O_2 (Figure 5-9F).

DISCUSSION

The processes affecting the consumption and production of sulfur gases in aphotic spring systems and associated microbial mats were studied by gas flux measurements and by incubations of native and homogenized microbial mats. Changes in $C_TS^=$ along the Upper Spring stream channel result from the combined effects of abiotic volatilization, autoxidation, and microbial processes, including biological production and consumption (microbial consumption includes both

catalyzed sulfide oxidation, as well as sulfur utilization for biosynthesis). VOSC production from incubations of the cave microbial mats, but low amounts measured from the habitat, suggest that the microbes in Lower Kane Cave, as well as other aphotic subsurface environments, play a role in VOSC flux to the atmosphere.

At the Upper Spring the observed $C_TS^=$ loss at the orifice is much faster than can be accounted for from the combined effects of abiotic autoxidation and volatilization loss mechanisms (Figure 5-3B). Based on the estimated autoxidation, and actual and theoretical volatilization rates alone, $C_TS^=$ at the cave entrance should be only slightly lower than the measured Upper Spring $C_TS^=$. In this anaerobic to disaerobic cave system, autoxidation $t_{1/2}$ is considerably slower ($t_{1/2} = $ 866 to 1250 hr) than measurements from air-saturated natural waters with low salinity (Avrahami and Golding, 1969; Chen and Morris, 1972) and several deep waters from anoxic marine basins, such as Framvaren Fjord ($t_{1/2} = $ 19-20 min) and the Chesapeake Bay ($t_{1/2} \sim 8.3$ min), where the autoxidation rates are enhanced as a result of reaction with dissolved constituents (e.g., metals) in the water and mixing with surface waters (Millero, 2001). Therefore, the observed rapid decrease in $C_TS^=$ near the mat terminus requires subaqueous microbial sulfide consumption.

Microbial consumption of $C_TS^=$ occurs under disaerobic to aerobic conditions in the cave stream (Figure 5-3A). Using the full-cycle 16S rRNA approach to describe the microbial communities in the Lower Kane Cave mats (refer to Chapters 2 and 3), mat biovolume is dominated by "*Epsilonproteobacteria*" (~70% of the bacterial biovolume), with minor assemblages of known sulfur-oxidizing bacterial groups belonging to the genera

168

Thiothrix and *Thiobacillus* (McDonald et al., 1996; Cha et al., 1999). Although cultures of the "*Epsilonproteobacteria*" from Lower Kane Cave have not been successfully established to date, closely-related taxonomic groups consume dissolved sulfide in culture (Fenchel and Glud, 1998; Gevertz et al., 2000; Campbell et al., 2001; Nemati et al., 2001; Kodama and Watanabe, 2003), and even at oxygen tensions as low as 1% (Takai et al., 2003). Qualitative assessment of microbial sulfide oxidation was done from the mat incubation experiments. In the M-, A-, and B-series incubations, there were low to non-detectable concentrations of headspace $H_2S_{(g)}$ when O_2 levels were >15%. Headspace $H_2S_{(g)}$ increased when O_2 decreased, suggesting that microbial sulfide consumption occurs over a narrow range of O_2 levels for aerobic to microaerophilic sulfide consumption. Microbial consumption could also be occurring at lower O_2 tensions, but consumption rates may not be as rapid nor as competitive compared to microbial $H_2S_{(g)}$ production by SRB, S^0RB, and fermenting bacteria at low O_2.

The observed $C_TS^=$ versus distance profile showing nearly constant $C_TS^=$ through the microbial mats (Figure 5-3A) and enhanced $H_2S_{(g)}$ flux directly over the microbial mats in the stream channel (Table 5-1) indicate that the mats in the cave stream are sites for in situ $H_2S_{(g)}$ production by SRB and S^0RB, and possibly, to a lesser extent, from sulfur assimilation or growth on dissolved thiosulfate by fermenting bacteria (Figure 5-4). MPN biomass estimates demonstrate that anaerobic metabolic guilds are ubiquitous in the microbial mats, and that SRB are the most abundant anaerobic metabolic guilds (refer to Chapter 4; Figure 4-1). The sulfur isotope values of the dissolved sulfide in Lower Kane Cave, averaging -

22.5‰, support autochthonous microbial sulfate reduction. The $\delta^{34}S$ values for dissolved sulfide in the spring waters indicate that dissimilatory sulfate reduction is the source of sulfide to the cave (refer to Chapter 2; Figure 2-6) (Canfield, 2001a). However, the decrease in $\delta^{34}S$ values at the end of the Upper Spring microbial mats suggests that sulfide, with a lighter $\delta^{34}S$ value, is being generated within the stream; in situ sulfate reduction would generate a decrease in the sulfide $\delta^{34}S$ composition.

MT, DMS, and COS generated in incubations were biogenic in origin because VOSC were not emitted from filtered spring water or killed microbial mat samples. The prevalence of MT production from cultures (Table 5-2), bulk mat incubations (Figure 5-5), and from the small flux from the cave stream suggest that MT is the most abundant VOSC in the cave. These results are in agreement with studies from other anoxic freshwater and marine settings where MT is also the dominant VOSC (Kiene, 1988; Kiene et al., 1990; Lomans et al., 1997; Bodenbender et al., 1999; Lomans et al., 1999a; Fritz and Bachofen, 2000).

Lomans et al. (1997) suggest that MT and DMS form from the methylation of $H_2S_{(g)}$ due to the degradation of sulfur-containing amino acids and methoxylated compounds by SRB during degradation of organic material in anoxic sediments. Some microbes can demethiolate methionine to MT (Taylor, 1991; Dias and Weimer, 1998); (Seiflein and Lawrence, 2001). Taylor (1991) describes that various enzymes are responsible for VOSC production from successive methylation of precursor sulfur gases. If these processes were occurring, a decrease in $H_2S_{(g)}$ would be expected. However, decreasing $H_2S_{(g)}$ could also be from microbial sulfide consumption. Only when aerobic or microaerophilic consumption was

170

lessened could the effects of methylation be resolved. For the M-series and B-series (Figures 5-5 and 5-7), decreases in $H_2S_{(g)}$ under anaerobic conditions could be correlated to MT increases. Therefore, MT production by the microbes from Lower Kane Cave may be due to both amino acid breakdown and sulfide methylation.

Disparate results for COS from the incubations of homogenized mat samples may be due to differences in the microbial populations within the sample, such that the Upper Spring sample (A-series) may have a greater abundance of methanogens compared to the Lower Spring sample (B-series). Previous research supports that COS is primarily derived from bacterial activity in marine environments, but COS can also form chemically in soil stimulated by thiocyanate (Conrad, 1996), from photochemical oxidation of CS_2 in the atmosphere (Bodenbender et al., 1999; Watts, 2000), or by autoclaving or γ-irradiating soils (Lehmann and Conrad, 1996). COS evolved in the headspace of two live mat incubations and BES-amended samples (Figures 5-6C and 5-7C), suggesting that COS may be produced by SRB or fermenters (Table 5-2). However, because the COS concentrations were relatively low for all of the incubations, additional work is required to verify microbial COS cycling.

VOSC consumption by microorganisms may be a mechanism by which VOSC concentrations are kept low in the cave. MT, and DMS to a lesser extent, were degraded under aerobic conditions (Figure 5-9B), which may have been due to microbial consumption. Previous work with sulfur-oxidizing bacteria, including *Thiobacillus thioparus* strain 5 and *Thiobacillus novellas* strain SRM, indicates that these organisms grow using DMS, MT, DMDS (Visscher et al., 1991). Some

171

sulfur-oxidizing bacteria (e.g., Smith and Kelly, 1988; Jordan et al., 1995; Conrad, 1996) and other metabolically diverse bacteria (e.g., Smith et al., 1991; Ensign, 1995; Seefeldt et al., 1995) can also grow using COS.

Headspace DMS remained relatively low during the incubations, except for the BES-amended bottles (e.g., Figure 5-6D) which may suggest that methanogens are important for DMS cycling. Several researchers suggest that methanogens are vital to VOSC cycling (Kiene et al., 1986; Rajagopal and Daniels, 1986; Lomans et al., 1999a; Lomans et al., 1999b). Specifically, Lomans et al. (1999a) demonstrate that high concentrations of VOSC result in methane production through methanogenesis in marine and brackish settings. Anaerobic heterotrophs, such as proteolytic (fermenting) clostridia, can also generate methane from methionine and MT (Rimbault et al., 1988). However, in the S-series incubations, aerobic consumption of DMS was evident (Figure 5-9D), and because the BES-amended sample had the same concentration profile as the unamended samples, DMS may also be consumed by SRB or aerobic bacteria, but not by methanogens. Moreover, rare methanogens were cultured from some of the Lower Kane Cave microbial mats (Chapter 4), and low levels of methane were measured from the cave spring water (Table 2-1). During the A- and B-series, however, methane levels did not increase above the background, which is expected if methanogenesis or proteolytic sulfur amino acid breakdown processes were occurring (Figures 5-6G and 5-7G).

In conclusion, microorganisms living in sulfur-rich, subterranean habitats contribute to sulfur gas cycling, and the terrestrial subsurface represents both a source and sink for $H_2S_{(g)}$ and VOSC. This research demonstrates for the first time

that H_2S and VOSC are cycled by microbial communities in an aphotic freshwater habitat. Photochemical degradation processes are absent in the cave, so the microbial contributions to gas cycling can be studied in detail. Even if microbial production is balanced by consumption, sulfur gas cycling by microorganisms may be important in subsurface ecosystems by providing additional sulfur substrates for the microbial communities. The results from Lower Kane Cave are consistent with those from previous studies from marine and freshwater habitats with SRB (e.g., Stoner et al., 1994; Lomans et al., 1997; Visscher et al., 2003). One notable exception of this work is that methanogenesis does not appear to be a significant process by which VOSC are degraded in Lower Kane Cave. Less than 10% of the world's karst is associated with sulfidic waters (Palmer, 1991), and yet caves like Lower Kane Cave can serve as a proxy for larger sulfidic aquifers that may be inaccessible for study. As groundwater in non-karst areas can often have high concentrations of dissolved sulfide, especially in regions near hydrocarbon reservoirs (Ulrich et al., 1998; Nemati et al., 2001; Kodama and Watanabe, 2002; Elshahed et al., 2003), the contribution of subterranean sulfur gas cycling is potentially significant globally.

Table 5-1: Aqueous geochemical data, observed $C_TS^=$, and theoretical and measured $H_2S_{(g)}$ volatilization flux. $C_TS^=$ and flux measurements were collected at different times over a three day time period, August 2003.

Site	Observed Parameters				2-film Theoretical Volatilization Model				Measured Volatilization				Mass Flux		Loss by Volatilization	
	O_2	$C_TS^=$	pH	Flux $C_TS^=$	K_H	$t_{1/2}$	Mean $H_2S_{(g)}$ Flux	Theoretical Flux	Discharge from chamber	[H_2S]	Vapor Flux	$H_2S_{(g)}$ flux	Mean	$t_{1/2}$	Actual $C_TS^=$	Theoretical $C_TS^=$
(m)	$\mu mol \cdot L^{-1}$	$\mu mol \cdot L^{-1}$		$\mu mol \cdot min^{-1}$	ppmv	min	$\mu mol \cdot m^{-2} \cdot min^{-1}$	$\mu mol \cdot m^{-2} \cdot min^{-1}$	$ml \cdot min^{-1}$	ppmv	$ml\ H_2S \cdot min^{-1}$	$\mu mol \cdot m^{-2} \cdot min^{-1}$	$\mu \mu ol \cdot m^{-2} \cdot min^{-1}$	min	$\mu mol \cdot L^{-1}$	$\mu mol \cdot L^{-1}$
190	0.00	26.67	7.36	9600				34.08	86	4.5	0.00038	10.58			26.67	26.67
191	0.00	26.24	7.36	8727	83.4	13.07	30.98	30.98	53	38.46	0.00204	55.74	9.13		26.58	26.59
191									80	30.38	0.00243	66.46				
191	0.00	26.2	7.36	8727	83.4	13.07	30.98	30.98	84	27.87	0.00234	64.02	48.5			
191									57	9.3	0.00053	14.50				
191									84	7.2	0.00061	16.54				
191									84	6.9	0.00058	15.85	15.62			
191									56	26.5	0.00148	40.58	40.58	11.7		
191									52	5.4	0.00028	7.68				
191									49	26.8	0.00131	35.91				
191									82	19.7	0.00161	44.17	41.43			
191									82	19.72	0.0016	44.22				
193	2.34	21.52	7.38	7964	73.9	13.07	27.43	26.68	54	47	0.0025	69.40			26.08	26.42
193									84	41.7	0.0035	95.78	87.52			
193									84	42.4	0.00356	97.39				
193									25	51.73	0.00129	35.36				
193									27	46.3	0.00125	34.18				
193									59	47.2	0.00278	76.15				
193									85	46.9	0.00399	109.01				
193									103	42.1	0.00433	118.58	84.48	4.38		
194	2.66	20.91	7.42	7745	67.6	13.07	25.09	24.39	57	46.43	0.00264	72.37			25.82	26.33
194									84	37.56	0.0031	86.27	62.43			
194									84	35.31	0.0030	81.11				
194									53	41.2	0.00218	59.71				
194									87	32.6	0.00284	77.56				
194									87	32.4	0.00282	77.08	71.45	4.21		
195	2.55	20.91	7.42	7527				24.39							25.57	26.25
196	2.19	18.79	7.42	6764				21.91							25.32	26.17
197	7.5	20.3	7.42	7309				23.68							25.17	26.08

Table 5-1: Continued.

Meter	Observed Parameters O_2	$C_{TS}^{=}$	pH	Flux $C_{TS}^{=}$	2-film Theoretical Volatilization Model K_H	$t_{1/2}$	Mean $H_2S_{(g)}$ Flux	Theor-etical Flux	Measured Volatilization Dis-charge from chamber	[H_2S]	Vapor Flux	$H_2S_{(g)}$ flux	Mass Flux Mean	$t_{1/2}$	Loss by Volatilization Actual $C_{TS}^{=}$	Theor-etical $C_{TS}^{=}$
m	μmol·L^{-1}	μmol·L^{-1}		μmol·min^{-1}	ppmv	min	μmol·m^{-2}·min^{-1}	μmol·m^{-2}·min^{-1}	ml·min^{-1}	ppmv	ml H_2S·min^{-1}	μmol·m^{-2}·min^{-1}	μmol·m^{-2}·min^{-1}	min	μmol·L^{-1}	μmol·L^{-1}
199	14.69	22.42	7.42	8073				26.16							25.02	25.92
200		0.67	7.43	7309	62.8	13.07	23.31	23.22	40	30.25	0.00121	33.09				
200		0.62	7.43	6764	58.1	13.07	21.57		63	24.8	0.00156	42.72	37.91			
200		0.64	7.36	6982	66.8	13.07	24.78		27	41.74	0.00113	30.82	46.61		24.88	25.83
200									84	27.17	0.00228	62.41				
200									44	29.3	0.00129	35.25				
200									84	22	0.0018	50.53				
200									84	20.7	0.00174	47.55				
201	19.38	10.09	7.34	6873				25.13							24.73	25.75
202	33.44	20.3	7.34	7309				26.72							24.59	25.67
203	40.31	0.51	7.34	5564	54.8	13.07	20.34	20.76	40	31	0.0012	33.91	44.44		24.44	25.59
203		0.54	7.43	5891	50.6	13.07	18.79		60	25.4	0.0015	41.67				
203		0.54	7.43	5891	50.6	13.07	18.79		85	19.9	0.00169	46.25	40.61	7.03		
203									42	27.1	0.00114	31.12				
203									42	25.7	0.00108	29.52				
203									80	18.3	0.00146	40.03				
203									80	17.7	0.00142	38.72		7.27		
205.5		0.44	7.4	4800	43.2	13.07	16.04		38	35	0.00133	36.37				
205.5		0.34	7.4	3709	33.4	13.07	12.39		57	34.4	0.00196	53.62	34.85			
205.5		0.41	7.4	4473	40.3	13.07	14.95		85	29	0.00246	67.40				
205.5									83	27.9	0.00231	63.32	55.18	4.14		
205.5									43	7.41	0.00031	8.71				
205.5									43	7.7	0.00033	9.05				
206	47.50	12.42	7.4	4473				14.46							23.95	25.38
207		0.35	7.44	3818	32.3	13.07	11.99	11.56	56	13.1	0.00073	20.06			23.81	25.27
207		0.32	7.43	3491	30.0	13.07	11.13		84	10.25	0.00086	23.54	21.80	7.25		
210		5.76	7.43	2073				6.61							23.41	25.03
215		3.33	7.43	1200												24.63

175

Table 5-2: Reduced sulfur gases produced from all enrichment cultures, listed per microbial mat site in the Lower Kane Cave.

Site (m) and Sample[a]	Group I SRB				Group II SRB				S°RB				Fermenters			
	H$_2$S	COS	MT	DMS	H$_2$S	COS	MT	DMS	H$_2$S	COS	MT	DMS	H$_2$S	COS	MT	DMS
189 orifice water	-[b]	-	-	-	-	-	-	-	-	-	-	-	-	-	-	-
215 orifice water	+	-	-	-	+	-	-	-	-	-	-	-	+	-	+	-
248 orifice water	+	-	-	-	+	-	-	-	-	-	-	-	+	-	-	-
189 gray orifice sediment	+	+	-	-	+	+	+	-	+	-	-	-	-	-	-	-
189 gray orifice sediment	+	+	+	-	+	-	+	-					+	+	+	-
189 gray orifice sediment	+	-	+	-	+	-	+	-					+	+	+	-
193 gray filaments	+	-	+	-	+	-	+	-	+	-	-	-	+	-	-	-
198 gray filaments	+	-	+	-	+	-	+	-	+	-	-	-	+	-	+	-
201 gray filaments	+	-	+	-	+	-	+	-	-	-	-	-	+	-	+	-
203 gray filaments	+	-	+	-	+	-	+	-	+	-	-	-	+	-	+	-
203 deep gray filaments	+	-	+	-	+	-	+	-	+	-	-	-	+	-	+	-
248 gray filaments	+	-	-	-	+	-	+	-	+	-	-	-	+	-	+	-
248 gray orifice sediment	+	-	+	-	+	-	+	-	+	-	-	-	+	-	-	-
198 white filaments	+	-	+	-	+	-	+	-	+	-	-	-	+	-	+	-
201 white filaments	+	-	+	-	+	-	+	-	+	-	-	-	+	-	+	-
203 white filaments	+	-	-	-	+	-	+	-	+	-	-	-	+	-	-	-
203 white filaments	+	-	+	-	+	-	+	+					+	+	+	+
248 white filaments	+	-	+	-	+	-	+	+	+	-	-	-	+	+	+	+
203 white webs	+	-	+	-	+	+	+	-	+	-	-	-	+	-	+	-
203 white feathers	+	-	+	-	+	-	+	-	+	-	-	-	+	-	-	-
249 feathers	+	-	+	-	+	-	+	-	+	-	-	-	+	-	+	-
203 yellow patches	+	-	+	-	+	-	-	-	-	-	-	-	-	-	-	-
249 yellow patches	+	-	+	-	+	+	+	-	+	-	-	-	+	-	+	-

[a]Repeated sampling sites represent replicate bottles scored for serial dilutions from different sampling trips.
[b] − gas not produced; + gas detected; no symbol represents a sample was not analyzed.

176

Figure 5-1: Gas chromatograph (GC) setup in Lower Kane Cave. (A) Passage below Upper Spring, with flux chamber in foreground and GC to the left (arrow). (B) Close-up of Teflon 16-cm² flux chamber (arrow). (C) Flux chambers over microbial mats and cave stream at 197 m. A copper tube was used to scrub incoming $H_2S_{(g)}$. (D) GC in Lower Kane Cave; flux chamber running in the background (arrow).
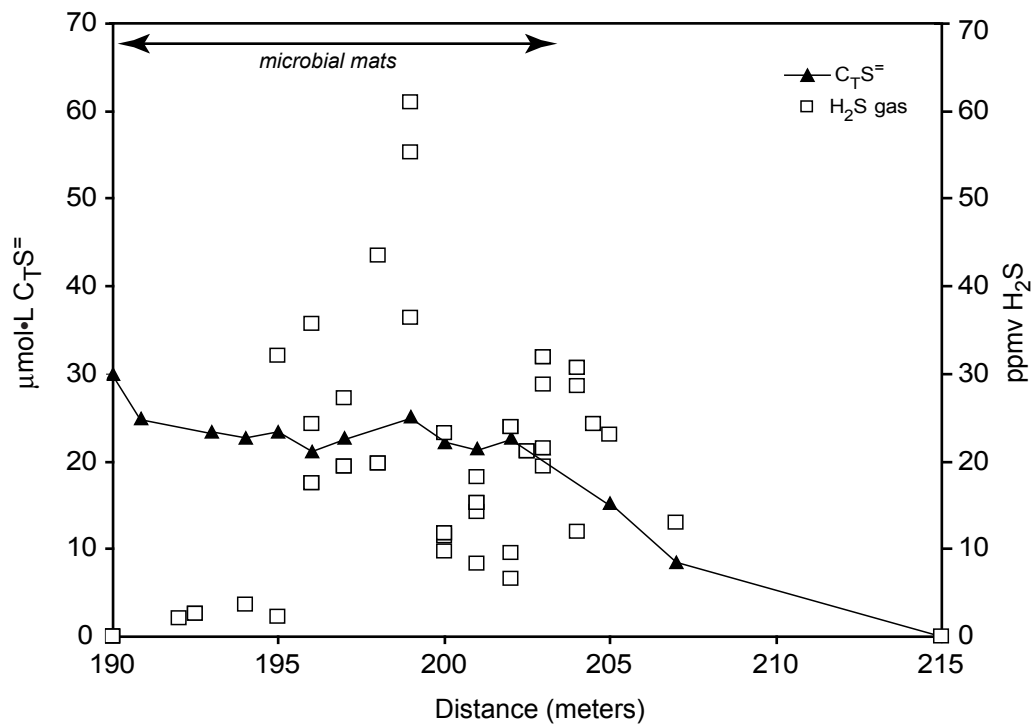
Figure 5-2: Total dissolved sulfide concentration ($C_TS^=$) and average H_2S gas concentrations measured along the Upper Spring flowpath in Lower Kane Cave, starting downstream from the spring orifice (189 m). Gas was measured by gas chromatography directly in the cave from individual gas samples collected from the air-water boundary layer.
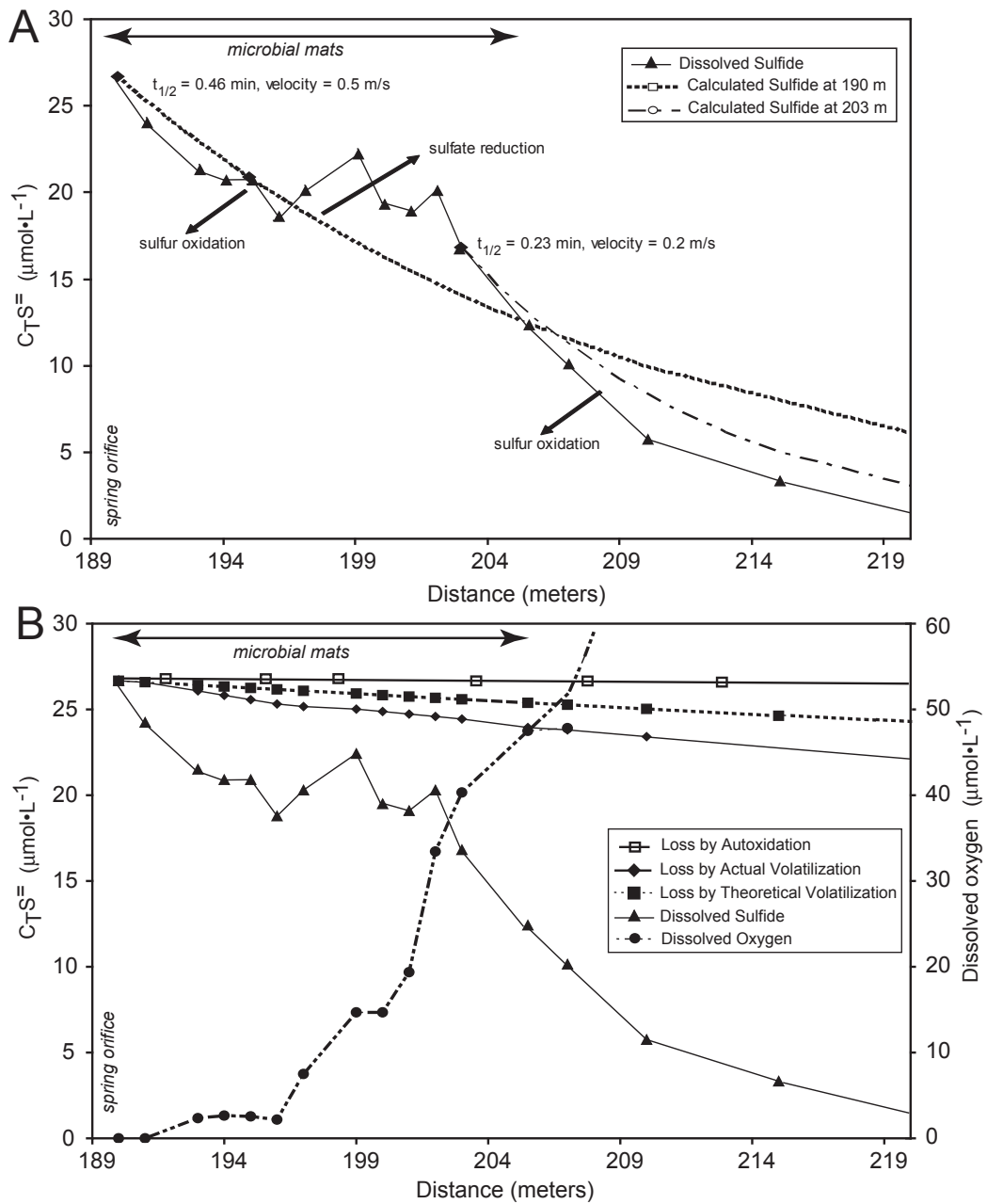
Figure 5-3: Total dissolved sulfide ($C_TS^=$) loss from the Upper Spring orifice through the microbial mats downstream. (A) Observed concave-down $C_TS^=$ vs. distance profile and two expected concave-up first-order loss profiles estimated from the initial $C_TS^=$ at the spring orifice (190) and $C_TS^=$ at 203 m. Microbial processes proposed responsible for offsetting the $C_TS^=$ are labeled. (B) Observed $C_TS^=$ and dissolved oxygen vs. distance profiles compared to volatilization and autoxidation loss profiles. Actual volatilization based on $H_2S_{(g)}$ flux measurements and theoretical volatilization loss curve estimated from 2-film Liss and Slater (1974) model.

179
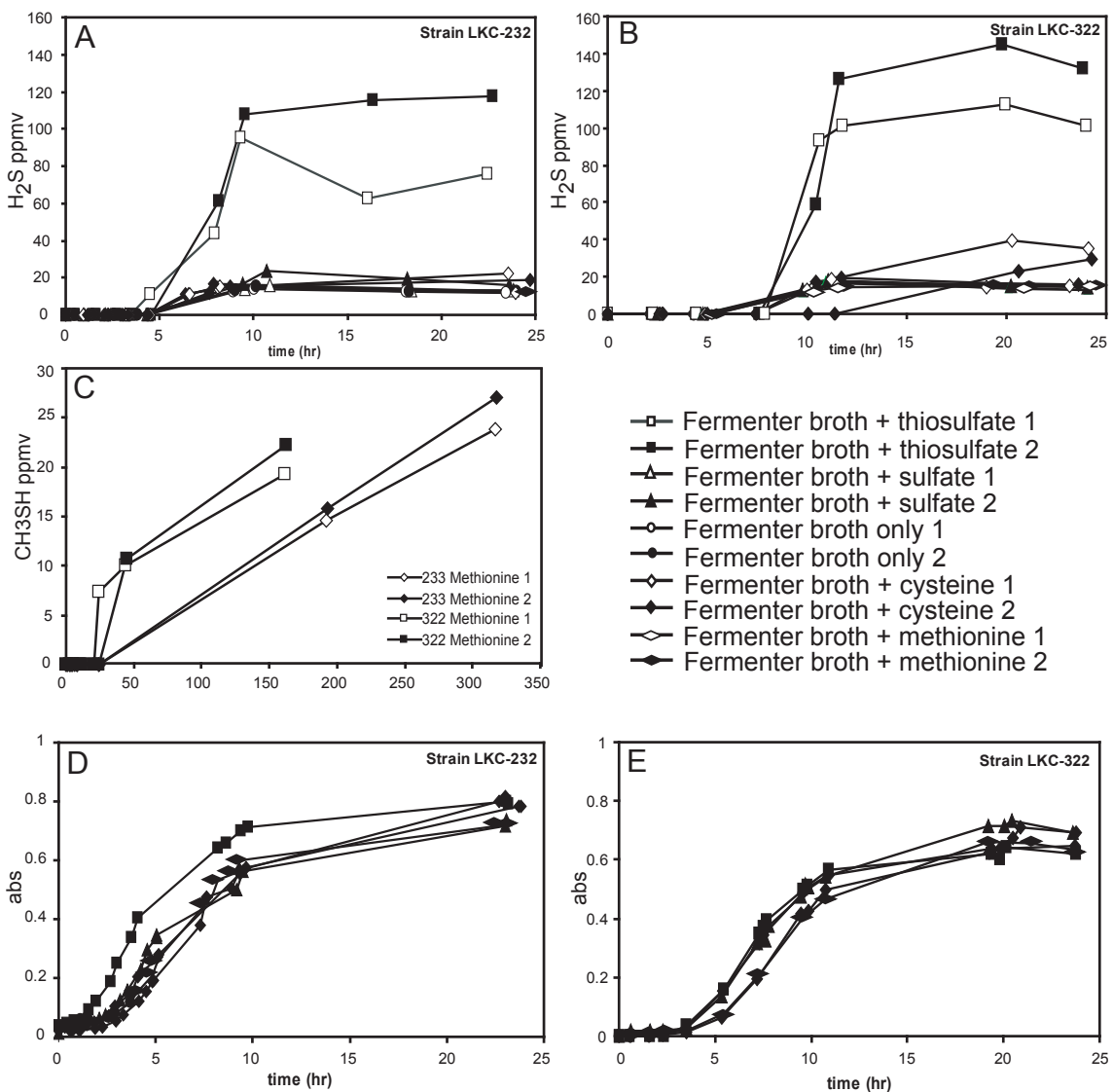
Figure 5-4: Time course series for two fermenting bacterial strains. (A and B) H$_2$S production was tested for using different inorganic and organic sulfur substrates. (C) Methanethiol production on methionine. (D and E) Growth curves measured by spectrophotometry.
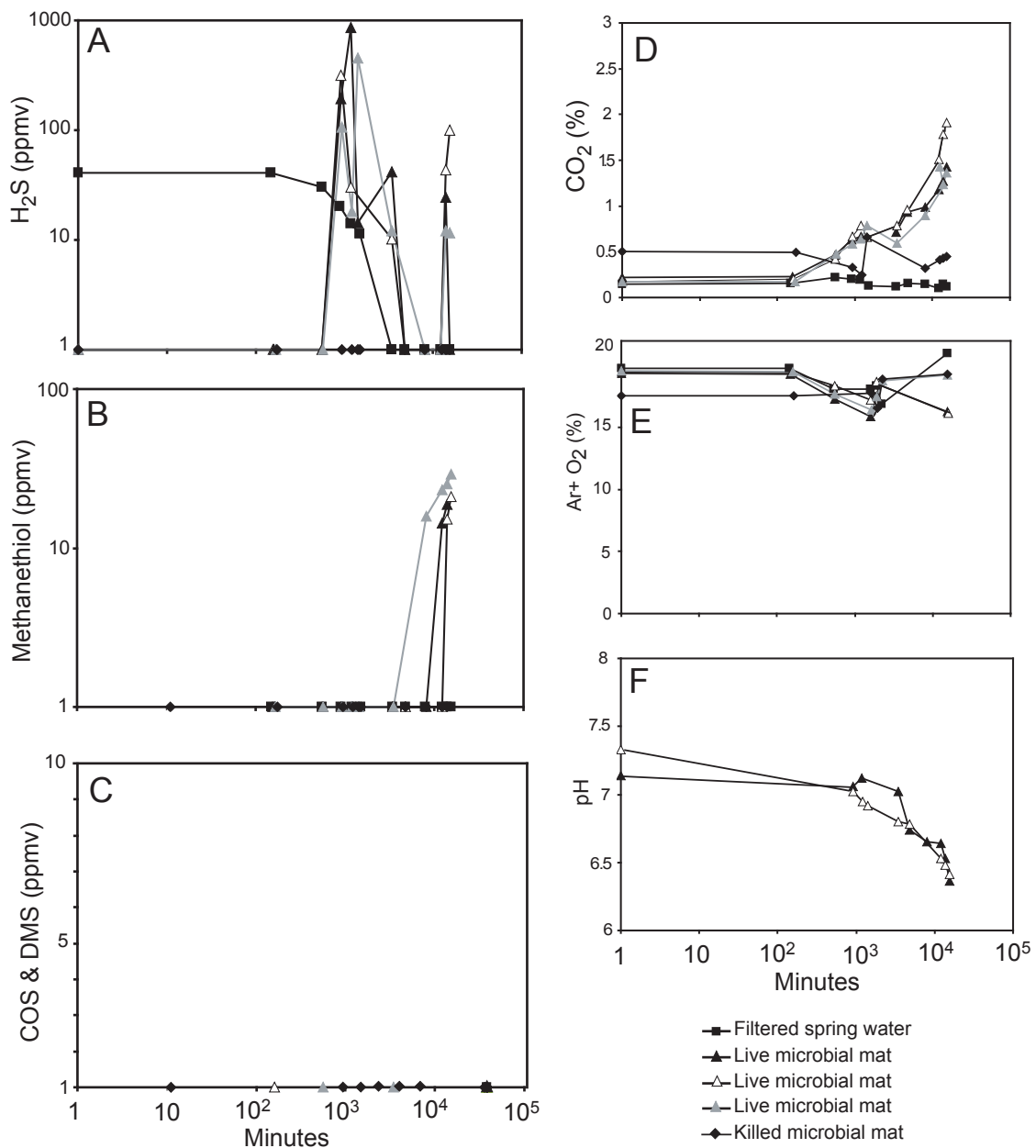
Figure 5-5: M-series time courses of gases and pH from Teflon reactor incubations prepared from natural microbial mat samples (Lower Kane Cave, 248 m mat sample). pH was monitored in reactor M2 and M3.
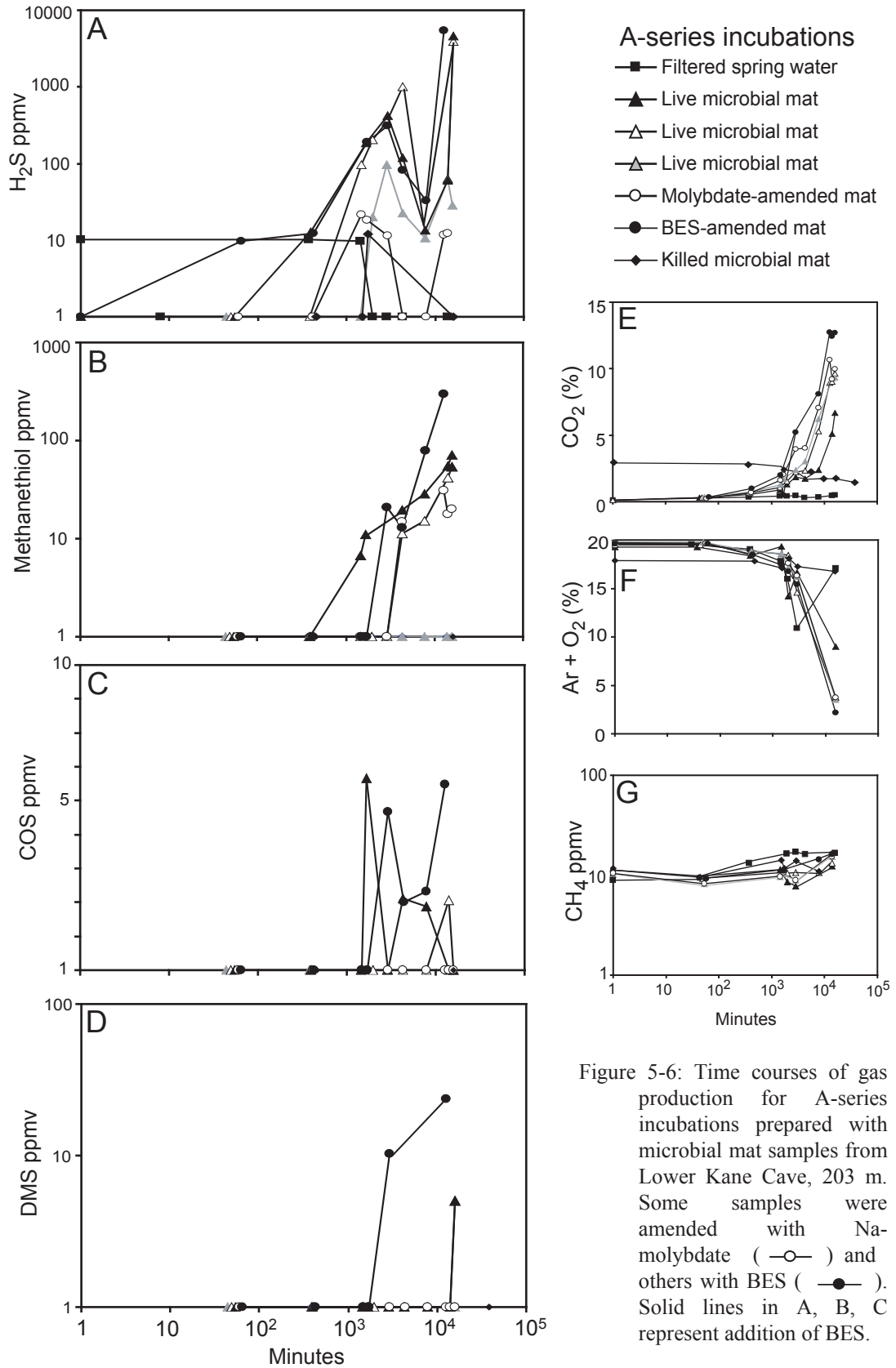
Figure 5-6: Time courses of gas production for A-series incubations prepared with microbial mat samples from Lower Kane Cave, 203 m. Some samples were amended with Na-molybdate (—○—) and others with BES (—●—). Solid lines in A, B, C represent addition of BES.

182

Figure 5-7: Time courses of gas production for B-series incubations prepared with microbial mat samples from Lower Kane Cave, 248 m. Some samples were amended with Na-molybdate (—○—) and others with BES (—●—).

183
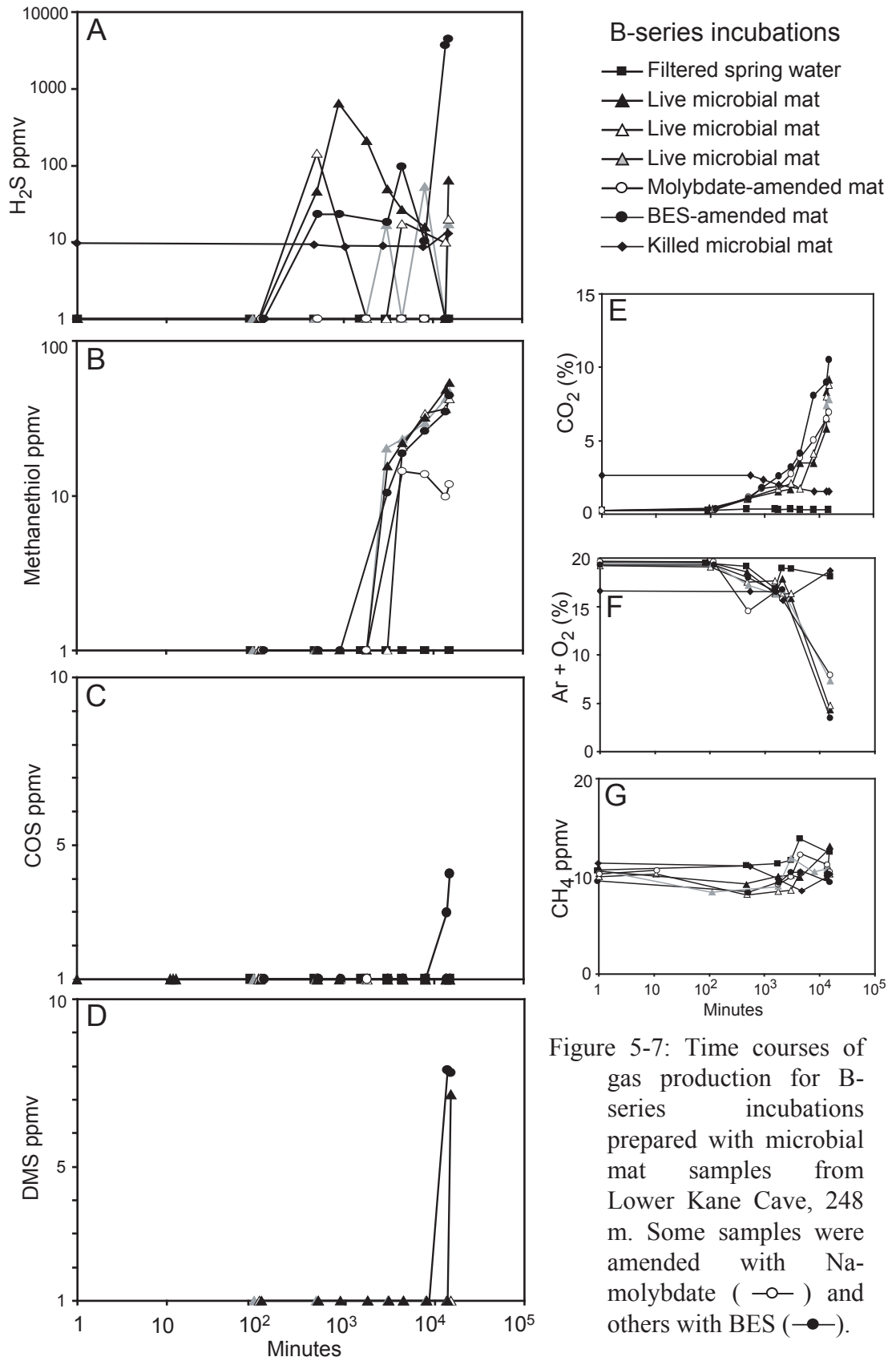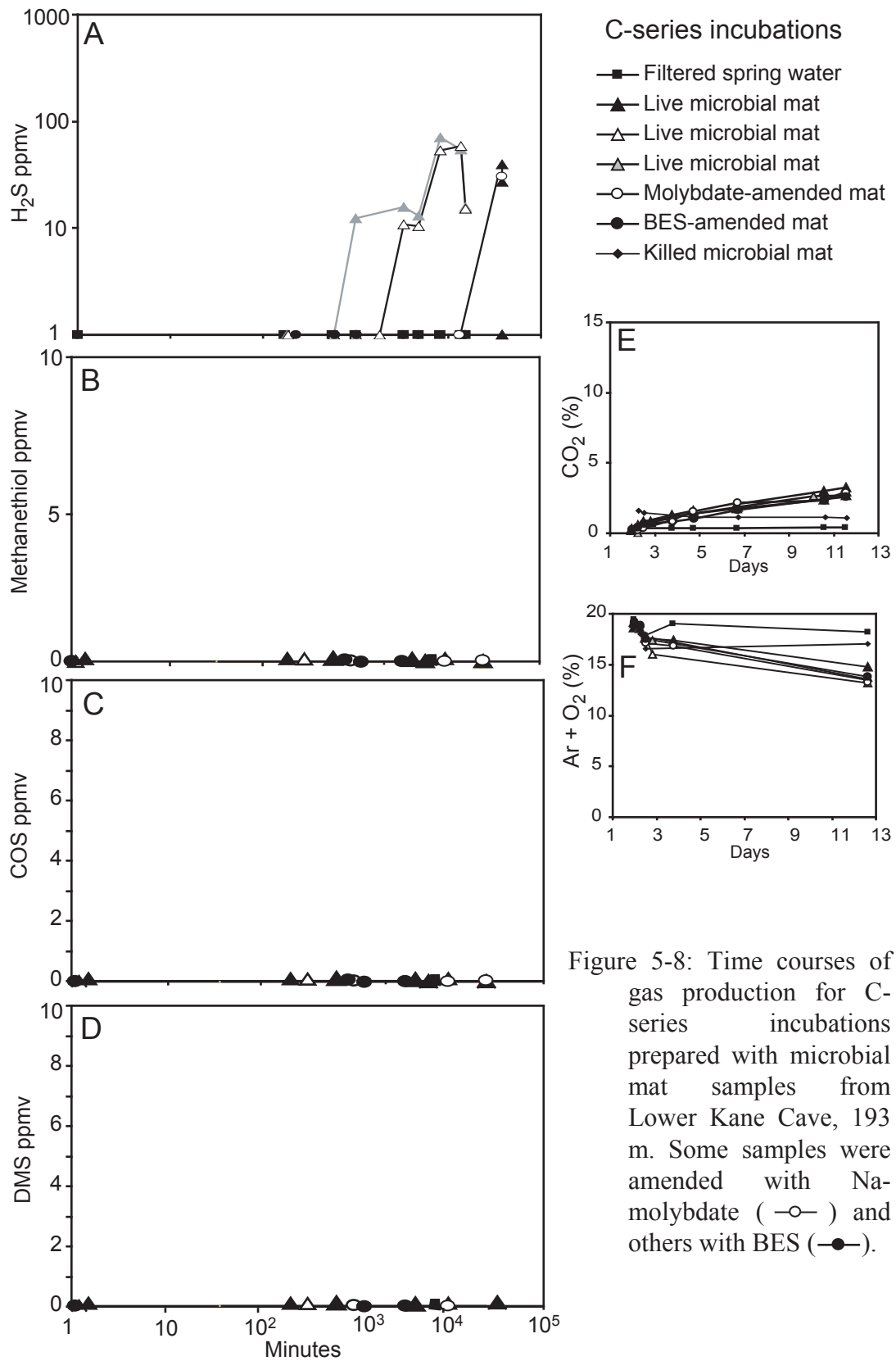
Figure 5-8: Time courses of gas production for C-series incubations prepared with microbial mat samples from Lower Kane Cave, 193 m. Some samples were amended with Na-molybdate (—○—) and others with BES (—●—).

184
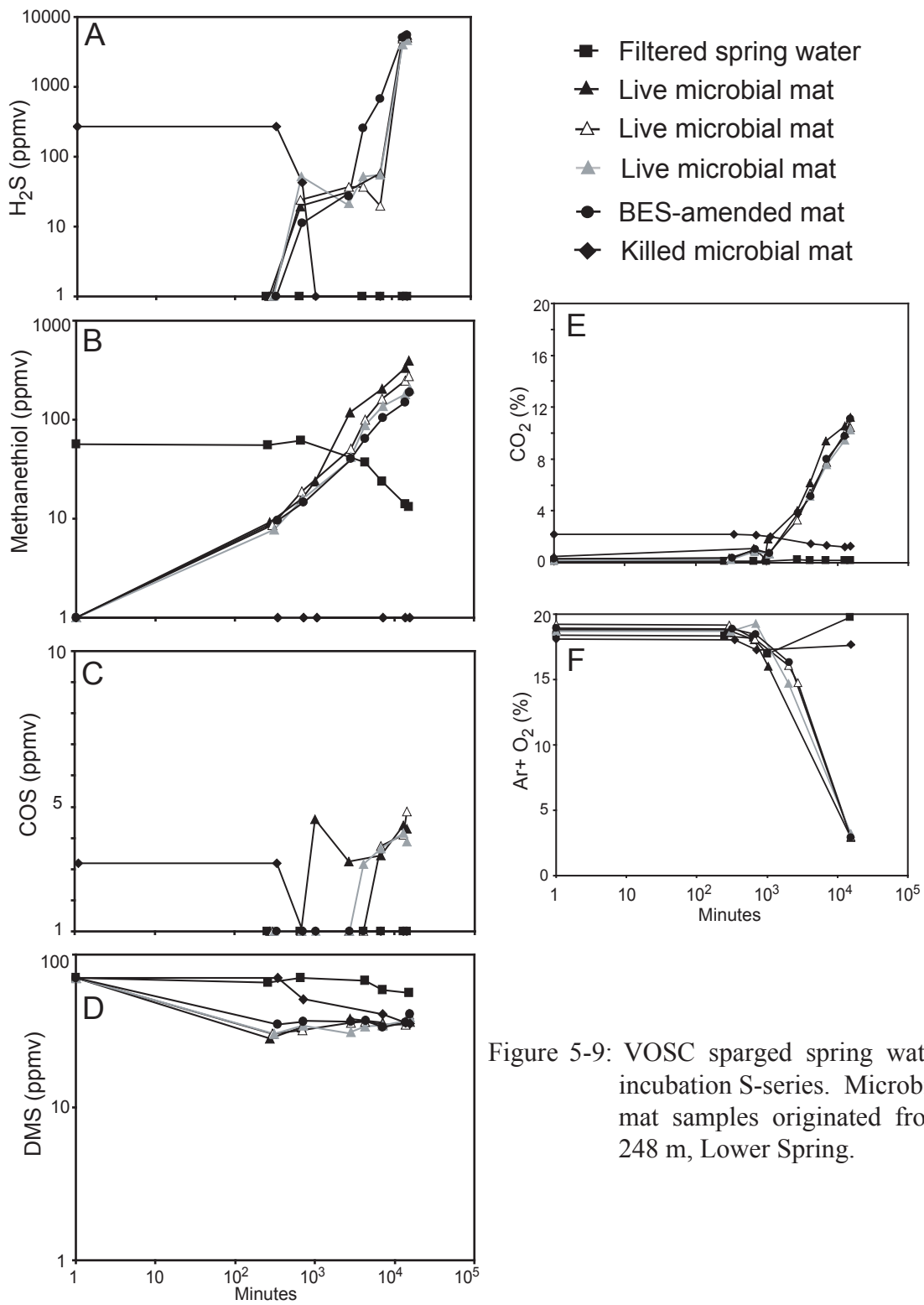
Figure 5-9: VOSC sparged spring water incubation S-series. Microbial mat samples originated from 248 m, Lower Spring.

185

Chapter 6: Microbial Contributions to Cave Formation:
New Insights into Sulfuric Acid Speleogenesis

ABSTRACT[1]

The sulfuric acid speleogenesis model was introduced in the early 1970s from observations of Lower Kane Cave, Wyoming, and was proposed as a cave enlargement process resulting primarily from H_2S autoxidation to sulfuric acid and replacement of carbonate by gypsum on subaerially exposed cave-wall surfaces. This sulfuric acid speleogenesis type-locality was reexamined using uniquely applied geochemical and microbiological methods. Little H_2S escapes into the cave atmosphere, or is lost by abiotic autoxidation, and instead the primary H_2S loss mechanism is from consumption of reduced sulfur compounds by subaqueous sulfur-oxidizing bacteria. Filamentous *"Epsilonproteobacteria"* and *Gammaproteobacteria,* characterized by fluorescence in situ hybridization, colonize carbonate surfaces and generate sulfuric acid as a metabolic byproduct. The bacteria focus carbonate dissolution by locally depressing pH. These exceptional findings show that sulfuric acid speleogenesis occurs in the shallow subaqueous cave environment, and potentially at much greater phreatic depths in carbonate aquifers, thereby offering new insights into the microbial roles in subsurface karstification.

INTRODUCTION

Karst landscapes form where soluble carbonate rocks dissolve by chemical solution, resulting in distinct geomorphic features including caves and conduit drainage systems (White, 1988; Ford and Williams, 1989). Karst comprises a significant percentage of the continental earth's surface, and karst formations are important resources for water, hydrocarbon energy, and tourism (see reviews by White, 1988; Ford and Williams, 1989; Palmer, 1991; Daoxian, 1998). The classic model for cave and karst development (speleogenesis) is one of carbonate rock dissolution by carbonic acid, generally at the water table or within the epikarst. Palmer (Palmer, 1991) estimates that <10% of karst globally has developed from hypogenic processes involving CO_2- or H_2S-rich fluids. Examples of extensive hypogenic karst include the caves of the Black Hills, South Dakota (Palmer and Palmer, 1989), the caves of the Guadalupe Mountains, New Mexico and Texas, including Carlsbad Cavern (Hill, 1996; Polyak et al., 1998), caves in Central Italy (Galdenzi and Menichetti, 1995), and the karst of the Caucasus Mountains (Shelley, 1956) and Turkmenistan (Maltsev, 1993). Many hypogenic caves are polygenic in origin (Hill, 1995; 1996), reflecting processes whereby mixing of meteoric water with waters enriched in CO_2 or H_2S has played a role in formational processes (e.g., Ford and Williams, 1989). Because of the complexity of speleogenesis processes, as well as the fact that many of these systems are no longer forming today, many of the mechanisms governing cave formation must be inferred.

Historically, several researchers have proposed that carbonates could dissolve by acids other than carbonic acid, including acids derived from inorganic or bacterial oxidation of sulfides or organic matter (Kaye, 1957; Howard, 1964). For many years, however, carbonate dissolution by sulfuric acid was considered insignificant, and more recently Lowe and Gunn (1995) suggest that sulfuric acid may be important for all nascent subsurface carbonate porosity generation. Palmer (1991; 1995) speculates that sulfuric acid dissolution, as a major cave formation process, is of more importance for the evolution of carbonate petroleum reservoirs than it is for the origin of caves. Indeed, sulfuric acid dissolution has been proposed for the karstification of significant hydrocarbon reservoirs, including the Lisburne field in Prudhoe Bay, Alaska (Jameson, 1994; Hill, 1995), and Mississippi Valley-type deposits (Hill, 1990). Recently, several active caves with hydrogen sulfide-rich groundwater, which discharges into the cave passages as springs, have been recognized (Hubbard et al., 1990; Galdenzi and Menichetti, 1995; Sarbu et al., 1996; Hose et al., 2000).

The process of sulfuric acid speleogenesis from the 'replacement-solution' process was proposed by Egemeier (Egemeier, 1981; Hill, 1990; Jagnow et al., 2000) from work in Lower Kane Cave, Wyoming. Dissolved hydrogen sulfide in the groundwater volatilizes into the cave atmosphere, where hydrogen sulfide oxidizes on moist, sub-aerial cave-wall surfaces to sulfuric acid;

$$H_2S + 2O_2 \rightarrow H_2SO_4 \qquad\qquad (5\text{-}1)$$

The acid reacts with and replaces limestone with gypsum ($CaSO_4 \cdot 2H_2O$),

$$CaCO_3 + H_2SO_4 + H_2O \rightarrow CaSO_4 \cdot 2H_2O + CO_2 \qquad\qquad (5\text{-}2)$$

188

which eventually dissolves into groundwater undersaturated with respect to gypsum. The net result is the removal of mass and an increase in void volume.

Hydrogen sulfide is a rich energy source for microorganisms, and sulfidic cave systems are often colonized by thick microbial mats (e.g., Angert et al., 1998; Hose et al., 2000; Engel et al., 2001). However, the potential role of sulfuric acid-generating microorganisms to cave formation has only been alluded to (Symk and Drzal, 1964; Hubbard et al., 1990; Hill, 1996; Angert et al., 1998; Hose et al., 2000; Vlasceanu et al., 2000; Engel et al., 2001). The present investigation reexamines the Lower Kane Cave sulfuric acid speleogenesis process by considering the presence of active microbial communities in subaqueous microbial mats, and in particular sulfur-oxidizing bacteria. Because only a small percentage of hydrogen sulfide volatilizes into the cave air, most of the dissolved sulfide is consumed within the subaqueous environment by microbial oxidation (refer to Chapter 5). This exceptional finding led to the hypothesis that speleogenesis within Lower Kane Cave occurs in the subaqueous environment, where sulfur-oxidizing bacteria directly contribute to carbonate dissolution.

MATERIALS AND METHODS

Aqueous Geochemistry

The focus of this chapter is on the Upper Spring transect and the 17 m of mat-filled outflow channel (Figure 1-2), although similar results were found at the other spring-stream complexes in the cave. Stream and gas chemistries were characterized seasonally over three years by standard field-based techniques, as well as by methods developed specifically for the cave environment. Unstable

aqueous parameters (pH, E_H, O_2, temperature) were determined in situ by electrode methods every meter along the spring outflow channel. Low-level dissolved oxygen and total dissolved sulfide ($C_TS^=$) were measured in the field by colorimetric analysis on a field spectrophotometer using Rhodazine D and Methylene Blue complex (CHEMetrics, VA), respectively. Dissolved, moderate-level oxygen was measured in the field also by colorimetry using the Indigo-Carmine method (CHEMetrics). Other dissolved constituents were determined as previously described in Chapter 2. Stream water dissolved solute speciation and activity, equilibrium gas partial pressure, and saturation state with respect to mineral phases were calculated from the in situ temperature, dissolved solute concentration, pH, and ionic strength using the geochemical speciation model PHREEQC (Parkhurst and Appelo, 1999).

Atmosphere Gases

As a result of the unstable and fugitive nature of some sulfur gases, gas measurements and H_2S flux were performed in the cave by direct-inject field gas chromatography (refer to Chapter 5).

Calcite Field Chambers and Microcosms

Sterile and non-sterile field chambers (in situ microcosms) containing chips (0.5 to 1 cm^3) of Iceland Spar calcite (Wards Scientific) and native Madison Limestone (mineralogy confirmed by x-ray diffraction) were deployed to test whether microorganisms or the bulk stream water chemistry controlled carbonate dissolution. Microcosms were constructed from 2.5 cm wide by 5 cm long PVC-pipes with screw-caps on either end. Sterile microcosms had 0.1 μm-PVDF

hydrophilic filters on the end (similar to 'peepers'), while non-sterile microcosms had 0.5 mm polyethylene mesh on either end to allow for fluid flow, and also for microbial colonization of the chips. Paired sterile and non-sterile microcosms were placed throughout the cave in the stream and within microbial mats, and remained in the cave to react for 2 weeks to nine months (Figure 6-1). Additionally, a technique similar to the buried-slide technique (Parkinson et al., 1971) was used: polished chips (with the largest surface areas being 1-2 cm^2) of limestone and pieces of Iceland Spar were surrounded by a 0.5 mm-mesh sack. At each microcosm site, a mesh sack was also deployed (which contained glass slides for structural support).

Electron Microscopy

When field chambers and mesh sacks were retrieved, the rock and mineral chips were processed separately and chips were preserved for microscopy, including conventional scanning electron microscopy (CSEM), environmental SEM (ESEM), and florescence in situ hybridization (FISH). Chips examined by ESEM were not preserved, but instead were frozen to -20°C. Unpreserved chips were examined using a Philips XL30 ESEM, with energy dispersive x-ray analysis system, and gaseous secondary and backscatter electron detectors. Chamber conditions were varied from 10%-95% relative humidity using a peltier cooling stage and variable water pressure (0.9 to 6.4 torr, with corresponding accelerating voltages from 4 to 20 kV). For CSEM, chips were fixed using a chemical critical-point drying method modified from Nation (1983). Chips were fixed in 2.5% gluteraldehyde, followed by dehydration in a series of ethanol washes to preserve

biological material on the surfaces. Air-dried samples were mounted on aluminum stubs, sputter-coated with gold for 30 sec, and examined using a JEOL JSM-T330A SEM with a 30 kV accelerating voltage.

Fluorescence In Situ Hybridization

Because filamentous sulfur-oxidizing bacteria are difficult to isolate or to grow in cultures, as well as to enumerate by standard culturing methodology, culture-independent phylogenetic characterization and quantification of microbial communities comprising the filamentous mats, including the construction of 16S rRNA gene sequence clone libraries (Chapter 2) and fluorescence in situ hybridization (FISH) using 16S rRNA-specific probes (Chapter 3; Engel et al., 2003), was done for Lower Kane Cave microbial mats. FISH probes were designed to target specific and dominant epsilonproteobacterial groups within the mats (Amann et al., 1995).

For fluorescence in situ hybridization (FISH), chips were fixed in two ways within 12 hr of collection: (i) with 4% paraformaldehyde for 3 hr, as described by Manz et al. (1996), and (ii) with 50% ice-cold ethanol according to Roller et al. (1994). Fixed chips were air-dried and dehydrated by sequential washes in 50, 80, and 100% ethanol for 3 min prior to hybridization. Previously synthesized oligonucleotide probes (LKC1006, GAM42a, and EUB338I-IIImix; Chapter 3) were applied to the chips using hybridization and washing buffers. Refer to Chapter 3 for details. Probe LKC1006 (5'-CTCCAATGTTTCCATCGG-3') was designed to target one epsilonproteobacterial group (LKC Group II) from the microbial mats; this group was the most abundant by biovolume using FISH (Table 3-4). Probe

192

GAM42a (5'-GCCTTCCCACATCGTTT-3') targeted *Gammaproteobacteria*, including *Thiothrix* spp. (Manz et al., 1996). Probe EUB338I-IIImix hybridized with *Eubacteria*, with equal concentrations of EUB338I (5'-GCTGCCTCCCGTAGGAGT-3') for *Eubacteria*, EUB338II (5'-GCAGCCACCCGTAGGTGT-3') specific for *Plantomycetes*, and EUB338III (5'-GCTGCCACCCGTAGGTGT-3') specific for *Verrucomicrobia* and other bacterial groups (Daims et al., 1999). A Leica TCS 4D confocal laser scanning microscope (CLSM) at the Institute for Cellular and Molecular Biology Core Facility, University of Texas at Austin, was used for three-channel simultaneous monitoring of fluorescence results. The CLSM was equipped with a Kr/Ar mixed gas laser and a UV laser, with DIC optics in an inverted microscope. The lasers supply the excitation wavelengths at 488, 568, and 647 nm. Examination was done using the 100x oil immersion objective. Image processing was done using software provided with the Leica instrument, with manual adjustment of contrast and brightness using Adobe Photoshop.

RESULTS AND DISCUSSION

Hydrogen Sulfide Transport and Reaction

Based on Egemeier's original work (Egemeier, 1973, 1981), it was hypothesized that subaerial replacement of limestone by gypsum was a significant mechanism for cave enlargement in Lower Kane Cave because most of the H_2S would quickly escape into the cave atmosphere. Volatilization was tested by measuring the dissolved and atmospheric gases, and by determining the actual flux of $H_2S_{(g)}$ from the cave water to the atmosphere (Chapter 5), and subsequently the

available $H_2S_{(g)}$ that could oxidize on the moist cave-wall surfaces (refer to Chapter 7 for additional information).

At the study spring (Upper Spring), anaerobic water has 34 $\mu mol \cdot L^{-1}$ total dissolved sulfide ($C_TS^=$) at 20.5 °C and pH 7.2 (40% H_2S:60% HS^-; pK= 7.04), (Table 6-1). The total flux of $C_TS^=$ at the Upper Spring, calculated from the stream velocity and the incoming concentration of sulfide, was ~8700 $\mu mol \cdot min^{-1}$, with an average $H_2S_{(g)}$ flux of 44 $\mu mol \cdot m^{-2} \cdot min^{-1}$ from the stream and microbial mats (Table 5-1 and 5-3). Therefore, over the entire length of the microbial mat at the Upper Spring, the transfer $H_2S_{(g)}$ to the cave atmosphere represents less than 8% of the total discharged $C_TS^=$, suggesting that the bulk of $C_TS^=$ is lost by other mechanisms in the subaqueous environment. One of those loss mechanisms is abiotic autoxidation, but it was found to be very slow in the disaerobic proximal stream water (Zhang and Millero, 1983; Millero et al., 1987), representing only ~0.014% of the potential abiotic loss.

Therefore, the $C_TS^=$ loss rate was much faster than could be accounted for by volatilization and autoxidation. The distinctly concave-down concentration vs. distance profile (Figure 5-3) is unlike the characteristic concave-up first-order loss profile expected for both abiotic loss mechanisms. At the mat terminus, however, the increase in dissolved O_2 concentration corresponds to rapid biotic consumption of $C_TS^=$ (Figure 5-3). Near the Upper Spring mat terminus, both allochthonous and autochthonous (see Chapter 5) sulfide is consumed by subaqueous biotic consumption, evidenced by the extremely rapid decrease in $C_TS^=$. The high

194

background $[SO_4^{2-}]$ in the stream water (Table 6-1), however, makes it impossible to measure small changes in oxidation byproducts.

Subaqueous Microbial Carbonate Dissolution

The dominant mechanism for $C_TS^=$ loss is subaqueous microbial oxidation, and most sulfur-oxidizing bacteria oxidize H_2S completely to sulfate with a substantial energy yield:

$$H_2S + 2O_2 \rightarrow SO_4^{2-} + 2H^+ \qquad (-798 \text{ kJ/reaction}) \qquad (6\text{-}3)$$

Others initially form elemental sulfur (S^0) as an intermediate that is stored intracellularly and further oxidized during periods of limiting sulfide:

$$HS^- + \tfrac{1}{2}O_2 + H^+ \rightarrow S^0 + H_2O \qquad (-209 \text{ kJ/reaction}) \qquad (6\text{-}4)$$

$$S^0 + H_2O + 1\tfrac{1}{2}O_2 \rightarrow SO_4^{2-} + 2H^+ \qquad (-587 \text{ kJ/reaction}) \qquad (6\text{-}5).$$

As a result of two of these three energetic oxidation reactions (Equations 6-3 and 6-5), acidity is generated in the form of sulfuric acid, attacking the geologic matrix supporting the community and modifying their ecological surroundings. Although some sulfur-oxidizers are acidophiles (Johnson, 1998), most are neutrophilic. Colonization of carbonate surfaces, therefore, buffers excess acidity and maintains pH homeostasis (Engel et al., 2001).

The dominant microorganisms in Lower Kane Cave are phylogenetically grouped within the "*Epsilonproteobacteria*", with lesser abundant sulfur-oxidizing communities of *Thiothrix* spp. (*Gammaproteobacteria*) and *Thiobacillus* spp. (*Betaproteobacteria*) (Chapter 2; Table 2-3). Although many "*Epsilonproteobacteria*", including those identified from Lower Kane Cave, have not been obtained in pure culture, many cultured epsilonproteobacterial groups

oxidize reduced sulfur compounds using molecular oxygen (under microaerophilic conditions) or alternative electron acceptors (such as nitrate or metals) (e.g., Campbell et al., 2001; Madrid et al., 2001; Lopez-Garcia et al., 2002; Takai et al., 2003). On the basis of phylogenetic affiliation, habitat geochemistry, and sulfur isotope data (Chapter 2), I hypothesize that the "*Epsilonproteobacteria*" in Lower Kane Cave are also sulfur-oxidizers. Most cultured *"Epsilonproteobacteria"* do not store sulfur intracellularly, in contrast to *Gammaproteobacteria*, specifically *Thiothrix* spp. (Larkin, 1989; Nielsen et al., 2000).

Deeply corroded native carbonate fragments (pebble- to cobble-size limestone clasts) were observed in the cave stream, with dissolution effects only on surfaces exposed to stream water and the filamentous microbial mats (Figure 6-2A). Gypsum replacement of these clasts is obvious above the water surface (Figure 6-2B). Examination of these rock surfaces by CSEM and ESEM revealed a complex reacting environment with dissolving carbonate surfaces, secondary gypsum, and a thick cover of predominately filamentous bacteria and exopolysaccharide material (Figure 6-3). The observed carbonate dissolution and gypsum precipitation associated with a surface biofilm suggests that sulfuric acid speleogenesis occurs within a mineral surface microenvironment maintained by the microbial community, rather than being caused by changes in bulk aqueous geochemistry.

The water exiting the Upper Spring pool had a calculated equilibrium partial pressure of CO_2 (pCO_2) of $10^{-1.95}$ atm, was only slightly undersaturated with respect to calcite ($SI_{cal} \sim 0.2$), but was significantly undersaturated with respect to

gypsum ($SI_{gyp} \sim {}^-1.5$) (Table 6-1). Within a few meters from the orifice, the cave waters became supersaturated with respect to calcite ($SI_{cal} = {}^+0.06$), and at the end of the microbial mat $SI_{cal} = {}^+0.2$ due to the volatilization of CO_2 and the contribution of alkalinity by dissimilatory sulfate reduction. The bulk waters were undersaturated with respect to gypsum ($SI_{gyp} = -1.54$ to -1.62) (Table 6-1).

Although the waters were in equilibrium or supersaturated with respect to calcite, SEM examination of the chamber calcite revealed etching localized where microbial filaments or biofilms were attached to the mineral surfaces (Figure 6-4A through 6-4E; Appendix E). Sterile calcite chips exposed to the stream water show no microbial colonization and no apparent dissolution (Figure 6-4F). Two filament types were observed on nonsterile calcite chips with ESEM, one containing sulfur globules and another without (Figure 6-5A). Dissolution trenches directly under filaments without sulfur (white arrows) were deeper than trenches associated with sulfur-containing filaments (black arrows) (Figure 6-5B). Differences in dissolution intensity at the microbial filament may correspond to the predominance of each of the two sulfide oxidation mechanisms (Equation 6-3 vs. Equation 6-4); greater localized acidity may be generated under the filaments that do not store sulfur (Equation 6-3).

FISH probes were used on the experimental chip surfaces to determine the identities of the filaments colonizing the surfaces. By using CLSM, the three FISH probes applied to rock and mineral surfaces showed positive hybridization signals to predominantly filamentous organisms (Figure 6-6). The topographic signal range was ~25 μm from the native limestone and 5 μm on the Iceland Spar surfaces.

However, these topographic variations in the surfaces, presumably because of dissolution of the carbonate during the experiment, made it difficult to obtain one focal plane with the CLSM. Exceptionally bright hybridization signals for each of the probes indicated high rRNA content, suggesting metabolically active populations when the samples were retrieved (Amann et al., 1995). Nearly all observed filaments simultaneously hybridized with the EUB338I–IIImix and LKC1006 probes on limestone surfaces (Figure 6-6A and 6-6B), and fewer filaments hybridized with the GAM42a and EUB338I–IIImix probes (Figure 6-6A and 6-6C). The FISH results genetically identify the two filamentous sulfur-oxidizing bacterial groups that colonize subaqueous carbonate surfaces, consistent with the ESEM observations of filaments with and without intracellular sulfur (Figure 6-5A).

A New Model for Microbial Sulfuric Acid Speleogenesis

The rapid loss of sulfide from the stream, carbonate dissolution associated with microbial filaments, and the dominance of *"Epsilonproteobacteria"* on the experimental limestone surfaces support the hypothesis that these organisms have a direct role in sulfuric acid speleogenesis by oxidizing sulfide to sulfuric acid. The classic sulfuric acid speleogenesis model relied in part on $H_2S_{(g)}$ volatilization from the cave stream to the cave atmosphere for replacement-solution processes to proceed (Egemeier, 1981; Palmer, 1991), yet negligible volatilization and abiotic autoxidation of $C_TS^=$ in the cave stream was measured in Lower Kane Cave (Chapter 5). Instead, $C_TS^=$ is consumed by subaqueous sulfur-oxidizing bacteria and cave enlargement occurs via microbially-enhanced dissolution of the cave

floor. In the cave stream, the system is very close to equilibrium, and the calcite dissolution rate is a function of $[Ca^{2+}]$, pCO_2, and solution pH. The rate has a non-linear dependence on the degree of undersaturation (Ω) that can be described as the difference between the actual and equilibrium saturation pH ($\Delta pH = 0.5 \log \Omega$) (e.g., (Morse and Berner, 1972; Berner and Morse, 1974). At conditions of small Ω ($\Delta pH < 0.15$), such as found in the bulk stream water receiving diffuse proton input from abiotic sulfide oxidation, calcite dissolution is very slow with little effect from small changes in pH. In contrast, where bacterial filaments are in contact with carbonate, excess acidity is focused at the reacting surface (Equation 3) and local Ω increases. Although the stream water is near calcite equilibrium, the $[Ca^{2+}]$ increases along the stream region where microbial growth is greatest, whereas $[SO_4^{2-}]$ increases only slightly (Table 6-1). These observations show that sulfur-oxidizing bacteria colonize subaqueous carbonates, localize dissolution by generating acidity, and therefore are integral to sulfuric acid speleogenesis.

CONCLUSIONS

While a microbial role to cave formation has been alluded to for sulfidic caves (Hubbard et al., 1990; Hill, 1996; Angert et al., 1998; Hose et al., 2000; Vlasceanu et al., 2000; Engel et al., 2001), previous explanations for sulfuric acid speleogenesis assumed abiotic chemical and hydrologic controls. These controls operate predominantly near a shallow groundwater table because of oxygen requirements for abiotic processes (e.g., Palmer and Palmer, 2000) or subaerially after H_2S volatilization on the basis of extensive gypsum in these cave systems

(e.g., Egemeier, 1981; Hill, 1990; Galdenzi and Menichetti, 1995; Hill, 2000). This work reexamined Lower Kane Cave and confirmed that some $H_2S_{(g)}$ does indeed volatilize into the cave atmosphere, and consequently subaerial speleogenesis does occur. However, the long-term rate is unknown. The $H_2S_{(g)}$ volatilization flux today cannot explain modern speleogenesis processes, but the volatilization loss into the cave atmosphere represents the maximum potential proton transfer to the cave walls, which affects subaerial cave-wall speleogenesis processes (Chapter 7).

Almost all $C_TS^=$ in Lower Kane Cave is consumed by subaqueous sulfur-oxidizing bacteria. These bacteria drive sulfuric acid speleogenesis by their attachment to carbonate surfaces and generation of sulfuric acid, which focuses local carbonate undersaturation and dissolution. As the sulfur-oxidizing "*Epsilonproteobacteria*" can be metabolically active under low oxygen tensions, they can catalyze sulfide oxidation in environments where autoxidation is kinetically limited. Therefore, microbial catalysis extends the phreatic depths to which porosity and conduit enlargement could occur in carbonate systems, including oil-field reservoirs and aquifers. One such setting for future investigations, and a location to test the microbial dissolution model, is within the Edwards Aquifer, Central Texas, where it has been proposed that a portion of the karstic aquifer has formed from sulfuric acid speleogenesis (Grubbs, 1991). The metabolic and geologic consequences of an active microbial ecosystem fundamentally change the model for sulfuric acid speleogenesis in the deep subsurface, which may shed light on carbonate porosity development in large aquifers and petroleum reservoirs.

200

Table 6-1: Aqueous geochemical data, total dissolved sulfide ($C_T S^=$), and saturation indices (SI) for calcite (SIcal) and gypsum (SIgyp) from Lower Kane Cave Upper Spring stream water.

Meter	pH	Ca^{2+}	Mg^{2+}	Na$^+$	Major Constituents HCO$_3^-$	SO$_4^{2-}$	O$_2$	C$_T$S$^=$	Saturation Index pCO$_2$	SIcal	SIgyp
(m)		mmol·L	mmol·L	mmol·L	mmol·L	mmol·L	μmol·L	μmol·L	Log Atm		
190	7.36						0.00	26.67			
191	7.36	1.583	0.94	0.25	3.39	1.13	0.00	24.24	-2.08	-0.06	-1.62
193	7.38						2.34	21.52			
194	7.42	1.637	0.98	0.25	3.38	1.11	2.66	20.91	-2.14	0.01	-1.62
195	7.42						2.55	20.91			
196	7.42						2.19	18.79			
197	7.42						7.50	20.30			
199	7.42						14.69	22.42			
200	7.36	1.762	0.99	0.26	3.38	1.12	14.69	19.49	-2.08	-0.02	-1.59
201	7.34						19.38	19.09			
202	7.34						33.44	20.30			
203	7.43	1.765	1.00	0.33	3.23	1.08	40.31	16.82	-2.17	0.03	-1.60
206	7.40	1.691	0.99	0.25	3.28	1.11	47.50	12.42	-2.13	-0.01	-1.61
207	7.43	1.890	0.97	0.31	3.41	1.14	47.81	10.15	-2.15	0.08	-1.56
210	7.43							5.76			
215	7.43	1.914	0.96	0.27	3.45	1.18		3.33	-2.14	0.09	-1.54
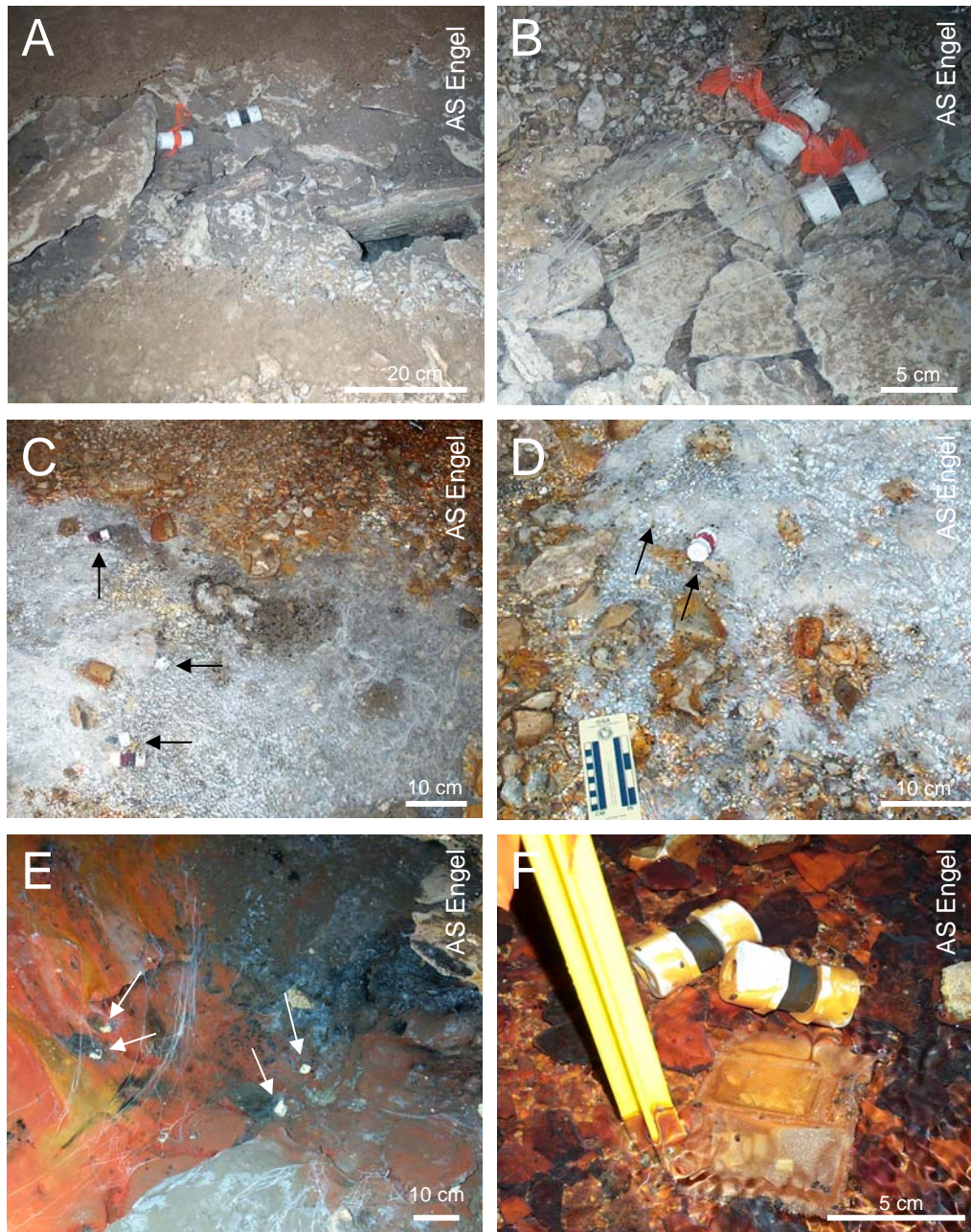
Figure 6-1: Examples of field chambers and buried slides used in Lower Kane Cave. (A) Fissure Spring orifice (hole at center right) at 118 m; (B) Microcosms at 127 m with sparse filaments; (C) Arrows point to microcosms covered by microbial mats at 203 m; (D) Exposed and buried microcosms at 249 m (arrows); (E) Arrows point to partially buried microcosms (white caps are showing) in Lower Spring orifice pool, 189 m; (F) Microcosms and buried slide mesh pouch in stream channel at 215 m.
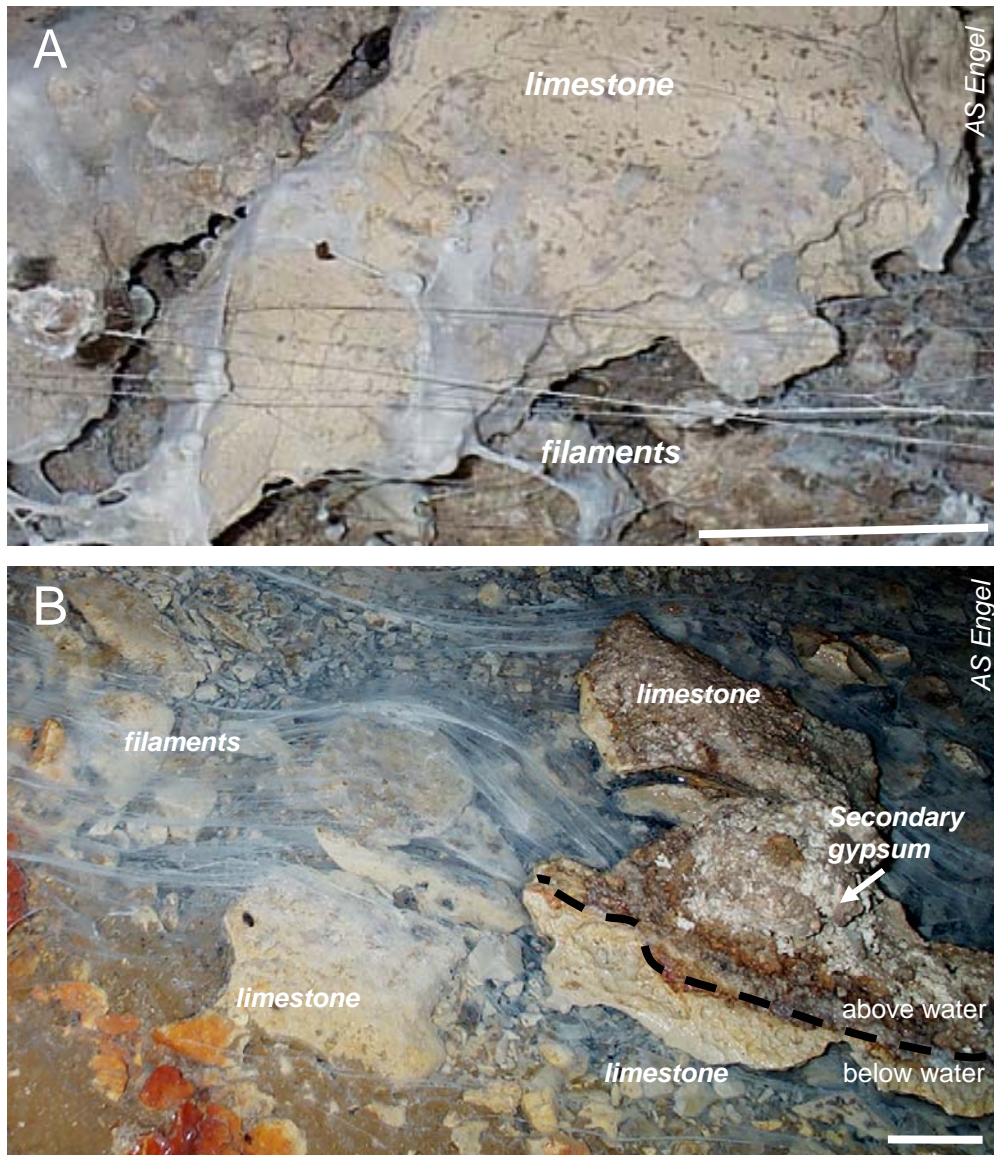
Figure 6-2: Examples of deeply corroded limestone cobbles in Fissure Spring stream channel. (A) Microbial filaments and webs discontinuously cover limestone clasts. (B) When limestone is exposed above the water surface, secondary gypsum replaces the limestone (lower right). Scale bars are 10 cm.
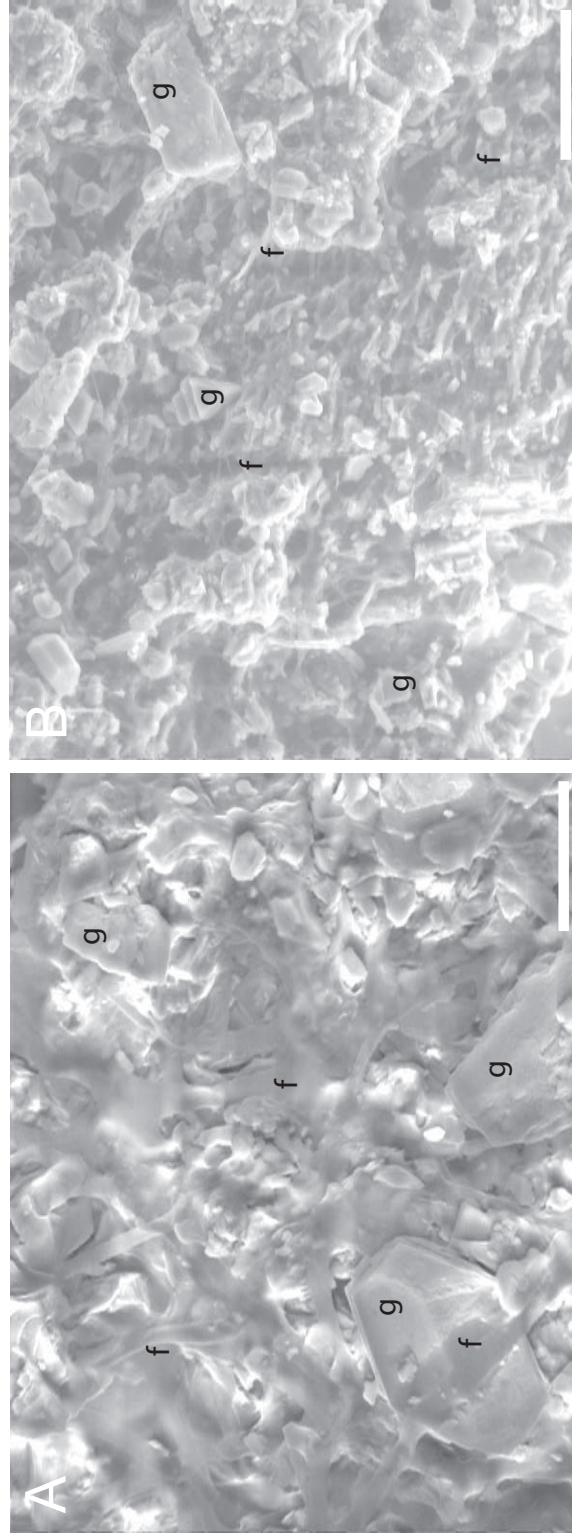
Figure 6-3: Environmental scanning electron photomicrographs showing surface textures of native limestone. (A) Biofilm and filaments (f) coating surface and gypsum (g) crystals on native limestone (0.9 torr, 12 kV). Scale bar represents 10 μm. (B) Biofilm showing deeply etched limestone surface filled with gypsum (6.4 torr, 20 kV). Scale bar represents 50 μm.
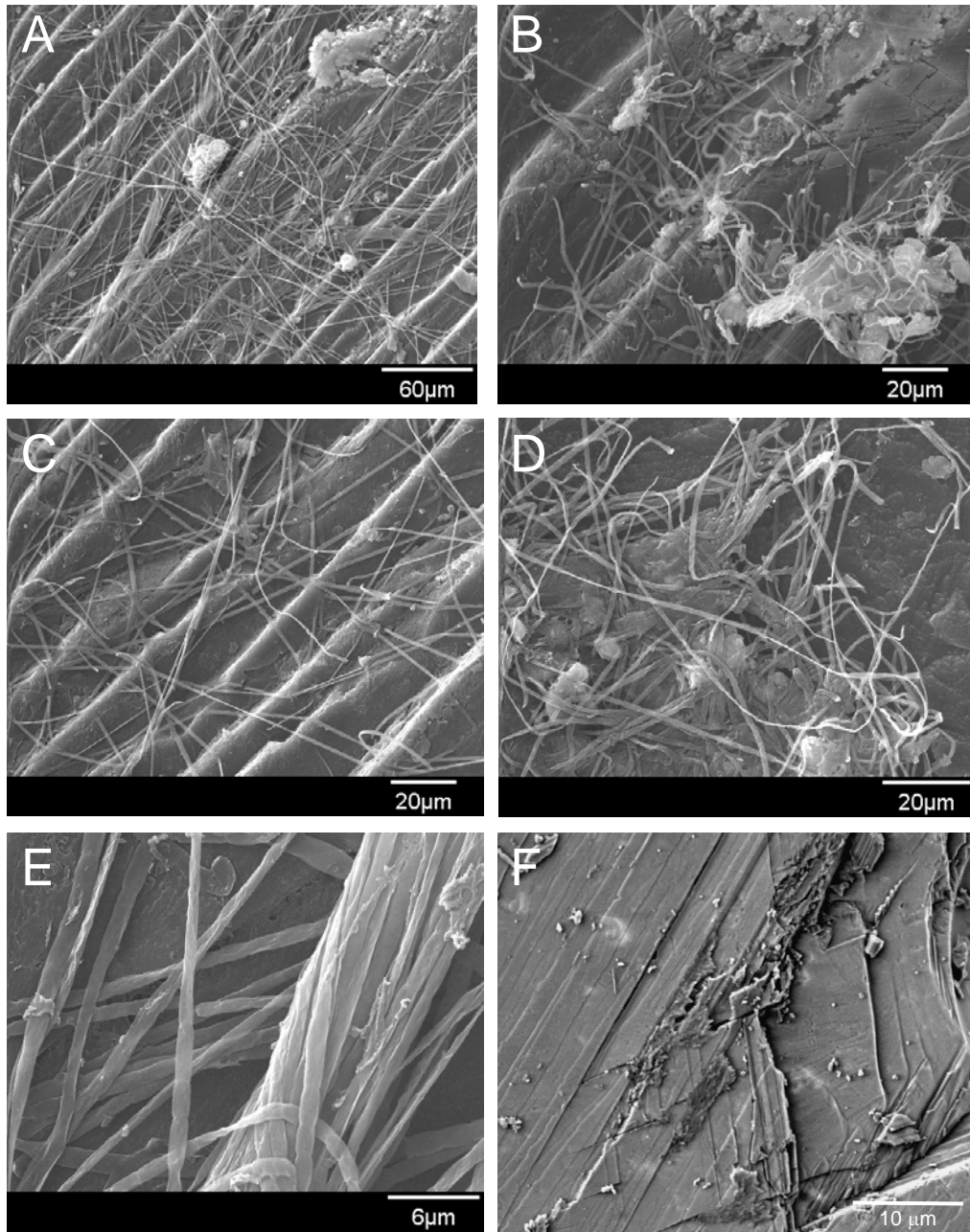
Figure 6-4: Scanning electron photomicrographs of calcite chip surfaces from in situ microcosm in microbial mats at 203 m. (A-E) Preserved chip examined with CSEM with 30 kV accelerating voltage. All strands are microbial filaments; calcite surface is etched. (F) Unpreserved chip examined with ESEM at 5 kV and 1.6 torr. Filaments and surface dissolution were not visible.
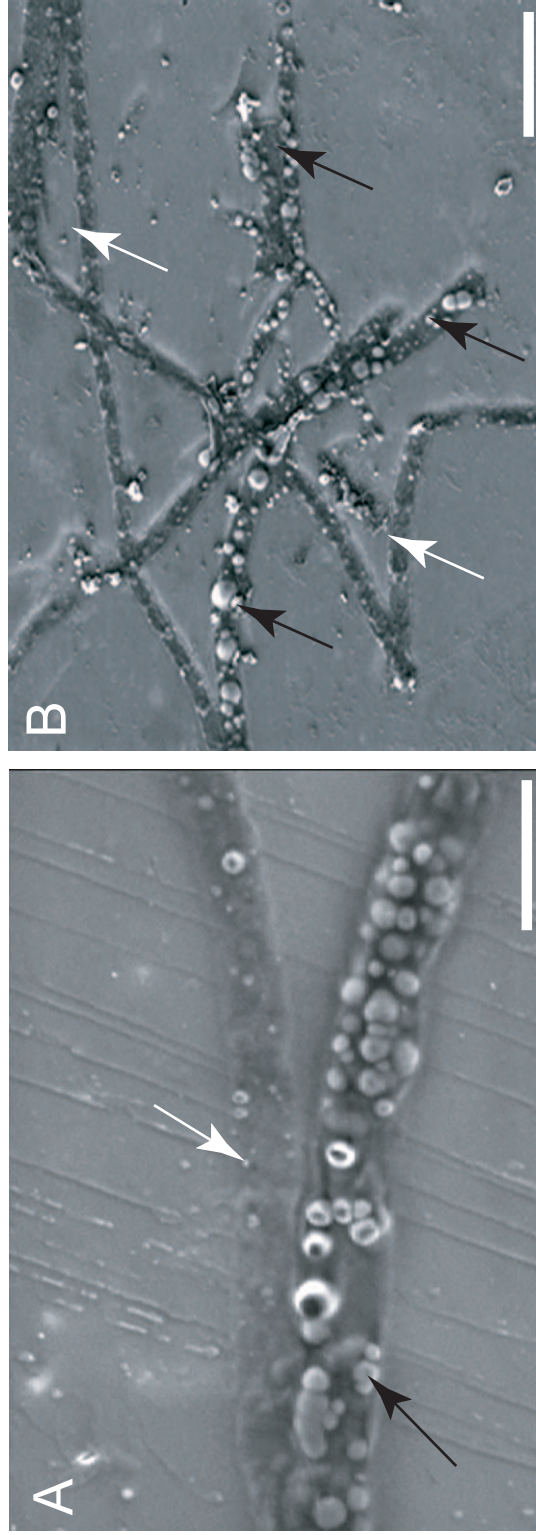
Figure 6-5: Environmental scanning electron photomicrographs of calcite chip surface from field microcosm. (A): Two filament morphologies, one with intracellular sulfur globules (black arrows) and another filament without (white arrows) (1.0 torr, 6.0 kV). Scale bar represents 5 μm. (B): Calcite chip surface with two filament morphologies showing deep trenches directly under filaments without intracellular sulfur (white arrows) in contrast to shallow trenches under filaments with sulfur (black arrows) (1.6 torr, 4.0 kV). Scale bar represents 20 μm.
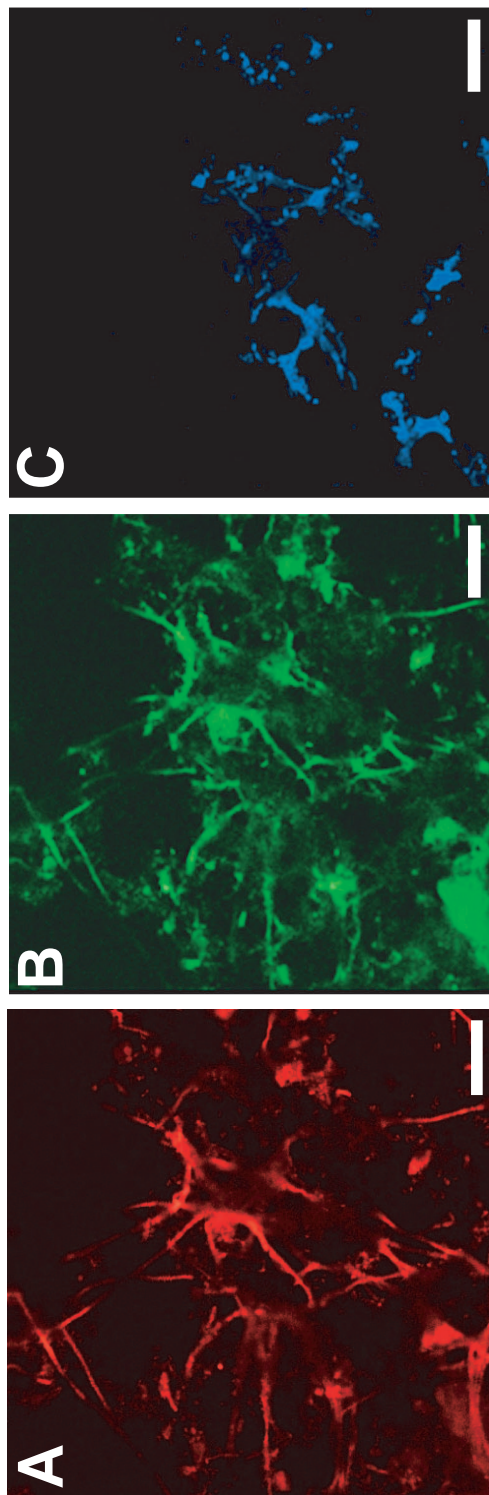
Figure 6-6: Fluorescence in situ hybridization (FISH) of filaments attached to polished chip of native limestone from mesh-covered buried slides with probes "*Epsilonproteobacteria*" LKC1006 (red), EUB338I–IIImix (green) specific for all Eubacteria, and GAM42a (light blue), specific for *Gammaproteobacteria*, including *Thiothrix* spp. Scale bar in all images represents 20 μm.

Chapter 7: Geochemistry and Interfacial Phenomena of Acidic Condensation Droplets on Cave-wall Surfaces: Implications for Authigenic Quartz Precipitation and Sulfuric Acid Speleogenesis

ABSTRACT

Volatilization of hydrogen sulfide in Lower Kane Cave, Wyoming, and sulfide oxidation to sulfuric acid on moist subaerial cave-wall surfaces causes carbonate rock dissolution and replacement by gypsum during sulfuric acid speleogenesis. A slight temperature gradient from the cave springs to the rock walls and high relative humidity contribute to condensation. Condensate forms on cave-wall surfaces, including gypsum and organic-rich reddish-brown crusts ($\delta^{13}C$ = -36.3 ‰; n = 11, 1σ = 0.84‰). The brown crusts discontinuously cover the gypsum throughout the cave and are composed principally of carbon, oxygen, and silicon. Average droplet pH is 1.7 (n = 40), ranging from pH 1.25 on brown crusts to 2.92 on gypsum. Droplets on crusts had pH values below the critical HSO_4^-:SO_4^{2-} pK as a result of crust hydrophobicity and acid-producing bacteria; droplets with a pH < 2 were undersaturated with respect to gypsum, while droplets with pH > 2 were in equilibrium with gypsum, as a result of buffering by the bisulfate-sulfate weak acid/base pair (pK = 1.92) combined with the gypsum-sulfate. Microbial cells and filaments, although evident from nucleic acid staining, are metabolically inactive based on application of 16S rRNA-specific oligonucleotide probes. Low pH droplets were supersaturated with respect to quartz (SI_{quartz} = +0.55, n = 4), and euhedral quartz microcrystals were found in the crusts. The cave-wall environment enhances silica mobilization from acid dissolution of the limestone and liberation

208

of insoluble residues (clays and feldspars). Quartz precipitation may be accelerated by bacterial cells and organic material acting as nucleation points for crystal growth, especially for the very small crystals. Armoring of the cave walls by gypsum and organic biofilms fundamentally affects how the cave enlarges during sulfuric acid speleogenesis. Microbial colonization of the low pH, moist gypsum habitat forms an organic film that eventually becomes impermeable through time. Condensation droplets become separated from the underlying gypsum, thereby precluding diffusion of sulfuric acid through the gypsum to the limestone, limiting or shutting off sulfuric acid dissolution completely. Subaerial sulfuric acid speleogenesis, as the replacement of the limestone by gypsum, will commence only when fresh limestone is exposed.

INTRODUCTION

Tiny authigenic quartz crystals have been found in gypsum deposits from ancient caves formed by sulfuric acid speleogenesis, including several caves in Italy (Forti, 1994), Turkmenistan (Maltsev et al., 1997), and Carlsbad Cavern, Lechuguilla Cave, and others in the Guadalupe Mountains, New Mexico (Polyak and Provencio, 2001; Polyak and Güven, 2004). In Carlsbad Cavern, micrometer- to deci-micrometer quartz crystals are found in unconsolidated powders in association with gypsum and carbonate mineralization (Polyak and Provencio, 2001; Polyak and Güven, 2004). These cave systems did not form under hydrothermal processes, and therefore quartz precipitation in the caves occurred at low, earth-surface temperatures. Moreover, as most of these cave systems are no

longer active, there has been little explanation for how the quartz crystals originated.

Quartz precipitation at low temperatures is a perplexing chemical and kinetic occurrence (e.g., Chafetz and Zhang, 1998). Although quartz is one of the most abundant minerals on the Earth, it is kinetically unreactive at low temperatures and it is unlikely to precipitate (or dissolve) at any significant rate without a catalyst (Rimstidt and Barnes, 1980; Rimstidt, 1997). Quartz precipitation from solution is hindered by the presence of humic acids, Al, Fe, and Ca, and removal of these impurities is necessary for precipitation (Thiry and Millot, 1987). There is evidence that microorganisms, acting as potential nucleation sites, catalyze silica precipitation at low pH, by cell wall sorption of H_4SiO_4 ions (Fortin and Beveridge, 1997).

In Lower Kane Cave, Wyoming, a small system actively forming from sulfuric acid speleogenesis (Egemeier, 1981), quartz microcrystals are found in brown organic-rich crusts associated with gypsum cave-wall mineralization and acidic condensation droplets. Sulfuric acid speleogenesis in Lower Kane Cave is principally by subaqueous hydrogen sulfide oxidation to sulfuric acid by microbial catalysis. A small percentage of hydrogen sulfide does volatilize into the cave atmosphere (refer to Chapters 5 and 6), and it is subsequently oxidized on moist cave-wall surfaces. The sulfuric acid on exposed cave-wall surfaces creates an aggressive solution that rapidly corrodes the carbonate host rock and replaces it with gypsum, the replacement-solution process of Egemeier (1981):

$$CaCO_3 + H_2SO_4 + H_2O \rightarrow CaSO_4 \cdot 2H_2O + CO_2 \qquad (7\text{-}1)$$

To date, sulfuric acid speleogenesis has been linked to the development of <10% of the carbonate karst worldwide (Palmer, 1991), including the formation of some of the world's largest caves such as Carlsbad Cavern, New Mexico (Hill, 1996), and the Frasassi Caves, Italy (Galdenzi and Menichetti, 1995). In some cave systems that are actively forming from sulfuric acid speleogenesis, microbial communities colonize subaqueous and subaerial habitats, including acidic cave-wall surfaces (Hose et al., 2000; Vlasceanu et al., 2000; Engel et al., 2001). Microbial life at pH <4 in natural and artificial environments has been characterized, as studies of life in extreme environments has surged recently (e.g., Johnson, 1998; Bond et al., 2000).

Warm (22.6 $^\circ$C) incoming sulfidic water and cooler (~21 $^\circ$C) cave walls enhance condensation on subaerial cave-wall surfaces in Lower Kane Cave. I hypothesized that the chemistry of condensation on cave walls influences limestone dissolution, and gypsum and authigenic quartz precipitation reactions. Subaerial condensation is significant not just for cave formation mechanisms and speleothem alteration or precipitation (Dublyansky and Dublyansky, 1998), but also for microbial communities that may colonize the cave-walls. Condensation has been noted in many different caves (e.g., Eraso, 1969; Dublyansky and Dublyansky, 1998), and several studies of caves forming by carbonic acid dissolution describe aggressive condensate chemistries (Gergedeva, 1970; Pasquini, 1973; Dublyansky and Dublyansky, 1998), demonstrating that condensed waters are responsible for carving cave features and even wide-scale speleogenesis. Understanding cave-wall condensate properties is important because the nature of condensate and the

211

surfaces upon which they form affect the dissolving or precipitating ability of the solution, as well as its ability to entrain gas(es).

The role of condensation in sulfuric acid speleogenesis and cave-wall modification has not been previously investigated. Moreover, there has not been demonstrable evidence of quartz precipitation from a naturally acidic, microbially-active environment. Therefore, the goals of this study were to characterize the physical and chemical nature of the subaerial cave-wall surfaces from Lower Kane Cave in order to speculate about the formation of quartz in other caves formed from sulfuric acid speleogenesis. The quartz may also serve as a biomarker for an environment in these ancient caves where microorganisms once lived.

MATERIALS AND METHODS

Study Site

Several caves in the Bighorn Basin, Wyoming, formed from sulfuric acid speleogenesis, including Lower Kane Cave (Egemeier, 1981). Lower Kane Cave air temperatures average ~21 ^{o}C with a relative humidity of 99-100%. The spring waters average 22.6 ^{o}C, and have a pH of ~7.3. Incoming total dissolved sulfide is ~34 μmol·L^{-1}, and volatilization of $H_2S_{(g)}$ is <8% of the total dissolved sulfide flux (refer to Chapter 5).

Crust and Gypsum Characterization

Moist and dry brown crusts and gypsum deposits were collected aseptically throughout Lower Kane Cave. Crusts were digested in warm HCl and HNO_3 for 4 hr and the acid solution was analyzed by inductively coupled plasma mass

spectroscopy (ICP-MS) for major cations and high pressure liquid chromatography (HPLC) for anions.

Crusts were fixed using a chemical critical-point drying method modified from Nation (1983); samples were washed overnight with 25% gluteraldehyde, and then dehydrated with a series of ethanol washes. Air-dried, preserved samples were mounted on aluminum stubs, sputter-coated with gold, and examined using a JEOL JSM-T330A scanning electron microscope (SEM) in conventional-mode (CSEM) at an accelerating voltage of 30 kV with electron dispersive analysis (EDS) system. A Philips XL30 SEM operated in environmental mode (ESEM) with EDS was used for visualizing hydrated crusts and EDS elemental mapping without gold-coating.

The brown crusts were HCl-acidified to ensure removal of carbonate mineral phases for carbon isotope ratio analysis. Most carbon isotope measurements were made by elemental analyzer interfaced with a continuous flow FinniganMAT Delta Plus mass spectrometer, but some measurements were also made by sealed tube combustion, vacuum purification, and dual-inlet VG Prism II mass spectrometer (refer to Chapter 2). Carbon isotope values are expressed in delta (δ) notation with respect to the international standard V-PDB.

Brown crusts were prepared with the stain 4',6-diamidino-2-phenylindole (DAPI) to visualize nucleic acids within the crusts. Some crust samples were also preserved in two ways with respect to the general requirements for successful fluorescence in situ hybridization (FISH) of various gram-negative and gram-positive bacteria: (i) with 4% (wt/vol) paraformaldehyde for 3 hr before final wash with saline phosphate buffer as described by Manz et al. (1992), and (ii) with one-

213

time 96% ice-cold ethanol according to Roller et al. (1994). Preserved crusts were attached to a thin agarose layer on Teflon-coated nonfluorescence slides and air-dried before dehydrating by sequential ethanol washes (refer to Chapter 3 for detailed FISH methodology). Hybridizations with multiple 16S rRNA-specific oligonucleotide probes to target specific taxa were preformed as described by Manz et al. (1992) (Table 7-1); following hybridization, DAPI was applied to the crusts for cross-referencing cells. DAPI and FISH results were visualized on an Olympus BX41 phase-contrast microscope with a reflected fluorescence system, and a 100x oil-immersion objective.

Droplet Collection and Characterization

Condensation droplets were drawn into a sterile, plastic, and non-reactive syringe, whereby ~1 ml of droplet solution over a 5-10 cm^2 area of the same substrate was collected and homogenized. Droplets from brown crusts and gypsum were collected separately. Condensate solutions were filtered to remove gypsum crystals. Solution chemistry was determined by HPLC and ICP-MS, and pH was measured from an aliquot with a IQ150 pH/mV/temperature meter with a stainless steel micro pH electrode (IQ Scientific Instruments, Inc., San Diego, CA) calibrated to pH 4, 2, and 1.8. Dissolved solute speciation and activity and saturation state with respect to mineral phases were calculated from in situ temperature, dissolved solute concentration, pH, and droplet ionic strength using the geochemical speciation model PHREEQC (Parkhurst and Appelo, 1999). pH of individual droplets in the cave was measured using the IQ150 pH microelectrode.

Surface free energy affects the saturation state of a solution with respect to mineral stability. Condensation droplet morphology was measured in the cave and interfacial tension was determined from digital images by measuring the contact angles droplets on brown crust (n = 21) and on gypsum (n = 3; droplets on gypsum were rare). In order to reduce complications between advancing and receding edge contact angles, because droplets did not form on completely flat surfaces and the inclination of the solid can deform the droplet (Extrand and Kumagai, 1995), only droplets that appeared to be free-hanging on nearly horizontal cave walls (ceilings) were measured. Interfacial tension was determined from a modified Young's relationship,

$$\gamma LV \cos\Theta = \gamma SV - \gamma SL \qquad (7\text{-}2),$$

such that the surface forces are of a liquid (L) drop on a surface (S) in contact with air (V), and a definite contact angle, Θ, between the liquid and solid phase. If the contact angle can be estimated, then an equation-of-state approach that relates γS and γLV can be derived. Kwok et al. (1998) suggest that, for a contact angle- based surface analysis, the measure of contact angles of a single liquid drop would suffice for determination of the surface tension of the underlying solid,

$$\cos \Theta = -1 + 2 \,(\gamma S \,/\, \gamma LV) \qquad (7\text{-}3)$$

Once the contact angle and γS are known, γSL can be calculated (Kwok et al., 2000). Using Equation 7-3 assumes a smooth, homogeneous, and incompressible solid, all aspects of natural systems that are difficult to quantify (e.g., solids are not completely smooth surfaces; adsorbed gas can reduce the solid-liquid interfacial

tension and smooth effective roughness at the solid surface). These calculations were used to estimate surface hydrophobicity, which would also serve as a measure for the potential reactions that could be occurring between the droplet and the underlying mineral or crust surface(s).

Quartz Separation and Cathodoluminescence Microscopy

Gypsum deposits and brown crusts were dissolved in dilute HCl to collect the insoluble residue phase. Gypsum was further dissolved by gentle shaking in distilled water with NaCl to complex free Ca^{2+}. Bedrock from several units within the Madison Limestone was digested with HCl and EDTA separately. Insoluble residues from the various digestions were centrifuged and the supernatants were removed by pipet. Residues from gypsum and the brown crusts were visually inspected by stereoscopic microscopy, and individual euhedral crystals were separated from quartz clusters. Residues from the limestone were analyzed by x-ray diffraction and quartz grains were separated.

Quartz crystals from the brown crusts, ~30 μm long (the lower limit for manual manipulation using a stereo-microscope), were mounted individually in epoxy and polished flat to obtain cross-sections of the crystals at random orientations. Clusters were also mounted in epoxy in several orientations and polished. Crystal sections were imaged by cathodoluminescence (CL) microscopy using the ESEM with a Philips PanaCL detector and RGB (red/green/blue) filters. Digital images were processed in Adobe Photoshop for RGB color merging, and brightness and contrast alterations.

RESULTS

Cave-wall Crusts and Condensate Morphology

The walls of the cave are nearly all replaced by gypsum (Figure 7-1A), formed as a result of active sulfuric acid speleogenesis; limestone is rarely exposed. Discontinuous patches of reddish-brown crusts cover the gypsum (Figure 7-1B). Acid digestion of the brown crusts revealed they were composed of 56% carbon by dry weight. ESEM with elemental mapping of crusts supported this, demonstrating dominance by carbon (Figure 7-2A), with rare sulfur and isolated areas of silicon (Figure 7-2B). Calcium was not detected in the brown crusts using ESEM, although there was 14% calcium detected by dry weight.

Condensation droplets, averaging 2-3 mm in diameter, were observed on brown crusts, gypsum, and rarely on freshly exposed limestone. The highest abundance of droplets was on brown crusts in areas of the cave directly over flowing stream water (Figure 7-3). Where there was no flowing stream water, condensation was not observed on the walls, and the brown crusts appeared dehydrated (i.e., cracked and pulling away from the gypsum underneath). Contact angle estimates for condensation droplets on brown crusts were $>90^{o}$, with an average angle of 121.6^{o} (n = 21; Table 7-2), and 20% of these droplets were noticeably cloudy. In contrast, the average contact angle of droplets on gypsum was 71° (n = 3) (Table 7-2).

The surface tension (γS) values for the brown crust were estimated using Equation 7-3, assuming that the γLV was pure water at 72.8 mJ·m^{-2} (although the ionic strength and the high concentration of sulfate-ions, speciated as sulfate and

bisulfate, would slightly decrease interfacial tension of the liquid (Zhou et al., 1998). For the crusts with contact angles >90°, the mean interfacial tension was 17.3 mJ·m^{-2}, while the average surface tension for droplets with contact angles <90° was higher at 47.5 mJ·m^{-2} (Table 7-2). The corresponding interfacial tension between the solid and water was 55.3 mJ·m^{-2} for droplets on brown crust, while droplets on gypsum had less γSL values, averaging 25.1 mJ·m^{-2} (Table 7-2). The small contact angles and tension estimates indicate that the brown crusts were more hydrophobic surfaces than the gypsum.

Condensate Geochemistry

Condensation droplets on brown crusts had a mean pH of 1.7 (n = 40), whereas gypsum droplets had pH values ~2-3. Higher pH droplets (~pH 4, n = 20) were measured from exposed limestone surfaces near the cave entrance. Condensation droplets were collected from fifteen locations for geochemical analysis. Table 7-3 summarizes overall droplet geochemistry.

Droplets with the lowest pH had the highest [SO_4^{2-}] and ionic strengths. Sulfate (as $C_TSO_4^{2-}$) was speciated using dissociation constants for sulfate-bisulfate-sulfuric acid (Stumm and Morgan, 1996). There was up to 85 mM HSO_4^- for the lowest pH droplet (Figure 7-4). The concentrations of metals increased with decreasing condensate pH, including Si (Figure 7-5A). Total Al^{3+} (measured as C_TAl) was complexed as $AlSO_4^+$ and $Al(SO4)_2^-$, at 0.047 and 0.011 mM, respectively (Figure 7-5B). Equilibrium calculations of condensate solutions showed that most droplets at pH >2 were in equilibrium with gypsum, while the droplets at pH <2 were undersaturated with respect to gypsum (Tables 7-3 and 7-4;

Figure 7-4). The droplets from gypsum that were not in equilibrium with gypsum have varying concentrations of Ca^{2+} in solution, and especially low concentrations. (Figure 7-4). Droplets on crusts and gypsum were undersaturated with respect to calcite (Table 7-4), but most of the droplets on brown crusts were supersaturated with respect to quartz (Table 7-4; Figure 7-5B).

Quartz

Quartz crystals observed from the brown crusts ranged in size from <1μm to 10 μm along the longest axis (Figure 7-6; Appendix F). Some crystals had organic debris covering them (Figure 7-6C), or were imbedded within a fibrous matrix (Figure 7-6E). The surfaces of the quartz crystals showed no evidence of abrasion or pitting common to detrital quartz. Crystal size ranged from <0.5 μm to >19 μm, and the median crystal length of crystals observed by ESEM was 1.28 μm (n = 495). All sizes fell within a statistically significant log-normal distribution (with four degrees of freedom) (Figure 7-7). Quartz crystals were also found within gypsum, in large complex clusters with odd morphologies; individual crystals could not be discerned (similar to Figure 7-6D). No euhedral quartz crystals were found in limestone, although chert fragments were identified and x-ray results showed a 'quartz' peak that most likely coincided with chert interference.

Fifteen quartz crystals or clusters ~30 μm or larger were examined using CL. It was not possible to examine thin sections of the averaged-size quartz crystals (1.28 μm), and the larger crystal size distribution was not measured using ESEM. Therefore, the significance of this size range is not known. The smallest crystal

219

analyzed by CL (~10 μm in length) had only dark brown to black luminescence color, indicating an authigenic phase (e.g., Pagel et al., 2000; Ramseyer and Mullis, 2000). In contrast, larger crystals showed authigenic overgrowths on a quartz core with higher luminescence color (Figure 7-8). High luminescence color is characteristic of detrital quartz grains (light blue) (Ramseyer and Mullis, 2000). Depending on the sectioning of an individual crystal, the overgrowth rim width varied, but an average thickness was <5 μm. In Figure 7-8, the detrital grain is fractured and two stages of authigenic overgrowth precipitation events were observed, one brown layer and another purplish-black layer.

Brown Crust Microbiology

Eleven brown crust samples were analyzed for the carbon isotope composition in order to determine if there was a signature of biological activity. The brown crusts had carbon isotope values of -36.3‰ (n = 11; 1σ = 0.84‰). The limestone had a carbon isotope composition of +0.95‰. The carbon isotope values for the crusts reflect significant discrimination against ^{13}C, typically exhibited by chemolithoautotrophic fractionation (Preuβ et al., 1989).

DAPI inspection of the crusts indicated a variety of microbial cell morphologies throughout the brown crusts had, including thin filaments ~1-2 μm wide and larger fungal hyphae with filament widths averaging 10 μm, and small rods and cocci (Figure 7-9). However, FISH with 16S rRNA-specific oligonucleotide probes was not successful. After multiple attempts, no fluorescence signals were observed with any of the probes hybridized to the brown crusts.

DISCUSSION

Sulfuric Acid Speleogenesis and the Role of Cave-wall Surfaces

Lower Kane Cave formation mechanisms, including mineral alteration or precipitation reactions, are affected by the properties of the solids and liquids on cave-wall surfaces and microorganisms using the cave-wall surfaces as habitat. The cave walls are coated with gypsum, formed from the dissolution of the host limestone by sulfuric acid produced via sulfide oxidation (either biotic or abiotic):

$$H_2S + 2O_2 \rightarrow HSO_4^- + H^+ \quad \text{(the dominant species at pH ~2)} \quad (7\text{-}4)$$

$$HSO_4^- + H^+ + CaCO_3 + H_2O \rightarrow 2CaSO_4 \cdot 2H_2O + CO_2 \quad (7\text{-}5)$$
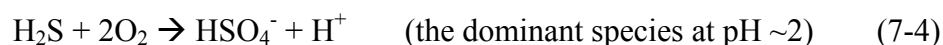
If the condensate solution is in contact with the underlying gypsum, the solution will approach pH 2, but typically will not go below this pH due to the buffering by the sulfate-bisulfate weak acid/base pair:

$$HSO_4^- \rightarrow H^+ + SO_4^{2-} \quad \text{(pKa = 1.98)} \quad (7\text{-}6)$$

and also from the gypsum-sulfate,

$$H^+ + HSO_4^- + CaSO_4 \cdot 2H_2O \rightarrow 2HSO_4^- + Ca^{2+} + 2H_2O \quad (7\text{-}7)$$

In contrast, droplets on brown crusts have pH values below the critical bisulfate-sulfate pKa, possibly as a result of sulfuric acid-producing bacteria, as well as crust hydrophobicity that physically separates the condensate from the gypsum and allows the pH to pass the bisulfate buffer point (Figure. 7-4). The γS values calculated for the brown crusts are as high as hydrophobic hydrocarbon or plastic surfaces (Stumm and Morgan, 1996).

Changes in surface tension resulting from the effects of solution pH and ionic strength have been previously investigated (Zhou et al., 1998). According to

221

Butkus and Grasso (1998), solution pH has two distinct effects on the interfacial energy between surfaces. pH indirectly affects hydration forces by changing surface charge, which also affects the magnitude of electrolyte adsorption. Additionally, solution pH changes surface functional group characteristics (Holmes-Farley et al., 1985). When the pH of water droplets decreased (as in the example provided by Holmes-Farley et al., 1985, from droplets on polyethylene carboxylic acid surfaces), there was an increase in the hydrophobicity of the surface and water contact angles increased due to the protonation of surface groups. This is further supported by the work of Hård and Johanson (1977) which demonstrated that the conjugate base of strong acids, and not the proton, may be responsible for decreases in surface tension, and that an increase in surface tension caused by the conjugate acid of a strong base is more pronounced than the decrease in surface tension caused by the conjugate base of a strong acid. In Lower Kane Cave, the droplets on brown crust had a lower pH and higher contact angles than those on gypsum, resulting in the crusts themselves being were more hydrophobic than the gypsum. Ionic strength will also influence contact angle, and consequently surface tension. The experiments by Butkus and Grasso (1998) demonstrate that an increase in ionic strength results in an increase in contact angle, approximately $2\text{-}5^{\circ}$ for a 10-fold increase in ionic strength. The highest ionic strength of the droplets with the lowest pH also had the lower surface tension value (Tables 7-2 and 7-3).

Speleogenetic Quartz Formation

At pH ~2 or less, total silica ($C_T Si$) was dominated by H_4SiO_4. As pH decreased, $C_T Si$ increased, as did the SI with respect to quartz (Tables 7-3 and 7-4),

222

indicating that the observation of quartz crystals in the brown crusts is matched by the saturation state of the solutions on the surfaces. The log-normal distribution in quartz crystal sizes suggests that the crystals have not grown uniformly on the cave walls. These differences may be due to variable adsorption of silica from the bulk condensate solution, depending on the surrounding physical surface chemistry of the gypsum or organic crusts, as well as the presence of microorganisms. Parks (1990) describes that if a solution is supersaturated with respect to quartz, quartz is expected to precipitate, but unless particles of quartz are already present, precipitation begins with nucleation of very small particles (<5 nm) (Iler, 1979). At this size, quartz is very soluble (Parks, 1990) and amorphous silica will precipitate, not quartz. If the rate of dissolution of amorphous silica is larger than the rates of nucleation and growth of quartz, then amorphous silica will precipitate. Conversely, precipitation in the presence of seed quartz crystals larger than 5 nm should allow quartz to grow directly. Quartz overgrowths on large detrital quartz grains suggest that the latter is true (Figure 7-8). As the authigenic, euhedral crystals are also quartz, this suggests that nucleation of small particles may have also occurred (Figure 7-6).

Sources of Silica

Several hypothetical sources of dissolved silica are evaluated to examine what processes may have contributed to high silica saturation states in the condensate solutions. Sources of silica from meteoric water, dissolving silicates, and weathering of insoluble clays are discussed.

Influx of quartz-saturated meteoric water

Surface waters are often supersaturated with respect to quartz because the reaction kinetics of quartz precipitation are slow compared to the dissolution rate of, for example, feldspars at temperatures <80°C (Rimstidt and Barnes, 1980; Rimstidt, 1997). However, Egemeier (1981) proposes that there is little infiltration of meteoric water into Lower Kane Cave because of the depth of the cave in Little Sheep Mountain and the low precipitation rates in the northern Bighorn Basin (<20 cm·yr^{-1}). Additionally, abundant cave gypsum would most likely not be preserved if meteoric water, typically undersaturated with respect to gypsum, percolated into the cave. Meteoric influx has caused gypsum to dissolve in the caves of the Guadalupe Mountains (Polyak and Provencio, 2001), as well as the Frasassi system, Italy (Galdenzi and Menichetti, 1995). If quartz-saturated meteoric water did flow along fractures into the cave, quartz would most likely be precipitating at the contact between limestone and gypsum, which was not observed. Therefore, the source of silica in the condensation droplets on the cave walls most primarily results from condensation of water vapor, and not a source outside into the cave.

Silicates dissolution

Dissolution of feldspars by hydrolysis (e.g., $KAlSi_3O_8$),

$$2KAlSi_3O_8 + 2H^+ + 9H_2O \rightarrow Al_2Si_2O_5(OH)_4 + 4H_4SiO_4 + 2K^+ \qquad (7\text{-}8)$$
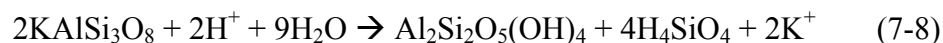
or precipitation of secondary clay minerals such as kaolinite or illite on the cave-wall surfaces, could be occurring.

$$KAlSi_3O_8 + Al_2Si_2O_5(OH)_4 \rightarrow KAl_3Si_3O_{10}(OH)_2 + 2SiO_2 + H_2O \qquad (7\text{-}9)$$
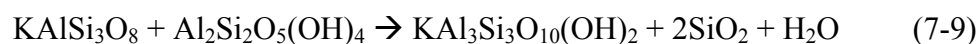
There is limited evidence of primary feldspar within the limestone or of significant

diagenetic clay precipitation within the gypsum deposits, as has been observed in Carlsbad Cavern (Polyak and Provencio, 2001). Clay minerals are most likely not forming because concentrations of accessory cations in condensate solutions are not high enough to reach mineral saturation, and SI values for various clays are extremely low. Therefore, the high silica concentrations in the cave condensate do not result from feldspar dissolution and precipitation of clays.

Weathering of insoluble (residual) clays

Dissolution of insoluble residues from the limestone during sulfuric acid speleogenesis could be occurring. Previous descriptions of the Madison Limestone suggest that the most dominant insoluble residues in the limestone units are clays, such as kaolinite and illite (Plummer et al., 1990). Clay solubility increases with decreasing pH, and as a result, silica could be released into solution (Nagy, 1995):

$$Al_2Si_2O_5(OH)_4 + 6H^+ \rightarrow 2Al^{3+} + 2H_2SiO_4 + H_2O \qquad (7\text{-}10)$$
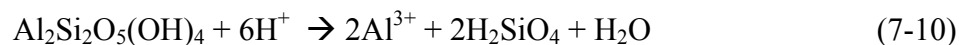
Aggressive condensate containing sulfuric acid would enhance clay mineral weathering. Organic acids and ligands may also increase clay dissolution by forming complexes with Al on the clay surface, weakening the Al-O-Si bonds (Nagy, 1995). Because rates of silica dissolution vary with changes in exposed surface area of a silicate mineral, and with changes in the volume of water reacting with the dissolving clays, the high surface area of dissolving clays would provide more silica to solution with constant reacting water volumes. For the Lower Kane Cave condensate solutions, liberation of Al during clay dissolution could inhibit the activity of silica (Iler, 1979). At pH values <4, Al exists as Al^{3+}, and in the lowest pH condensate solution, free Al^{3+} is almost completely complexed with sulfate

(Figure 7-5B). Therefore, of the possible silica sources, clay weathering during sulfuric acid dissolution of the host carbonates is the most likely.

Significance of Microorganisms to Cave Formation and Quartz Precipitation

Authigenic quartz formation at earth-surface temperatures is extremely slow, and not typically considered an important process. Kinetic barriers still must be overcome to precipitate quartz in the cave. Because metals (e.g., Ca and Al) that would otherwise poison quartz precipitation are complexed with sulfate, it is hypothesized that organic matter, and specifically microorganisms that once were metabolically active on the cave walls and formed organic biofilms, may have acted as catalysts for quartz precipitation.

Any microorganisms living on the cave-walls are most likely acidophilic bacteria. DAPI staining suggests that microbes are present in the wall crusts (Figure 7-9), but FISH might suggest that they are not metabolically active. As the FISH probes target rRNA, perhaps the lack of positive hybridization indicates the metabolic status (or lack thereof) of the organisms in the low-pH environment when the samples were collected and preserved (Amann et al., 1990; Amann et al., 1995). Previous investigations of 16S rRNA gene sequences retrieved from cave-wall biofilms in other active sulfidic caves demonstrated the occurrence of known sulfur-oxidizing bacteria, including *Thiobacillus* and *Sulfobacillus* (Vlasceanu et al., 2000), and *Thiobacillus* spp. and *Acidomicrobium* (Hose et al., 2000). However, the metabolic viability of these organisms was not established. Acidic biofilms also have been reported from mines, and cultures of *Leptospirillum*, *Acidomicrobium*,

Ferromicrobium acidophilus, and the Archaean *Thermoplasmales* have been obtained (Bond et al., 2000).

The occurrence of quartz within the organic crusts may not be coincidental. Acidophilic sulfur-oxidizing bacteria generate sulfuric acid, which is important for maintaining an acidic habitat, but cells may also function as nucleation sites for quartz precipitation. Fortin and Beveridge (1997) suggest that sorption of silicate ions (speciated as H_4SiO_4) onto acidophiles (e.g., *Thiobacillus* spp.) serves as a nucleation surface, possibly by templating, for the precipitation of *amorphous silica* at pH ~2 - 3. Metal-bridging of multivalent cations on bacterial cells also has been shown to promote aluminosilicate precipitation by enhancing silicate anion binding (Urrutia and Beveridge, 1993). Currently, however, there is no known relationship between microbes and quartz precipitation at any temperature range,

Microbes that colonization the subaerial cave-wall surfaces play a role in speleogenesis by forming a thick organic biofilm on the gypsum. These biofilms have high surface tensions relative to the gypsum, which eventually creates an impermeable surface layer on the cave walls. This hydrophobic surface precludes diffusion of sulfuric acid through to the gypsum and, consequently, to the underlying limestone.

CONCLUSIONS

Low-temperature euhedral quartz crystals found in caves formed from sulfuric acid speleogenesis indicate potentially microbially active acidic environments during periods of cave formation. While it is possible that the speleogenetic quartz precipitated in Lower Kane Cave prior to the cave formation,

it is more likely, based on condensate geochemistry and the association of the quartz with gypsum and brown crust, that the quartz formed since cave inception. The relationship between euhedral quartz and the cave-wall surfaces colonized by microorganisms (active or not) suggests that the rate of quartz precipitation might be enhanced by biologically active surfaces or microbially-produced ligands. This finding would be a fundamental discovery for both geomicrobiology and geochemistry. Identification of quartz, as a geologically stable signature of acid-sulfur bacterial metabolism, could then be used to identify such integrated bio- and geo- processes in ancient cave systems, or other more diverse terrestrial or extraterrestrial systems, modern or ancient.

Table 7-1: Oligonucleotide probes used to screen cave-wall biofilms using fluorescence in situ hybridization.

Probe	Target group	Probe sequence (5' → 3')	Target Site[a]	FA[b]	Reference
EUB338	*Eubacteria*	GCT GCC TCC CGT AGG AGT	16S (338)	0-40	Daims et al., 1999
EUB338-II	*Planctomycetes*	GCA GCC ACC CGT AGG TGT	16S (338)	0-40	Daims et al., 1999
EUB338-III	*Verrucomicrobia* (and others)	GCT GCC ACC CGT AGG TGT	16S (338)	0-40	Daims et al., 1999
NonEUB	Negative control	ACT CCT ACG GGA GGC AGC	16S (338)	0	Wallner et al., 1993
ARCH344	*Archaea*	TCG CGC CTG CTG CIC CCC GT	16S (344)	0	Raskin et al., 1994
ALF968	*Alphaproteobacteria*	GGT AAG GTT CTG CGC GTT	16S (968)	20	Neef et al., 1998
BET42a	*Betaproteobacteria*	GCC TTC CCA CTT CGT TT	23S (1027)	35	Manz et al., 1992
GAM42a	*Gammaproteobacteria*	GCC TTC CCA CAT CGT TT	23S (1027)	35	Manz et al., 1992
HGC69a	*Actinobacteria*	TAT AGT TAC CAC CGC CGT	23S (1901)	25	Roller et al., 1994
LGC345mix	*Firmicutes* (together with two other probes)	TGG AAG ATT CCC TAC TGC	16S (354)	20	Meier et al., 1999
CF319a	Some members of "*Flavobacteria*"	TGG TCC GTG TCT CAG TAC	16S (319)	35	Manz et al., 1996

[a] *E. coli* rRNA position (Brosius et al., 1981).
[b] Formamide percentage (vol/vol) in the FISH hybridization buffer

Table 7-2: Contact angles of condensation droplets on brown crust and gypsum measured from digital images, with corresponding surface tension (γS) and interfacial tension (γSL) calculations between the solid and liquid droplets.

Contact Angle[a]	γS (mJ·m^{-2})	γSL (mJ·m^{-2})
Brown Crust		
101.5	29.06	43.53
102.5	28.44	44.15
105	26.9	45.69
115	20.96	51.64
115	20.96	51.64
115.5	20.67	51.92
116.5	20.1	52.58
117	19.82	52.78
120	18.15	54.55
120	18.15	54.45
121.5	17.33	55.37
123	16.53	56.07
124	16	56.6
127.5	14.2	58.4
130	12.97	59.64
130	12.97	59.64
131	12.48	60.11
131.5	12.24	60.48
132.5	11.78	60.83
133.5	11.31	61.28
141	8.09	64.51
Gypsum		
62	53.34	19.16
74	46.3	26.29
80	42.72	30.11

[a] To avoid complications with receding versus advancing contact angles, contact angles were measured from droplets with equal (within 0.5°) angles on both sides.

Table 7-3: Major geochemical constituents for condensation droplets. Cave air temperature was 21°C. Analyses are reported in mg·L^{-1}.

pH	Substrate[a]	SO$_4^{2-}$	Na	K	Ca	Mg	Fe	Mn	Sr	Zn	Al	Si	IS[b]
1.17	BC	3679	22.4	3.9	338	81.2	0.40	0.46	1.17	0.14	0.47	14.5	0.06
1.24	BC	1297	7.6	8.2	400	259	1.06	0.38	1.46	0.11	1.20	15.2	0.05
1.24	BC	9491	2.4	0.72	309.1	71.8	1.12	0.14	0.57	0.13	1.85	5.77	0.14
1.45	BC	6221	25.3	1.13	427.3	110.3	0.38	0.50	1.40	0.04	1.67	15.84	0.10
1.5	BC	4339	2.7	1.18	319.0	65.1	2.56	0.11	1.62	0.06	5.54	17.62	0.08
2.01	G	2281	2.1	0.24	572.1	37.0	0.67	0.04	0.78	0.07	1.71	6.66	0.05
2.15	G	1955	21.2	2.3	545	141	0.15	0.05	1.06	0.03	0.45	6.8	0.05
2.35	G	3297	4.0	0.0	517	19.7	0.10	0.08	1.05	0.05	0.18	8.3	0.04
2.45	G	1835	1.8	0.22	536.5	20.2	0.60	0.03	0.24	--[c]	2.83	5.00	0.05
2.55	G	1760	6.1	0.33	63.1	24.0	0.01	--	0.74	--	0.10	4.26	0.03
2.72	G	919	1.6	0.0	470	11.6	2.02	0.07	0.36	0.03	0.19	1.6	0.03
2.92	G	1493	2.1	0.10	578.3	5.1	0.08	0.01	0.18	0.01	0.10	2.13	0.04

[a] Substrate from which droplets were collected: BC, brown crust; G, gypsum.
[b] Ionic strength.
[c] not determined.

Table 7-4: Calculated mineral saturation indices (SI)[a] for condensation droplets. Modeled using the web-based PHREEQC (ver. 2) computer software (Parkhurst et al., 1999).

Droplet pH	Calcite SI[b]	Gypsum SI[c]	Quartz SI[c]
1.17	-4.33	-0.48	0.59
1.2	-7.71	-0.27	0.04
1.24	-2.79	-0.49	0.61
1.45	-7.08	-0.11	0.48
1.55	-7.05	-0.28	0.52
2.01	-5.72	-0.04	0.09
2.15	-4.15	-0.21	0.26
2.35	-4.15	-0.28	0.35
2.45	-4.97	-0.04	-0.03
2.55	--[d]	--	--
2.72	-3.36	-0.41	-0.37
2.92	-4.41	-0.03	-0.4

[a]SI = (log IAP/K_{sp}), where IAP is ion activity product and K_{sp} is the equilibrium constant
[b]Modeled as pre-batch reaction with a CO_2–phase
[c]Modeled as post-batch reaction
[d]Not modeled due to charge balance problems.

Figure 7-1: (A) Gypsum coatings ("paste") and condensation droplets from the cave ceiling. Scale bar = 2 mm. (B) Clear and mucous-like droplets on brown cave-wall crust. White area to the upper left of the center droplet is gypsum. Scale bar = 2 mm.
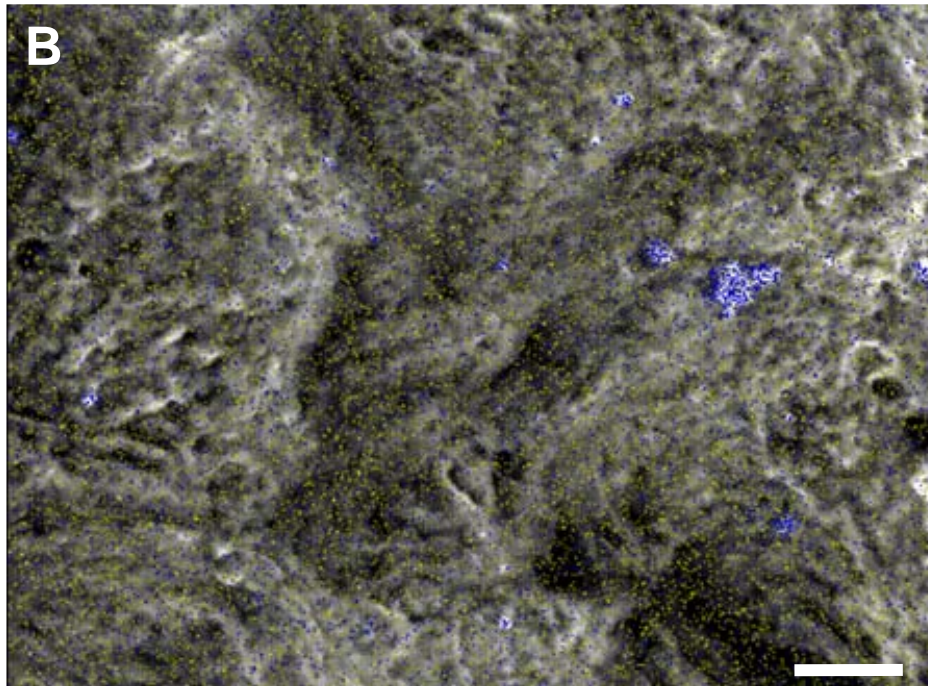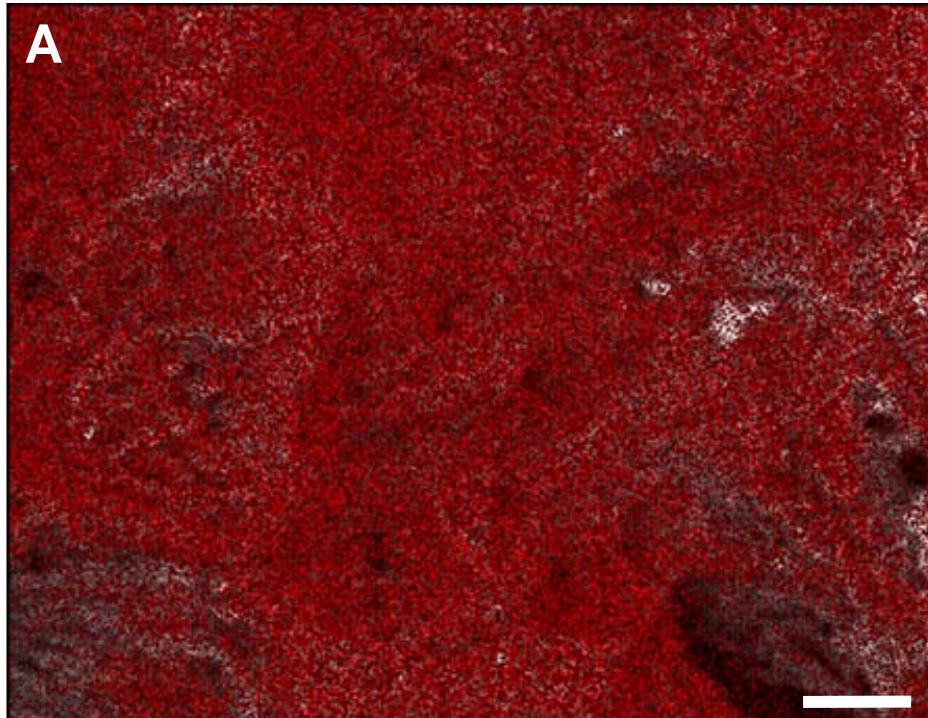
Figure 7-2: ESEM photomicrographs of brown crust combined with elemental mapping. (A) Map of carbon (red). (B) Map of sulfur (yellow) and silicon (blue). Scale bar = 10 μm.

Figure 7-3: Condensation droplets on brown crusts (hydrated and dehydrated) on gypsum-covered cave-wall surface in Lower Kane Cave, Wyoming. Droplets are roughly 2 mm wide.
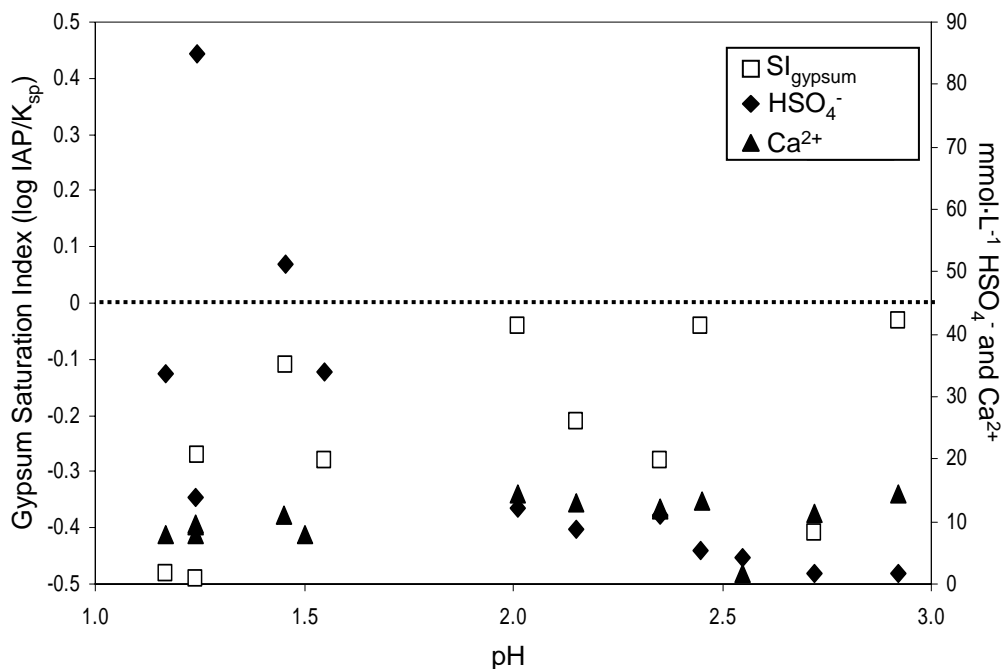
Figure 7-4: Condensation droplet chemistry, with HSO_4^-, speciated from C_TSO_4, C_TCa, and Saturation Index (SI) with respect gypsum versus pH of the droplets. $[HSO_4^-]$ increases with decreasing pH. Droplets near pH 2 are at the the pKa of the weak acid-base pair $HSO_4^-:SO_4^{2-}$ (pKa = 1.98) and are in equilibrium with respect to gypsum. Deviations from equilibrium are due to the low concentration of C_TCa for that droplet.
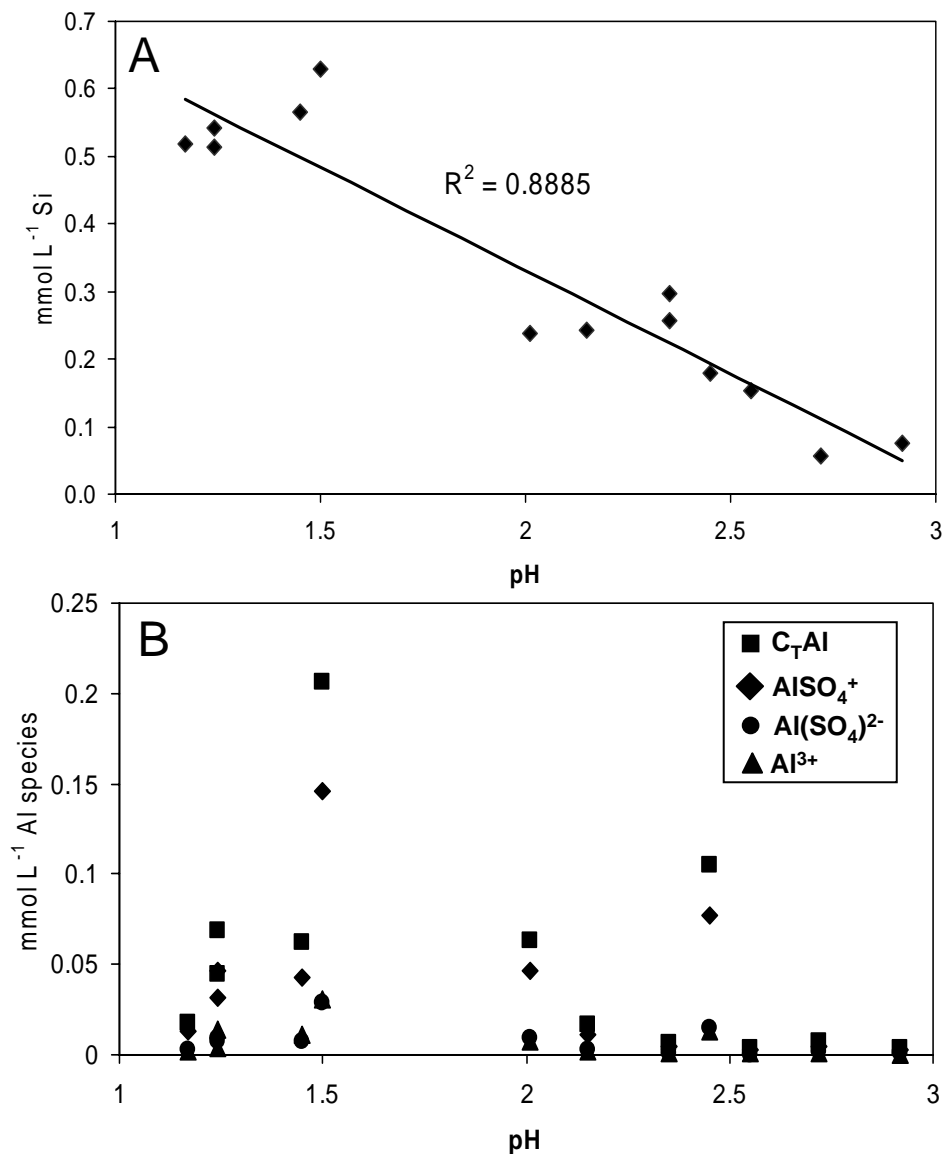
Figure 7-5: Si and Al concentrations in condensation droplets. (A) The [Si] from the condensation droplets strongly correlates to decreasing pH. (B) Al and Al-SO$_4$ complexes modeled by PHREEQC; free Al (Al^{3+}) has negligible concentrations in the droplets, as a result of Al complexation with sulfate. There is no correlation with Al-species and pH.
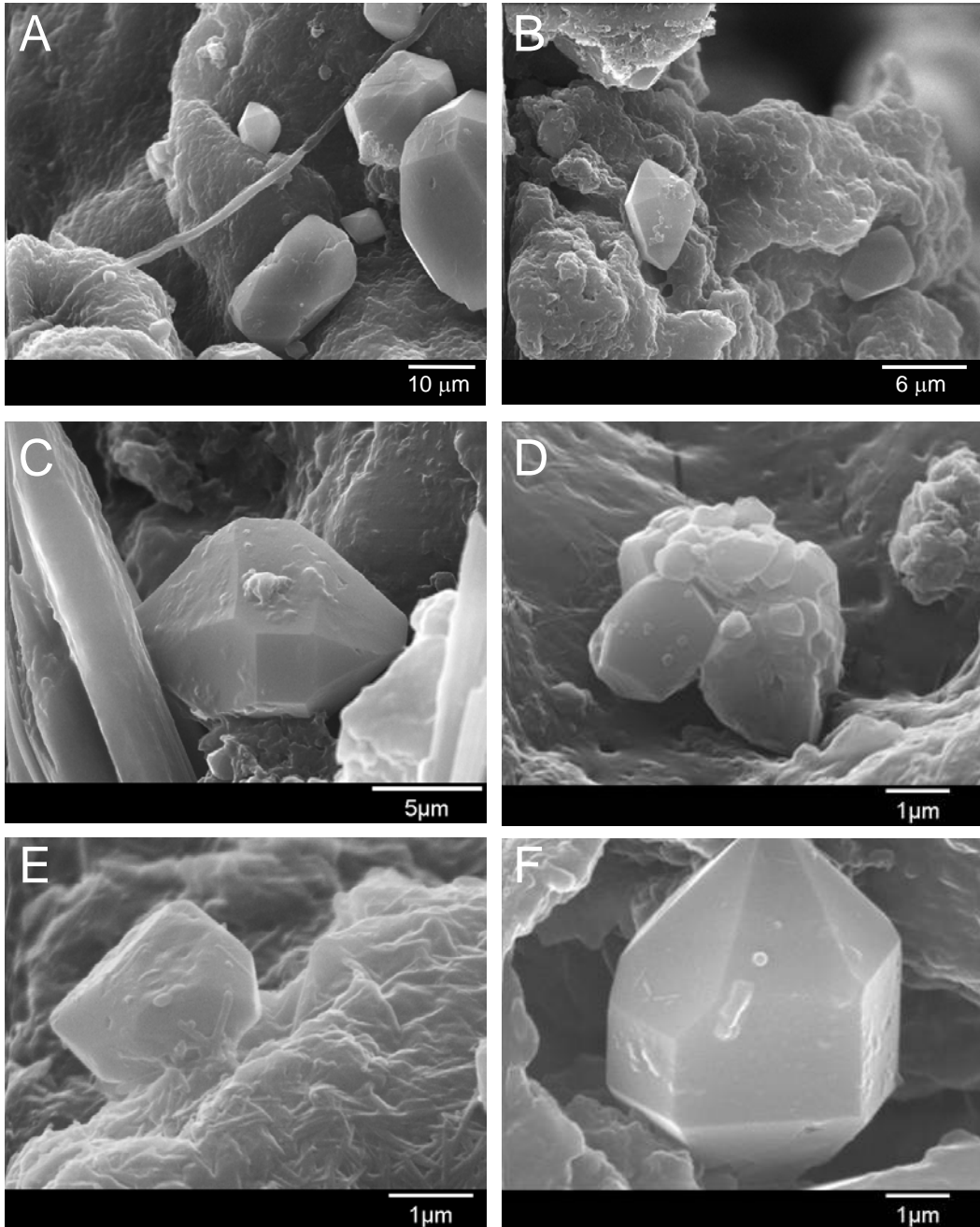
Figure 7-6: Scanning electron photomicrographs of authigenic quartz crystals from brown crusts on cave-wall surfaces.
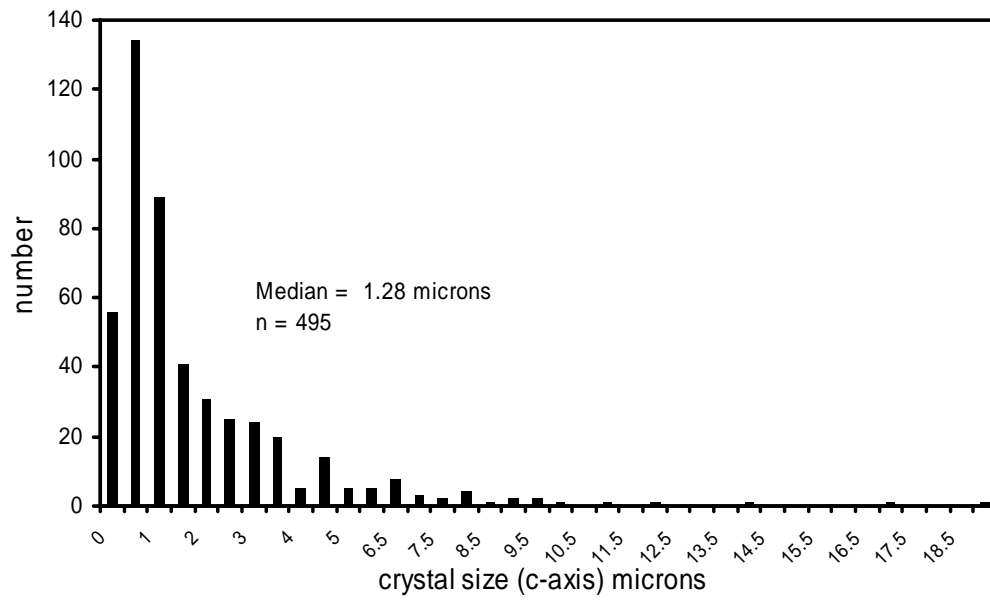
Figure 7-7: Quartz crystal lengths measured using ESEM.
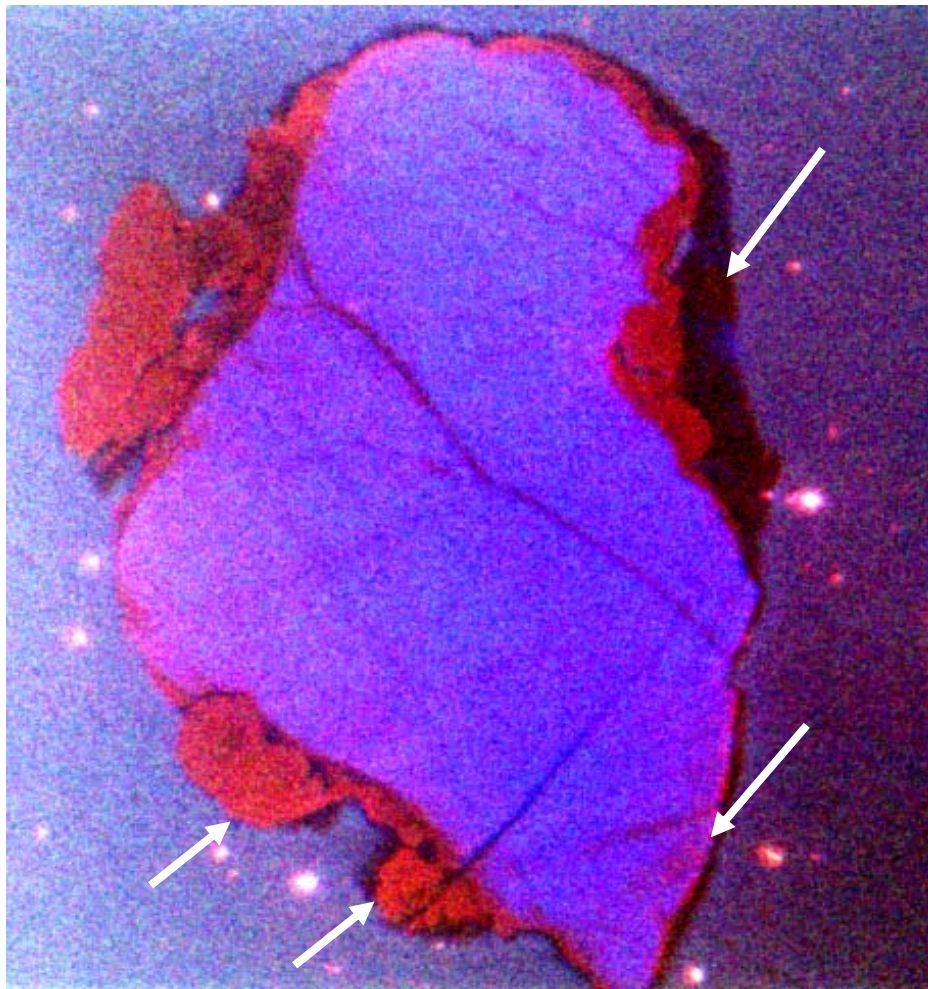
Figure 7-8: Cathodoluminescence image of polished quartz crystal imaged by ESEM. The crystal is approximately 50 mm wide. The core of the crystal is a fractured detrital quartz grain, although quartz was rarely found in the limestone as an insoluble phase. Two stages of authigenic overgrowths occurred on this grain (dark purple and dark orange-red). The overgrowths are not evenly distributed around the grain, possibly due to polishing artifact or to authigenic growth in the brown crust.
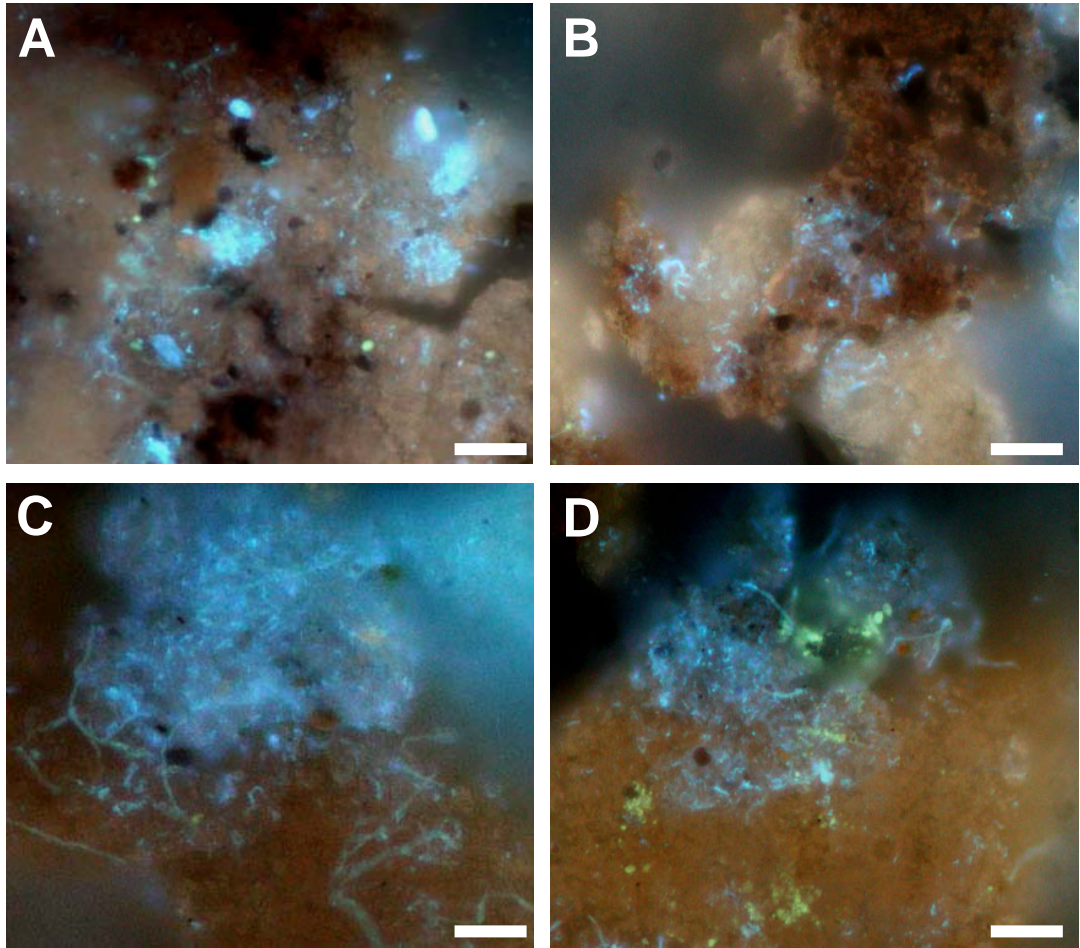
Figure 7-9: Fluorescence photomicrographs of brown crust stained with DAPI.
Bright blue areas are those that have nucleic acids and bright yellow
areas (D) are those with elemental sulfur. Scale bar = 10 μm.

Chapter 8: Conclusions

The subsurface is a major habitat for diverse microbial communities, as reactive rock surfaces and mineral-rich groundwater provide a variety of energy sources for microorganisms. Caves, although typically <50 m below the earth's surface, offer a valuable opportunity to examine biologic-geologic interactions under subsurface conditions. In Lower Kane Cave, Wyoming, groundwater bearing dissolved hydrogen sulfide, but negligible allochthonous carbon, discharges as springs into the cave passage. Both subaqueous and subaerial microbial communities inhabit this cave system, and the microbial ecology and geochemistry of both of these habitats were investigated.

The bulk of the subaqueous microbial mats has high sulfur content and expresses chemolithoautotrophic metabolism. 16S rDNA sequences retrieved from these mats indicate low overall taxonomic diversity, and the mats are dominated by several novel evolutionary lineages within the class "*Epsilonproteobacteria*". Lower Kane Cave represents the first non-marine natural system demonstrably driven by the metabolic activity of "*Epsilonproteobacteria*". The epsilonproteobacterial groups identified from Lower Kane Cave are not endemic to Lower Kane Cave, as molecular evidence suggests that these epsilonproteobacterial groups occupy a variety of terrestrial sulfidic habitats, both under photic and aphotic conditions. These results expand the geographic and ecological diversity of "*Epsilonproteobacteria*", suggesting that geographic isolation may not be a driving factor in speciation based on minimal genetic divergence among these groups.

242

Ecologically, the "*Epsilonproteobacteria*" are chemolithoautotrophic sulfur-oxidizing bacteria. As they diversify genetically and metabolically, they create habitats within the microbial mats for other bacterial groups. The biomass of the diverse anaerobic microbial groups, within the interior of the microbial mats, is substantially less than the total biomass of the microbial mat. Stream geochemistry and the spatial relationship of aerobic and anaerobic metabolic guilds allow for tight carbon and sulfur cycling constrained by redox boundaries within the mat environment. A significant component of autotrophically produced carbon is cycled through a detrital microbial loop, demonstrating the ecological importance of these anaerobes. The physical model of carbon and sulfur nutrient spiraling is based on the energy transfer between redox environments, and without aerobic and anaerobic metabolic complexity, nutrient spiraling would not occur. Specifically, chemoautotrophically-fixed carbon produced by the sulfur-oxidizers is degraded by the fermenting bacteria, as well as transported downstream. Fermenters produce a variety of breakdown products that are consumed by different sulfate-reducing bacterial groups, methanogens, and other microbial groups such as iron-reducers or denitrifiers. In turn, the sulfate-, sulfur- and fermenting bacteria generate autochthonous hydrogen sulfide and other volatile organosulfur gases that are consumed primarily by sulfur-oxidizers. Active VOSC cycling by microbial communities from an aphotic habitat has not been previously demonstrated. Sulfur gases produced in terrestrial subsurface habitats, such as sulfidic groundwater, can be important potential sources to the global sulfur cycle.

Almost all of the dissolved sulfide coming into the cave is consumed by subaqueous sulfur-oxidizing bacteria within the microbial mats, including the "*Epsilonproteobacteria*", but also *Gammaproteobacteria* (e.g., *Thiothrix* spp.) and *Betaproteobacteria* (e.g., *Thiobacillus* spp.). These bacteria drive subaqueous sulfuric acid speleogenesis by attachment to carbonate surfaces and generation of sulfuric acid, which focuses local carbonate undersaturation and dissolution. As the "*Epsilonproteobacteria*" can be metabolically active under low oxygen tensions, these organisms can potentially catalyze sulfide oxidation where autoxidation would be kinetically limited, such as in deep anoxic aquifers. Prior to this work, sulfuric acid speleogenesis was considered a subaerial process (e.g., Egemeier, 1981; Hill, 1990; Galdenzi et al., 1995; Hill, 2000) or a process limited to shallow groundwater environments because of oxygen requirements for abiotic autoxidation mechanisms (e.g., Palmer, 2000). However, chemolithoautotrophy and microbial sulfur oxidation under microaerophilic conditions extend the phreatic depths to which porosity and conduit enlargement can occur in carbonate systems. Groundwater in karst and non-karst areas can often have high concentrations of dissolved sulfide, especially in regions near hydrocarbon reservoirs (Ulrich et al., 1998; Nemati et al., 2001; Kodama et al., 2002; Elshahed et al., 2003), making the contribution of sulfur cycling and microbially enhanced carbonate dissolution more significant globally. As "*Epsilonproteobacteria*" are the major microbial groups so far identified in many sulfidic habitats associated with carbonate caves and springs, these organisms may not only be responsible for sulfuric acid speleogenesis in Lower Kane Cave, but may also be important for carbonate porosity development

globally. The metabolic and geologic consequences of an active microbial ecosystem in the subsurface fundamentally change the model for sulfuric acid speleogenesis.

APPENDIX A

Scanning Electron Photomicrographs and
16S rRNA Gene Sequence Clone Libraries:
Chapter 2 Supplement

File SEM5201usm_b.doc

Date May 2, 2001

Sample   upper spring white mat – bottom jelly mat

Sample # LKB-O1M – OO3b (jelly mat)

Description brown-golden to darkbrw mat under
white mats at Site 3

Duration in place

Date emplaced

Date retrieved March 2001

Method of preservation gluteraldehyde, frozen in N2,
Cracked, freeze-dried overnight

Coating material gold

Time of coating 2x 15 sec

Accelerating voltage 30 kv

Are bugs present?☒ Singles?☐ Groups?☐

No. types present [ ] cocci☒ rods☒ branchy☒

Radius of bugs [ ]   Length [ ]

Etching?☐   Secondary minerals?☒

EDAX ☐ File names [ ]

No. photomicrographs 20 File names M2_upb2_*.tif

Comments: Pictures from two sample stubs

White mat – bottom jelly brown mat – slimy with some sediment (evidence of fine-grained stuff (50-100 um) stuff inside of mat). Lots of filaments on the mineral substrates – and it looks like the filaments are ordered structurally on the substrates – in a lattice structure. Really strange – thick filaments are oriented in one direction, with smaller ones in between them (1 um wide)- may be for nutrient acquisition ("closest- packing" arrangement)

Need to look for more of this

Saw spiky mineral (calcite?)- within the mats – maybe dissolving – maybe precipitating…. Other strange mineral forms – maybe sulfur globules

REALLY AWESOME spiral-guys… but very very very small (100-200 um wide) but long… free-floating in filament matrix but also adhered to substrates (last pic)
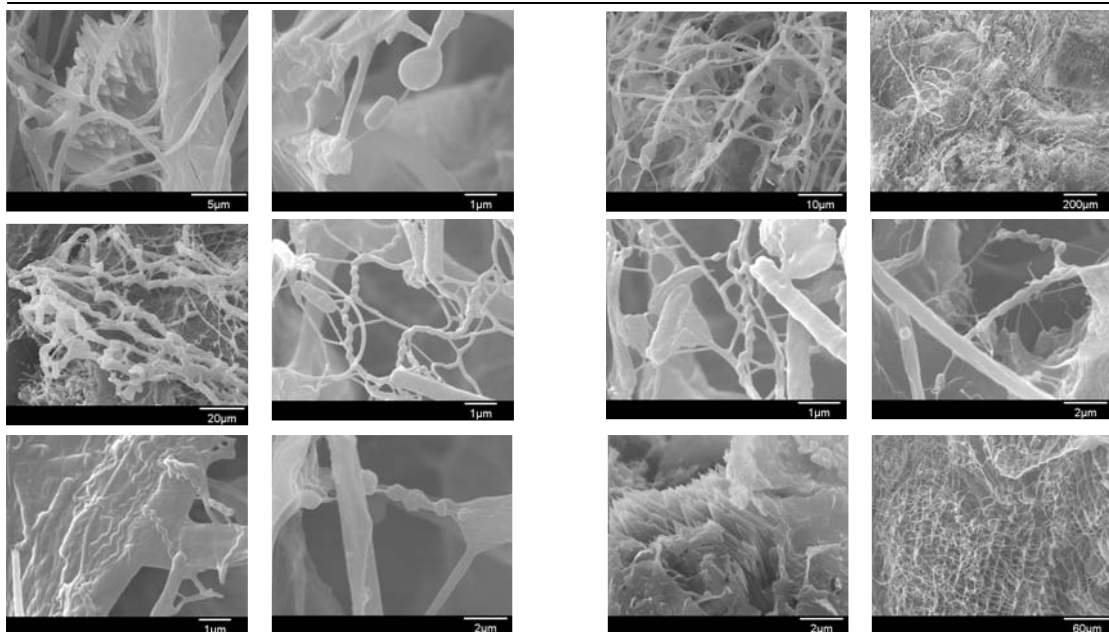
File SEM5201usm.doc

Date 5-2-01

Sample   Upper Spring White Mat – top layer

Sample # LKB-01M-003a

Description white filamentous mat from U Spg

Duration in place

Date emplaced

Date retrieved March 2001

Method of preservation gluteraldehyde, N2frozen, fractured w/ exacto, froze whole bottle in N2, Then freeze-dried overnight (~ 15 hrs)

Coating material gold

Time of coating 2x 15 sec

Accelerating voltage 30 KV

Are bugs present?☒ Singles?☐ Groups?☒

No. types present ☐ cocci☐ rods☒ branchy☐

Radius of bugs   Length

Etching?☐   Secondary minerals?☐

EDAX ☐ File names

Comments:
 White mat preserved in gluteraldehyde in field – collected from 203 m (same spot as always – Site 3)

Mat is very slimy and difficult to pull apart – had to cut sections to look at in freeze-dry and look at

Lots of filaments – very dense mat – size of filaments is generally the same (between 3 and 1 μm). Larger filaments look a little rough on the outside, but smaller (around 1 um wide) are very smooth

See some minerals – like the spiky calcite and other rhombs within filament matrix

Sulfur globules

248
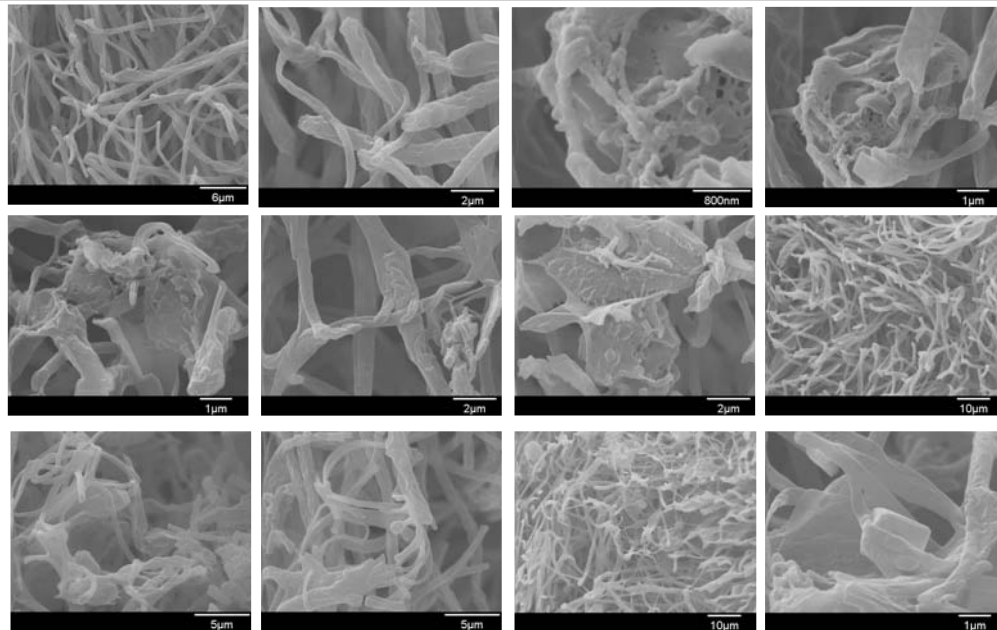
File SEM21301framdoc

Date 2-13-01

Sample Upper Spring Gray sediment – top layer

Sample # LKC-01M-004

Description gray sediment from U Spg orifice area

Duration in place

Date emplaced

Date retrieved March 2001

Method of preservation gluteraldehyde, N2frozen,

fractured w/ exacto, froze whole bottle in N2,

Then freeze-dried overnight (~ 15 hrs)

Coating material gold

Time of coating 2x 15 sec

Accelerating voltage 30 KV

Are bugs present?☒ Singles?☐ Groups?☒

No. types present 3 cocci☒ rods☒ branchy☒

Etching?☐ Secondary minerals?☐

EDAX ☒ File names attached – peaks Fe and S (small peak)

Comments:
Gray sediment mat preserved in gluteraldehyde in field – collected from 189 m (pool bottom)

Sediment is very flocky

Lots of black specs – Fe-S stuff
Not many biological things- some filaments and cocci "sacks" – lots of framboids and crystallites
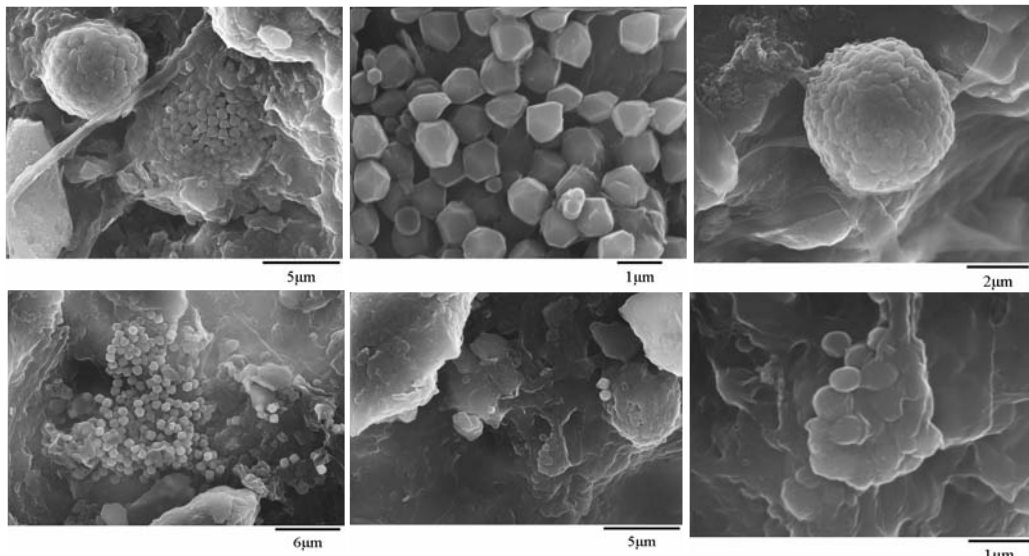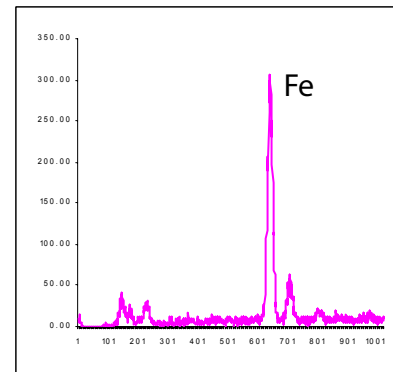
249

File SEM62601_up_red.doc

Date 6-26-01

Sample up spg 189 m, blood red mat next to black

Sample # lkb-01m-004r

Description blood red, thin biofilm/mat near black

Duration in place

Date emplaced

Date retrieved 3-01 trip

Method of preservation glut, freeze-fract, freeze-dry

Coating material gold

Time of coating 30 sec

Accelerating voltage 30 kv

Are bugs present? ☒   Singles? ☐   Groups? ☒

No. types present ____ cocci ☒ rods ☒ branchy ☒

Radius of bugs variable   Length   variable

Etching? ☐   Secondary minerals? ☐

Comments:
Upper Spring orifice 189 m (Figure 1-6A). Most impt images were the first ones (esp the third in the 1st row), showing that a framboid is associated with limestone (Ca, and shows extensive dissolution). Perhaps the framboids ARE coming from the limestone…. Need to look at hostrock in SEM to see b/c thin sections show Fe present…. Some of the framboid crystals are "coated" compared to others, maybe they are being replaced?

 Rest of the sample showed thick glycocaylx with lots and lots of cells (mostly cocci <1mm), but also with some rods 1-2 mm long. The biofilm is generally thin. Some evidence for filamentous cells, but could be sheaths – what is making the blood red color? Saw lots of small framboids also encased in biofilm (looked for density/composition variation in TV with contrast turned way up…. Very dark objects were framboids!).
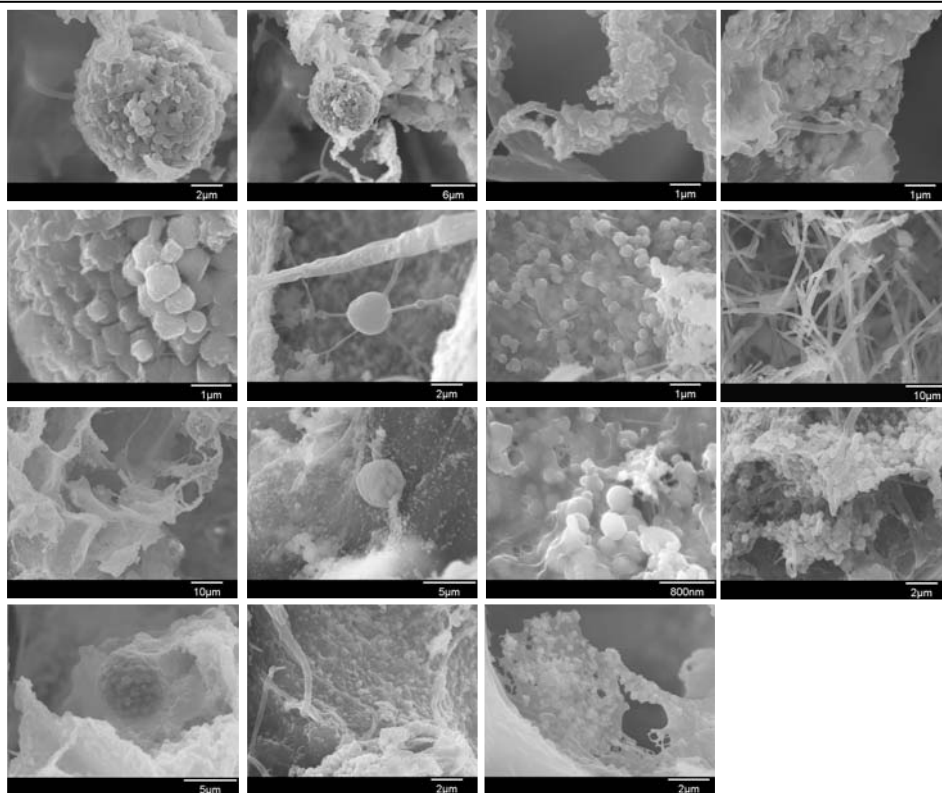
ile SEM62601org.doc

Date 6-26-01

Sample   189 m , up spg, orange mat next to black

Sample # lkb-01m-004o

Description rusty org mat in Upper Spg pool, near blk

Duration in place

Date emplaced

Date retrieved 3-01 trip

Method of preservation 2.5% glut, freeze-fracture, Freeze-dry

Coating material gold

Time of coating 30 sec

Accelerating voltage 30 KV

Are bugs present?☒ Singles?☐ Groups?☒

No. types present ☐ cocci☒ rods☒ branchy☒

Radius of bugs ☐   Length ☐

Etching?☐   Secondary minerals?☐

EDAX ☐ File names ☐

No. photomicrographs

File names 626site4org1 thu 9.tif

Comments:
Upper Spring orange film next to gray and red.

Really bad charging problems and the SEM was jumping all over the place- drifting and jumping during picture-capture. Sample was really really porous.

For the most part, it looked like the samples from the red mats at Site 1, with sheaths. Didn't see any *Gallionella*-like stuff. There was a thick biofilm on solid particles (sediment?), with clumps of cocci, less then 1 μm across. Some indication of spirochetes.

Red stuff on right (whole picture ~0.75 m wide).
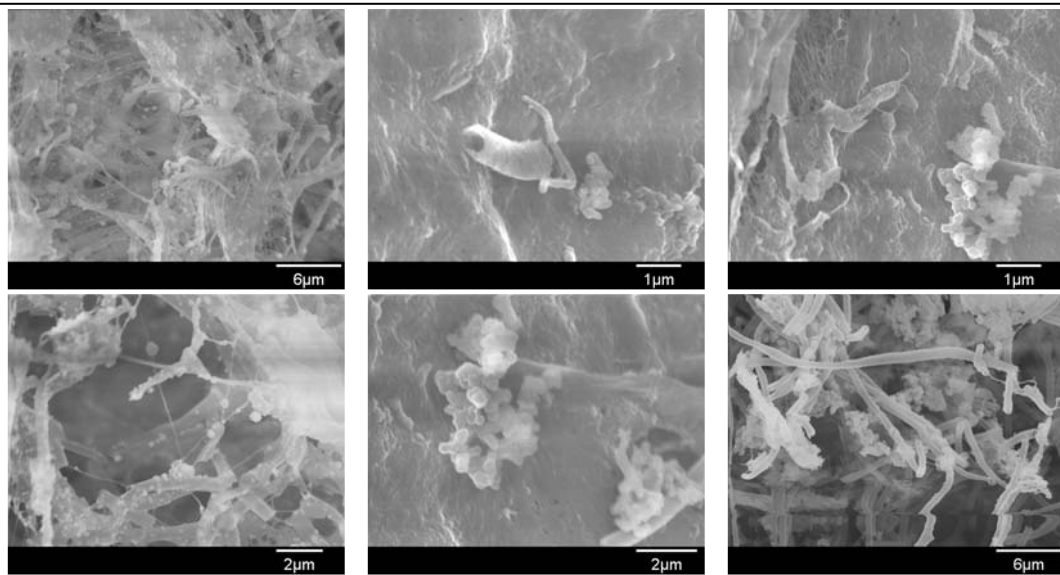
File SEM62601red

Date 6-26-01

Sample   215 m red mats discharing into stream

Sample # lkb-01m-001

Description red mats at 215 m, sampled from top 2 cm

Duration in place [   ]

Date emplaced [   ]

Date retrieved 3-01 trip

Method of preservation 2.5% glut, freeze-fracture,

Freeze-dry for at least 18 hours

Coating material gold

Time of coating 30 sec

Accelerating voltage 30 KV

Are bugs present?☒   Singles?☒   Groups?☒

No. types present [   ] cocci ☒ rods☒ branchy☒

Radius of bugs ~ 1μm   Length see comments

Etching?☐   Secondary minerals? Mostly Fe

EDAX ☐ just general , mostly Fe

Comments:
 215 m red mats (Figure 1-8), thick goopy stuff – freeze-dried sample was very soft and porous, little bit of charging problem, but not too bad over all.

Lots and lots of sheaths (*Leptothrix*) – this sample didn't have as much of the bumpy stuff all over it like before (maybe too much gold before?) – clumps of cocci and rods in between sheaths. Sheaths have broken ends, but couldn't find growing tips. Sheaths approx 1μm across, and more than 20 μm long, avg about 10 μm, but this is probably a function of breaking them up.

Thin filaments, about 100 nm across, twisted around each other and sheaths (see image below!) – perhaps *Gallionella*…very nice twisty segments, no more than about 10 μm long, but could have been broken
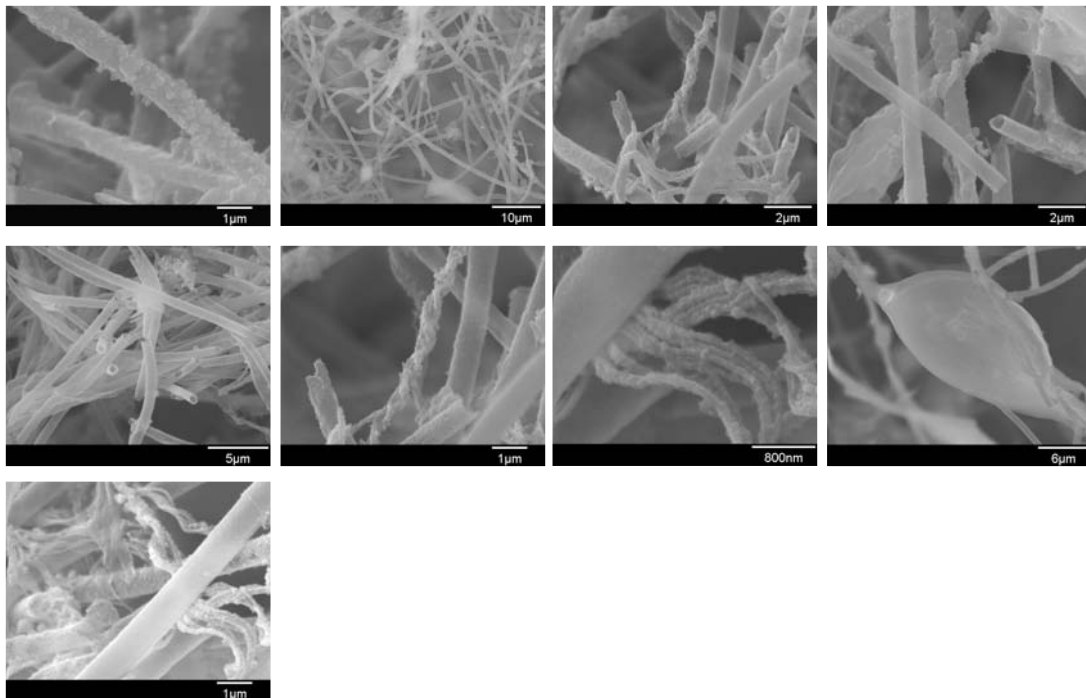
File SEM2201p

Date 2-2-01

Sample pumpkin guts - ~72 m

Sample #

Description red mats @ 72 m- very dense

Duration in place

Date emplaced

Date retrieved 9-00 trip

Method of preservation tube-glut-ethanol

Coating material gold

Time of coating 30 sec

Accelerating voltage 30 Kv

Are bugs present?☒ Singles?☒ Groups?☒

No. types present ?? cocci ☒ rods☒ spiral ☒

Sheaths ☒

Radius of bugs varies   Length varies

Etching?☐ Secondary minerals?☐

EDAX ☒ File names pumpEDS.xls

No. photomicrographs 7

Comments:

Pumpkin guts from stream channel at 72 m – charge a little, have to reduce spot size and brightness- concentrate on small areas, then move because of charge – need to coat better

Seems to be just a sheath matrix with balls (or cells) all around. Really cool stuff- oriented? Sheaths - look at mats under Epi or confocal to see (but might not stain…?)

EDS of ball material has Fe

Groups/clumps of stuff – mineral matter-mixed with
Sheaths… don't know what it is?

Spiral sheaths – maybe *Gallionella* – but don't know because diameter is pretty small

Straight sheaths – *Leptothrix*-like
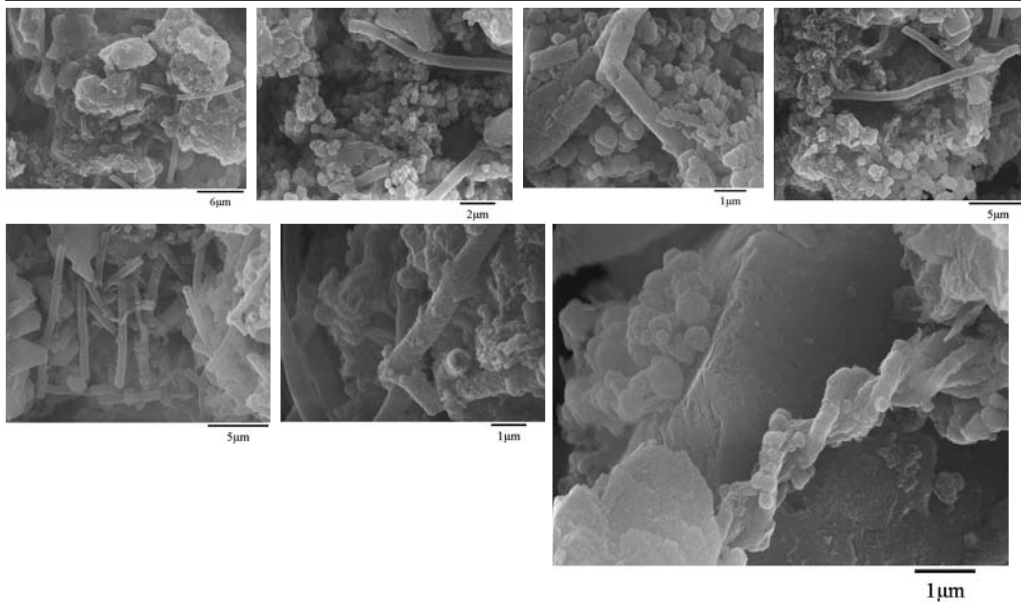
253

Restriction fragment length polymorphism results

LKC19_31-45

Clone Library 19 (124 m filaments)	
Pattern	Number
1	3
2	36
4	3
5	7
6	2
7	1
12	1
13	1
17	1
X	19
Total	74

LKC19_73.76

LKC19_16-30

LKC19_61-72

LKC19_1-15

LKC19_46-60

Restriction fragment length polymorphism results

LKC19B_33-47

LKC19B_16,17,19,20,22-32

LKC19B_63-71

LKC19B_1-15

LKC19B_48-62
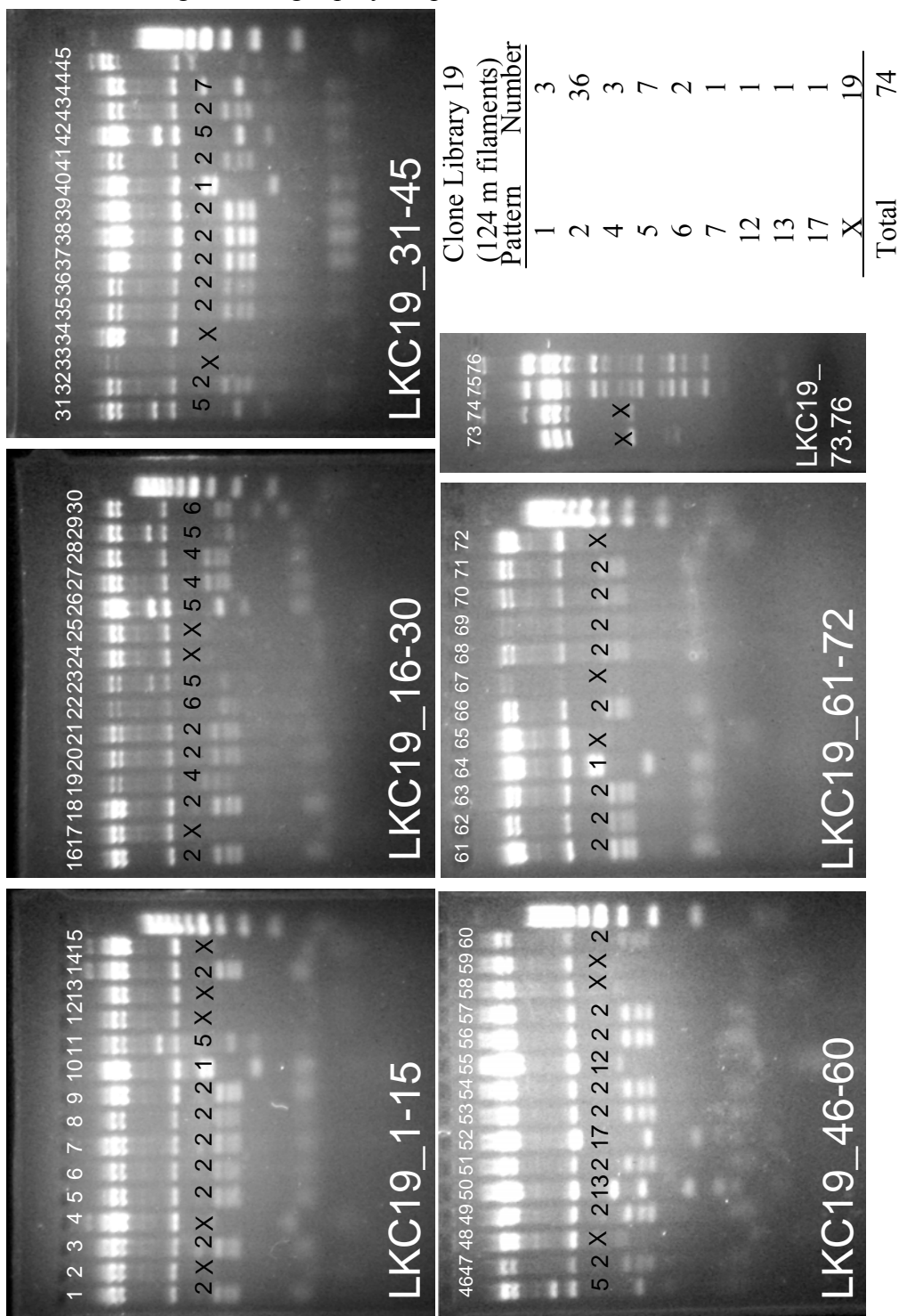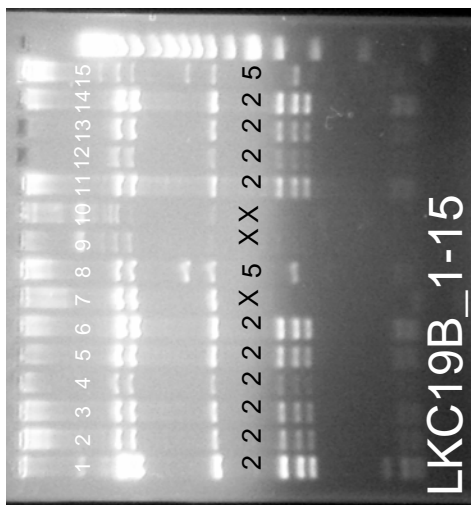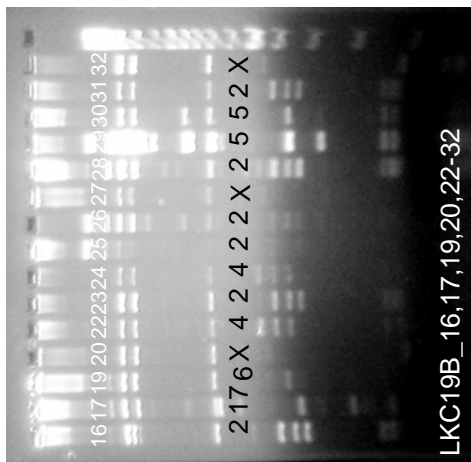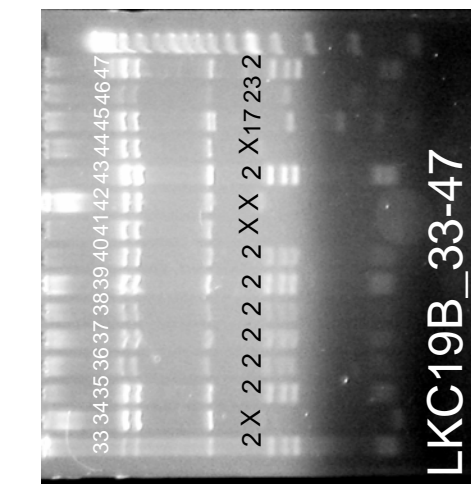
Clone Library 19B
(124 m filaments)

Pattern	Number
1	1
2	44
4	2
5	5
6	1
17	2
23	1
X	13
Total	69
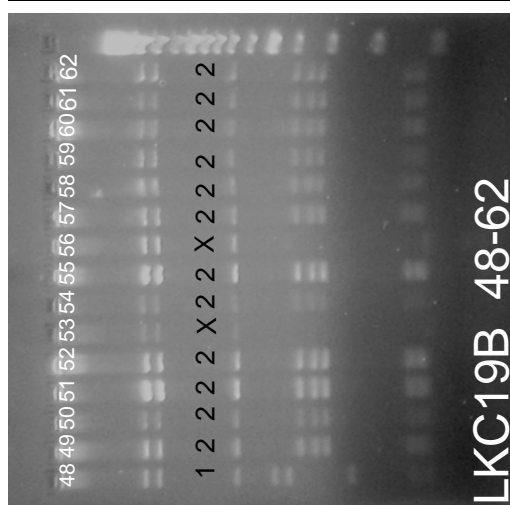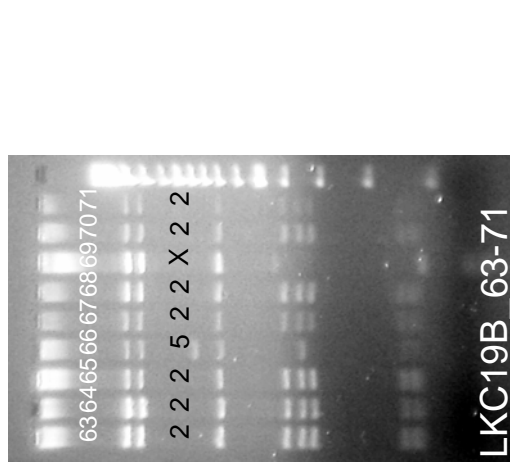
Restriction fragment length polymorphism results
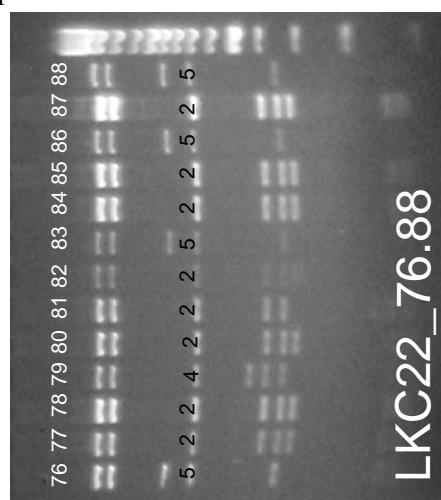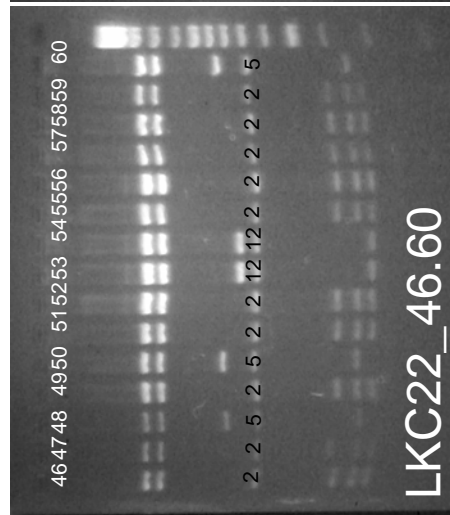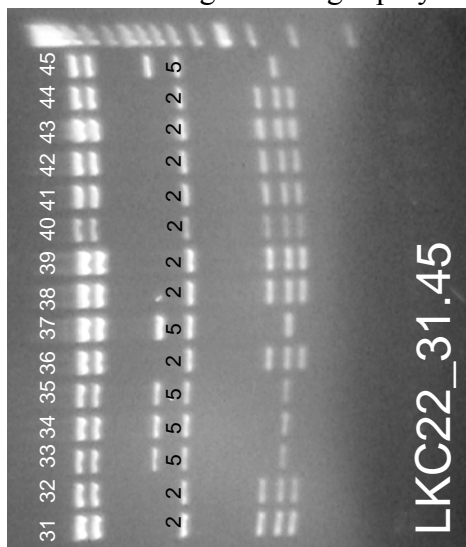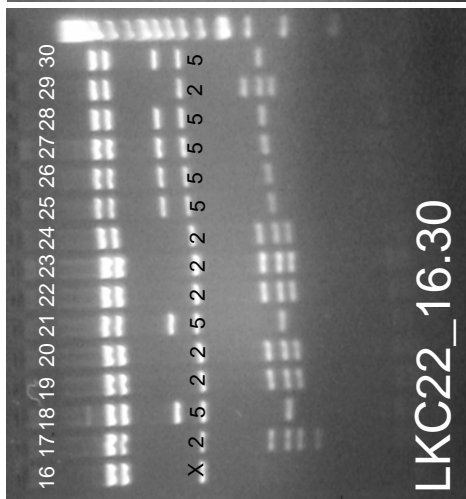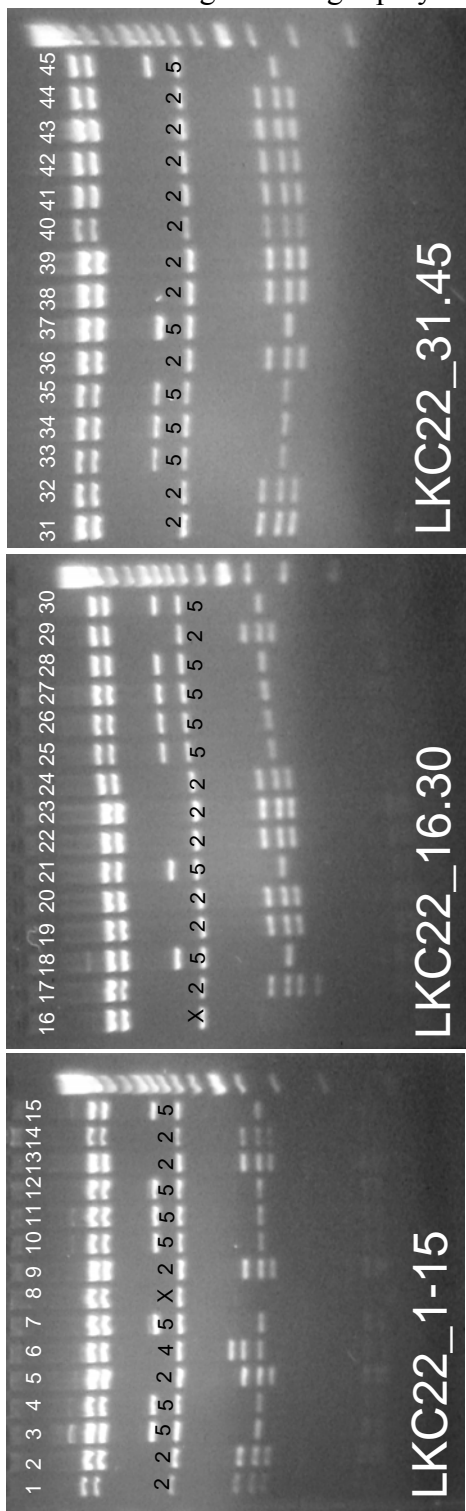
LKC22_31.45

LKC22_76.88

LKC22_16.30

LKC22_61.75

LKC22_1-15

LKC22_46.60

Restriction fragment length polymorphism results

Clone Library 22
(127 m filaments)

Pattern	Number
2	61
4	4
5	36
12	2
X	3
Total	106

LKC22_104-106

LKC22_89-103
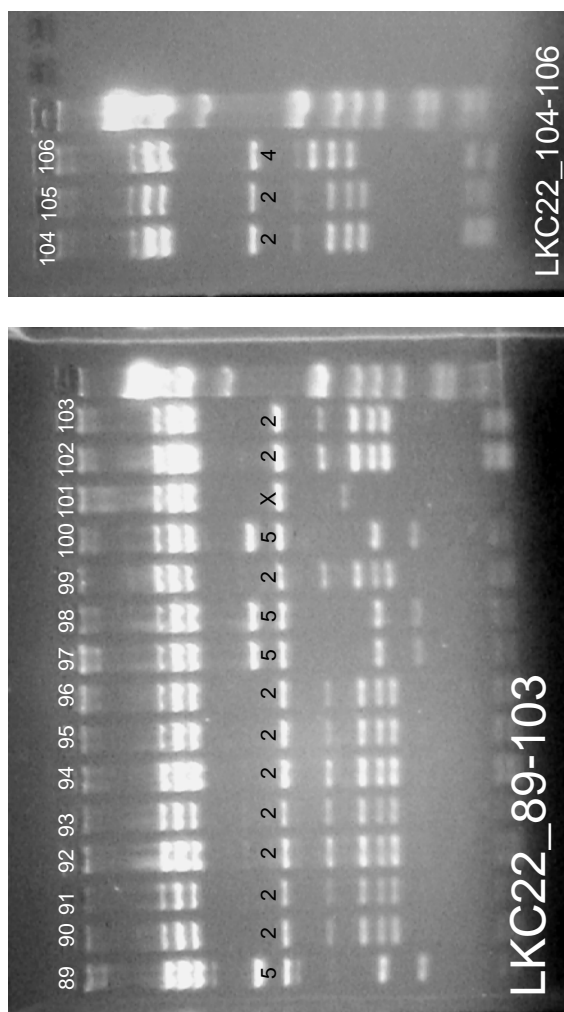
Restriction fragment length polymorphism results
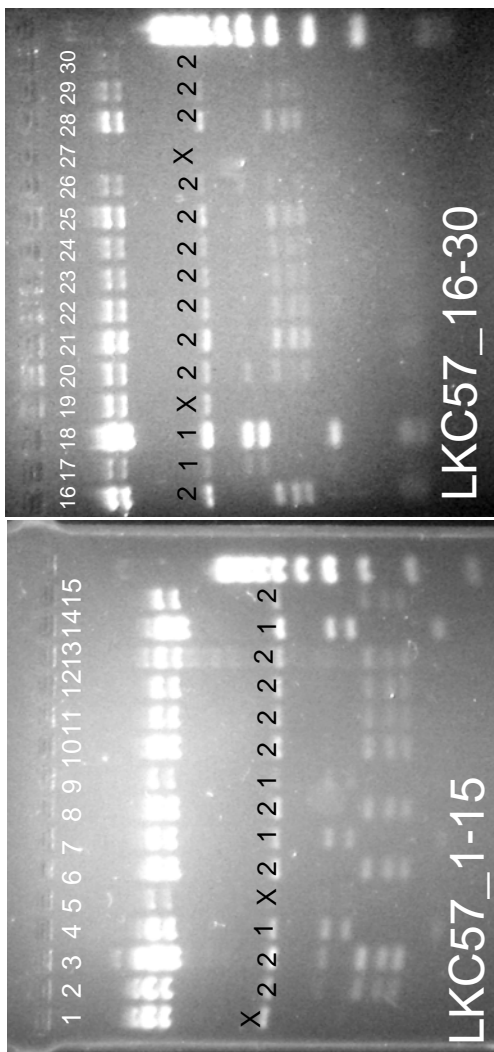
Clone Library 57
(190 m filaments)

Pattern	Number
1	7
2	24
X	25
Total	56
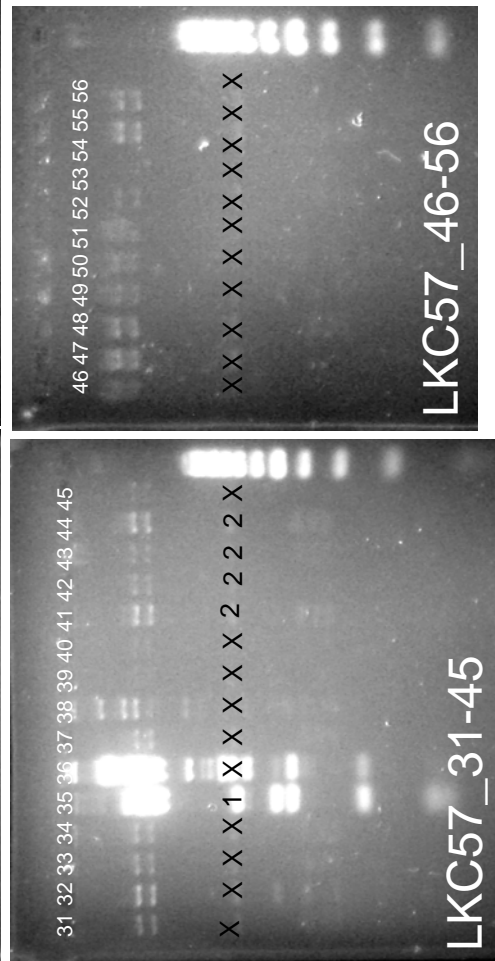
Clone Library 57C (not shown)
(190 m filaments)

Pattern	Number
1	16
2	16
4	2
8	6
10	2
Total	42

Restriction fragment length polymorphism results

LKC57B_31-45

LKC57B_16-30

LKC57B_1-15

LKC57B_61-72

LKC57B_46-60

Clone Library 57B
(190 m filaments)

Pattern	Number
1	6
2	39
4	4
5	4
8	1
9	2
10	2
12	1
X	13
Total	72

Restriction fragment length polymorphism results

LKC270_31-45

LKC270_76.87

Pattern	Number
X	4
Total	87

LKC270_16-30

LKC270_49.60_73.75

Pattern	Number
9	1
10	3
24	1

Pattern	Number
5	4
7	2
8	4

LKC270_1-15

LKC270_46.48_61.72
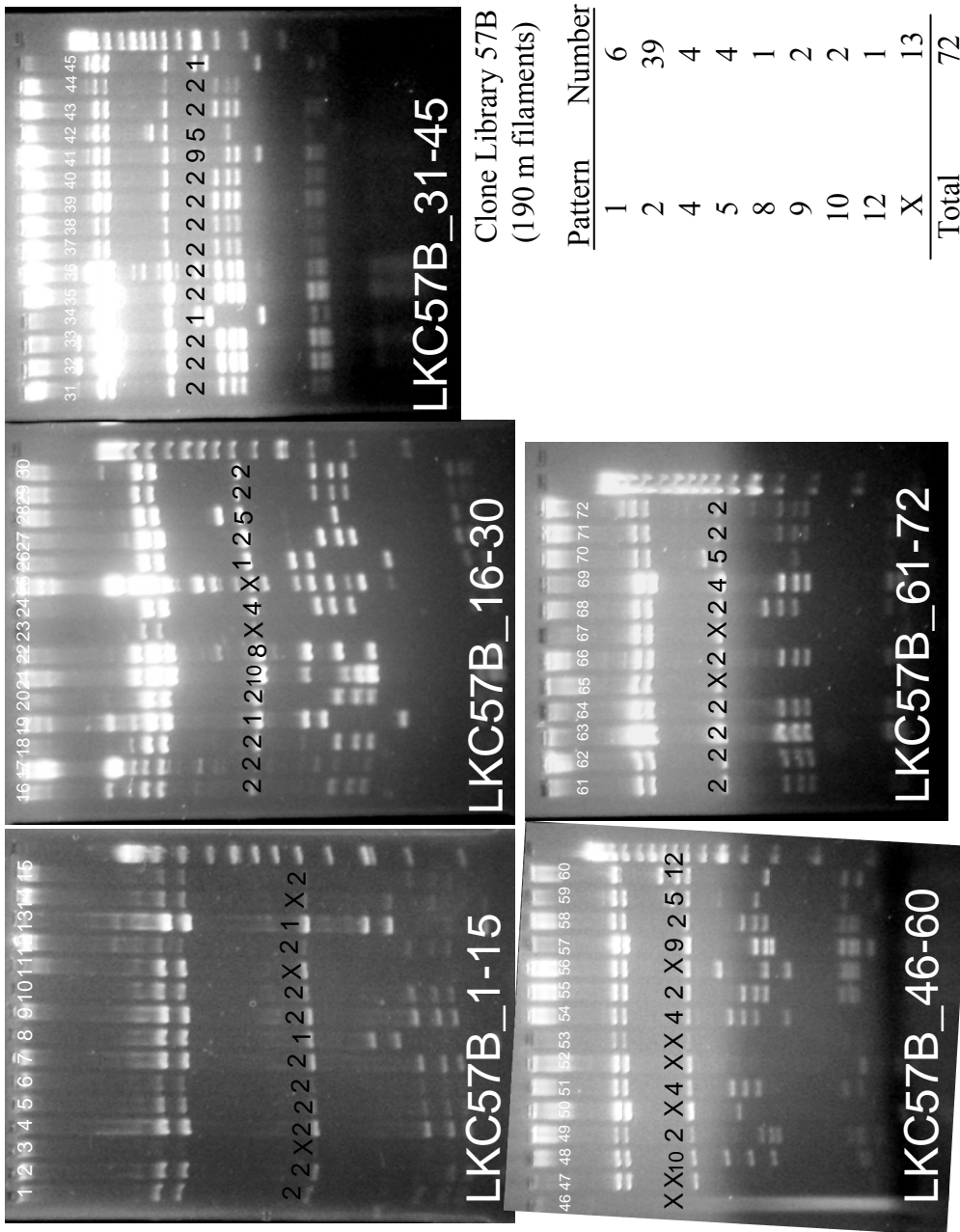
Pattern	Number
1	27
2	38
4	3
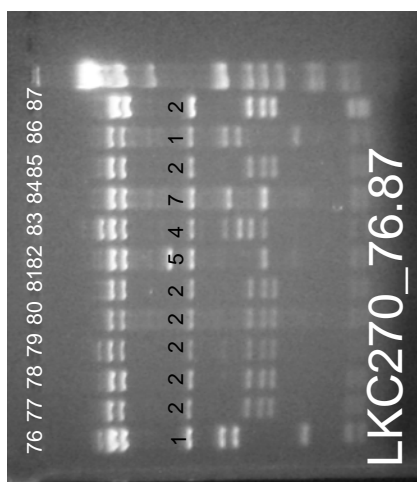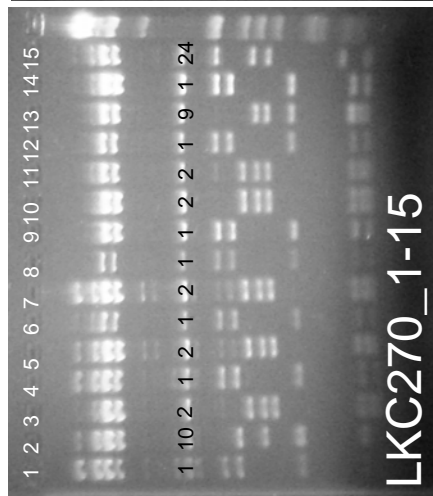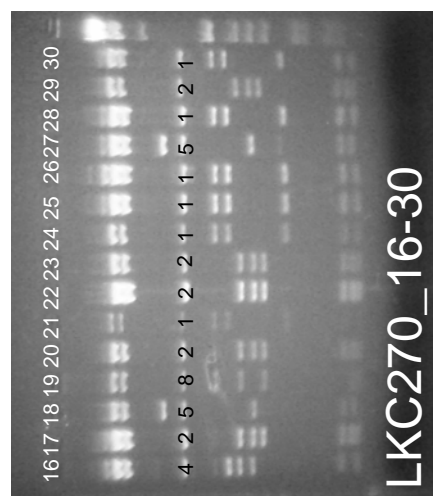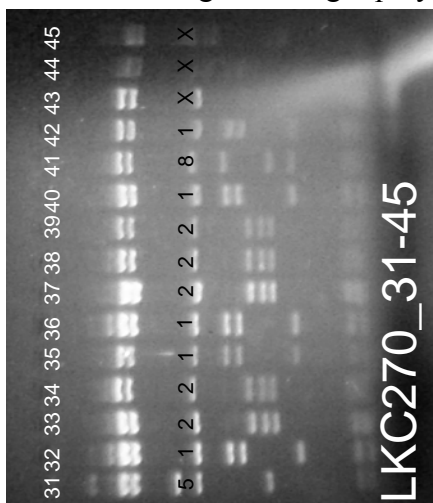
Clone Library 270
(195 m filaments)

260

Restriction fragment length polymorphism results
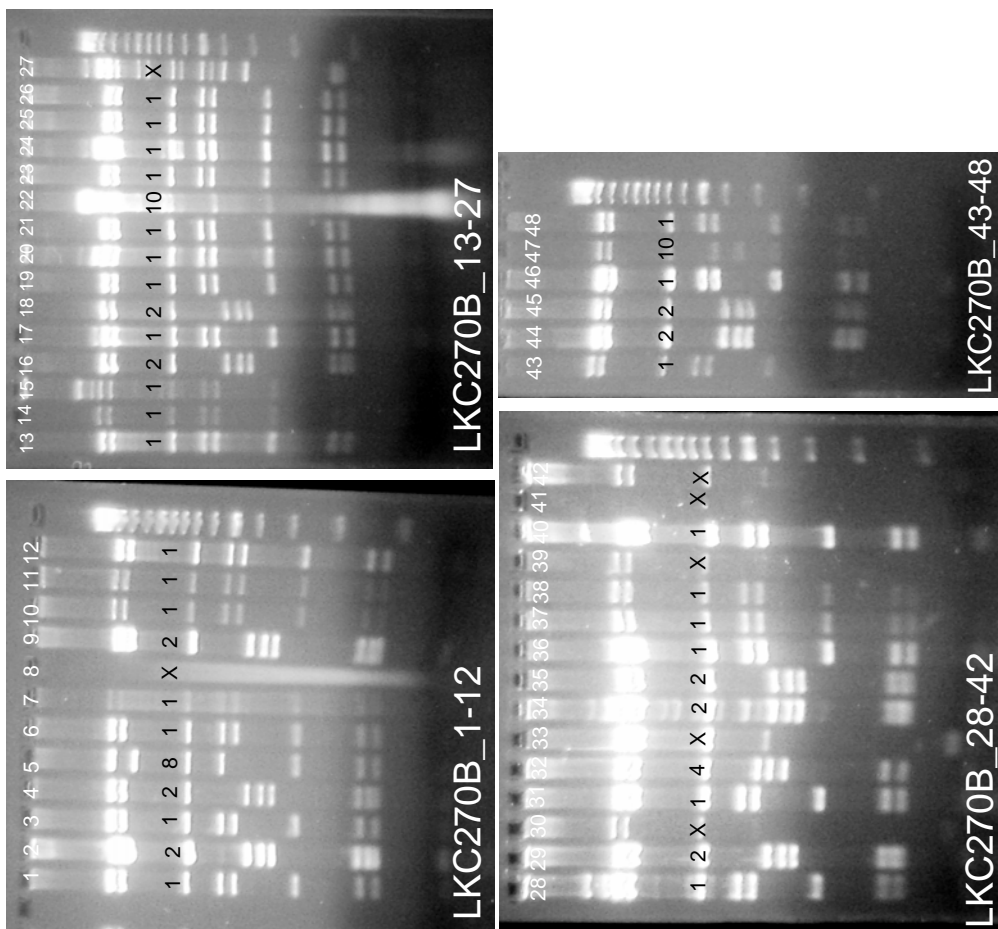
Clone Library 270B
(195 m filaments)

Pattern	Number
1	27
2	10
4	1
8	1
10	2
X	7
Total	48

LKC270B_13-27

LKC270B_43-48

LKC270B_1-12

LKC270B_28-42

Restriction fragment length polymorphism results

LKC190_31-45

LKC190_91-94

LKC190_76-90

LKC190_46-60

Clone Library 190*
(198 m filaments)

Pattern	Number
1	81
11	6
X	5
Total	92

* Additional gels not shown

Restriction fragment length polymorphism results
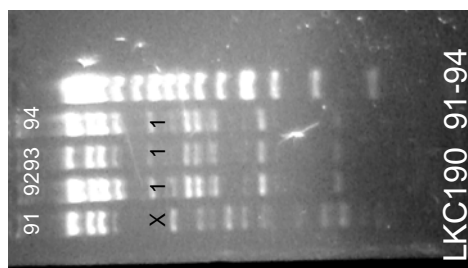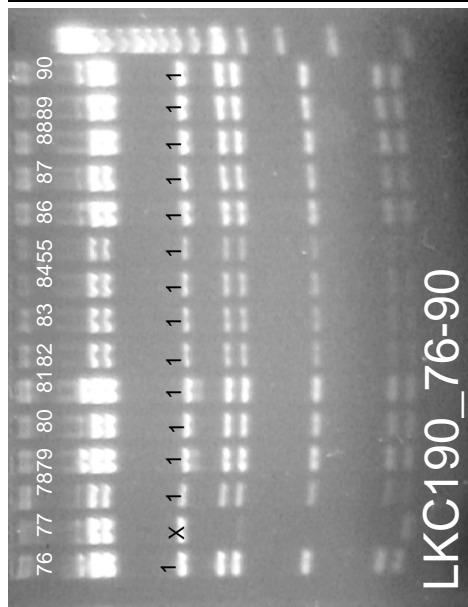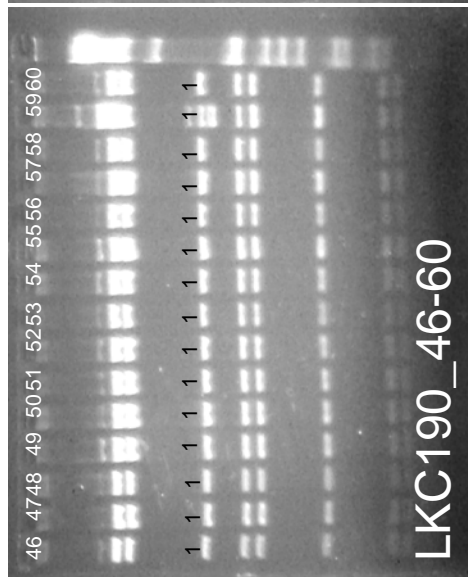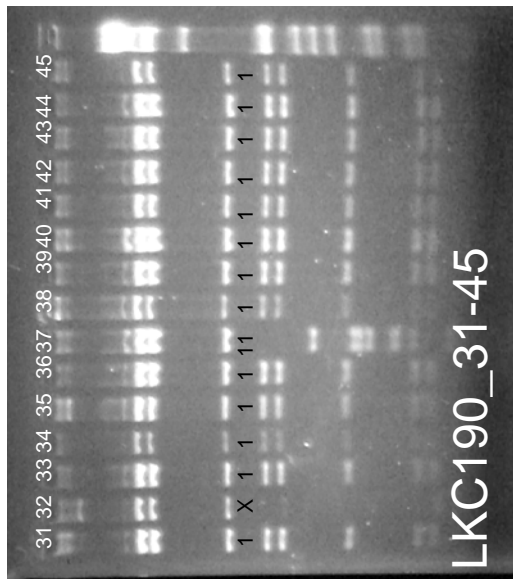
Clone Library 127 (203 m filaments)	
Pattern	Number
1	13
2	9
4	10
5	12
7	2
10	3
13	1
X	10
Total	60

LKC127_16-30

LKC127_1-15

LKC127_46-60

LKC127_31-45

Restriction fragment length polymorphism results

LKC127B_16-30

LKC127B_1-15
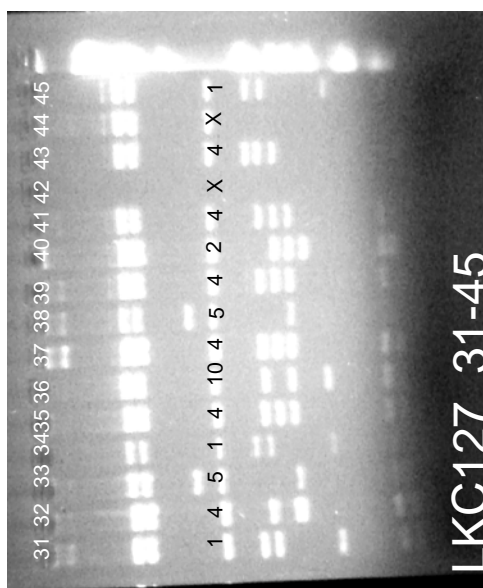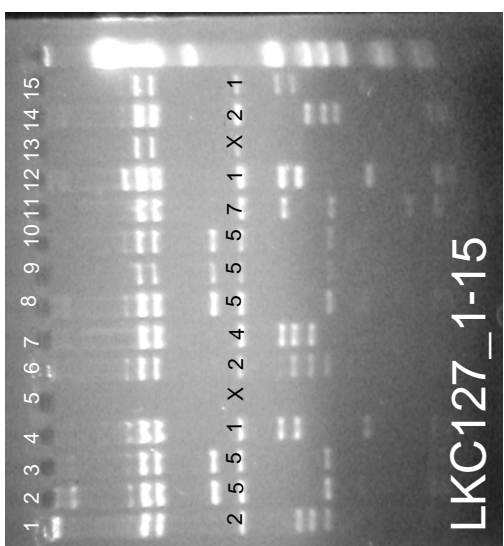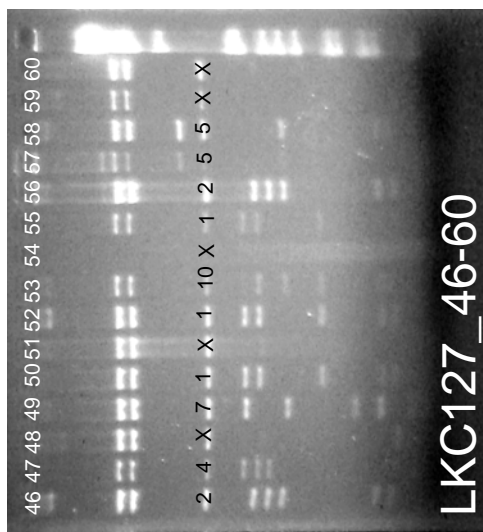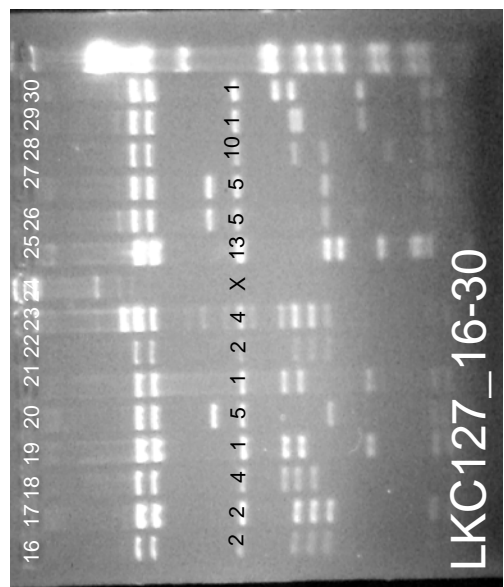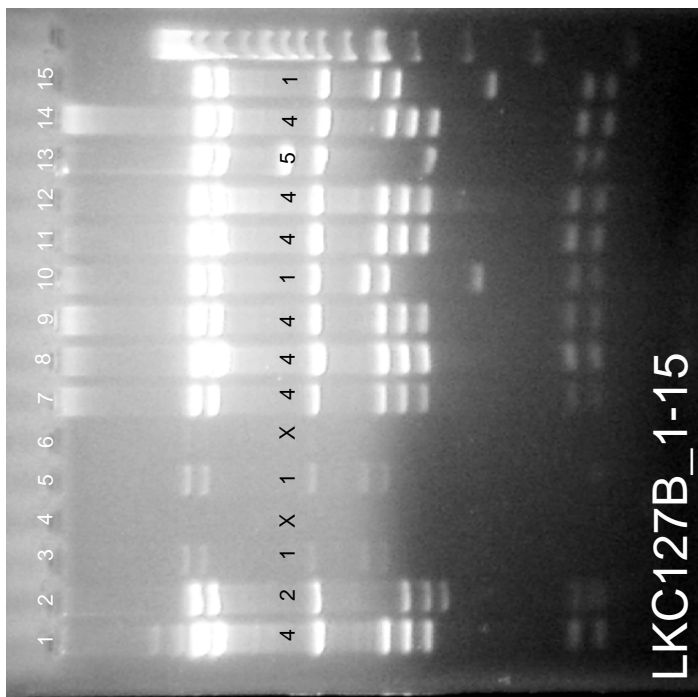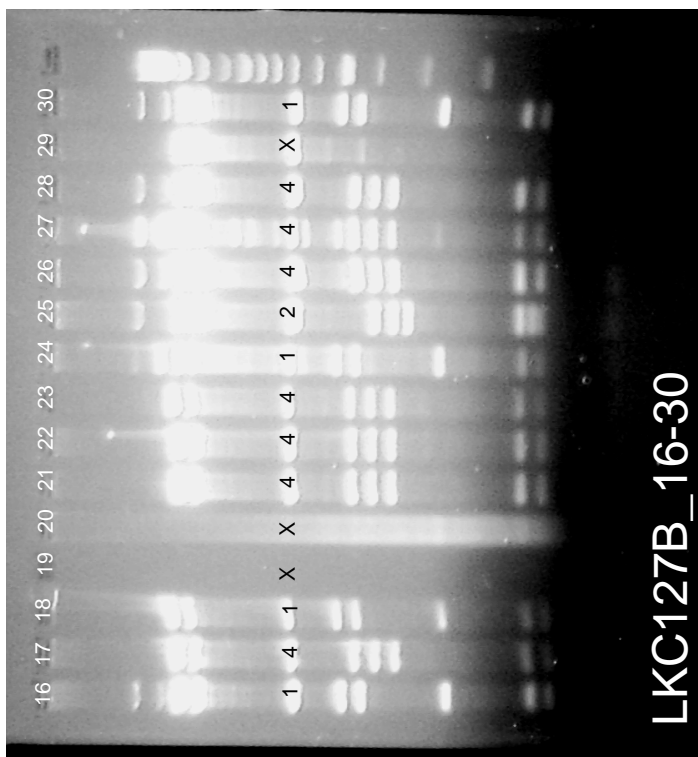
Pattern	Number
1	8
2	2
4	14
5	1
X	5
Total	30

Clone Library 127B
(203 m filaments)

Restriction fragment length polymorphism results

Clone Library 159
(counted with library 127)
(203 m filament)

Pattern	Number
1	6
5	1
7	1
X	4
Total	12

LKC159_1.12

Restriction fragment length polymorphism results

LKC156_31-45

LKC156_16-30

LKC156_1-15

LKC156_76-80

LKC156_61-75

LKC156_46-60
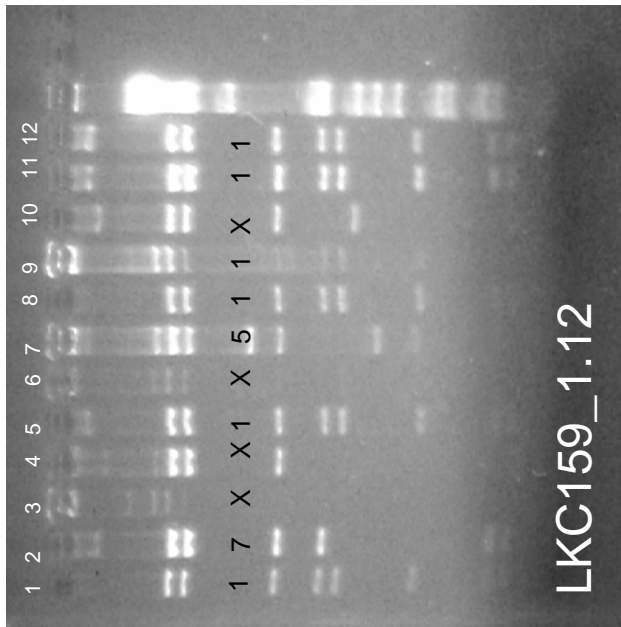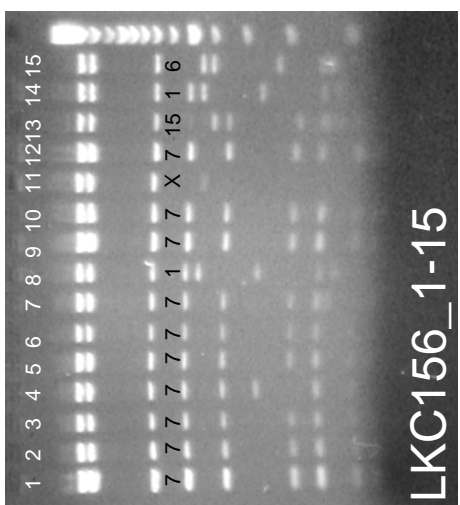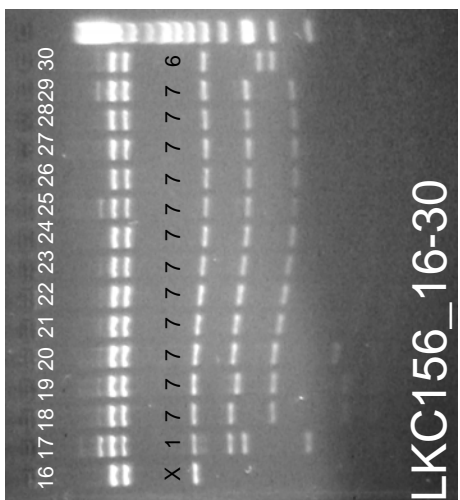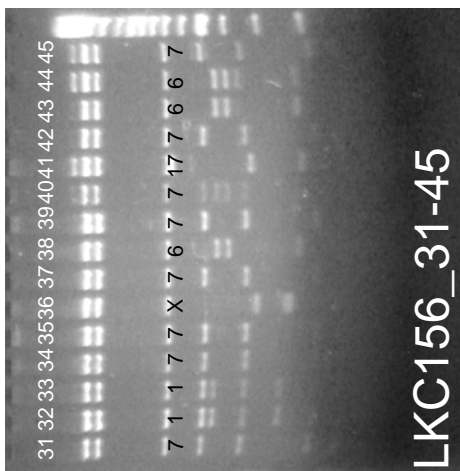
Clone Library 156
(203 m white webs)

Pattern	Number
1	7
5	1
6	12
7	49
11	2
15	1
16	1
17	3
X	4
Total	80

266

Restriction fragment length polymorphism results

LKC102_16-30

16 17 18 19 20 21 22 23 24 25 26 27 28 29 30

29 X 29 7 29 1 11 X X X 29 29 29 29

LKC102_1-15

1 2 3 4 5 6 7 8 9 10 11 12 13 14 15

29 29 29 29 29 X X XX X 29 7 X X

LKC102_31-45

31 32 33 34 35 36 37 38 39 40 41 42 43 44 45

X X X X X 2929 29 29 292929X
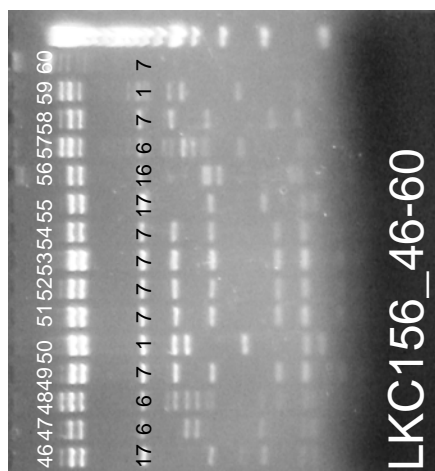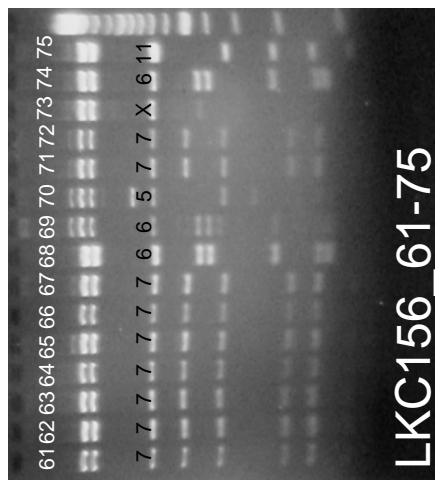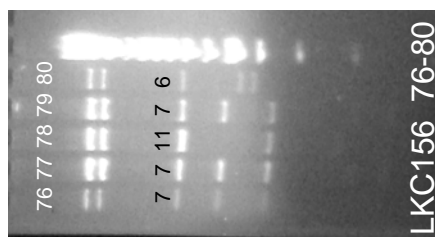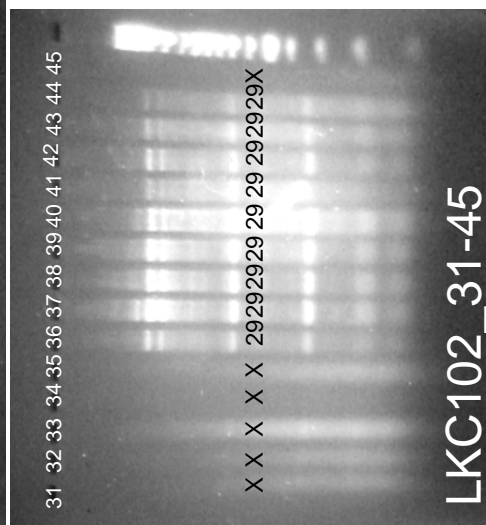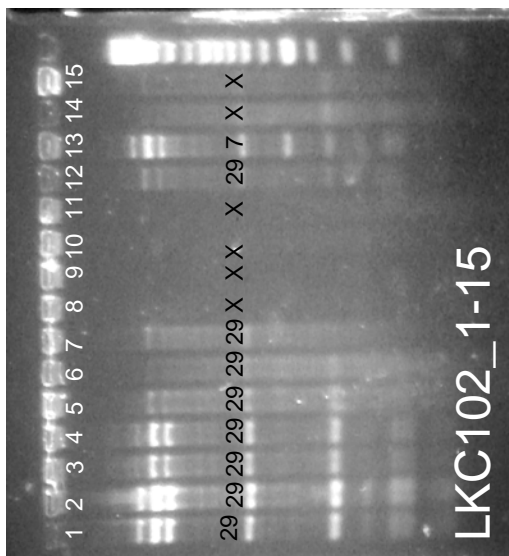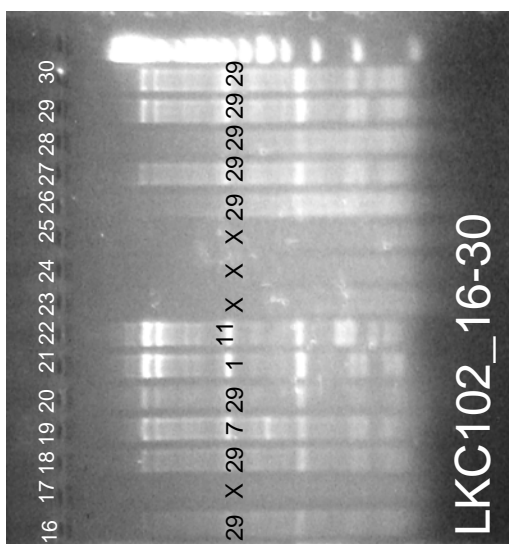
Clone Library 102
(203 m yellow patches)

Pattern	Number
1	1
7	2
11	1
29	26
X	15
Total	45

267

Restriction fragment length polymorphism results

LKC102B_31-45

LKC102B_16-30

LKC102B_1-15

LKC102B_61-68, 71-72

LKC102B_46-60
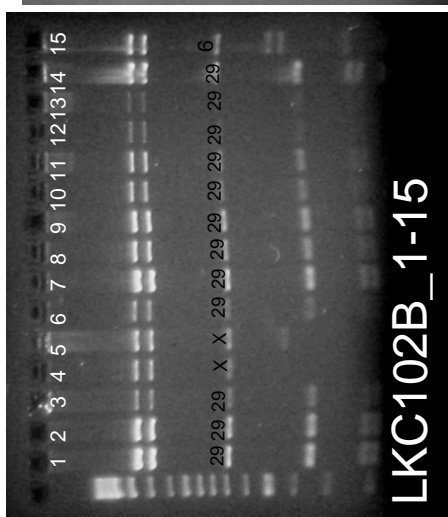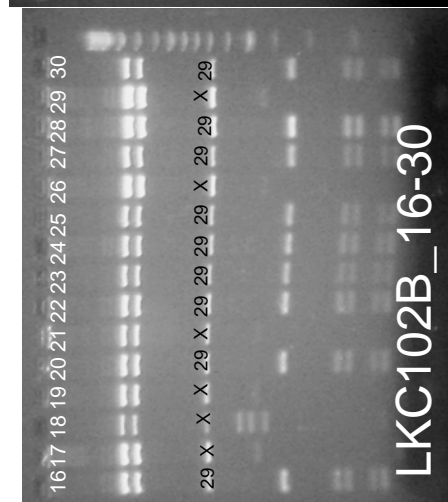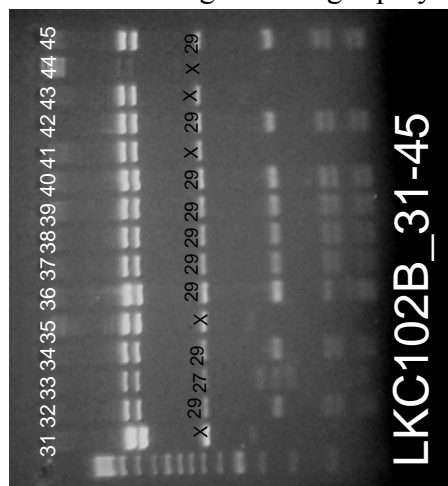
Clone Library 102B
(203 m yellow patches)

Pattern	Number
6	2
7	1
19	1
27	1
28	1
29	47
X	17
Total	70

Restriction fragment length polymorphism results

LKC125_31-45

LKC125_16-30

LKC125_61-72

LKC125_1-15r

LKC102B_46-60
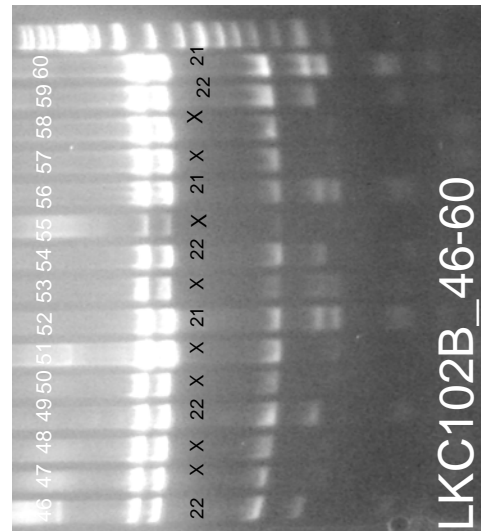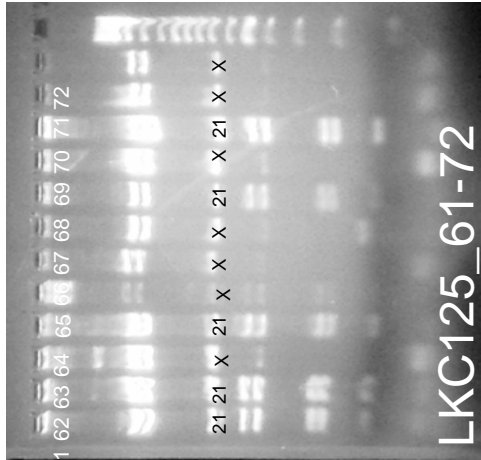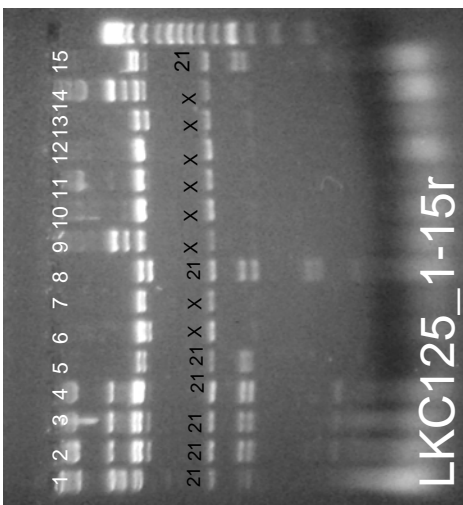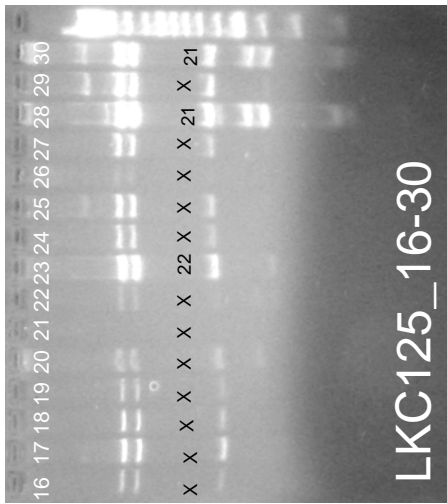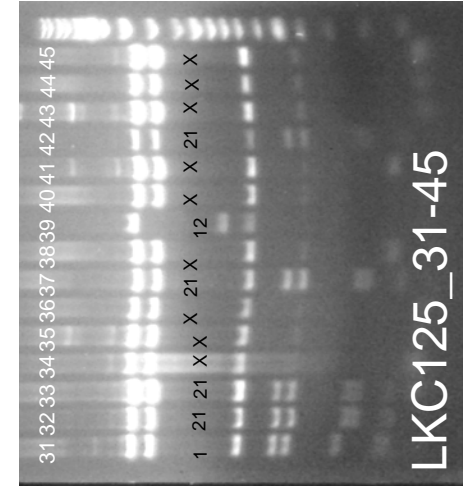
Clone Library 125B
(203 m gray filaments)

Pattern	Number
1	1
12	1
21	20
22	6
X	44
Total	26
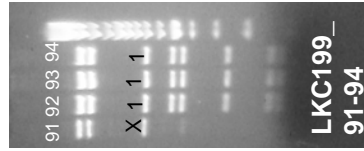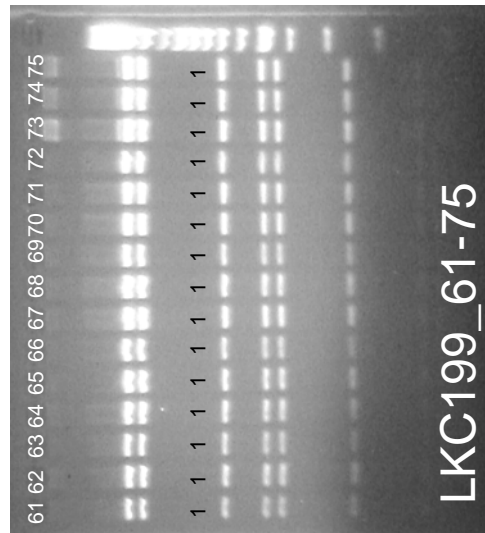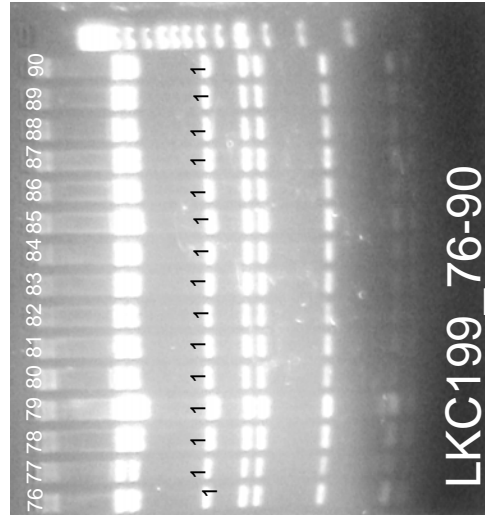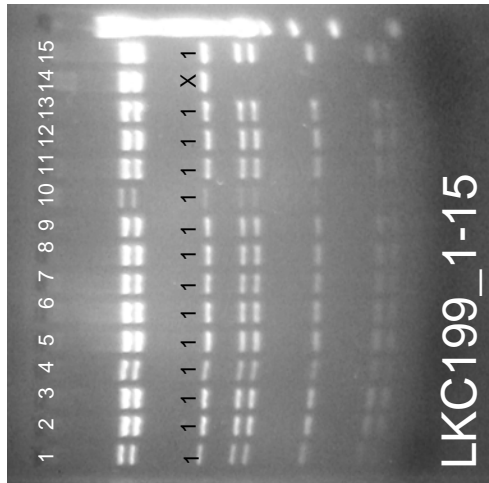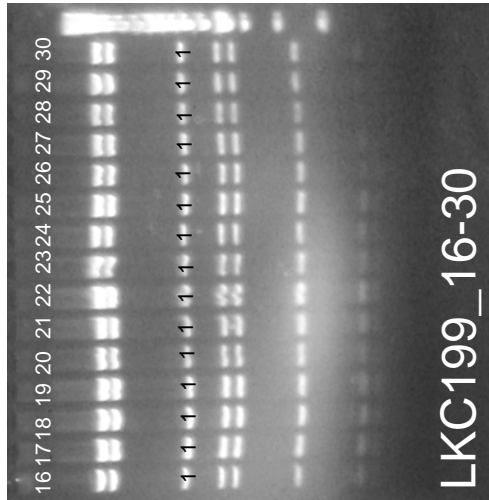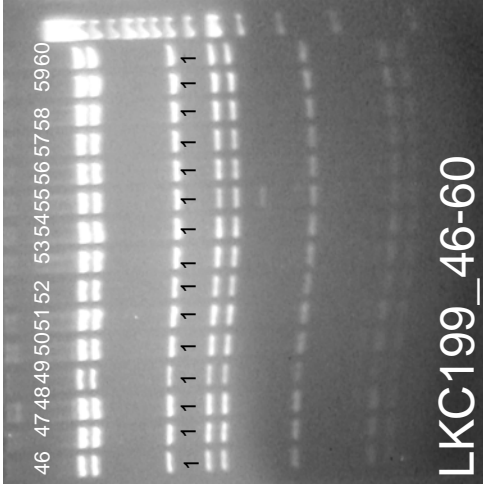
269

Restriction fragment length polymorphism results

LKC199_46-60

LKC199_16-30

LKC199_1-15

LKC199_91-94

LKC199_76-90

LKC199_61-75

Restriction fragment length polymorphism results

LKC198_30.44

LKC198_15.29

LKC198_1-14

LKC198_75.76

LKC198_60.74

LKC198_45.59
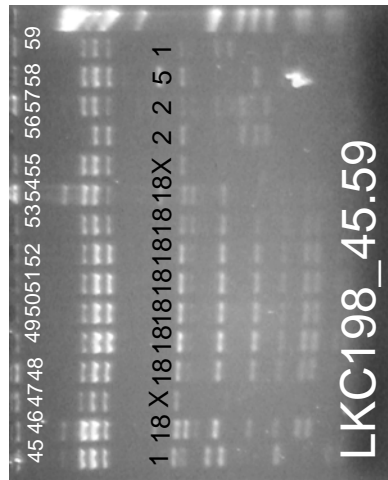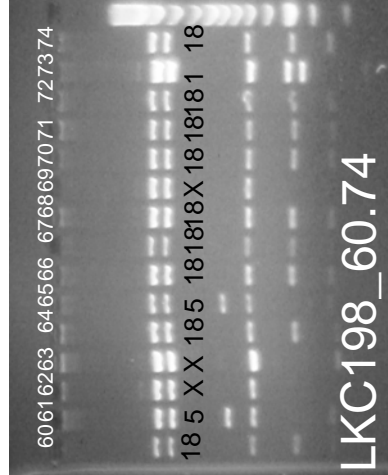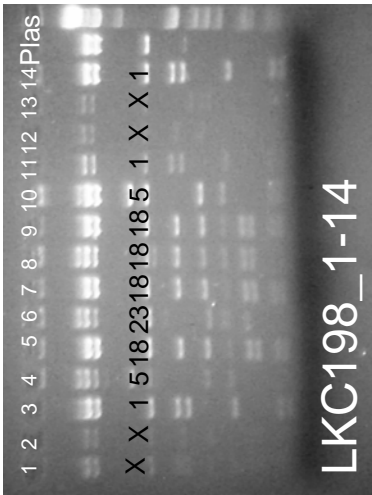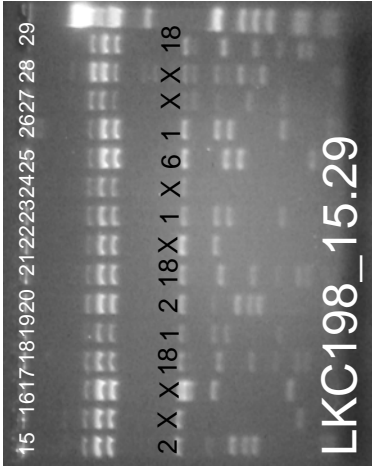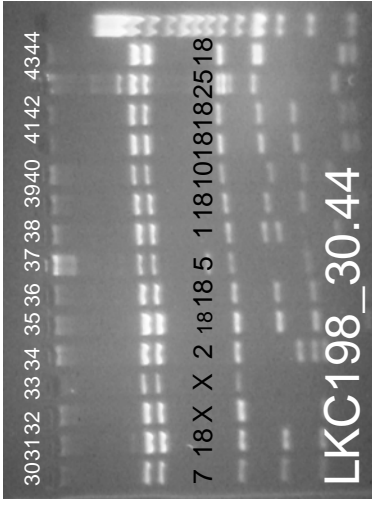
Clone Library 198
(248 m yellow-white mat)

Pattern	Number
1	11
2	5
5	6
6	1
7	1
18	31
23	1
25	1
X	18
Total	75

271

Restriction fragment length polymorphism results

Clone Library 198B
(248 m yellow-white mat)

Pattern	Number
1	5
2	5
5	1
7	1
10	1
11	1
18	8
23	3
X	22
Total	47
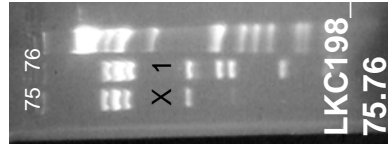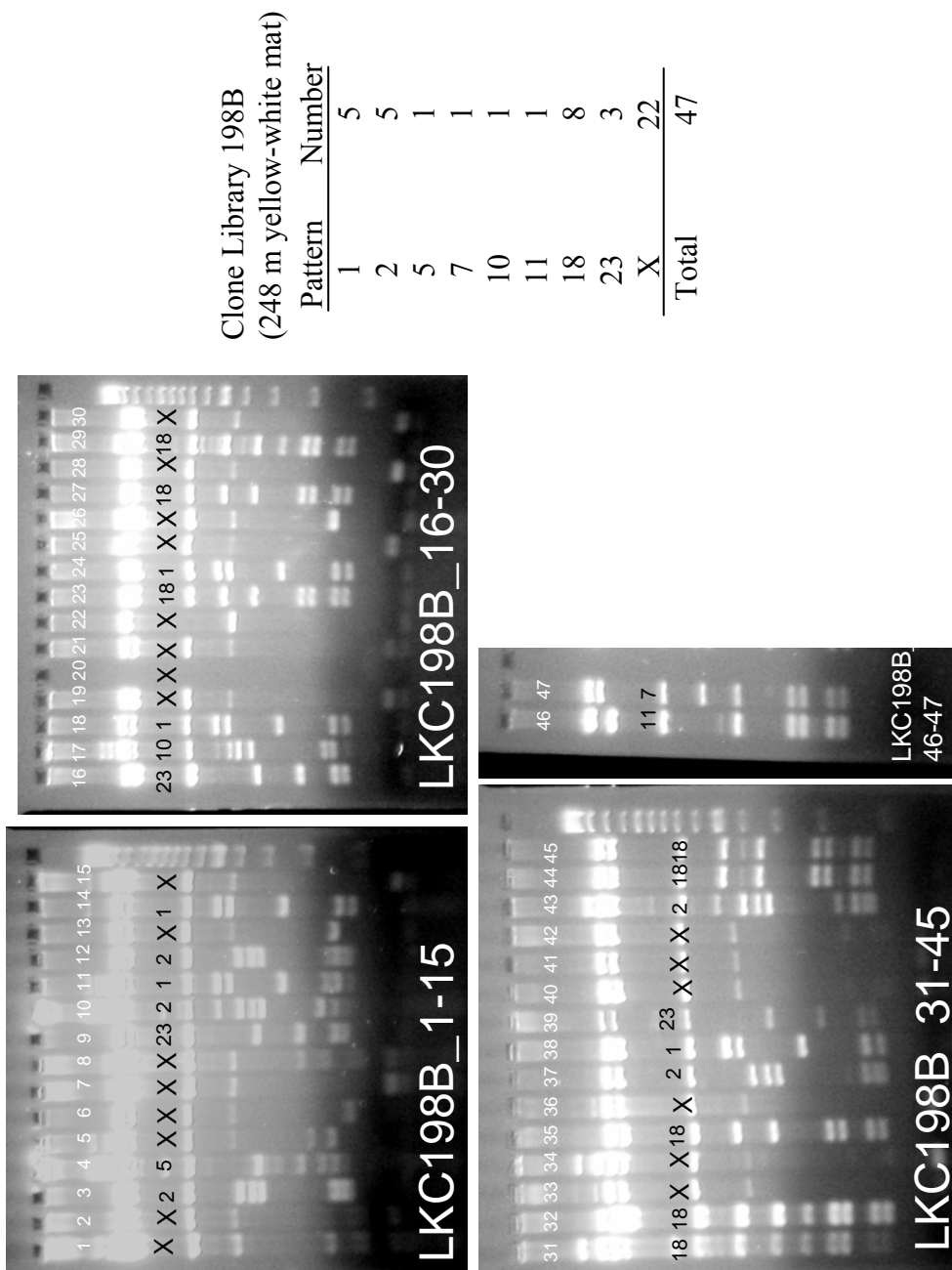
Table A-1: Clone 16S rRNA gene sequences from Lower Kane Cave libraries with phylogenetic affiliations and percent sequence similarity to closest relative. LKC clone accession numbers in Chapter 2.

Library	Clone[a]	RFLP Pattern	Closest relatives[b]	Percent Similarity[c]
124m filament	LKC3_19.29 LKC3_19B.29	5	Sulfidic spring clone sipK4 [AJ307933]	99
	LKC3_19.39	2	Sulfidic spring clone sipK119 [AJ307940]	99
	LKC3_19.50	13	*Rifta* clone R76-B13 [AF449261]	91
	LKC3_19B.17 LKC3_19B.45	17	*Beggiatoa* 'Bay of Concepcion' strain [AF035956]	90
127m filament	LKC3_22.9 LKC3_22.13 LKC3_22.5 LKC3_22.81	2	Groundwater clone FTL212 [AF529098] Groundwater clone 1043 [AB030601]	98-99
	LKC3_22.3 LKC3_22.17 LKC3_22.33 LKC3_22.73 LKC3-22.89	5	Sulfidic spring clone sipK4 [AJ307933]	99
	LKC3_22.72	4	Groundwater clone 1043 [AB030601]	98
	LKC3_22.6	4	*Wolinella succinogenes* [AF273252]	90
	LKC3_22.53 LKC3_22.54	12	Sulfidic spring clone sipK119 [AJ307940] Groundwater clone FTL212 [AF529098]	98-99
190m filament	LKC3_57B.17 LKC3_57B.49 LKC3_57.8 LKC3_57.20 LKC3_57C.15 LKC3_57C.33 LKC3_57B.57 LKC3_57B.2	2	Sulfidic spring clone sipK119 [AJ307940]	99
	LKC3_57.4 LKC3_57C.13	1	Sulfidic spring clone sipK94 [AJ307941]	98
	LKC3_57B.54	4	Groundwater clone FTL212 [AF529098]	97
	LKC3_57B.22 LKC3_57C.10	8	Sulfidic spring clone sipK119 [AJ307940]	99
	LKC3_57B.41	9	Groundwater clone FTL212 [AF529098] Sulfidic spring clone sipK119 [AJ307940]	97-98
195m filament	LKC3_270.5 LKC3-270.64	2	Sulfidic spring clone sipK119 [AJ307940]	99
	LKC3-270.57	1	Sulfidic spring clone sipK94 [AJ307941]	98
	LKC3_270.16 LKC3_270.58	4	Groundwater clone 1043 [AB030601]	97-98
	LKC3_270.18	5	Sulfidic spring clone sipK4 [AJ307933]	100
	LKC3_270.19	8	Groundwater clone 1028 [AB030605]	96
	LKC3_270.13	9	Sulfidic spring clone sipK119 [AJ307940]	95
	LKC3_270.15	24	*Bacteroides* sp. ECP-C1 [AF529225]	94
198m filament	LKC3_190.31	1	Sulfidic spring clone sipK94 [AJ307941]	98

Table	*A-1 (Continued).*			
Library	**Clone**	**RFLP Pattern**	**Closest relatives**[a]	**Percent Similarity**[b]
198m filament	LKC3-190.28	11	*Desulfocapsa* sp. Cad626 [AJ511275]	96-97
	LKC3_190.63		*Desulfocapsa thiozymogenes* [X95181]	
	LKC3_190.37		Lake clone SRB-348 [AJ389628]	
	LKC3_190.75			
203m filament	LKC3_127.47	19	Groundwater clone G1070 [AB030590]	94-95
	LKC3_127.18		Sulfidic spring clone sipK94 [AJ307941]	
	LKC3_127.7	19	*Campylobacter* sp. [L14632]	98
	LKC3_127B.2	2	Sulfidic spring clone sipK119 [AJ307940]	99
	LKC3_127.11	7	Groundwater clone SJA-36 [AJ009461]	98
	LKC3_127.25	13	Polychaete clone P.palmA10 [AJ441240]	90
	LKC3_127.4	1	Sulfidic spring clone sipK94 [AJ307941]	97-98
	LKC3_159.2			
	LKC3_159.10			
	LKC3_159.12			
	LKC3-127.29			
	LKC3_127.1	4	Groundwater clone FTL212 [AF529098]	96-98
	LKC3_127.6		Sulfidic spring clone sipK119 [AJ307940]	
	LKC3_127.23		Groundwater clone 1043 [AB030601]	
	LKC3_127.32			
	LKC3_127.14			
	LKC3_127.39			
	LKC3_127.40			
	LKC3_127.43			
	LKC3_127.46			
	LKC3_127B.26			
	LKC3_127B.27			
	LKC3_127.2	5	Sulfidic spring clone sipK4 [AJ307933]	99-100
	LKC3_127.33			
	LKC3_159.7			
	LKC3_127.27			
	LKC3_127.26			
	LKC3_127.28	10	Sulfidic spring clone sipK94 [AJ307941]	98
	LKC3_127.36			92
	LKC3_127.53			95
203m web	LKC3_156.14	1	Sulfidic spring clone sipK94 [AJ307941]	98
	LKC3_156.17			
	LKC3_156.1	7	Groundwater clone SJA-36 [AJ009461]	97
	LKC3_156.4			
	LKC3_156.19			
	LKC3_156.13	15	Groundwater clone SJA-36 [AJ009461]	96
	LKC3_156.15	6	Acid mine clone 44a-B1-1 [AY082456]	95-96
	LKC3_156.38			
	LKC3_156.74			
	LKC3_156.46	17	*Beggiatoa* sp. strain MS-81-1c [AF110276]	90-91
	LKC3_156.55			
	LKC3_156.41		*Beggiatoa* 'Bay of Concepcion' strain [AF035956]	
	LKC3_156.56	16	Clone vadinHA54 [U81722]	92

Table	A-1 (Continued).			
Library	**Clone**	**RFLP Pattern**	**Closest relatives**[a]	**Percent Similarity**[b]
203m yellow	LKC3-102B.15 LKC3-102B.55	6	Acid mine clone 44a-B1-40 [AY082468]	95
	LKC3_102B.2 LKC3_102B.27L KC3 _102B.25 LKC3_102B.28	29	*Thiobacillus aquaesulis* [U58019] Groundwater clone FW119 [AF523954] Forest-wetland soil clone FW119 [AF523954]	93-95
	LKC3_102.21	1	Sulfidic spring clone sipK94 [AJ307941]	97
	LKC3_102.22	11	Lake clone SRB-348 [AJ389628]	97
	LKC3_102B.18	19	Acid mine clone 44a-B1-40 [AY082468]	97
	LKC3-102B.33	27	Clone WCHA1-01 [AF050541]	91
	LKC3_102B.59	28	*Cytophagales* clone Hyd-B2-1 [AJ535256]	96
203m gray filament	LKC3_125.2 LKC3_125.3 LKC3_125.60	21	*Pantoea agglomerans* [AB004691] Uncultured clone p-2172-s959-3 [AF371852]	99
	LKC3_125.31	1	Sulfidic spring clone sipK94 [AJ307941]	98
	LKC3_125.46 LKC3_125.59	22	*Serratia marcescens* strain CPO1(4)CU [AJ296308]	99
248m filament	LKC3_199.1	1	Sulfidic spring clone sipK94 [AJ307941]	98
248m yellow-white	LKC3_198.8 LKC3_198.29 LKC3_198.31 LKC3_198.35 LKC3_198.44	18	Uncultured clone RB7C6 [AF407385] *Leptothrix discophora* (SS-1) [L33975] Acid mine clone 44a-B2-21 [AY082471]	94
	LKC3_198.17	10	Sulfidic spring clone sipK94 [AJ307941]	96
	LKC3_198.15 LKC3_198.20	2	Groundwater clone FTL212 [AF529098]	98
	LKC3_198.17	14	Lake clone TLM10/TLMdgge01 [AF534434]	91
	LKC3_198.26	1	Sulfidic spring clone sipK94 [AJ307941]	98
	LKC3_198.43	25	Marsh clone FSA6 [AY193038]	97

[a] Twelve clone sequences were found to be chimera based on results from the CHECK_CHIMERA program in the RDP.
[b] Based on BLAST search. GenBank accession numbers in brackets.
[c] Based on alignable base pairs.

APPENDIX B

Supplemental Information for Chapter 3

DESCRIPTION OF ADDITIONAL SAMPLING SITES FOR CHAPTER 3

Sulfidic Caves

Hellspont Cave, Big Horn County, Wyoming

This small cave (20 m long) is located along the Bighorn River downstream from Lower Kane Cave, but across the river (Figure 1-3; Figure B-1). Hellspont Cave has one spring orifice at the back of the cave (Egemeier, 1981), and microbial mat filament bundles are suspended in the stream water column discharging from the spring (~15 cm deep). There is a thick white microbial mat at the entrance of the cave. A gypsum crust of moist white gypsum and discontinuous patches of elemental sulfur cover the walls. Mat samples from inside the cave and at the entrance were collected on several occasions in 2000 through 2002.

Cesspool Cave, Allegheny County, Virginia

Cesspool Cave is a small opening (<20 m of passage) developed in a travertine-marl complex of Quaternary age located along the Sweet Springs Creek (Hubbard et al., 1986, 1990; Engel et al., 2001). A sulfidic, non-thermal spring discharges into a back pool, flows out of the cave, and resurges into a surface pond. The hydrogen sulfide is thought to originate from oil-field brine solutions that flow up-dip along local faults (Hubbard et al., 1990). Some incidental sunlight reaches the back pool area due to the limited passage length and large surface entrance. The white filamentous microbial mats in the cave and resurgent spring were previously sampled (Engel et al., 2001), and two groups of "*Epsilonproteobacteria*" were identified from 16S rDNA gene sequences. Both of these groups were closely

related to the Lower Kane Cave group I (Figure 3-1), and glycerol-preserved samples and samples stored at -80°C were used to verify that the LKC group I PCR primer could amplify this group.

Big Sulphur Cave, Trigg County, Kentucky

The only entrance to Big Sulphur Cave, near Cadiz, Kentucky, is as a resurgence spring, approximately 5 m above the south side of the Little River. Big Sulphur Cave is large, with 15,750 ft of passage. A very small side passage, with a sulfidic stream, feeds into the main cave trunk passage within approximately 100 m of the entrance. Sulfide is only detected in this small side passage, but $H_2S_{(g)}$ can be smelled from the entrance and in the vicinity of the side passage within the main trunk passage. The side channel is relatively small (no more than 0.5 m wide x 1-0.3 m high) and white filamentous microbial mats are attached to cobbles in the stream. The mats are discontinuous along the stream bed, and first occur 5-6 m from the main trunk passage (Figure B-2). Due to passage constriction, it was not possible to see a spring orifice, if there is any, or even where the sulfidic water was originating from (e.g., a spring orifice or from a fissure in the stream bed). Collembolan, flatworms, crayfish and a significantly large population of isopods, were associated with the mats. Gypsum and elemental sulfur were observed on small exposed limestone cobbles in the sulfidic stream. Mat samples were acquired in 2002.

278

Surface-discharging Mesothermal Sulfidic Springs

Frasassi Caves and resurgence, Genga, Italy

The Frasassi Caves, including Grotta Grande del Vento, Grotta del Fiume, and Grotta Sulfurea, have been studied extensively by Italian speleologists, and Galdenzi and Menichetti (1995) suggest that the caves formed from sulfuric acid speleogenesis. An active sulfidic stream flows through lower levels of the system, originating beyond the passages in Grotta Grande del Vento. Abundant gypsum and sulfur accumulations occur throughout the entire cave system at all cave passage elevation levels. Subaqueous white microbial mats, as discontinuous patches of filaments and webs, have developed within an anaerobic, sulfidic cave stream in two different portions of the cave (Grotta del Fiume and Grotta Sulfurea), and filamentous mats again occur at the resurgence cave spring into the Sentio River (Figure B-3). Samples from the cave microbial mats were acquired in 1998 and frozen at -80 ^{o}C prior to DNA extraction. Resurgent spring samples were collected in 2001.

White Sulphur Springs, Schoharie County, New York

White Sulphur Springs is part of a circa 1805-1940s resort in Sharon Springs, New York. A sulfidic spring discharges from a large pool inside an unused bathhouse behind the White Sulphur Temple (Figure B-4), and the water overflows from the floor of the bathhouse, under the walls of the building, and into a small stream outside the building. Thin white filaments covered the outflow basin from the bathhouse. Other sampling locations included two cisterns, one that was covered and another that was open to sunlight; both had white filaments and web-

279

like microbial mats. Elemental sulfur deposits were common on surfaces above the water level and the cistern walls. Samples were collected in 2002.

Palmetto Spring, Gonzolas County, Texas

Sulfidic water discharges from an artificial (concrete) basin in the parking lot of a picnic area in Palmetto State Park, Texas (Figure B-5). A thin white filamentous mat forms over the concrete, and discontinuous white filament bundles occur ~ 5 m from the concrete basin, although green phototrophic material was also present. White mat samples were collected in 2003.

Surface-discharging thermal Sulfidic Springs

Thermopolis Hot Springs, Hot Springs County, Wyoming

Sulfidic water flows along faults in the Thermopolis anticline and emerge from the Madison Limestone, discharging into the Bighorn River within Hot Springs State Park, Thermopolis, Wyoming (Figure B-6). Water flows from one orifice at 7000 $m^3 \cdot day^{-1}$. Thick white microbial mats occur in the upper reaches of the spring before the water spills over travertine pools and dams. Samples were collected in 2002 and 2003.

Glenwood Springs, Garfield County, Colorado

The hot spring at Glenwood Springs, Colorado, is also known as Yampah Hot Springs, and feeds an extremely large swimming pool at the resort. Before reaching the pool there is a cooling pond, piping, a small cistern (referred to as the Drinking Spring), and more pipe work. Microbial mat samples were collected at the cistern (Figure B-7).

Pah Tempe, Washington County, and Fifth Water, Utah County, Utah

Sulfidic water at Pah Tempe Mineral Hot Springs discharges along the Hurricane Fault in Quaternary basalts near the Virgin River, Hurricane, Utah, and the water flows through underground faults. The resort was closed due to groundwater pumping along the river, and hot spring flow has diminished. Microbial mats form on the artificial (concrete) pool bottoms, as well as below breaks in the pool walls where a stream developed (Figure B-8). Mats are suspended on the water surface, supported by large bubbles. Megan L. Porter and Katharina de la Cruz-Dittmar, Brigham Young University (BYU), sampled the mats from these springs in 2002. M.L. Porter extracted total environmental DNA and amplified the epsilonproteobacterial groups using specific PCR primers; universal bacterial primers were also used. Springs at Fifth Water Hot spring, also known as Diamond Fork hot springs, in Utah County, Utah, were also sampled by M.L. Porter and used in this study.

Soda Dam Spring, Sandoval County, New Mexico

Numerous active fumeroles, hot springs, and mudpots attest to active thermalism in the Valles Caldera, associated with the Rio Grande rift (Rzonca et al., 2003). At the Soda Dam near Jemez Pueblo, water discharges from a fault where Precambrian granite juxtaposes Paleozoic carbonates (Madera Limestone, Pennsylvanian). Waters are characterized as Na-Cl-HCO_3 type with minor sulfate concentrations (Goff et al., 1982). A small outlet opposite the Travertine Dam has a small microbial mat (referred to here as Soda Dam Spring) (Figure B-9), which is mostly green from phototrophic organisms; thin patches of white filaments are

found closest to the orifice. Samples were collected in 2001 and 2003. Rzonca and Schulze-Makuch (2003) describe the microbiology of numerous spring waters from the region, finding evidence that an organism genetically related to the Lower Kane Cave groups were present in the water coming out at the spring, although the resulting sequence from the study has not been deposited into GenBank to verify taxonomic relatedness.

Lazio Volcanic Province

Hot springs in central Italy occur along the flanks of the Monte Cimino caldera near the city of Viterbo. Sulfidic waters emerge at the Bagnaccio, Bullicame, Paliano, and Le Zitelle Springs, where white and salmon-colored microbial mats and secondary travertine deposits are common (Figure B-10). Microbial mats from Le Zitelle were sampled in 2001, and were included in this study. Thick white microbial mats occur in the upper reaches of the spring before the waters spill over travertine pools and dams.
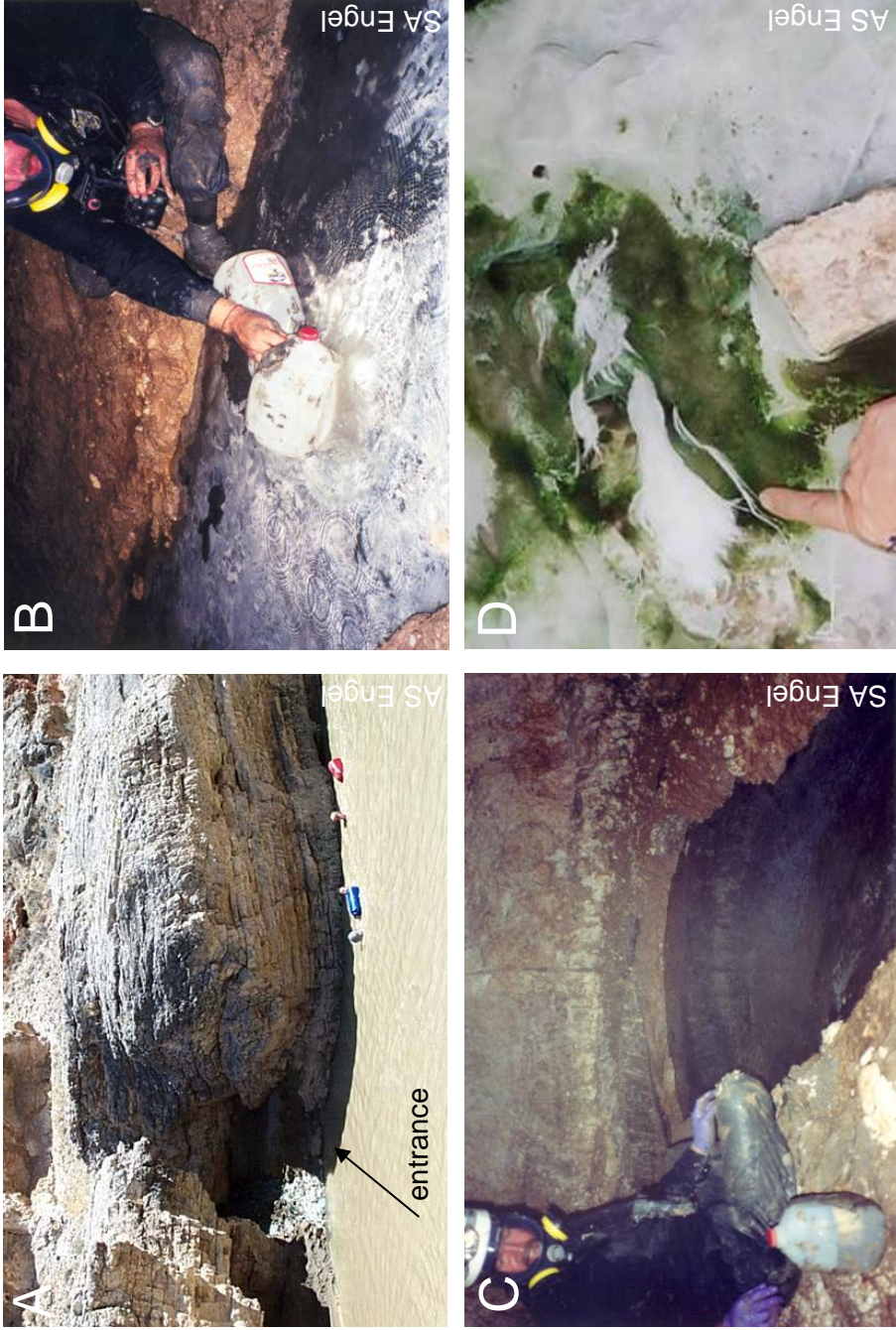
Figure B-1: (A) Entrance of Hellspont Cave, Bighorn Co., Wyoming, on the eastern side of the Bighorn River. (B) White filamentous microbial mats on bottom of stream. (C) Spring at back of cave. Full-face respirators are required because the concentration of H_2S is very high. (D) White filaments and phototrophs at entrance at river level.

283
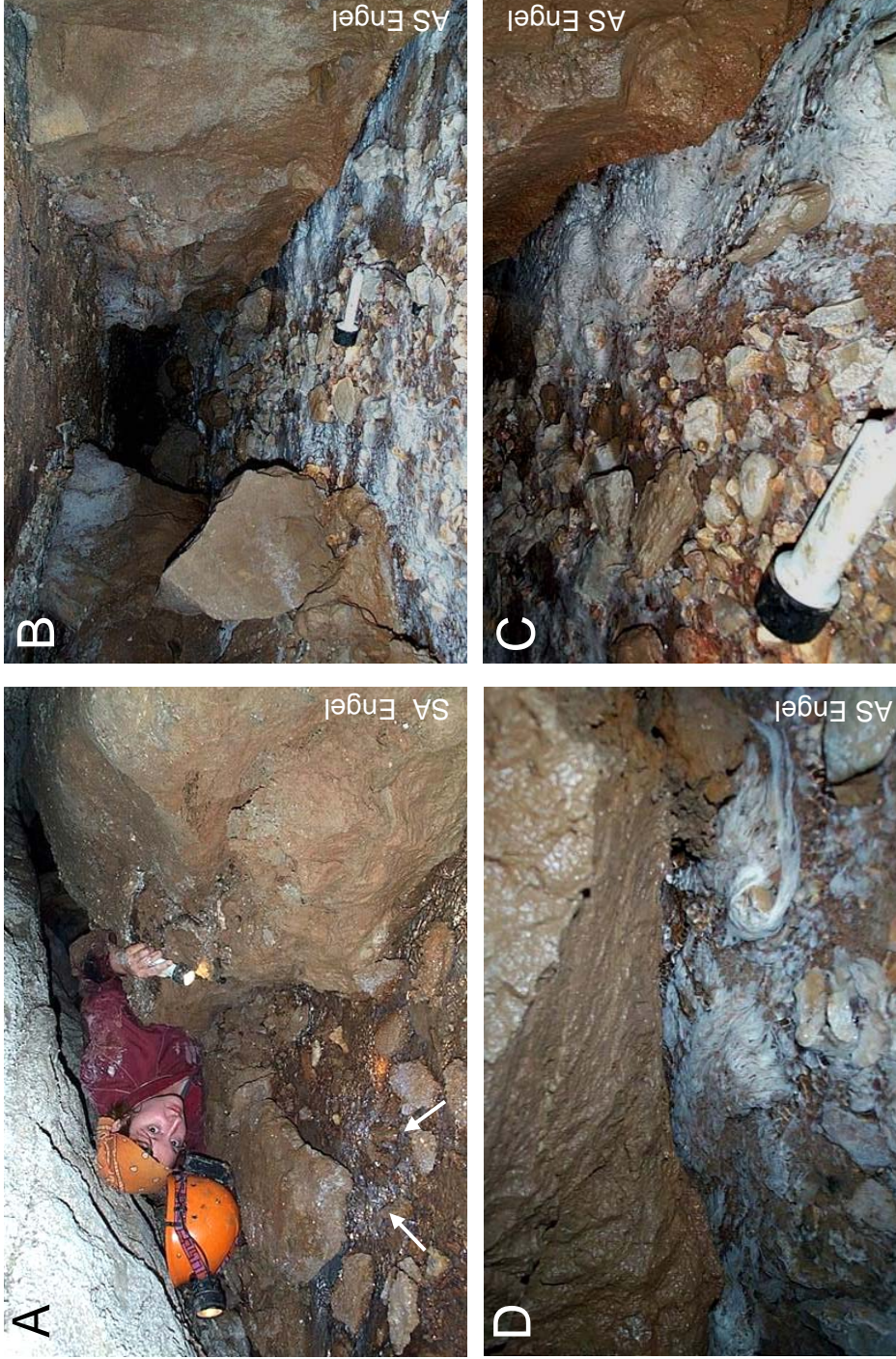
Figure B-2: Microbial mats in Big Sulphur Cave, Trigg Co., Kentucky. (A) Very small side passage. (B) Microbial mats. (C) Closeup of mats and mud. (D) Flashlight next to mats for scale. Isopods are commonly found in the mats.
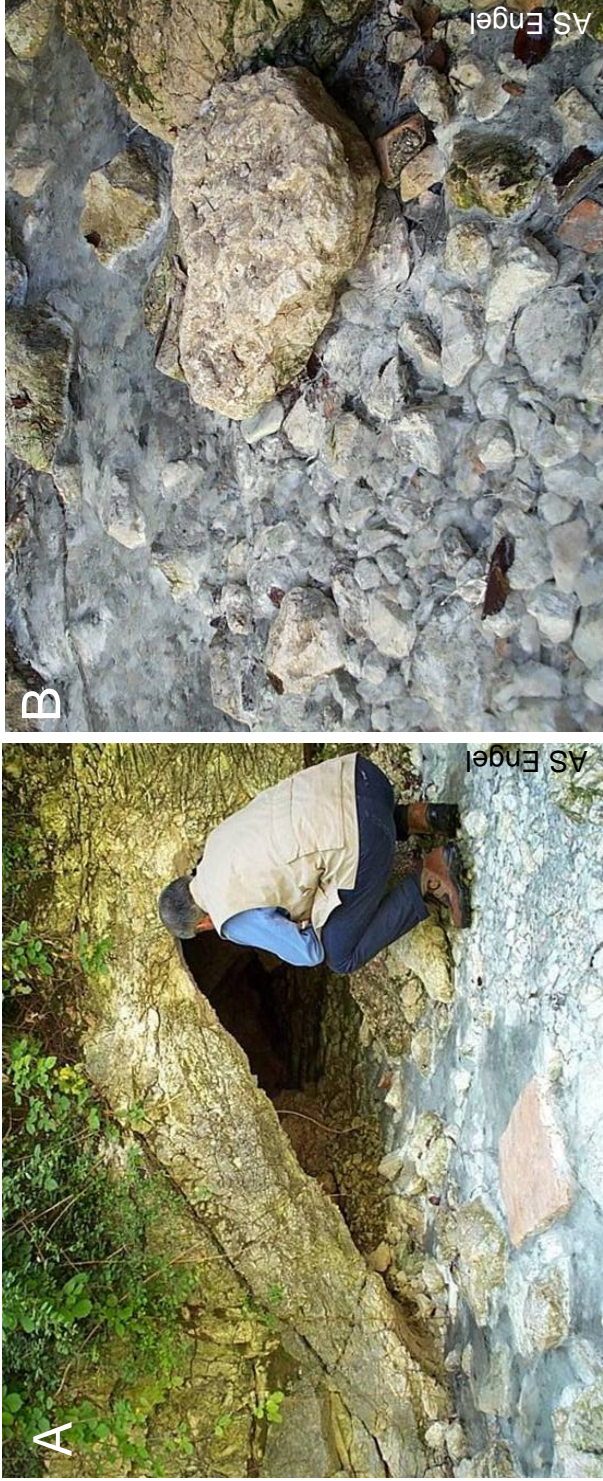
Figure B-3: Microbial mats at Frasassi Cave resurgence spring, Genga, Italy. (A) The spring discharges from a cave passages ~ 0.5 m high. (B) White microbial mats extend for 20 m inside the passage.

285

Figure B-4: (A) Microbial mats coating a concrete discharge pool from the Sulphur Temple bathhouse, White Sulphur Springs, Sharon Springs, Schoharie Co., New York. (B) The pipes running from the bathhouse were exposed under access panels. (C) Long filaments on concrete.

286
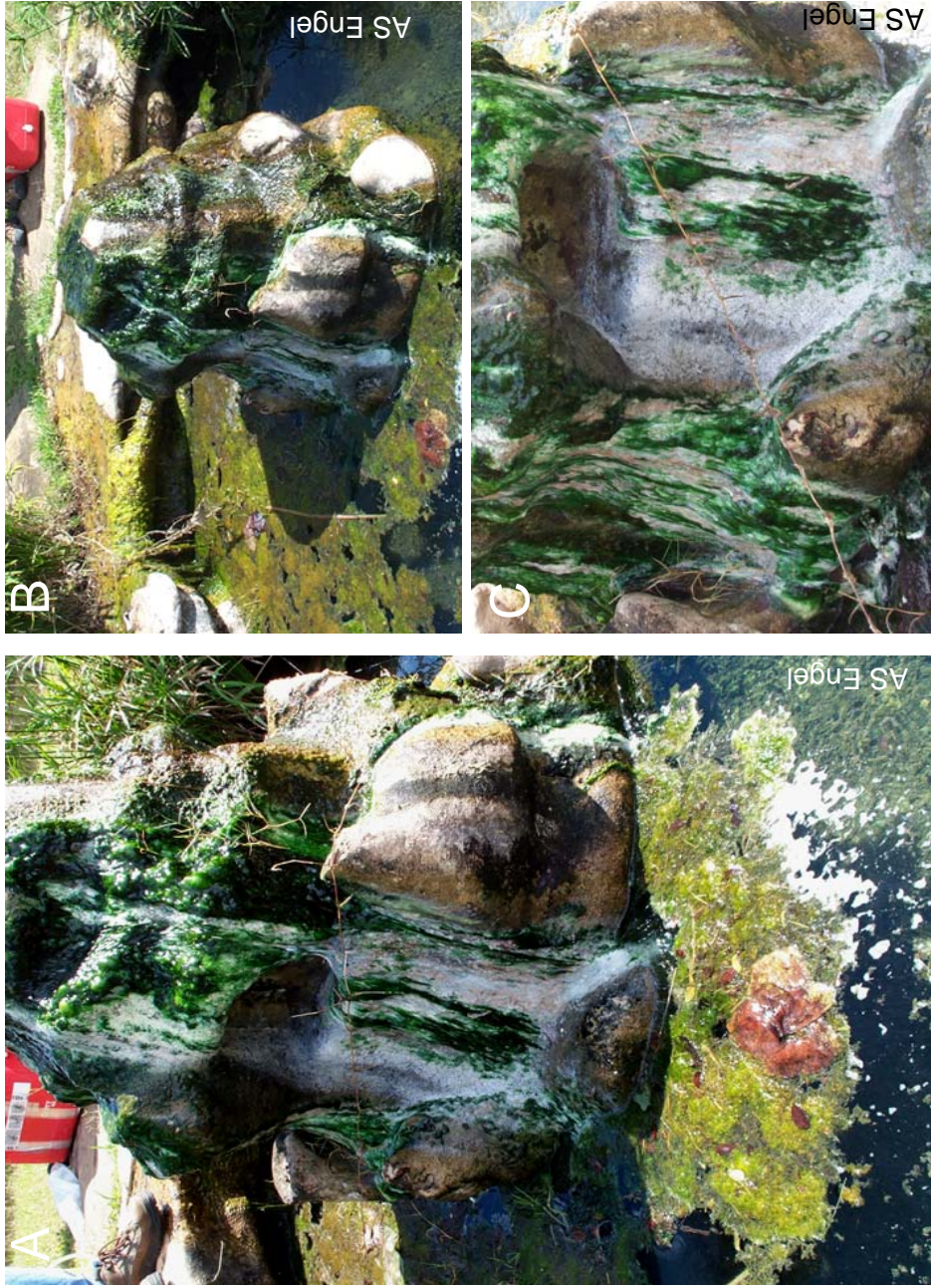
Figure B-5: Microbial mats associated with an artificial concrete mound at Palmetto Spring, Gonzales Co., Texas. White mats were also found ~3 m downstream in a small creek.
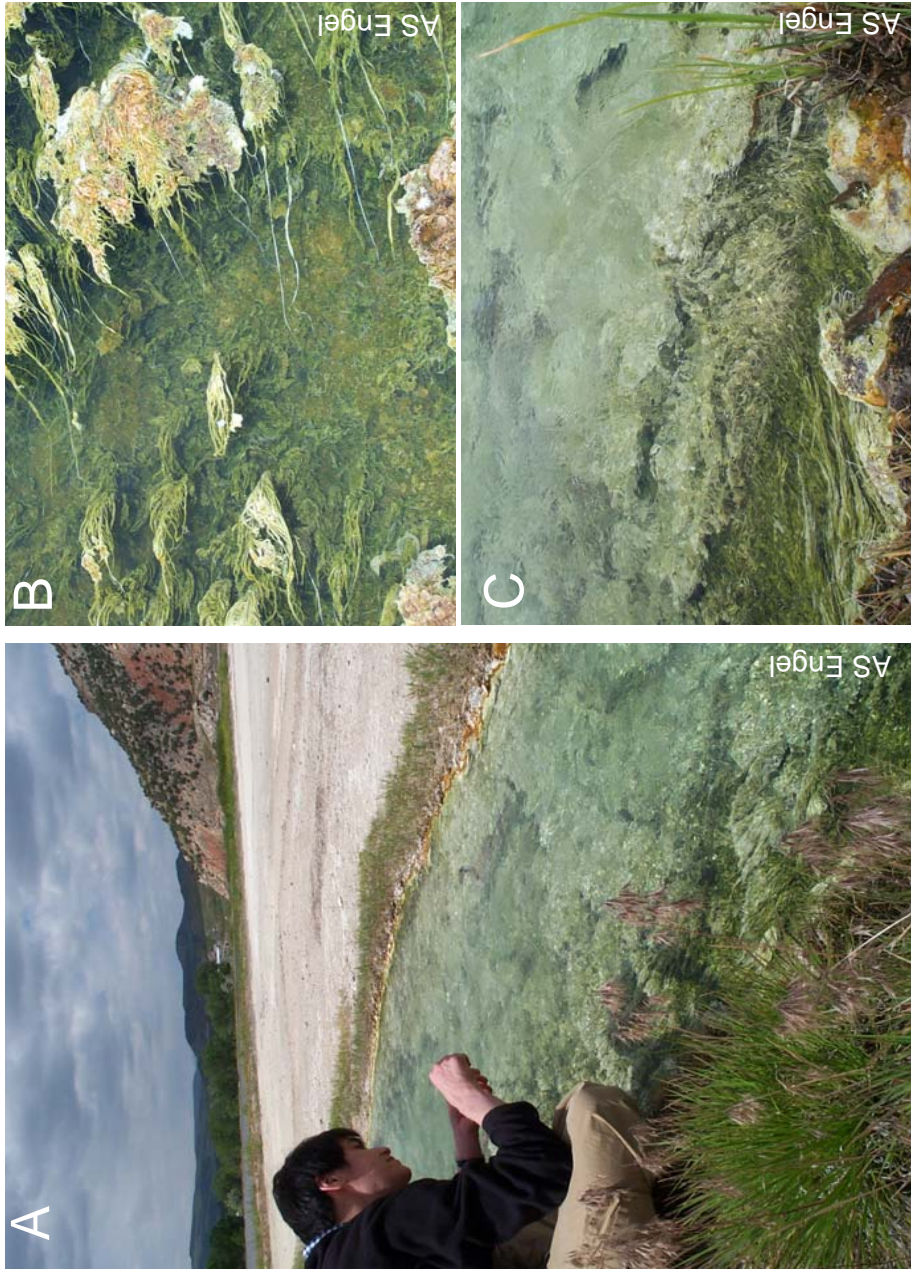
Figure B-6: (A) Microbial mats in stream channel discharging from one of the hot springs at Thermopolis Hot Springs, Hot Spring Co., Wyoming. (B) Floating organic matter with white filaments. (C) Thick white filaments on cobbles in stream.
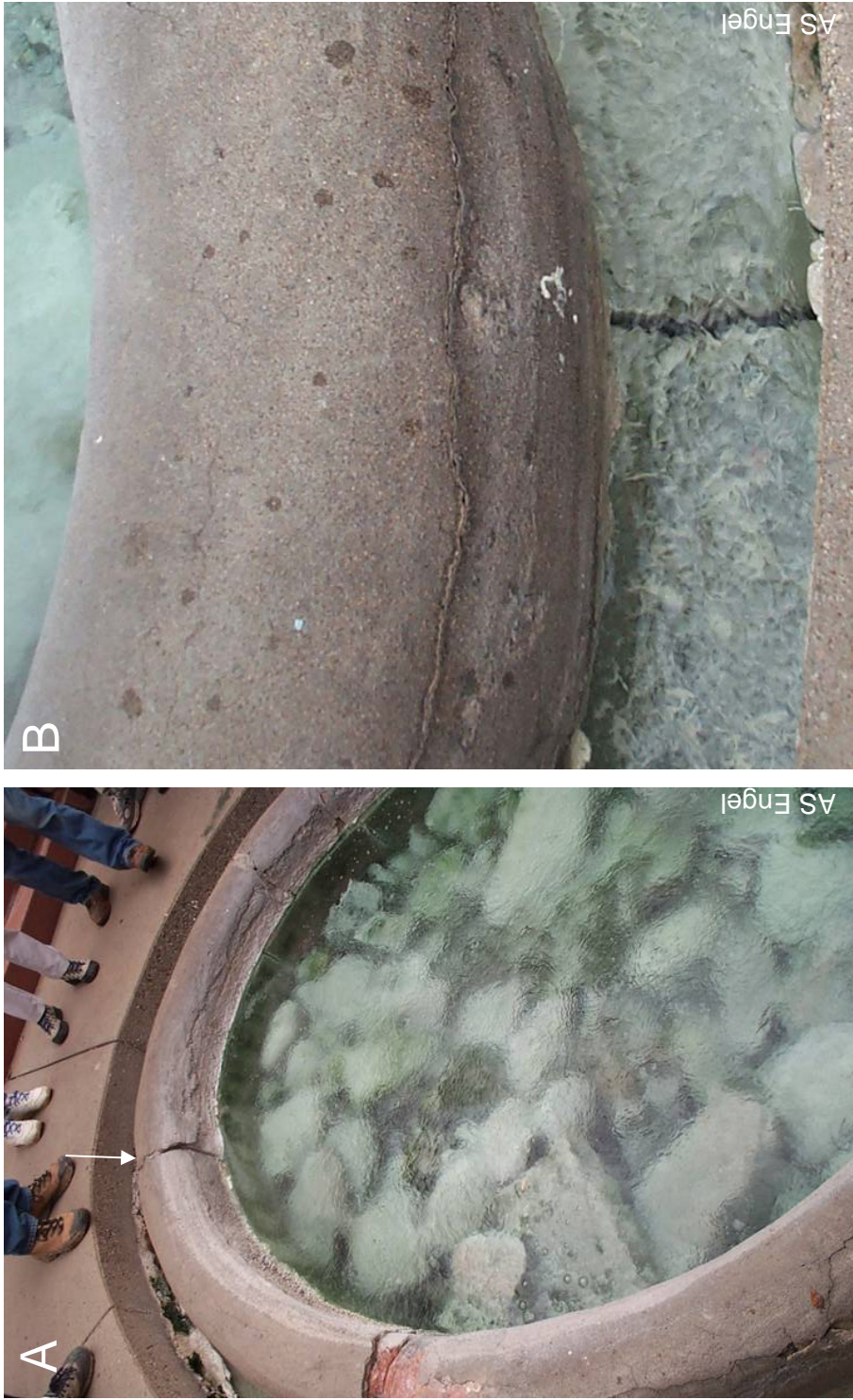
Figure B-7: Drinking Spring cistern, Glenwood Springs, Garfield Co., Colorado. (A) Water discharges in the upper center (arrow) from a pipe under the platform and flows into a channel ringing the cistern pool. (B) Channel around pool with white filaments.
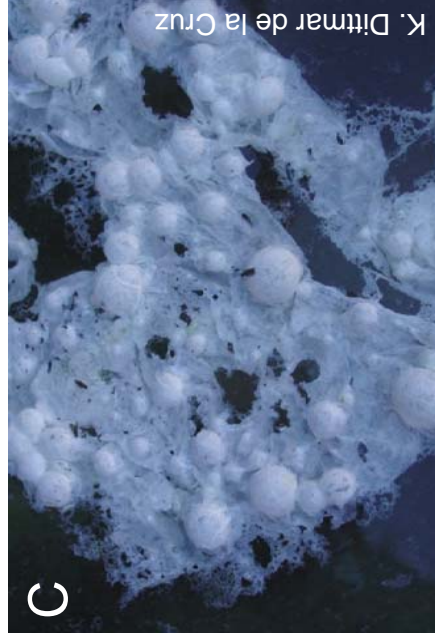
Figure B-8: Microbial mats consisting of webs and bubbles floating on the surface of the water at Pah Tempe hot Springs, Washington Co., Utah. (A) Sampling mats. (B) Filamentous mat where wading pool wall was broken. (C) Floating mat, webs and bubbles.
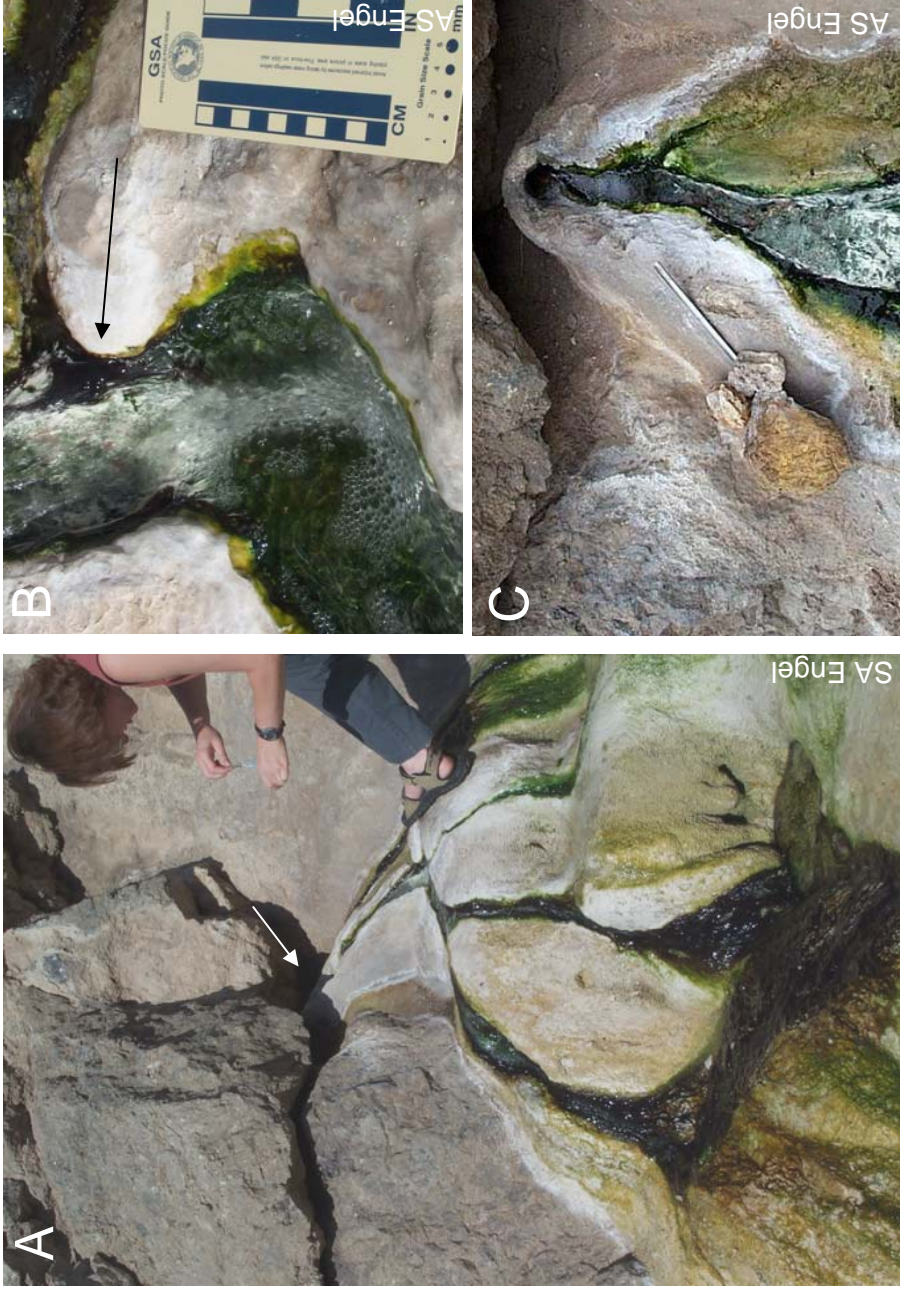
Figure B-9: Microbial mats at Soda Dam Spring, Jemez Co., New Mexico. (A) Small discharge hole (~2 in diameter) in travertine (arrow). (B) Closeup of white filamentous area (arrow) in mostly a phototrophic mat. (C) Small discharge hole (probably from a pipe) and minor rivulet with white filaments.
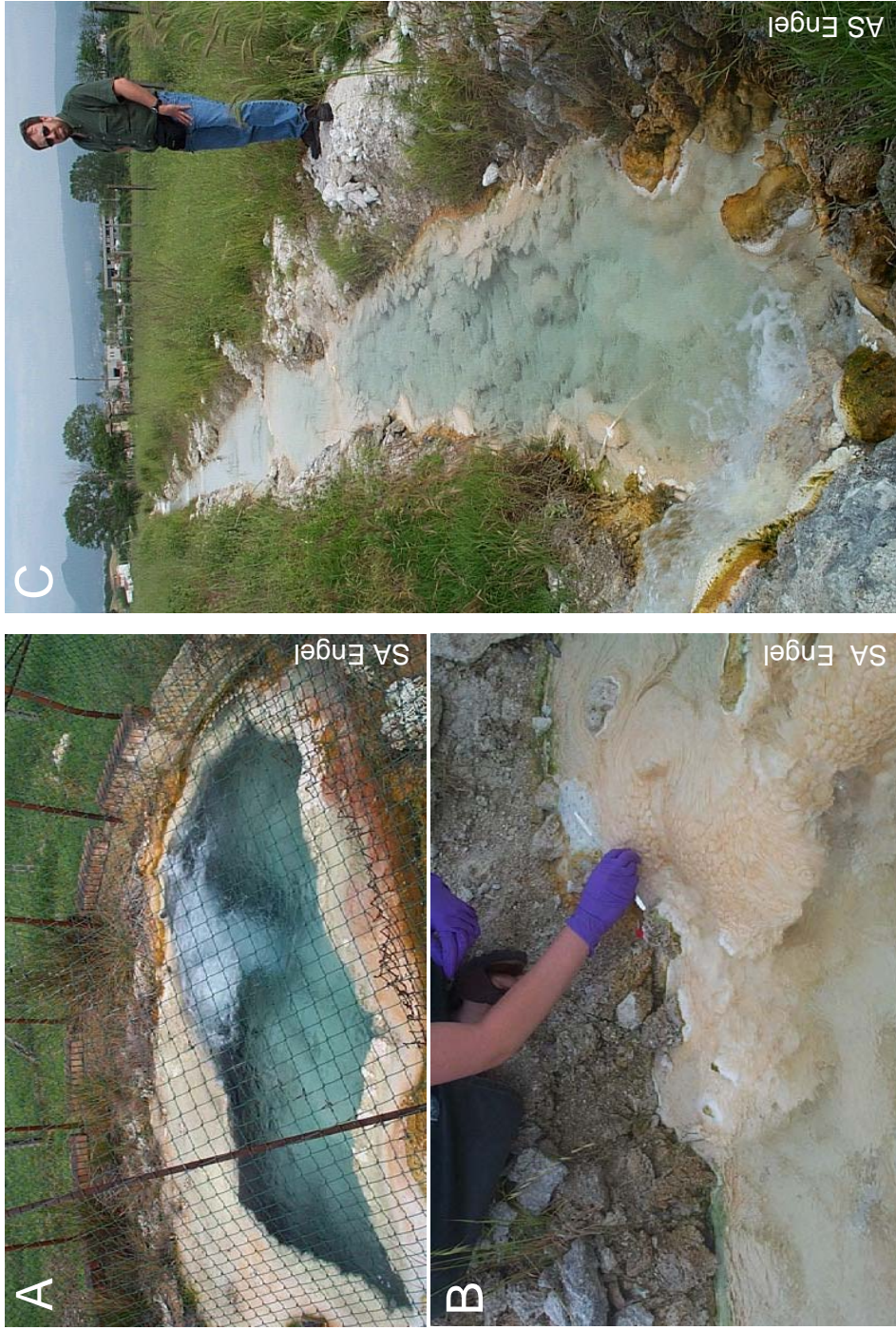
Figure B-10: Microbial mats at Zitelle mineral hot springs, near Viterbo, Italy. (A) Orifice with boiling spring. (B) Sampling white filaments on channel edge with travertine. (C) Channel below spring.

Gel B1 – Both LKC groups

PCR conditions:
2 min hot start
47°C annealing temperature

Columns:
MW- molecular weight marker
I - eps59f/1492r primers
II - eps174f/1492r primers
ND – no DNA control

Samples:
DKS - Drinking Spring, CO
PS – Palmetto Spring, TX
BSC - Big Sulphur Cave, KY
JM - Soda Dam Spring, NM
SS - White Sulphur Spring, NY
LKC - Lower Kane Cave, WY
Frasassi – Frasassi resurgence
           spring, Italy
FC – Frasassi Cave, Italy
CC - Cesspool Cave, VA
LeZit – Le Zitelle Spring, Italy

DKS-02-001A   PS-03-002Aa   BSC-02-002   JM-01-002   SS-02-003B
MW   I   II   I   II   I   II   I   II   I   II

2000
1000

LKC-02-1   BSC-02-004   Frasassi-5A
MW   I   II   I   II   I   II

2000
1000

FC-01-01   CC-00-01   LeZit-01-1A   ND
MW   I   II   I   II   I   II
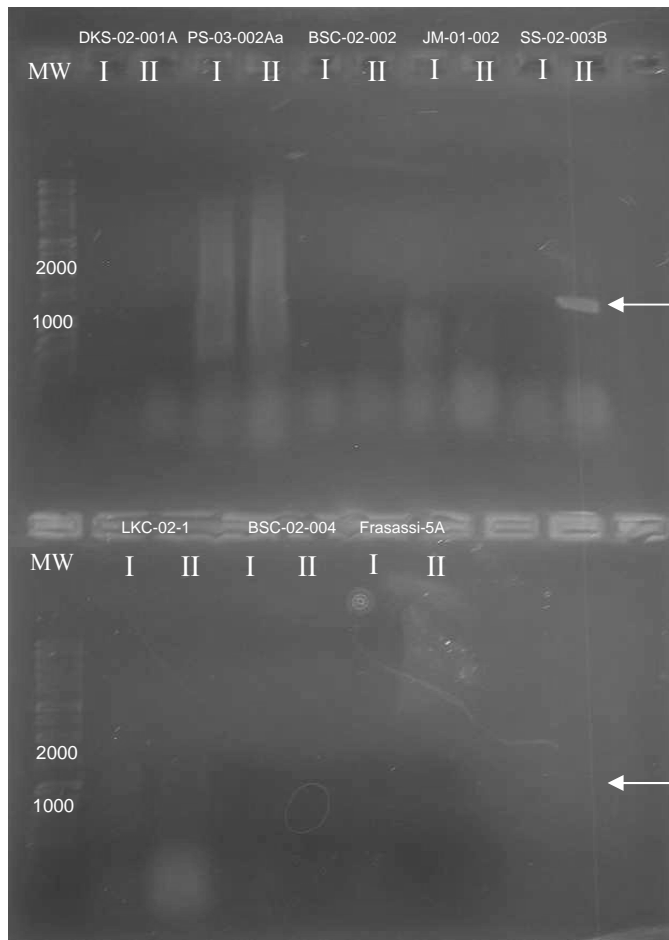
Gel B2 – LKC group I

PCR conditions:
2 min hot start
47°C annealing temperature

Columns:
MW- molecular weight marker
ND – no DNA control
Primer sets used are labeled.

Samples:
CC - Cesspool Cave, VA
DKS - Drinking Spring, CO
JM - Soda Dam Spring, NM
SS - White Sulphur Spring, NY
PS – Palmetto Spring, TX
BSC - Big Sulphur Cave, KY
SOX - Edwards church well, TX

294
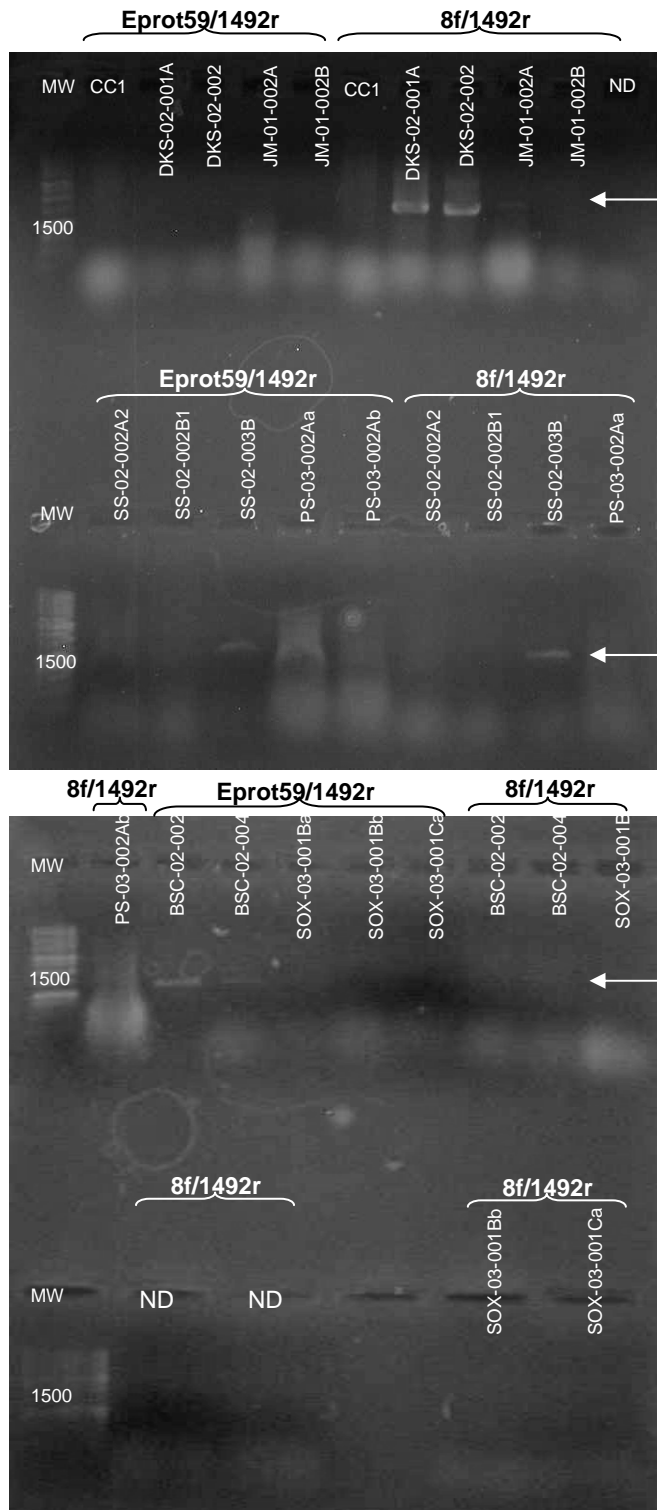
Gel B3 – LKC group II

PCR conditions:
2 min hot start
47°C annealing temperature

Columns:
MW- molecular weight marker
ND – no DNA control
Primer sets used are labeled.

Samples:
LKC - Lower Kane Cave, WY
Frasassi – Frasassi resurgence
 spring, Italy
LeZit – Le Zitelle Spring, Italy
DKS- Drinking Spring, CO
FC – Frasassi Cave, Italy
PS – Palmetto Spring, TX
BSC - Big Sulphur Cave, KY
SS - White Sulphur Spring, NY
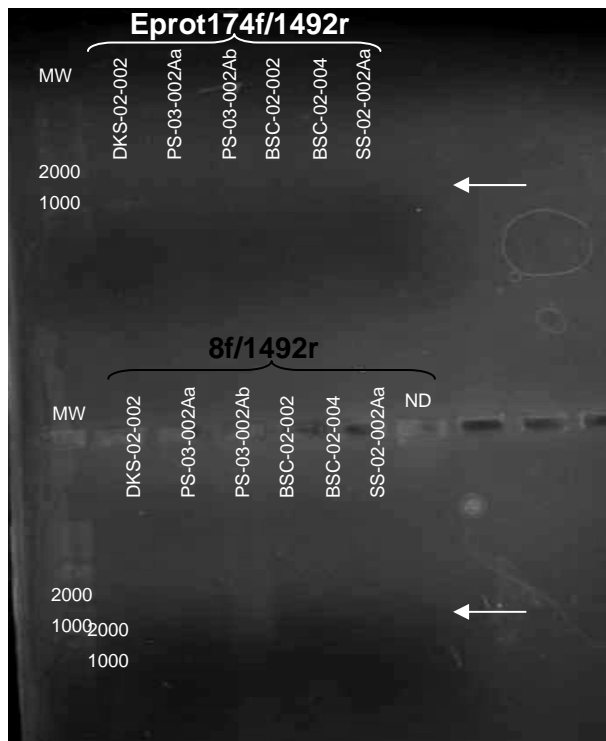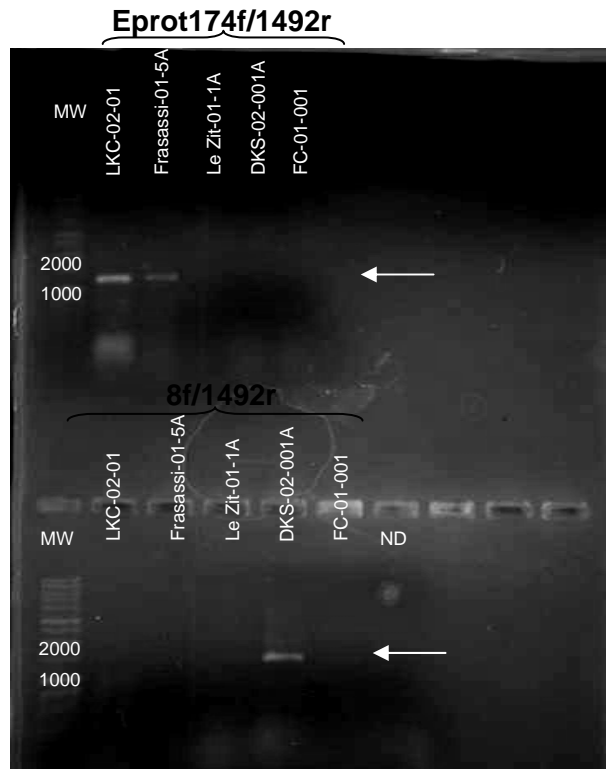
Gel B4 – LKC group I and II

2 min hot start
47°C annealing temperature

Columns:
MW- molecular weight marker
ND – no DNA control
Primer sets used are labeled.

Samples:
DKS- Drinking Spring, CO
SS - White Sulphur Spring, NY
JM – Soda Dam Spring, NM
PS – Palmetto Spring, TX
BSC - Big Sulphur Cave, KY
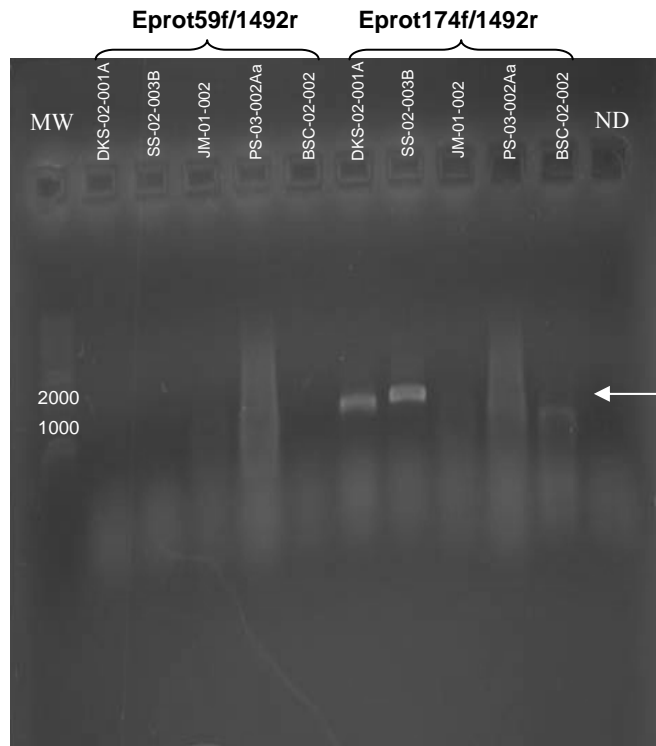
Gel B5 – LKC Group I and II

PCR conditions:
2 min hot start
45°C annealing temperature

Columns:
MW- molecular weight marker
ND – no DNA control
Primer sets used are labeled.

Samples:
PS – Palmetto Spring, TX
BSC - Big Sulphur Cave, KY
JM – Soda Dam Spring, NM

297
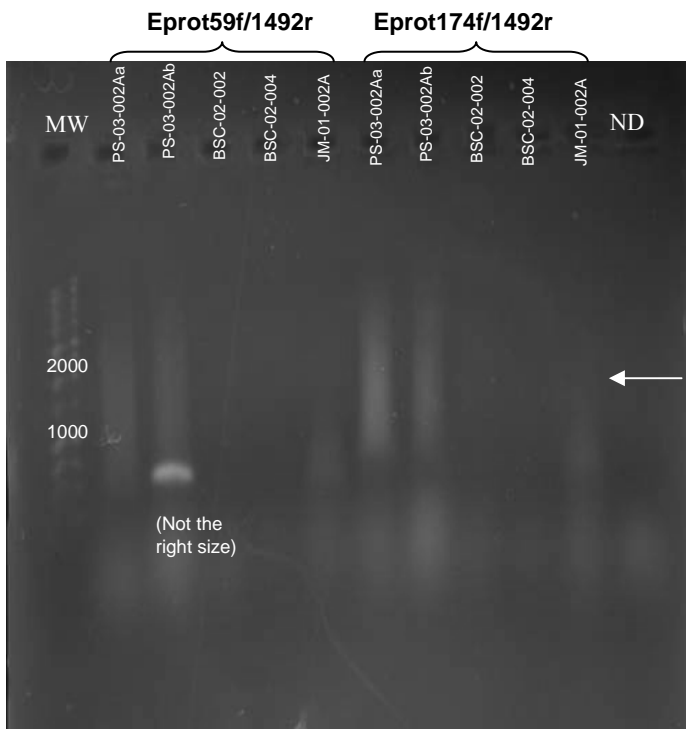
Table B-1: Screening Lower Kane Cave microbial mat samples and experimental FISH plan.

Probe	Target	FA%	Samples[a]	Comments
EUBI-FP	General *Bacteria*	0	22, 11, 189w, 189g	(13-03-02) needed to repeat with different samples
EUBII-cy3	*Planctomyces*		22, 11, 203g, 198w	(22-03-02) nothing, filaments to EUBI, tiny spots EUBII
EUBIII-cy5	*Verrucomicrobium*			
Arch915-cy3	*Archaea*	0	22, 11, 189w, 189g	(13-03-02) needed to repeat with different samples and
EUBmix-cy5			22, 11, 203g, 198w	filaments….
				(22-03-02) filaments, very weird
ALF968-cy3	*Alphaproteobacteria*	35	22, 11, 203g, 198w	(18-03-02) nothing
EUBmix-cy5				
Bet42a- cy3	*Betaproteobacteria*	35	22, 11, 203g, 198w	(24-03-02) Beta weak to single cells, gamma to filaments
Gam42a- cy5	*Gammaproteobacteria*			
EUBmix-FP				
Bet42a- cy5	*Betaproteobacteria*	35	22, 11, 203g, 198w	(18-03-02) Beta weak, gamma strong to filaments
Gam42a – cy3	*Gammaproteobacteria*			
EUBmix – FP				
CF19a-cy3	*Cytophaga*	35	22, 11, 203g, 198w	(24-03-02) nothing
EUBmix-cy5				
EUK516-cy3	Eukaryotes	0	22, 11, 203g, 198w	(18-03-02) nothing
EUBmix-cy5				
G123T-cy3	*Thiothrix*	40	22, 11, 203g, 198w	(18-03-02) many thick filaments
EUBmix-cy5				
HGC69a-cy3	Gram+ high GC	35	22, 11, 203g, 198w	(24-03-02) nothing
LGCmix-cy3	Gram+ low GC	20	22, 11, 203g, 198w	(24-03-02) nothing
Gam42a –cy5	*Gammaproteobacteria*	35	22, 11, 203g, 198w	(18-03-02) many thick filaments
G123T-cy3	*Thiothrix*			
EUBmix-FP				
EUBmix– cy5	Bacteria to all cells		22, 11, 203g, 198w, 15, 10, 9, 12, 1, 3, 4, 28, 29	(21-03-02) more cells with SyberGreen than with EUB – calculated percentages of EUB biovolume to SyberGreen (sample quantification)
SyberGreen				
onEUB-cy3	Controls	0	22, 11, 203g, 198w	(21-03-02) test autofluorescence, nothing
EUBmix-FP				

Probe	Target	FA%	Samples	Comments
Nonsense-cy3 EUBmix – FP	Controls, test autofluorescence	0	22, 11, 203g, 198w	(21-03-02) nothing
Eprot549-cy3 Eprot549-cy5 EUBmix - FP	All (maybe) *Epsilonproteobacteria*	0,10,20 25,30, 40,50	22, 11	(20-03-02 to 27-03-02) lots of different filaments, had to repeat with higher FA concentrations to get optimal (optimal FA 20-30%)
EPS710-cy3 Eprot549-cy5 EUBmix-FP	LKC group I and if there are other epsilons	0,10,20 25,30, 40,50	22, 11	(20-03-02 to 22-03-02) lots, EPS710 optimal FA 20%, some EPS710 not hybridized to Eprot549
LKC1006-cy3 Eprot549-cy5 EUBmix-FP	LKC group II and if there are other epsilons	0,10,20 30,40, 50	22, 11	(25-03-02) lots, LKC1006 optimal FA 30%
LKC174-cy3 Eprot549-cy5 EUBmix-FP	LKC group II, different target site	0-xx	22, 11	(20-03-02) didn't hybridize, so didn't repeat for FA optimization; use for PCR primer
GNSB-941-cy3 EUBmic-cy5	Nongreen sulfur bacteria	35	22, 11	(21-03-02) maybe a couple of filaments
CFX1223-cy3 GNSB941-cy5 EUBmix-FP	Nongreen sulfur bacteria	23	22, 11	(21-03-02) maybe a couple of filaments
LKC1006 –cy3 EPS710-cy5 EUBmix-FP	LKC group I and Group II	20	22, 11	(21-03-02) LKC1006 and EPS710 to different filaments (no overlap)
EPS710-cy5 Eprot549-cy3 EUBmix-FP	LKC group I and all epsilons	20	22, 11	(21-03-02) EPS710 and Eprot549 overlap, but a couple of thin filaments with EPS710 didn't hybridize to Eprot549… hmmm
EUBI-FP EUBII-cy3 EUBIII-cy5	Bacteria	0	Sewage sludge	(24-03-02) Used to see how all three Eubacterial groups are in sludge
Arch915-cy3 EUBmix-cy5	*Archaea*	0	Sewage sludge	(24-03-02) Used to see how all three Eubacterial groups are in sludge
EUK516-cy3 EUBmix-cy5	Eukaryotes	0	Sewage sludge	(24-03-02) Used to see how all three Eubacterial groups are in sludge
ALF968-cy3 EUBmix-cy5	*Alphaproteobacteria*	35	Sewage sludge	(24-03-02) Used to see how all three Eubacterial groups are in sludge

Table B-1: *Continued*

Probe	Target	FA%	Samples	Comments
Bet42a- cy3 / Gam42a- cy5 / EUBmix-FP	*Betaprotoebacteria* / *Gammaproteobacteria*	35	Sewage sludge	(24-03-02) Used to see how all three Eubacterial groups are in sludge
Bet42a- cy5 / Gam42a – cy3 / EUBmix – FP	*Betaprotoebacteria* / *Gammaproteobacteria*	35	Sewage sludge	(24-03-02) Used to see how all three Eubacterial groups are in sludge
CF19a-cy3 / EUBmix-cy5	*Cytophaga*	35	Sewage sludge	(24-03-02) See how all three Eubacterial groups in sludge
HGC69a-cy3	Gram+ high GC	35	Sewage sludge	(24-03-02) See how all three Eubacterial groups in sludge
LGCmix-cy3	Gram+ low GC	20	Sewage sludge	(24-03-02) See how all three Eubacterial groups in sludge
LKCl006-cy3 / EPS710-cy5 / EUBmix-FP	LKC group I and II	30	10, 9, 15, 12, 20, 11	(26-03-02) Probe screening and quantification
LKCl006-cy3 / EUBmix-cy5	LKC group II	30	11	(26-03-02) quantification; lots of filaments, very clean sample
LKCl006-cy3 / EUBmix-cy5	LKC group II	30	20	(26-03-02) quantification; thinner filaments and weaker signals, clean sample, some sulfur crystals and rosettes
LKCl006-cy3 / EUBmix-cy5	LKC group II	30	10	(26-03-02) quantification; sediment blobs, lots of samples and too many crystals (Fe-S stuff), few filaments
LKCl006-cy3 / EUBmix-cy5	LKC group II	30	9	(26-03-02) quantification; only 2 fields that had filaments
LKCl006-cy3 / EUBmix-cy5	LKC group II	30	12	(26-03-02) quantification; little sediments and a lot of filaments, very thin, hard to get good pictures because sample was too thick
LKCl006-cy3 / EUBmix-cy5	LKC group II	30	15	(26-03-02) quantification; lots of filaments, clean sample
LKCl006-cy3 / EUBmix-cy5	LKC group II	30	1	(29-03-02) quantification; lots of filaments, clean sample
LKCl006-cy3 / EUBmix-cy5	LKC group II	30	3	(29-03-02) quantification; lots of filaments, clean sample
LKCl006-cy3 / EUBmix-cy5	LKC group II	30	29	(29-03-02) quantification; lots of filaments, clean sample
LKCl006-cy3 / EUBmix-cy5	LKC group II	30	4	(29-03-02) quantification; lots of filaments, clean sample

300

Probe	Target	FA%	Samples	Comments
LKC1006-cy3 EUBmix-cy5	LKC group II	30	28	(29-03-02) quantification; no filaments anywhere in the sample (just sediment)
LKC1006-cy3 EUBmix-cy5	LKC group II	30	22	(26-03-02) quantification; lots and lots of sediment, impossible to get a good pictures (too much topography), lots of filaments, too
LKC59-cy3 EPS710-cy5 EUBmix-FP	LKC group I to large epsilon group	0	11, 22	(28-03-02) check that LKC59 and EPS710 overlap, they do
LKC59-cy3 LKC1006-cy5 EUBmix-FP	LKC group I to LKC group II to show they don't overlap	30	11, 22	(28-03-02) check that probes don't overlap (they don't)
LKC59-cy3 EUBmix-cy5	LKC group I	0, 10, 20 25,30,35 40, 50	11	(29-03-02) FA optimization for LKC59 probe (30% optimal FA)
LKC59-cy3 EUBmix-cy5	LKC group I	30	11	(29-03-02) quantification; lots of filaments, clean sample
LKC59-cy3 EUBmix-cy5	LKC group I	30	15	(29-03-02) quantification; lots of filaments, lots of sediment
LKC59-cy3 EUBmix-cy5	LKC group I	30	20	(29-03-02) quantification; background very high, short small filaments
LKC59-cy3 EUBmix-cy5	LKC group I	30	1	(29-03-02) quantification; very few filaments, weak signal
LKC59-cy3 EUBmix-cy5	LKC group I	30	3	(29-03-02) quantification; poor signal with lots of sediment
LKC59-cy3 EUBmix-cy5	LKC group I	30	29	(29-03-02) quantification; lots of filaments, clean sample
LKC59-cy3 EUBmix-cy5	LKC group I	30	10	(29-03-02) quantification; some filaments, background high
LKC59-cy3 EUBmix-cy5	LKC group I	30	9	(29-03-02) quantification; too much sediment and couldn't see filaments
LKC59-cy3 EUBmix-cy5	LKC group I	30	12	(29-03-02) quantification; like sample 9, not a good sample because of too much sediment, topography too high
LKC59-cy3 EUBmix-cy5	LKC group I	30	22	(29-03-02) quantification; lots of filaments, clean sample

Table B-1:	Continued		
Probe	**Target**	**FA%**	**Comments**
LKC59-cy3	LKC group I	30	4	(29-03-02) quantification; nothing obvious
EUBmix-cy5			
LKC59-cy3	LKC group I	30	28	(29-03-02) quantification; no hybridized filaments
EUBmix-cy5			

[a] Samples numbers are listed on Table B-2.

Table B-2: Sample numbers listed in Table B-1 and corresponding location and microbial mat morphotype. Samples that were labeled 1 though 29 were fixed in the Munich laboratory within two days after collection, while other samples were fixed in the field immediately.

Sample	Location in Cave	Mat type
1	248	White filaments in orifice
3	248	White and yellow mat near orifice
4	248	Gray mat beneath sample #3
9	190	Gray orifice sediment
10	190	White filaments floating in orifice water
11	194	White filaments, side of channel
12	194	Gray filaments in center of channel
15	198	White and gray filaments in channel
20	203	White surface webs on mat
22	203	Gray mat beneath white
28	123	Gray sediment near orifice
29	123	White filaments floating in water near orifice
203g	203	Gray filaments beneath white, fixed later
198w	198	White filaments in channel
189w	189	White filaments floating in orifice water
189g	189	Gray orifice sediment

APPENDIX C

Most Probable Number Results

Chapter 4 Supplement

Locations of sampling sites

meter	location	mat type
118	Fissure Spring orifice	water, gray sediment, white filaments
125	Fissure Spring stream	water, gray sediment, white filaments
189	Upper Spring orifice	water, gray sediment, white filaments
193	Upper Spring stream	gray filaments
195	Upper Spring stream	gray filaments white filaments
197	Upper Spring stream	gray filaments, white filaments
198	Upper Spring stream	gray filaments, white filaments
201	Upper Spring stream	white webs, white filaments, gray filaments
203	Upper Spring stream	knobby web
203	Upper Spring stream	white filaments
203	Upper Spring stream	white feathers
203	Upper Spring stream	yellow patches on mat surface
203	Upper Spring stream	gray filaments, directly under white
203	Upper Spring stream	gray filaments, deeper in mat
248	Lower Spring orifice	water, gray sediment, white filaments
248	Lower Spring orifice	white filaments, gray filaments, yellow
Cave-wall	175 m cave wall biofilm	
Hellspont	gray filaments and sediment from back of cave	
PBS	white filaments and mat mixutre from surface spring	

305

Most Probable Number Results for Lower Kane Cave and Hellspont Cave

March 2001 Fermenters

meter	cells ml-1
216 (red)	7.60E+00
215 (water)	4.00E+03
203 (white)	5.40E+03
189 (black)	2.60E+02

July-August 2001 Fermenters

meter	cell ml-1	95% UL	95%LL
orifice	8.20E+02	1.60E+01	4.30E+00
black	7.60E+00	0.37	0.15
white	5.10E+03	1.10E+02	2.30E+01
stream	2.70E+03	5.50E+02	1.40E+02
red	1.10E+02	2.10E+01	5.80E+00
248 (Lspg gray)	1.60E+02	3.10E+01	8.70E+00
248 (LSpg white)	1.30E+02	2.50E+01	7.10E+00
Hellspont	1.50E+04	2.70E+03	8.60E+02
PBS Spg	1.30E+06	2.50E+05	7.10E+04

March 2001 Heterotrophs

meter	cells ml-1
216	4.00E+04
215	1.50E+02
203	4.00E+03
189	2.80E+03

August 2001 Heterotrophs

meter	cells ml-1	95% UL	95%LL
189 (water)	3.60E+07	6.40E+07	2.00E+06
189 (gray)	1.20E+01	2.40E+00	0.59
203 (white)	7.20E+08	1.20E+09	4.20E+08
215 (water)	2.20E+03	4.00E+03	1.20E+03
216 (red)	9.30E+00	4.7	0.18
Hellspont	2.20E+03	4.00E+03	1.20E+03
PBS Spring	1.60E+06	3.10E+06	8.60E+05
248 (gray)	7.20E+09	1.20E+10	4.20E+09
248 (white)	3.70E+00	1.20E+01	1.20E+00
Cave-wall biofilm	0.024	0.006	0.096

August 2002 Fermenters

meter	cells ml-1	UL	LL	
118water	1.50E-02	1.10E-01		2.10E-03
118g	5.90E+04	1.10E+05		2.90E+05
125w	5.90E+04	1.10E+05		2.90E+04
189water	3.10E-02	1.20E-01		0.0077
189g	5.70E+03	1.10E+04		2.90E+03
193g	2.80E+02	5.30E+02		1.50E+02
195w				
195g				
198w	5.90E+06	1.00E+06		2.90E+06
198g	4.30E+06	8.10E+06		2.20E+06
201w				
201g	5.90E+06	1.10E+07		2.90E+06
203kw	5.90E+04	1.10E+05		2.90E+04
203kw	5.70E+06	1.10E+07		2.90E+06
203fe	5.90E+04	1.10E+05		2.90E+04
203fil	5.90E+06	1.10E+07		2.90E+06
203y	5.90E+04	1.10E+05		2.90E+04
203g				
203g	5.70E+04	1.10E+05		2.90E+04
203dg	5.90E+04	1.10E+05		2.90E+04
215water	2.40E+02	4.50E+02		1.20E+02
248water	2.90E+03	5.40E+03		1.50E+03
248g	5.90E+05	1.10E+06		2.90E+05

August 2001 Iron-reducers

meter	cells ml-1	UL	LL	
189 water	0.023	0.07		0.0072
189 gray sediment	7.70E+01	1.60E+01		3.80E+00
203 white mat	1.60E+02	3.10E+02		8.70E+01
215 water	4.10E-01	9.90E-01		1.70E-01
248 gray sediment	1.60E+02	3.10E+02		8.70E+01
248 white mats	1.60E+02	3.10E+02		8.70E+01
Hellspont Cave	2.80E+03			
PBS Spring	2.70E+03	5.50E+03		1.40E+03

August 2001 MPN Results

location	H-SRB	95% UL	95%LL	Ac-SRB	95% UL	95%LL
U.S. orifice	2.40E+00	0.96	0.06	1.00E+01	2.30E+01	4.60E+00
U.S. black	1.00E+00	2.30	0.46	1.90E+01	37.00	9.40E+00
U.S. white	0.01	0.10	0.00	2.20E+04	4.00E+04	1.20E+04
stream	0.45	0.14	0.014	5.70E+05		
red	0.00	1.40E-01	1.50E-02	1.00E+01	2.30E+00	0.46
L.S. black	1.90E+03	3.70E+03	9.40E+02	2.90E+02	5.60E+02	1.60E+02
L.S. white	1.50E+01	3.10E+01	7.60E+00	2.60E+04	4.60E+04	1.40E+04
Hellspont	3.30E+04	6.10E+04	1.70E+04	5.70E+05		
PBS Spring	5.70E+05			5.70E+05		

August 2001 MPN Results

location	LF-SRB	95% UL	95%LL	TSRB	95% UL	95%LL
U.S. orifice	0.63	1.70	0.23	1.30E+01	2.70E+01	6.00E+00
U.S. black	2.20E+01	4.30E+01	1.20E+01	2.20E+02	4.30E+02	1.20E+02
U.S. white	1.00E+02	2.30E+02	4.60E+00	4.40E+05	8.00E+05	2.40E+05
stream	1.90E+02	3.70E+02	9.40E+01	5.70E+05		
red	0.46	1.40	0.15	1.10E+00	2.30E+00	4.60E-01
L.S. black	2.20E+02	430.00	100.00	1.40E+05	7.70E+05	2.20E+04
L.S. white	1.90E+02	3.70E+02	9.40E+01	2.60E+05	5.00E+05	1.40E+05
Hellspont	5.40E+05	1.10E+05	2.70E+04	5.70E+05		
PBS Spring	5.70E+05			5.70E+05		

August 2003 S^{o}RB

location	cells ml-1	UL	LL
189 orifice water	0		
189 gray sediment	0.023	0.16	0.0032
193 gray filaments	5.20E+00	2.10E+01	1.30E+00
195 white filaments	1.70E+02		
195 gray filaments	9.30E+01	3.00E+02	2.90E+01
198 white filaments	5.20E+00	2.10E+01	1.30E+00
198 gray filaments	5.20E+00	2.10E+01	1.30E+00
201 white filaments	1.70E+02		
201 gray filaments	9.30E+01	3.00E+02	2.90E+01
203 white webs	1.70E+02		
203 filaments	9.30E+01	3.00E+02	2.90E+01
203 gray filaments	1.70E+02		
215 stream water	0		

August 2002 SRB

Acetate	SRB		
meter	cells ml-1	UL 95%	LL 95%
118water			
118g			
125w			
189water	0.015	1.1	0.0021
189g	5.70E+03	1.10E+04	2.90E+03
193g	1.60E+01	3.30E+01	8.00E+00
195w	6.00E+03	1.20E+04	3.00E+03
195g	1.40E+01	3.00E+01	6.60E+00
198w	5.90E+06		
198g	1.00E+06	1.80E+06	6.10E+05
201w	3.60E+04	6.70E+04	1.90E+04
201g	2.00E+03	4.00E+03	1.00E+03
203kw	5.90E+06		
203kw	4.50E+05	8.50E+05	2.40E+05
203fe	5.90E+05		
203fil	6.00E+06		
203y	5.90E+05		
203g	3.60E+06	6.70E+06	1.90E+06
203g			
203dg			
215water	3.20E-01	7.70E-01	1.30E-01
248water	0		
248g	5.90E+05		

August 2001 Methanogens

meter	H-Met	95% UL	95% LL	Ac-Met	95% UL	95%LL
orifice	0.00E+00	1.40E-01	1.50E-02	0.00E+00	1.40E-01	1.50E-02
black	0.00E+00	1.40E-01	1.50E-02	1.40E-02	1.00E-01	0.002
white	1.40E-02	1.00E-01	0.002	0.00E+00	1.40E-01	1.50E-02
stream	1.40E-02	1.00E-01	0.002	0.00E+00	1.40E-01	1.50E-02
red	0.00E+00	1.40E-01	1.50E-02	0.00E+00	1.40E-01	1.50E-02
Hellspont	3.30E+02	6.10E+02	1.70E+02	1.50E+01	3.10E+01	7.60E+00
PBS Spring	2.30E+03	4.40E+03	1.20E+03	2.20E+02	4.30E+02	1.20E+02
248 (Lspg gray)	0.00E+00	1.40E-01	1.50E-02	0.00E+00	1.40E-01	1.50E-02
248 (LSpg white)	0.00E+00	1.40E-01	1.50E-02	0.00E+00	1.40E-01	1.50E-02

August 2002 SRB

meter	Lactate/Formate SRB cells ml-1	UL 95%	LL 95%	Hydrogen SRB cells ml-1	UL 95%	LL 95%
118water						
118g						
125w						
189water	0.015	1.1	0.0021	0		
189g	4.30E+03	8.10E+03	2.20E+03	6.70E-01	1.80E+00	2.50E-01
193g	2.00E+02	3.90E+02	1.00E+02	6.70E-01	1.80E+00	2.50E-01
195w	3.60E+02	6.70E+02	1.90E+02	1.70E+01	3.40E+01	8.30E+00
195g	0.05	0.15	0.016	0.05	0.15	0.016
198w	5.90E+06			3.40E+03	6.40E+03	1.80E+03
198g	5.90E+05			9.60E+00	2.30E+01	4.00E+00
201w	3.60E+04	6.70E+04	1.90E+04	2.90E+02	5.50E+02	1.60E+02
201g	1.70E+03	3.40E+03	8.30E+02	2.00E+01	4.00E+01	1.00E+01
203kw	5.90E+06					
203kw	6.00E+06			2.40E+02	4.70E+02	1.30E+02
203fe	5.90E+05					
203fil	2.90E+05	5.50E+05	1.60E+05	3.60E+02	6.70E+02	1.90E+02
203y	5.90E+05			5.90E+05		
203g	1.70E+03	3.40E+03	8.30E+02	1.70E+01	3.40E+01	8.30E+00
203g						
203dg						
215water	6.90E+01	1.30E+02	3.70E+01	3.20E-01	7.70E-01	1.30E-01
248water	0			0		
248g	5.90E+05			5.30E+01	1.10E+02	2.60E+01

August 2001 Methanogens

meter	F-Met	95% UL	95%LL
orifice	0.00E+00	1.40E-01	1.50E-02
black	0.00E+00	1.40E-01	1.50E-02
white	0.00E+00	1.40E-01	1.50E-02
stream	0.00E+00	1.40E-01	1.50E-02
red	0.00E+00	1.40E-01	1.50E-02
Hellspont	1.90E+01	3.70E+01	9.40E+00
PBS Spring	1.50E+01	3.10E+01	7.60E+00
248 (Lspg gray)	0.00E+00	1.40E-01	1.50E-02
248 (LSpg white)	2.90E-02	1.20E-01	7.20E-03

2001

S-Oxidizers	March	UL	LL	August	UL	LL
orifice				8.20E+00	2.00E+01	3.40E+00
black	1.10E+01	8.10E+01	1.60E+00	0.00E+00	1.40E-01	1.50E-02
white	1.00E+08	1.60E+07	2.70E+06	1.90E+03	3.50E+03	1.00E+03
stream	0.04	0.11	0.01	5.60E+00	1.60E+01	5.60E+00
red	1.40E+06	2.70E+06	7.10E+05	5.80E+08	6.40E+08	2.00E+08
Hellspont				5.00E+06	1.30E+06	1.90E+05
PBS Spring				0.00E+00	1.40E-01	1.50E-02
Cave-wall biofilm				0.00E+00	1.40E-01	1.50E-02
248 (gray)				0.00E+00	1.40E-01	1.50E-02
248 (white)				0.00E+00	1.40E-01	1.50E-02

2002 Sulfur-oxidizers

meter	cells ml	UL	LL
118g	1.40E+00	3.00E+00	6.60E-01
125w	2.40E+05	4.40E+05	1.30E+05
189g	2.40E+01	4.70E+01	1.30E+01
193g	2.10E+02	3.90E+02	1.10E+02
195w	2.00E+01	4.00E+01	1.00E+01
195g	1.50E+05	3.00E+05	7.90E+04
198w	2.40E+02	4.40E+02	1.30E+02
198g	2.40E+04	4.70E+04	1.30E+04
201w	3.30E+03	5.90E+03	1.90E+03
201g	2.80E+02	5.10E+02	1.60E+02
203kw	2.00E+01	4.00E+01	1.00E+01
203kw	2.00E+01	4.00E+01	1.00E+01
203fe	2.90E+02	5.50E+02	1.60E+02
203fil	2.00E+02	5.10E+02	1.60E+02
203y	2.00E+01	4.00E+01	1.00E+01
203g	2.80E+02	5.10E+02	1.60E+02
203g	2.40E+01	4.70E+01	1.30E+01
203dg	2.10E+02	3.90E+02	1.10E+02
248g	2.00E+01	4.00E+01	1.00E+01

APPENDIX D

Chapter 6 Supplement

Appendix D - Chapter 5 Gas chromatography data from Nov 2003

FPD Results

SAMPLE	SAMPLE	INJECT SIZE	date	time	cum time	cum time (min)	gas	reten	area	conc	units	gas	reten	area	conc	units	gas	reten	area	conc	units	gas	reten	area	conc	units	gas	reten	area	conc
	A-1				11/23/03 8:00 PM	1.00				10.2						1					1 ppm					1 ppm				10.2
Nov03-FPD61.chr	A-1	250	11/24/2003	2:15:30	11/24/03 2:15:30 AM	375.00	H2S	2.65	3.77	10.163	ppm	COS	0	0	0	1 ppm	CH3SH	0	0	0	1 ppm	DMS	0	0	0	1 ppm	DMDS	0	0	0
Nov03-FPD106.chr	A-1		11/24/2003	8:04:27	11/24/03 8:04:27 AM	1444.00	H2S	2.633	2.56	9.737	ppm	COS	0	0	0	1 ppm	CH3SH	0	0	0	1 ppm	DMS	0	0	0	1 ppm	DMDS	0	0	0
Nov03-FPD158.chr	A-1		11/24/2003	16:26:23	11/24/03 4:26 PM	1950.00	H2S	0	0	0	ppm	COS	0	0	0	1 ppm	CH3SH	0	0	0	1 ppm	DMS	0	0	0	1 ppm	DMDS	0	0	0
Nov03-FPD197.chr	A-1		11/25/2003	12:24:20	11/25/03 12:24 PM	2852.00	H2S	0	0	0	1 ppm	COS	0	0	0	1 ppm	CH3SH	0	0	0	1 ppm	DMS	0	0	0	1 ppm	DMDS	0	0	0
Nov03-FPD237.chr	A-1		11/26/2003	12:04:10	11/26/03 12:04 PM	4270.00	H2S	0	0	0	1 ppm	COS	0	0	0	1 ppm	CH3SH	0	0	0	1 ppm	DMS	0	0	0	1 ppm	DMDS	0	0	0
Nov03-FPD368.chr	A-1		12/2/2003	17:53:08	12/2/03 5:53 PM	13976.00	H2S	0	0	0	1 ppm	COS	0	0	0	1 ppm	CH3SH	0	0	0	1 ppm	DMS	0	0	0	1 ppm	DMDS	0	0	0
Nov03-FPD428.chr	A-1		12/4/2003	17:04:53	12/4/03 5:04 PM	15847.00	H2S	0	0	0	1 ppm	COS	0	0	0	1 ppm	CH3SH	0	0	0	1 ppm	DMS	0	0	0	1 ppm	DMDS	0	0	0
	A-2				11/23/03 8:00 PM	1.00				1						1					1 ppm					1 ppm				1
Nov03-FPD24.chr	A-2		11/23/2003	20:44:03	11/23/03 8:44 PM	44.00	H2S	0	0	0	1 ppm	COS	0	0	0	1 ppm	CH3SH	0	0	0	1 ppm	DMS	0	0	0	1 ppm	DMDS	0	0	0
Nov03-FPD62.chr	A-2		11/24/2003	2:23:06	11/24/03 2:23 AM	383.00	H2S	0	0	0	1 ppm	COS	0	0	0	1 ppm	CH3SH	0	0	0	1 ppm	DMS	0	0	0	1 ppm	DMDS	0	0	0
Nov03-FPD107.chr	A-2		11/24/2003	8:09:44	11/24/03 8:09 AM	1449.00	H2S	0	0	0	1 ppm	COS	0	0	0	1 ppm	CH3SH	0	0	0	1 ppm	DMS	0	0	0	1 ppm	DMDS	0	0	0
Nov03-FPD159.chr	A-2		11/24/2003	16:31:05	11/24/03 4:31 PM	1954.00	H2S	2.641	42.67	19.858	ppm	COS	0	0	0	1 ppm	CH3SH	0	0	0	1 ppm	DMS	0	0	0	1 ppm	DMDS	0	0	0
Nov03-FPD198.chr	A-2		11/25/2003	12:30:36	11/25/03 12:30 PM	2858.00	H2S	2.616	1038.64	95.79	ppm	COS	0	0	0	1 ppm	CH3SH	0	0	0	1 ppm	DMS	0	0	0	1 ppm	DMDS	0	0	0
Nov03-FPD238.chr	A-2		11/26/2003	12:08:54	11/26/03 12:08 PM	4274.00	H2S	2.633	55.95	22.375	ppm	COS	0	0	0	1 ppm	CH3SH	0	0	0	1 ppm	DMS	0	0	0	1 ppm	DMDS	0	0	0
Nov03-FPD283.chr	A-2		11/28/2003	10:21:19	11/28/03 10:21 AM	7775.00	H2S	2.6	5.25	10.682	ppm	COS	0	0	0	1 ppm	CH3SH	0	0	0	1 ppm	DMS	0	0	0	1 ppm	DMDS	0	0	0
Nov03-FPD369.chr	A-2		12/2/2003	18:07:16	12/2/03 6:07 PM	13981.00	H2S	2.633	441.88	61.82	ppm	COS	0	0	0	1 ppm	CH3SH	7.475	4.75	0	1 ppm	DMS	0	0	0	1 ppm	DMDS	0	0	0
Nov03-FPD429.chr	A-2		12/4/2003	17:09:45	12/4/03 5:09 PM	15852.00	H2S	2.625	94.04	28.45	ppm	COS	0	0	0	1 ppm	CH3SH	0	0	0	1 ppm	DMS	0	0	0	5 ppm	DMDS	0	0	0
	A-3				11/23/03 8:00 PM	1.00				1						1					1 ppm					1 ppm				1
Nov03-FPD25.chr	A-3		11/23/2003	20:49:46	11/23/03 8:49 PM	49.00	H2S	0	0	0	1 ppm	COS	0	0	0	1 ppm	CH3SH	0	0	0	1 ppm	DMS	0	0	0	1 ppm	DMDS	0	0	0
Nov03-FPD63.chr	A-3		11/24/2003	2:29:01	11/24/03 2:29 AM	389.00	H2S	0	0	0	1 ppm	COS	0	0	0	1 ppm	CH3SH	0	0	0	1 ppm	DMS	0	0	0	1 ppm	DMDS	0	0	0
Nov03-FPD108.chr	A-3	100	11/24/2003	8:15:11	11/24/03 8:15 AM	1455.00	H2S	2.625	1076.3	97.617	ppm	COS	0	0	0	1 ppm	CH3SH	0	0	0	1 ppm	DMS	0	0	0	1 ppm	DMDS	0	0	0
Nov03-FPD160.chr	A-3		11/24/2003	16:40:21	11/24/03 4:40 PM	1965.00	H2S	2.608	765.96	204.82	ppm	COS	0	0	0	1 ppm	CH3SH	0	0	0	1 ppm	DMS	0	0	0	1 ppm	DMDS	0	0	0
Nov03-FPD199.chr	A-3		11/25/2003	12:40:16	11/25/03 12:40 PM	2868.00	H2S	2.6	6248.68	348.37	ppm	COS	0	0	0	1 ppm	CH3SH	0	0	0	1 ppm	DMS	0	0	0	1 ppm	DMDS	0	0	0
Nov03-FPD239.chr	A-3		11/26/2003	12:18:57	11/26/03 12:18 PM	4284.00	H2S	2.6	19663.39	998.706	ppm	COS	0	0	0	1 ppm	CH3SH	7.416	5.56	11.183	ppm	DMS	0	0	0	1 ppm	DMDS	0	0	0
Nov03-FPD284.chr	A-3		11/28/2003	10:32:23	11/28/03 10:32 AM	7786.00	H2S	2.575	16.27	0	ppm	COS	0	0	0	1 ppm	CH3SH	7.408	12.77	15.159	ppm	DMS	0	0	0	1 ppm	DMDS	0	0	0
Nov03-FPD370.chr	A-3		12/2/2003	18:27:04	12/2/03 6:27 PM	14001.00	H2S	2.6	465.77	63.507	ppm	COS	0	0	0	1 ppm	CH3SH	7.433	129.59	41.767	ppm	DMS	0	0	0	1 ppm	DMDS	0	0	0
Nov03-FPD430.chr	A-3		12/4/2003	17:24:32	12/4/03 5:24 PM	15867.00	H2S	2.516	80749.2	3960.104	ppm	COS	4.191	2.68	3.071	1 ppm	CH3SH	7.433	224.71	54.103	ppm	DMS	0	0	0	5 ppm	DMDS	0	0	0
	A-4				11/23/03 8:00 PM	1.00				1						1					1 ppm					1 ppm				1
Nov03-FPD26.chr	A-4		11/23/2003	20:54:50	11/23/03 8:54 PM	54.00	H2S	0	0	0	1 ppm	COS	0	0	0	1 ppm	CH3SH	0	0	0	1 ppm	DMS	0	0	0	1 ppm	DMDS	0	0	0
Nov03-FPD64.chr	A-4		11/24/2003	2:35:47	11/24/03 2:35 AM	395.00	H2S	2.625	12.4	12.796	ppm	COS	4.075	3.77	0	1 ppm	CH3SH	7.225	5.32	6.775	ppm	DMS	0	0	0	1 ppm	DMDS	0	0	0
Nov03-FPD109.chr	A-4		11/24/2003	8:24:58	11/24/03 8:24 AM	1464.00	H2S	2.583	26130.2	0	ppm	COS	0	0	0	1 ppm	CH3SH	7.433	2.41	11.092	ppm	DMS	0	0	0	1 ppm	DMDS	0	0	0
Nov03-FPD161.chr	A-4		11/24/2003	16:50:56	11/24/03 4:50 PM	1675.00	H2S	2.583	2871.07	184.626	ppm	COS	4.258	8.79	6.672	1 ppm	CH3SH	7.225	6.06	11.092	ppm	DMS	0	0	0	1 ppm	DMDS	0	0	0
Nov03-FPD200.chr	A-4		11/25/2003	12:48:29	11/25/03 12:48 PM	2876.00	H2S	2.616	7784.12	422.807	ppm	COS	0	0	0	1 ppm	CH3SH	7.433	23.45	19.482	ppm	DMS	0	0	0	1 ppm	DMDS	0	0	0
Nov03-FPD240.chr	A-4		11/26/2003	12:33:54	11/26/03 12:33 PM	4299.00	H2S	2.583	1503.09	118.307	ppm	COS	4.191	2.74	3.109	1 ppm	CH3SH	7.408	56.4	28.53	ppm	DMS	0	0	0	1 ppm	DMDS	0	0	0
Nov03-FPD285.chr	A-4		11/28/2003	10:49:20	11/28/03 10:49 AM	7803.00	H2S	2.575	14.6	13.396	ppm	COS	4.058	2.39	2.877	1 ppm	CH3SH	7.408	237.01	55.488	ppm	DMS	0	0	0	1 ppm	DMDS	0	0	0
Nov03-FPD371.chr	A-4		12/2/2003	18:43:54	12/2/03 6:43 PM	14017.00	H2S	2.616	422.18	60.407	ppm	COS	0	0	0	1 ppm	CH3SH	7.433	394.24	70.851	ppm	DMS	0	0	0	1 ppm	DMDS	0	0	0
Nov03-FPD431.chr	A-4		12/4/2003	17:42:59	12/4/03 5:42 PM	15885.00	H2S	2.441	93429.38	4574.831	ppm	COS	0	0	0	1 ppm	CH3SH	0	0	0	1 ppm	DMS	0	0	0	5 ppm	DMDS	0	0	0
	A-5				11/23/03 8:00 PM	1.00				1						1					1 ppm					1 ppm				1
Nov03-FPD27.chr	A-5		11/23/2003	21:00:52	11/23/03 9:00 PM	60.00	H2S	0	0	0	1 ppm	COS	0	0	0	1 ppm	CH3SH	0	0	0	1 ppm	DMS	0	0	0	1 ppm	DMDS	0	0	0
Nov03-FPD65.chr	A-5		11/24/2003	2:57:06	11/24/03 2:57 AM	417.00	H2S	0	0	0	1 ppm	COS	0	0	0	1 ppm	CH3SH	0	0	0	1 ppm	DMS	0	0	0	1 ppm	DMDS	0	0	0
Nov03-FPD110.chr	A-5		11/24/2003	8:34:36	11/24/03 8:34 AM	1474.00	H2S	2.616	50.75	21.389	ppm	COS	0	0	0	1 ppm	CH3SH	0	0	0	1 ppm	DMS	0	0	0	1 ppm	DMDS	0	0	0
Nov03-FPD162.chr	A-5		11/24/2003	17:02:35	11/24/03 5:02 PM	1687.00	H2S	2.633	34.74	18.235	ppm	COS	0	0	0	1 ppm	CH3SH	0	0	0	1 ppm	DMS	0	0	0	1 ppm	DMDS	0	0	0
Nov03-FPD201.chr	A-5		11/25/2003	12:55:22	11/25/03 12:55 PM	2889.00	H2S	2.616	7.79	11.536	ppm	COS	0	0	0	1 ppm	CH3SH	7.425	12.14	14.861	ppm	DMS	0	0	0	1 ppm	DMDS	0	0	0
Nov03-FPD241.chr	A-5		11/26/2003	12:48:46	11/26/03 12:48 PM	4314.00	H2S	0	0	0	1 ppm	COS	0	0	0	1 ppm	CH3SH	0	0	0	1 ppm	DMS	0	0	0	1 ppm	DMDS	0	0	0
Nov03-FPD286.chr	A-5		11/28/2003	11:09:46	11/28/03 11:09 AM	7823.00	H2S	2.625	8.06	11.607	ppm	COS	0	0	0	1 ppm	CH3SH	0	0	0	1 ppm	DMS	0	0	0	1 ppm	DMDS	0	0	0
Nov03-FPD331.chr	A-5		12/1/2003	19:27:24	12/1/03 7:27 PM	12650.00	H2S	0	0	0	1 ppm	COS	0	0	0	1 ppm	CH3SH	7.408	66.7	30.779	ppm	DMS	0	0	0	1 ppm	DMDS	14.666	0	24.73
Nov03-FPD372.chr	A-5		12/2/2003	18:58:12	12/2/03 6:58 PM	14032.00	H2S	2.6	10.42	12.254	ppm	COS	0	0	0	1 ppm	CH3SH	7.416	18.54	17.63	ppm	DMS	0	0	0	1 ppm	DMDS	0	0	0
Nov03-FPD432.chr	A-5		12/4/2003	17:58:55	12/4/03 5:58 PM	15901.00	H2S	2.608	17.36	14.153	ppm	COS	0	0	0	1 ppm	CH3SH	7.433	24.58	19.854	ppm	DMS	0	0	0	1 ppm	DMDS	0	0	0
	A-6				11/23/03 8:00 PM	1.00				1						1					1 ppm					1 ppm				1
Nov03-FPD28.chr	A-6		11/23/2003	21:05:55	11/23/03 9:05 PM	65.00	H2S	2.7	2.22	9.616	ppm	COS	0	0	0	1 ppm	CH3SH	0	0	0	1 ppm	DMS	0	0	0	1 ppm	DMDS	0	0	0
Nov03-FPD66.chr	A-6		11/24/2003	3:06:11	11/24/03 3:06 AM	425.00	H2S	2.6	10.1	12.165	ppm	COS	0	0	0	1 ppm	CH3SH	0	0	0	1 ppm	DMS	0	0	0	1 ppm	DMDS	0	0	0
Nov03-FPD111.chr	A-6	100	11/24/2003	8:44:25	11/24/03 8:44 AM	1484.00	H2S	2.591	14141.16	0	ppm	COS	0	0	0	1 ppm	CH3SH	0	0	0	1 ppm	DMS	0	0	0	1 ppm	DMDS	0	0	0
Nov03-FPD163.chr	A-6	100	11/24/2003	17:12:45	11/24/03 5:12 PM	1697.00	H2S	2.55	654.82	189.05	ppm	COS	0	0	0	1 ppm	CH3SH	7.416	27.18	20.71	ppm	DMS	10.333	7.43	10.334	ppm	DMDS	0	0	0
Nov03-FPD202.chr	A-6		11/25/2003	13:04:06	11/25/03 1:04 PM	2898.00	H2S	2.591	5522.48	313.164	ppm	COS	0	0	0	1 ppm	CH3SH	7.416	8.56	13.012	ppm	DMS	10.316	8	0	ppm	DMDS	0	0	0
Nov03-FPD242.chr	A-6		11/26/2003	13:04:19	11/26/03 1:04 PM	4338.00	H2S	2.591	754.84	81.317	ppm	COS	0	0	0	1 ppm	CH3SH	7.425	482.94	78.927	ppm	DMS	0	0	0	ppm	DMDS	0	0	0
Nov03-FPD287.chr	A-6		11/28/2003	11:18:06	11/28/03 11:18 AM	7832.00	H2S	2.625	125.22	32.706	ppm	COS	0	0	0	1 ppm	CH3SH	0	0	0	ppm	DMS	0	0	0	ppm	DMDS	0	0	0
Nov03-FPD332.chr	A-6		12/1/2003	20:05:10	12/1/03 8:05 PM	12682.00	H2S	2.441	111725.16	5461.798	ppm	COS	0	0	0	1 ppm	CH3SH	7.4	2863.3	295.653	ppm	DMS	10.325	47.55	23.527	ppm	DMDS	0	0	0
Nov03-FPD373.chr	A-6		12/2/2003	19:13:33	12/2/03 7:13 PM	14047.00	H2S	2.425	120501.83	5887.285	ppm	COS	0	0	0	1 ppm	CH3SH	7.416	3739.37	375.417	ppm	DMS	10.325	47.73	23.571	ppm	DMDS	0	0	0
Nov03-FPD433.chr	A-6		12/4/2003	18:08:45	12/4/03 6:08 PM	15911.00	H2S	2.458	122894.42	5988.732	ppm	COS	0	0	0	1 ppm	CH3SH	7.425	4330.08	429.2	ppm	DMS	10.325	52.15	24.553	ppm	DMDS	0	0	72
	A-7				11/23/03 8:00 PM	1.00				1						1					1 ppm					1 ppm				1
Nov03-FPD29.chr	A-7		11/23/2003	21:11:08	11/23/03 9:11 PM	71.00	H2S	2.616	27.36	16.583	ppm	COS	0	0	0	1 ppm	CH3SH	0	0	0	1 ppm	DMS	0	0	0	1 ppm	DMDS	14.57	0	0
Nov03-FPD67.chr	A-7		11/24/2003	3:12:17	11/24/03 3:12 AM	431.00	H2S	0	0	0	1 ppm	COS	0	0	0	1 ppm	CH3SH	0	0	0	1 ppm	DMS	0	0	0	1 ppm	DMDS	0	0	0
Nov03-FPD112.chr	A-7	100	11/24/2003	8:54:50	11/24/03 8:54 AM	1494.00	H2S	2.616	26220.69	3291.4975	ppm	COS	0	0	0	1 ppm	CH3SH	0	0	0	1 ppm	DMS	0	0	0	1 ppm	DMDS	0	0	0

313

Chromatography data table (all concentration units in ppm). Gas groups left→right: H2S, COS, CHSH, DMS, DMDS.

file	SAMPLE	INJECT SIZE	date	time	cum time (min)	cum time	H2S reten	H2S area	H2S conc	COS reten	COS area	COS conc	CHSH reten	CHSH area	CHSH conc	DMS reten	DMS area	DMS conc	DMDS gas	DMDS reten	DMDS area	DMDS conc
Nov03-FPD164.chr	A-7	100	11/24/2003	17:24:07	1709.00	11/24/03 5:24 PM	2.541	43385.81	5371.8825	0	0	1	0	0	1	0	0	1	DMDS	0	0	0
Nov03-FPD165.chr	A-7	50	11/24/2003	17:35:58	1720.00	11/24/03 5:35 PM	2.625	19347.1	9833.72	0	0	1	0	0	1	0	0	1	DMDS	0	0	0
Nov03-FPD203.chr	A-7	50	11/25/2003	13:25:07	2919.00	11/25/03 1:25 PM	2.691	2.56		0	0	1	0	0	1	0	0	1	DMDS	0	0	0
Nov03-FPD204.chr	A-7	50	11/25/2003	13:30:28	2924.00	11/25/03 1:30 PM	2.641	21067.82	10667.92	0	0	1	0	0	1	0	0	1	DMDS	0	0	0
Nov03-FPD243.chr	A-7		11/26/2003	13:24:18	4364.00	11/26/03 1:24 PM	2.458	88644.86	4342.881	4.158	6.33	5.49	7.425	221.2	53.696	10.325	4.23	8.272	DMDS	0	0	0
Nov03-FPD288.chr	A-7		11/28/2003	11:37:50	7851.00	11/28/03 11:37 AM	2.491	94740.1	4638.373	4.191	7.63	6.141	7.425	865.72	113.778	10.325	9.35	11.432	DMDS	0	0	0
Nov03-FPD333.chr	A-7		12/1/2003	20:27:08	12714.00	12/1/03 8:27 PM	2.5	101224.29	4952.723	4.2	12.61	8.414	7.425	1534.54	174.673	10.316	9.61	11.573	DMDS	0	0	0
Nov03-FPD374.chr	A-7		12/2/2003	19:30:48	14064.00	12/2/03 7:30 PM	2.458	105060.58	5138.704	4.166	11.38	7.851	7.425	1766.45	195.788	10.316	9.61	11.573	DMDS	0	0	0
Nov03-FPD434.chr	A-7		12/4/2003	18:40:21	16943.00	12/4/03 6:40 PM	2.491	97804.95	4786.955	4.183	16.74	9.875	7.425	1384.68	161.028	10.291	8.67	11.035	DMDS	0	0	0
Nov03-FPD30.chr	A-8		11/23/2003	21:16:22	76.00	11/23/03 9:16 PM	0	0		0	0	1	0	0	0	0	0	0	DMDS	0	0	0
Nov03-FPD68.chr	A-8		11/24/2003	3:24:51	443.00	11/24/03 3:24 AM	2.7	2.51	9.717	0	0	1	0	0	0	0	0	0	DMDS	0	0	0
Nov03-FPD113.chr	A-8	250	11/24/2003	9:04:57	1504.00	11/24/03 9:04 AM	2.608	6.63	11.165	0	0	1	7.416	3.23	9.29	0	0	0	DMDS	0	0	0
Nov03-FPD166.chr	A-8	250	11/24/2003	17:42:06	1721.00	11/24/03 5:42 PM	2.625	43.26	19.969	0	0	1	7.391	3.46	9.481	0	0	0	DMDS	0	0	0
Nov03-FPD205.chr	A-8	250	11/25/2003	13:39:50	2938.00	11/25/03 1:39 PM	2.608	17.09	14.078	0	0	1	7.416	19.87	18.147	0	0	0	DMDS	0	0	0
Nov03-FPD244.chr	A-8		11/26/2003	13:38:59	4378.00	11/26/03 1:38 PM	2.566	9.54	12.014	0	0	1	7.433	414.12	72.661	0	0	0	DMDS	0	0	0
Nov03-FPD289.chr	A-8		11/28/2003	12:00:51	7874.00	11/28/03 12:00 PM	2.633	7.93	11.572	0	0	1	7.425	345.82	66.443	0	0	0	DMDS	0	0	0
Nov03-FPD334.chr	A-8		12/1/2003	20:50:59	12737.00	12/1/03 8:50 PM	0	0		0	0	1	0	0	1	11.4	112		DMDS	11.4	112	112
Nov03-FPD375.chr	A-8		12/2/2003	19:48:37	14076.00	12/2/03 7:48 PM	0	0		0	0	1	0	0	1	0	0	1	DMDS	0	0	0
Nov03-FPD435.chr	A-8		12/4/2003	18:58:56	15961.00	12/4/03 6:58 PM	2.533	9.47	11.995	0	0	1	7.408	139.3	43.2	10.33	2.69	6.9	DMDS	0	0	0
Nov03-FPD31.chr	A-9		11/23/2003	21:22:57	82.00	11/23/03 9:22 PM	0	0		0	0	1	0	0	1	0	0	1	DMDS	0	0	0
Nov03-FPD69.chr	A-9	100	11/24/2003	3:31:17	450.00	11/24/03 3:31 AM	2.625	557.08	69.601	0	0	1	0	0	1	0	0	1	DMDS	0	0	0
Nov03-FPD114.chr	A-9		11/24/2003	9:10:45	1510.00	11/24/03 9:10 AM	2.625	721.96	198.745	0	0	1	0	0	1	0	0	1	DMDS	0	0	0
Nov03-FPD167.chr	A-9	50	11/24/2003	17:48:55	1727.00	11/24/03 5:48 PM	2.616	11641.38	6098.04	0	0	1	0	0	1	0	0	1	DMDS	0	0	0
Nov03-FPD206.chr	A-9	50	11/25/2003	13:49:38	2948.00	11/25/03 1:49 PM	2.6	23189.37	11696.43	0	0	1	0	0	1	0	0	1	DMDS	0	0	0
Nov03-FPD245.chr	A-9		11/26/2003	13:51:43	4391.00	11/26/03 1:51 PM	2.45	88643.38	4342.809	4.15	4.62	4.354	7.441	23.8	19.598	0	0	1	DMDS	0	0	0
Nov03-FPD290.chr	A-9		11/28/2003	12:21:00	7895.00	11/28/03 12:21 PM	2.5	93667.81	4586.39	4.2	6.77	5.752	7.425	75.93	32.659	0	0	1	DMDS	0	0	0
Nov03-FPD376.chr	A-9		12/2/2003	20:03:36	14081.00	12/2/03 8:03 PM	2.458	108564.95	5308.593	4.2	11.33	7.829	7.425	389.89	70.455	10.308	5.16	9.045	DMDS	0	0	0
Nov03-FPD436.chr	A-9		12/4/2003	19:13:00	15976.00	12/4/03 7:13 PM	2.45	104552.85	5114.089	4.158	9.99	7.217	7.425	418.46	73.056	10.316	5.37	9.168	DMDS BIG	0	0	0
Nov03-FPD70.chr	A-10		11/24/2003	3:41:07	460.00	11/24/03 3:41 AM	0	0		0	0	1	0	0	1	0	0	1	DMDS	0	0	0
Nov03-FPD115.chr	A-10	250	11/24/2003	9:20:03	1524.00	11/24/03 9:20 AM	0	0		0	0	1	0	0	1	0	0	1	DMDS	0	0	0
Nov03-FPD168.chr	A-10	250	11/24/2003	17:59:10	1738.00	11/24/03 5:59 PM	2.575	9.42	11.979	0	0	1	0	0	1	0	0	1	DMDS	0	0	0
Nov03-FPD437.chr	A-10		12/4/2003	19:33:04	15996.00	12/4/03 7:33 PM	0	0		0	0	1	0	0	1	0	0	1	DMDS	0	0	0
Nov03-FPD60.chr	AIR		11/24/2003	2:09:21			0	0		0	0	1	0	0	0	0	0	0	DMDS	0	0	0
Nov03-FPD105.chr	AIR		11/24/2003	7:57:51			0	0		0	0	1	0	0	0	0	0	0	DMDS	0	0	0
Nov03-FPD189.chr	AIR		11/24/2003	20:15:37			2.808	4.73	10.496	0	0	1	0	0	0	0	0	0	DMDS	0	0	0
Nov03-FPD279.chr	AIR		11/28/2003	9:06:10			2.408	2.62	9.757	0	0	1	10.491	3.39	7.55	10.491	3.39	7.55	CS2	11.783	13.18	7.55
Nov03-FPD335.chr	AIR		12/2/2003	9:25:26			0	0		0	0	1	7.675	3.16	9.228	7.675	3.16	9.228	DMS	10.125	6.46	9.781
Nov03-FPD32.chr	B-1		11/23/2003	21:29:21	89.00	11/23/03 9:29 PM	0	0		0	0	1	0	0	0	0	0	0	DMDS	0	0	0
Nov03-FPD71.chr	B-1		11/24/2003	3:46:32	465.00	11/24/03 3:46 AM	0	0		0	0	1	0	0	0	0	0	0	DMDS	0	0	0
Nov03-FPD116.chr	B-1	250	11/24/2003	9:25:12	1529.00	11/24/03 9:25 AM	0	0		0	0	1	0	0	0	0	0	0	DMDS	0	0	0
Nov03-FPD169.chr	B-1		11/24/2003	18:04:13	1743.00	11/24/03 6:04 PM	0	0		0	0	1	0	0	0	0	0	0	DMDS	0	0	0
Nov03-FPD209.chr	B-1		11/25/2003	14:26:43	2983.00	11/25/03 2:26 PM	0	0		0	0	1	0	0	0	0	0	0	DMDS	0	0	0
Nov03-FPD247.chr	B-1		11/26/2003	14:20:41	4420.00	11/26/03 2:20 PM	0	0		0	0	1	0	0	0	0	0	0	DMDS	0	0	0
Nov03-FPD292.chr	B-1		11/28/2003	12:58:33	7932.00	11/28/03 12:58 PM	0	0		0	0	1	0	0	0	0	0	0	DMDS	0	0	0
Nov03-FPD382.chr	B-1		12/3/2003	10:06:51	15012.00	12/3/03 10:06 AM	0	0		0	0	1	0	0	0	0	0	0	DMDS	0	0	0
Nov03-FPD33.chr	B-2		11/23/2003	21:35:22	94.00	11/23/03 9:35 PM	0	0		0	0	1	0	0	1	0	0	1	DMDS	0	0	0
Nov03-FPD72.chr	B-2		11/24/2003	3:53:32	472.00	11/24/03 3:53 AM	0	0		0	0	1	0	0	1	0	0	1	DMDS	0	0	0
Nov03-FPD171.chr	B-2	250	11/24/2003	18:17:30	1756.00	11/24/03 6:17 PM	0	0		0	0	1	0	0	1	0	0	1	DMDS	0	0	0
Nov03-FPD210.chr	B-2		11/25/2003	14:32:50	2990.00	11/25/03 2:32 PM	2.625	28.54	16.846	0	0	1	7.441	25.64	20.201	0	0	1	DMDS	0	0	0
Nov03-FPD248.chr	B-2		11/26/2003	14:27:14	4427.00	11/26/03 2:27 PM	2.633	329.87	53.268	0	0	1	7.425	35.37	23.203	0	0	1	DMDS	0	0	0
Nov03-FPD293.chr	B-2		11/28/2003	13:02:22	7936.00	11/28/03 1:02 PM	2.633	31.22	17.446	0	0	1	7.408	60.78	29.514	11.525	2.04	1	CS2	11.525	2.04	9.393
Nov03-FPD383.chr	B-2		12/3/2003	10:15:04	15021.00	12/3/03 10:15 AM	0	0		0	0	1	7.433	132.35	42.174	10.3	5.77	1	DMS	10.408	5.77	9.393
Nov03-FPD34.chr	B-3		11/23/2003	21:50:17	109.00	11/23/03 9:50 PM	0	0		0	0	1	0	0	1	0	0	1	DMDS	0	0	0
Nov03-FPD74.chr	B-3		11/24/2003	4:09:55	488.00	11/24/03 4:09 AM	2.608	2016.86	143.214	0	0	1	0	0	1	0	0	1	DMDS	0	0	0
Nov03-FPD172.chr	B-3	100	11/24/2003	18:27:56	1766.00	11/24/03 6:27 PM	0	0		0	0	1	0	0	1	0	0	1	DMDS	0	0	0
Nov03-FPD212.chr	B-3		11/25/2003	14:48:21	3006.00	11/25/03 2:48 PM	2.625			0	0	1	7.425		20.667	10.408		1	CS2	10.408	10.3	3.54
Nov03-FPD249.chr	B-3		11/26/2003	14:41:01	4441.00	11/26/03 2:41 PM	2.625	30.39	17.261	0	0	1	7.425	27.05	20.667	0	0	1	CS2	11.433	3.47	3.47

The following is a dense multi-column gas-chromatography data table. Each sample (B-3 through B-10) lists chromatogram files with date/time, cumulative time (min), and for each target gas (H2S, COS, CH3SH, DMS/CS2, DMDS) the retention time, peak area, concentration and units (ppm).

file	SAMPLE	INJECT SIZE	date	time	cum time	cum time (min)	H2S reten	H2S area	H2S conc	units	COS reten	COS area	COS conc	units	CH3SH reten	CH3SH area	CH3SH conc	units	gas	reten	area	conc	units	gas (DMDS)	reten	area	conc
Nov03-FPD294.chr	B-3		11/28/2003	13:24:29	11/28/03 1:24 PM	7988.00	2.558	46700		ppm	COS	0	0	1 ppm	CH3SH 7.425	82.58	33.914	ppm	DMS	0	0	0	1	DMDS	0	0	0
Nov03-FPD338.chr	B-3		12/2/2003	10:51:22	12/2/03 10:51 AM	13651.00	2.575	3.21	9.963	ppm	COS	0	0	1 ppm	CH3SH 7.416	96.52	36.436	ppm	DMS	10.325	0	0	1	DMDS	10.325	2.96	7.177
Nov03-FPD384.chr	B-3		12/3/2003	10:30:07	12/3/03 10:30 AM	15036.00	2.591	42.72	19.867	ppm	COS	0	0	1 ppm	CH3SH 7.433	132.68	42.223	ppm	DMS	10.358	0	0	1	DMDS	10.358	2.94	7.168
	B-4				11/23/03 8:00 PM	1.00	H2S		1		COS		1		CH3SH		1		DMS			1		DMDS			1
Nov03-FPD35.chr	B-4		11/23/2003	21:55:52	11/23/03 9:55 PM	114.00	0	0	0	1 ppm	COS 0	0	0	1 ppm	CH3SH 0	0	1	ppm	DMS 0	0	0	1		DMDS 0	0	0	0
Nov03-FPD75.chr	B-4		11/24/2003	4:19:01	11/24/03 4:19 AM	498.00	2.6	250.58	46.304	1 ppm	COS 0	0	0	1 ppm	CH3SH 0	0	1	ppm	DMS 0	0	0	1		DMDS 0	0	0	0
Nov03-FPD119.chr	B-4	250	11/24/2003	9:50:00	11/24/03 9:50 AM	867.00	2.625	12294.77	641.48	1 ppm	COS 0	0	0	1 ppm	CH3SH 0	0	1	ppm	DMS 0	0	0	1		DMDS 0	0	0	0
Nov03-FPD173.chr	B-4	100	11/24/2003	18:38:08	11/24/03 6:38 PM	1777.00	2.575	821.38	212.285	1 ppm	COS 0	0	0	1 ppm	CH3SH 7.408	13.57	15.538	ppm	DMS 0	0	0	1		DMDS 0	0	0	0
Nov03-FPD213.chr	B-4		11/25/2003	14:58:11	11/25/03 2:58 PM	3016.00	2.583	282.53	49.228	1 ppm	COS 0	0	0	1 ppm	CH3SH 7.416	30.84	21.911	ppm	DMS 10.333	2.68		1		DMDS 10.333	2.68	6.939
Nov03-FPD250.chr	B-4		11/26/2003	15:01:03	11/26/03 3:01 PM	4461.00	2.591	82.63	26.794	1 ppm	COS 0	0	0	1 ppm	CH3SH 7.433	72.62	31.985	ppm	DMS 10.391	3.27		1		DMDS 10.391	3.27	7.446
Nov03-FPD295.chr	B-4		11/28/2003	13:40:14	11/28/03 1:40 PM	7984.00	2.625	23.59	15.737	1 ppm	COS 0	0	0	1 ppm	CH3SH 7.416	180	48.72	ppm	DMS 10.525	3.07		1		DMDS 10.525	3.07	7.273
Nov03-FPD339.chr	B-4		12/2/2003	11:11:49	12/2/03 11:11 AM	13671.00	0	0	0	1 ppm	COS 0	0	0	1 ppm	CH3SH 7.416	222.29	53.823	ppm	DMS 10.325	2.93		1		DMDS 10.325	2.93	7.157
Nov03-FPD385.chr	B-4		12/3/2003	10:46:15	12/3/03 10:46 AM	15042.00	2.65	478.47	64.404	1 ppm	COS 0	0	0	1 ppm	CH3SH 7.433			ppm	DMS			2.93	7.157 ppm				
	B-5				11/23/03 8:00 PM	1.00	H2S		1		COS		1		CH3SH		1		DMS			1		DMDS			1
Nov03-FPD36.chr	B-5		11/23/2003	22:01:45	11/23/03 10:01 PM	120.00	0	0	0	1 ppm	COS 0	0	0	1 ppm	CH3SH 0	0	1	ppm	DMS 0	0	0	1		DMDS 0	0	0	0
Nov03-FPD76.chr	B-5		11/24/2003	4:24:49	11/24/03 4:24 AM	503.00	0	0	0	1 ppm	COS 0	0	0	1 ppm	CH3SH 0	0	1	ppm	DMS 0	0	0	1		DMDS 0	0	0	0
Nov03-FPD174.chr	B-5	250	11/24/2003	18:48:52	11/24/03 6:48 PM	1787.00	0	0	0	1 ppm	COS 0	0	0	1 ppm	CH3SH 0	0	1	ppm	DMS 0	0	0	1		DMDS 0	0	0	0
Nov03-FPD251.chr	B-5		11/26/2003	15:14:27	11/26/03 3:14 PM	4474.00	0	0	0	1 ppm	COS 0	0	0	1 ppm	CH3SH 7.416	11.22	14.422	ppm	DMS 0	0	0	1		DMDS 0	0	0	0
Nov03-FPD296.chr	B-5		11/28/2003	13:58:38	11/28/03 1:58 PM	8002.00	0	0	0	1 ppm	COS 0	0	0	1 ppm	CH3SH 7.416	9.63	13.663	ppm	DMS 10.325	2.82	0	0 ppm		DMDS 10.325	2.82	7.064
Nov03-FPD340.chr	B-5		12/2/2003	11:50:54	12/2/03 11:50 AM	13710.00	0	0	0	1 ppm	COS 0	0	0	1 ppm	CH3SH 7.191	3.81	9.777	ppm	CS2 0	0	0	0 ppm		CS2 0	3.31	0
Nov03-FPD386.chr	B-5		12/3/2003	11:01:11	12/3/03 11:01 AM	15057.00	0	0	0	1 ppm	COS 0	0	0	1 ppm	CH3SH 7.45	6.62	11.831	ppm	DMS 10.341	0	0	0		DMS 10.341	3.31	7.484
	B-6				11/23/03 8:00 PM	1.00	H2S		1		COS		1		CH3SH		1		DMS			1		DMDS			1
Nov03-FPD37.chr	B-6		11/23/2003	22:06:59	11/23/03 10:06 PM	125.00	0	0	0	1 ppm	COS 0	0	0	1 ppm	CH3SH 0	0	1	ppm	DMS 0	0	0	1		DMDS 0	0	0	0
Nov03-FPD77.chr	B-6		11/24/2003	4:30:32	11/24/03 4:30 AM	509.00	2.625	60.26	23.142	1 ppm	COS 0	0	0	1 ppm	CH3SH 0	0	1	ppm	DMS 0	0	0	1		DMDS 0	0	0	0
Nov03-FPD121.chr	B-6	250	11/24/2003	10:04:16	11/24/03 10:04 AM	897.00	2.65	60.26	23.142	1 ppm	COS 0	0	0	1 ppm	CH3SH 0	0	1	ppm	DMS 0	0	0	1		DMDS 0	0	0	0
Nov03-FPD215.chr	B-6		11/25/2003	15:34:17	11/25/03 3:34 PM	3053.00	2.625	34.68	18.222	1 ppm	COS 0	0	0	1 ppm	CH3SH 7.416	4.52	10.382	ppm	CS2 11.35	2.69	0	0 ppm		CS2 11.35	2.69	
Nov03-FPD252.chr	B-6		11/26/2003	15:34:17	11/26/03 3:34 PM	4494.00	2.625	1046.35	96.164	1 ppm	COS 0	0	0	1 ppm	CH3SH 7.433	21.21	18.67	ppm	DMS 0	0	0	0		DMDS 0	2.74	6.993
Nov03-FPD341.chr	B-6		11/28/2003	14:17:56	11/28/03 1:58 PM	8011.00	2.625	4.29	10.343	1 ppm	COS 0	0	0	1 ppm	CH3SH 7.425	46.05	26.06	ppm	DMS 10.333	3.78	7.884 ppm			DMS 10.3	3.78	7.884
Nov03-FPD342.chr	B-6		12/2/2003	12:10:16	12/2/03 12:10 PM	13730.00	2.483	75465.76	3703.967	2.972 ppm	COS 4.183	2.54	2.972	1 ppm	CH3SH 7.416	86.89	34.716	ppm	DMS 10.3	10.3	7.884	ppm		DMS 10.3	3.78	7.884
Nov03-FPD387.chr	B-6		12/3/2003	11:15:21	12/3/03 11:15 AM	15071.00	2.45	90361.91	4426.122	4.13 ppm	COS 4.125	4.28	4.13	1 ppm	CH3SH 7.433	147.94	44.433	ppm	DMS 10.341	10.341	7.804 ppm			DMS 10.341	3.69	7.804
	B-7				11/23/03 8:00 PM	1.00	H2S		1		COS		1		CH3SH		1		DMS			1		DMDS			1
Nov03-FPD38.chr	B-7		11/23/2003	22:13:58	11/23/03 10:13 PM	132.00	0	0	0	1 ppm	COS 0	0	0	1 ppm	CH3SH 0	0	1	ppm	DMS 0	0	0	1		DMDS 0	0	0	0
Nov03-FPD78.chr	B-7		11/24/2003	4:36:07	11/24/03 4:36 AM	515.00	2.608	319.67	52.404	1 ppm	COS 0	0	0	1 ppm	CH3SH 0	0	1	ppm	DMS 0	0	0	1		DMDS 0	0	0	0
Nov03-FPD122.chr	B-7	100	11/24/2003	10:13:54	11/24/03 10:13 AM	906.00	2.591	4715.74	685.135	1 ppm	COS 0	0	0	1 ppm	CH3SH 0	0	1	ppm	CS2 0	0	0	1 ppm		CS2 0	0	0
Nov03-FPD216.chr	B-7	100	11/24/2003	19:05:41	11/24/03 7:05 PM	1799.00	2.625	183.98	99.0125	1 ppm	COS 0	0	0	1 ppm	CH3SH 0	0	1	ppm	DMS 10.575	3.95	8.032	1 ppm		DMS 10.575	3.95	8.032
Nov03-FPD253.chr	B-7		11/25/2003	17:02:20	11/25/03 5:02 PM	3209.00	2.6	87.56	27.51	1 ppm	COS 0	0	0	1 ppm	CH3SH 7.425	15.12	16.272	ppm	DMS 0	0	0	1		DMDS 0	0	0	0
Nov03-FPD298.chr	B-7		11/26/2003	15:49:52	11/26/03 3:49 PM	4650.00	2.566	1278.34	107.411	1 ppm	COS 0	0	0	1 ppm	CH3SH 7.433	44.04	25.553	ppm	DMS 0	0	0	1		DMDS 0	0	0	0
Nov03-FPD342.chr	B-7		11/28/2003	14:31:55	11/28/03 2:31 PM	8026.00	2.583	10.93	12.392	1 ppm	COS 0	0	0	1 ppm	CH3SH 7.425	103.46	37.624	ppm	DMS 0	0	0	1		DMDS 0	0	0	0
Nov03-FPD388.chr	B-7		12/2/2003	12:28:26	12/2/03 12:28 PM	13744.00	2.616	386.34	57.723	1 ppm	COS 0	0	0	1 ppm	CH3SH 7.425	204.55	51.755	ppm	DMS 10.283	2.36		1		DMS 10.283	2.36	6.664
	B-7		12/3/2003	11:35:06	12/3/03 11:35 AM	15091.00	2.508	72655.36	3567.721	1 ppm	COS 0	0	0	1 ppm	CH3SH			ppm	DMS									
	B-8				11/23/03 8:00 PM	1.00	H2S		1		COS		1		CH3SH		1		DMS			1		DMDS			1
Nov03-FPD39.chr	B-8		11/23/2003	22:18:59	11/23/03 10:18 PM	137.00	0	0	0	1 ppm	COS 0	0	0	1 ppm	CH3SH 0	0	1	ppm	DMS 0	0	0	1		DMDS 0	0	0	0
Nov03-FPD79.chr	B-8		11/24/2003	4:41:38	11/24/03 4:41 AM	520.00	2.533	60018.5	2955.094	1 ppm	COS 0	0	0	1 ppm	CH3SH 0	0	1	ppm	DMS 0	0	0	1		DMDS 0	0	0	0
Nov03-FPD123.chr	B-8	250	11/24/2003	10:24:56	11/24/03 10:24 AM	536.00	2.566	37842.06	4699.9875	1 ppm	COS 0	0	0	1 ppm	CH3SH 0	0	1	ppm	DMS 0	0	0	1		DMDS 0	0	0	0
Nov03-FPD178.chr	B-8	250	11/24/2003	19:17:25	11/24/03 7:17 PM	541.00	2.641	8693	4668.69	1 ppm	COS 0	0	0	1 ppm	CH3SH 0	0	1	ppm	DMS 0	0	0	1		DMDS 0	0	0	0
Nov03-FPD217.chr	B-8	250	11/25/2003	17:24:57	11/25/03 5:24 PM	3231.00	2.533	67171.91	8254.7175	1 ppm	COS 0	0	0	1 ppm	CH3SH 0	0	1	ppm	DMS 0	0	0	1		DMDS 0	0	0	0
Nov03-FPD254.chr	B-8		11/26/2003	16:03:02	11/26/03 4:03 PM	4664.00	2.458	105144.81	5142.787	1 ppm	COS 4	20.9	3.942	1 ppm	CH3SH 0	0	1	ppm	DMS 0	0	0	1		DMDS 0	0	0	0
Nov03-FPD299.chr	B-8		11/28/2003	14:52:58	11/28/03 2:52 PM	8047.00	2.416	117171.04	5725.81	1 ppm	COS 4.175	11.321		1 ppm	CH3SH 0	0	1	ppm	DMS 7.13	7.13		1		DMS 10.164	7.13	10.164
Nov03-FPD343.chr	B-8		12/2/2003	12:48:22	12/2/03 12:48 PM	13764.00	2.508	95692.66	11711.383	14.5125 ppm	COS 4.191	6.89	14.5125	1 ppm	CH3SH 0	0	8.989 ppm		DMS 0	0	0	1		DMDS 0	0	0	0
Nov03-FPD389.chr	B-8		12/3/2003	11:50:27	12/3/03 11:50 AM	15106.00	2.391	132370.1	6462.65	12.706 ppm	COS 4.158	25.81	12.706	1 ppm	CH3SH		10.975 ppm		DMS 2.88	2.88	8.989	1		DMS	5.22	10.975
	B-9				11/23/03 8:00 PM	1.00	H2S		10.7		COS		1		CH3SH		1		DMS			1		DMDS			1
Nov03-FPD40.chr	B-9		11/23/2003	22:24:45	11/23/03 10:24 PM	143.00	0	0	0	1 ppm	COS 0	0	0	1 ppm	CH3SH 0	0	1	ppm	DMS 0	0	0	1		DMDS 0	0	0	0
Nov03-FPD80.chr	B-9	250	11/24/2003	4:47:35	11/24/03 4:47 AM	526.00	2.525	5.27	10.688	1 ppm	COS 0	0	0	1 ppm	CH3SH 0	0	1	ppm	DMS 0	0	0	1		DMDS 0	0	0	0
Nov03-FPD81.chr	B-9	100	11/24/2003	4:57:48	11/24/03 4:57 AM	536.00	2.5	5.19	10.659	1 ppm	COS 0	0	0	1 ppm	CH3SH 0	0	1	ppm	DMS 0	0	0	1		DMDS 0	0	0	0
Nov03-FPD82.chr	B-9	50	11/24/2003	5:02:22	11/24/03 5:02 AM	541.00	2.625	5.38	10.727	1 ppm	COS 0	0	0	1 ppm	CH3SH 0	0	1	ppm	DMS 0	0	0	1		DMDS 0	0	0	0
Nov03-FPD124.chr	B-9	100	11/24/2003	10:31:41	11/24/03 10:31 AM	924.00	2.583	12.18	12.734	1 ppm	COS 0	0	0	1 ppm	CH3SH 0	0	1	ppm	DMS 0	0	0	0		DMDS 0	6.84	
Nov03-FPD218.chr	B-9		11/25/2003	17:39:08	11/25/03 5:39 PM	3246.00	2.6	18.86	14.563	3.942 ppm	COS 4.05	4	3.942	1 ppm	CH3SH 22.7	19.236	ppm	CS2 11.625	11.625	6.84	ppm		CS2 11.625	6.84	
Nov03-FPD300.chr	B-9		11/28/2003	15:08:22	11/28/03 3:08 PM	8063.00	2.416			11.321 ppm	COS 4.175	20.9	11.321	1 ppm	CH3SH 78.54	33.163	ppm	DMS 10.35	10.35	8.132 ppm			DMS 10.35	4.07	8.132
Nov03-FPD344.chr	B-9	100	12/2/2003	13:00:26	12/2/03 1:00 PM	13776.00	2.508			14.5125 ppm	COS 4.191	6.89	14.5125	1 ppm	CH3SH 14.63	40.105	ppm	DMS 0	0	0	1		DMDS 0	0	0	0
Nov03-FPD390.chr	B-9		12/3/2003	12:04:14	12/3/03 12:04 PM	15120.00	2.391			12.706 ppm	COS 4.158	25.81	12.706	1 ppm	CH3SH 110.26	38.755	ppm	DMS 10.35	10.35	8.815 ppm			DMS 10.35	4.86	8.815
	B-10				11/23/03 8:00 PM	1.00	H2S		10.7		COS		1		CH3SH		1		DMS			1		DMDS			1
Nov03-FPD83.chr	B-10	250	11/24/2003	5:06:54	11/24/03 5:06 AM	545.00	2.525	5.27	10.688	1 ppm	COS 0	0	0	1 ppm	CH3SH 0	0	1	ppm	DMS 0	0	0	1		DMDS 0	0	0	0
Nov03-FPD126.chr	B-10	250	11/24/2003	10:52:55	11/24/03 10:52 AM	945.00	2.5	5.19	10.659	1 ppm	COS 0	0	0	1 ppm	CH3SH 0	0	1	ppm	DMS 0	0	0	1		DMDS 0	0	0	0
Nov03-FPD180.chr	B-10	250	11/24/2003	19:24:49	11/24/03 7:24 PM	1818.00	2.625	5.38	10.727	1 ppm	COS 0	0	0	1 ppm	CH3SH 0	0	1	ppm	DMS 0	0	0	1		DMDS 0	0	0	0
Nov03-FPD301.chr	B-10		11/28/2003	15:27:31	11/28/03 3:27 PM	8074.00	2.583	12.18	12.734	1 ppm	COS 0	0	0	1 ppm	CH3SH 0	0	1	ppm	DMS 10.366	6.63	9.879 ppm			DMS 10.366	6.63	9.879
Nov03-FPD391.chr	B-10		12/3/2003	12:22:59	12/3/03 12:22 PM	15138.00	2.6	18.86	14.563	1 ppm	COS 0	0	0	1 ppm	CH3SH 0	0	1	ppm	DMS 0	0	0	1		DMDS 0	0	0	0

315

Data table of chromatography results (gas analyses: H2S, COS, CH3SH, DMS, DMDS). Columns: file, SAMPLE, INJECT SIZE, date, time, cum time, cum time (min), then for each gas: gas, reten, area, conc, units.

file	SAMPLE	INJECT SIZE	date	time	cum time	cum time (min)	H2S gas	H2S reten	H2S area	H2S conc	H2S units	COS gas	COS reten	COS area	COS conc	COS units	CH3SH gas	CH3SH reten	CH3SH area	CH3SH conc	CH3SH units	DMS gas	DMS reten	DMS area	DMS conc	DMS units	DMDS gas	DMDS reten	DMDS area	DMDS conc	DMDS units
					11/23/03 8:00 PM	1.00																									
Nov03-FPD45.chr	C-1		11/23/2003	22:55:01	11/23/03 10:55 PM	174.01	H2S	0	0	0	1 ppm	COS	0	0	0	1 ppm	CH3SH	0	0	0	1 ppm	DMS	0	0	0	1 ppm	DMDS	0	0	0	1
Nov03-FPD89.chr	C-1		11/24/2003	5:39:49	11/24/03 5:29 AM	568.00	H2S	0	0	0	1 ppm	COS	0	0	0	1 ppm	CH3SH	0	0	0	1 ppm	DMS	0	0	0	1 ppm	DMDS	0	0	0	1
Nov03-FPD132.chr	C-1		11/24/2003	11:44:47	11/24/03 11:44 AM	997.00	H2S	0	0	0	1 ppm	COS	0	0	0	1 ppm	CH3SH	0	0	0	1 ppm	DMS	0	0	0	1 ppm	DMDS	0	0	0	1
Nov03-FPD219.chr	C-1		11/25/2003	17:57:28	11/25/03 5:57 PM	3262.00	H2S	0	0	0	1 ppm	COS	0	0	0	1 ppm	CH3SH	0	0	0	1 ppm	DMS	0	0	0	1 ppm	DMDS	0	0	0	1
Nov03-FPD257.chr	C-1		11/26/2003	16:54:11	11/26/03 4:54 PM	4715.00	H2S	2.566	12.08		1 ppm	COS	0	0	0	1 ppm	CH3SH	0	0	0	1 ppm	DMS	0	0	0	1 ppm	DMDS	0	0	0	1
Nov03-FPD302.chr	C-1		11/28/2003	15:46:37	11/28/03 3:46 PM	8101.00	H2S	2.641	5.74		1 ppm	COS	0	0	0	1 ppm	CH3SH	0	0	0	1 ppm	DMS	0	0	0	1 ppm	DMDS	0	0	0	1
Nov03-FPD346.chr	C-1		12/2/2003	13:24:47	12/2/03 1:24 PM	13800.00	H2S	0	0	0	1 ppm	COS	0	0	0	1 ppm	CH3SH	0	0	0	1 ppm	DMS	0	0	0	1 ppm	DMDS	0	0	0	1
Nov03-FPD392.chr	C-1		12/3/2003	12:37:05	12/3/03 12:37 PM	15153.00	H2S	0	0	0	1 ppm	COS	0	0	0	1 ppm	CH3SH	0	0	0	1 ppm	DMS	0	0	0	1 ppm	DMDS	0	0	0	1
					11/23/03 8:00 PM	1.00																									
Nov03-FPD46.chr	C-2		11/23/2003	23:03:13	11/23/03 11:03 PM	182.00	H2S	0	0	0	1 ppm	COS	0	0	0	1 ppm	CH3SH	0	0	0	1 ppm	DMS	0	0	0	1 ppm	DMDS	0	0	0	1
Nov03-FPD90.chr	C-2		11/24/2003	5:45:32	11/24/03 5:45 AM	584.00	H2S	0	0	0	1 ppm	COS	0	0	0	1 ppm	CH3SH	0	0	0	1 ppm	DMS	0	0	0	1 ppm	DMDS	0	0	0	1
Nov03-FPD133.chr	C-2		11/24/2003	11:49:00	11/24/03 11:49 AM	1002.00	H2S	2.65	11.1	12.441	1 ppm	COS	0	0	0	1 ppm	CH3SH	0	0	0	1 ppm	DMS	0	0	0	1 ppm	DMDS	0	0	0	1
Nov03-FPD220.chr	C-2		11/25/2003	18:07:09	11/25/03 6:07 PM	3272.00	H2S	2.591	23.82	15.788	1 ppm	COS	0	0	0	1 ppm	CH3SH	0	0	0	1 ppm	DMS	0	0	0	1 ppm	DMDS	0	0	0	1
Nov03-FPD258.chr	C-2		11/26/2003	17:05:07	11/26/03 5:05 PM	4722.00	H2S	2.6	13.89	13.203	1 ppm	COS	0	0	0	1 ppm	CH3SH	0	0	0	1 ppm	DMS	0	0	0	1 ppm	DMS	10.183	3.04	7.249	1
Nov03-FPD303.chr	C-2		11/28/2003	16:03:04	11/28/03 4:03 PM	8118.00	H2S	2.633	568.01	70.293	1 ppm	COS	0	0	0	1 ppm	CH3SH	0	0	0	1 ppm	DMS	0	0	0	1 ppm	DMDS	0	0	0	1
Nov03-FPD347.chr	C-2		12/2/2003	13:30:58	12/2/03 1:30 PM	13806.00	H2S	2.65	340.19	54.091	1 ppm	COS	0	0	0	1 ppm	CH3SH	0	0	0	1 ppm	DMS	0	0	0	1 ppm	DMDS	0	0	0	1
Nov03-FPD393.chr	C-2		12/3/2003	12:45:31	12/3/03 12:45 PM	15160.00	H2S	2.658	23.31	15.674	1 ppm	COS	0	0	0	1 ppm	CH3SH	0	0	0	1 ppm	DMS	0	0	0	1 ppm	DMDS	0	0	0	1
					11/23/03 8:00 PM	1.00																									
Nov03-FPD47.chr	C-3		11/23/2003	23:08:28	11/23/03 11:08 PM	187.00	H2S	0	0	0	1 ppm	COS	0	0	0	1 ppm	CH3SH	0	0	0	1 ppm	DMS	0	0	0	1 ppm	DMDS	0	0	0	1
Nov03-FPD91.chr	C-3		11/24/2003	5:50:54	11/24/03 5:50 AM	589.00	H2S	0	0	0	1 ppm	COS	0	0	0	1 ppm	CH3SH	0	0	0	1 ppm	DMS	0	0	0	1 ppm	DMDS	0	0	0	1
Nov03-FPD134.chr	C-3		11/24/2003	11:53:05	11/24/03 11:53 AM	1006.00	H2S	0	0	0	1 ppm	COS	0	0	0	1 ppm	CH3SH	0	0	0	1 ppm	DMS	0	0	0	1 ppm	DMDS	0	0	0	1
Nov03-FPD183.chr	C-3		11/24/2003	19:36:15	11/24/03 7:36 PM	1830.00	H2S	0	0	0	1 ppm	COS	0	0	0	1 ppm	CH3SH	0	0	0	1 ppm	DMS	0	0	0	1 ppm	DMDS	0	0	0	1
Nov03-FPD221.chr	C-3		11/25/2003	18:16:38	11/25/03 6:16 PM	3281.00	H2S	2.591	5.63	10.812	1 ppm	COS	0	0	0	1 ppm	CH3SH	0	0	0	1 ppm	DMS	0	0	0	1 ppm	DMDS	0	0	0	1
Nov03-FPD259.chr	C-3		11/26/2003	17:20:05	11/26/03 5:20 PM	4737.00	H2S	2.658	4.6	10.452	1 ppm	COS	0	0	0	1 ppm	CH3SH	0	0	0	1 ppm	DMS	0	0	0	1 ppm	DMDS	0	0	0	1
Nov03-FPD304.chr	C-3		11/28/2003	16:19:14	11/28/03 4:19 PM	8134.00	H2S	2.625	338.91	53.988	1 ppm	COS	0	0	0	1 ppm	CH3SH	0	0	0	1 ppm	DMS	0	0	0	1 ppm	DMDS	0	0	0	1
Nov03-FPD348.chr	C-3	100	12/2/2003	13:44:53	12/2/03 1:44 PM	13820.00	H2S	2.65	63.34	59.1175	1 ppm	COS	0	0	0	1 ppm	CH3SH	0	0	0	1 ppm	DMS	0	0	0	1 ppm	DMDS	0	0	0	1
Nov03-FPD394.chr	C-3		12/3/2003	12:57:12	12/3/03 12:57 PM	15172.00	H2S	2.625	21.09	15.173	1 ppm	COS	0	0	0	1 ppm	CH3SH	0	0	0	1 ppm	DMS	0	0	0	1 ppm	DMDS	0	0	0	1
					11/23/03 8:00 PM	1.00																									
Nov03-FPD48.chr	C-4		11/23/2003	23:21:02	11/23/03 11:21 PM	200.00	H2S	0	0	0	1 ppm	COS	0	0	0	1 ppm	CH3SH	0	0	0	1 ppm	DMS	0	0	0	1 ppm	DMS	10.458	3.43	7.682	1
Nov03-FPD92.chr	C-4		11/24/2003	5:56:34	11/24/03 5:56 AM	595.00	H2S	0	0	0	1 ppm	COS	0	0	0	1 ppm	CH3SH	0	0	0	1 ppm	DMS	0	0	0	1 ppm	DMDS	0	0	0	1
Nov03-FPD135.chr	C-4		11/24/2003	11:58:02	11/24/03 11:58 AM	1011.00	H2S	0	0	0	1 ppm	COS	0	0	0	1 ppm	CH3SH	0	0	0	1 ppm	DMS	0	0	0	1 ppm	DMDS	0	0	0	1
Nov03-FPD182.chr	C-4		11/24/2003	19:32:48	11/24/03 7:32 PM	1834.00	H2S	0	0	0	1 ppm	COS	0	0	0	1 ppm	CH3SH	0	0	0	1 ppm	DMS	0	0	0	1 ppm	DMDS	0	0	0	1
Nov03-FPD222.chr	C-4		11/25/2003	18:26:20	11/25/03 6:26 PM	3291.00	H2S	0	0	0	1 ppm	COS	0	0	0	1 ppm	CH3SH	0	0	0	1 ppm	DMS	0	0	0	1 ppm	DMDS	0	0	0	1
Nov03-FPD260.chr	C-4		11/26/2003	17:28:05	11/26/03 5:28 PM	4745.00	H2S	2.625	83.77	26.96	1 ppm	COS	0	0	0	1 ppm	CH3SH	0	0	0	1 ppm	CS2	0	0	0	1 ppm	DMS	0	0	0	1 ppm
Nov03-FPD305.chr	C-4		11/28/2003	16:33:18	11/28/03 4:33 PM	8148.00	H2S	2.625	184.34	39.644	1 ppm	COS	0	0	0	1 ppm	CH3SH	0	0	0	1 ppm	DMS	0	0	0	1 ppm	DMDS	0	0	0	1
Nov03-FPD349.chr	C-4		12/2/2003	13:56:15	12/2/03 1:56 AM	13832.00	H2S	2.641	107.36	30.385	1 ppm	COS	0	0	0	1 ppm	CH3SH	0	0	0	1 ppm	DMS	0	0	0	1 ppm	DMDS	0	0	0	1
					11/23/03 8:00 PM	1.00																									
Nov03-FPD49.chr	C-5		11/23/2003	23:40:24	11/23/03 11:40 PM	219.00	H2S	0	0	0	1 ppm	COS	0	0	0	1 ppm	CH3SH	0	0	0	1 ppm	DMS	0	0	0	1 ppm	DMDS	0	0	0	1
Nov03-FPD93.chr	C-5		11/24/2003	6:02:27	11/24/03 6:02 AM	601.00	H2S	0	0	0	1 ppm	COS	0	0	0	1 ppm	CH3SH	0	0	0	1 ppm	DMS	0	0	0	1 ppm	DMDS	0	0	0	1
Nov03-FPD136.chr	C-5		11/24/2003	12:05:29	11/24/03 12:05 PM	1018.00	H2S	0	0	0	1 ppm	COS	0	0	0	1 ppm	CH3SH	0	0	0	1 ppm	CS2	0	0	0	1 ppm	DMS	0	0	0	1 ppm
Nov03-FPD223.chr	C-5		11/25/2003	18:34:10	11/25/03 6:34 PM	3299.00	H2S	0	0	0	1 ppm	COS	0	0	0	1 ppm	CH3SH	0	0	0	1 ppm	DMS	0	0	0	1 ppm	DMDS	0	0	0	1
Nov03-FPD261.chr	C-5		11/26/2003	17:37:58	11/26/03 5:37 PM	4754.00	H2S	0	0	0	1 ppm	COS	0	0	0	1 ppm	CH3SH	0	0	0	1 ppm	DMS	0	0	0	1 ppm	DMDS	0	0	0	1
Nov03-FPD306.chr	C-5		11/28/2003	16:48:52	11/28/03 4:48 PM	8163.00	H2S	2.566	192.5	40.52	1 ppm	COS	0	0	0	1 ppm	CH3SH	0	0	0	1 ppm	DMS	0	0	0	1 ppm	DMDS	0	0	0	1
Nov03-FPD350.chr	C-5		12/2/2003	14:05:59	12/2/03 2:05 PM	13841.00	H2S	2.616	4435.59	260.473	1 ppm	COS	0	0	0	1 ppm	CH3SH	0	0	0	1 ppm	DMS	0	0	0	1 ppm	DMDS	0	0	0	1
Nov03-FPD396.chr	C-5		12/3/2003	13:18:55	12/3/03 1:18 PM	15193.00	H2S	2.658	2066.67	145.629	1 ppm	COS	0	0	0	1 ppm	CH3SH	0	0	0	1 ppm	DMS	0	0	0	1 ppm	DMS	10.275	3.46	7.614	1
					11/23/03 8:00 PM	1.00																									
Nov03-FPD50.chr	C-6		11/23/2003	23:46:26	11/23/03 11:46 PM	225.00	H2S	0	0	0	1 ppm	COS	0	0	0	1 ppm	CH3SH	0	0	0	1 ppm	DMS	0	0	0	1 ppm	DMDS	0	0	0	1
Nov03-FPD94.chr	C-6		11/24/2003	6:07:46	11/24/03 6:07 AM	606.00	H2S	0	0	0	1 ppm	COS	0	0	0	1 ppm	CH3SH	0	0	0	1 ppm	DMS	0	0	0	1 ppm	DMDS	0	0	0	1
Nov03-FPD137.chr	C-6		11/24/2003	12:10:09	11/24/03 12:10 PM	1023.00	H2S	0	0	0	1 ppm	COS	0	0	0	1 ppm	CH3SH	0	0	0	1 ppm	DMS	0	0	0	1 ppm	DMDS	0	0	0	1
Nov03-FPD224.chr	C-6		11/25/2003	18:45:45	11/25/03 6:45 PM	3310.00	H2S	0	0	0	1 ppm	COS	0	0	0	1 ppm	CH3SH	0	0	0	1 ppm	DMS	0	0	0	1 ppm	DMDS	0	0	0	1
Nov03-FPD262.chr	C-6		11/26/2003	17:44:09	11/26/03 5:44 PM	4761.00	H2S	0	0	0	1 ppm	COS	0	0	0	1 ppm	CH3SH	0	0	0	1 ppm	DMS	0	0	0	1 ppm	DMDS	0	0	0	1
Nov03-FPD397.chr	C-6		12/3/2003	13:32:48	12/3/03 1:32 PM	15207.00	H2S	0	0	0	1 ppm	COS	0	0	0	1 ppm	CH3SH	0	0	0	1 ppm	DMS	0	0	0	1 ppm	DMDS	0	0	0	1
					11/23/03 8:00 PM	1.00																									
Nov03-FPD51.chr	C-7		11/23/2003	23:53:44	11/23/03 11:53 PM		H2S	0	0	0	1 ppm	COS	0	0	0	1 ppm	CH3SH	0	0	0	1 ppm	DMS	0	0	0	1 ppm	DMDS	0	0	0	1
Nov03-FPD95.chr	C-7		11/24/2003	6:13:17	11/24/03 6:13 AM		H2S	0	0	0	1 ppm	COS	0	0	0	1 ppm	CH3SH	0	0	0	1 ppm	DMS	0	0	0	1 ppm	DMDS	0	0	0	1
Nov03-FPD138.chr	C-7		11/24/2003	12:14:16	11/24/03 12:14 PM		H2S	0	0	0	1 ppm	COS	0	0	0	1 ppm	CH3SH	0	0	0	1 ppm	DMS	0	0	0	1 ppm	DMDS	0	0	0	1
Nov03-FPD181.chr	C-7		11/24/2003	19:28:41	11/24/03 7:28 PM		H2S	0	0	0	1 ppm	COS	0	0	0	1 ppm	CH3SH	0	0	0	1 ppm	DMS	0	0	0	1 ppm	DMDS	0	0	0	1
Nov03-FPD225.chr	C-7		11/25/2003	18:58:39	11/25/03 6:58 PM		H2S	0	0	0	1 ppm	COS	0	0	0	1 ppm	CH3SH	0	0	0	1 ppm	DMS	0	0	0	1 ppm	DMDS	0	0	0	1
Nov03-FPD263.chr	C-7		11/26/2003	17:52:21	11/26/03 12:00 PM		H2S	0	0	0	1 ppm	COS	0	0	0	1 ppm	CH3SH	0	0	0	1 ppm	CS2	0	0	0	1 ppm	DMS	0	0	0	1 ppm
Nov03-FPD308.chr	C-7		11/28/2003	17:17:51	11/28/03 5:17 PM		H2S	0	0	0	1 ppm	COS	0	0	0	1 ppm	CH3SH	0	0	0	1 ppm	DMS	0	0	0	1 ppm	DMDS	0	0	0	1
Nov03-FPD352.chr	C-7		12/2/2003	14:20:25	12/2/03 2:20 PM		H2S	0	0	0	1 ppm	COS	0	0	0	1 ppm	CH3SH	0	0	0	1 ppm	DMS	0	0	0	1 ppm	DMDS	0	0	0	1
Nov03-FPD398.chr	C-7		12/3/2003	13:40:37	12/3/03 1:40 PM		H2S	0	0	0	1 ppm	COS	0	0	0	1 ppm	CH3SH	0	0	0	1 ppm	DMS	0	0	0	1 ppm	DMDS	0	0	0	1
					11/23/03 8:00 PM	1.00																									
Nov03-FPD52.chr	C-8		11/24/2003	0:02:26	11/24/03 12:02 AM		H2S	0	0	0	1 ppm	COS	0	0	0	1 ppm	CH3SH	0	0	0	1 ppm	DMS	0	0	0	1 ppm	DMDS	0	0	0	1
Nov03-FPD96.chr	C-8		11/24/2003	6:18:38	11/24/03 6:18 AM		H2S	0	0	0	1 ppm	COS	0	0	0	1 ppm	CH3SH	0	0	0	1 ppm	DMS	0	0	0	1 ppm	DMDS	0	0	0	1
Nov03-FPD139.chr	C-8		11/24/2003	12:18:02	11/24/03 12:18 PM		H2S	0	0	0	1 ppm	COS	0	0	0	1 ppm	CH3SH	0	0	0	1 ppm	DMS	0	0	0	1 ppm	DMDS	0	0	0	1

Dense chromatography data table (rotated). Best-effort transcription.

SAMPLE	INJECT SIZE	pH	date	time	cum time	cum time (min)	gas	reten	area	conc	units	gas	reten	area	conc	units	gas	reten	area	conc	units	gas	reten	area	conc	units	gas	reten	area	conc
Nov03-FPD264.chr	C-8		11/26/2003	18:03:42	11/26/03 6:03 PM		H2S	2.525	15.45	13.629	ppm	COS		0	0	ppm	CHSH		0	0	ppm	DMS		0	0	ppm	DMDS		0	0
Nov03-FPD309.chr	C-8		11/28/2003	17:27:40	11/28/03 5:27 PM		H2S	2.591	2.71	9.787	ppm	COS		0	0	ppm	CHSH		0	0	ppm	DMS		0	0	ppm	DMDS		0	0
Nov03-FPD353.chr	C-8		12/2/2003	14:30:57	12/2/03 2:30 PM		H2S	2.591	0		ppm	COS		0	0	ppm	CHSH		0	0	ppm	DMS		0	0	ppm	DMDS		0	0
Nov03-FPD399.chr	C-8		12/3/2003	13:55:01	12/3/03 1:55 PM	1.00	H2S		0		ppm	COS		0	0	ppm	CHSH		0	0	ppm	DMS		0	0	ppm	DMDS		0	0
Nov03-FPD53.chr	C-9		11/24/2003	0:09:34	11/24/03 12:09 AM		H2S		0		ppm	COS		0	0	ppm	CHSH		0	0	ppm	DMS		0	0	ppm	DMDS		0	0
Nov03-FPD97.chr	C-9		11/24/2003	6:24:00	11/24/03 6:24 AM		H2S		0		ppm	COS		0	0	ppm	CHSH		0	0	ppm	DMS		0	0	ppm	DMDS		0	0
Nov03-FPD140.chr	C-9		11/24/2003	12:23:53	11/24/03 12:23 PM		H2S		0		ppm	COS		0	0	ppm	CHSH		0	0	ppm	DMS		0	0	ppm	DMDS		0	0
Nov03-FPD273.chr	C-9		11/26/2003	19:51:11	11/26/03 7:51 PM		H2S	2.508	3.92	10.214	ppm	COS		0	0	ppm	CHSH		0	0	ppm	DMS		0	0	ppm	DMDS		0	0
Nov03-FPD310.chr	C-9		11/28/2003	17:38:06	11/28/03 5:38 PM		H2S	2.591	1026	95.178	ppm	COS		0	0	ppm	CHSH		0	0	ppm	DMS		0	0	ppm	DMDS		0	0
Nov03-FPD354.chr	C-9		12/2/2003	14:39:31	12/2/03 2:39 PM		H2S	2.65	10919.29	574.798	ppm	COS		0	0	ppm	CHSH		0	0	ppm	DMS		0	0	ppm	DMDS		0	0
Nov03-FPD400.chr	C-9		12/3/2003	14:06:58	12/3/03 2:06 PM		H2S	2.633	29295.99	1465.688	ppm	COS		0	0	ppm	CHSH		0	0	ppm	DMS		0	0	ppm	DMDS		0	0
Nov03-FPD98.chr	C-10		11/24/2003	6:29:28	11/24/03 6:29 AM	628.00	H2S	0	0		ppm	COS		0	0	ppm	CHSH		0	0	ppm	DMS		0	0	ppm	DMDS		0	0
Nov03-FPD141.chr	C-10		11/24/2003	12:27:25	11/24/03 12:27 PM	1040.00	H2S	0	0		ppm	COS		0	0	ppm	CHSH		0	0	ppm	DMS		0	0	ppm	DMDS		0	0
Nov03-FPD275.chr	C-10		11/26/2003	20:17:14	11/26/03 8:17 PM		H2S	0	0		ppm	COS		0	0	ppm	CHSH		0	0	ppm	DMS		0	0	ppm	DMDS		0	0
Nov03-FPD311.chr	C-10		11/28/2003	17:48:53	11/28/03 5:48 PM	8223.00	H2S	0	0		ppm	COS		0	0	ppm	CHSH		0	0	ppm	DMS		0	0	ppm	DMDS		0	0
Nov03-FPD401.chr	C-10		12/3/2003	14:18:36	12/3/03 2:18 PM	15253.00	H2S	0	0		ppm	COS		0	0	ppm	CHSH		0	0	ppm	DMS		0	0	ppm	DMDS		0	0
Nov03-FPD377.chr	DRY BLANK		12/3/2003	9:00:13			H2S	2.8	4.44	10.396	ppm	COS	4.308	4.24	4.105	ppm	CHSH	7.516	3.38	9.415	ppm	DMS				ppm	DMDS	11.391	4	
Nov03-FPD413.chr	DRY BLANK		12/4/2003	9:31:22			H2S	2.416	2.8	9.819	ppm	COS	3.991	7.05	5.88	ppm	CHSH	7.466	3.6	9.599	ppm	DMS				ppm	DMDS	10.366	2.28	6.597
Nov03-FPD379.chr	h2s STAND		12/3/2003	9:54:23			H2S	2.625	774.53	82.399	ppm	COS	4.225	7.12	5.909	ppm	CHSH		0	1	ppm	DMS				ppm	DMDS		0	0
Nov03-FPD143.chr	INTAKE TUBE		11/24/2003	12:38:09			H2S	2.625	5.44	10.747	ppm	COS	4.175	717.25	70.999	ppm	CHSH	7.391	570.2	68.509	ppm	DMS				ppm	DMDS	10.291	1372.63	74.985
Nov03-FPD150.chr	INTAKE TUBE		11/24/2003	14:49:08			H2S		0		ppm	COS	4.166	565.64	66.523	ppm	CHSH	7.416	359.42	68.556	ppm	DMS				ppm	DMDS	10.3	498.29	74.997
Nov03-FPD190.chr	INTAKE TUBE		11/24/2003	20:24:13			H2S	2.491	8.88	11.832	ppm	COS	4.183	457.26	59.629	ppm	CHSH	7.416	327.77	65.567	ppm	DMS	10.3	425.89	69.319	ppm	DMDS	11.35	2.25	25.677
Nov03-FPD193.chr	INTAKE TUBE		11/25/2003	9:57:40			H2S	2.8	2.46	9.702	ppm	COS	4.158	346.02	51.611	ppm	CHSH	7.416	190.95	50.575	ppm	DMS				ppm	DMDS	10.316	58.98	25.677
Nov03-FPD196.chr	INTAKE TUBE		11/25/2003	10:55:17		41.1	H2S	0	0	1	ppm	COS	4.191	140.75	32.209	ppm	CHSH	7.416	108	38.396	ppm	DMS				ppm	DMDS	10.308	171.66	43.131
Nov03-FPD41.chr	M-1		11/23/2003	22:30:09	11/23/03 10:30 PM	150.00	H2S	2.608	198.69	41.185	ppm	COS		0	0	ppm	CHSH		0	0	ppm	DMS		0	0	ppm	DMDS		0	0
Nov03-FPD84.chr	M-1		11/24/2003	5:12:09	11/24/03 5:12 AM	555.00	H2S	2.616	104.84	30.019	ppm	COS		0	0	ppm	CHSH		0	0	ppm	DMS		0	0	ppm	DMDS		0	0
Nov03-FPD127.chr	M-1		11/24/2003	10:57:13	11/24/03 10:57 AM	900.00	H2S	2.666	43.56	20.025	ppm	COS		0	0	ppm	CHSH		0	1	ppm	DMS		0	0	ppm	DMDS		0	0
Nov03-FPD153.chr	M-1		11/24/2003	15:45:50	11/24/03 3:45 PM	1182.00	H2S	2.625	16.96	14.044	ppm	COS		0	0	ppm	CHSH		0	0	ppm	DMS		0	0	ppm	DMDS		0	0
Nov03-FPD184.chr	M-1		11/24/2003	19:40:39	11/24/03 7:40 PM	1507.00	H2S	2.683	7.08	11.322	ppm	COS		0	0	ppm	CHSH		0	0	ppm	DMS		0	0	ppm	DMDS		0	0
Nov03-FPD231.chr	M-1		11/25/2003	20:24:22	11/25/03 8:24 PM	3431.00	H2S		0		ppm	COS		0	0	ppm	CHSH		0	0	ppm	DMS		0	0	ppm	DMDS		0	0
Nov03-FPD271.chr	M-1		11/26/2003	19:26:02	11/26/03 7:26 PM	4813.00	H2S		0		ppm	COS		0	0	ppm	CHSH		0	0	ppm	DMS		0	0	ppm	DMDS		0	0
Nov03-FPD318.chr	M-1		11/28/2003	20:34:08	11/28/03 8:34 PM	8035.00	H2S		0		ppm	COS		0	0	ppm	CHSH		0	0	ppm	DMS		0	0	ppm	DMDS		0	0
Nov03-FPD325.chr	M-1		12/1/2003	14:21:22	12/1/03 2:21 PM	12136.00	H2S		0		ppm	COS		0	0	ppm	CHSH		0	0	ppm	DMS		0	0	ppm	DMDS		0	0
Nov03-FPD363.chr	M-1		12/2/2003	16:50:51	12/2/03 4:50 PM	13806.00	H2S	2.666	226.19	43.951	ppm	COS		0	0	ppm	CHSH		0	0	ppm	DMS		0	0	ppm	DMDS		0	0
Nov03-FPD408.chr	M-1		12/3/2003	16:06:49	12/3/03 4:06 PM	15362.00	H2S	2.65	1108.11	99.159	ppm	COS		0	0	ppm	CHSH		0	0	ppm	DMS		0	0	ppm	DMDS		0	0
Nov03-FPD42.chr	M-2	7.33	11/23/2003	22:36:08	11/23/03 10:36 PM	156.00	H2S	2.608	0		ppm	COS		0	0	ppm	CHSH		0	0	ppm	DMS		0	0	ppm	DMDS		0	0
Nov03-FPD85.chr	M-2		11/24/2003	5:17:29	11/24/03 5:17 AM	560.00	H2S		0		ppm	COS		0	0	ppm	CHSH		0	0	ppm	DMS		0	0	ppm	DMDS		0	0
Nov03-FPD128.chr	M-2	7.06	11/24/2003	11:07:27	11/24/03 11:07 AM	910.00	H2S	2.608	5551.21	314.557	ppm	COS		0	0	ppm	CHSH		0	1	ppm	DMS		0	0	ppm	DMDS		0	0
Nov03-FPD154.chr	M-2	7.12	11/24/2003	15:50:32	11/24/03 3:50 PM	1187.00	H2S	2.641	106.54	30.265	ppm	COS		0	0	ppm	CHSH		0	0	ppm	DMS		0	0	ppm	DMDS		0	0
Nov03-FPD232.chr	M-2	7.02	11/25/2003	20:36:28	11/25/03 8:36 PM	3441.00	H2S	2.616	3.62	10.108	ppm	COS		0	0	ppm	CHSH		0	0	ppm	DMS		0	0	ppm	DMDS		0	0
Nov03-FPD265.chr	M-2	6.74	11/26/2003	18:11:08	11/26/03 6:11 PM	4768.00	H2S		0		ppm	COS		0	0	ppm	CHSH		0	0	ppm	DMS		0	0	ppm	DMDS		0	0
Nov03-FPD319.chr	M-2	6.65	11/28/2003	20:45:29	11/28/03 8:45 PM	8046.00	H2S		0		ppm	COS		0	0	ppm	CHSH		0	0	ppm	DMS		0	0	ppm	DMDS		0	0
Nov03-FPD326.chr	M-2	6.64	12/1/2003	14:35:26	12/1/03 2:35 PM	12150.00	H2S		0		ppm	COS		0	0	ppm	CHSH	7.425	11.19	14.41	ppm	DMS		0	0	ppm	DMDS		0	0
Nov03-FPD364.chr	M-2	6.53	12/2/2003	16:55:29	12/2/03 4:55 PM	13811.00	H2S	2.666	226.19	43.951	ppm	COS		0	0	ppm	CHSH	7.441	21.19	18.659	ppm	DMS		0	0	ppm	DMDS		0	0
Nov03-FPD409.chr	M-2	6.36	12/3/2003	16:12:55	12/3/03 4:12 PM	15368.00	H2S	2.65	1108.11	99.159	ppm	COS		0	0	ppm	CHSH	7.425	34.88	23.062	ppm	DMS		0	0	ppm	DMDS		0	0
Nov03-FPD43.chr	M-3	7.33	11/23/2003	22:48:21?	11/23/03 10:42 PM	162.00	H2S		0		ppm	COS		0	0	ppm	CHSH		0	0	ppm	DMS		0	0	ppm	DMDS		0	0
Nov03-FPD86.chr	M-3		11/24/2003	5:22:48	11/24/03 5:22 AM	565.00	H2S		0		ppm	COS		0	0	ppm	CHSH		0	0	ppm	DMS		0	0	ppm	DMDS		0	0
Nov03-FPD129.chr	M-3	7.02	11/24/2003	11:17:31	11/24/03 11:17 AM	920.00	H2S	2.6	3078.81	194.697	ppm	COS		0	0	ppm	CHSH		0	0	ppm	DMS		0	0	ppm	DMDS		0	0
Nov03-FPD155.chr	M-3	6.95	11/24/2003	16:00:06	11/24/03 4:00 PM	1197.00	H2S	2.616	16705.94	855.331	ppm	COS		0	0	ppm	CHSH		0	0	ppm	DMS		0	0	ppm	DMDS		0	0
Nov03-FPD186.chr	M-3	6.92	11/24/2003	19:56:29	11/24/03 7:56 PM	1421.00	H2S	2.7	17.75	14.26	ppm	COS		0	0	ppm	CHSH		0	0	ppm	DMS		0	0	ppm	DMDS		0	0
Nov03-FPD233.chr	M-3	6.8	11/25/2003	20:45:04	11/25/03 8:45 PM	3450.00	H2S	2.608	201.3	41.465	ppm	COS		0	0	ppm	CHSH		0	0	ppm	DMS		0	0	ppm	DMDS		0	0
Nov03-FPD266.chr	M-3	6.78	11/26/2003	18:18:02	11/26/03 6:18 PM	4775.00	H2S		0		ppm	COS		0	0	ppm	CHSH		0	0	ppm	DMS		0	0	ppm	DMDS		0	0
Nov03-FPD327.chr	M-3	6.53	12/1/2003	14:53:57	12/1/03 2:53 PM	12172.00	H2S		0		ppm	COS		0	0	ppm	CHSH		0	0	ppm	DMS		0	0	ppm	DMDS		0	0
Nov03-FPD365.chr	M-3	6.48	12/2/2003	17:11:20	12/2/03 5:11 PM	13827.00	H2S	2.616	68.42	24.483	ppm	COS		0	0	ppm	CHSH	7.433	12.94	15.241	ppm	DMS		0	0	ppm	DMDS		0	0
Nov03-FPD410.chr	M-3	6.41	12/3/2003	16:23:07	12/3/03 4:23 PM	15379.00	H2S		0		ppm	COS		0	0	ppm	CHSH	7.366	28.37	21.1	ppm	DMS		0	0	ppm	DMDS		0	0
Nov03-FPD44.chr	M-4		11/23/2003	22:48:21	11/23/03 10:48 PM	168.00	H2S		0		ppm	COS		0	0	ppm	CHSH		0	0	ppm	DMS		0	0	ppm	DMDS		0	0
Nov03-FPD87.chr	M-4		11/24/2003	5:28:36	11/24/03 5:28 AM	571.00	H2S		0		ppm	COS		0	0	ppm	CHSH		0	0	ppm	DMS		0	0	ppm	DMDS		0	0
Nov03-FPD130.chr	M-4		11/24/2003	11:27:04	11/24/03 11:27 AM	930.00	H2S	2.633	1249.04	105.991	ppm	COS		0	0	ppm	CHSH		0	0	ppm	DMS		0	0	ppm	DMDS		0	0
Nov03-FPD156.chr	M-4		11/24/2003	16:10:56	11/24/03 4:10 PM	1207.00	H2S	2.65	33.59	17.978	ppm	COS		0	0	ppm	CHSH		0	0	ppm	DMS		0	0	ppm	DMDS		0	0

Annotations on sheet: "pH", "7.14", "DS"

file	SAMPLE	INJECT SIZE	date	time	cum time	cum time (min)	H2S reten	H2S area	H2S conc	units	COS reten	COS area	COS conc	units	CH3SH reten	CH3SH area	CH3SH conc	units	DMS reten	DMS area	DMS conc	units	DMDS reten	DMDS area	DMDS conc
Nov03-FPD187.chr	M-4		11/24/2003	20:00:55	11/24/03 8:00 PM	1424.00	2.65	8353.19	450.395	ppm		0	0	ppm		0	0	ppm		0	0	ppm		0	0
Nov03-FPD234.chr	M-4		11/25/2003	20:54:40	11/25/03 8:54 PM	3459.00	2.6	9.8	12.085	ppm		0	0	ppm		0	0	ppm		0	0	ppm		0	0
Nov03-FPD321.chr	M-4		11/28/2003	21:26:05	11/28/03 9:26 PM	8087.00		0	0	ppm		0	0	ppm		0	0	ppm		0	0	ppm		0	0
Nov03-FPD328.chr	M-4		12/1/2003	18:33:14	12/1/03 6:33 PM	12392.00		0	0	ppm		0	0	ppm		0	0	ppm		0	0	ppm		0	0
Nov03-FPD366.chr	M-4		12/2/2003	17:27:13	12/2/03 5:27 PM	13843.00	2.6	9.56	12.019	ppm		0	0	ppm		0	0	ppm		0	0	ppm		0	0
Nov03-FPD411.chr	M-4		12/3/2003	16:35:02	12/3/03 4:35 PM	15391.00	2.65	8.04	11.604	ppm		0	0	ppm		0	0	ppm		0	0	ppm		0	0
					11/23/03 8:00 PM	1.00				1				1 ppm				1 ppm				1 ppm			
Nov03-FPD088.chr	M-5		11/24/2003	5:34:09	11/24/03 5:34 AM	174.00		0	0	ppm		0	0	ppm		0	0	ppm		0	0	ppm		0	0
Nov03-FPD131.chr	M-5		11/24/2003	11:37:39	11/24/03 11:37 AM	940.00		0	0	ppm		0	0	ppm		0	0	ppm		0	0	ppm		0	0
Nov03-FPD157.chr	M-5		11/24/2003	16:20:30	11/24/03 4:20 PM	1217.00		0	0	ppm		0	0	ppm		0	0	ppm		0	0	ppm		0	0
Nov03-FPD188.chr	M-5		11/24/2003	20:11:16	11/24/03 8:11 PM	1435.00		0	0	ppm		0	0	ppm		0	0	ppm		0	0	ppm		0	0
Nov03-FPD235.chr	M-5		11/25/2003	21:06:57	11/25/03 9:06 PM	1490.00		0	0	ppm		0	0	ppm		0	0	ppm		0	0	ppm		0	0
Nov03-FPD269.chr	M-5		11/26/2003	19:00:32	11/26/03 7:00 PM	4817.00		0	0	ppm		0	0	ppm		0	0	ppm		0	0	ppm		0	0
Nov03-FPD322.chr	M-5		11/28/2003	21:48:05	11/28/03 9:48 PM	8109.00		0	0	ppm		0	0	ppm		0	0	ppm		0	0	ppm		0	0
Nov03-FPD329.chr	M-5		12/1/2003	18:53:40	12/1/03 6:53 PM	12412.00		0	0	ppm		0	0	ppm		0	0	ppm		0	0	ppm		0	0
Nov03-FPD367.chr	M-5		12/2/2003	17:43:03	12/2/03 5:43 PM	13859.00		0	0	ppm		0	0	ppm		0	0	ppm		0	0	ppm		0	0
Nov03-FPD412.chr	M-5		12/3/2003	16:52:34	12/3/03 4:52 PM	15408.00		0	0	ppm		0	0	ppm		0	0	ppm		0	0	ppm		0	0
Nov03-FPD151.chr	MIDPOINT		11/24/2003	15:08:06			2.583	4.16	10.296	ppm	4.158	524.86	64.007	1 ppm	7.425	120.21	40.612	ppm	10.308	455.71	71.71	ppm	11.558	2.2	0
Nov03-FPD191.chr	MIDPOINT		11/24/2003	20:46:42				0	0	ppm	4.2	427.02	57.546	ppm	7.425	168.6	47.662	ppm	10.316	0	0	ppm	10.316	398.79	67.064
Nov03-FPD211.chr	MIX 33 STAND?		11/25/2003	14:42:38				0	0	ppm		0	0	ppm		0	0	ppm		0	0	ppm		0	0
Nov03-FPD144.chr	OUTTAKE TUBE		11/24/2003	12:57:58				0	0	ppm	4.175	588.13	64.251	ppm	7.416	18.24	12.46	ppm	10.316	482.42	73.776	ppm	10.308	522.11	46.276
Nov03-FPD152.chr	OUTTAKE TUBE		11/24/2003	15:30:52				0	0	ppm	4.2	521.64	63.805	ppm	7.441	29.47	21.298	ppm	10.325	0	0	ppm	11.375	2.04	0
Nov03-FPD192.chr	OUTTAKE TUBE		11/24/2003	21:09:15				0	0	ppm	4.208	449.13	59.069	ppm	7.433	81.28	33.8	ppm		0	0	ppm	10.325	422.41	69.041
Nov03-FPD194.chr	OUTTAKE TUBE		11/25/2003	10:24:12				0	0	ppm	4.191	89.57	25.328	ppm	7.425	115.9	39.91	ppm	10.308	339.23	61.841	ppm	11.525	2.35	0
Nov03-FPD195.chr	s-GAS STAND		11/25/2003	10:39:45				0	0	ppm	4.183	479.59	61.099	ppm	7.416	369.15	68.567	ppm	10.308	537.5	75.035	ppm	11.416	2.56	0
Nov03-FPD236.chr	s-GAS STAND		11/26/2003	11:43:48			2.525	12.13	12.721	ppm	4.125	439.45	58.402	ppm	7.375	299.97	62.071	ppm	10.283	196.24	45.999	ppm	11.466	3.31	0
Nov03-FPD280.chr	s-GAS STAND		11/28/2003	9:26:27			2.391	3.48	10.058	ppm	4.208	6.08	5.325	ppm	7.283	3.93	9.883	ppm	7.516	8.92	13.227	ppm			0
Nov03-FPD281.chr	s-GAS STAND		11/28/2003	9:40:55			2.408	7.72	11.514	ppm	4.183	334.31	50.698	ppm	7.416	271.27	59.163	ppm	10.308	0	0	ppm	10.308	363.2	61.969
Nov03-FPD323.chr	s-GAS STAND		12/1/2003	13:40:47			2.433	2.44	9.692	ppm	4.258	2.14	2.602	ppm	7.333	5.18	10.947	ppm	10.308	3.03	7.237	ppm	10.458	3.09	7.296
Nov03-FPD324.chr	s-GAS STAND		12/1/2003	13:58:56			2.758	11.68	12.599	ppm	4.175	533.34	64.541	ppm	7.425	365.97	68.277	ppm	10.325	391.2	64.248	ppm	10.325	438.64	67.934
Nov03-FPD336.chr	s-GAS STAND		12/2/2003	9:56:01			2.85	2.67	9.775	ppm	4.175	410.33	56.376	ppm	7.416	281.82	60.264	ppm	10.308	391.2	64.248	ppm	11.541	3.1	0
Nov03-FPD378.chr	s-GAS STAND		12/3/2003	9:20:47			2.583	0	0	ppm	4.15	472.49	60.631	ppm	7.425	361.13	67.836	ppm	10.325	516.1	73.544	ppm	10.316	516.1	73.544
Nov03-FPD054.chr	SOX-1		11/24/2003	0:16:11	11/24/03 12:16 AM	256.00		0	0	ppm		0	0	ppm	7.4	195.95	55.416	ppm	10.3	398.56	65.997	ppm	10.3	398.56	65.997
Nov03-FPD099.chr	SOX-1		11/24/2003	6:35:47	11/24/03 6:35 AM	667.00		0	0	ppm		0	0	ppm	7.425	244.04	61.745	ppm	10.308	452.69	70.209	ppm	10.308	452.69	70.209
Nov03-FPD268.chr	SOX-1		11/26/2003	18:41:59	11/26/03 6:41 PM	4237.00		0	0	ppm		0	0	ppm	7.416	98.12	36.709	ppm	10.316	429.16	67.213	ppm	10.316	429.16	67.213
Nov03-FPD312.chr	SOX-1		11/28/2003	18:11:26	11/28/03 6:11 PM	7087.00		0	0	ppm		0	0	ppm	7.433	37.27	23.745	ppm	10.308	320.99	58.356	ppm	11.716	3.94	0
Nov03-FPD362.chr	SOX-1		12/2/2003	16:35:19	12/2/03 4:35 PM	13781.00		0	0	ppm		0	0	ppm	7.441	10.16	13.921	ppm	10.3	521.91	73.948	ppm	10.3	521.91	73.948
Nov03-FPD402.chr	SOX-1		12/3/2003	14:25:33	12/3/03 2:25 PM	15341.00		0	0	ppm		0	0	ppm	7.425	8.95	13.246	ppm	10.3	294.85	56.002	ppm	11.733	2.33	
Nov03-FPD055.chr	SOX-2		11/24/2003	0:34:08	11/24/03 12:34 AM	274.00		0	0	ppm		0	0	ppm	7.408	4.78	9.282	ppm	10.3	67.25	28.096	ppm	10.3	67.25	28.096
Nov03-FPD100.chr	SOX-2		11/24/2003	6:49:12	11/24/03 6:49 AM	681.00		0	0	ppm		0	0	ppm	7.416	14.95	15.883	ppm	10.316	98.09	33.592	ppm	10.316	98.09	33.592
Nov03-FPD145.chr	SOX-2		11/24/2003	13:18:44	11/24/03 1:18 PM	1019.00		0	0	ppm	4.141	3.62	4.612	ppm	7.425	66.8	23.636	ppm	10.308	116.42	21.893	ppm	10.308	116.42	21.893
Nov03-FPD270.chr	SOX-2		11/26/2003	19:06:18	11/26/03 7:06 PM	2783.00	2.591	37590.4	58.593	ppm	4.275	2.95	3.249	ppm	7.425	911.73	117.967	ppm	10.316	129.97	37.748	ppm	10.316	129.97	37.748
Nov03-FPD313.chr	SOX-2		11/28/2003	18:29:29	11/28/03 6:29 PM	7069.00	2.575	397.96	5205.913	ppm	4.158	3.24	3.441	ppm	7.408	1845.83	203.015	ppm	10.316	118.28	36.116	ppm	10.316	118.28	36.116
Nov03-FPD357.chr	SOX-2		12/2/2003	15:00:50	12/2/03 3:00 PM	13686.00	2.5	106446.95	5205.913	ppm	4.191	4.68	4.393	ppm	7.425	3314.53	336.736	ppm	10.233	673.87	84.534	ppm	10.233	673.87	84.534
Nov03-FPD403.chr	SOX-2		12/3/2003	14:43:55	12/3/03 2:43 PM	15359.00	2.483	111671.57	5459.2	ppm	4.191	4.6	4.3	ppm	7.433	3968.38	396.269	ppm	10.316	152.62	40.764	ppm	11.416	3.64	0
Nov03-FPD056.chr	SOX-3		11/24/2003	0:55:51	11/24/03 12:55 AM	295.00		0	0	ppm		0	0	ppm	7.45	4.03	8.627	ppm	10.308	78.01	30.159	ppm	10.308	78.01	30.159
Nov03-FPD101.chr	SOX-3		11/24/2003	7:02:11	11/24/03 7:02 AM	694.00	2.6	64.72	23.874	ppm		0	0	ppm	7.425	21.58	18.941	ppm	10.316	89.13	32.093	ppm	10.316	89.13	32.093
Nov03-FPD228.chr	SOX-3		11/25/2003	19:32:27	11/25/03 7:32 PM	2809.00	2.591	160.78	37.03	ppm		0	0	ppm	7.425	195.19	50.61	ppm	10.308	116.65	35.878	ppm	10.308	116.65	35.878
Nov03-FPD272.chr	SOX-3		11/26/2003	19:32:41	11/26/03 7:32 PM	4249.00	2.608	156.47	36.523	ppm		0	0	ppm	7.425	720.23	100.532	ppm	10.316	119.6	36.301	ppm	10.316	119.6	36.301
Nov03-FPD314.chr	SOX-3		11/28/2003	18:46:16	11/28/03 6:46 PM	7086.00	2.633	41.22	19.582	ppm		0	0	ppm	7.416	1395.15	161.981	ppm	10.316	109.86	34.844	ppm	10.316	109.86	34.844
Nov03-FPD358.chr	SOX-3		12/2/2003	15:20:38	12/2/03 3:20 PM	13706.00	2.391	100270.95	4906.505	ppm		0	0	ppm	7.4	2347.12	248.656	ppm	10.316	111.33	35.068	ppm	10.316	111.33	35.068
Nov03-FPD404.chr	SOX-3		12/3/2003	15:04:04	12/3/03 3:04 PM	15380.00	2.458	103325.71	5054.598	ppm		0	0	ppm	7.416	2675.2	278.527	ppm	10.308	119.5	36.286	ppm	10.308	119.5	36.286
Nov03-FPD057.chr	SOX-4		11/24/2003	1:09:26	11/24/03 1:09 AM	309.00		0	0	ppm		0	0	ppm	7.4	3.17	7.727	ppm	10.325	78.67	30.274	ppm	10.325	78.67	30.274
Nov03-FPD102.chr	SOX-4		11/24/2003	7:16:12	11/24/03 7:16 AM	708.00	2.6	319.22	52.366	ppm		0	0	ppm	7.416	15.31	16.072	ppm	10.308	102.77	34.332	ppm	10.308	102.77	34.332
Nov03-FPD147.chr	SOX-4	100	11/24/2003	13:52:16	11/24/03 1:52 PM	1053.00	2.6	17202.31		ppm		0	0	ppm	7.425	8.14		ppm	10.308	23.11	3.16	ppm	11.616	23.11	3.16
Nov03-FPD229.chr	SOX-4		11/25/2003	19:47:29	11/25/03 7:47 PM	2824.00	2.608	50.65	21.371	ppm		0	0	ppm	7.425	130.8	41.946	ppm	10.3	86.71	31.146	ppm	11.408	3.14	0
Nov03-FPD274.chr	SOX-4		11/26/2003	19:57:46	11/26/03 7:57 PM	4274.00	2.616	308.59	51.46	ppm		0	0	ppm	7.416	582.18	87.962	ppm	10.308	104.43	34.015	ppm	10.308	104.43	34.015
Nov03-FPD315.chr	SOX-4		11/28/2003	19:15:45	11/28/03 7:15 PM	7115.00	2.633	348.2	54.729	ppm		0	0	ppm	7.416	1114.53	136.432	ppm	10.308	107.38	34.465	ppm	10.308	107.38	34.465
Nov03-FPD359.chr	SOX-4		12/2/2003	15:41:11	12/2/03 3:41 PM	13727.00	2.483	83083.34	4073.262	ppm		0	0	ppm	7.425	1614.77	181.978	ppm	10.325	122.58	36.716	ppm	10.325	122.58	36.716
Nov03-FPD405.chr	SOX-4		12/3/2003	15:21:17	12/3/03 3:21 PM	15397.00	2.45	95023.72	4652.123	ppm		0	0	ppm	7.416	1855.84	203.926	ppm	10.316	140.41	39.191	ppm	11.716	2.59	0
Nov03-FPD058.chr	SOX-5		11/24/2003	1:32:57	11/24/03 2:38 AM	340.00		0	0	ppm		0	0	ppm	7.408	5.19	9.635	ppm	10.316	106.98	34.996	ppm	10.316	106.98	34.996

SAMPLE	SAMPLE	INJECT SIZE	date	time	cum time	cum time (min)	gas	reten	area	conc	units	gas	reten	area	conc	units	gas	reten	area	conc	units	gas	reten	area	conc	units	gas	reten	area	conc
Nov03-FPD103.chr	SOX-5		11/24/2003	7:29:34	11/24/03 7:29 AM	721.00	H2S	2.6	6.59	11.152	ppm	COS	0	0	0	1 ppm	CH3SH	7.4	12.33	14.483	ppm	DMS	10.316	114.93	36.232	ppm	DMDS	10.316	114.93	36.232
Nov03-FPD148.chr	SOX-5	100	11/24/2003	14:07:34	11/24/03 2:07 PM	1068.00	H2S	2.6	5502.59		ppm	COS	0	0	0	1 ppm	CH3SH	7.408	7.83		ppm	DMS	10.3	20.68		ppm	DMDS	10.3	20.68	9.284
Nov03-FPD230.chr	SOX-5		11/25/2003	20:09:47	11/25/03 8:09 PM	2846.00	H2S	2.633	83.19	26.876	ppm	COS	0	0	0	1 ppm	CH3SH	7.425	121.44	40.526	ppm	DMS	10.316	120.86	36.476	ppm	DMDS	10.316	120.86	36.476
Nov03-FPD276.chr	SOX-5		11/26/2003	20:23:06	11/26/03 8:23 PM	4310.00	H2S	2.625	4329.38	255.324	ppm	COS	0	0	0	1 ppm	CH3SH	7.433	318.86	63.909	ppm	DMS	10.308	123.48	36.842	ppm	DMDS	10.308	123.48	36.842
Nov03-FPD316.chr	SOX-5		11/28/2003	19:36:47	11/28/03 7:36 PM	7136.00	H2S	2.608	12774.36	664.731	ppm	COS	0	0	0	1 ppm	CH3SH	7.425	763.77	104.496	ppm	DMS	10.316	101.74	33.605	ppm	DMDS	10.316	101.74	33.605
Nov03-FPD360.chr	SOX-5		12/2/2003	16:08:56	12/2/03 4:08 PM	13754.00	H2S	2.508	102164.49	4998.303	ppm	COS	0	0	0	1 ppm	CH3SH	7.433	1245.94	148.396	ppm	DMS	10.316	117.89	36.062	ppm	DMDS	10.316	117.89	36.062
Nov03-FPD406.chr	SOX-5		12/3/2003	15:37:16	12/3/03 3:37 PM	15403.00	H2S	2.433	111627.62	5457.069	ppm	COS	0	0	0	1 ppm	CH3SH	7.416	1675.86	187.539	ppm	DMS	10.316	151.7	40.646	ppm	DMDS	11.566	2.94	0
					11/23/03 8:00 PM	1.00				269.544	1				3.2						1				70.05					
Nov03-FPD59.chr	SOX-6		11/24/2003	1:49:14	11/24/03 1:49 AM	340.00	H2S	2.575	4622.72	269.544	ppm	COS	4.175	3.59	3.184	1 ppm	CH3SH	0	0	0	1 ppm	DMS	10.316	450.58	70.05	ppm	DMDS	10.316	450.58	70.05
Nov03-FPD104.chr	SOX-6		11/24/2003	7:44:04	11/24/03 7:44 AM	721.00	H2S	2.6	218.73	43.214	ppm	COS	0	0		1 ppm	CH3SH	0	0		1 ppm	DMS	10.308	234.31	51.004	ppm	DMDS	10.308	234.31	51.004
Nov03-FPD149.chr	SOX-6		11/24/2003	14:29:15	11/24/03 2:29 PM	1068.00	H2S	0	0		1 ppm	COS	0	0		1 ppm	CH3SH	0	0		1 ppm	DMS	10.308	202.9		ppm	DMDS	10.308	202.9	28.878
Nov03-FPD277.chr	SOX-6		11/26/2003	20:43:23	11/26/03 8:43 PM	7136.00	H2S	0	0		1 ppm	COS	0	0		1 ppm	CH3SH	0	0		1 ppm	DMS	10.316	151.66	40.64	ppm	DMDS	11.658	3.58	0
Nov03-FPD317.chr	SOX-6		11/28/2003	19:59:35	11/28/03 7:59 PM	13754.00	H2S	0	0		1 ppm	COS	0	0		1 ppm	CH3SH	0	0		1 ppm	DMS	10.333	118.31	36.121	ppm	DMDS	10.333	118.31	36.121
Nov03-FPD407.chr	SOX-6		12/3/2003	15:52:06	12/3/03 3:52 PM	15403.00	H2S	0	0		1 ppm	COS	0	0		1 ppm	CH3SH	0	0		1 ppm	DMS	10.325	114.09	35.489	ppm	DMDS	10.325	114.09	35.489
Nov03-FPD380.chr	1000PPM co2		12/3/2003	10:00:58			H2S	0	0	0	0 ppm	COS	0	0	0	0 ppm	CH3SH	0	0	0	0 ppm	DMS	0	0	0	0 ppm	DMDS	0	0	0
Nov03-FPD381.chr	98.6 ch4		12/3/2003	10:04:19			H2S	0	0	0	0 ppm	COS	0	0	0	0 ppm	CH3SH	0	0	0	0 ppm	DMS	0	0	0	0 ppm	DMDS	0	0	0

Appendix D - Chapter 5 Gas chromatography data from Nov 2003
TCD Results

	SAMPLE	InJ SIZE	date	time	cum time	cum minutes	gas	reten	area	conc	units
					11/23/03 20:00	1				0.1	
Nov03-TCD61.chr	A-1		11/24/2003	2:15:30	11/24/03 2:15	375	CO2	1.975	2.8	0.359	%vol
Nov03-TCD106.chr	A-1		11/24/2003	8:04:27	11/24/03 8:04	1444	CO2	1.975	3.31	0.419	%vol
Nov03-TCD158.chr	A-1		11/24/2003	16:26:23	11/24/03 16:26	1950	CO2	1.983	3.28	0.415	%vol
Nov03-TCD197.chr	A-1		11/25/2003	12:24:20	11/25/03 12:24	2852	CO2	1.958	3.59	0.452	%vol
Nov03-TCD237.chr	A-1		11/26/2003	12:04:10	11/26/03 12:04	4270	CO2	1.958	3.02	0.325	%vol
Nov03-TCD282.chr	A-1		11/28/2003	10:01:11	11/28/03 10:01	7755	CO2	1.975	3.18	0.339	%vol
Nov03-TCD368.chr	A-1		12/2/2003	17:53:08	12/2/03 17:53	13976	CO2	2.008	4.45	0.457	%vol
Nov03-TCD428.chr	A-1		12/4/2003	17:04:53	12/4/03 17:04	15847	CO2	1.966	4.74	0.484	%vol
					11/23/03 20:00	1				0.1	
Nov03-TCD24.chr	A-2	250	11/23/2003	20:44:03	11/23/03 20:44	44	CO2	1.958	2.2	0.288	%vol
Nov03-TCD62.chr	A-2		11/24/2003	2:23:06	11/24/03 2:23	383	CO2	1.975	4.2	0.524	%vol
Nov03-TCD107.chr	A-2		11/24/2003	8:09:44	11/24/03 8:09	1449	CO2	1.975	7.31	0.891	%vol
Nov03-TCD159.chr	A-2		11/24/2003	16:31:05	11/24/03 16:31	1954	CO2	1.975	10.9	1.313	%vol
Nov03-TCD198.chr	A-2		11/25/2003	12:30:36	11/25/03 12:30	2858	CO2	1.958	15.24	1.825	%vol
Nov03-TCD238.chr	A-2		11/26/2003	12:08:54	11/26/03 12:08	4274	CO2	1.991	18.05	1.718	%vol
Nov03-TCD283.chr	A-2		11/28/2003	10:21:19	11/28/03 10:21	7775	CO2	1.958	25.06	2.368	%vol
Nov03-TCD369.chr	A-2		12/2/2003	18:07:16	12/2/03 18:07	13981	CO2	1.975	54.38	5.088	%vol
Nov03-TCD429.chr	A-2		12/4/2003	17:09:45	12/4/03 17:09	15852	CO2	1.975	71.67	6.692	%vol
					11/23/03 20:00	1				0.1	
Nov03-TCD25.chr	A-3		11/23/2003	20:49:46	11/23/03 20:49	49	CO2	1.95	2.43	0.315	%vol
Nov03-TCD63.chr	A-3		11/24/2003	2:29:01	11/24/03 2:29	389	CO2	1.958	5.21	0.643	%vol
Nov03-TCD108.chr	A-3		11/24/2003	8:15:11	11/24/03 8:15	1455	CO2	1.966	8.82	1.069	%vol
Nov03-TCD160.chr	A-3	100	11/24/2003	16:40:21	11/24/03 16:40	1965	CO2	1.958	5.02	1.55	%vol
Nov03-TCD199.chr	A-3		11/25/2003	12:40:16	11/25/03 12:40	2868	CO2	1.958	18.74	2.237	%vol
Nov03-TCD239.chr	A-3		11/26/2003	12:18:57	11/26/03 12:18	4284	CO2	1.958	24.65	2.331	%vol
Nov03-TCD284.chr	A-3		11/28/2003	10:32:23	11/28/03 10:32	7786	CO2	1.941	56.47	5.282	%vol
Nov03-TCD330.chr	A-3		12/1/2003	19:07:14	12/1/03 19:07	12653	CO2	1.941	95.83	8.933	%vol
Nov03-TCD370.chr	A-3		12/2/2003	18:27:04	12/2/03 18:27	14001	CO2	1.95	96.56	9.001	%vol
Nov03-TCD430.chr	A-3		12/4/2003	17:24:32	12/4/03 17:24	15867	CO2	1.941	103.45	9.64	%vol
						1				0.1	
Nov03-TCD26.chr	A-4		11/23/2003	20:54:50	11/23/03 20:54	54	CO2	1.966	2.57	0.332	%vol
Nov03-TCD64.chr	A-4		11/24/2003	2:35:47	11/24/03 2:35	395	CO2	1.966	5.8	0.713	%vol
Nov03-TCD109.chr	A-4		11/24/2003	8:24:58	11/24/03 8:24	1464	CO2	1.958	10.57	1.275	%vol
Nov03-TCD161.chr	A-4		11/24/2003	16:50:56	11/24/03 16:50	1675	CO2	1.941	14.18	1.7	%vol
Nov03-TCD200.chr	A-4		11/25/2003	12:48:29	11/25/03 12:48	2876	CO2	1.958	19.8	2.362	%vol
Nov03-TCD240.chr	A-4		11/26/2003	12:33:54	11/26/03 12:33	4299	CO2	1.95	31.99	3.012	%vol
Nov03-TCD285.chr	A-4		11/28/2003	10:49:20	11/28/03 10:49	7803	CO2	1.933	66.52	6.214	%vol
Nov03-TCD371.chr	A-4		12/2/2003	18:43:54	12/2/03 18:43	14017	CO2	1.958	99.08	9.235	%vol
Nov03-TCD431.chr	A-4		12/4/2003	17:42:59	12/4/03 17:42	15885	CO2	1.941	100.1	9.329	%vol
						1				0.1	
Nov03-TCD27.chr	A-5		11/23/2003	21:00:52	11/23/03 21:00	60	CO2	1.95	1.6	0.218	%vol
Nov03-TCD65.chr	A-5		11/24/2003	2:57:06	11/24/03 2:57	417	CO2	1.975	5.53	0.68	%vol
Nov03-TCD110.chr	A-5		11/24/2003	8:34:36	11/24/03 8:34	1474	CO2	1.975	13.52	1.622	%vol
Nov03-TCD162.chr	A-5		11/24/2003	17:02:35	11/24/03 17:02	1687	CO2	1.975	17.08	2.041	%vol
Nov03-TCD201.chr	A-5		11/25/2003	12:55:22	11/25/03 12:55	2889	CO2	1.958	33.17	3.936	%vol
Nov03-TCD241.chr	A-5		11/26/2003	12:48:46	11/26/03 12:48	4314	CO2	1.941	42.85	4.019	%vol
Nov03-TCD286.chr	A-5		11/28/2003	11:09:46	11/28/03 11:09	7823	CO2	1.966	75.72	7.067	%vol
Nov03-TCD331.chr	A-5		12/1/2003	19:27:24	12/1/03 19:27	12650	CO2	1.933	114.45	10.66	%vol
Nov03-TCD372.chr	A-5		12/2/2003	18:58:12	12/2/03 18:58	14032	CO2	1.933	98.88	9.216	%vol
Nov03-TCD432.chr	A-5		12/4/2003	17:58:55	12/4/03 17:58	15901	CO2	1.95	106.9	9.96	%vol
						1				0.1	
Nov03-TCD28.chr	A-6		11/23/2003	21:05:55	11/23/03 21:05	65	CO2	1.966	2.59	0.335	%vol
Nov03-TCD66.chr	A-6		11/24/2003	3:06:11	11/24/03 3:06	425	CO2	1.966	8.22	0.997	%vol
Nov03-TCD111.chr	A-6	100	11/24/2003	8:44:25	11/24/03 8:44	1484	CO2	1.95	6.5	1.99	%vol
Nov03-TCD163.chr	A-6	100	11/24/2003	17:12:45	11/24/03 17:12	1697	CO2	1.866	1.47	0.505	%vol
Nov03-TCD202.chr	A-6		11/25/2003	13:04:06	11/25/03 13:04	2898	CO2	1.933	43.99	5.211	%vol
Nov03-TCD242.chr	A-6		11/26/2003	13:04:19	11/26/03 13:04	4338	CO2	1.958	17.83		%vol
Nov03-TCD287.chr	A-6		11/28/2003	11:18:06	11/28/03 11:18	7832	CO2	1.958	86.8	8.095	%vol
Nov03-TCD332.chr	A-6		12/1/2003	20:05:10	12/1/03 20:05	12682	CO2	1.916	136.83	12.736	%vol
Nov03-TCD373.chr	A-6		12/2/2003	19:13:33	12/2/03 19:13	14047	CO2	1.933	133.5	12.427	%vol
Nov03-TCD433.chr	A-6		12/4/2003	18:08:45	12/4/03 18:08	15911	CO2	1.958	136.24	12.681	%vol
						1				18.6	
Nov03-TCD29.chr	A-7		11/23/2003	21:11:08	11/23/03 21:11	71	CO2	1.916	156.95	18.517	%vol
Nov03-TCD67.chr	A-7		11/24/2003	3:12:17	11/24/03 3:12	431	CO2	1.925	139.3	16.438	%vol
Nov03-TCD112.chr	A-7	100	11/24/2003	8:54:50	11/24/03 8:54	1494	CO2	1.95	52.08	15.41	%vol
Nov03-TCD164.chr	A-7	100	11/24/2003	17:24:07	11/24/03 17:24	1709	CO2	1.916	48.77	5.774	%vol
Nov03-TCD165.chr	A-7	50	11/24/2003	17:35:58	11/24/03 17:35	1720	CO2	1.958	28.4	33.75	%vol
Nov03-TCD204.chr	A-7	50	11/25/2003	13:30:28	11/25/03 13:30	2919	CO2	1.966	19.81	23.63	%vol
Nov03-TCD243.chr	A-7		11/26/2003	13:24:18	11/26/03 13:24	4364	CO2	1.925	129.46	12.052	%vol
Nov03-TCD288.chr	A-7		11/28/2003	11:37:50	11/28/03 11:37	7851	CO2	1.95	134.97	12.564	%vol
Nov03-TCD333.chr	A-7		12/1/2003	20:27:08	12/1/03 20:27	12714	CO2	1.958	136.25	12.683	%vol
Nov03-TCD374.chr	A-7		12/2/2003	19:30:48	12/2/03 19:30	14064	CO2	1.941	139.95	13.026	%vol
Nov03-TCD434.chr	A-7		12/4/2003	18:40:21	12/4/03 18:40	15943	CO2	1.941	125.5	11.685	%vol
						1				18.6	
Nov03-TCD30.chr	A-8		11/23/2003	21:16:22	11/23/03 21:16	76	CO2	1.916	155.36	18.329	%vol
Nov03-TCD68.chr	A-8		11/24/2003	3:24:51	11/24/03 3:24	443	CO2	1.908	143.91	16.981	%vol
Nov03-TCD113.chr	A-8	250	11/24/2003	9:04:57	11/24/03 9:04	1504	CO2	1.925	123.87	14.621	%vol
Nov03-TCD166.chr	A-8	250	11/24/2003	17:42:06	11/24/03 17:42	1721	CO2	1.941	111.72	13.19	%vol
Nov03-TCD205.chr	A-8	250	11/25/2003	13:39:50	11/25/03 13:39	2938	CO2	1.925	118.85	14.03	%vol
Nov03-TCD244.chr	A-8		11/26/2003	13:38:59	11/26/03 13:38	4378	CO2	1.916	113.49	10.571	%vol

	SAMPLE	INJECT S	date	time	cum time	cum minutes	gas	reten	area	conc	units
Nov03-TCD289.chr	A-8		11/28/2003	12:00:51	11/28/03 12:00	7874	CO2	1.95	125.63	11.697	%vol
Nov03-TCD334.chr	A-8		12/1/2003	20:50:59	12/1/03 20:50	12737	CO2	1.941	151.88	14.132	%vol
Nov03-TCD375.chr	A-8		12/2/2003	19:48:37	12/2/03 19:48	14076	CO2	1.941	160.3	14.913	%vol
Nov03-TCD435.chr	A-8		12/4/2003	18:58:56	12/4/03 18:58	15961	CO2	1.916	141.01	13.123	%vol
						1				19.5	
Nov03-TCD31.chr	A-9		11/23/2003	21:22:57	11/23/03 21:22	82	CO2	1.908	162.66	19.189	%vol
Nov03-TCD69.chr	A-9		11/24/2003	3:31:17	11/24/03 3:31	450	CO2	1.925	140.8	16.615	%vol
Nov03-TCD114.chr	A-9	100	11/24/2003	9:10:45	11/24/03 9:10	1510	CO2	1.958	52.56	15.55	%vol
Nov03-TCD167.chr	A-9	50	11/24/2003	17:48:55	11/24/03 17:48	1727	CO2	1.95	31.35	37.22	%vol
Nov03-TCD206.chr	A-9	50	11/25/2003	13:49:38	11/25/03 13:49	2948	CO2	1.941	23.67	28.17	%vol
Nov03-TCD207.chr	A-9	250	11/25/2003	14:01:58	11/25/03 14:01	4391	CO2	1.925	121.33	14.322	%vol
Nov03-TCD245.chr	A-9		11/26/2003	13:51:43	11/26/03 13:51	7895	CO2	1.908	111.19	10.357	%vol
Nov03-TCD376.chr	A-9		12/2/2003	20:03:36	12/2/03 20:03	14081	CO2	1.95	132.37	12.323	%vol
Nov03-TCD436.chr	A-9		12/4/2003	19:13:00	12/4/03 19:13	15976	CO2	1.941	128	11.917	%vol
						1				2.9	
Nov03-TCD70.chr	A-10		11/24/2003	3:41:07	11/24/03 3:41	460	CO2	1.933	23.99	2.855	%vol
Nov03-TCD115.chr	A-10	250	11/24/2003	9:20:03	11/24/03 9:20	1524	CO2	1.975	22.28	2.654	%vol
Nov03-TCD168.chr	A-10	250	11/24/2003	17:59:10	11/24/03 17:59	1738	CO2	1.933	20.16	2.404	%vol
Nov03-TCD208.chr	A-10		11/25/2003	14:15:28	11/25/03 14:15	2965	CO2	1.958	19.05	2.273	%vol
Nov03-TCD246.chr	A-10		11/26/2003	14:04:15	11/26/03 14:04	4699	CO2	1.958	17.66	1.682	%vol
Nov03-TCD291.chr	A-10		11/28/2003	12:49:41	11/28/03 12:49	7923	CO2	1.975	18.17	1.73	%vol
Nov03-TCD437.chr	A-10		12/4/2003	19:33:04	12/4/03 19:33	15996	CO2	1.95	18.17	1.729	%vol
Nov03-TCD60.chr	AIR		11/24/2003	2:09:21			CO2	1.95	0.6	0.1	%vol
Nov03-TCD105.chr	AIR		11/24/2003	7:57:51			CO2	1.966	0.7	0.111	%vol
Nov03-TCD189.chr	AIR		11/24/2003	20:15:37			CO2	1.991	0.95	0.141	%vol
						1				0.244	
Nov03-TCD32.chr	B-1		11/23/2003	21:29:21	11/23/03 21:29	89	CO2	1.958	1.82	0.244	%vol
Nov03-TCD71.chr	B-1		11/24/2003	3:46:32	11/24/03 3:46	465	CO2	1.958	2.79	0.358	%vol
Nov03-TCD116.chr	B-1	250	11/24/2003	9:25:12	11/24/03 9:25	1529	CO2	1.975	2.78	0.356	%vol
Nov03-TCD169.chr	B-1		11/24/2003	18:04:13	11/24/03 18:04	1743	CO2	1.975	2.08	0.275	%vol
Nov03-TCD209.chr	B-1		11/25/2003	14:26:43	11/25/03 14:26	2983	CO2	1.975	2.81	0.361	%vol
Nov03-TCD247.chr	B-1		11/26/2003	14:20:41	11/26/03 14:20	4420	CO2	1.958	2.64	0.289	%vol
Nov03-TCD292.chr	B-1		11/28/2003	12:58:33	11/28/03 12:58	7932	CO2	1.975	2.69	0.294	%vol
Nov03-TCD382.chr	B-1		12/3/2003	10:06:51	12/3/03 10:06	15012	CO2	1.991	2.62	0.287	%vol
					11/23/03 20:00	1				0.244	
Nov03-TCD33.chr	B-2		11/23/2003	21:35:22	11/23/03 21:35	94	CO2	1.958	2.95	0.376	%vol
Nov03-TCD72.chr	B-2		11/24/2003	3:53:32	11/24/03 3:53	472	CO2	1.925	8.65	1.048	%vol
Nov03-TCD117.chr	B-2	100	11/24/2003	9:28:55	11/24/03 9:28	1756	CO2	1.975	4.99	1.5425	%vol
Nov03-TCD170.chr	B-2	50	11/24/2003	18:12:15	11/24/03 18:12	2990	CO2	1.933	1.19	1.7	%vol
Nov03-TCD210.chr	B-2		11/25/2003	14:32:50	11/25/03 14:32	4427	CO2	1.958	29.4	3.492	%vol
Nov03-TCD248.chr	B-2		11/26/2003	14:27:14	11/26/03 14:27	7936	CO2	1.958	36.86	3.464	%vol
Nov03-TCD293.chr	B-2		11/28/2003	13:02:22	11/28/03 13:02	13631	CO2	1.958	62.55	5.846	%vol
Nov03-TCD337.chr	B-2		12/2/2003	10:31:52	12/2/03 10:31	13641	CO2	1.941	89.34	8.331	%vol
Nov03-TCD383.chr	B-2		12/3/2003	10:15:04	12/3/03 10:15	15021	CO2	1.966	98.56	9.186	%vol
					11/23/03 20:00	1				0.244	
Nov03-TCD34.chr	B-3		11/23/2003	21:50:17	11/23/03 21:50	109	CO2	1.941	2.83	0.362	%vol
Nov03-TCD74.chr	B-3		11/24/2003	4:09:55	11/24/03 4:09	488	CO2	1.958	8.85	1.072	%vol
Nov03-TCD118.chr	B-3	100	11/24/2003	9:39:45	11/24/03 9:39	1766	CO2	1.941	5.62	1.7275	%vol
Nov03-TCD172.chr	B-3	100	11/24/2003	18:27:56	11/24/03 18:27	3006	CO2	1.958	6.81	2.0775	%vol
Nov03-TCD212.chr	B-3		11/25/2003	14:48:21	11/25/03 14:48	4441	CO2	1.966	18.57	1.767	%vol
Nov03-TCD249.chr	B-3		11/26/2003	14:41:01	11/26/03 14:41	7968	CO2	1.966	43.95	4.121	%vol
Nov03-TCD294.chr	B-3		11/28/2003	13:24:29	11/28/03 13:24	13651	CO2	1.958	69.66	6.505	%vol
Nov03-TCD338.chr	B-3		12/2/2003	10:51:22	12/2/03 10:51	13661	CO2	1.941	85.96	8.017	%vol
Nov03-TCD384.chr	B-3		12/3/2003	10:30:07	12/3/03 10:30	15036	CO2	1.95	94.44	8.804	%vol
					11/23/03 20:00	1				0.244	
Nov03-TCD35.chr	B-4		11/23/2003	21:55:52	11/23/03 21:55	113	CO2	1.983	2.57	0.332	%vol
Nov03-TCD75.chr	B-4		11/24/2003	4:19:01	11/24/03 4:19	498	CO2	1.958	8.53	1.034	%vol
Nov03-TCD119.chr	B-4	250	11/24/2003	9:50:00	11/24/03 9:50	867	CO2	1.975	13.08	1.57	%vol
Nov03-TCD173.chr	B-4	100	11/24/2003	18:38:08	11/24/03 18:38	1777	CO2	1.95	3.87	1.215	%vol
Nov03-TCD213.chr	B-4		11/25/2003	14:58:11	11/25/03 14:58	3016	CO2	1.958	29.9	2.817	%vol
Nov03-TCD250.chr	B-4		11/26/2003	15:01:03	11/26/03 15:01	4461	CO2	1.958	38.51	3.617	%vol
Nov03-TCD295.chr	B-4		11/28/2003	13:40:14	11/28/03 13:40	7984	CO2	1.958	56.91	5.323	%vol
Nov03-TCD339.chr	B-4		12/2/2003	11:11:49	12/2/03 11:11	13671	CO2	1.95	79.72	7.439	%vol
Nov03-TCD385.chr	B-4		12/3/2003	10:46:15	12/3/03 10:46	15042	CO2	1.983	84.08	7.843	%vol
					11/23/03 20:00	1				0.244	
Nov03-TCD36.chr	B-5		11/23/2003	22:01:45	11/23/03 22:01	120	CO2	1.966	2.2	0.289	%vol
Nov03-TCD76.chr	B-5		11/24/2003	4:24:39	11/24/03 4:24	503	CO2	1.941	9.43	1.14	%vol
Nov03-TCD120.chr	B-5	250	11/24/2003	10:00:03	11/24/03 10:00	877	CO2	1.983	14.65	1.755	%vol
Nov03-TCD174.chr	B-5	250	11/24/2003	18:48:52	11/24/03 18:48	1797	CO2	1.975	16.03	1.917	%vol
Nov03-TCD214.chr	B-5		11/25/2003	15:15:28	11/25/03 15:15	3033	CO2	1.958	28.83	2.719	%vol
Nov03-TCD251.chr	B-5		11/26/2003	15:14:27	11/26/03 15:14	4474	CO2	1.958	40.87	3.835	%vol
Nov03-TCD296.chr	B-5		11/28/2003	13:58:38	11/28/03 13:58	8002	CO2	1.933	53.75	5.03	%vol
Nov03-TCD340.chr	B-5		12/2/2003	11:50:54	12/2/03 11:50	13710	CO2	1.916	69.56	6.497	%vol
Nov03-TCD386.chr	B-5		12/3/2003	11:01:11	12/3/03 11:01	15057	CO2	1.975	74.41	6.946	%vol
					11/23/03 20:00	1				0.244	
Nov03-TCD37.chr	B-6		11/23/2003	22:06:59	11/23/03 22:06	125	CO2	1.966	2.6	0.335	%vol
Nov03-TCD77.chr	B-6		11/24/2003	4:30:32	11/24/03 4:30	509	CO2	1.966	8.65	1.048	%vol
Nov03-TCD121.chr	B-6	250	11/24/2003	10:04:16	11/24/03 10:04	881	CO2	1.983	15	1.796	%vol
Nov03-TCD175.chr	B-6	250	11/24/2003	18:53:58	11/24/03 18:53	1802	CO2	1.975	21.6	2.573	%vol
Nov03-TCD215.chr	B-6		11/25/2003	15:35:21	11/25/03 15:35	3053	CO2	1.958	34.12	3.209	%vol
Nov03-TCD252.chr	B-6		11/26/2003	15:34:17	11/26/03 15:34	4494	CO2	1.958	43.99	4.125	%vol
Nov03-TCD297.chr	B-6		11/28/2003	14:17:56	11/28/03 14:17	8011	CO2	1.95	86.73	8.089	%vol
Nov03-TCD341.chr	B-6		12/2/2003	12:10:16	12/2/03 12:10	13730	CO2	1.933	96.26	8.973	%vol
Nov03-TCD387.chr	B-6		12/3/2003	11:15:21	12/3/03 11:15	15071	CO2	1.925	112.98	10.523	%vol

	SAMPLE	INJECT S	date	time	cum time	cum minutes	gas	reten	area	conc	units
						1					19.5
Nov03-TCD38.chr	B-7		11/23/2003	22:13:58	11/23/03 22:13	132	CO2	1.908	164.85	19.447	%vol
Nov03-TCD78.chr	B-7		11/24/2003	4:36:07	11/24/03 4:36	515	CO2	1.908	151.92	17.925	%vol
Nov03-TCD122.chr	B-7	100	11/24/2003	10:13:54	11/24/03 10:13	906	CO2	1.933	55.46	16.405	%vol
Nov03-TCD253.chr	B-7		11/26/2003	15:49:52	11/26/03 15:49	4650	CO2	1.908	134.34	12.505	%vol
Nov03-TCD298.chr	B-7		11/28/2003	14:31:55	11/28/03 14:31	8026	CO2	1.925	141.99	13.215	%vol
Nov03-TCD342.chr	B-7		12/2/2003	12:28:26	12/2/03 12:28	13744	CO2	1.933	153.2	14.254	%vol
Nov03-TCD388.chr	B-7		12/3/2003	11:35:06	12/3/03 11:35	15091	CO2	1.925	186.88	17.379	%vol
					11/23/03 20:00	1					19.5
Nov03-TCD39.chr	B-8		11/23/2003	22:18:59	11/23/03 22:18	137	CO2	1.925	162.58	19.18	%vol
Nov03-TCD79.chr	B-8		11/24/2003	4:41:38	11/24/03 4:41	520	CO2	1.908	142.5	16.815	%vol
Nov03-TCD123.chr	B-8	250	11/24/2003	10:24:56	11/24/03 10:24	917	CO2	1.941	138.97	16.399	%vol
Nov03-TCD178.chr	B-8	250	11/24/2003	19:17:25	11/24/03 19:17	1811	CO2	1.95	113.09	13.35	%vol
Nov03-TCD217.chr	B-8		11/25/2003	17:24:57	11/25/03 17:24	3231	CO2	1.95	129.03	12.012	%vol
Nov03-TCD254.chr	B-8		11/26/2003	16:03:02	11/26/03 16:03	4664	CO2	1.933	126.55	11.783	%vol
Nov03-TCD299.chr	B-8		11/28/2003	14:52:58	11/28/03 14:52	8047	CO2	1.933	137.96	12.841	%vol
Nov03-TCD343.chr	B-8		12/2/2003	12:48:22	12/2/03 12:48	13764	CO2	1.95	146.81	13.662	%vol
Nov03-TCD389.chr	B-8		12/3/2003	11:50:27	12/3/03 11:50	15106	CO2	1.958	162.38	15.106	%vol
					11/23/03 20:00	1					19.5
Nov03-TCD40.chr	B-9		11/23/2003	22:24:45	11/23/03 22:24	143	CO2	1.933	162.84	19.211	%vol
Nov03-TCD80.chr	B-9		11/24/2003	4:47:35	11/24/03 4:47	526	CO2	1.908	152.21	17.959	%vol
Nov03-TCD81.chr	B-9	100	11/24/2003	4:57:48	11/24/03 4:57	536	CO2	1.916	62.37	18.4425	%vol
Nov03-TCD82.chr	B-9	50	11/24/2003	5:02:22	11/24/03 5:02	541	CO2	1.966	25.72	30.58	%vol
Nov03-TCD124.chr	B-9	100	11/24/2003	10:31:41	11/24/03 10:31	924	CO2	1.95	58.91	17.4225	%vol
Nov03-TCD179.chr	B-9	100	11/24/2003	19:20:41	11/24/03 19:20	1814	CO2	1.941	59.94	17.725	%vol
Nov03-TCD218.chr	B-9		11/25/2003	17:39:08	11/25/03 17:39	3246	CO2	1.925	133.25	12.404	%vol
Nov03-TCD255.chr	B-9		11/26/2003	16:14:50	11/26/03 16:14	4675	CO2	1.925	126.82	11.808	%vol
Nov03-TCD300.chr	B-9		11/28/2003	15:08:22	11/28/03 15:08	8063	CO2	1.925	145.33	13.524	%vol
Nov03-TCD344.chr	B-9	100	12/2/2003	13:00:26	12/2/03 13:00	13776	CO2	1.983	56.43	13.1975	%vol
Nov03-TCD390.chr	B-9		12/3/2003	12:04:14	12/3/03 12:04	15120	CO2	1.916	162.88	15.153	%vol
					11/23/03 20:00	1					2.65
Nov03-TCD83.chr	B-10	250	11/24/2003	5:06:54	11/24/03 5:06	545	CO2	1.95	22.03	2.624	%vol
Nov03-TCD126.chr	B-10	250	11/24/2003	10:52:55	11/24/03 10:52	945	CO2	1.983	19.77	2.358	%vol
Nov03-TCD180.chr	B-10	250	11/24/2003	19:24:49	11/24/03 19:24	1818	CO2	1.966	16.84	2.013	%vol
Nov03-TCD301.chr	B-10		11/28/2003	15:27:31	11/28/03 15:27	8074	CO2	1.95	16.03	1.531	%vol
Nov03-TCD345.chr	B-10	250	12/2/2003	13:16:52	12/2/03 13:16	13789	CO2	1.966	15.97	1.526	%vol
Nov03-TCD391.chr	B-10		12/3/2003	12:22:59	12/3/03 12:22	15138	CO2	1.975	16.12	1.54	%vol
					11/23/03 20:00	1					0.15
Nov03-TCD41.chr	M-1		11/23/2003	22:30:09	11/23/2003 22:30	150	CO2	1.958	1.1	0.158	%vol
Nov03-TCD84.chr	M-1	250	11/24/2003	5:12:09	11/24/2003 5:12	555	CO2	1.95	1.6	0.218	%vol
Nov03-TCD127.chr	M-1		11/24/2003	10:57:13	11/24/2003 10:57	900	CO2	2	1.47	0.203	%vol
Nov03-TCD153.chr	M-1		11/24/2003	15:45:50	11/24/2003 15:45	1182	CO2	1.975	1.35	0.188	%vol
Nov03-TCD184.chr	M-1		11/24/2003	19:40:39	11/24/2003 19:40	1507	CO2	1.966	0.87	0.132	%vol
Nov03-TCD231.chr	M-1		11/25/2003	20:24:22	11/25/2003 20:24	3431	CO2	1.941	0.83	0.121	%vol
Nov03-TCD271.chr	M-1		11/26/2003	19:26:02	11/26/2003 19:26	4813	CO2	1.925	1.16	0.152	%vol
Nov03-TCD318.chr	M-1		11/28/2003	20:34:08	11/28/2003 20:34	8035	CO2	1.95	1.07	0.143	%vol
Nov03-TCD325.chr	M-1		12/1/2003	14:21:22	12/1/2003 14:21	12136	CO2	2	0.62	0.101	%vol
Nov03-TCD363.chr	M-1		12/2/2003	16:50:51	12/1/2003 16:50	13806	CO2	1.975	1.1	0.146	%vol
Nov03-TCD408.chr	M-1		12/3/2003	16:06:49	12/3/2003 16:06	15362	CO2	1.966	0.78	0.117	%vol
					11/23/03 20:00	1					0.22
Nov03-TCD42.chr	M-2		11/23/2003	22:36:08	11/23/2003 22:36	156	CO2	1.95	1.67	0.226	%vol
Nov03-TCD85.chr	M-2		11/24/2003	5:17:29	11/24/2003 5:17	560	CO2	1.966	3.72	0.468	%vol
Nov03-TCD128.chr	M-2		11/24/2003	11:07:27	11/24/2003 11:07	910	CO2	1.975	5.09	0.629	%vol
Nov03-TCD154.chr	M-2		11/24/2003	15:50:32	11/24/2003 15:50	1187	CO2	1.991	5.45	0.671	%vol
Nov03-TCD185.chr	M-2		11/24/2003	19:52:19	11/24/2003 19:52		CO2	1.95	3.17	0.403	%vol
Nov03-TCD232.chr	M-2		11/25/2003	20:36:28	11/25/2003 20:36	3441	CO2	1.958	7.21	0.713	%vol
Nov03-TCD265.chr	M-2		11/26/2003	18:11:08	11/26/2003 18:11	4768	CO2	1.95	9.62	0.937	%vol
Nov03-TCD319.chr	M-2		11/28/2003	20:45:29	11/28/2003 20:45	8046	CO2	1.958	10.17	0.988	%vol
Nov03-TCD326.chr	M-2		12/1/2003	14:35:26	12/1/2003 14:35	12150	CO2	1.966	12.22	1.178	%vol
Nov03-TCD364.chr	M-2		12/2/2003	16:55:29	12/2/2003 16:55	13811	CO2	2.008	13.2	1.269	%vol
Nov03-TCD409.chr	M-2		12/3/2003	16:12:55	12/3/2003 16:12	15368	CO2	1.991	14.87	1.424	%vol
					11/23/03 20:00	1					0.17
Nov03-TCD43.chr	M-3		11/23/2003	22:42:37	11/23/2003 22:42	162	CO2	1.966	1.43	0.198	%vol
Nov03-TCD86.chr	M-3		11/24/2003	5:22:48	11/24/2003 5:22	565	CO2	1.95	3.31	0.419	%vol
Nov03-TCD129.chr	M-3		11/24/2003	11:17:31	11/24/2003 11:17	920	CO2	1.966	5.4	0.666	%vol
Nov03-TCD155.chr	M-3		11/24/2003	16:00:06	11/24/2003 16:00	1197	CO2	1.975	6.44	0.788	%vol
Nov03-TCD186.chr	M-3		11/24/2003	19:56:29	11/24/2003 19:56	1421	CO2	2	5.38	0.663	%vol
Nov03-TCD233.chr	M-3		11/25/2003	20:45:04	11/25/2003 20:45	3450	CO2	1.966	8.02	0.789	%vol
Nov03-TCD266.chr	M-3		11/26/2003	18:18:02	11/26/2003 18:18	4775	CO2	1.95	9.85	0.958	%vol
Nov03-TCD320.chr	M-3		11/28/2003	21:07:46	11/28/2003 21:07		CO2	1.983	11.22	1.085	%vol
Nov03-TCD327.chr	M-3		12/1/2003	14:53:57	12/1/2003 14:53	12172	CO2	1.966	15.83	1.513	%vol
Nov03-TCD365.chr	M-3		12/2/2003	17:11:20	12/2/2003 17:11	13827	CO2	1.975	18.79	1.787	%vol
Nov03-TCD410.chr	M-3		12/3/2003	16:23:07	12/3/2003 16:23	15379	CO2	1.966	20.17	1.915	%vol
					11/23/03 20:00	1					0.17
Nov03-TCD44.chr	M-4		11/23/2003	22:48:21	11/23/2003 22:48	168	CO2	1.95	1.25	0.177	%vol
Nov03-TCD87.chr	M-4		11/24/2003	5:28:36	11/24/2003 5:28	571	CO2	1.941	3.78	0.475	%vol
Nov03-TCD130.chr	M-4		11/24/2003	11:27:04	11/24/2003 11:27	930	CO2	1.983	4.75	0.589	%vol
Nov03-TCD156.chr	M-4		11/24/2003	16:10:56	11/24/2003 16:10	1207	CO2	1.991	5.21	0.643	%vol
Nov03-TCD187.chr	M-4		11/24/2003	20:00:55	11/24/2003 20:00	1424	CO2	1.983	6.4	0.783	%vol
Nov03-TCD234.chr	M-4		11/25/2003	20:54:40	11/25/2003 20:54	3459	CO2	1.966	5.88	0.59	%vol
Nov03-TCD267.chr	M-4		11/26/2003	18:34:23	11/26/2003 18:34		CO2	1.941	9.22	0.899	%vol
Nov03-TCD321.chr	M-4		11/28/2003	21:26:05	11/28/2003 21:26	8087	CO2	1.975	14.83	1.42	%vol
Nov03-TCD328.chr	M-4		12/1/2003	18:33:14	12/1/2003 18:33	12392	CO2	1.95	14.95	1.431	%vol
Nov03-TCD366.chr	M-4		12/2/2003	17:27:13	12/2/2003 17:27	13843	CO2	1.975	12.87	1.238	%vol
Nov03-TCD411.chr	M-4		12/3/2003	16:35:02	12/3/2003 16:35	15391	CO2	1.975	14.18	1.36	%vol
					11/23/03 20:00	1					0.5
Nov03-TCD88.chr	M-5		11/24/2003	5:34:09	11/24/2003 5:34		CO2	1.933	3.94	0.494	%vol
Nov03-TCD131.chr	M-5		11/24/2003	11:37:39	11/24/2003 11:37	940	CO2	1.966	2.55	0.33	%vol
Nov03-TCD157.chr	M-5		11/24/2003	16:20:30	11/24/2003 16:20	1217	CO2	1.975	1.88	0.251	%vol

	SAMPLE	INJECT S	date	time	cum time		gas	reten	area	conc	units
Nov03-TCD188.chr	M-5		11/24/2003	20:11:16	11/24/2003 20:11	1435	CO2	1.95	5.38	0.662	%vol
Nov03-TCD322.chr	M-5		11/28/2003	21:48:05	11/28/2003 21:48	8109	CO2	1.975	2.96	0.319	%vol
Nov03-TCD329.chr	M-5		12/1/2003	18:53:40	12/1/2003 18:53	12412	CO2	1.941	3.99	0.415	%vol
Nov03-TCD367.chr	M-5		12/2/2003	17:43:03	12/2/2003 17:43	13859	CO2	1.983	4.11	0.426	%vol
Nov03-TCD412.chr	M-5		12/3/2003	16:52:34	12/3/2003 16:52	15408	CO2	2	4.37	0.449	%vol
Nov03-TCD151.chr	MIDPOINT		11/24/2003	15:08:06			CO2	0	0	0	%vol
Nov03-TCD191.chr	MIDPOINT		11/24/2003	20:46:42			CO2	0	0	0	%vol
Nov03-TCD211.chr	MIX 33 STAND?		11/25/2003	14:42:38			CO2	1.958	10.3	1.243	%vol
Nov03-TCD144.chr	OUTTAKE TUBE		11/24/2003	12:57:58			CO2	0	0	0	%vol
Nov03-TCD152.chr	OUTTAKE TUBE		11/24/2003	15:30:52			CO2	0	0	0	%vol
Nov03-TCD192.chr	OUTTAKE TUBE		11/24/2003	21:09:15			CO2	0	0	0	%vol
Nov03-TCD194.chr	OUTTAKE TUBE		11/25/2003	10:24:12			CO2	0	0	0	%vol
Nov03-TCD195.chr	s-GAS STAND		11/25/2003	10:39:45			CO2	0	0	0	%vol
Nov03-TCD236.chr	s-GAS STAND		11/26/2003	11:43:48			CO2	0	0	0	%vol
Nov03-TCD280.chr	s-GAS STAND		11/28/2003	9:26:27			CO2	0	0	0	%vol
Nov03-TCD281.chr	s-GAS STAND		11/28/2003	9:40:55			CO2	0	0	0	%vol
Nov03-TCD323.chr	s-GAS STAND		12/1/2003	13:40:47			CO2	0	0	0	%vol
Nov03-TCD324.chr	s-GAS STAND		12/1/2003	13:58:56			CO2	0	0	0	%vol
Nov03-TCD336.chr	s-GAS STAND		12/2/2003	9:56:01			CO2	0	0	0	%vol
Nov03-TCD378.chr	s-GAS STAND		12/3/2003	9:20:47			CO2	0	0	0	%vol
					11/23/03 20:00	1					0.1
Nov03-TCD54.chr	SOX-1		11/24/2003	0:16:11	11/24/2003 0:16	256	CO2	1.95	0.76	0.119	%vol
Nov03-TCD99.chr	SOX-1		11/24/2003	6:35:47	11/24/2003 6:35	651	CO2	1.95	0.61	0.101	%vol
Nov03-TCD142.chr	SOX-1		11/24/2003	12:31:13	11/24/2003 12:31	1007	CO2	1.966	0.72	0.114	%vol
Nov03-TCD226.chr	SOX-1		11/25/2003	19:11:41	11/25/2003 19:11	2727	CO2	1.941	2.32	0.259	%vol
Nov03-TCD268.chr	SOX-1		11/26/2003	18:41:59	11/26/2003 18:41	4077	CO2	1.966	1.47	0.181	%vol
Nov03-TCD312.chr	SOX-1		11/28/2003	18:11:26	11/28/2003 18:11	6927	CO2	1.975	1.38	0.172	%vol
Nov03-TCD356.chr	SOX-1		12/2/2003	14:55:07	12/2/2003 14:55	12622	CO2	1.983	1.39	0.173	%vol
Nov03-TCD402.chr	SOX-1		12/3/2003	14:25:33	12/3/2003 14:25	15260	CO2	1.983	1.54	0.187	%vol
					11/23/03 20:00	1					0.5
Nov03-TCD100.chr	SOX-2		11/24/2003	6:49:12	11/24/2003 6:49	665	CO2	1.941	8.88	1.076	%vol
Nov03-TCD55.chr	SOX-2		11/24/2003	0:34:08	11/24/2003 11:34	944	CO2	1.958	2.6	0.336	%vol
Nov03-TCD145.chr	SOX-2		11/24/2003	13:18:44	11/24/2003 13:18	1055	CO2	1.95	15.29	1.831	%vol
Nov03-TCD227.chr	SOX-2		11/25/2003	19:18:09	11/25/2003 19:18	2734	CO2	1.975	42.82	4.016	%vol
Nov03-TCD270.chr	SOX-2		11/26/2003	19:06:18	11/26/2003 19:06	4102	CO2	1.95	66.17	6.182	%vol
Nov03-TCD313.chr	SOX-2		11/28/2003	18:29:29	11/28/2003 18:29	6945	CO2	1.908	100.84	9.398	%vol
Nov03-TCD357.chr	SOX-2		12/2/2003	15:00:50	12/2/2003 15:00	12627	CO2	1.958	113.44	10.566	%vol
Nov03-TCD403.chr	SOX-2		12/3/2003	14:43:55	12/3/2003 14:43	15278	CO2	1.975	120.19	11.193	%vol
					11/23/03 20:00	1					0.3
Nov03-TCD56.chr	SOX-3		11/24/2003	0:55:51	11/24/2003 0:55	295	CO2	1.983	2.92	0.374	%vol
Nov03-TCD101.chr	SOX-3		11/24/2003	7:02:11	11/24/2003 7:02	678	CO2	1.95	7.95	0.966	%vol
Nov03-TCD146.chr	SOX-3	100	11/24/2003	13:33:31	11/24/2003 13:33	1077	CO2	1.975	6.14	0.753	%vol
Nov03-TCD228.chr	SOX-3		11/25/2003	19:32:27	11/25/2003 19:32	2748	CO2	1.95	34.81	3.274	%vol
Nov03-TCD272.chr	SOX-3		11/26/2003	19:32:41	11/26/2003 19:32	4128	CO2	1.933	57.6	5.387	%vol
Nov03-TCD314.chr	SOX-3		11/28/2003	18:46:16	11/28/2003 18:46	6962	CO2	1.958	83.14	7.756	%vol
Nov03-TCD358.chr	SOX-3		12/2/2003	15:20:38	12/2/2003 15:20	12647	CO2	1.925	107.57	10.022	%vol
Nov03-TCD404.chr	SOX-3		12/3/2003	15:04:16	12/3/2003 15:04	15299	CO2	1.958	111.86	10.42	%vol
					11/23/03 20:00	1					0.2
Nov03-TCD57.chr	SOX-4		11/24/2003	1:09:26	11/24/2003 1:09	309	CO2	1.966	2.03	0.269	%vol
Nov03-TCD102.chr	SOX-4		11/24/2003	7:16:12	11/24/2003 7:16	682	CO2	1.958	7.1	0.865	%vol
Nov03-TCD147.chr	SOX-4	100	11/24/2003	13:52:16	11/24/2003 13:52	1096	CO2	1.975	5.26	0.649	%vol
Nov03-TCD229.chr	SOX-4		11/25/2003	19:47:29	11/24/2003 19:47		CO2	1.95	31.61	2.976	%vol
Nov03-TCD274.chr	SOX-4		11/26/2003	19:57:46	11/26/2003 19:57	4143	CO2	1.95	54.89	5.136	%vol
Nov03-TCD315.chr	SOX-4		11/28/2003	19:15:45	11/28/2003 19:15	6991	CO2	1.95	81.12	7.568	%vol
Nov03-TCD359.chr	SOX-4		12/2/2003	15:41:11	12/2/2003 15:41	12668	CO2	1.95	101.72	9.479	%vol
Nov03-TCD405.chr	SOX-4		12/3/2003	15:21:17	12/3/2003 15:21	15316	CO2	1.941	109.89	10.237	%vol
					11/23/03 20:00	1					0.3
Nov03-TCD58.chr	SOX-5		11/24/2003	1:32:57	11/24/2003 1:31	331	CO2	1.975	2.97	0.379	%vol
Nov03-TCD103.chr	SOX-5		11/24/2003	7:29:34	11/24/2003 7:29	695	CO2	1.966	8.34	1.011	%vol
Nov03-TCD148.chr	SOX-5	100	11/24/2003	14:07:34	11/24/2003 14:07	1111	CO2	1.966	5.82	0.715	%vol
Nov03-TCD230.chr	SOX-5		11/25/2003	20:09:47	11/25/2003 20:09	2785	CO2	1.983	40.67	3.817	%vol
Nov03-TCD276.chr	SOX-5		11/26/2003	20:23:06	11/26/2003 20:23	4169	CO2	1.958	54.69	5.117	%vol
Nov03-TCD316.chr	SOX-5		11/28/2003	19:36:47	11/28/2003 19:36	7012	CO2	1.95	85.79	8.002	%vol
Nov03-TCD360.chr	SOX-5		12/2/2003	16:08:56	12/2/2003 16:08	12695	CO2	1.966	104.99	9.782	%vol
Nov03-TCD406.chr	SOX-5		12/3/2003	15:37:16	12/3/2003 15:37	15332	CO2	1.941	119.15	11.096	%vol
					11/23/03 20:00	1					2.22
Nov03-TCD59.chr	SOX-6		11/24/2003	1:49:14	11/24/2003 1:49	349	CO2	1.941	18.53	2.212	%vol
Nov03-TCD104.chr	SOX-6		11/24/2003	7:44:04	11/24/2003 7:44	710	CO2	1.966	17.66	2.109	%vol
Nov03-TCD149.chr	SOX-6		11/24/2003	14:29:15	11/24/2003 14:29	1133	CO2	1.983	16.8	2.008	%vol
Nov03-TCD277.chr	SOX-6		11/26/2003	20:43:23	11/26/2003 20:43	4189	CO2	1.966	15.53	1.485	%vol
Nov03-TCD317.chr	SOX-6		11/28/2003	19:59:35	11/28/2003 19:59	7035	CO2	1.991	14.14	1.355	%vol
Nov03-TCD361.chr	SOX-6		12/2/2003	16:27:38	12/2/2003 16:27	12714	CO2	1.975	12.91	1.242	%vol
Nov03-TCD407.chr	SOX-6		12/3/2003	15:52:06	12/3/2003 15:52	15347	CO2	1.975	13.44	1.291	%vol

Appendix D - Chapter 5 Gas chromatography data from Nov 2003

FID Results

	SAMPLE	INJECT	date	time	cum time	cum min	gas	conc	units
Nov03-FID381.chr	98.6 ch4		12/3/2003	10:04:19			Methane	101.34	ppm
					11/23/03 20:00	1.00			
Nov03-FID61.chr	A-1		11/24/2003	2:15:30	11/24/2003 2:15	375.00	Methane	13.2	ppm
Nov03-FID106.chr	A-1		11/24/2003	8:04:27	11/24/2003 8:04	1444.00	Methane		ppm
Nov03-FID158.chr	A-1		11/24/2003	16:26:23	11/24/2003 16:26	1950.00	Methane	16.33	ppm
Nov03-FID197.chr	A-1		11/25/2003	12:24:20	11/25/2003 12:24	2852.00	Methane	17	ppm
Nov03-FID237.chr	A-1		11/26/2003	12:04:10	11/26/2003 12:04	4270.00	Methane	16.2	ppm
Nov03-FID282.chr	A-1		11/28/2003	10:01:11	11/28/2003 10:01	7755.00	Methane		ppm
Nov03-FID368.chr	A-1		12/2/2003	17:53:08	12/2/2003 17:53	13976.00	Methane		ppm
Nov03-FID428.chr	A-1		12/4/2003	17:04:53	12/4/2003 17:04	15847.00	Methane	16.7	ppm
					11/23/03 20:00	1.00			
Nov03-FID24.chr	A-2	250	11/23/2003	20:44:03	11/23/2003 20:44	44.00	Methane		ppm
Nov03-FID62.chr	A-2		11/24/2003	2:23:06	11/24/2003 2:23	383.00	Methane	9.6	ppm
Nov03-FID107.chr	A-2		11/24/2003	8:09:44	11/24/2003 8:09	1449.00	Methane		ppm
Nov03-FID159.chr	A-2		11/24/2003	16:31:05	11/24/2003 16:31	1954.00	Methane	11.4	ppm
Nov03-FID198.chr	A-2		11/25/2003	12:30:36	11/25/2003 12:30	2858.00	Methane	8.6	ppm
Nov03-FID238.chr	A-2		11/26/2003	12:08:54	11/26/2003 12:08	4274.00	Methane	7.78	ppm
Nov03-FID283.chr	A-2		11/28/2003	10:21:19	11/28/2003 10:21	7775.00	Methane		ppm
Nov03-FID369.chr	A-2		12/2/2003	18:07:16	12/2/2003 18:07	13981.00	Methane		ppm
Nov03-FID429.chr	A-2		12/4/2003	17:09:45	12/4/2003 17:09	15852.00	Methane	12.3	ppm
					11/23/03 20:00	1.00			
Nov03-FID25.chr	A-3		11/23/2003	20:49:46	11/23/2003 20:49	49.00	Methane		ppm
Nov03-FID63.chr	A-3		11/24/2003	2:29:01	11/24/2003 2:29	389.00	Methane	9.3	ppm
Nov03-FID108.chr	A-3		11/24/2003	8:15:11	11/24/2003 8:15	1455.00	Methane		ppm
Nov03-FID160.chr	A-3	100	11/24/2003	16:40:21	11/24/2003 16:40	1965.00	Methane		ppm
Nov03-FID199.chr	A-3		11/25/2003	12:40:16	11/25/2003 12:40	2868.00	Methane	10.46	ppm
Nov03-FID239.chr	A-3		11/26/2003	12:18:57	11/26/2003 12:18	4284.00	Methane	10.6	ppm
Nov03-FID284.chr	A-3		11/28/2003	10:32:23	11/28/2003 10:32	7786.00	Methane		ppm
Nov03-FID330.chr	A-3		12/1/2003	19:07:14	12/1/2003 19:07	12653.00	Methane	10.7	ppm
Nov03-FID370.chr	A-3		12/2/2003	18:27:04	12/2/2003 18:27	14001.00	Methane		ppm
Nov03-FID430.chr	A-3		12/4/2003	17:24:32	12/4/2003 17:24		Methane	13.2	ppm
					11/23/03 20:00	1.00			
Nov03-FID26.chr	A-4		11/23/2003	20:54:50	11/23/2003 20:54	54.00	Methane		ppm
Nov03-FID64.chr	A-4		11/24/2003	2:35:47	11/24/2003 2:35	395.00	Methane	8.2	ppm
Nov03-FID109.chr	A-4		11/24/2003	8:24:58	11/24/2003 8:24	1464.00	Methane		ppm
Nov03-FID161.chr	A-4		11/24/2003	16:50:56	11/24/2003 16:50	1675.00	Methane	9.7	ppm
Nov03-FID200.chr	A-4		11/25/2003	12:48:29	11/25/2003 12:48	2876.00	Methane	10.7	ppm
Nov03-FID240.chr	A-4		11/26/2003	12:33:54	11/26/2003 12:33	4299.00	Methane	8.9	ppm
Nov03-FID285.chr	A-4		11/28/2003	10:49:20	11/28/2003 10:49	7803.00	Methane		ppm
Nov03-FID371.chr	A-4		12/2/2003	18:43:54	12/2/2003 18:43	14017.00	Methane		ppm
Nov03-FID431.chr	A-4		12/4/2003	17:42:59	12/4/2003 17:42	15885.00	Methane	15.4	ppm
					11/23/03 20:00	1.00			
Nov03-FID27.chr	A-5		11/23/2003	21:00:52	11/23/2003 21:00	60.00	Methane		ppm
Nov03-FID65.chr	A-5		11/24/2003	2:57:06	11/24/2003 2:57	417.00	Methane	8.4	ppm
Nov03-FID110.chr	A-5		11/24/2003	8:34:36	11/24/2003 8:34	1474.00	Methane		ppm
Nov03-FID162.chr	A-5		11/24/2003	17:02:35	11/24/2003 17:02	1687.00	Methane	12.6	ppm
Nov03-FID201.chr	A-5		11/25/2003	12:55:22	11/25/2003 12:55	2889.00	Methane	17.5	ppm
Nov03-FID241.chr	A-5		11/26/2003	12:48:46	11/26/2003 12:48	4314.00	Methane	17.55	ppm
Nov03-FID286.chr	A-5		11/28/2003	11:09:46	11/28/2003 11:09	7823.00	Methane		ppm
Nov03-FID331.chr	A-5		12/1/2003	19:27:24	12/1/2003 19:27	12650.00	Methane	20.26	ppm
Nov03-FID372.chr	A-5		12/2/2003	18:58:12	12/2/2003 18:58	14032.00	Methane		ppm
Nov03-FID432.chr	A-5		12/4/2003	17:58:55	12/4/2003 17:58	15901.00	Methane	20.4	ppm
					11/23/03 20:00	1.00			
Nov03-FID28.chr	A-6		11/23/2003	21:05:55	11/23/2003 21:05	65.00	Methane		ppm
Nov03-FID66.chr	A-6		11/24/2003	3:06:11	11/24/2003 3:06	425.00	Methane	9.2	ppm
Nov03-FID111.chr	A-6	100	11/24/2003	8:44:25	11/24/2003 8:44	1484.00	Methane		ppm
Nov03-FID163.chr	A-6	100	11/24/2003	17:12:45	11/24/2003 17:12	1697.00	Methane		ppm
Nov03-FID202.chr	A-6		11/25/2003	13:04:06	11/25/2003 13:04	2898.00	Methane	11.05	ppm
Nov03-FID242.chr	A-6		11/26/2003	13:04:19	11/26/2003 13:04	4338.00	Methane		ppm
Nov03-FID287.chr	A-6		11/28/2003	11:18:06	11/28/2003 11:18	7832.00	Methane		ppm
Nov03-FID332.chr	A-6		12/1/2003	20:05:10	12/1/2003 20:05	12682.00	Methane	14.3	ppm
Nov03-FID373.chr	A-6		12/2/2003	19:13:33	12/2/2003 19:13	14047.00	Methane		ppm
Nov03-FID433.chr	A-6		12/4/2003	18:08:45	12/4/2003 18:08	15911.00	Methane	16.3	ppm
					11/23/03 20:00	1.00			
Nov03-FID29.chr	A-7		11/23/2003	21:11:08		71.00	Methane		ppm
Nov03-FID67.chr	A-7		11/24/2003	3:12:17		431.00	Methane	7.05	ppm
Nov03-FID112.chr	A-7	100	11/24/2003	8:54:50		1494.00	Methane		ppm
Nov03-FID164.chr	A-7	100	11/24/2003	17:24:07		1709.00	Methane		ppm
Nov03-FID165.chr	A-7	50	11/24/2003	17:35:58		1720.00	Methane		ppm
Nov03-FID203.chr	A-7	50	11/25/2003	13:25:07		1720.00	Methane		ppm

	SAMPLE	INJECT	date	time		gas		conc	units
Nov03-FID243.chr	A-7		11/26/2003	13:24:18		4364.00	Methane	9.75	ppm
Nov03-FID288.chr	A-7		11/28/2003	11:37:50		7851.00	Methane		ppm
Nov03-FID333.chr	A-7		12/1/2003	20:27:08		12714.00	Methane	15	ppm
Nov03-FID374.chr	A-7		12/2/2003	19:30:48		14064.00	Methane		ppm
Nov03-FID434.chr	A-7		12/4/2003	18:40:21		15943.00	Methane	8.1	ppm
					11/23/03 20:00	1.00			
Nov03-FID30.chr	A-8		11/23/2003	21:16:22		76.00	Methane		ppm
Nov03-FID68.chr	A-8		11/24/2003	3:24:51		443.00	Methane	7.29	ppm
Nov03-FID113.chr	A-8	250	11/24/2003	9:04:57		1504.00	Methane		ppm
Nov03-FID166.chr	A-8	250	11/24/2003	17:42:06		1721.00	Methane	13.9	ppm
Nov03-FID205.chr	A-8	250	11/25/2003	13:39:50		2938.00	Methane	18.32	ppm
Nov03-FID244.chr	A-8		11/26/2003	13:38:59		4378.00	Methane	22.3	ppm
Nov03-FID289.chr	A-8		11/28/2003	12:00:51		7874.00	Methane		ppm
Nov03-FID334.chr	A-8		12/1/2003	20:50:59		12737.00	Methane	28.1	ppm
Nov03-FID375.chr	A-8		12/2/2003	19:48:37		14076.00	Methane		ppm
Nov03-FID435.chr	A-8		12/4/2003	18:58:56		15961.00	Methane	28	ppm
					11/23/03 20:00	1.00			
Nov03-FID31.chr	A-9		11/23/2003	21:22:57		82.00	Methane		ppm
Nov03-FID69.chr	A-9		11/24/2003	3:31:17		450.00	Methane	7.94	ppm
Nov03-FID114.chr	A-9	100	11/24/2003	9:10:45		1510.00	Methane		ppm
Nov03-FID167.chr	A-9	50	11/24/2003	17:48:55		1727.00	Methane		ppm
Nov03-FID207.chr	A-9	250	11/25/2003	14:01:58		2948.00	Methane	9.9	ppm
Nov03-FID245.chr	A-9		11/26/2003	13:51:43		4391.00	Methane	13.4	ppm
Nov03-FID290.chr	A-9		11/28/2003	12:21:00		7895.00	Methane	8.1	ppm
Nov03-FID376.chr	A-9		12/2/2003	20:03:36		14081.00	Methane		ppm
Nov03-FID436.chr	A-9		12/4/2003	19:13:00		15976.00	Methane	11	ppm
					11/23/03 20:00	1.00			
Nov03-FID70.chr	A-10		11/24/2003	3:41:07	11/24/2003 3:41	460.00	Methane	11.71	ppm
Nov03-FID115.chr	A-10	250	11/24/2003	9:20:03	11/24/2003 9:20	1524.00	Methane		ppm
Nov03-FID168.chr	A-10	250	11/24/2003	17:59:10	11/24/2003 17:59	1738.00	Methane	14.2	ppm
Nov03-FID208.chr	A-10		11/25/2003	14:15:28	11/25/2003 14:15	2952.00	Methane	11.66	ppm
Nov03-FID246.chr	A-10		11/26/2003	14:04:15	11/26/2003 14:04	4699.00	Methane	14	ppm
Nov03-FID291.chr	A-10		11/28/2003	12:49:41	11/28/2003 12:49	7923.00	Methane		ppm
Nov03-FID437.chr	A-10		12/4/2003	19:33:04	12/4/2003 19:33	15996.00	Methane	10.89	ppm
					11/23/03 20:00	1.00			
Nov03-FID32.chr	B-1		11/23/2003	21:29:21	11/23/2003 21:29	89.00	Methane		ppm
Nov03-FID71.chr	B-1		11/24/2003	3:46:32	11/24/2003 3:46	465.00	Methane	12.9	ppm
Nov03-FID116.chr	B-1	250	11/24/2003	9:25:12	11/24/2003 9:25	1529.00	Methane		ppm
Nov03-FID169.chr	B-1		11/24/2003	18:04:13	11/24/2003 18:04	1743.00	Methane	13.5	ppm
Nov03-FID209.chr	B-1		11/25/2003	14:26:43	11/25/2003 14:26	2983.00	Methane	14.7	ppm
Nov03-FID247.chr	B-1		11/26/2003	14:20:41	11/26/2003 14:20	4420.00	Methane	24.4	ppm
Nov03-FID292.chr	B-1		11/28/2003	12:58:33	11/28/2003 12:58	7932.00	Methane		ppm
Nov03-FID382.chr	B-1		12/3/2003	10:06:51	12/3/2002 10:06	15012.00	Methane	17.9	ppm
					11/23/03 20:00	1.00			
Nov03-FID33.chr	B-2		11/23/2003	21:35:22	11/23/2003 21:35	94.00	Methane		ppm
Nov03-FID72.chr	B-2		11/24/2003	3:53:32	11/24/2003 3:52	472.00	Methane	8.3	ppm
Nov03-FID117.chr	B-2	100	11/24/2003	9:28:55	11/24/2003 9:28	1532.00	Methane		ppm
Nov03-FID170.chr	B-2	50	11/24/2003	18:12:15	11/24/2003 18:12	1756.00	Methane		ppm
Nov03-FID171.chr	B-2	250	11/24/2003	18:17:30	11/24/2003 18:17	1761.00	Methane	10	ppm
Nov03-FID210.chr	B-2		11/25/2003	14:32:50	11/25/2003 14:32	2990.00	Methane	10.3	ppm
Nov03-FID248.chr	B-2		11/26/2003	14:27:14	11/26/2003 14:27	4427.00	Methane	9.7	ppm
Nov03-FID293.chr	B-2		11/28/2003	13:02:22	11/28/2003 13:02	7936.00	Methane		ppm
Nov03-FID337.chr	B-2		12/2/2003	10:31:52	12/2/2003 10:31	13631.00	Methane	9.75	ppm
Nov03-FID383.chr	B-2		12/3/2003	10:15:04	12/3/2003 10:15	15021.00	Methane	20.4	ppm
					11/23/03 20:00	1.00			
Nov03-FID34.chr	B-3		11/23/2003	21:50:17	11/23/2003 21:50	109.00	Methane		ppm
Nov03-FID74.chr	B-3		11/24/2003	4:09:55	11/24/2003 4:09	488.00	Methane	6.5	ppm
Nov03-FID118.chr	B-3	100	11/24/2003	9:39:45	11/24/2003 9:39	1543.00	Methane		ppm
Nov03-FID172.chr	B-3	100	11/24/2003	18:27:56	11/24/2003 18:27	1766.00	Methane	6.98	ppm
Nov03-FID212.chr	B-3		11/25/2003	14:48:21	11/25/2003 14:48	3006.00	Methane	7.2	ppm
Nov03-FID249.chr	B-3		11/26/2003	14:41:01	11/26/2003 14:41	4441.00	Methane	11.1	ppm
Nov03-FID294.chr	B-3		11/28/2003	13:24:29	11/28/2003 13:24	7968.00	Methane		ppm
Nov03-FID338.chr	B-3		12/2/2003	10:51:22	12/2/2003 10:51	13661.00	Methane	12.9	ppm
Nov03-FID384.chr	B-3		12/3/2003	10:30:07	12/3/2003 10:30	15028.00	Methane	10.5	ppm
					11/23/03 20:00	1.00			
Nov03-FID35.chr	B-4		11/23/2003	21:55:52	11/23/2003 21:55	113.00	Methane	10.5	ppm
Nov03-FID75.chr	B-4		11/24/2003	4:19:01	11/24/2003 4:19	498.00	Methane	6.9	ppm
Nov03-FID119.chr	B-4	250	11/24/2003	9:50:00	11/24/2003 9:50	867.00	Methane		ppm
Nov03-FID173.chr	B-4	100	11/24/2003	18:38:08	11/24/2003 18:38	1777.00	Methane		ppm
Nov03-FID213.chr	B-4		11/25/2003	14:58:11	11/25/2003 14:58	3016.00	Methane	7.97	ppm
Nov03-FID250.chr	B-4		11/26/2003	15:01:03	11/26/2003 15:01	4461.00	Methane	15.2	ppm

	SAMPLE	INJECT	date	time		gas	conc	units
Nov03-FID295.chr	B-4		11/28/2003	13:40:14	11/28/2003 13:40	7984.00 Methane		ppm
Nov03-FID339.chr	B-4		12/2/2003	11:11:49	12/2/2003 11:11	13671.00 Methane	11.2	ppm
Nov03-FID385.chr	B-4		12/3/2003	10:46:15	12/3/2003 10:46	15042.00 Methane	12	ppm
					11/23/03 20:00	1.00		
Nov03-FID36.chr	B-5		11/23/2003	22:01:45	11/23/2003 22:01	120.00 Methane		ppm
Nov03-FID76.chr	B-5		11/24/2003	4:24:39	11/24/2003	503.00 Methane	6.8	ppm
Nov03-FID120.chr	B-5	250	11/24/2003	10:00:03	11/24/2003 10:00	877.00 Methane		ppm
Nov03-FID174.chr	B-5	250	11/24/2003	18:48:52	11/24/2003 18:48	1797.00 Methane	8.3	ppm
Nov03-FID214.chr	B-5		11/25/2003	15:15:28	11/25/2003 15:15	3033.00 Methane	9.9	ppm
Nov03-FID251.chr	B-5		11/26/2003	15:14:27	11/26/2003 15:14	4474.00 Methane	16.6	ppm
Nov03-FID296.chr	B-5		11/28/2003	13:58:38	11/28/2003 13:58	8002.00 Methane		ppm
Nov03-FID340.chr	B-5		12/2/2003	11:50:54	12/2/2003 11:50	13710.00 Methane	13.1	ppm
Nov03-FID386.chr	B-5		12/3/2003	11:01:11	12/3/2003 11:01	15057.00 Methane	11.2	ppm
					11/23/03 20:00	1.00		
Nov03-FID37.chr	B-6		11/23/2003	22:06:59	11/23/2003 22:06	125.00 Methane		ppm
Nov03-FID77.chr	B-6		11/24/2003	4:30:32	11/24/2003 4:30	509.00 Methane	6.8	ppm
Nov03-FID121.chr	B-6	250	11/24/2003	10:04:16	11/24/2003 10:04	881.00 Methane		ppm
Nov03-FID175.chr	B-6	250	11/24/2003	18:53:58	11/24/2003 18:53	1802.00 Methane	8.6	ppm
Nov03-FID215.chr	B-6		11/25/2003	15:35:21	11/25/2003 15:35	3053.00 Methane	10.97	ppm
Nov03-FID252.chr	B-6		11/26/2003	15:34:17	11/26/2003 15:34	4494.00 Methane	10.96	ppm
Nov03-FID297.chr	B-6		11/28/2003	14:17:56	11/28/2003 14:17	8011.00 Methane		ppm
Nov03-FID341.chr	B-6		12/2/2003	12:10:16	12/2/2003 12:10	13730.00 Methane	10.1	ppm
Nov03-FID387.chr	B-6		12/3/2003	11:15:21	12/3/2003 11:15	15071.00 Methane	8.7	ppm
						1.00		
Nov03-FID38.chr	B-7		11/23/2003	22:13:58		132.00 Methane		ppm
Nov03-FID78.chr	B-7		11/24/2003	4:36:07		515.00 Methane	6.7	ppm
Nov03-FID122.chr	B-7	100	11/24/2003	10:13:54		906.00 Methane		ppm
Nov03-FID176.chr	B-7	100	11/24/2003	19:05:41		1814.00 Methane		ppm
Nov03-FID216.chr	B-7		11/25/2003	17:02:20		3140.00 Methane	9.48	ppm
Nov03-FID253.chr	B-7		11/26/2003	15:49:52		4650.00 Methane	15.1	ppm
Nov03-FID298.chr	B-7		11/28/2003	14:31:55		8026.00 Methane		ppm
Nov03-FID342.chr	B-7		12/2/2003	12:28:26		13744.00 Methane	17.6	ppm
Nov03-FID388.chr	B-7		12/3/2003	11:35:06		15091.00 Methane	9.2	ppm
						1.00		
Nov03-FID39.chr	B-8		11/23/2003	22:18:59		137.00 Methane		ppm
Nov03-FID79.chr	B-8		11/24/2003	4:41:38		520.00 Methane		ppm
Nov03-FID123.chr	B-8	250	11/24/2003	10:24:56		917.00 Methane		ppm
Nov03-FID177.chr	B-8	250	11/24/2003	19:15:45		1811.00 Methane		ppm
Nov03-FID178.chr	B-8	250	11/24/2003	19:17:25		1813.00 Methane	6.5	ppm
Nov03-FID217.chr	B-8		11/25/2003	17:24:57		3231.00 Methane	6.97	ppm
Nov03-FID254.chr	B-8		11/26/2003	16:03:02		4664.00 Methane	7.2	ppm
Nov03-FID299.chr	B-8		11/28/2003	14:52:58		8047.00 Methane		ppm
Nov03-FID343.chr	B-8		12/2/2003	12:48:22		13764.00 Methane	7.4	ppm
Nov03-FID389.chr	B-8		12/3/2003	11:50:27		15106.00 Methane	9.4	ppm
						1.00		
Nov03-FID40.chr	B-9		11/23/2003	22:24:45		143.00 Methane		ppm
Nov03-FID80.chr	B-9		11/24/2003	4:47:35		526.00 Methane	6.3	ppm
Nov03-FID81.chr	B-9	100	11/24/2003	4:57:48		536.00 Methane		ppm
Nov03-FID82.chr	B-9	50	11/24/2003	5:02:22		541.00 Methane		ppm
Nov03-FID124.chr	B-9	100	11/24/2003	10:31:41		924.00 Methane		ppm
Nov03-FID125.chr	B-9	50	11/24/2003	10:46:35		929.00 Methane		ppm
Nov03-FID179.chr	B-9	100	11/24/2003	19:20:41		1814.00 Methane		ppm
Nov03-FID218.chr	B-9		11/25/2003	17:39:08		3246.00 Methane	9.58	ppm
Nov03-FID255.chr	B-9		11/26/2003	16:14:50		4675.00 Methane		ppm
Nov03-FID300.chr	B-9		11/28/2003	15:08:22		8063.00 Methane		ppm
Nov03-FID344.chr	B-9	100	12/2/2003	13:00:26		13776.00 Methane		ppm
Nov03-FID390.chr	B-9		12/3/2003	12:04:14		15120.00 Methane	8.1	ppm
						1.00		
Nov03-FID83.chr	B-10	250	11/24/2003	5:06:54	11/24/2003 5:06	545.00 Methane	12.7	ppm
Nov03-FID126.chr	B-10	250	11/24/2003	10:52:55	11/24/2003 10:52	945.00 Methane		ppm
Nov03-FID180.chr	B-10	250	11/24/2003	19:24:49	11/24/2003 19:24	1818.00 Methane	9.2	ppm
Nov03-FID256.chr	B-10		11/26/2003	16:37:22	11/26/2003 16:37	4698.00 Methane	7.1	ppm
Nov03-FID301.chr	B-10		11/28/2003	15:27:31	11/28/2003 15:27	8074.00 Methane		ppm
Nov03-FID345.chr	B-10	250	12/2/2003	13:16:52	12/2/2003 13:16	13789.00 Methane	10.8	ppm
Nov03-FID391.chr	B-10		12/3/2003	12:22:59	12/3/2003 12:22	15138.00 Methane	10.5	ppm
Nov03-FID45.chr	C-1		11/23/2003	22:55:01		Methane		ppm
Nov03-FID89.chr	C-1		11/24/2003	5:39:49		Methane	14.2	ppm
Nov03-FID132.chr	C-1		11/24/2003	11:44:47		Methane		ppm
Nov03-FID219.chr	C-1		11/25/2003	17:57:28		Methane	17.5	ppm
Nov03-FID257.chr	C-1		11/26/2003	16:54:11		Methane	25	ppm
Nov03-FID302.chr	C-1		11/28/2003	15:46:37		Methane		ppm
Nov03-FID346.chr	C-1		12/2/2003	13:24:47		Methane	18.9	ppm

	SAMPLE	INJECT	date	time		gas	conc	units
Nov03-FID392.chr	C-1		12/3/2003	12:37:05		Methane	20.1	ppm
Nov03-FID98.chr	C-10		11/24/2003	6:29:28		Methane	13.59	ppm
Nov03-FID141.chr	C-10		11/24/2003	12:27:25		Methane		ppm
Nov03-FID275.chr	C-10		11/26/2003	20:17:14		Methane		ppm
Nov03-FID311.chr	C-10		11/28/2003	17:48:53		Methane		ppm
Nov03-FID355.chr	C-10		12/2/2003	14:51:33		Methane	12.3	ppm
Nov03-FID401.chr	C-10		12/3/2003	14:18:36		Methane	11.9	ppm
Nov03-FID46.chr	C-2		11/23/2003	23:03:13		Methane		ppm
Nov03-FID90.chr	C-2		11/24/2003	5:45:32		Methane	12.04	ppm
Nov03-FID133.chr	C-2		11/24/2003	11:49:00		Methane		ppm
Nov03-FID220.chr	C-2		11/25/2003	18:07:09		Methane	12.79	ppm
Nov03-FID258.chr	C-2		11/26/2003	17:05:07		Methane	15.8	ppm
Nov03-FID303.chr	C-2		11/28/2003	16:03:04		Methane		ppm
Nov03-FID347.chr	C-2		12/2/2003	13:30:58		Methane	14	ppm
Nov03-FID393.chr	C-2		12/3/2003	12:45:31		Methane	12.9	ppm
Nov03-FID47.chr	C-3		11/23/2003	23:08:28		Methane		ppm
Nov03-FID91.chr	C-3		11/24/2003	5:50:54		Methane	11.25	ppm
Nov03-FID134.chr	C-3		11/24/2003	11:53:05		Methane		ppm
Nov03-FID183.chr	C-3		11/24/2003	19:36:15		Methane	10.76	ppm
Nov03-FID221.chr	C-3		11/25/2003	18:16:38		Methane	13	ppm
Nov03-FID259.chr	C-3		11/26/2003	17:20:05		Methane	13.9	ppm
Nov03-FID304.chr	C-3		11/28/2003	16:19:14		Methane		ppm
Nov03-FID348.chr	C-3	100	12/2/2003	13:44:53		Methane	7.5	ppm
Nov03-FID394.chr	C-3		12/3/2003	12:57:12		Methane	11.5	ppm
Nov03-FID48.chr	C-4		11/23/2003	23:21:02		Methane		ppm
Nov03-FID92.chr	C-4		11/24/2003	5:56:34		Methane		ppm
Nov03-FID135.chr	C-4		11/24/2003	11:58:02		Methane		ppm
Nov03-FID182.chr	C-4		11/24/2003	19:32:48		Methane	10	ppm
Nov03-FID222.chr	C-4		11/25/2003	18:26:20		Methane	10.7	ppm
Nov03-FID260.chr	C-4		11/26/2003	17:28:05		Methane	14.3	ppm
Nov03-FID305.chr	C-4		11/28/2003	16:33:18		Methane		ppm
Nov03-FID349.chr	C-4		12/2/2003	13:56:15		Methane	17.6	ppm
Nov03-FID395.chr	C-4		12/3/2003	13:12:59		Methane	11.1	ppm
Nov03-FID49.chr	C-5		11/23/2003	23:40:24		Methane		ppm
Nov03-FID93.chr	C-5		11/24/2003	6:02:27		Methane	10.2	ppm
Nov03-FID136.chr	C-5		11/24/2003	12:05:29		Methane		ppm
Nov03-FID223.chr	C-5		11/25/2003	18:34:10		Methane	12.3	ppm
Nov03-FID261.chr	C-5		11/26/2003	17:37:58		Methane	10.1	ppm
Nov03-FID306.chr	C-5		11/28/2003	16:48:52		Methane		ppm
Nov03-FID350.chr	C-5		12/2/2003	14:05:59		Methane	12.6	ppm
Nov03-FID396.chr	C-5		12/3/2003	13:18:55		Methane	11.99	ppm
Nov03-FID50.chr	C-6		11/23/2003	23:46:26		Methane		ppm
Nov03-FID94.chr	C-6		11/24/2003	6:07:46		Methane	8.8	ppm
Nov03-FID137.chr	C-6		11/24/2003	12:10:09		Methane		ppm
Nov03-FID224.chr	C-6		11/25/2003	18:45:45		Methane	10.96	ppm
Nov03-FID262.chr	C-6		11/26/2003	17:44:09		Methane	12.1	ppm
Nov03-FID307.chr	C-6		11/28/2003	17:03:37		Methane		ppm
Nov03-FID351.chr	C-6		12/2/2003	14:09:32		Methane	8.4	ppm
Nov03-FID397.chr	C-6		12/3/2003	13:32:48		Methane	10.5	ppm
Nov03-FID51.chr	C-7		11/23/2003	23:53:44		Methane		ppm
Nov03-FID95.chr	C-7		11/24/2003	6:13:17		Methane	7.6	ppm
Nov03-FID138.chr	C-7		11/24/2003	12:14:16		Methane		ppm
Nov03-FID181.chr	C-7		11/24/2003	19:28:41		Methane	7.9	ppm
Nov03-FID225.chr	C-7		11/25/2003	18:58:39		Methane	9.5	ppm
Nov03-FID263.chr	C-7		11/26/2003	17:52:21		Methane	8	ppm
Nov03-FID308.chr	C-7		11/28/2003	17:17:51		Methane		ppm
Nov03-FID352.chr	C-7		12/2/2003	14:20:25		Methane	9.5	ppm
Nov03-FID398.chr	C-7		12/3/2003	13:40:37		Methane	9.3	ppm
Nov03-FID52.chr	C-8		11/24/2003	0:02:26		Methane		ppm
Nov03-FID96.chr	C-8		11/24/2003	6:18:38		Methane	8.7	ppm
Nov03-FID139.chr	C-8		11/24/2003	12:18:02		Methane		ppm
Nov03-FID264.chr	C-8		11/26/2003	18:03:42		Methane	11	ppm
Nov03-FID309.chr	C-8		11/28/2003	17:27:40		Methane		ppm
Nov03-FID353.chr	C-8		12/2/2003	14:30:57		Methane	9	ppm
Nov03-FID399.chr	C-8		12/3/2003	13:55:01		Methane	7.6	ppm
Nov03-FID53.chr	C-9		11/24/2003	0:09:34		Methane		ppm
Nov03-FID97.chr	C-9		11/24/2003	6:24:00		Methane	6.7	ppm
Nov03-FID140.chr	C-9		11/24/2003	12:23:53		Methane		ppm
Nov03-FID273.chr	C-9		11/26/2003	19:51:11		Methane		ppm
Nov03-FID310.chr	C-9		11/28/2003	17:38:06		Methane		ppm
Nov03-FID354.chr	C-9		12/2/2003	14:39:31		Methane	7.4	ppm
Nov03-FID400.chr	C-9		12/3/2003	14:06:58		Methane		ppm

	SAMPLE	INJECT	date	time		gas	conc	units
Nov03-FID41.chr	M-1		11/23/2003	22:30:09		Methane		ppm
Nov03-FID84.chr	M-1	250	11/24/2003	5:12:09		Methane	7.8	ppm
Nov03-FID127.chr	M-1		11/24/2003	10:57:13		Methane		ppm
Nov03-FID153.chr	M-1		11/24/2003	15:45:50		Methane	7.2	ppm
Nov03-FID184.chr	M-1		11/24/2003	19:40:39		Methane		ppm
Nov03-FID231.chr	M-1		11/25/2003	20:24:22		Methane	6.8	ppm
Nov03-FID271.chr	M-1		11/26/2003	19:26:02		Methane	10.8	ppm
Nov03-FID318.chr	M-1		11/28/2003	20:34:08		Methane		ppm
Nov03-FID325.chr	M-1		12/1/2003	14:21:22		Methane	7.8	ppm
Nov03-FID363.chr	M-1		12/2/2003	16:50:51		Methane		ppm
Nov03-FID408.chr	M-1		12/3/2003	16:06:49		Methane		ppm
Nov03-FID42.chr	M-2		11/23/2003	22:36:08		Methane		ppm
Nov03-FID85.chr	M-2		11/24/2003	5:17:29		Methane	7.99	ppm
Nov03-FID128.chr	M-2		11/24/2003	11:07:27		Methane		ppm
Nov03-FID154.chr	M-2		11/24/2003	15:50:32		Methane	7.8	ppm
Nov03-FID185.chr	M-2		11/24/2003	19:52:19		Methane	7.8	ppm
Nov03-FID232.chr	M-2		11/25/2003	20:36:28		Methane	9.7	ppm
Nov03-FID265.chr	M-2		11/26/2003	18:11:08		Methane	7.3	ppm
Nov03-FID319.chr	M-2		11/28/2003	20:45:29		Methane		ppm
Nov03-FID326.chr	M-2		12/1/2003	14:35:26		Methane	8.37	ppm
Nov03-FID364.chr	M-2		12/2/2003	16:55:29		Methane		ppm
Nov03-FID409.chr	M-2		12/3/2003	16:12:55		Methane	8.6	ppm
Nov03-FID43.chr	M-3		11/23/2003	22:42:37		Methane		ppm
Nov03-FID86.chr	M-3		11/24/2003	5:22:48		Methane	8.88	ppm
Nov03-FID129.chr	M-3		11/24/2003	11:17:31		Methane		ppm
Nov03-FID155.chr	M-3		11/24/2003	16:00:06		Methane	9.2	ppm
Nov03-FID186.chr	M-3		11/24/2003	19:56:29		Methane		ppm
Nov03-FID233.chr	M-3		11/25/2003	20:45:04		Methane	9.5	ppm
Nov03-FID266.chr	M-3		11/26/2003	18:18:02		Methane	9.6	ppm
Nov03-FID320.chr	M-3		11/28/2003	21:07:46		Methane		ppm
Nov03-FID327.chr	M-3		12/1/2003	14:53:57		Methane	10.8	ppm
Nov03-FID365.chr	M-3		12/2/2003	17:11:20		Methane		ppm
Nov03-FID410.chr	M-3		12/3/2003	16:23:07		Methane	6.66	ppm
Nov03-FID44.chr	M-4		11/23/2003	22:48:21		Methane		ppm
Nov03-FID87.chr	M-4		11/24/2003	5:28:36		Methane	9.76	ppm
Nov03-FID130.chr	M-4		11/24/2003	11:27:04		Methane		ppm
Nov03-FID156.chr	M-4		11/24/2003	16:10:56		Methane	6.7	ppm
Nov03-FID187.chr	M-4		11/24/2003	20:00:55		Methane		ppm
Nov03-FID234.chr	M-4		11/25/2003	20:54:40		Methane	6.56	ppm
Nov03-FID267.chr	M-4		11/26/2003	18:34:23		Methane	9	ppm
Nov03-FID321.chr	M-4		11/28/2003	21:26:05		Methane		ppm
Nov03-FID328.chr	M-4		12/1/2003	18:33:14		Methane		ppm
Nov03-FID366.chr	M-4		12/2/2003	17:27:13		Methane		ppm
Nov03-FID411.chr	M-4		12/3/2003	16:35:02		Methane		ppm
Nov03-FID88.chr	M-5		11/24/2003	5:34:09		Methane		ppm
Nov03-FID131.chr	M-5		11/24/2003	11:37:39		Methane		ppm
Nov03-FID157.chr	M-5		11/24/2003	16:20:30		Methane	7.7	ppm
Nov03-FID188.chr	M-5		11/24/2003	20:11:16		Methane		ppm
Nov03-FID235.chr	M-5		11/25/2003	21:06:57		Methane		ppm
Nov03-FID269.chr	M-5		11/26/2003	19:00:32		Methane		ppm
Nov03-FID322.chr	M-5		11/28/2003	21:48:05		Methane		ppm
Nov03-FID329.chr	M-5		12/1/2003	18:53:40		Methane		ppm
Nov03-FID367.chr	M-5		12/2/2003	17:43:03		Methane		ppm
Nov03-FID412.chr	M-5		12/3/2003	16:52:34		Methane	7.3	ppm
Nov03-FID151.chr	MIDPOINT		11/24/2003	15:08:06		Methane	0	ppm
Nov03-FID191.chr	MIDPOINT		11/24/2003	20:46:42		Methane	0	ppm
Nov03-FID144.chr	)UTTAKE TUBE		11/24/2003	12:57:58		Methane	0	ppm
Nov03-FID152.chr	)UTTAKE TUBE		11/24/2003	15:30:52		Methane	0	ppm
Nov03-FID192.chr	)UTTAKE TUBE		11/24/2003	21:09:15		Methane	0	ppm
Nov03-FID194.chr	)UTTAKE TUBE		11/25/2003	10:24:12		Methane	0	ppm
Nov03-FID195.chr	s-GAS STAND		11/25/2003	10:39:45		Methane	0	ppm
Nov03-FID236.chr	s-GAS STAND		11/26/2003	11:43:48		Methane	0	ppm
Nov03-FID280.chr	s-GAS STAND		11/28/2003	9:26:27		Methane	0	ppm
Nov03-FID281.chr	s-GAS STAND		11/28/2003	9:40:55		Methane	0	ppm
Nov03-FID323.chr	s-GAS STAND		12/1/2003	13:40:47		Methane	0	ppm
Nov03-FID324.chr	s-GAS STAND		12/1/2003	13:58:56		Methane	0	ppm
Nov03-FID336.chr	s-GAS STAND		12/2/2003	9:56:01		Methane	0	ppm
Nov03-FID378.chr	s-GAS STAND		12/3/2003	9:20:47		Methane	0	ppm
Nov03-FID54.chr	SOX-1		11/24/2003	0:16:11		Methane		ppm
Nov03-FID99.chr	SOX-1		11/24/2003	6:35:47		Methane	8.9	ppm
Nov03-FID142.chr	SOX-1		11/24/2003	12:31:13		Methane	8.9	ppm

	SAMPLE	INJECT	date	time		gas	conc	units
Nov03-FID226.chr	SOX-1		11/25/2003	19:11:41		Methane	9.9	ppm
Nov03-FID268.chr	SOX-1		11/26/2003	18:41:59		Methane		ppm
Nov03-FID312.chr	SOX-1		11/28/2003	18:11:26		Methane		ppm
Nov03-FID356.chr	SOX-1		12/2/2003	14:55:07		Methane	9.5	ppm
Nov03-FID362.chr	SOX-1		12/2/2003	16:35:19		Methane		ppm
Nov03-FID402.chr	SOX-1		12/3/2003	14:25:33		Methane		ppm
Nov03-FID55.chr	SOX-2		11/24/2003	0:34:08		Methane		ppm
Nov03-FID100.chr	SOX-2		11/24/2003	6:49:12		Methane	11.3	ppm
Nov03-FID145.chr	SOX-2		11/24/2003	13:18:44		Methane	7.3	ppm
Nov03-FID227.chr	SOX-2		11/25/2003	19:18:09		Methane		ppm
Nov03-FID270.chr	SOX-2		11/26/2003	19:06:18		Methane	8.8	ppm
Nov03-FID313.chr	SOX-2		11/28/2003	18:29:29		Methane		ppm
Nov03-FID357.chr	SOX-2		12/2/2003	15:00:50		Methane	10.9	ppm
Nov03-FID403.chr	SOX-2		12/3/2003	14:43:55		Methane	10.7	ppm
Nov03-FID56.chr	SOX-3		11/24/2003	0:55:51		Methane		ppm
Nov03-FID101.chr	SOX-3		11/24/2003	7:02:11		Methane	10.2	ppm
Nov03-FID146.chr	SOX-3	100	11/24/2003	13:33:31		Methane		ppm
Nov03-FID228.chr	SOX-3		11/25/2003	19:32:27		Methane	6.3	ppm
Nov03-FID272.chr	SOX-3		11/26/2003	19:32:41		Methane	9.2	ppm
Nov03-FID314.chr	SOX-3		11/28/2003	18:46:16		Methane		ppm
Nov03-FID358.chr	SOX-3		12/2/2003	15:20:38		Methane	14.3	ppm
Nov03-FID404.chr	SOX-3		12/3/2003	15:04:16		Methane	7.3	ppm
Nov03-FID57.chr	SOX-4		11/24/2003	1:09:26		Methane		ppm
Nov03-FID102.chr	SOX-4		11/24/2003	7:16:12		Methane	7.3	ppm
Nov03-FID147.chr	SOX-4	100	11/24/2003	13:52:16		Methane		ppm
Nov03-FID229.chr	SOX-4		11/25/2003	19:47:29		Methane	10.75	ppm
Nov03-FID274.chr	SOX-4		11/26/2003	19:57:46		Methane	6.7	ppm
Nov03-FID315.chr	SOX-4		11/28/2003	19:15:45		Methane		ppm
Nov03-FID359.chr	SOX-4		12/2/2003	15:41:11		Methane	8.1	ppm
Nov03-FID405.chr	SOX-4		12/3/2003	15:21:17		Methane	7.6	ppm
Nov03-FID58.chr	SOX-5		11/24/2003	1:32:57		Methane		ppm
Nov03-FID103.chr	SOX-5		11/24/2003	7:29:34		Methane	7.1	ppm
Nov03-FID148.chr	SOX-5	100	11/24/2003	14:07:34		Methane		ppm
Nov03-FID230.chr	SOX-5		11/25/2003	20:09:47		Methane	9.04	ppm
Nov03-FID276.chr	SOX-5		11/26/2003	20:23:06		Methane	7.2	ppm
Nov03-FID316.chr	SOX-5		11/28/2003	19:36:47		Methane		ppm
Nov03-FID360.chr	SOX-5		12/2/2003	16:08:56		Methane	9.4	ppm
Nov03-FID406.chr	SOX-5		12/3/2003	15:37:16		Methane	9.9	ppm
Nov03-FID59.chr	SOX-6		11/24/2003	1:49:14		Methane		ppm
Nov03-FID104.chr	SOX-6		11/24/2003	7:44:04		Methane	7.07	ppm
Nov03-FID149.chr	SOX-6		11/24/2003	14:29:15		Methane	6.7	ppm
Nov03-FID277.chr	SOX-6		11/26/2003	20:43:23		Methane	9.1	ppm
Nov03-FID317.chr	SOX-6		11/28/2003	19:59:35		Methane		ppm
Nov03-FID407.chr	SOX-6		12/3/2003	15:52:06		Methane	7	ppm

329

Appendix D - Chapter 5 Gas chromatography data from Nov 2003
HP-TCD Results

100 MICRO-L INJECTS

SAMPLE	date	time	time	cum minutes	gas	reten	area	conc	units	gas	reten	area	conc	units
			11/23/03 20:00	1					**19.6**					
03NOV-HPTCD-22.CHR	11/23/2003	20:29:53	11/23/03 20:29	29	O2 + Ar	0.916	6372.4435	19.5679	%vol	Nitrogen	1.708	26211.733	76.3095	%vol
03NOV-HPTCD-61.CHR	11/24/2003	2:09:04	11/24/03 2:09	369	O2 + Ar	0.916	6195.0685	19.0232	%vol	Nitrogen	1.708	25669.079	74.7297	%vol
03NOV-HPTCD-104.CHR	11/24/2003	7:56:51	11/24/03 7:56	1434	O2 + Ar	0.925	5794.721	17.7939	%vol	Nitrogen	1.716	24076.7835	70.0941	%vol
03NOV-HPTCD-152.CHR	11/24/2003	16:14:34	11/24/03 16:14	1936	O2 + Ar	0.925	5203.4348	15.9782	%vol	Nitrogen	1.716	21759.224	63.347	%vol
03NOV-HPTCD-180.CHR	11/25/2003	12:20:45	11/25/03 12:20	2848	O2 + Ar	0.95	3548.783	10.8973	%vol	Nitrogen	1.775	14844.501	43.2164	%vol
03NOV-HPTCD-209.CHR	12/4/2003	13:00:04	12/4/03 13:00	15603	O2 + Ar	1.008	5573.0185	17.1131	%vol	Nitrogen	1.766	23088.3142	67.2164	%vol
			11/23/03 20:00	1					**19.3**					
03NOV-HPTCD-23.CHR	11/23/2003	20:37:06	11/23/03 20:37	37	O2 + Ar	0.925	6268.8295	19.2497	%vol	Nitrogen	1.716	25814.957	75.1544	%vol
03NOV-HPTCD-62.CHR	11/24/2003	2:17:24	11/24/03 2:17	377	O2 + Ar	0.916	5992.8325	18.4022	%vol	Nitrogen	1.716	24928.814	72.5746	%vol
03NOV-HPTCD-105.CHR	11/24/2003	8:04:40	11/24/2003 8:04	1444	O2 + Ar	0.925	6300.809	19.3479	%vol	Nitrogen	1.716	26435.691	76.9615	%vol
03NOV-HPTCD-153.CHR	11/24/2003	16:25:12	11/24/2003 16:25	1947	O2 + Ar	0.925	4628.213	14.2119	%vol	Nitrogen	1.725	19723.8765	57.4216	%vol
03NOV-HPTCD-181.CHR	11/25/2003	12:26:43	11/25/2003 12:26	2854	O2 + Ar	0.95	5412.637	16.6206	%vol	Nitrogen	1.766	23490.1682	68.3863	%vol
03NOV-HPTCD-210.CHR	12/4/2003	13:05:23	12/4/2003 13:05	15608	O2 + Ar	1.008	2928.2768	8.9919	%vol	Nitrogen	1.775	26193.9698	76.2578	%vol
			11/23/03 20:00	1					**19.5**					
03NOV-HPTCD-24.CHR	11/23/2003	20:43:31	11/23/2003 20:43	42	O2 + Ar	0.916	6345.6467	19.4856	%vol	Nitrogen	1.708	26119.646	76.0414	%vol
03NOV-HPTCD-63.CHR	11/24/2003	2:23:34	11/24/2003 2:23	383	O2 + Ar	0.916	6140.283	18.855	%vol	Nitrogen	1.708	25528.574	74.3206	%vol
03NOV-HPTCD-106.CHR	11/24/2003	8:09:59	11/24/2003 8:09	1449	O2 + Ar	0.925	6046.6165	18.5674	%vol	Nitrogen	1.725	25440.8795	74.0653	%vol
03NOV-HPTCD-154.CHR	11/24/2003	16:31:48	11/24/2003 16:31	1953	O2 + Ar	0.925	6011.8353	18.4606	%vol	Nitrogen	1.716	25715.3418	74.8644	%vol
03NOV-HPTCD-182.CHR	11/25/2003	12:34:17	11/25/2003 12:34	2864	O2 + Ar	0.95	4745.4828	14.572	%vol	Nitrogen	1.766	21132.4392	61.5223	%vol
03NOV-HPTCD-211.CHR	12/4/2003	13:10:55	12/4/2003 13:10	15613	O2 + Ar	1.008	1212.2842	3.7226	%vol	Nitrogen	1.775	27199.6195	79.1855	%vol
			11/23/03 20:00	1					**19.8**					
03NOV-HPTCD-25.CHR	11/23/2003	20:49:18	11/23/2003 20:49	48	O2 + Ar	0.916	6436.567	19.7648	%vol	Nitrogen	1.708	26473.852	77.0726	%vol
03NOV-HPTCD-64.CHR	11/24/2003	2:30:27	11/24/2003 2:30	390	O2 + Ar	0.908	6137.004	18.8449	%vol	Nitrogen	1.7	25495.8518	74.2254	%vol
03NOV-HPTCD-107.CHR	11/24/2003	8:16:56	11/24/2003 8:16	1456	O2 + Ar	0.925	6052.7513	18.5862	%vol	Nitrogen	1.725	25572.3678	74.4481	%vol
03NOV-HPTCD-155.CHR	11/24/2003	16:37:02	11/24/2003 16:37	1959	O2 + Ar	0.916	5585.2025	17.1505	%vol	Nitrogen	1.708	24146.183	70.2961	%vol
03NOV-HPTCD-183.CHR	11/25/2003	12:42:40	11/25/2003 12:42	2872	O2 + Ar	0.958	5280.75	16.2156	%vol	Nitrogen	1.775	24000.966	69.8733	%vol
03NOV-HPTCD-212.CHR	12/4/2003	13:16:26	12/4/2003 13:16	15619	O2 + Ar	1.008	1148.7438	3.5275	%vol	Nitrogen	1.766	26123.8305	76.0536	%vol
			11/23/03 20:00	1					**19.7**					
03NOV-HPTCD-26.CHR	11/23/2003	20:54:48	11/23/2003 20:54	53	O2 + Ar	0.916	6399.4045	19.6507	%vol	Nitrogen	1.708	26347.583	76.705	%vol
03NOV-HPTCD-65.CHR	11/24/2003	2:51:59	11/24/2003 2:51	411	O2 + Ar	0.908	6010.037	18.455	%vol	Nitrogen	1.708	25178.1375	73.3004	%vol
03NOV-HPTCD-108.CHR	11/24/2003	8:22:58	11/24/2003 8:22	1462	O2 + Ar	0			%vol	Nitrogen	0	0	0	%vol
03NOV-HPTCD-156.CHR	11/24/2003	16:56:19	11/24/2003 16:56	1978	O2 + Ar	0.916	5739.417	17.6241	%vol	Nitrogen	1.708	25263.887	73.5501	%vol
03NOV-HPTCD-184.CHR	11/25/2003	12:49:52	11/25/2003 12:49	2879	O2 + Ar	0.95	5309.045	16.3025	%vol	Nitrogen	1.766	25817.545	75.1619	%vol
03NOV-HPTCD-213.CHR	12/4/2003	13:20:47	12/4/2003 13:20	15623	O2 + Ar	1.008	1225.805	3.7641	%vol	Nitrogen	1.766	26493.2155	77.129	%vol
			11/23/03 20:00	1					**19.61**					
03NOV-HPTCD-27.CHR	11/23/2003	21:00:40	11/23/2003 21:00	59	O2 + Ar	0.908	6383.5835	19.6021	%vol	Nitrogen	1.708	26350.4635	76.7134	%vol
03NOV-HPTCD-66.CHR	11/24/2003	3:00:15	11/24/2003 3:00	420	O2 + Ar	0.908	6020.0188	18.4857	%vol	Nitrogen	1.7	25400.1813	73.9468	%vol
03NOV-HPTCD-109.CHR	11/24/2003	8:29:08	11/24/2003 8:29	1469	O2 + Ar	0.925	5672.559	17.4188	%vol	Nitrogen	1.716	24583.661	71.5697	%vol
03NOV-HPTCD-157.CHR	11/24/2003	17:06:28	11/24/2003 17:06	1988	O2 + Ar	0.908	5461.2275	16.7698	%vol	Nitrogen	1.7	25351.4653	73.805	%vol
03NOV-HPTCD-185.CHR	11/25/2003	12:58:38	11/25/2003 12:58	2888	O2 + Ar	0.958	5019.5918	15.4137	%vol	Nitrogen	1.775	26562.0405	77.3293	%vol
03NOV-HPTCD-214.CHR	12/4/2003	13:25:11	12/4/2003 13:25	15628	O2 + Ar	1.008	709.9075	2.1799	%vol	Nitrogen	1.775	25117.183	73.123	%vol
			11/23/03 20:00	1					**12.1**					
03NOV-HPTCD-28.CHR	11/23/2003	21:05:48	11/23/2003 21:05	64	O2 + Ar	0.916	3928.4915	12.0632	%vol	Nitrogen	1.716	16221.895	47.2264	%vol
03NOV-HPTCD-67.CHR	11/24/2003	3:06:41	11/24/2003 3:06	426	O2 + Ar	0.9	3688.3035	11.3257	%vol	Nitrogen	1.708	15448.073	44.9735	%vol
03NOV-HPTCD-110.CHR	11/24/2003	8:38:51	11/24/2003 8:38	1478	O2 + Ar	0.916	3345.188	10.2721	%vol	Nitrogen	1.725	14194.979	41.3255	%vol
03NOV-HPTCD-158.CHR	11/24/2003	17:17:29	11/24/2003 17:17	1999	O2 + Ar	0.891	3323.7345	10.2062	%vol	Nitrogen	1.691	14335.588	41.7348	%vol

	SAMPLE	date	time	time	gas	reten	area	conc	units	gas	reten	area	conc	units
03NOV-HPTCD-186.CHR	A-7	11/25/2003	13:18:41	11/25/2003 13:18	2908 O2 + Ar	0.958	3403.0655	10.4498	%vol	Nitrogen	1.783	15053.205	43.824	%vol
03NOV-HPTCD-215.CHR	A-7	12/4/2003	13:28:42	12/4/2003 13:28	15631 O2 + Ar	1.016	2623.498	8.056	%vol	Nitrogen	1.783	14844.3685	43.216	%vol
				11/23/03 20:00				11.4						
03NOV-HPTCD-29.CHR	A-8	11/23/2003	21:11:05	11/23/2003 21:11	70 O2 + Ar	0.916	3700.7635	11.3639	%vol	Nitrogen	1.716	15284.905	44.4985	%vol
03NOV-HPTCD-68.CHR	A-8	11/24/2003	3:18:36	11/24/2003 3:18	438 O2 + Ar	0.916	3430.9972	10.5356	%vol	Nitrogen	1.716	14361.946	41.8115	%vol
03NOV-HPTCD-111.CHR	A-8	11/24/2003	8:45:45	11/24/2003 8:45	1485 O2 + Ar	0.925	3255.0385	9.9953	%vol	Nitrogen	1.725	13774.7728	40.1021	%vol
03NOV-HPTCD-159.CHR	A-8	11/24/2003	17:36:17	11/24/2003 17:36	2018 O2 + Ar	0.925	1446.568	4.442	%vol	Nitrogen	1.733	6263.814	18.2357	%vol
03NOV-HPTCD-187.CHR	A-8	11/25/2003	13:28:25	11/25/2003 13:28	2918 O2 + Ar	0.958	3413.768	10.4827	%vol	Nitrogen	1.783	15244.8375	44.3819	%vol
03NOV-HPTCD-216.CHR	A-8	12/4/2003	13:32:30	12/4/2003 13:32	15365 O2 + Ar	1	362.2887	1.1125	%vol	Nitrogen	1.775	17638.2948	51.3499	%vol
				11/23/03 20:00	1			11.1						
03NOV-HPTCD-30.CHR	A-9	11/23/2003	21:17:27	11/23/2003 21:17	76 O2 + Ar	0.916	3590.2253	11.0245	%vol	Nitrogen	1.716	14863.6177	43.272	%vol
03NOV-HPTCD-69.CHR	A-9	11/24/2003	3:25:47	11/24/2003 3:25	445 O2 + Ar	0.933	3304.6332	10.1476	%vol	Nitrogen	1.733	13927.6228	40.5471	%vol
03NOV-HPTCD-112.CHR	A-9	11/24/2003	8:59:09	11/24/2003 8:59	1499 O2 + Ar	0.933	3472.6768	10.6636	%vol	Nitrogen	1.741	14832.7925	43.1823	%vol
03NOV-HPTCD-160.CHR	A-9	11/24/2003	17:43:24	11/24/2003 17:43	2038 O2 + Ar	0.916	3487.292	10.7084	%vol	Nitrogen	1.716	15185.2925	44.2085	%vol
03NOV-HPTCD-188.CHR	A-9	11/25/2003	13:41:29	11/25/2003 13:41	2931 O2 + Ar	0.958	2858.0507	8.7762	%vol	Nitrogen	1.783	12765.0015	37.1624	%vol
03NOV-HPTCD-217.CHR	A-9	12/4/2003	13:36:22	12/4/2003 13:36	15369 O2 + Ar	1.016	2639.2848	8.1045	%vol	Nitrogen	1.783	15032.7618	43.7645	%vol
				11/23/03 20:00				17.9						
03NOV-HPTCD-70.CHR	A-10	11/24/2003	3:32:57	11/24/2003 3:32	452 O2 + Ar	0.933	5809.707	17.8399	%vol	Nitrogen	1.725	25221.0745	73.4254	%vol
03NOV-HPTCD-113.CHR	A-10	11/24/2003	9:06:35	11/24/2003 9:06	1506 O2 + Ar	0.933	5565.06	17.0887	%vol	Nitrogen	1.725	24074.739	70.0881	%vol
03NOV-HPTCD-161.CHR	A-10	11/24/2003	17:52:44	11/24/2003 17:52	2047 O2 + Ar	0.908	5890.327	18.0875	%vol	Nitrogen	1.7	25886.9975	75.3641	%vol
03NOV-HPTCD-189.CHR	A-10	11/25/2003	13:55:29	11/25/2003 13:55	2945 O2 + Ar	0.95	5617.3975	17.2494	%vol	Nitrogen	1.766	24862.6195	72.3819	%vol
03NOV-HPTCD-218.CHR	A-10	12/4/2003	13:39:46	12/4/2003 13:39	15372 O2 + Ar	1.008	5451.4083	16.7397	%vol	Nitrogen	1.766	24385.3023	70.9923	%vol
03NOV-HPTCD-60.CHR	AIR	11/24/2003	2:04:15		O2 + Ar	0.908	6160.159	18.916	%vol	Nitrogen	1.708	25261.609	73.5434	%vol
03NOV-HPTCD-103.CHR	AIR	11/24/2003	7:44:22		O2 + Ar	0.925	5777.087	17.7397	%vol	Nitrogen	1.725	23799.475	69.2868	%vol
03NOV-HPTCD-190.CHR	AIR	11/25/2003	14:14:42		O2 + Ar	0.95	6212.341	19.0763	%vol	Nitrogen	1.766	25581.5663	74.4749	%vol
03NOV-HPTCD-200.CHR	AIR	11/26/2003	14:46:18		O2 + Ar	0	0	0	%vol	Nitrogen	0	0	0	%vol
03NOV-HPTCD-205.CHR	AIR	12/4/2003	12:35:13		O2 + Ar	1.008	5001.955	15.3595	%vol	Nitrogen	1.775	20177.9475	58.7435	%vol
03NOV-HPTCD-206.CHR	AIR	12/4/2003	12:40:36		O2 + Ar	1.008	4470.7825	13.7285	%vol	Nitrogen	1.775	18006.6285	52.4222	%vol
				11/23/03 20:00	1			19.5						
03NOV-HPTCD-32.CHR	B-1	11/23/2003	21:24:21	11/23/2003 21:24	83 O2 + Ar	0.908	6344.385	19.4817	%vol	Nitrogen	1.7	26146.025	76.1182	%vol
03NOV-HPTCD-71.CHR	B-1	11/24/2003	3:41:06	11/24/2003 3:41	461 O2 + Ar	0.925	6243.012	19.1704	%vol	Nitrogen	1.716	25868.326	75.3097	%vol
03NOV-HPTCD-114.CHR	B-1	11/24/2003	9:16:08	11/24/2003 9:16	1516 O2 + Ar	0.925	5485.106	16.8431	%vol	Nitrogen	1.725	22779.3335	66.3168	%vol
03NOV-HPTCD-162.CHR	B-1	11/24/2003	17:58:42	11/24/2003 17:58	2053 O2 + Ar	0.908	6176.254	18.9654	%vol	Nitrogen	1.7	25711.862	74.8542	%vol
03NOV-HPTCD-191.CHR	B-1	11/25/2003	14:23:00	11/25/2003 14:23	2987 O2 + Ar	0.941	6145.759	18.8718	%vol	Nitrogen	1.758	25446.6195	74.082	%vol
03NOV-HPTCD-219.CHR	B-1	12/4/2003	13:46:16	12/4/2003 13:46	15379 O2 + Ar	1.016	5892.8425	18.0952	%vol	Nitrogen	1.775	23951.874	69.7304	%vol
				11/23/03 20:00				19.7						
03NOV-HPTCD-33.CHR	B-2	11/23/2003	21:30:20	11/23/2003 21:30	89 O2 + Ar	0.916	6392.2215	19.6286	%vol	Nitrogen	1.708	26350.516	76.7135	%vol
03NOV-HPTCD-72.CHR	B-2	11/24/2003	3:47:56	11/24/2003 3:47	467 O2 + Ar	0.916	6049.5525	18.5764	%vol	Nitrogen	1.708	25444.959	74.0772	%vol
03NOV-HPTCD-115.CHR	B-2	11/24/2003	9:21:34	11/24/2003 9:21	1521 O2 + Ar	0.925	5328.569	16.3625	%vol	Nitrogen	1.725	22705.738	66.1026	%vol
03NOV-HPTCD-163.CHR	B-2	11/24/2003	18:06:34	11/24/2003 18:06	2061 O2 + Ar	0.908	5809.9173	17.8405	%vol	Nitrogen	1.7	25776.3105	75.0419	%vol
03NOV-HPTCD-192.CHR	B-2	11/25/2003	14:27:35	11/25/2003 14:27	2991 O2 + Ar	0.883	5154.509	15.828	%vol	Nitrogen	1.7	24523.3805	71.3957	%vol
03NOV-HPTCD-220.CHR	B-2	12/4/2003	13:51:16	12/4/2003 13:51	15384 O2 + Ar	1.008	1406.967	4.3204	%vol	Nitrogen	1.775	27734.17	80.7417	%vol
				11/23/03 20:00	1			19.2						
03NOV-HPTCD-34.CHR	B-3	11/23/2003	21:43:36	11/23/2003 21:43	102 O2 + Ar	0.916	6224.673	19.1141	%vol	Nitrogen	1.708	25663.724	74.7141	%vol
03NOV-HPTCD-73.CHR	B-3	11/24/2003	3:57:20	11/24/2003 3:57	477 O2 + Ar	0.916	5711.7665	17.5391	%vol	Nitrogen	1.708	23895.488	69.5663	%vol
03NOV-HPTCD-116.CHR	B-3	11/24/2003	9:32:24	11/24/2003 9:32	1530 O2 + Ar	0.925	5740.327	17.6268	%vol	Nitrogen	1.725	24310.8363	70.7755	%vol
03NOV-HPTCD-164.CHR	B-3	11/24/2003	18:23:45	11/24/2003 18:23	2074 O2 + Ar	0.925	5307.3435	16.2973	%vol	Nitrogen	1.716	23146.1545	67.3848	%vol
03NOV-HPTCD-193.CHR	B-3	11/25/2003	14:44:34	11/25/2003 14:44	3008 O2 + Ar	0.941	5314.239	16.3185	%vol	Nitrogen	1.758	24655.34	71.7784	%vol
03NOV-HPTCD-201.CHR	B-3	11/26/2003	14:55:31	11/26/2003 14:55	4459 O2 + Ar	0	0		%vol	Nitrogen	0	0	0	%vol
03NOV-HPTCD-221.CHR	B-3	12/4/2003	13:55:40	12/4/2003 13:55	15388 O2 + Ar	1.008	1553.3185	4.7698	%vol	Nitrogen	1.766	26214.4125	76.3173	%vol

SAMPLE	date	time	time	gas	reten	area	conc	units	gas	reten	area	conc	units
03NOV-HPTCD-221.CHR · B-3	12/4/2003	13:55:40	12/4/2003 13:55	15388 O2 + Ar	1.008	1553.3185	4.7698	%vol	Nitrogen	1.766	26214.4125	76.3173	%vol
			11/23/03 20:00	1			19.5						
03NOV-HPTCD-35.CHR · B-4	11/23/2003	21:50:37	11/23/2003 21:50	109 O2 + Ar	0.916	6331.624	19.4425	%vol	Nitrogen	1.708	26076.852	75.9168	%vol
03NOV-HPTCD-75.CHR · B-4	11/24/2003	4:13:29	11/24/2003 4:13	493 O2 + Ar	0.916	5587.7305	17.1583	%vol	Nitrogen	1.708	23481.011	68.3596	%vol
03NOV-HPTCD-117.CHR · B-4	11/24/2003	9:43:18	11/24/2003 9:43	1550 O2 + Ar	0.925	5306.9515	16.2961	%vol	Nitrogen	1.725	22654.1575	65.9524	%vol
03NOV-HPTCD-165.CHR · B-4	11/24/2003	18:29:27	11/24/2003 18:29	2080 O2 + Ar	0.916	5457.7127	16.759	%vol	Nitrogen	1.708	24147.6947	70.3005	%vol
03NOV-HPTCD-222.CHR · B-4	12/4/2003	14:02:33	12/4/2003 14:02	15395 O2 + Ar	1.016	2378.334	7.3032	%vol	Nitrogen	1.775	27261.6427	79.3661	%vol
			11/23/03 20:00	1			19.6						
03NOV-HPTCD-36.CHR · B-5	11/23/2003	21:56:15	11/23/2003 21:56	115 O2 + Ar	0.916	6381.5743	19.5959	%vol	Nitrogen	1.716	26348.358	76.7072	%vol
03NOV-HPTCD-76.CHR · B-5	11/24/2003	4:19:13	11/24/2003 4:19	499 O2 + Ar	0.916	4718.9835	14.4906	%vol	Nitrogen	1.716	20036.626	58.3321	%vol
03NOV-HPTCD-118.CHR · B-5	11/24/2003	9:52:53	11/24/2003 9:52	1559 O2 + Ar	0.925	5379.4378	16.5187	%vol	Nitrogen	1.725	23194.4083	67.5252	%vol
03NOV-HPTCD-166.CHR · B-5	11/24/2003	18:45:02	11/24/2003 18:45	2096 O2 + Ar	0.925	5127.3562	15.7446	%vol	Nitrogen	1.716	23131.2038	67.3412	%vol
03NOV-HPTCD-223.CHR · B-5	12/4/2003	14:06:58	12/4/2003 14:06	15399 O2 + Ar	1.008	2579.266	7.9202	%vol	Nitrogen	1.766	23929.1055	69.6641	%vol
			11/23/03 20:00	1			19.3						
03NOV-HPTCD-37.CHR · B-6	11/23/2003	22:01:43	11/23/2003 22:01	120 O2 + Ar	0.916	6269.315	19.2512	%vol	Nitrogen	1.708	25828.213	75.193	%vol
03NOV-HPTCD-77.CHR · B-6	11/24/2003	4:25:18	11/24/2003 4:25	499 O2 + Ar	0.916	5848.2185	17.9581	%vol	Nitrogen	1.716	24551.459	71.476	%vol
03NOV-HPTCD-119.CHR · B-6	11/24/2003	9:58:39	11/24/2003 9:58	1565 O2 + Ar	0.933	5377.797	16.5136	%vol	Nitrogen	1.725	22874.414	66.5936	%vol
03NOV-HPTCD-167.CHR · B-6	11/24/2003	18:53:42	11/24/2003 18:53	2104 O2 + Ar	0.925	5448.8888	16.7319	%vol	Nitrogen	1.716	24328.531	70.827	%vol
03NOV-HPTCD-224.CHR · B-6	12/4/2003	14:10:19	12/4/2003 14:10	15403 O2 + Ar	1.008	1127.2893	3.4616	%vol	Nitrogen	1.791	27848.4827	81.0745	%vol
			11/23/03 20:00	1			10.5						
03NOV-HPTCD-38.CHR · B-7	11/23/2003	22:07:59	11/23/2003 22:07	126 O2 + Ar	0.925	3412.0053	10.4773	%vol	Nitrogen	1.725	14101.2498	41.0526	%vol
03NOV-HPTCD-78.CHR · B-7	11/24/2003	4:30:55	11/24/2003 4:30	504 O2 + Ar	0.908	3278.882	10.0685	%vol	Nitrogen	1.716	13795.521	40.1625	%vol
03NOV-HPTCD-120.CHR · B-7	11/24/2003	10:05:54	11/24/2003 10:05	1562 O2 + Ar	0.933	3122.7753	9.5891	%vol	Nitrogen	1.733	13425.1213	39.0842	%vol
03NOV-HPTCD-168.CHR · B-7	11/24/2003	19:01:30	11/24/2003 19:01	2112 O2 + Ar	0.925	3398.8525	10.4369	%vol	Nitrogen	1.725	15092.819	43.9393	%vol
03NOV-HPTCD-202.CHR · B-7	11/26/2003	15:54:56	11/26/2003 15:54	4518 O2 + Ar	0	0	0	%vol	Nitrogen	1.491	13479.8755	39.2436	%vol
03NOV-HPTCD-225.CHR · B-7	12/4/2003	14:16:16	12/4/2003 14:16	15409 O2 + Ar	1	356.335	1.0942	%vol	Nitrogen	1.783	17854.216	51.9785	%vol
			11/23/03 20:00	1			10.9						
03NOV-HPTCD-39.CHR · B-8	11/23/2003	22:13:50	11/23/2003 22:13	132 O2 + Ar	0.916	3525.6903	10.8264	%vol	Nitrogen	1.725	14580.044	42.4465	%vol
03NOV-HPTCD-79.CHR · B-8	11/24/2003	4:36:29	11/24/2003 4:36	508 O2 + Ar	0.916	3153.3565	9.683	%vol	Nitrogen	1.716	13157.247	38.3043	%vol
03NOV-HPTCD-121.CHR · B-8	11/24/2003	10:11:49	11/24/2003 10:11	1568 O2 + Ar	0.933	3268.291	10.036	%vol	Nitrogen	1.733	13756.154	40.0479	%vol
03NOV-HPTCD-169.CHR · B-8	11/24/2003	19:10:15	11/24/2003 19:10	2121 O2 + Ar	0.925	2998.2935	9.2069	%vol	Nitrogen	1.733	12812.92	37.3019	%vol
03NOV-HPTCD-226.CHR · B-8	12/4/2003	14:20:45	12/4/2003 14:20	15414 O2 + Ar	1.008	1331.9778	4.0901	%vol	Nitrogen	1.783	14810.3018	43.1168	%vol
			11/23/03 20:00	1			10.9						
03NOV-HPTCD-40.CHR · B-9	11/23/2003	22:19:28	11/23/2003 22:19	138 O2 + Ar	0.916	3532.2733	10.8466	%vol	Nitrogen	1.725	14614.34	42.5463	%vol
03NOV-HPTCD-80.CHR · B-9	11/24/2003	4:42:11	11/24/2003 4:42	524 O2 + Ar	0.925	3460.498	10.6262	%vol	Nitrogen	1.725	14566.538	42.4072	%vol
03NOV-HPTCD-122.CHR · B-9	11/24/2003	10:18:57	11/24/2003 10:18	1575 O2 + Ar	0.933	3123.812	9.5923	%vol	Nitrogen	1.733	13388.8353	38.9785	%vol
03NOV-HPTCD-170.CHR · B-9	11/24/2003	19:16:27	11/24/2003 19:16	2127 O2 + Ar	0.925	2794.618	8.5814	%vol	Nitrogen	1.725	12315.855	35.8548	%vol
03NOV-HPTCD-227.CHR · B-9	12/4/2003	14:25:25	12/4/2003 14:25	15419 O2 + Ar	1.016	2325.518	7.141	%vol	Nitrogen	1.783	13466.113	39.2035	%vol
03NOV-HPTCD-81.CHR · B-10	11/24/2003	5:01:27	11/24/2003 5:01	535 O2 + Ar	0.9	5388.5585	16.5467	%vol	Nitrogen	1.7	23097.337	67.2426	%vol
03NOV-HPTCD-123.CHR · B-10	11/24/2003	10:26:17	11/24/2003 10:26	1588 O2 + Ar	0.925	5377.345	16.5122	%vol	Nitrogen	1.716	23078.1865	67.1869	%vol
			11/23/03 20:00	1			16.6						
03NOV-HPTCD-171.CHR · B-10	11/23/2003	19:23:12	11/23/2003 19:23	2134 O2 + Ar	0.925	5081.1708	15.6028	%vol	Nitrogen	1.716	21889.1712	63.7253	%vol
03NOV-HPTCD-228.CHR · B-10	12/4/2003	14:30:50	12/4/2003 14:30	15423 O2 + Ar	1.008	6085.134	18.6856	%vol	Nitrogen	1.766	25669.836	74.7319	%vol
			11/23/03 20:00	1			19.8						
03NOV-HPTCD-41.CHR · M-1	11/23/2003	22:24:52	11/23/2003 22:24	143 O2 + Ar	0.916	6442.0927	19.7818	%vol	Nitrogen	1.708	26516.294	77.1962	%vol
03NOV-HPTCD-82.CHR · M-1	11/24/2003	5:06:53	11/24/2003 5:06	540 O2 + Ar	0.925	5904.5285	18.1311	%vol	Nitrogen	1.716	24372.0098	70.9536	%vol
03NOV-HPTCD-124.CHR · M-1	11/24/2003	10:31:46	11/24/2003 10:31	1593 O2 + Ar	0.925	5887.648	18.0792	%vol	Nitrogen	1.716	24422.053	71.0992	%vol
03NOV-HPTCD-147.CHR · M-1	11/24/2003	15:35:36	11/24/2003 15:35	1897 O2 + Ar	0.916	5979.7785	18.3621	%vol	Nitrogen	1.716	24793.374	72.1803	%vol
03NOV-HPTCD-175.CHR · M-1	11/24/2003	19:55:32	11/24/2003 19:55	2211 O2 + Ar	0.933	5504.84	16.9037	%vol	Nitrogen	1.725	22793.322	66.3576	%vol
03NOV-HPTCD-245.CHR · M-1	12/4/2003	17:03:40	12/4/2003 17:03	15456 O2 + Ar	1.008	6841.472	21.0081	%vol	Nitrogen	1.766	27589.1445	80.3195	%vol

	SAMPLE	date	time	time	gas	reten	area	conc	units	gas	reten	area	conc	units
				11/23/03 20:00	1				19.4					
03NOV-HPTCD-42.CHR	M-2	11/23/2003	22:30:46	11/23/2003 22:30	149 O2 + Ar	0.925	6285.711	19.3016	%vol	Nitrogen	1.716	25872.8925	75.323	%vol
03NOV-HPTCD-83.CHR	M-2	11/24/2003	5:12:10	11/24/2003 5:12	546 O2 + Ar	0.908	5632.678	17.2963	%vol	Nitrogen	1.708	23396.5262	68.1137	%vol
03NOV-HPTCD-125.CHR	M-2	11/24/2003	10:48:46	11/24/2003 10:48	1610 O2 + Ar	0.925	5187.4047	15.929	%vol	Nitrogen	1.716	21696.3858	63.1641	%vol
03NOV-HPTCD-148.CHR	M-2	11/24/2003	15:41:57	11/24/2003 15:41	1903 O2 + Ar	0.925	5718.879	17.561	%vol	Nitrogen	1.716	24088.078	70.127	%vol
03NOV-HPTCD-176.CHR	M-2	11/24/2003	20:05:19	11/24/2003 20:05	2221 O2 + Ar	0.925	6110.4395	18.7634	%vol	Nitrogen	1.716	25761.9895	75.0002	%vol
03NOV-HPTCD-204.CHR	M-2	11/26/2003	18:08:49	11/26/2003 18:08	4760 O2 + Ar	0	0		%vol	Nitrogen	1.5	8590.3295	25.0088	%vol
03NOV-HPTCD-246.CHR	M-2	12/4/2003	17:09:52	12/4/2003 17:09	15462 O2 + Ar	1.016	5310.0725	16.3057	%vol	Nitrogen	1.775	21910.0968	63.7863	%vol
									19.5					
				11/23/03 20:00	1									
03NOV-HPTCD-43.CHR	M-3	11/23/2003	22:37:28	11/23/2003 22:37	156 O2 + Ar	0.916	6338.988	19.4652	%vol	Nitrogen	1.708	26112.07	76.0193	%vol
03NOV-HPTCD-84.CHR	M-3	11/24/2003	5:17:39	11/24/2003 5:17	551 O2 + Ar	0.908	5993.1188	18.4031	%vol	Nitrogen	1.708	24903.757	72.5016	%vol
03NOV-HPTCD-126.CHR	M-3	11/24/2003	10:56:00	11/24/2003 10:56	1610 O2 + Ar	0.933	5615.3685	17.2431	%vol	Nitrogen	1.733	23655.4175	68.8674	%vol
03NOV-HPTCD-149.CHR	M-3	11/24/2003	15:49:28	11/24/2003 15:49	1911 O2 + Ar	0.916	6088.7148	18.6966	%vol	Nitrogen	1.708	25724.136	74.89	%vol
03NOV-HPTCD-177.CHR	M-3	11/24/2003	20:18:30	11/24/2003 20:18	2234 O2 + Ar	0.925	2262.35		%vol	Nitrogen	1.733	9658.599	28.1188	%vol
03NOV-HPTCD-247.CHR	M-3	12/4/2003	17:13:17	12/4/2003 17:13	15666 O2 + Ar	1.016	5270.659	16.1846	%vol	Nitrogen	1.775	22782.859	66.3271	%vol
									19.6					
				11/23/03 20:00	1									
03NOV-HPTCD-44.CHR	M-4	11/23/2003	22:42:36	11/23/2003 22:42	161 O2 + Ar	0.916	6363.0715	19.5391	%vol	Nitrogen	1.708	26195.587	76.2625	%vol
03NOV-HPTCD-85.CHR	M-4	11/24/2003	5:23:20	11/24/2003 5:23	557 O2 + Ar	0.908	5766.313	17.7066	%vol	Nitrogen	1.708	23987.0887	69.8329	%vol
03NOV-HPTCD-127.CHR	M-4	11/24/2003	11:20:15	11/24/2003 11:20	1641 O2 + Ar	0.925	5342.94	16.4066	%vol	Nitrogen	1.725	22454.116	65.37	%vol
03NOV-HPTCD-150.CHR	M-4	11/24/2003	16:00:21	11/24/2003 16:00	1920 O2 + Ar	0.925	5710.426	17.535	%vol	Nitrogen	1.716	24014.227	69.912	%vol
03NOV-HPTCD-178.CHR	M-4	11/24/2003	20:28:14	11/24/2003 20:28	2244 O2 + Ar	0.916	6114.2275	18.775	%vol	Nitrogen	1.708	25733.075	74.916	%vol
03NOV-HPTCD-248.CHR	M-4	12/4/2003	17:20:44	12/4/2003 17:20	15612 O2 + Ar	1.008	6260.0563	19.2228	%vol	Nitrogen	1.766	26644.4048	77.5691	%vol
									17.6					
03NOV-HPTCD-86.CHR	M-5	11/24/2003	5:28:49	11/24/2003 5:28	166 O2 + Ar	0.916	5725.0423	17.5799	%vol	Nitrogen	1.708	23867.291	69.4842	%vol
03NOV-HPTCD-128.CHR	M-5	11/24/2003	11:28:07	11/24/2003 11:28	1649 O2 + Ar	0.925	5784.22	17.7616	%vol	Nitrogen	1.716	24055.082	70.0309	%vol
03NOV-HPTCD-151.CHR	M-5	11/24/2003	16:06:50	11/24/2003 16:06	1926 O2 + Ar	0.925	5404.796	16.5965	%vol	Nitrogen	1.716	22401.4735	65.2168	%vol
03NOV-HPTCD-179.CHR	M-5	12/4/2003	20:42:42	11/24/2003 20:42	2258 O2 + Ar	0.916	6158.451	18.9108	%vol	Nitrogen	1.708	25523.645	74.3063	%vol
03NOV-HPTCD-249.CHR	M-5	12/4/2003	17:26:37	12/4/2003 17:26	15618 O2 + Ar	1.008	6280.155	19.2845	%vol	Nitrogen	1.766	25135.873	73.1774	%vol
03NOV-HPTCD-141.CHR	OUTTAKE	11/24/2003	12:51:07		O2 + Ar	0.933	2060.334	6.3267	%vol	Nitrogen	1.8	31354.618	91.2818	%vol
									18.4					
				11/23/03 20:00	1									
03NOV-HPTCD-54.CHR	SOX-1	11/24/2003	0:09:20	11/24/2003 0:09	249 O2 + Ar	0.916	5979.884	18.3625	%vol	Nitrogen	1.708	24779.341	72.1394	%vol
03NOV-HPTCD-97.CHR	SOX-1	11/24/2003	6:30:27	11/24/2003 6:30	646 O2 + Ar	0.908	5904.5885	18.1312	%vol	Nitrogen	1.7	24681.9195	71.8558	%vol
03NOV-HPTCD-139.CHR	SOX-1	11/24/2003	12:31:55	11/24/2003 12:31	1007 O2 + Ar	0.925	5517.309	16.942	%vol	Nitrogen	1.725	22426.5255	65.2897	%vol
03NOV-HPTCD-239.CHR	SOX-1	12/4/2003	15:19:58	12/4/2003 15:19	15314 O2 + Ar	1.008	6436.2473	19.7638	%vol	Nitrogen	1.766	26302.6853	76.5743	%vol
									18.8					
03NOV-HPTCD-55.CHR	SOX-2	11/24/2003	0:27:28	11/24/2003 0:27	269 O2 + Ar	0.916	6121.3975	18.797	%vol	Nitrogen	1.708	25350.529	73.8023	%vol
03NOV-HPTCD-98.CHR	SOX-2	11/24/2003	6:42:57	11/24/2003 6:42	658 O2 + Ar	0.9	5875.46	18.0418	%vol	Nitrogen	1.691	24896.234	72.4797	%vol
03NOV-HPTCD-142.CHR	SOX-2	11/24/2003	13:03:45	11/24/2003 13:03	1039 O2 + Ar	0.925	5217.5922	16.0217	%vol	Nitrogen	1.725	22822.0907	66.4413	%vol
03NOV-HPTCD-240.CHR	SOX-2	12/4/2003	15:24:04	12/4/2003 15:24	15319 O2 + Ar	1	956.4325	2.9369	%vol	Nitrogen	1.766	24688.643	71.8754	%vol
									19.2					
03NOV-HPTCD-56.CHR	SOX-3	11/24/2003	0:50:43	11/24/2003 0:50	292 O2 + Ar	0.916	6249.548	19.1905	%vol	Nitrogen	1.708	25878.911	75.3406	%vol
03NOV-HPTCD-99.CHR	SOX-3	11/24/2003	6:56:04	11/24/2003 6:56	672 O2 + Ar	0.925	5896.148	18.1053	%vol	Nitrogen	1.716	24931.193	72.5815	%vol
03NOV-HPTCD-143.CHR	SOX-3	11/24/2003	13:17:16	11/24/2003 13:17	2032 O2 + Ar	0.925	5232.758	16.0683	%vol	Nitrogen	1.725	22314.8168	64.9645	%vol
03NOV-HPTCD-199.CHR	SOX-3	11/25/2003	19:30:58	11/25/2003 19:30	2746 O2 + Ar	0.95	4802.71	14.7477	%vol	Nitrogen	1.766	24263.642	70.6381	%vol
03NOV-HPTCD-241.CHR	SOX-3	12/4/2003	15:27:32	12/4/2003 15:27	15322 O2 + Ar	1.008	977.072	3.0003	%vol	Nitrogen	1.775	23920.724	69.6397	%vol
									18.9					
03NOV-HPTCD-57.CHR	SOX-4	11/24/2003	1:02:58	11/24/2003 1:02	304 O2 + Ar	0.908	6088.5797	18.6962	%vol	Nitrogen	1.7	25184.0333	73.3176	%vol
03NOV-HPTCD-100.CHR	SOX-4	11/24/2003	7:08:54	11/24/2003 7:08	684 O2 + Ar	0.916	6281.786	19.2895	%vol	Nitrogen	1.708	26469.823	77.0609	%vol
03NOV-HPTCD-144.CHR	SOX-4	11/24/2003	13:22:27	11/24/2003 13:22	2037 O2 + Ar	0.933	4785.231	14.694	%vol	Nitrogen	1.725	20248.747	58.9496	%vol
03NOV-HPTCD-242.CHR	SOX-4	12/4/2003	15:31:12	12/4/2003 15:31	15326 O2 + Ar	1.008	1037.5573	3.186	%vol	Nitrogen	1.775	24779.7048	72.1405	%vol
				11/23/03 20:00	1				18.9					

333

	SAMPLE	date	time	time	gas	reten	area	conc	units	gas	reten	area	conc	units
03NOV-HPTCD-58.CHR	SOX-5	11/24/2003	1:21:47	11/24/2003 1:21	323 O2 + Ar	0.9	6139.1925	18.8516	%vol	Nitrogen	1.7	25529.983	74.3247	%vol
03NOV-HPTCD-101.CHR	SOX-5	11/24/2003	7:20:31	11/24/2003 7:20	696 O2 + Ar	0.925	6006.2172	18.4433	%vol	Nitrogen	1.716	25464.8662	74.1352	%vol
03NOV-HPTCD-145.CHR	SOX-5	11/24/2003	13:29:23	11/24/2003 13:29	2044 O2 + Ar	0.925	5308.872	16.302	%vol	Nitrogen	1.716	22818.3603	66.4305	%vol
03NOV-HPTCD-243.CHR	SOX-5	12/4/2003	15:34:37	12/4/2003 15:34	15329 O2 + Ar	1	953.292	2.9273	%vol	Nitrogen	1.766	25386.557	73.9072	%vol
				11/23/03 20:00	1			18.1						
03NOV-HPTCD-59.CHR	SOX-6	11/24/2003	1:42:21	11/24/2003 1:42	345 O2 + Ar	0.916	5880.251	18.0565	%vol	Nitrogen	1.708	25068.775	72.982	%vol
03NOV-HPTCD-102.CHR	SOX-6	11/24/2003	7:34:15	11/24/2003 7:34	710 O2 + Ar	0.925	5612.537	17.2344	%vol	Nitrogen	1.725	24079.1885	70.1011	%vol
03NOV-HPTCD-146.CHR	SOX-6	11/24/2003	14:04:35	11/24/2003 14:04	3079 O2 + Ar	0.933	2703.701		%vol	Nitrogen	1.733	11699.2315	34.0596	%vol
03NOV-HPTCD-244.CHR	SOX-6	12/4/2003	15:39:29	12/4/2003 15:39	15334 O2 + Ar	1.016	5758.275	17.682	%vol	Nitrogen	1.775	24744.987	72.0394	%vol
03NOV-HPTCD-207.CHR	STAND	12/4/2003	12:47:56		O2 + Ar	1	9457.303	29.0406	%vol	Nitrogen	1.825	36355.533	105.8409	%vol
03NOV-HPTCD-208.CHR	STAND	12/4/2003	12:53:45		O2 + Ar	1.016	5907.526	18.1403	%vol	Nitrogen	1.775	26365.0505	76.7558	%vol
03NOV-HPTCD-194.CHR		11/25/2003	15:07:18		O2 + Ar	0.941	4989.735	15.322	%vol	Nitrogen	1.758	24331.901	70.8368	%vol
03NOV-HPTCD-195.CHR		11/25/2003	17:48:10		O2 + Ar	0.941	2906.063	8.9237	%vol	Nitrogen	1.766	13132.159	38.2313	%vol

APPENDIX E

Chapter 6 Supplement

File microcosm10-chip1.doc
Date May 3, 2002
Sample   upper spring white mat
Description chip from microcosm at 203 m
white mats at Site 3
Duration in place 4 months
Date emplaced Aug 2002
Date retrieved Dec 2002
Method of preservation gluteraldehyde, ethanol series
Coating material gold
Time of coating 2x 15 sec
Accelerating voltage 30 kv
Are bugs present?☒   Singles?☒   Groups?☒
No. types present lots cocci☒   rods☒   branchy☒
Radius of bugs ☐   Length ☐
Etching?☒   Secondary minerals?☒

Comments:
Pics from calcite chip from microcosm at 203 m

Calcite chip deeply corroded and severely etched where filaments were covering surface

Rare, strange quartz within biofilms…. Don't know if this is from the wall crusts that fell into mats and was incorporated into mat, or if the euhedral quartz formed within the mat authigenically (saw only 2 crystals within the mat)

File microcosm10-chip2.doc
Date May 3, 2002
Sample   upper spring white mat
Sample #
Description chip2 from microcosm at 203 m
white mats at Site 3
Duration in place 4 months
Date emplaced Aug 2002
Date retrieved Dec 2002
Method of preservation gluteraldehyde, ethanol series
Coating material gold
Time of coating 2x 15 sec
Accelerating voltage 30 kv
Are bugs present?☒   Singles?☒   Groups?☒
No. types present lots cocci☒   rods☒   branchy☒
Etching?☒   Secondary minerals?☒

Comments:
Pics from calcite chip 2 from microcosm at 203 m
 Calcite chip deeply corroded and severely etched where filaments were covering surface
Filaments covering surface- crosscutting cleavage surfaces – embedded filaments and cocci in dissolving calcite
Two types of filaments – one with septa and another without. Cocci very small and attached to filaments, or embedding within glycocaylx – lot of slime on surfaces
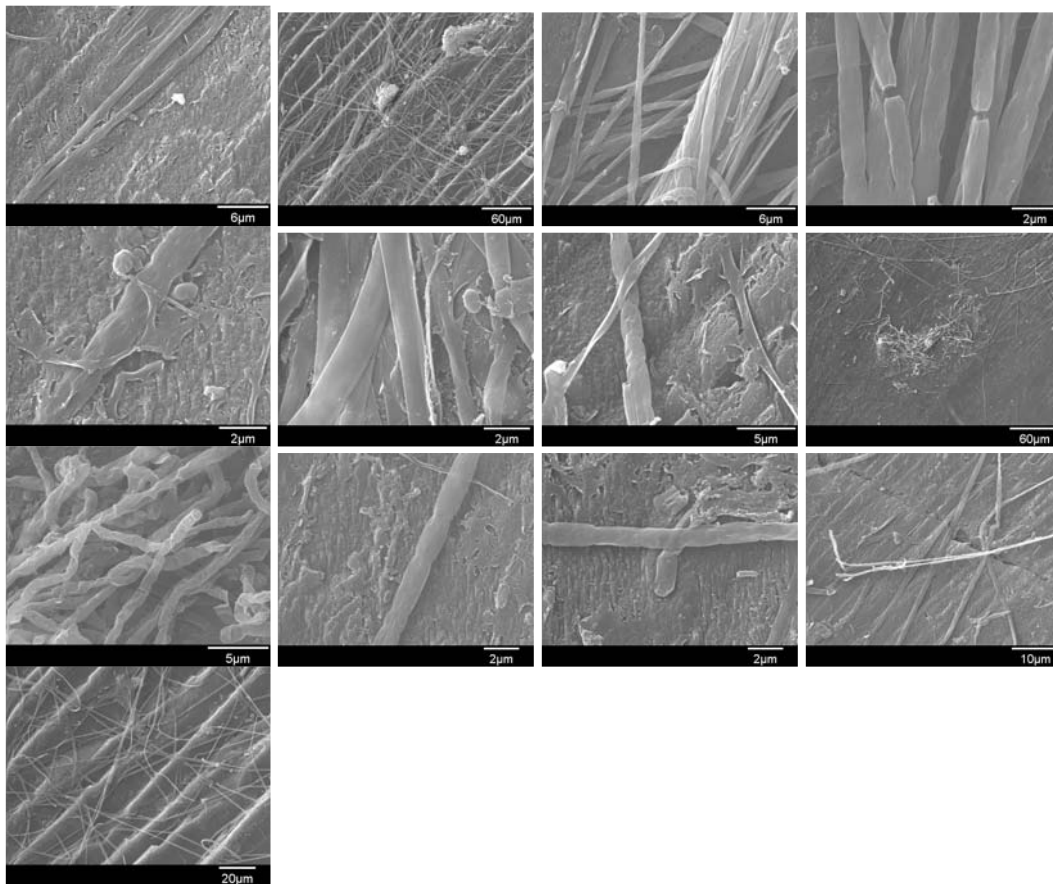
337

File ESEMmicro_chip3.doc

Date Aug 29, 2002

Sample   upper spring white mat- ESEM

Description "Chip3" from microcosm at 203 m

white mats at Site 3

Duration in place 4-5 months

Date emplaced March 2002

Date retrieved Aug 2002

Method of preservation samples collected and frozen

Coating material nothing

Time of coating ------

Accelerating voltage several stages

Are bugs present?☒   Singles?☒   Groups?☒

No. types present lots cocci☒ rods☒ branchy☒

Etching?☒   Secondary minerals?☒

Comments:
ESEM Pics from calcite chip 3 from microcosm at 203 m (aken by Phil and Libby)

Calcite chip corroded where filaments were covering surface

Filaments covering surface- crosscutting cleavage surfaces – embedded filaments in dissolving calcite

Dissolution under sulfur- filaments less than dissolution under non-sulfur-filaments

Two types of filaments – one with septa and another without, and one with intracellular sulfur and another without.
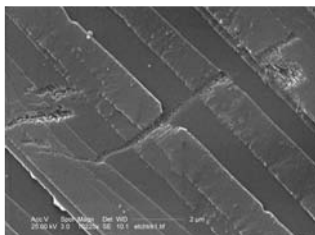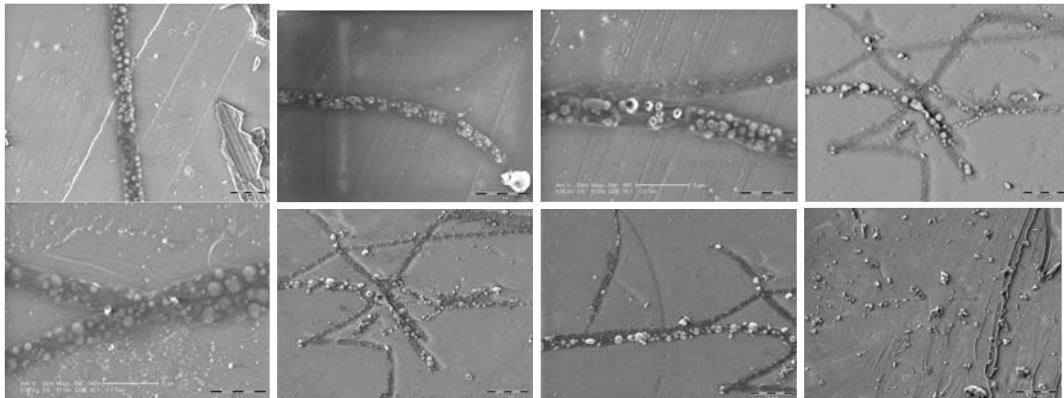
APPENDIX F

Chapter 7 Supplement

Date 2-1-01

Sample   wall crust

Sample # 175 m

Description red crust on wall – pH 0-1

Date retrieved 9-00 trip

Method of preservation bag-glut-ethanol

Coating material gold

Time of coating 30 sec

Accelerating voltage 30 Kv

Are bugs present?☒   Singles?☐   Groups?☒

No. types present ☐1 cocci☐ rods☒ branchy☐

Radius of bugs ~1 um Length ~1um

No. photomicrographs 2

File names wall-1   File names wall-2 (in order below)

Comments:
Problem with charging, so only took 2 pictures

Nice Si xtals – no etching or signs of weathering – no pitting… embedded in biofilm matrix. Most of the xtals are gypsum (Ca and S) – long tabular gypsum needles/xtals

Cells are mixed with matrix- if there are any real cells it's hard to tell

2μm
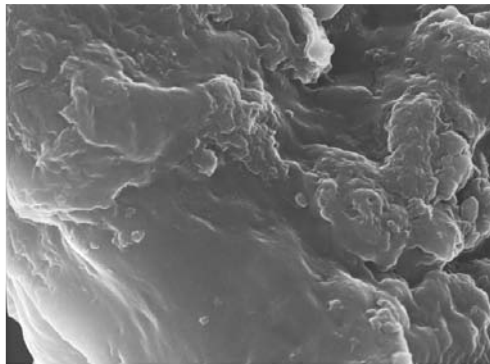
wall biofilm, no descrip (some cells)

10μm
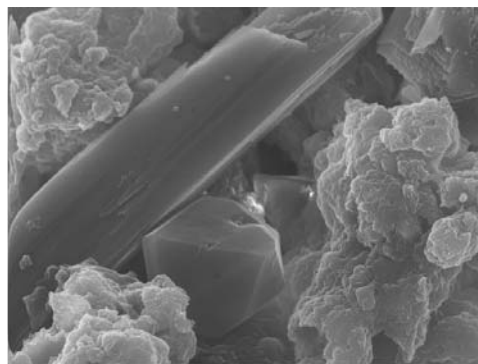
gypsum (big xtal in back) and Si (nice xtal in front) with biofilm

340

Date 2-2-01

Sample wall mat

Sample # 175 m

Description red crust on gysum walls, pH 0-1 site

Date retrieved 9-00 trip

Method of preservation bag – glut-ethanol

Coating material gold

Time of coating 30 sec

Accelerating voltage 30 Kv

Are bugs present? ☒ Singles?☐ Groups?☒

No. types present 1 cocci☐ rods☒ branchy☐

Radius of bugs <1 um Length <1 um hard to measure

Etching?☐ Secondary minerals?☐

EDAX ☐ File names WallEDS2-1

(Si, CaS, SiS,etc.)

Comments:
Si xtals on and within biofilms. Biofilm made up of rods and filaments embedded in matrix (Ca,Si, Fe, S composition, see EDS). Quartz xtals range in size from 200 nm to about 5-10 um, and some xtals may be bigger (about 20 um). Most show nice clean surfaces, no etching or pitting… and very awesome euhedral shapes (see below).

Cells hard to measure because the shapes are hidden in the biofilm matrix, but most cells appear to be about 1 um long, but others look like cocci (short and stubby)…. Only a few "fat" rods >1 um

341
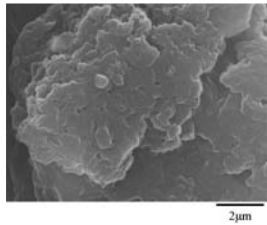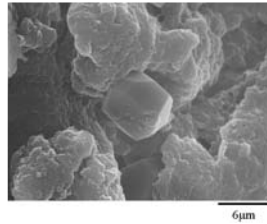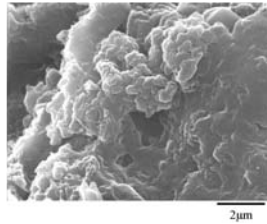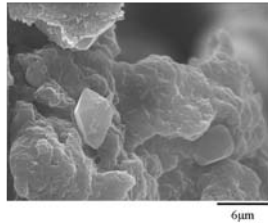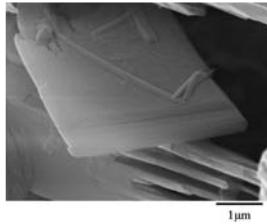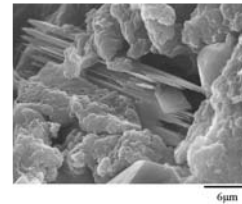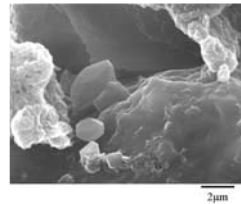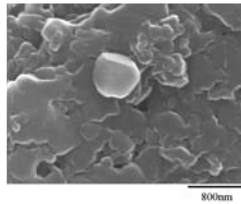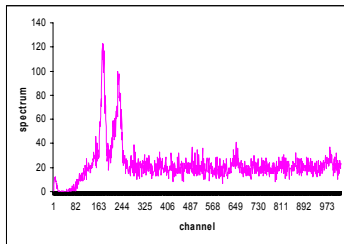
File SEM5701acid
Date 5-7-01
Sample wall mat, acid crust near Up Spg
Sample # lkb-01m-007
Description gyp and rusty-colored crust on wall, acid
Date retrieved 3-01 trip
Method of preservation glut
Coating material gold
Time of coating 30 sec
Accelerating voltage 30 KV
Are bugs present?☒ Singles?☒ Groups?☒
No. types present ☐ cocci☒ rods☒ branchy☐
Radius of bugs small, <1 μm) Length 1μm
Etching?☐ Secondary minerals? Quartz

Comments:

Acid wall crust, more pictures of beautiful quartz crystals…. And strange thin filaments that grow around and near some of them (Folk thinks that it may be palygorskite?). Quartz ranges from about 1mm long to about 5 mm long, some having doubly-terminated ends (quite euhedral and longer than wide), while others are round. Some faces appear to be coated – maybe with a biofilm….

Cells few and far between, although where they are present, and are clumped in a biofilm – hard to get size, but avg 1 μm long as rods. The whole background substrate is a biofilm, bumpy with cells, and quartz is either resting on or struck through it.
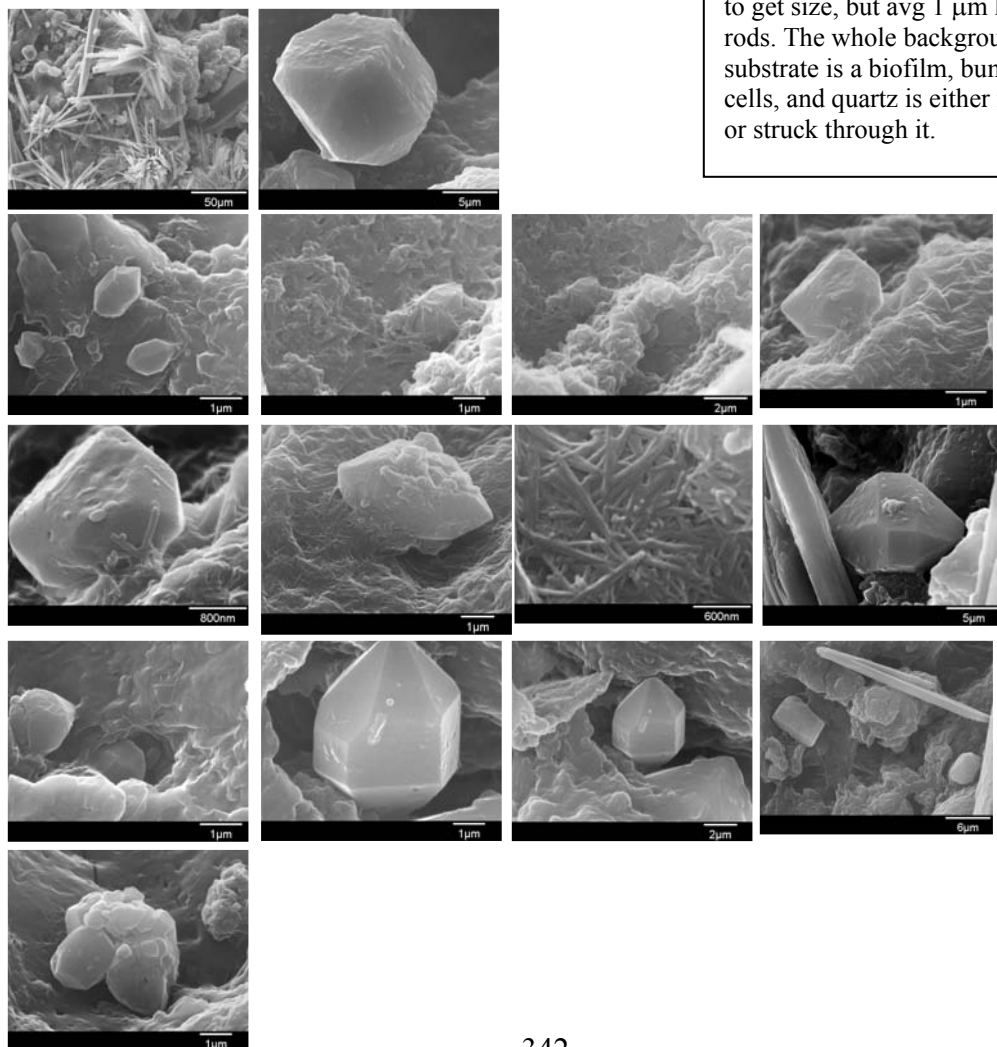
Bibliography

Airoldi, L., Southward, A.J., Niccolai, I., and Cinelli, F., 1997, Sources and pathways of particulate organic carbon in a submarine cave with sulphur water springs: Water, Air, and Soil Pollution, v. 99, p. 353-362.

Alain, K., Olagnon, M., Desbruyeres, D., Page, A., Barbier, G., Juniper, S.K., Quérellou, J., and Cambon-Bonavita, M.-A., 2002a, Phylogenetic characterization of the bacterial assemblage associated with mucous secretions of the hydrothermal vent polychaete *Paralvinella palmiformis*: FEMS Microbiology Ecology, v. 42, p. 463-476.

Alain, K., Quérellou, J., Lesongeur, F., Pignet, P., Crassous, P., Raguenes, G., Cueff, V., and Cambon-Bonavita, M.-A., 2002b, *Caminibacter hydrogeniphilus* gen. nov., sp. nov., a novel thermophilic, hydrogen-oxidizing bacterium isolated from an East Pacific Rise hydrothermal vent: International Journal of Systematic and Evolutionary Microbiology, v. 52, p. 1317-1323.

Alain, K., Zbinden, M., Le Bris, N., Lesongeur, F., Quérellou, J., Gaill, F., and Cambon-Bonavita, M.-A., 2004, Early steps in microbial colonization processes at deep-sea hydrothermal vents: Environmental Microbiology, v. 6, p. 227-241.

Alfreider, A., Vogt, C., Hoffman, D., and Babel, W., 2003, Diversity of ribulose-1,5-bisphosphate carboxylase/oxygenase large-subunit from groundwater and aquifer microorganisms: Microbial Ecology, v. 45, p. 317-328.

Allan, J.D., 1995, Stream Ecology: Structure and function of running waters: New York, Chapman & Hall, 388 p.

Alm, E.W., Oerther, D.B., Larsen, N., Stahl, D.A., and Raskin, L., 1996, The oligonucleotide probe database: Applied and Environmental Microbiology, v. 62, p. 3557-3559.

Amann, R.I., Krumholz, L., and Stahl, D.A., 1990, Fluorescent-oligonucleotide probing of whole cells for determinative, phylogenetic, and environmental studies in microbiology: Journal of Bacteriology, v. 172, p. 762-770.

Amann, R.I., Ludwig, W., and Schleifer, K.H., 1995, Phylogenetic identification and in situ detection of individual microbial cells without cultivation: Microbiological Reviews, v. 59, p. 143-169.

Andreae, M.O., and Andreae, T.W., 1988, The cycle of biogenic sulfur compounds over the Amazon Basin. 1. Dry season: Journal of Geophysical Research, v. 93, p. 1487-1497.

Angert, E.R., Northup, D.E., Reysenbach, A.L., Peek, A.S., Goebel, B.M., and Pace, N.R., 1998, Molecular phylogenetic analysis of a bacterial community in Sulphur River, Parker Cave, Kentucky: American Mineralogist, v. 83, p. 1583-1592.

Ausubel, F., Brent, R., Kingston, R., Moore, D., Seidman, J., Smith, H., and Strujil, K., 1990, Current protocols in molecular biology, Volume 1: New York, Greene Publishing Associates and Wiley-Interscience, p. 1.6.1-1.6.2.

Avrahami, M., and Golding, R.M., 1969, The oxidation of the sulfide ion at very low concentrations in aqueous solutions: Chemical Society (A), p. 647-651 (no volumes).

Bachofen, R., Ferloni, P., and Flynn, I., 1998, Microorganisms in the subsurface: Microbiological Research, v. 153, p. 1-22.

Bak, F., and Pfenning, N., 1991, Sulfate-reducing bacteria in littoral sediment of Lake Constance: FEMS Microbiology Ecology, v. 85, p. 43-52.

Barns, S.M., Takala, S.L., and Kuske, C.R., 1999, Wide distribution and diversity of members of the bacterial kingdom Acidobacterium in the environment: Applied and Environmental Microbiology, v. 65, p. 1731-1737.

Barton, H.A., Luiszer, F., and Pace, N.R., 2002, Unique microbial diversity in an aphotic cave hot spring, *in* Stokowski, S., Jr., ed., National Speleological Society: Camden, Maine, p. A-3.

Barton, H.A., Taylor, M.R., and Pace, N.R., 2004, Molecular phylogenetic analysis of a bacterial community in an oligotrophic cave environment: Geomicrobiology Journal, v. 21, p. 11-20.

Bates, T.S., Lamb, B.K., Guenther, A., Dignon, J., and Stoiber, R.E., 1992, Sulfur emissions to the atmosphere from natural sources: Journal of Atmospheric Chemistry, v. 14, p. 315-337.

Beauchamp, R.O., Bus, J.S., Popp, J.A., Boreiko, C.J., and Andejelkovich, D.A., 1984, A critical review of the literature on hydrogen sulfide toxicity: Critical Reviews in Toxicity, v. 13, p. 25-97.

Bekins, B.A., Godsy, E.M., and Warren, E., 1999, Distribution of microbial physiologic types in an aquifer contaminated by crude oil: Microbial Ecology, v. 37, p. 263-275.

Ben-Ari, E.T., 2002, Microbiology and geology: solid marriage made on Earth: ASM News, v. 68, p. 13-18.

Berner, R.C., and Morse, J.W., 1974, Dissolution kinetics of calcium carbonate in sea water; IV, Theory of calcite dissolution: American Journal of Science, v. 274, p. 108-134.

Biggs, P., and Espach, R.H., 1960, Petroleum and natural gas fields in Wyoming, U.S. Bur. Mines Bull. 582, 538 p.

Bodenbender, J., Wassmann, R., Papen, H., and Rennenberg, H., 1999, Temporal and spatial variation of sulfur-gas-transfer between coastal marine sediments and the atmosphere: Atmospheric Environment, v. 33, p. 3487-3502.

Bond, P.L., Smriga, S.P., and Banfield, J.F., 2000, Phylogeny of microorganisms populating a thick, subaerial, predominantly lithotrophic biofilm at an extreme acid mine drainage site: Applied and Environmental Microbiology, v. 66, p. 3843-3849.

Boschker, H.T.S., Nold, S.C., Wellsbury, P., Bos, D., de Graaf, W., Pel, R., Parkes, R.J., and Cappenberg, T.E., 1998, Direct linking of microbial populations to specific biogeochemical processes by 13C-labelling of biomarkers: Nature, v. 392, p. 801-805.

Boschker, H.T.S., and Middelburg, J.J., 2002, Stable isotopes and biomarkers in microbial ecology: FEMS Microbiology Ecology, v. 40, p. 85-95.

Boston, P.J., Spilde, M.N., Northup, D.E., Melim, L.A., Soroka, D.S., Kleina, L.G., Lavoie, K.H., Hose, L.D., Mallory, L.M., Dahm, C.N., Crossey, L.J., and Schelble, R.T., 2001, Cave biosignature suites: microbes, minerals, and Mars: Astrobiology, v. 1, p. 25-55.

Bratbak, G., and Dundas, I., 1984, Bacterial dry matter content and biomass estimations: Applied and Environmental Microbiology, v. 48, p. 755.

Breckenridge, R.M., and Hinckley, B.S., 1978, Thermal Springs of Wyoming: Geological Survey of Wyoming Bulletin 60, 104 p.

Brezonik, P.L., 1994, Chemical Kinetics and Process Dynamics in Aquatic Systems: Boca Raton, Lewis Publishers, 754 p.

Brigmon, R.L., Martin, H.W., Morris, T.L., Britton, G., and Zam, S.G., 1994, Biogeochemical ecology of *Thiothrix* spp. in underwater limestone caves: Geomicrobiology Journal, v. 12, p. 141-159.

Brigmon, R.L., Furlong, M., and Whitman, W.B., 2003, Identification of *Thiothrix unzii* in two distinct ecosystems: Letters in Applied Microbiology, v. 36, p. 88-91.

Brimacombe, R., Atmadja, J., Stiege, W., and Schüler, D., 1988, A detailed model of the three-dimensional structure of *Escherichia coli* 16S ribosomal RNA in situ in the 30S subunit: Journal of Molecular Biology, v. 199, p. 115-136.

Brinkhoff, T., and Muyzer, G., 1997, Increased species diversity and extended habitat range of sulfur-oxidizing *Thiomicrospira* spp.: Applied and Environmental Microbiology, v. 63, p. 3789-3796.

Brinkhoff, T., Siebert, S.M., Kuever, J., and Muyzer, G., 1999, Distribution and diversity of *Thiomicrospira* spp. at a shallow-water hydrothermal vent in the Aegean Sea (Milos, Greece): Applied and Environmental Microbiology, v. 65, p. 3843-3849.

Brosius, J., Dull, T.L., Sletter, D.D., and Noller, H.F., 1981, Gene organization and primary structure of a ribosomal operon from *Escherichia coli*: Journal of Molecular Biology, v. 148, p. 107-127.

Brown, A.V., Pierson, W.K., and Brown, K.B., 1994, Organic carbon and the payoff-risk relationship in cave ecosystems: 2nd International Conference on Ground Water Ecology, USEPA, p. 67-76.

Brunet, R.C., and Garcia-Gil, L.J., 1996, Sulfide-induced dissimilatory nitrate reduction to ammonia in anaerobic freshwater sediments: FEMS Microbiology Ecology, v. 21, p. 131-138.

Butkus, M.A., and Grasso, D., 1998, Impact of aqueous electrolytes on interfacial energy: Journal of Colloid Interface Science, v. 200, p. 172-181.

Campbell, B.J., Jeanthon, C., Kostka, J.E., Luther, I., G.W. , and Cary, S.C., 2001, Growth and phylogenetic properties of novel bacteria belonging to the Epsilon subdivision of the *Proteobacteria* enriched from *Alvinella pompejana* and deep-sea hydrothermal vents: Applied and Environmental Microbiology, v. 67, p. 4566-4572.

Canfield, D.E., 2001a, Biogeochemistry of sulfur isotopes, Stable Isotope Geochemistry, Volume 43: Reviews in Mineralogy, p. 607-636.

Canfield, D.E., 2001b, Isotope fractionation by natural populations of sulfate-reducing bacteria: Geochimica et Cosmochimica Acta, v. 65, p. 1117-1124.

Carmody, R., Plummer, L., Busenberg, E., and Coplen, T., 1998, Methods of collection of dissolved sulfate and sulfide and analysis of their sulfur isotopic composition. US Geological Survey Open-File Report, 97-234.

Cary, S.C., Cottrell, M.T., Stein, J.L., Camacho, F., and Desbruyeres, D., 1997, Molecular identification and localization of a filamentous symbiotic bacteria associated with the hydrothermal vent annelid *Alvinella pompejana*: Applied and Environmental Microbiology, v. 63, p. 1124-1130.

Caumartin, V., 1963, Review of the microbiology of underground environments: Bulletin of the National Speleological Society, v. 25, p. 1-14.

Cha, J.M., Cha., W.S., and Lee, J., 1999, Removal of organo-sulphur odour compounds by *Thiobacillus novellas* SRM, sulphur-oxidizing microorganisms: Process Biochemistry, v. 34, p. 659-665.

Chafetz, H.S., and Zhang, J., 1998, Authigenic euhedral megaquartz crystals in a Quaternary dolomite: Journal of Sedimentary Research, v. 68, p. 994-1000.

Chapelle, F.H., Vroblesky, D.A., Woodward, J.C., and Lovley, D.R., 1997, Practical considerations for measuring hydrogen concentrations in groundwater: Environmental Science and Technology, v. 31, p. 2873-2877.

Chen, K.Y., and Morris, J.C., 1972, Kinetics of oxidation of aqueous sulfide by O_2: Environmental Science and Technology, v. 6. , p. 529-537.

Chesson, P., Pacala, S.W., and Neuhauser, C., 2002, Environmental niches and ecosystem functioning, *in* Kinzig, A.P., Pacala, S.W., and Tilman, D., eds., The Functional Consequences of Biodiversity: Monographs in Population Biology, p. 213-245.

Conrad, R., 1996, Soil microorganisms as controllers of atmospheric trace gases (H_2, CO, CH_4, OCS, N_2O, and NO): Microbiological Reviews, v. 60, p. 609-640.

Coplen, T.B., Hopple, J.A., Böhlke, J.K., Peiser, H.S., Rieder, S.E., Krouse, H.R., Rosman, K.J.R., Ding, T., Vocke, R.D., Jr., Révész, K.M., Lamberty, A.,

Taylor, P., and De Bièvre, P., 2002, Compilation of Minimum and Maximum Isotopic Ratios of Selected Elements in Naturally Occurring Terrestrial Materials and Reagents: Reston, Virginia, US Geological Survey Water-Resources Investigations Report 01-4222, 98p.

Corre, E., Reysenbach, A.-L., and Prieur, D., 2001, ε-*Proteobacterial* diversity from a deep-sea hydrothermal vent on the Mid-Atlantic Ridge: FEMS Microbiology Letters, v. 205, p. 329-335.

Culver, D., and Sket, B., 2000, Hotspots of subterranean biodiversity in caves and wells: Journal of Cave and Karst Studies, v. 62, p. 11-17.

Daims, H., Bruhl, A., Amann, R., Schleifer, K.H., and Wagner, M., 1999, The Domain-specific probe EUB338 is insufficient for the detection of all Bacteria: development and evaluation of a more comprehensive probe set: Systematic and Applied Microbiology, v. 22, p. 434-444.

Daoxian, Y., 1998, Basic ideas, methodologies, and major results of IGCP 299, in Daoxian, Y. and Zaihua, L. Global Karst Correlation., *in* Daoxian, Y.a.Z., L., ed., UNESCO/IUGS International Geological Correlation Program Project 299: Geology, Climate, Hydrology, and Karst Formation (1990-1994) Final Report.: Beijing, Science Press, p. 1-32.

Davis, D.G., 1980, Cave development in the Guadalupe Mountains: a critical review of recent hypotheses: National Speleological Society Bulletin, v. 42, p. 42-48.

DeBont, J.A.M., van Dijken, J.P., and Harder, W., 1981, Dimethyl sulphoxide and dimethyl sulphide as a carbon, sulphur, and energy source for growth of *Hyphomicrobium*: S. J. General Microbiology, v. 127, p. 315-323.

DeLaune, R.D., Devai, I., and Lindau, C.W., 2002, Flux of reduced sulfur gases along a salinity gradient in Louisiana coastal marshes: Estuarine, Coastal, and Shelf Science, v. 54, p. 1003-1011.

Dias, B., and Weimer, B., 1998, Conversion of methionine to thiols by lactococci, lactobacilli, and *Brevibacteria*: Applied and Environmental Microbiology, v. 64, p. 3320-3326.

Dickson, G.W., and Kirk, Jr., P.W., 1976, Distribution of heterotrophic microorganisms in relation to detritivores in Virginia caves (with supplemental bibliography on cave mycology and microbiology), *in* Parker, B.C., Roane, M.K., eds., The distributional history of the biota of the

Southern Appalachians, Part IV, Algae and fungi: Charlottesville, VA, University Press of Virginia, p. 205-226.

Dublyansky, V.N., and Dublyansky, Y.V., 1998, The problem of condensation in karst studies: Journal of Cave and Karst Studies, v. 60, p. 3-17.

Egemeier, S.J., 1973, Cavern development by thermal waters with a possible bearing on ore deposition [Unpublished Ph.D. dissertation thesis], Stanford University.

Egemeier, S.J., 1981, Cavern development by thermal waters: National Speleological Society Bulletin, v. 43, p. 31-51.

Egemeier, S.J., 1987, A theory for the origin of Carlsbad Caverns: National Speleological Society Bulletin, v. 49, p. 73-76.

Ehrlich, H.L., 1995, Bacterial mineralization of organic carbon under anaerobic conditions, *in* Bollag, J.-M., and Stotzky, G., eds., Soil Biochemistry, Volume 8: New York, Marcel Dekker, Inc., p. 219-247.

Ehrlich, H.L., 1996, Geomicrobiology: New York, Marcel Dekker, 719 p.

Eiler, A., Langenheder, S., Bertilsson, S., and Tranvik, L.J., 2003, Heterotrophic bacterial growth efficiency and community structure at different natural organic carbon concentrations: Applied and Environmental Microbiology, v. 69, p. 3701–3709.

Elshahed, M.S., Senko, J.M., Najar, F.Z., Kenton, S.M., Roe, B.A., Dewers, T.A., Spear, J.R., and Krumholz, L.R., 2003, Bacterial diversity and sulfur cycling in a mesophilic sulfide-rich spring: Applied and Environmental Microbiology, v. 69, p. 5609-5621.

Engberg, J., On, S.L., Harrington, C.S., and Gerner-Smidt, P., 2000, Prevalence of *Campylobacter, Arcobacter, Helicobacter,* and *Sutterella* spp. in human fecal samples as estimated by a reevaluation of isolation methods for Campylobacters: Journal of Clinical Microbiology, v. 38, p. 286-291.

Engel, A.S., Porter, M.L., Kinkle, B.K., and Kane, T.C., 2001, Ecological assessment and geological significance of microbial communities from Cesspool Cave, Virginia: Geomicrobiology Journal, v. 18, p. 259-274.

Engel, A.S., Lee, N., Porter, M.L., Stern, L.A., Bennett, P.C., and Wagner, M., 2003, Filamentous "*Epsilonproteobacteria*" dominate microbial mats from

sulfidic cave springs: Applied and Environmental Microbiology, v. 69, p. 5503-5511.

Engel, A.S., Porter, M.L., Stern, L.A., Quinlan, S., and Bennett, P.C., Bacterial diversity and ecosystem function of filamentous microbial mats from aphotic (cave) springs dominated by chemolithoautotrophic "*Epsilonproteobacteria*": FEMS Microbiology Ecology, accepted 2004.

Ensign, S.A., 1995, Reactivity of carbon monoxide dehydrogenase from *Rhodospirillum rubrum* with carbon dioxide, carbonyl sulfide, and carbon disulfide: Biochemistry, v. 34, p. 5372-5381.

Eraso, A., 1969, La corrósion climática en las cavernas: Bol. Geol. y Minero, v. 80, p. 564-581.

Extrand, C.W., and Kumagai, Y., 1995, Liquid drops on an inclined plane: the relation between contact angles, drop shape, and retentive force: Journal of Colloid and Interface Science, v. 170, p. 515-521.

Fagerbakke, K.M., Heldal, M., and Norland, S., 1996, Content of carbon, nitrogen, oxygen, sulfur, and phosphorous in native aquatic and cultured bacteria: Aquatic Microbial Ecology, v. 10, p. 15-27.

Fenchel, T., and Glud, R.N., 1998, Veil architecture in a sulphide-oxidizing bacterium enhances countercurrent flux: Nature, v. 394, p. 367-369.

Finster, K., Liesack, W., and Tindall, B.J., 1997, *Sulfurospirillum arcachonense* sp. nov., a new-microaerophilic sulfur-reducing bacterium: International Journal of Systematic Bacteriology, v. 47, p. 1212-1217.

Ford, D., and Williams, P., 1989, Karst Geomorphology and Hydrology: London, Unwin Hyman, 601 p.

Forti, P., 1994, The role of sulfate-sulfide reactions in gypsum speleogenesis, *in* Sasowsky I.D., and Palmer, M.V., eds., Breakthroughs in Karst Geomicrobiology and Redox Geochemistry, Volume Sp. Pub. 1: Colorado Springs, Colorado, Karst Waters Institute, p. 21-22.

Fortin, D., and Beveridge, T.J., 1997, Role of the bacterium *Thiobacillus* in the formation of silicates in acidic mine tailings: Chemical Geology, v. 141, p. 235-250.

France, R., 1995, Carbon-13 enrichment in benthic compared to planktonic algae: food web implications: Marine Ecology Progress Series, v. 124, p. 307-312.

France, R., and Cattaneo, A., 1998, δ^{13}C variability of benthic algae: effects of water colour via modulation by stream current: Freshwater Biology, v. 39, p. 617-622.

Francis, C.A., Obraztsova, A.Y., and Tebo, B.M., 2000, Dissimilatory metal reduction by the facultative anaerobe *Pantoea agglomerans* SP1: Applied and Environmental Microbiology, v. 66, p. 543-548.

Fritz, M., and Bachofen, R., 2000, Volatile organic sulfur compounds in a meromictic alpine lake: Acta Hydrochimica et Hydrobiologica, v. 28, p. 185-192.

Fry, B., Gest, H., and Hayes, J.M., 1986, Sulfur isotope effects associated with protonation of HS$^-$ and volatilization of H$_2$S: Chemical Geology, v. 58, p. 253-258.

Fry, B., Ruf, W., Gest, H., and Hayes, J.M., 1988, Sulfur isotope effects associated with oxidation of sulfide by O$_2$ in aqueous solution.: Chemical Geology, v. 73, p. 205-210.

Fuhrman, J.A., and Campbell, L., 1998, Microbial microdiversity: Nature, v. 393, p. 410-411.

Galdenzi, S., and Menichetti, M., 1995, Occurrence of hypogenic caves in a karst region: examples from Central Italy: Environmental Geology, v. 26, p. 39-47.

Garcia, J.-L., Patel, B.K.C., and Ollivier, B., 2000, Taxonomic, phylogenetic, and ecological diversity of methanogenic Archaea: Anaerobe, v. 6, p. 205-226.

Garman, K.M., 2002, Biodiversity associated with anoxic, sulfidic environments in West Central Florida cave systems, *in* Martin, J.B., Wicks, C.M., and Sasowsky, I.D., eds., Hydrology and Biology of Post-Paleozoic Carbonate Aquifers: Karst Frontiers. Florida and Related Environments: Gainesville, Florida, Karst Waters Institute, p. 64-65.

Gergedeva, B.A., 1970, The role of condensation and infiltration waters in cave origin: Trudi. Vses. Geograficheskogo Obshchestva, v. 102, p. 196-198.

Gevertz, D., Telang, A.J., Voordouw, G., and Jenneman, G.E., 2000, Isolation and characterization of strains CVO and FWKOB, two novel nitrate-reducing, sulfide-oxidizing bacteria isolated from oil field brine: Applied and Environmental Microbiology, v. 66, p. 2491-2501.

Glendon, A.L., 1989, Hydrogeology of the Leadville Limestone and other Paleozoic rocks in northwestern Colorado, with results of aquifer tests at Glenwood Springs: U.S. Geological Survey Water-Resources Investigations Report 87-4195, 96p.

Goff, F., and Grigsby, C.O., 1982, Valles Caldera geothermal systems, New Mexico, U.S.A.: Journal of Hydrology, v. 56, p. 119-136.

Gold, T., 1999, The Deep Hot Biosphere: New York, Spinger-Verlag, 235 p.

Gray, N.D., and Head, I.M., 2001, Linking genetic identity and function in communities of uncultured bacteria: Environmental Microbiology, v. 3, p. 481-492.

Gregory, S.V., 1983, Plant-herbivore interactions in stream ecosystems, in Barnes, J.R., and Minshall, G.W., eds., Stream Ecology: New York, Plenum Press, p. 157-190.

Grubbs, A., 1991, Sulfur bacteria and the deep phreatic environment of the Edwards Aquifer: National Speleological Society Bulletin, v. 53, p. 41.

Gugliandolo, C., and Maugeri, T.L., 1998, Temporal variations in heterotrophic mesophilic bacteria from a marine shallow hydrothermal vent off the Island of Volcano (Eolian Islands, Italy): Microbial Ecology, v. 36, p. 13-22.

Gundersen, J.K., Jorgensen, B.B., Larsen, E., and Jannasch, H.W., 1992, Mats of giant sulphur bacteria on deep-sea sediments due to fluctuating hydrothermal flow: Nature, v. 360, p. 454-456.

Haddad, A., Camacho, F., Durand, P., and Cary, S.C., 1995, Phylogenetic characterization of the epibiotic bacteria associated with the hydrothermal vent polychaete *Alvinella pompejana*: Applied and Environmental Microbiology, v. 61, p. 1679-1687.

Hajna, A.A., 1945, Triple-sugar iron medium for the identification of the intestinal group of bacteria: Journal Bacteriology, v. 49, p. 516-517.

Hård, S., and Johansson, K., 1977, Journal of Colloid and Interface Science, v. 60, p. 467.

Hassan, A.A., 1982, Methodologies for extraction of dissolved inorganic carbon for stable carbon isotope studies: evaluation and alternatives: US Geological Survey Water Resources Investigations 82-6.

Hays, J.M., 2001, Fractionation of carbon and hydrogen isotopes in biosynthetic processes, *in* Valley, J.W., Cole, D.R., eds., Stable Isotope Geochemistry, Reviews in Mineralogy and Geochemistry, vol. 43: Washington, D.C., Mineralogical Society of America, 225-277.

Head, I.M., Saunders, J.R., and Pickup, R.W., 1998, Microbial evolution, diversity, and ecology: A decade of ribosomal RNA analysis of uncultivated microorganisms: Microbial Ecology, v. 35, p. 1-21.

Heasler, H.P., and Hinckley, B.S., 1985, Geothermal resources of the Bighorn Basin, Wyoming: Laramie, The Geological Survey of Wyoming, Report of Investigations 29, p. 28.

Heck, K.L., Jr., G. Van Belle, and D. Simberloff, 1975. Explicit calculation of the rarefaction diversity measurement and the determination of sufficient sample size: Ecology, v. 56, p. 1459-1461.

Hill, C., Sutherland, W., and Tierney, L., 1976, Caves of Wyoming: Laramie, University of Wyoming, 229 p.

Hill, C.A., 1990, Sulfuric acid speleogenesis of Carlsbad Cavern and its relationship to hydrocarbons, Delaware Basin, New Mexico and Texas: American Association of Petroleum Geologists Bulletin, v. 74, p. 1685-1694.

Hill, C.A., 1995, H2S-related porosity and sulfuric acid oil-field karst, in Budd, D.A., Saller, A.H., and Harris, P.M., eds., Unconformities in carbonate strata: Their recognition and the significance of associated porosity, American Association of Petroleum Geologists Memoir 61, p. 301-306.

Hill, C.A., 1996, Geology of the Delaware Basin, Guadalupe, Apache, and Glass Mountains, New Mexico and West Texas, Permian Basin Section- SEPM, 480 p.

Hill, C.A., 2000, Overview of the geologic history of cave development in the Guadalupe Mountains, New Mexico: Journal of Cave and Karst Studies, v. 62, p. 60-71.

Hill, C.A., and Forti, P., 1997, Cave Minerals of the World: Huntsville, Alabama, National Speleological Society, 463 p.

Hill, T.C.J., Walsh, K.A., Harris, J.A., and Moffett, B.F., 2003, Using ecological diversity measures with bacterial communities: FEMS Microbiology Ecology, v. 43, p. 1-11.

Holdman, L.V., and Moore, W.E.C., 1972, Anaerobe Laboratory Manual: Blacksburg, Virginia, Virginia Polytechnic Institute and State University.

Holmes, A.J., Tujula, N.A., Holley, M., Contos, A., James, J.M., Rogers, P., and Gillings, M.R., 2001, Phylogenetic structure of unusual aquatic microbial formations in Nullarbor caves, Australia: Environmental Microbiology, v. 3, p. 256-264.

Holmes-Farley, S.R., Reamey, R.H., McCarthy, T.J., Deutch, J., and Whitesides, G.M., 1985, Langmuir, v. 1, p. 725.

Horner-Devine, M.C., Leibold, M.A., Smith, V. H., and Bohannan, B.J.M., 2003, Bacterial diversity patterns along a gradient of primary productivity: Ecology Letters, v. 6, p. 613-622.

Hose, L.D., Palmer, A.N., Palmer, M.V., Northup, D.E., Boston, P.J., and DuChene, H.R., 2000, Microbiology and geochemistry in a hydrogen-sulphide rich karst environment: Chemical Geology, v. 169, p. 399-423.

Howard, A.D, 1964, Processes of limestone cave development: International Journal of Speleology, v. 1, p. 47-60.

Howarth, R., Unz, R.F., Seviour, E.M., Seviour, R.J., Blackall, L.L., Pickup, R.W., Jones, J.G., Yaguchi, J., and Head, I.M., 1999, Phylogenetic relationships of filamentous sulfur bacteria (*Thiothrix* spp. and Eikelboom type 021N bacteria) isolated from wastewater-treatment plants and description of *Thiothrix eikelboomii* sp. nov., *Thiothrix unzii* sp. nov., *Thiothrix fructosivorans* sp. nov. and *Thiothrix defluvii* sp. nov.: International Journal of Systematic Bacteriology, v. 49, p. 1817-1827.

Hubbard, D.A., Herman, J.S., and Bell, P.E., 1986, The role of sulfide oxidation in the genesis of Cesspool Cave, Virginia, USA, *in* Comissio Organitzadora del IX Congres Internacional d'Espeleologia, ed., 9th International Congress of Speleology, Volume 1: Barcelona, Spain, p. 255-257.

Hubbard, D.A., Herman, J.S., and Bell, P.E., 1990, Speleogenesis in a travertine scarp: observations of sulfide oxidation in the subsurface, *in* Herman, J.S., Hubbard, D.A., ed., Travertine-Marl: Stream Deposits in Virginia: Charlottesville, Department of Mines, Minerals and Energy, Division of Mineral Resources, p. 177-184.

354

Huelsenbeck, J.P., and Crandall, K.A., 1997, Phylogeny estimation and hypothesis testing using maximum likelihood: Annual Review of Ecology and Systematics, v. 28, p. 437-466.

Hughes, J.B., Hellmann, J.J., Ricketts, T.H., and Bohannan, B.L.M., 2001, Counting the uncountable: statistical approaches to estimating microbial diversity: Applied and Environmental Microbiology, v. 67, p. 4399-4406.

Hurely, M.A., and Roscoe, M.E., 1983, Automated statistical analysis of microbial enumeration by dilution series: Journal of Applied Bacteriology, v. 55, p. 157-164.

Hurlbert, S.H., 1971. The nonconcept of species diversity: a critique and alternative parameters: Ecology, v. 52, p. 577-586.

Hutchens, E., Radajewski, S., Dumont, M.G., McDonald, I.R., and Murrell, J.C., 2004, Analysis of methanotrophic bacteria in Movile Cave by stable isotope probing: Environmental Microbiology, v. 6, p. 111-120.

Iler, R.K., 1979, The chemistry of silica: Solubility, Polymerization, Colloid and Surface Properties and biochemistry: New York, John Wiley and Sons, 866 p.

Jagnow, D.H., Hill, C.A., Davis, D.G., DuChene, H.R., Cunningham, K.I., Northup, D.E., and Queen, J.M., 2000, History of the sulfuric acid theory of speleogenesis in the Guadalupe Mountains, New Mexico: Journal of Cave and Karst Studies, v. 62, p. 54-59.

Jameson, J., 1994, Models of porosity formation and their impact on reservoir description in the Lisburne field, Prudhoe Bay, Alaska: American Association of Petroleum Geologists, v. 78, p. 1651-1678.

Janssen, P.H., Schuhmann, A., Bak, F., and Liesack, W., 1996, Disproportionation of inorganic sulfur compounds by the sulfate-reducing bacterium *Desulfocapsa thiozymogenes* gen. nov., sp. nov.: Archives in Microbiology, v. 166, p. 184-192.

Jarvis, T., 1986, Regional hydrology of the Paleozoic aquifer systems, southeastern Bighorn Basin, Wyoming, with an impact analysis on Hot Springs State Park: [Unpublished Masters thesis] Laramie, University of Wyoming, 224p.

Johnson, D.B., 1998, Biodiversity and ecology of acidophilic microorganisms: FEMS Microbiology Ecology, v. 27, p. 307-317.

Jordan, S.L., Kracziewicz-Dowajat, A.J., Kelly, D.P., and Wood, A.P., 1995, Novel eubacteria able to grow on carbon disulfide: Archives in Microbiology, v. 163, p. 131-137.

Kanagawa, T., and Kelly, D.P., 1986, Breakdown of dimethyl sulfide by mixed cultures and by *Thiobacillus thioparus*: FEMS Microbiology Letters, v. 34, p. 13-19.

Kanagawa, T., Kamagata, Y., Aruga, S., Kohno, T., Horn, M., and Wagner, M., 2000, Phylogenetic analysis of and oligonucleotide probe development for Eikelboom Type 021N filamentous bacteria isolated from bulking activated sludge: Applied and Environmental Microbiology, v. 66, p. 5043-5052.

Kaplan, I.R., and Rittenberg, S.C., 1964, Microbiological fractionation of sulfur isotopes: Journal of General Microbiology, v. 34, p. 195-212.

Kaye, C.A., 1957, The effects of solvent motion on limestone solution: Journal of Geology, v. 65, p. 35-46.

Kelly, D.P., and Harrison, A.P., 1989, The genus *Thiobacillus*, *in* Staley, J.T., Pfenning, N., Bryant, M.P., and Holdt, J.G., eds., Bergey's Manual of Determinative Bacteriology, Volume 3: Baltimore, Williams and Wilkins, p. 1842-1858.

Kelly, D.P., Wood, A.P., Jordan, S.L., Padden, A.N., Gorlenko, V.M., and Dubinina, G.A., 1994, Biological production and consumption of gaseous sulphur compounds: Biochemical Society Transactions, Atmospheric Gas Production and Consumption, v. 22, p. 1011-1014.

Kiene, R.P., 1988, Dimethyl sulfide metabolism in salt marsh sediments: FEMS Microbial Ecology, v. 53, p. 71-78.

Kiene, R.P., Malloy, K.D., and Taylor, B.F., 1990, Sulfur-containing amino acids as precursors of thiols in anoxic coastal sediments: Applied and Environmental Microbiology, v. 56, p. 156-161.

Kiene, R.P., Oremland, R.S., Catena, A., Miller, L.G., and Capone, D.G., 1986, Metabolism of reduced methylated sulfur compounds in anaerobic sediments and by a pure culture of an estuarine methanogens: Applied and Environmental Microbiology, v. 52, p. 1037-1045.

Kinkle, B., and Kane, T.C., 2000, Chemolithoautotrophic micro-organisms and their potential role in subsurface environments, *in* Wilkens, H., Culver,

D.C., Humphreys, W.F., eds., Ecosystems of the World 30: Amsterdam, Elsevier, p. 309-318.

Kirchman, D.L., Keil, R.G., Simon, M., and Welschmeyer, N.A., 1993, Biomass and production of heterotrophic bacterioplankton in the oceanic subarctic Pacific: Deep-Sea Research, p. 967-988.

Klimchouk, A.B., Ford, D.C., Palmer, A.N., Dreybrodt, W. (eds.), 2000, Speleogenesis: Evolution of Karst Aquifers: Huntsville, National Speleological Society, Inc., p.527.

Kodama, Y., and Watanabe, K., 2002, Production of sulfate from petroleum by a sulfur-oxidizing anaerobic chemolithotroph, *in* Albrechtsen, H.-J., and Aamand, J., eds., International Symposium on Subsurface Microbiology: Copenhagen, Denmark, p. 67.

Kodama, Y., and Watanabe, K., 2003, Isolation and characterization of a sulfur-oxidizing chemolithotroph growing on crude oil under anaerobic conditions: Applied and Environmental Microbiology, v. 69, p. 107-112.

Kolmos, H.J., and Schmidt, J., 1987, Failure to detect hydrogen-sulphide production in lactose/sucrose-fermenting Enterobacteriaceae, using triple sugar iron agar: Acta Pathol. Microbiol. Immunol. Scand. [B], v. 95, p. 85-87.

Kristensen, E., Bodenbender, J., Jensen, M.H., Rennenberg, H., and Jensen, K.M., 2000, Sulfur cycling of intertidal Wadden Sea sediments (Konigshafen Island of Sylt, Germany): sulfate reduction and sulfur gas emission: Journal of Sea Research, v. 43, p. 93-104.

Kwok, D.Y., Lam, C.N.C., Li, A., Leung, A., Wu, R., Mok, E., and Neumann, A.W., 1998, Measuring and interpreting contact angles: a complex issue: Colloids and Surfaces A: Physicochemical and Engineering Aspects, v. 142, p. 219-235.

Kwok, D.Y., Ng, H., and Neumann, A.W., 2000, Experimental study on contact angle patterns: liquid surface tensions less than solid surface tensions: Journal of Colloid and Interface Science, v. 225, p. 323-328.

Lane, D.J., 1991, 16S/23S rRNA sequencing, *in* Stackebrandt, E., and Goodfellow, M., eds., Nucleic Acid Techniques in Bacterial Systematics: New York, Wiley, p. 115-175.

Larkin, L.M., 1989, Genus II. *Thiothrix* Winogradsky 1888., *in* Staley, J.P., Bryant, M.P., Pfenning, N., and Holt, J.G., eds., Bergey's Manual of Systematic Bacteriology, Volume 3: Baltimore, Williams and Wilkins, p. 2098-2101.

Leff, L.G., Dana, J.R., McArthur, J.V., and Shimkets, L.J., 1995, Comparison of methods of DNA extraction from stream sediments: Applied and Environmental Microbiology, v. 61, p. 1141-1143.

Legrand, M., Feniet-Saigne, C., Saltzman, E.S., Germain, C., Barkov, N.I., and Petrov, V.N., 1991, Ice-core record of oceanic emission of dimethylsulfide during the last climate cycle: Nature, v. 350, p. 144-146.

Lemmon, A.R., and Milimkovitch, M.C., 2002, The metapopulation genetic algorithm: An efficient solution for the problem of large phylogeny estimation: Proceedings of the National Academy of Science USA, v. 99, p. 10516-10521.

Li, L., Guezennec, J., Nichols, P., Henry, P., Yanagibayashi, M., and Kato, C., 1999a, Microbial diversity in Nankai Trough sediments at a depth of 3,843 m: Journal of Oceanography, v. 55, p. 635-642.

Li, L., Kato, C., and Horikoshi, K., 1999b, Bacterial diversity in deep-sea sediments from different depths: Biodiversity and Conservation, v. 8, p. 659-667.

Liles, M.R., Manske, B.F., Bintrim, S.B., Handelsman, J., and Goodman, R.M., 2003, A census of rRNA genes and linked genomic sequences within a soil metagenomic library: Applied and Environmental Microbiology, v. 69, p. 2684-2691.

Lomans, B.P., Smolders, A.L., Intven, L.M., Pol, A., Op den Camp, H.J.M., and van der Drift, C., 1997, Formation of dimethyl sulfide and methanethiol in anoxic freshwater sediments: Applied and Environmental Microbiology, v. 63, p. 4741-4747.

Lomans, B.P., Op den Camp, H.J.M., Pol, A., van der Drift, C., and Vogels, G.D., 1999a, Role of methanogens and other bacteria in degradation of dimethyl sulfide and methanethiol in anoxic freshwater sediments: Applied and Environmental Microbiology, v. 65, p. 2116-2121.

Lomans, B.P., Op den Camp, H.J.M., Pol, A., and Vogels, G.D., 1999b, Anaerobic and aerobic degradation of dimethyl sulfide and methanethiol in anoxic freshwater sediments: Applied and Environmental Microbiology, v. 65, p. 438-443.

Longnecker, K., and Reysenbach, A.-L., 2001, Expansion of the geographic distribution of a novel lineage of epsilon-*Proteobacteria* to a hydrothermal vent site on the Southern East Pacific Rise: FEMS Microbiology Ecology, v. 35, p. 287-293.

López-Garcia, P., Gaill, F., and Moreira, D., 2002, Wide bacterial diversity associated with tubes of the vent worm *Riftia pachyptila*: Environmental Microbiology, v. 4, p. 204-215.

López-García, P., Duperron, S., Philippot, P., Foriel, J., Susini, J., and Moreira, D., 2003, Bacterial diversity in hydrothermal sediment and epsilonproteobacterial dominance in experimental microcolonizers at the Mid-Atlantic Ridge: Environmental Microbiology, v. 5, p. 961-976.

Luijten, M.L.G.C., de Weert, J., Smidt, H., Boschker, H.T.S., de Vos, W.M., Schraa, G., and Stams, A.J.M., 2003, Description of *Sulfurospirillum halorespirans* sp. nov., an anaerobic tetrachloroethene-respiring bacterium, and transfer of *Dehalospirillum multivorans* to the genus *Sulfurospirillum* as *Sulfurospirillum multivorans* comb. nov.: International Journal of Systematic and Evolutionary Microbiology, v. 53, p. 787-793.

Lovely, D.R., 2001, Reduction of iron and humics in subsurface environments, in Fredrickson, J.K., and Fletcher, M., eds., Subsurface Microbiology and Biogeochemistry: New York, Wiley-Liss, p. 193-217.

Lovley, D.R., and Phillips, E.J.P., 1986, Organic matter mineralization with reduction of ferric iron in anaerobic sediments: Applied and Environmental Microbiology, v. 51, p. 683-689.

Lowe, D., and Gunn, J., 1995, The role of strong acid in speleo-inception and subsequent cavern development, *in* Barany-Kevei, I., and Mucsi, L., eds., Special Issue Acta Geographica (Szeged), v. 34, p. 33-60.

Loy, A., Horn, M., and Wagner, M., 2003, probeBase - an online resource for rRNA-targeted oligonucleotide probes: Nucleic Acids Research, v. 31, p. 514-416.

Ludwig, W., and Strunk, O., 1996, ARB: a software environment for sequence data. Department of Microbiology, Technical University of Munich, Munich, Germany.

MacFarlane, G.T., and Gibson, G.R., 1991, Anaerobic Microbiology: a practical approach: Oxford, Oxford University Press, 201-222 p.

Madrid, V.M., Taylor, G.T., Scranton, M.I., and Chistoserdov, A.Y., 2001, Phylogenetic diversity of bacterial and Archaeal communities in the anoxic zone of the Cariaco Basin: Applied and Environmental Microbiology, v. 67, p. 1663-1674.

Maidak, B.L., Cole, J.R., Lilburn, T.G., Parker, C.T., Jr., Saxman, P.R., Farris, R.J., and al., e., 2001, The RDP-II (Ribosomal database project): Nucleic Acids Research, v. 29, p. 173-174.

Maltsev., V., 1993, Minerals of the Cupp-Coutunn karst cave systems, southeast Turkmenistan: World of Stones, v. 2., p. 5-30.

Maltsev, V., Korshynov, V., and Semikolennykh, A., 1997, Cave chemolithotrophic soils, *in* Jeannin, P., ed., 12th International Congress of Speleology, Volume 1: La-Chaux-de-Fonds, Switzerland, p. 29-32.

Manz, W., Amann, R., Ludwig, W., Vancanneyt, M., and Schleifer, K.-H., 1996, Application of a suite of 16S rRNA-specific oligonucleotide probes designed to investigate bacteria of the phylum *Cytophaga-Flavobacter-Bacteriodes* in the natural environment: Microbiology, v. 142, p. 1097-1106.

Manz, W., Amann, R., Ludwig, W., Wagner, M., and Schleifer, K.-H., 1992, Phylogenetic oligodeoxynucleotide probes for the major subclasses of *Proteobacteria*: problems and solutions: Systematic and Applied Microbiology, v. 15, p. 593-600.

Martin, A.P., 2002, Phylogenetic approaches for describing and comparing the diversity of microbial communities: Applied and Environmental Microbiology, v. 68, p. 3673-3682.

Mattison, R., Abbiati, M., Dando, P., Fitzsimons, M., Pratt, S., Southward, A., and Southward, E., 1998, Chemoautotrophic microbial mats in submarine caves with hydrothermal sulphidic springs at Cape Palinuro, Italy: Microbial Ecology, v. 35, p. 58-71.

McCrea, J.M., 1950, On the isotopic chemistry of carbonates and a paleotemperature scale: Journal of Chemical Physics, v. 18, p. 849-857.

McDougald, D., Rice, S., Weichart, D., and Kjelleberg, S., 1998, Nonculturablility: adaptation or debilitation?: FEMS Microbiology Ecology, v. 25, p. 1-9.

McDonald, I.R., Kelly, D.P., Murrell, J.C., and Wood, A.P., 1996, Taxonomic relationships of *Thiobacillus halophilus*, *T. aquaesulis*, and other species of *Thiobacillus*, as determined using 16S rDNA sequencing: Archives in Microbiology, v. 166, p. 394-398.

McMahon, R.F., 1975, Growth, reproduction and bioenergetic variation in three natural populations of a freshwater limpit *Laevapex fuscus* (C.B. Adams): Proceedings of Malacol. Society of London, v. 41, p. 331-342.

Meier, H., Amann, R., Ludwig, W., and Schleifer, K.-H., 1999, Oligonucleotide probes for in situ detection of a major group of Gram-positive bacteria with low DNA G+C content: Systematic and Applied Microbiology, v. 22, p. 186-196.

Mikell, A.T., Smith, C.L., and Richardson, J.C., 1996, Evaluation of media and techniques to enumerate heterotrophic microbes from karst and sand aquifer springs: Microbial Ecology, v. 31, p. 115-124.

Millero, F.J., 2001, Physical Chemistry of Natural Waters: New York, Wiley-Interscience, p. 654.

Millero, F.J., Hubinger, S., Fernandez, M., and Garnett, S., 1987, Oxidation of H_2S in seawater as a function of temperature, pH, and ionic strength: Environmental Science and Technology, v. 21, p. 439-443.

Minz, D., Fishbain, S., Green, S.J., Muyzer, G., Cohen, Y., Rittmann, B.E., and Stahl, D.A., 1999a, Unexpected population distribution in a microbial mat community: sulfate-reducing bacteria localized to the highly oxic chemocline in contrast to a eukaryotic preference for anoxia: Applied and Environmental Microbiology, v. 65, p. 4659-4665.

Minz, D., Flax, J.L., Green, S.J., Muyzer, G., Cohen, Y., Wagner, M., Rittmann, B.E., and Stahl, D.A., 1999b, Diversity of sulfate-reducing bacteria in oxic and anoxic regions of a microbial mat characterized by comparative analysis of dissimilatory sulfite reductase genes: Applied and Environmental Microbiology, v. 65, p. 4666-4671.

Miroshnichenko, M.L., Kostrikina, N.A., L'Haridon, S., Jeanthon, C., Hippe, H., Stackebrandt, E., and Bonch-Osmolovskaya, E.A., 2002, *Nautilia lithotrophica* gen. nov., sp. nov., a thermophilic sulfur-reducing ε-proteobacterium isolated from a deep-sea hydrothermal vent: International Journal of Systematic and Evolutionary Microbiology, v. 52, p. 1299-1304.

361

Miroshnichenko, M.L., L'Haridon, S., Schumann, P., Spring, S., Bonch-Osmolovskaya, E.A., Jeanthon, C., and Stackebrandt, E., 2004, *Caminibacter profundus* sp. nov., a novel thermophile of *Nautiliales* ord. nov. within the class "*Epsilonproteobacteria*", isolated from a deep-sea hydrothermal vent: International Journal of Systematic and Evolutionary Microbiology, v. 54, p. 41-45.

Moissl, C., Rudolph, C., and Huber, R., 2002, Natural communities of novel Archaea and bacteria with a string-of-pearls-like morphology: molecular analysis of the bacterial partners: Applied and Environmental Microbiology, v. 68, p. 933-937.

Morris, C.E., Bardin, M., Berge, O., Frey-Klett, P., Fromin, N., Girardin, H., Guinebretière, M.-H., Lebaron, P., Thiéry, J.M., and Troussellier, M., 2002, Microbial biodiversity: approaches to experimental design and hypothesis testing in primary scientific literature from 1975 to 1999: Microbiology and Molecular Biology Reviews, v. 66, p. 592-616.

Morse, J.W., and Berner, R.C., 1972, Dissolution kinetics of calcium carbonate in sea water; I, A kinetic origin for the lysocline: American Journal of Science, v. 272, p. 840-851.

Moyer, C.L., Dobbs, F.C., and Karl, D.M., 1995, Phylogenetic diversity of the bacterial communities from a microbial mat at an active, hydrothermal vent system, Loihi Seamount, Hawaii: Applied and Environmental Microbiology, v. 61, p. 1555-1562.

Muyzer, G., Teske, A., Wirsen, C.O., and Jannasch, H.W., 1995, Phylogenetic relationships of *Thiomicrospira* species and their identification in deep-sea hydrothermal vent sample by denaturing gradient gel electrophoresis of 16S rDNA fragments: Archives in Microbiology, v. 164, p. 165-172.

Naeem, S., 2002, Autotrophic-heterotrophic interactions and their impacts on biodiversity and ecosystem functioning, *in* Kinzig, A.P., Pacala, S.W., and Tilman, D., eds., The Functional Consequences of Biodiversity: Empirical progress and theoretical extensions. Monographs in Population Biology 33: Princeton, Princeton University Press, p. 96-119.

Naganuma, T., Kato, C., Hirayama, H., Moriyama, N., Hashimoto, J., and Horikoshi, K., 1997, Intracellular occurrence of ε-Proteobacterial 16S rDNA sequences in the vestimentiferan trophosome: Journal of Oceanography, v. 53, p. 193-197.

Nagy, K.L., 1995, Dissolution and precipitation kinetics of sheet silicates, *in* White, A.F., and Brantley, S.L., eds., Chemical Weathering Rates of Silicate Minerals, Volume Reviews in Mineralogy, vol. 31: Washington D.C., Mineralogical Society of America, p. 173-233.

Nation, J.L., 1983, A new method using hexamethyldisilazane for preparation of insect soft tissues for scanning electron microscopy: Stain Technology, v. 58, p. 347-351.

Neef, A., Amann, R., Schlesner, H., and Schleifer, K.-H., 1998, Monitoring a widespread bacterial group: in situ detection of *Planctomycetes* with 16S rRNA-targeted probes: Microbiology, v. 144, p. 3257-3266.

Nelson, D.C., Revsbech, N.P., and Jorgensen, B.B., 1986, Microoxic-anoxic niche of *Beggiatoa* spp.: microelectrode survey of marine and freshwater strains: Applied and Environmental Microbiology, v. 52, p. 161-168.

Nemati, M., Jenneman, G.E., and Voordouw, G., 2001, Mechanistic study of microbial control of hydrogen sulfide production in oil reservoirs: Biotechnology and Bioengineering, v. 74, p. 424-434.

Newbold, J.D., Elwood, J.W., O'Neill, R.V., and Van Winkle, W., 1981, Measuring nutrient spiraling in streams: Canadian Journal of Fishery and Aquatic Science, v. 38, p. 860-863.

Newbold, J.D., Mulholland, P.J., Elwood, J.W., and O'Neill, R.V., 1982, Organic carbon spiraling in stream ecosystems: Oikos, v. 38, p. 266-272.

Newbold, J.D., O'Neill, R.V., Elwood, J.W., and Van Winkle, W., 1982, Nutrient spiraling in streams: Implications for nutrient limitation and invertebrate activity: American Naturalist, v. 120, p. 628-652.

Newman, D.K., and Banfield, J.F., 2002, Geomicrobiology: How molecular-scale interactions underpin biogeochemical systems: Science, v. 296, p. 1071-1077.

Nielsen, P.H., Aquino de Muro, M., and Nielsen, J.L., 2000, Studies of the in situ physiology of *Thiothrix* spp. present in activated sludge: Environmental Microbiology, v. 2, p. 389-398.

Northup, D.E., and Lavoie, K.H., 2001, Geomicrobiology of caves: a review: Geomicrobiology Journal, v. 18, p. 199-222.

Northup, D.E., Barns, S.M., Yu, L.E., Spilde, M.N., Schelble, R.T., Dano, K.E., Crossey, L.J., Connolly, C.A., Boston, P.J., Natvig, D.O., and Dahm, C.N., 2003, Diverse microbial communities inhabiting ferromanganese deposits in Lechuguilla and Spider Caves: Environmental Microbiology, v. 5, p. 1071-1086.

Nübel, U., Garcia-Pichel, F., Kuhl, M., and Muyzer, G., 1999, Quantifying microbial diversity: morphotypes, 16S rRNA genes, and carotenoids of oxygenic phototrophs in microbial mats: Applied and Environmental Microbiology, v. 65, p. 422-430.

Nübel, U., Bateson, M.M., Madigan, M.T., Kuhl, M., and Ward, D.M., 2001, Diversity and distribution in hypersaline microbial mats of bacteria related to *Chloroflexus* spp.: Applied and Environmental Microbiology, v. 67, p. 4365-4371.

Olson, R., and Thompson, D., 1988, Scanning electron microscopy and energy dispersive x-ray analysis of artificial and natural substrates from the Phantom flowstone of Sulphur River in Parker Cave, Kentucky: National Speleological Society Bulletin, v. 50, p. 47-53.

On, S.L.W., 2001, Taxonomy of *Campylobacter, Arcobacter, Helicobacter*, and related bacteria: current status, future prospects and immediate concerns: Journal of Applied Microbiology, v. 90, p. 1S-15S.

Oremland, R.S., and Capone, D.G., 1988, Use of "specific" inhibitors in biogeochemistry and microbial ecology: Advances in Microbial Ecology, v. 10, p. 285-383.

Otte, S., Kuenen, J.G., Nielsen, L.P., Paerl, H.W., Zopfi, J., Schulz, H.N., Teske, A., Strotmann, B., Gallardo, V.A., and Jorgense, B.B., 1999, Nitrogen, carbon, and sulfur metabolism in natural *Thioploca* samples: Applied and Environmental Microbiology, v. 65, p. 3148-3157.

Pagel, M., Barbin, V., Blanc, P., and Ohnenstetter, D., eds., 2000, Cathodoluminescence in Geosciences: Berlin, Springer-Verlag, 514p.

Palleroni, N.J., 1997, Prokaryotic diversity and the importance of culturing: Antonie van Leeuwenhoek, v. 72, p. 3-19.

Palmer, A.N., 1991, Origin and morphology of limestone caves: Geological Society of America Bulletin, v. 103, p. 1-21.

Palmer, A.N., 1995, Geochemical models for the origin of macroscopic solution porosity in carbonate rocks, *in* Budd, A., Saller, A., and Harris, P., eds., Unconformities and Porosity in Carbonate Strata: Memoir 63: Tulsa, AAPG, p. 77-101.

Palmer, A., and Palmer, M.V., 1989, Geologic history of the Black Hills caves, South Dakota: National Speleological Society Bulletin, v. 51, p. 72-99.

Palmer, A., and Palmer, M.V, 2000, Hydrochemical interpretation of cave patterns in the Guadalupe Mountains, New Mexico: Journal of Cave and Karst Studies, v. 62, p. 91-108.

Papke, R.T., Ramsing, N.B., Bateson, M.M., and Ward, D.M., 2003, Geographical isolation in hot spring cyanobacteria: Environmental Microbiology, v. 5, p. 650–659.

Parkhurst, D.L., and Appelo, C.A.J., 1999, User's guide to PHREEQC (version 2) - a computer program for speciation, batch-reaction, one-dimensional transport, and inverse geochemical calculations, U.S. Geological Survey Water-Resources Investigations Report, p. 312.

Parkinson, D., Gray, T.R.G., and Williams, S.T., 1971, Methods for Studying the Ecology of Soil Micro-organisms: Oxford, Blackwell Scientific Publications, p. 30-31.

Parks, G.A., 1990, Surface energy and adsorption at mineral-water interfaces: an introduction, *in* Hochella, J., M.F., and White, A.F., eds., Mineral-Water Interface Geochemistry, Volume 23: Washington, D.C., Mineralogical Society of America, p. 133-175.

Pasquini, G., 1973, Aggressive condensation, Proceedings of the 6th International Congress of Speleology, Volume 8, p. 315-318.

Paul, E.A., and Clark, F.E., 1996, Soil Microbiology and Biochemistry: San Diego, Academic Press, 340 p.

Pedersen, K., Hallbeck, L., Arlinger, J., Erlandson, A.C., and Jahromi, N., 1997, Investigations of the potential for microbial contamination of deep granitic aquifers during drilling using 16S rRNA gene sequencing and culturing methods: Journal of Microbiological Methods, v. 30, p. 179-192.

Pedersen, K., 2001, Exploration of deep intraterrestrial microbial life: current perspectives: FEMS Microbiology Letters, v. 185, p. 9-16.

Plummer, L.N., Busby, F., Lee, R.W., and Hanshaw, B.B., 1990, Geochemical modeling of the Madison Aquifer in parts of Montana, Wyoming, and South Dakota: Water Resources Res., v. 26, p. 1981-2014.

Polyak, V.J., and Güven, N., 2004, Silicates in carbonate speleothems, Guadalupe Mountains, New Mexico, U.S.A., *in* Sasowsky, I.D., and Mylroie, J., Studies of Cave Sediments: Physical and Chemical Records of Paleoclimate: New York, Kluwer Academic/Plenum Publishers, p. 303-311.

Polyak, V.J., and Provincio, P., 2001, By-product materials related to H_2S-H_2SO_4-influenced speleogenesis of Carlsbad, Lechuguilla, and other caves of the Guadalupe Mountains, New Mexico: Journal of Cave and Karst Studies, v. 63, p. 23-32.

Polyak, V.J., McIntosh, W.C., Güven, N., and Provencio, P., 1998, Age and origin of Carlsbad Cavern and related caves from 40Ar/39Ar of alunite: Science, v. 279, p. 1919-1922.

Polz, M.F., and Cavanaugh, C.M., 1995, Dominance of one bacterial phylotype at a mid-Atlantic ridge hydrothermal vent site: Proceedings of the National Academy of Sciences USA, v. 92, p. 7232-7236.

Porter, M.L., 1999, Ecosystem Energetics of Sulfidic Karst [Unpublished Masters thesis]: Cincinnati, Cincinnati, 52p.

Posada, D., and Crandall, K.A., 1998, Modeltest: testing the model of DNA substitution: Bioinformatics, v. 14, p. 817-818.

Poulson, T.L., and Lavoie, K.H., 2000, The trophic basis of subsurface ecosystems, *in* Wilkens, H., Culver, D.C., and Humphreys, W.F., eds., Ecosystems of the World 30: Subterranean Ecosystems: Amsterdam, Elsevier, p. 231-249.

Preuß, A., Schauder, R., and Fuchs, G., 1989, Carbon isotope fractionation by autotrophic bacteria with three different CO_2 fixation pathways: Z. Naturforsch, v. 44c, p. 397-402.

Rajagopal, B.S., and Daniels, L., 1986, Investigation of mercaptans, organic sulfides, and inorganic sulfur compounds as sulfur sources for the growth of methanogenic bacteria: Current Microbiology, v. 14, p. 137-144.

Ramseyer, K., and Mullis, J., 2000, Geologic application of cathodoluminescence of silicates, *in* Pagel, M., Barbin, V., Blanc, P., and Ohnenstetter, D. (eds.), Cathodoluminescence in Geosciences: Berlin, Springer-Verlag, p. 177-191.

Reheis, M.C., 1984, Drainage history of the Northern Bighorn Basin: Chronology and tectonic effect, *in* Reheis, M.C., Ritter, D.F., and Palmquist, R.C., eds., Late Cenozoic History and Soil Development, Northern Bighorn Basin, Wyoming and Montana, Guidebook for the Joint Field Trip of the Friends of the Pleistocene, Rocky Mountain Cell, and the American Quaternary Association, p. 11-49.

Reichenbach, H., 1992, The order *Cytophagales*, *in* Balows, A., Truper, H.G., Dworkin, M., Harder, W., and Schleifer, K.-H., eds., The Prokaryotes, Volume IV: New York, Springer-Verlag, p. 3631-3675.

Reysenbach, A.-L., Longnecker, K., and Kirshtein, J., 2000, Novel bacterial and archaeal lineages from an in situ growth chamber deployed at a Mid-Atlantic Ridge hydrothermal vent: Applied and Environmental Microbiology, v. 66, p. 3798-2806.

Ricotta, C., 2003, Parametric scaling from species relative abundances to absolute abundances in the computation of biological diversity: a first proposal using Shannon's entropy: Acta Biotheoretica, v. 51, p. 181-188.

Rimbault, A., Niel, P., Virelizier, H., Carbord, J.C., and Leluan, G., 1988, L-methionine, a precursor of trace methane in some proteolytic clostridia: Applied and Environmental Microbiology, v. 54, p. 1581-1586.

Rimstidt, J.D., 1997, Quartz solubility at low temperatures: Geochimica et Cosmochimica Acta, v. 61, p. 2553-2558.

Rimstidt, J.D., and Barnes, H.L., 1980, The kinetics of silica-water reactions: Geochimica et Cosmochimica Acta, v. 44, p. 1683-1699.

Rios-Hernandez, L.A., Gieg, L.M., and Suflita, J.M., 2003, Biodegradation of an alicyclic hydrocarbon by a sulfate-reducing enrichment from a gas condensate-contaminated aquifer: Applied and Environmental Microbiology, v. 69, p. 434-443.

Robinson, J.J., and Cavanaugh, C.M., 1995, Expression of form I and form II Rubisco in chemoautotrophic symbioses: Implications for the interpretation of stable carbon isotope values: Limnology and Oceanography, v. 40, p. 1496-1502.

Roller, C., Wagner, M., Amann, R., Ludwig, W., and Schleifer, K.-H., 1994, In situ probing of gram-positive bacteria with high DNA G+C content using 23S rRNA-targeted oligonucleotides: Microbiology, v. 140, p. 2849-2858.

367

Ronquist, F., and Huelsenbeck, J.P., 2003, MrBayes 3: Bayesian phylogenetic inference under mixed models A: Bioinformatics, v. 19, p. 1572-1574.

Rousseau, R., and Van Hecke, P., 1999, Measuring biodiversity: Acta Biotheoretica, v. 47, p. 1-5.

Ruby, E.G., Jannasch, H.W., and Dueser, W.G., 1987, Fractionation of stable carbon isotopes during chemoautotrophic growth of sulfur-oxidizing bacteria: Applied and Environmental Microbiology, v. 53, p. 1940-1943.

Rudolph, C., Wanner, G., and Huber, R., 2001, Natural communities of novel Archaea and Bacteria growing in cold sulfurous springs with a string-of-pearls-like morphology: Applied and Environmental Microbiology, v. 67, p. 2336-2344.

Rzonca, B., and Schulze-Makuch, 2003, Correlation between microbiological and chemical parameters of some hydrothermal springs in New Mexico, USA: Journal of Hydrology, v. 280, p. 272-284.

Sarbu, S.M., Kane, T.C., and Kinkle, B.K., 1996, A chemoautotrophically based cave ecosystem: Science, v. 272, p. 1953-1955.

Sarbu, S.M., Galdenzi, S., Menichetti, M., and Gentile, G., 2000, Geology and biology of Grotte di Frasassi (Frasassi Caves) in Central Italy, an ecological multi-disciplinary study of a hypogenic underground karst system, *in* Wilkens, H., Culver, D., Humphreys, S., ed., Ecosystems of the World: Subterranean Ecosystems, Volume 30: Oxford, Elsevier Science, p. 361-381.

Schabereiter-Gurtner, C., Saiz-Jimenez, C., Piñar, G., Lubitz, W., and Rölleke, S., 2002, Phylogenetic 16S rRNA analysis reveals the presence of complex and partly unknown bacterial communities in Tito Bustillo Cave, Spain, and on its Palaeolithic paintings: Environmental Microbiology, v. 4, p. 392-400.

Schabereiter-Gurtner, C., Saiz-Jimenez, C., Piñar, G., Lubitz, W., and Rölleke, S., 2003, Phylogenetic diversity of bacteria associated with Paleolithic paintings and surrounding rock walls in two Spanish caves (Llonín and La Garma): FEMS Microbiology Ecology, v. 1606, p. 1-13.

Schmid, M., Twachtmann, U., Klein, M., Strous, M., Juretschko, S., Jettem, M.S.M., Metzger, J.W., Schleifer, K.-H., and Wagner, M., 2000, Molecular evidence for genus level diversity of bacteria capable of catalyzing anaerobic ammonium oxidation: Systematic and Applied Microbiology, v. 23, p. 93-106.

Scholten, J.C.M., Conrad, R., and Stams, A.J.M., 2000, Effect of 2-bromo-ethane sulfonate, molybdate and chloroform on acetate consumption by methanogenic and sulfate-reducing populations in freshwater sediment: FEMS Microbiology and Ecology, v. 32, p. 35-42.

Scholten, J.C.M., van Bodegom, P.M., Vogelaar, J., van Ittersum, A., Hordijk, K., Roelofsen, W., and Stams, A.J.M., 2002, Effect of sulfate and nitrate on acetate conversion by anaerobic microorganisms in a freshwater sediment: FEMS Microbiology Ecology, v. 42, p. 375-385.

Schopf, J.W., 1983, Earth's Earliest Biosphere: It's Origin and Evolution: Princeton, Princeton University Press.

Shelley, M., 1956, Karst and Caves of the Caucasus. University of Miami [Unpublished thesis], 72p.

Simenstad, C.A., Duggins, D.O., and Quay, P.D., 1993, High turnover of inorganic carbon in kelp habitats as a source of $\delta^{13}C$ variability in marine food webs: Marine Biology, v. 116, p. 147-160.

Simon, K.S., Benfield, E.F., and Macko, S.A., 2003, Food web structure and the role of epilithic biofilms in cave streams: Ecology, v. 84, p. 2395-2406.

Skirnisdottir, S., Hreggvidsson, G.O., Hjorleifsdottir, S., Marteinsson, V.T., Petursdottir, S.K., Holst, O., and Kristjansson, J.K., 2000, Influence of sulfide and temperature on species composition and community structure of hot spring microbial mats: Applied and Environmental Microbiology, v. 66, p. 2835-2841.

Smyk, B., and Drzal, M., 1964, Research on the influence of microorganisms on the development of karst phenomena: Geographica Polonica, v. 2, p. 57-60.

Snaider, J., Amann, R., Huber, I., Ludwig, W., and Scheifer, K.-H., 1997, Phylogenetic analysis and in situ identification of bacteria in activated sludge: Applied and Environmental Microbiology, v. 63, p. 2884-2896.

Speksnijder, A.G.C.L., Kowalchuk, G.A., De Jong, S., Kline, E., Stephen, J.R., and Laanbroek, H.J., 2001, Microvariation artifacts introduced by PCR and cloning of closely related 16S rRNA gene sequences: Applied and Environmental Microbiology, v. 67, p. 469-472.

Spencer, S.A., 1986, Groundwater movement in the Paleozoic rocks and impact of petroleum production on water levels in the southwestern Bighorn Basin, Wyoming: Laramie, [Unpublished thesis] University of Wyoming.

Stackebrandt, E., and Goebel, B.M., 1994, Taxonomic note: a place for DNA-DNA reassociation and 16S rRNA sequence analysis in the present species definition in bacteriology: International Journal of Systematic Bacteriology, v. 44, p. 846-849.

Stanier, R.Y., Ingraham, L.J., Wheelis, M.L., and Painter, P.R., 1986, The Microbial World, 5th ed.: New Jersey, Prentice Hall, 689 p.

Stevens, T.O., and McKinley, J.P., 1995, Lithoautotrophic microbial ecosystems in deep basalt aquifers: Science, v. 270, p. 450-454.

Stevens, T.O., 1997, Lithoautotrophy in the subsurface: FEMS Microbiology Reviews, v. 20, p. 327-337.

Stoessell, R.K., Moore, Y.H., and Coke, J.G., 1993, The occurrence and effect of sulfate reduction and sulfide oxidation on coastal limestone dissolution in Yucatan cenotes: Ground Water, v. 31, p. 566-575.

Stolz, J.F., Ellis, D.J., Blum, J.S., Ahmann, D., Lovley, D.R., and Oremland, R.S., 1999, *Sulfurospirillum barnsii* sp. nov. and *Sulfurospirillum arsenophilum* sp. nov., new members of the *Sulfurospirillum* clade of the epsilon *Proteobacteria*: International Journal of Systematic Bacteriology, v. 49, p. 1177-1180.

Stone, D.S., 1967, Theory of Paleozoic oil and gas accumulation in Big Horn basin, Wyoming: American Association of Petroleum Geologists Bulletin, v. 51, p. 2056-2114.

Stumm, W., and Morgan, J.J., 1996, Aquatic Chemistry: New York, John Wiley and Sons, Inc., 1022 p.

Su, L.-H., Ou, J.T., Leu, H.-S., Chiang, P.-C., Chiu, Y.-P., Chia, J.-H., Kuo, A.-J., Chiu, C.-H., Chu, C., Wu, T.-L., Sun, C.-F., Riley, T.V., Chang, B.J., and Group, T.I.C., 2003, Extended epidemic of nosocomial urinary tract infections caused by *Serratia marcescens*: Journal of Clinical Microbiology, v. 41, p. 4726-4732.

Swofford, D.L., 2000, PAUP* Phylogenetic analysis using parsimony and other methods (v4.0b10): Sunderland, Mass., Sinauer Associates.

Swofford, D.L., 2002, PAUP* Phylogenetic analysis using parsimony (*and other methods) (version 4): Sunderland, Mass., Sinauer Associates.

Symk, B., and Drzal, M., 1964, Research on the influence of microorganisms on the development of karst phenomena: Geographia Polonica, v. 2, p. 57-60.

Takai, K., Inagaki, F., Nakagawa, S., Hirayama, H., Nunoura, T., Sako, Y., Nealson, K.H., and Horikoshi, K., 2003, Isolation and phylogenetic diversity of members of previously uncultivated ε-*Proteobacteria* in deep-sea hydrothermal fields: FEMS Microbiology Letters, v. 218, p. 167-174.

Taylor, B.F., 1991, Bacterial transformation of organic sulfur compounds in marine environments, *in* Oremland, R.S., ed., Biogeochemistry of Global Change: Radiatively active trace gases: Selected papers from the 10th International Symposium of Environmental Biogeochemistry, San Francisco, Champman-Hall, p. 745-781.

Taylor, C.D., Wirsen, C.O., and Gaill, F., 1999, Rapid microbial production of filamentous sulfur mats at hydrothermal vents: Applied and Environmental Microbiology, v. 65, p. 2253-2255.

Thiry, M., and Millot, G., 1987, Mineralogical forms of silica and their sequence of formation in silcretes: Journal of Sedimentary Petrology, v. 57, p. 343-352.

Thompson, J.D., and Olson, R., 1988, A preliminary survey of the protozoa and bacteria from Sulphur River in Parkers Cave, Kentucky: National Speleological Society Bulletin, v. 50, p. 42-46.

Thompson, J.D., Gibson, T.J., Plewniak, F., Jeanmougin, F., and Higgins, D.G., 1997, The ClustalX windows interface: flexible strategies for multiple sequence alignment aided by quality analysis tools: Nucleic Acids Research, v. 24, p. 4876-4882.

Timmer-ten Hoor, A., 1975, A new type of thiosulfate-oxidizing, nitrate-reducing microorganism: *Thiomicrospira denitrificans* sp. nov.: Neth. Journal of Sea Research, v. 9, p. 343-351.

Todorov, J.R., Chistoserdov, A.Y., and Aller, J.Y., 2000, Molecular analysis of microbial communities in mobile deltaic muds of Southeastern Papua New Guinea: FEMS Microbiology Ecology, v. 33, p. 147-155.

Tonolla, M., Demarta, A., Peduzzi, S., Hahn, D., and Peduzzi, R., 2000, In situ analysis of sulfate-reducing bacteria related to *Desulfocapsa thiozymogenes*

in the chemocline of meromictic Lake Cadagno (Switzerland): Applied and Environmental Microbiology, v. 66, p. 820-824.

Toran, L., and Harris, R.F., 1989, Geochimica et Cosmochimica Acta, v. 53, p. 2341-2348.

Ulrich, G.A., Martino, D., Burger, K., Routh, J., Grossman, E.L., Ammerman, J.W., and Suflita, J.M., 1998, Sulfur cycling in the terrestrial subsurface: commensal interactions, spatial scales, and microbial heterogeneity: Microbial Ecology, v. 36, p. 141-151.

Urrutia, M.M., and Beveridge, T., 1993, Mechanism of silicate binding to the bacterial cell wall in *Bacillus subtilis*: Journal of Bacteriology, v. 175, p. 1936-1945.

Van Everdingen, R.O., Shakur, M.A., and Krouse, H.R., 1985, Role of corrosion by H_2SO_4 fallout in cave development in a travertine deposit - evidence from sulfur and oxygen isotopes: Chemical Geology, v. 49, p. 205-211.

Vandamme, P., and De Ley, J., 1991, Proposal for a new family, Campylobacteraceae: International Journal of Systematic Bacteriology, v. 41, p. 451-455.

Visscher, P.T., Quist, P., and van Gemerden, H., 1991, Methylated sulfur compounds in microbial mats: in situ concentrations and metabolism by a colorless sulfur bacterium: Applied and Environmental Microbiology, v. 57, p. 1758-1763.

Visscher, P.T., Baumgartner, L.K., Buckley, D.H., Rogers, D.R., Hogan, M.E., Raleigh, C.D., Turk, K.A., and Des Marais, D.J., 2003, Dimethyl sulfide and methanethiol formation in microbial mats: potential pathways for biogenic signatures: Environmental Microbiology, v. 5, p. 296-308.

Vlasceanu, L., Popa, R., and Kinkle, B., 1997, Characterization of *Thiobacillus thioparus* LV43 and its distribution in a chemoautotrophically based groundwater ecosystem: Applied and Environmental Microbiology, v. 63, p. 3123-3127.

Vlasceanu, L., Sarbu, S.M., Engel, A.S., and Kinkle, B.K., 2000, Acidic cave-wall biofilms located in the Frasassi Gorge, Italy: Geomicrobiology Journal, v. 17, p. 125-139.

von Wintzingerode, F., Gobel, U.B., and Stackebrandt, E., 1997, Determination of microbial diversity in environmental samples: Pitfalls of PCR-based rRNA analysis: FEMS Microbiology Reviews, v. 21, p. 213-229.

von Wintzingerode, F., Selent, B., Hegemann, W., and Gobel, U.B., 1999, Phylogenetic analysis of an anaerobic, trichlorobenzene-transforming microbial consortium: Applied and Environmental Microbiology, v. 65, p. 283-286.

Voordouw, G., Armstrong, S.M., Reimer, M.F., Fouts, B., Telang, A.J., Shen, Y., and Gevertz, D., 1996, Characterization of 16S rRNA genes from oil field microbial communities indicates the presence of a variety of sulfate-reducing, fermentative, and sulfide-oxidizing bacteria: Applied and Environmental Microbiology, v. 62, p. 1623-1629.

Wagner, M., Amann, R., Kämpfer, P., Assmus, B., Hartmann, A., Hutzler, P., Springer, N., and Schleifer, K.-H., 1994, Identification and in situ detection of gram-negative filamentous bacteria in activated sludge: Systematic and Applied Microbiology, v. 17, p. 405-417.

Wallner, G., Amann, R., and Beisker, W., 1993, Optimizing fluorescent in situ hybridization with rRNA-targeted oligonucleotide probes for flow cytometric identification of microorganisms: Cytometry, v. 14, p. 136-143.

Wardle, D.A., 2002, Communities and Ecosystem: linking the aboveground and belowground components: New Jersey, Princeton University Press, 392 p.

Watanabe, K., Kodama, Y., and Kaku, N., 2002, Diversity and abundance of bacteria in an underground oil-storage cavity: BMC Microbiology, v. 2, p.23 [online].

Watanabe, K., Watanabe, K., Kodama, Y., Syutsubo, K., and Harayama, S., 2000, Molecular characterization of bacterial populations in petroleum-contaminated groundwater discharged from underground crude oil storage cavities: Applied and Environmental Microbiology, v. 66, p. 4803-4809.

Watts, S.F., 2000, The mass budgets of carbonyl sulfide, dimethyl sulfide, carbon disulfide, and hydrogen sulfide: Atmospheric Environment, v. 34, p. 761-779.

White, W., 1988, Geomorphology and Hydrology of Karst Terrains: New York, Oxford University Press, 464 p.

Widdel, F., and Bak, F., 1992, Gram-negative mesophilic sulfate-reducing bacteria, *in* Balows, A., Truper, H., Dworkin, M., Harder, W., and Schleifer, K.-H., eds., The Prokaryotes: New York, Springer-Verlag, p. 3352-3378.

Wilson, W.H., 1960, Radioactive mineral deposits of Wyoming: Laramie, Geological Survey of Wyoming, Report of Investigations 7, p. 41.

Wind, T., Stubner, S., and Conrad, R., 1999, Sulfate-reducing bacteria in rice field soil and on rice roots: Systematic and Applied Microbiology, v. 22, p. 269-279.

Wirsen, C.O., Sievert, S.M., Cavanaugh, C.M., Molyneaux, S.J., Ahmad, A.T., L.T., DeLong, E.F., and Taylor, C.D., 2002, Characterization of an autotrophic sulfide-oxidizing marine *Arcobacter* sp. that produces filamentous sulfur: Applied and Environmental Microbiology, v. 68, p. 316-325.

Vita

Annette Summers Engel, born Annette Marie Summers in Akron, Ohio, on December 21, 1972, was the first child to Ronald Lee and Marie Alice Summers. After graduating from Marlington High School in Alliance, Ohio, in 1991, she attended Wittenberg University in Springfield, Ohio, from 1991-1995. She majored in Geology, went caving nearly every weekend, and graduated *cum laude* with a Bachelor of Arts degree in May, 1995. Annette met Scott Allen Engel at a Wittenberg caving function, and they were married November 4, 1995. Scott and Annette moved to Cincinnati, Ohio, where Annette attended graduate school at the University of Cincinnati from 1995-1999. She received a Masters of Science from the Department of Geology in 1997, with the thesis "The Speleogenesis of Movile Cave, Southern Dobrogea, Romania," and followed that degree with a Masters of Science from the Department of Biological Sciences in 1999 for completing the thesis work entitled "The Geomicrobiology of Sulfidic Cave Systems." Annette entered the University of Texas at Austin in the Fall of 1999 where she began her doctoral research in the Department of Geological Sciences with Philip C. Bennett. She and Scott look forward to the future when they will have more time to explore wild places.

Permanent address: 2400 Stone River Drive, Austin, Texas 78745

This dissertation was typed by the author.